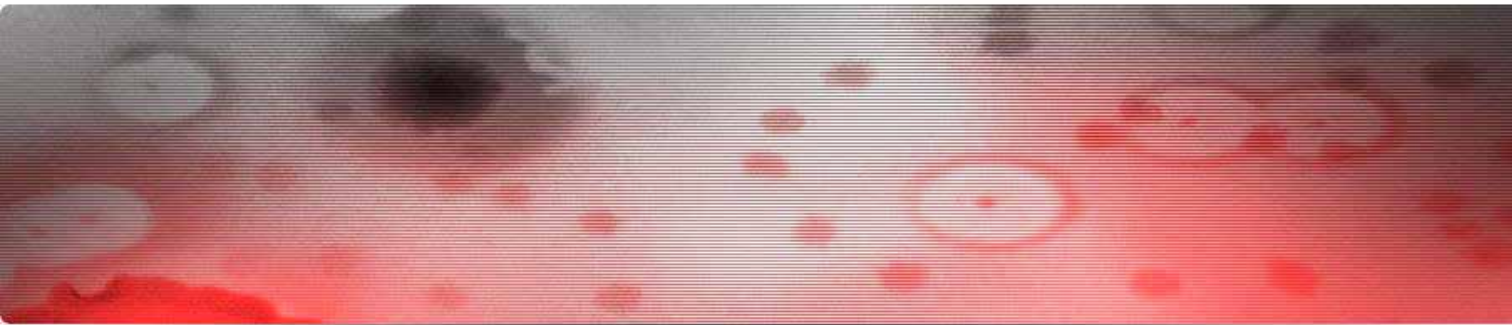


Thomas Clavel

Microbiologist



Gut microbiome in health and diseases: From ecosystem description to functional studies

Gut microbiome in health and diseases:

From ecosystem description to functional studies

Habilitationsschrift

vorgelegt von

Dr. rer. nat. Thomas Clavel

Nachwuchsgruppe Intestinales Mikrobiom

Zentralinstitut für Ernährungs- und Lebensmittelforschung (ZIEL)

Lehrstuhl für Ernährung und Immunologie

Fakultät Wissenschaftszentrum Weihenstephan für

Ernährung, Landnutzung und Umwelt

Freising-Weihenstephan



Technische Universität München

2014

Acknowledgements

For me, science is curiosity and the wish to understand and discover. But, most of all, science is made by human beings. Hence, one major driving factor in science is the exchange of knowledge, ideas, opinions, and emotions (which can be sometimes unfortunate if emotions are too negative, ignored or not under control). Many individuals in and outside scientific communities have influenced my career to date, and in many different ways. Due to space limitation and the fear to forget anyone, I will not draw here an exhaustive list. I will name just a few, knowing that all the persons who know me and have accompanied me on this journey will recognize themselves when reading these lines.

Over the last twelve years, I have had the privilege to be mentored by three outstanding scientists: Dr. Joël Doré, Prof. Michael Blaut, and Prof. Dirk Haller. In my opinion, they are outstanding for different reasons, and I am very grateful to have had the chance to learn from each of them. Joël, thanks to your wise guidance and your kindness, you have been a model in early steps of my career and throughout thereafter; thank you! Michael, your unconditional support, and your sense of loyalty and accurateness are exemplary: thank you! Dirk, your exhaustless dynamism, your clarity of vision, and your determination have always been very inspiring; thank you!

As already said, there are far too many names to be quoted here. I wish to express my gratitude to all professors, faculty members, colleagues and friends in Jouy, Potsdam, and Freising, who have supported me with my research and far beyond! I am also thankful to the colleagues and friends from partner institutions for fruitful exchanges and for making research so enjoyable.

My life, and thus my research, finds its source in all my friends, my family, and Julia: Thanks for all the shared moments, love, energy, and for showing me ways I would not have explored.

Table of contents

Prelude	5
<i>Curriculum vitae</i>	6
List of publications	7
Summary	11
Zusammenfassung	12
Résumé	13
PART I	14
Chapter 1 - Introduction	14
1 Background information	14
2 Questions and objectives	19
Chapter 2 - Main research activities and achievements	20
1 Microbiota diversity	21
1.1 Culturing is worth the effort.....	22
1.2 The need for molecular studies.....	27
2 Nutrition and microbiome	33
3 Microbe-host interaction: The gut-liver axis.....	39
Chapter 3 - Conclusion	43
Cited literature	44
PART II	50
Selected publications.....	50

Prelude

The present manuscript summarizes the outputs of my research activities in the field of gut microbial ecology since the official start of my Habilitation in May 2010. It is a cumulative work based on scientific papers published within the last 4 years. There should be no need of saying this, but as the rewards of collaborative effort in science get sometimes lost, I wish to make this clear from the start: I have been the major driver of the research outputs presented throughout the text, but I received of course intellectual, technical and infrastructural input from mentors, colleagues, team members in my junior group, and external collaborators, most of whom appear in the author lists of selected publications.

Part I of this Habilitation manuscript is divided into three chapters that respectively introduces some key concepts in the field, summarizes results, and gives some perspectives. Chapter 2 (the presentation of results and my research strategy) is the core of part I and is also divided into three sections according to my main research interests: (1) Microbiota diversity; (2) Nutrition and microbiome; and (3) Microbe-Host interaction. For the sake of clarity, each page of these sections is marked with the appropriate number (1, 2 or 3) in the right margin. In each of these three sections, I not only present major findings of my research on the corresponding topic, I also explain the rationale behind the work, detail some major accomplishments, and give opinions. That is, the present manuscript can be considered as the foundation of my research in the next few years.

Part II is the compilation of peer-reviewed original work published in scientific journals or as book chapters, which make up the backbone of part I. These publications are sorted as well into the three sections (1) “Microbiota diversity”, (2) “Nutrition and microbiome”, and (3) “Microbe-host interaction”. As in part I, for the sake of clarity, each page of these papers is numbered in the right margin according to the section to which the given publication belongs.

Curriculum vitae

Dr. rer. nat Thomas Clavel

Born on October 6th 1978 in Toulon (France)

RESEARCH ACTIVITIES:

- Present Junior Research Group Leader - Intestinal Microbiome (TUM, ZIEL)
- 2006-2011 Postdoctoral Research Associate; Dirk Haller's lab (TUM)
- 2002-2006 German-French joint PhD project; Michael Blaut's lab (DfE)
- 2002 Master project; Joël Doré's lab (INRA)

ACADEMIC QUALIFICATIONS:

- Present Ongoing habilitation (TUM)
- Feb 2006 PhD in microbiology (University of Potsdam and Châtenay-Malabry)
- Sept 2002 M.Sc. in Agricultural Sciences and Human Nutrition (ENSAR)
- May 1999 B.Sc. in biology (University of Toulouse)
- July 1997 French Scientific Baccalaureate (specialised in Mathematics)

AWARDS:

- Apr 2013 Grant holder of the European Nutrition Leadership program (advanced)
- July 2009 Travel awards (DAAD, SMI)
- May 2009 Travel awards (Danone Institute and SGM)
- Sept 2008 Stipend for research visits (BFHZ and SGM)
- June 2007 1st price for excellent PhD (University of Châtenay-Malabry)
- Apr 2006 Travel grant (SGM)
- Oct 2004 Scholarship holder of the DAAD Academic Exchange Service

List of publications

Total number published: 29; citations: ca. 1260; cumulative impact factor: ca. 140; h-index: 16

Peer-reviewed original work as principal investigator:

1. T Clavel,* C. Desmarchelier, D Haller, P Gérard, S Rohn, P Lepage, H Daniel (2014) Intestinal microbiota in metabolic diseases: from bacterial community structure and functions to species of pathophysiological relevance, *Gut Microbes* 5:544 (IF = 2.2); (* corresponding author)
2. H Daniel, A Moghaddas Gholami, D Berry, C Desmarchelier, H Hahne, G Loh, S Mondot, P Lepage, M Rothballer, A Walker, C Böhm, M Wenning, M Wagner, M Blaut, P Schmitt-Kopplin, B Kuster, D Haller, T Clavel (2014) High-fat diet alters gut microbiota physiology in mice, *ISME J* 8:295 (IF = 9.0; 14 citations)
3. K Kläring, L Hanske, N Bui, C Charrier, M Blaut, D Haller, CM Plugge, T Clavel (2013) *Intestinimonas butyriciproducens* gen. nov., sp. nov., a novel butyrate-producing bacterium from the mouse intestine, *Int J Syst Evol Microbiol* 63:4606 (IF = 2.1)
4. T Clavel,* C Charrier, M Wenning, D Haller (2013) *Parvibacter caecicola* gen. nov., sp. nov., a new bacterium of the family *Coriobacteriaceae* isolated from the caecum of a mouse, *Int J Syst Evol Microbiol* 63:2642 (IF = 2.1); (* corresponding author)
5. T Clavel,* C Charrier, D Haller (2013) *Streptococcus danieliae* sp. nov., a novel bacterium from the caecum of a mouse, *Arch Microbiol* 195:43 (IF = 2.1; 3 citations); (* corresponding author)
6. N Pfeiffer, C Desmarchelier, M Blaut, H Daniel, D Haller, T Clavel (2012) *Acetatifactor muris* gen. nov., sp. nov., a novel acetate- and butyrate-producing bacterium isolated from the intestine of an obese mouse, *Arch Microbiol* 194:901 (IF = 2.1; 3 citations)
7. T Clavel,* A Saalfrank, C Charrier, D Haller (2010) Isolation of bacteria from mouse cecal samples and description of *Bacteroides sartorii* sp. nov., *Arch Microbiol* 192:427 (IF = 2.1; 7 citations); (* corresponding author)

Peer-reviewed original work as principal investigator (prior to habilitation):

8. T Clavel,* W Duck, C Charrier, C Elson, D Haller (2009) *Enterorhabdus caecimuris* sp. nov., a novel member of the family *Coriobacteriaceae* isolated from a mouse model of spontaneous colitis, *Int J Syst Evol Microbiol* 60:1527 (IF = 2.1; 3 citations); (* corresponding author)
9. T Clavel,* C Charrier, A Braune, M Wenning, M Blaut, D Haller (2009) Isolation of bacteria from the ileal mucosa of TNF^{deltaARE} mice and description of *Enterorhabdus mucosicola* gen. nov., sp. nov., *Int J Syst Evol Microbiol* 59:1805 (IF = 2.1; 17 citations); (* corresponding author)
10. A Matthies, T Clavel,* M Gütschow, W Engst, D Haller, M Blaut, A Braune (2008) Conversion of daidzein and genistein by an anaerobic bacterium newly isolated from the mouse intestine, *Appl Environ Microbiol* 74:4847 (IF = 4.4; 42 citations) (* shared first authorship)
11. T Clavel, R Lippmann, F Gavini, J Doré, M Blaut (2007) *Clostridium saccharogumia* sp. nov. and *Lactonifactor longoviformis* gen. nov., sp. nov., two novel human faecal bacteria involved in the conversion of the dietary phytoestrogen secoisolariciresinol diglucoside, *Syst Appl Microbiol* 30: 16 (IF = 3.5; 44 citations)
12. T Clavel, G Henderson, W Engst, J Doré, M Blaut (2006) Phylogeny of human intestinal bacteria that activate the dietary lignan secoisolariciresinol diglucoside, *FEMS Microbiol Ecology* 55:471-8 (IF = 3.6; 69 citations)

13. T Clavel, D Borrmann, A Braune, J Doré, M Blaut (2006) Occurrence and activity of human intestinal bacteria involved in the conversion of dietary lignans, *Anaerobe* 12:140 (IF = 2.3; 70 citations)
14. T Clavel, G Henderson, C-A Alpert, C Philippe, L Rigottier-Gois, J Doré, M Blaut (2005) Intestinal bacterial communities that produce active estrogen-like compounds enterodiol and enterolactone in humans, *Appl Environ Microbiol* 71: 6077 (IF = 4.4; 89 citations)
15. T Clavel, M Fallani, P Lepage, F Levenez, J Mathey, V Rochet, M Sérézat, M Sutren, G Henderson, C Bennetau-Pelissero, F Tondu, M Blaut, J Doré, V Coxam (2005) Isoflavones and functional foods alter dominant intestinal microbiota in humans. *J Nutr* 135:2786 (IF = 4.2; 42 citations)

Peer-reviewed original work as collaborator:

1. M Wolf, A Adili, K Piotrowitz, Z Abdullah, Y Boege, K Stemmer, M Ringelhan, N Simonavicius, M Sigg, D Wohlleber, A Lorentzen, C Einer, S Schulz, T Clavel, U Protzer, C Thiele, H Zischka, H Moch, M Tschöp, AV Tumanov, D Haller, K Unger, M Karin, M Kopf, P Knolle, A Weber, M Heikenwalder2 (2014) Metabolic activation of intrahepatic CD8+ and NKT-cells causes nonalcoholic steatohepatitis and hepatocellular carcinoma via cross-talk with hepatocytes, *Cancer Cell* 26:549 (IF = 27.1)
2. J Hemmerling, K Heller, G Hörmannspenger, M Bazanella, T Clavel, G Kollias, D Haller (2014) Fetal exposure to maternal inflammation does not affect postnatal development of genetically driven ileitis and colitis, *PLoSone* 9:e98237 (IF = 3.7)
3. ME Perez-Munoz, K Bergstrom, V Peng, R, Schmaltz, R Jimenez-Cardona, N Marsteller, S McGee, T Clavel, L Xia, DA Peterson (2014) Discordance between dysbiosis and pathogenicity in a mouse model of spontaneous colitis, *Gut Microbes* 5:286 (IF = 2.2)
4. H Mabrok, R Klopffleisch, K Ghanem, T Clavel, M Blaut, G Loh (2011) Lignan transformation by gut bacteria lowers tumor burden in a gnotobiotic rat model of breast cancer, *Carcinogenesis* 33:203 (IF = 5.6; 14 citations)
5. J Mapesa, N Waldschmitt, I Schmoeller, C Blume, T Hofmann, S Mahungu, T Clavel, D Haller (2011) Catechols in caffeic acid phenethyl ester are essential for inhibition of TNF-mediated IP-10 expression through NF-kB-dependent but HO-1- and p38-independent mechanisms in mouse intestinal epithelial cells, *Mol Nutr Food Res* 55:1850 (IF = 4.3; 5 citations)
6. T Werner, S Wagner, I Martinez, J Walter, S Chang, T Clavel, S Kisling, K Schümann, D Haller (2011) Depletion of luminal iron alters the gut microbiota and prevents Crohn's disease-like ileitis, *Gut* 60:325 (IF = 10.7; 76 citations)
7. A Woting, T Clavel, G Loh, M Blaut (2010) Bacterial transformation of dietary lignans in gnotobiotic rats, *FEMS Microbiol Ecol* 72:507 (IF = 3.6; 19 citations)

Peer-reviewed original work as collaborator (prior to habilitation):

8. G Hörmannspenger, T Clavel, M Hoffmann, C Reiff, D Kelly, G Loh, M Blaut, G Hölzlwimmer, M Laschinger, D Haller (2009) Post-translational inhibition of IP-10 secretion in intestinal epithelial cells by probiotic bacteria: Impact on chronic inflammation, *PLoS One* 4:e4365 (IF = 3.7; 50 citations)
9. S Mueller, K Saunier, C Hanisch, E Norin, L Alm, T Midtvedt, A Cresci, S Silvi, C Orpianesi, M Verdenelli, T Clavel, C Koebnick, H-J Zunft, J Doré, M Blaut (2006) Differences in the fecal microbiota in different European study populations in relation to age, gender and country - a cross sectional study, *Appl Environ Microbiol* 72:1027 (IF = 4.4; 301 citations)

Review articles:

1. G Hörmannspurger, ^{*} T Clavel, ^{*} D Haller (2012) Gut matters: intestinal microbial ecology in allergic diseases, *J Allergy Clin Immunol* 129:1452 (IF = 12.1; 29 citations); (^{*} shared first authorship)

Review articles (prior to habilitation):

2. T Clavel, J Doré, M Blaut (2007) Bioavailability of lignans in human subjects, *Nutr Res Rev* 19:187 (IF = 2.2; 37 citations)
3. M Blaut, T Clavel (2007) Metabolic diversity of the intestinal microbiota: Implications for health and disease, *J Nutr* 137:751S (IF = 4.2; 180 citations)
4. T Clavel, D Haller (2007) Bacteria- and host-derived mechanisms to control intestinal epithelial cell homeostasis: implications for chronic intestinal inflammation, *IBD* 13:1153 (IF = 5.5; 78 citations)
5. T Clavel, D Haller (2007) Molecular interactions between bacteria, the epithelium and the mucosal immune system in the intestinal tract: Implications for chronic inflammation, *Curr Issues Intest Microbiol* 8:25 (IF = 3.7; 53 citations)

Book chapters:

1. T Clavel, P Lepage, C Charrier (2014) Family *Coriobacteriaceae*, In *The Prokaryotes*, 4th Edition, E Rosenberg, EF DeLong, F Thompson, S Lory, E Stackebrand (Eds), Springer, ISBN 978-3-642-30137-7
2. T Clavel, JO Mapesa (2013) Phenolics in human nutrition: importance of the intestinal microbiome for isoflavone and lignan bioavailability, In *Handbook of Natural Products*, KG Ramawat, JM Merillon (Eds), Elsevier, ISBN 978-3-642-221-43-9/44-6

Book (prior to habilitation):

1. T Clavel (2006) Metabolism of the dietary lignan secoisolariciresinol diglucoside by human intestinal bacteria, Logos Verlag Berlin, ISBN 3-8325-1192-X (PhD thesis)

Oral communications:

1. Alterations of fecal microbiota and metabolite landscape after oral or intravenous iron therapy in patients with IBD (**talk**), 2nd World Congress on Targeting Microbiota, 16-17 Oct 2014, Paris, France
2. MiBC: The Mouse intestinal Bacterial Collection (**talk and poster**), Herrenhausen Conference "Beyond the Intestinal Microbiome", 8-10 Oct 2014, Hannover, Germany
3. Microbes in prevention and therapy of chronic diseases (**invited talk**), 42nd Congress of the Germany Society for Rheumatology, 18th Sept 2014, Düsseldorf, Germany
4. Minimal bacterial consortia & the gut liver axis (**invited talk**), DSMZ, 8th July 2014, Braunschweig, Germany
5. Alterations of fecal microbiota and metabolite landscape after oral or intravenous iron therapy in patients with IBD (**talk**), 7th DGHM meeting "Microbiota, Probiota and Host", 4-6 July 2014, Seeon, Germany
6. Forgotten cultivable bugs: diversity and functions of novel mouse intestinal bacteria (**poster**), 9th Joint INRA-RRI Symposium on Gut Microbiology, 16-19 June 2014, Aberdeen, Scotland
7. Environmental factors - inflammation/antibiotics - triggers of microbiota composition and function (**invited talk**), Spring Conference of the German Society for Gastroenterology, Digestive and metabolic diseases, 23rd May 2014, Berlin, Germany
8. A microbial world within us: diversity and role of the gut microbiota in chronic inflammatory diseases (**invited talk**; in French), Rencontres de l'IMAD, 28th March 2014, CHU Nantes, France
9. Diet-induced obesity in mice: from community functions to single bacteria (**invited talk**), 23rd Oct 2013, Wageningen University, The Netherlands

10. Gut microbiota in mice: from communities to simplified models (**invited talk**), 18th Sept **2013**, INRA, Jouy, France
11. Regulation of metabolic processes by the gut microbiota: implications for the onset and treatment of metabolic disorders (**invited talk**; in German), Gastroenterology and visceral surgery congress, 11-14 Sept **2013**, Nürnberg, Germany
12. Functional analysis of the intestinal microbiota in a mouse model for Crohn's disease-like ileitis (**talk**), 6th DGHM meeting "Microbiota, Probiota and Host", 28-30 June **2013**, Seon, Germany
13. Alteration of the gut microbiota protects TNF^{deltaARE} mice from Crohn's disease-like ileitis (**poster**), Cell Symposia: Microbiome & Host Health, 12-14 May **2013**, Lisbon, Portugal
14. High energy diets alter the composition, proteome and metabolome of the mouse gut microbiota (**talk**), 8th Joint INRA-RRI Symposium on Gut Microbiology, 17-20th June **2012**, Clermont-Ferrand, France
15. Gut bacterial diversity in the TNF^{deltaARE} mouse model of ileitis (**talk**), 3rd DGHM meeting "Microbiota, Probiota and Host", 18-20 June **2010**, Seon, Germany

Oral communications (prior to habilitation):

16. Molecular chaperone networks in the gut: A study on novel bacteria from the intestine of TNF^{deltaARE} mice (**talk**), 14th International Congress of Mucosal Immunology, 5-9 July **2009**, Boston, USA
17. Molecular chaperone networks in the gut: A study on novel mouse and human intestinal bacteria (**poster**), EMBO Conference Series, The Biology of Molecular Chaperones, 23-28 May **2009**, Dubrovnik, Croatia
18. Forgotten cultivable bugs: Identity and functions of novel mouse intestinal bacteria (**poster**), 2nd DGHM meeting "Microbiota, Probiota and Host", 23-25 April **2009**, Seon, Germany
19. Intestinal bacteria in chronic inflammation (**invited talk**), LABHealth meeting, 31st March **2009**, INRA, Jouy, France
20. Endoplasmic reticulum and energy stress in intestinal epithelial cells under chronic inflammation: inhibitory effect of interleukin 10 (**talk**), 13th International Congress of Mucosal Immunology, 6-12 July **2007**, Tokyo, Japan
21. Lignan-converting human intestinal bacteria (**poster**), 158th SGM Meeting, 3-4 April **2006**, Warwick, England
22. Microbial conversion of dietary lignans in the human intestinal tract (**talk**), Annual VAAM Conference, 19-22 March **2006**, Jena, Germany
23. Metabolism of lignans by human intestinal bacteria (**poster**), 2nd International Conference on Polyphenols and Health, 4-7 Oct **2005**, Davis, USA
24. Metabolism of secoisolariciresinol by human intestinal bacteria (**talk**), 4th Joint INRA-RRI Symposium on Gut Microbiology, 21-24 June **2004**, Clermont-Ferrand, France

Summary

The gut microbiota refers to the communities of microorganisms living in our intestine. When taking their genomes into account, the term in use is microbiome. Pioneering work with germfree animals already highlighted the importance of the gut microbiota for host physiology in the 1960's. However, it has received a lot of attention again over the last decade, mainly due to major developments in the field of metagenomics. However, the time has come to provide specific and mechanistic evidence for the role of gut microbes in health, which must go beyond general and descriptive assessment of the ecosystem.

My primary interests in the field of microbial ecology are the study of intestinal bacterial diversity and the interactions between commensal bacteria and their environment (diet and host). I now see the chance to build on my expertise in the study of gut microbiota using both molecular and classical techniques in order to develop new lines of research on the implementation of novel metagenomics and culture-based approaches, as well as the impact of gut microbiota on molecular mechanisms underlying metabolic disorders. In the present work, my aim is to highlight the importance of cultivating bacteria, besides the need to improve the resolution of molecular tools (*in vitro* and *in silico*) for description of global and sample-specific diversity. I will show that the study of diversity can serve the purpose of translational research in experimental models for investigating specific features of the gut microbial ecosystem in relation to diet and the host. In particular, I will present data on the interaction between bacteria and plant polyphenols as well as the effect of dietary fat on bacterial communities, thereby highlighting special features of one specific bacterial family in the mammalian gut, the *Coriobacteriaceae*.

Zusammenfassung

Der Mensch besteht aus körpereigenen Zellen und Billionen von Mikroorganismen, die viele seiner Körperteile kolonisieren. Der Darm beherbergt das dichteste dieser mikrobiellen Ökosysteme, die sogenannte Darmmikrobiota. Bakterien sind Hauptbestandteile dieser Mikrobiota und haben komplexe und dynamische Wechselwirkungen mit dem Darm-assoziierten Immunsystem. Darüber hinaus steht die Physiologie des Wirtes unter permanentem Einfluss des Wechselspiels zwischen Bakterien im Darm und Lebensmittelbestandteilen aus der Nahrung. Dadurch beeinflussen Darmbakterien die Entstehung von vielen Infektionen und chronisch entzündlichen Erkrankungen (z.B. Allergien, Krebs, Darmentzündungen und Diabetes). Die Einsetzung therapeutischer bzw. präventiver Interventionen zur gezielten Modulierung der Darmmikrobiota scheint vielversprechend zu sein, ist aber aus zwei Hauptgründen eingeschränkt:

- Viele Bakterien im Darm sind immer noch unbekannt. Neuste Entwicklungen im Bereich der molekularen Analyse von mikrobiellen Populationen haben wichtige Einsichten in die Vielfalt der Darmmikrobiota ermöglicht, jedoch auf Kosten von klassischen Kultivierungsmethoden. Weitere Untersuchungen zur Identifizierung und Beschreibung von Darmbakterien durch die Kombination von molekularen und Kultur-abhängigen Techniken sind notwendig.
- Studien über das Zusammenspiel zwischen Nahrung und Darmbakterien und über die Rolle der Darmmikrobiota für die Aufrechterhaltung der Gesundheit bzw. die Entstehung chronisch entzündlicher Erkrankungen sind sehr häufig deskriptiv, d.h. unterliegende molekulare Mechanismen bleiben unerforscht. Untersuchungen müssen spezifisch werden und dazu dienen, dass mehr detaillierte mikrobielle Mechanismen zur Regulierung von gezielten Wirtsfunktionen identifiziert werden.

Zusammenfassend lässt sich sagen, dass die Erforschung der Darmmikrobiota von höchster Relevanz für die Gesundheit des Menschen ist. Diese Habilitationsschrift fasst die Ergebnisse meiner Arbeit der letzten vier Jahren im Bereich der bakteriellen Diversität, der Interaktion zwischen Nahrung und Darmbakterien, und der Rolle von Darmbakterien in metabolischen Erkrankungen zusammen.

Résumé

Le microbiote intestinal des mammifères est un écosystème complexe et dynamique, qui regroupe une diversité très importante de microorganismes, notamment des bactéries. Ces bactéries jouent un rôle prépondérant dans la régulation d'une multitude de fonctions physiologiques de l'espèce hôte, telles que les réponses immunitaires et les réactions métaboliques. Ces dix dernières années, l'avènement de techniques moléculaires d'analyse à haut-débit du microbiote intestinal a révolutionné notre vision de la complexité et du potentiel fonctionnel des communautés bactériennes. Cela a logiquement conduit à un regain d'intérêt pour le microbiote intestinal vis-à-vis de possibles applications dans le domaine de l'alimentation et de la médecine. Cependant, la recherche dans le domaine a d'ores et déjà atteint certaines limites, notamment par l'accumulation de données purement descriptives et le manque d'évidences fonctionnelles détaillant les mécanismes précis d'interaction entre l'hôte et son microbiote.

Ce manuscrit résume les résultats de mes recherches dans le domaine du microbiote intestinal au cours des quatre dernières années. Ces résultats ont pour but d'illustrer l'importance de développer de nouvelles approches robustes d'analyse du microbiote, non seulement vis-à-vis de l'exploitation des quantités massives de données accumulées dans les bases de données, mais aussi de la pertinence d'intensifier les efforts de recherche sur la base de techniques traditionnelles de culture. En effet, les travaux de culture permettent d'accroître notre connaissance de la diversité bactérienne ainsi que les possibilités d'études transverses dans le domaine de la nutrition et de la santé. Je vais ainsi présenter mes travaux en cours sur l'établissement de consortiums bactériens modélisant un écosystème complexe basé sur la première collection-type de souches originaires de l'intestin de souris. Je vais également exposer les données obtenues sur l'interaction entre le microbiote, les micronutriments (polyphénols) et surtout les macronutriments (acides gras) de l'alimentation, détaillant plus particulièrement l'intérêt d'étudier le métabolisme de composés dérivés du cholestérol par une famille particulière de bactéries, les *Coriobacteriaceae*.

PART I

Chapter 1 - Introduction

1 Background information

Mammals are supra-organisms.

Microorganisms are fascinating from many aspects: they are precursor forms of life that are found everywhere on earth;^{1, 2} they represent a tremendous biomass and their incredible diversity, boosted by the ability to evolve rapidly, make them a timeless reservoir of life;^{3, 4} and, they have accompanied the emergence of more complex organisms and thereby developed a wide array of relationship behaviors with them, from parasitism to symbiosis.⁵ Following the work of pioneers such as Louis Pasteur and Robert Koch, the last century of research on microorganisms has been dominated by medical microbiology.⁶ The heritage thereof was the consent that communities of endogenous bacteria, referred to as “microflora”, are present yet functionally not very important. In other words, many microbes explore niches for growth in and on our body and are ignored (or tolerated) by the immune system, but their functions were not given any particular attention. It has changed! Over the last 20 years, thanks to innovative technology-driven and experimental approaches, the

importance of mammalian body microbiota has become undeniable.⁷ From an evolutionary perspective, the human body can thus be considered as a supra-organism made of not only own eukaryotic cells, but also the hundred trillions of microorganisms that colonize various body sites such as the skin and the genital, respiratory and gastrointestinal (GI) tract. The GI microbiota is referred to as the assemblage of microbial communities and associated genomes (the microbiome) colonizing all niches from the oral cavity to the rectum. These communities represent a large pool of immune-activating molecules and carry out important metabolic functions such as the conversion of host- and food-derived substrates, thereby producing a broad variety of bioactive metabolites. For these reasons, the GI microbiota is known to influence host physiology, in particular metabolic and immune homeostasis.^{8, 9}

The gut microbiota is a complex and dynamic ecosystem.

In our intestine, communities of microbes are heterogeneous from proximal to distal parts and from luminal to mucosal sites. However, a hallmark of these communities along the GI tract is the dominance of bacteria, even though *Archaea* (e.g. the methane-producing species *Methanobrevibacter smithii*), eukaryotic microorganisms such as fungi and protozoa as well as viruses are also present. When compared to other environments, the intestinal microbiota consists primarily of only five of the 30 known bacterial phyla, i.e., the highest taxonomic level within the superkingdom Bacteria (see www.bacterio.cict.fr or www.ncbi.nlm.nih.gov/Taxonomy), namely: the *Firmicutes*, *Bacteroidetes*, *Actinobacteria*, *Proteobacteria*, and *Verrucomicrobia*.¹⁰ However, the diversity at low taxonomic levels is relatively high. Most recent molecular studies refer to a thousand different bacterial species in total and even more individual strains. This speaks in favor of intricate co-evolutionary forces that have shaped microbe-host relationships in the gut. It is important to keep in mind that most of the GI microbiome research has been performed on fecal communities. However, much of the dynamics occurring in the gut is most likely not reflected by this type of analysis. Hence, the spatial distribution of intestinal bacterial populations is a main issue that has started to be addressed in details.^{11, 12}

As often in biology, the efficacy of one complex system (the GI microbiota) is greater than the sum of its biologically active parts (bacterial strains). For instance, one key asset of the high diversity of our intestinal microbiota is that several bacterial species can carry out one given function. This is referred to as “functional redundancy” (one bacterium can take over the function of another if under environmental pressure the latter is deemed to disappear), which ensures flexibility and is crucial to achieve stability and ecosystem equilibrium overtime upon influence of various exogenous stimuli.¹³ Hence, this is the high diversity of our intestinal microbiota that helps us coping with the high diversity of exogenous chemical compounds that we ingest, and helps us also priming our immune system properly. Still, in spite of this high diversity, there are a few bacterial species (approx. 50), and by extension a few associated bacterial functions, that make up the so called “core microbiome”, *i.e.*, the assemblage of species/functions that are dominant (occur at high density) and show a high prevalence (they are found in most individuals).^{10, 14} Despite this notion of a core microbiome, each human being harbors its own GI microbiota, as in the sense of a personalized fingerprint. There are large inter-individual differences in both intestinal bacterial composition (proportion of taxa) and diversity (qualitative pattern of taxa), *i.e.*, even dominant bacterial groups are characterized by marked quantitative variations between gut samples from different individuals.^{10, 15, 16}

Individual GI microbiota profiles in adulthood depend on series of events affecting the ecosystem throughout life, especially early life. At birth, the human body gets colonized by microorganisms from the environment. Primary colonizers (aerobic or facultative anaerobic bacteria) help establishing a reduced environment suitable for subsequent colonization by strict anaerobes, which largely dominate the ecosystem in adulthood. In infants below 1-2 years of age, the GI microbiota is unstable and composition highly fluctuates.¹⁷ Environmental factors have of course a key influence in shaping gut bacterial communities, and nutrition plays an important role. For instance, breast- vs. formula-feeding influences microbial colonization patterns,^{18, 19} and the introduction of solid food has a strong impact on the diversity and functions of the GI microbiome.²⁰ In adults too, diet-microbiome interactions play important roles. Fifteen years ago, the consensus was that the GI ecosystem is stable overtime without major changes in diet.^{16, 21} Next-generation sequencing generated the concept that microbiota diversity and composition are associated with long-term

dietary habits,²² but most of all that diet can also rapidly create important shifts in the GI microbiota.²³ One likely interpretation of these discrepancy is that diet-induced variations in the GI microbiota depend on bacterial populations (most prevalent and dominant species are likely to be more stable) and on the amplitude of changes in diet (daily variations in food intake do not drastically change individual-specific GI microbiota profiles, at least as analyzed in a cumulative manner in fecal materials). Nevertheless, it is also very likely that variations within the ecosystem follow a much faster dynamic at the functional level.^{24, 25}

The GI microbiome influences health, but molecular mechanisms are not well characterized.

Environmental factors that shape the gut microbiota are of course not restricted to nutrition. The old-friends hypothesis states that the loss of stimuli by exogenous microbes in Western societies, due for instance to high hygiene status and the abusive use of antibiotics in the last decades, has perturbed hard-wired molecular mechanisms that control host physiology development, thereby contributing to the increasing incidence of chronic immune-mediated and metabolic diseases such as diabetes, allergies, inflammatory bowel diseases, and even neurodegenerative disorders.²⁶ This is supported for example by the fact that infants born in rural vs. urban environments in developed countries are at lower risk for allergic disorders such as asthma.²⁷ Delivery mode at birth (vaginal delivery vs. caesarian section) influences microbial colonization patterns,²⁸ and children born by caesarian section have a higher risk to develop allergies, showing that early life events can dictate the health becoming of an individual.²⁹ In infancy, and very often thereafter, the intestinal ecosystem is challenged by infectious agents and antibiotic therapies. In most cases in adult subjects, the ecosystem shows resilience thanks to its diversity, *i.e.*, it comes back to its original state after challenge. However, in some cases, and likely more frequently during infancy where microbial populations are not yet fully stabilized, the ecosystem or at least specific community niches can be permanently affected.³⁰ Altogether, this variety of colonization and challenging events partly explains why certain individuals harbor specific bacteria in their gut and others do not, and the latter group of subjects obviously lacks the functions expressed by absent or subdominant bacterial species. In combination with genetic predispositions, this can favor the development of chronic diseases.

The use of potentially beneficial bacteria (primarily from food) to improve health was investigated more than a century ago.³¹ However, our understanding of the importance of endogenous microflora really started to change in the 1960's. By using innovative approaches based on anaerobic culture techniques and gnotobiology, pioneer scientists including Dubos, Holdemann, Hungate, Moore, Savage, and Schaedler generated important findings on the role of commensal bacteria in the control of host physiology, including energy homeostasis and the exclusion of pathogens.³²⁻³⁵ This work has been overruled in recent years by the incredibly high interest in the scientific community and broadcast media driven by major advances in molecular microbial ecology and by the establishment of large-scale research consortia studying microbiomes.^{7, 10} However, this came at a cost: whereas the research community has been really good at describing the gut microbial ecosystem in depth, there is still a paucity of functional data on microbial components of particular importance and associated mechanisms of actions. The use of antibiotics, fecal microbial transplantation, and gnotobiology has demonstrated the causal role of microbiomes in health. For instance, studies on the transfer of gut contents to recipient hosts proved that the presence of specific exogenous microbial communities in the intestine can cause changes in host metabolic phenotypes.³⁶ Moreover, state-of-the-art experimental studies highlighting the role of certain types of bacteria and component thereof in regulating immune responses and metabolism have also been published: short-chain fatty acids produced in the gut by bacterial fermentation have multiple bioactive properties such as cell cycle regulation or modulation of inflammatory and metabolic responses via the GPR41 receptor;³⁷ polysaccharide A from *Bacteroides fragilis* was reported to influence CD4+ T-cells differentiation;³⁸ segmented filamentous bacteria are very effective in inducing Th17 responses;³⁹ a consortium of clostridia was shown to trigger expansion of Treg populations;⁴⁰ and other bacteria such as *Akkermansia muciniphila* and *Faecalibacterium prausnitzii* may be beneficial to the host with respect to metabolic health and inflammatory processes.^{41, 42} Nevertheless, the field has drawn a lot of attention on the complexity and importance of gut microbiomes, and the challenge is now to provide more functional proof and to explain molecular mechanisms in details.

2 Questions and objectives

We know to date that the gut microbiota is a complex ecosystem that is important for health. We can also describe the ecosystem at the functional level (genes, proteins, or metabolites), and have good knowledge of many of its dominant bacterial members. Moreover, a number of particular species and associated mechanisms of interactions with the host have been identified. In other words, the field is in good shape, but a lot remains to be done. There is still a lot of microbial diversity that is unexplored. Moreover, contradictory data have been published on the impact of diet on GI microbial communities. Also, strong statements have been made on the major impact of gut microorganisms on a variety of diseases, which contrasts with the few corresponding molecular mechanisms that have been described, especially in the field of obesity and associated co-morbidities. Hence, at least three main question categories are still highly relevant to the field:

- Which bacteria other than species already described are in the gut and what do they do? To what extent can we improve our view of gut microbial ecosystems via the implementation of innovative culture-based and molecular approaches?
- What is the impact of dietary components on microbial communities, and inversely what is the impact of bacterial metabolism on the fate of dietary compounds?
- Which molecular mechanisms explain that the GI microbiome influences energy homeostasis and the development of metabolic diseases such as type-2 diabetes?

In agreement with the questions addressed above, my main motivations in the field are the study of gut bacterial diversity (from generation of hypotheses using descriptive molecular tools to functionality using culture), the impact of dietary components (primarily polyphenols, fat, fibers, pre- and probiotics) on intestinal bacterial communities, and the impact of gut microbiota on host health, in particular energy homeostasis and the development of metabolic diseases. The latter aspect of my research relies on the use of state-of-the art human cohorts for assessment of the clinical relevance of specific gut microbes for glucose homeostasis, and of experimental models for translational research towards the understanding of molecular mechanisms, especially via the establishment of model bacterial consortia and the study of the gut-liver axis by using *Coriobacteriaceae* as models. In the next chapter, I present milestones of my research of the last 4 years on these topics.

Chapter 2 - Main research activities and achievements

This chapter gives an overview of main results that I obtained recently doing research on the gut microbiome. It is primarily based on the findings contained in the compilation of publications shown below in part II, including primarily own projects but also work in collaboration (*e.g.* paper 7 and 8). However, the chapter also goes beyond these findings as I present some of my main achievements at TUM, include some yet unpublished data, and put results into perspectives. Hence, chapter 2 is the core of the present Habilitation manuscript and can be seen as the foundation of my research in the very near future. According to the objectives aforementioned, chapter 2 is divided into the following three main sections (selected publications in part II are categorized using these sections too): 1) the study of bacterial diversity in gut environments using both culture-based and molecular approaches; 2) the interaction between diet and the gut microbiome, including the biotransformation of dietary components by gut bacteria and the impact of dietary factors on bacterial communities; and 3) molecular mechanisms underlying microbe-host interactions in health and diseases, with a primary focus on metabolic disorders and the gut-liver axis. Of course, work in all three areas is inter-connected, *i.e.*, the study of microbiota diversity and composition by sequencing helps generating hypotheses and the use of culture-based approaches is helpful to obtain specific bacteria, both of which are relevant to topic 2 and 3. As a consequence, selected publications may be relevant to several aspects of my research although placed in only one specific section in part II.

1 Microbiota diversity

For a microbial ecologist, one prime, yet so far still unachievable quest is to gain an exhaustive view of all community members in a given environment. To know what types of microorganisms are present in a sample is a good start for appreciating the functional potential of the community. Both culture-based and molecular techniques allow description of diversity at various levels, each having particular strengths and weaknesses as detailed below. The advent of high-throughput molecular methods combined with explorative bioinformatics approaches now challenge the rationale and conventions behind classical taxonomy to favor genome-wide function-based classification of microorganisms. Scientists may argue about the most efficient and unbiased system to be used for microbial classification, but one can at least agree on the necessity to divide the continuum of highly variable microbial entities in a specific environment into units that share a given similarity so as to have a common ground for exchange of information. That being said, one should always remember that microbial systems are in motion, for example via rapid exchange of genetic materials, and do not mind classification norms established by microbiologists for the sake of clarity. One additional point worth addressing here is that microbial ecosystems consist of various microorganisms, including not only bacteria, but also viruses, fungi and protozoa. Especially in the field of gut microbiology, the shortcut from microbiota to bacteria is very often made. Even though bacteria seem to be most dominant members of intestinal microbial communities, and bacteria are the focus of my research, the influence of other types of microorganisms should always be considered. In this context, in the next two sub-sections, I will detail the work I have been doing on the description of gut bacterial diversity and composition using both culture methods and *omics* technologies.

1.1 *Culturing is worth the effort*

Gut bacteria are indeed very important for health homeostasis and the development of chronic inflammatory diseases, and molecular tools have revolutionized our way to look at gut microbial ecosystems. However, the massive accumulation and resource-demanding analysis of data obtained in the course of non-targeted, high-throughput molecular work has become a very narrow bottleneck. Major challenges of the current post-omics era not only relate to meaningful interpretation of large-scale descriptive datasets obtained by non-targeted studies (see below; sub-section 1.2; p22), but also to the mechanistic understanding of ecological processes underlying microbe-microbe and microbe-host interactions in hypothesis-driven manners. In the latter case, classical culture-based approaches are very important. However, the study of mammalian gut bacteria using culture techniques has been neglected in recent years. The rush on using new molecular tools led to the misleading assumption that culturing bacteria is not worth the effort. Obtaining bacteria in culture is not only of benefit to *omics* approaches in the long run thanks to the amendment of genomic databases via description and characterization of novel taxa, it is also essential for the establishment of simplified models to study bacterial functions of particular relevance. I believe that the field does need classic microbiological expertise to feed requirements for state-of-the-art functional studies.

When compared with frequent and misleading statements made in the literature on the vast majority of gut bacterial communities being not cultivable, state-of-the-art work by Goodman *et al.*⁴³ reported that 56 % of 16S rRNA reads in a human fecal sample belong to readily cultured species, and this proportion will increase thanks to additional culturing effort.⁴⁴ A recent review paper by Walker and colleagues⁴⁵ also nicely illustrated that most of the dominant molecular species detected by molecular analysis actually have representative strains in culture. That being said, many less dominant species, which may also carry out important metabolic functions for instance, are still unknown. It is of course also true that culture-based work is biased; but so is molecular description of the ecosystem. Instead of repeatedly stating that bacteria are not cultivable, we must take on the challenge to discover new taxa for the purpose of improving our view of bacterial diversity. One of my main contributions to the field of gut microbial ecology in recent years has been the identification and

characterization of novel bacteria from the human and mouse intestine, including the study of their genomes and metabolic functions. Hence, I have described new species and genera within the phylum *Firmicutes*, e.g., *Acetatifactor muris* (**PAPER 3**) and *Streptococcus danieliae* (**PAPER 5**). I have also contributed to the recent bloom in description of novel members of the family *Coriobacteriaceae*, with for example the new genera *Enterorhabdus* (**PAPER 2**) and *Parvibacter* (**PAPER 4**). More details on this particular family of bacteria is provided below in section 3 (from p35 on).

As an example of the relevance of culturing bacteria for downstream analysis of their functions *in vitro*, we have isolated and characterized one novel butyrate producer from the mouse gut, *Intestinimonas butyriciproducens* (**PAPER 6**). Interestingly, collaborators at the Wageningen University isolated one strain of the same species from human feces. Since there is evidence from the literature that the origin of bacterial strains matters for the development of immune functions and the adaptation of bacteria to colonization,^{46, 47} I currently focus on comparative functional analysis of these bacteria as well as the effect of colonization of mice by the two strains (human vs. mouse). One other example refers to the study of inflammation onset in an experimental model. Collaborators at the John Hopkins School of Medicine in Baltimore used our new species *Bacteroides sartorii* (**PAPER 1**) and showed that it was less efficient in colonizing the gut and did not induce spontaneous colitis when compared with the type strain of *Bacteroides thetaiotaomicron* in mice deficient in core 1-derived O-glycans, which have a defective mucus layer.⁴⁸ Although mechanisms remain unknown, these findings support the notion of differential effects in the ability to colonize and trigger inflammation depending on strains.

As a spin-off of the work aforementioned at the level of single strains, taking into account the reported importance of the host species of origin of bacterial strains,^{46, 47} and that it is still very difficult for researchers that study molecular mechanisms underlying bacteria-host interactions in gnotobionts to gain easy access to gut bacterial isolates for the sake of experimental studies, I am currently in the process of establishing the Mouse intestinal Bacterial Collection (MiBC). Thereby, I aim at providing the first exhaustive repository of bacterial species and strains from the mouse intestine in collaboration with colleagues from the German Collection of Microorganisms and Cell cultures (DSMZ) and from the priority program SPP 1656 of

the German Research Foundation. The collection includes so far more than 80 species and 24 families across the 6 phyla known to cover most of the bacterial diversity in the mouse gut: *Firmicutes*, *Bacteroidetes*, *Actinobacteria*, *Proteobacteria*, *Verrucomicrobia*, and *Tenericutes*. The phylogenetic distribution of MiBC members reflects the dominance of *Firmicutes* in the mouse gut. Within this phylum, orders that are best represented in the collection (*i.e.*, they contain a substantial number of species) include the *Clostridiales* and *Lactobacillales*. A closer look at the phylogeny and taxonomy of members of the *Lachnospiraceae* revealed the urgent need to re-classify many species in this family. Importantly, already 15 isolates from the collection represent novel taxa on the basis of nearly full length 16S rRNA gene sequence analysis, and these isolates are currently under description. All species of the collection will have validated names with standing in nomenclature and the genome of most dominant and prevalent members as well as novel taxa will be deposited for the sake of database implementation.

MiBC will of course serve the purpose of own key functional projects to study particular metabolic or pathophysiological relevant functions of candidate bacterial strains *in vivo*, but will also open ways for fruitful collaborations taking into account the strong interest of many researchers in obtaining mouse bacterial commensals. One logical application of MiBC is the establishment of a model minimal microbiome that best mimics the entire ecosystem. Indeed, the high diversity of the gut microbial ecosystem and the substantial proportion of still unknown gut bacteria hampers good understanding of basic principles behind microbe-microbe interactions and changes affecting communities in relation to dietary challenges or pathological conditions. The idea of establishing such a model microbiome is of course not new, and bacterial consortia such as the altered Schaedlar flora⁴⁹ or the simplified human intestinal microbiota (SIHUMI)⁵⁰ have been described. However, there is room for improvement in several aspects: 1) in the case of the Schaedlar flora, strains are not easily accessible, which prevents wide-spread use of the model; 2) SIHUMI consists of strains from the human gut, which may show some limitations in mouse models; 3) in both cases, the selection of species was based on rational thinking with respect to the dominance and functional importance of bacteria, yet we propose that true ecological and genome-based analysis of the candidate species will provide a better model. Hence, we will assess the prevalence and abundance of all species from the

collection using existing gut sample datasets. Preliminary analysis of the prevalence of a subset of MiBC strains is shown below in **Figure 1**. Selection will subsequently be refined by functional analysis of most dominant, prevalent, and mouse-specific species on the basis of metagenomic coverage.

To conclude this part, it is important to remember that culture studies are biased and time-consuming, but that they allow to fill holes in the puzzle of diversity and that they open ways to very useful functional studies *in vitro* and *in vivo*. Especially in the gut, cultivability is not as limiting as in environmental ecosystems (e.g. soil, water). In any cases, it is unfair to deny the use of culture-based approaches on the sole reason that they are old-fashioned and laborious, especially with respect to strictly anaerobic species. Nevertheless, although innovative approaches with a high-throughput potential have been developed,⁴³ culture reaches its limits when comes the time to analyses large number of samples and make interpretation on the functional potential of ecosystems. Moreover, the boundaries created by bacterial taxonomy (which by the way have dreadful consequences also for the interpretation of 16S rRNA gene amplicon datasets) do not reflect the spectrum of diversity and dynamism inherent to gut bacterial communities. In these respects, the need for molecular methods is undeniable as it allows global assessment of microbial community functions.

1.2 *The need for molecular studies*

As already introduced above, the development of tools and approaches that bypass bottlenecks inherent to traditional culturing techniques (growth impairment, low throughput) revolutionized the study of microbial communities.⁵² Analysis of the model phylogenetic marker in use to date, the 16S ribosomal RNA gene, started already in the 1980's.⁵³ However, advances in the field of molecular microbial ecology have been boosted in the last decade by breakthroughs in new generation sequencing and mass spectrometry technologies. Most of all, these developments have allowed investigations at the functional level, thereby providing novel insights into so far unexplored facets of microbial communities.

Nevertheless, there is still a lack of gold standards in metagenomics with respect to sample collection and processing as well as data analysis, which hampers comparative analysis between studies and contributes to the accumulation of doubtful sequence datasets. This lack of standards is partly due to the various technologies available, to the complexity of the workflow and ensuing high number of steps to be considered, and to the fact that this is a very quickly evolving field of research. Hence, there is an urgent need for the sustainment of expertise to accommodate the increasing demand by the research community for analysis of microbial communities using next-generation sequencing in a multitude of research areas. One top-priority task of my work over the last year has been the establishment of a sequencing platform for 16S-based molecular analysis of intestinal samples based on the Illumina technology. I supervised the establishment of experimental workflows (from sample collection and preparation to data analysis) that are now used for high-throughput analysis of samples from own and third party studies. A schematic view of the platform and main methodological features are presented below in **Figure 2**.

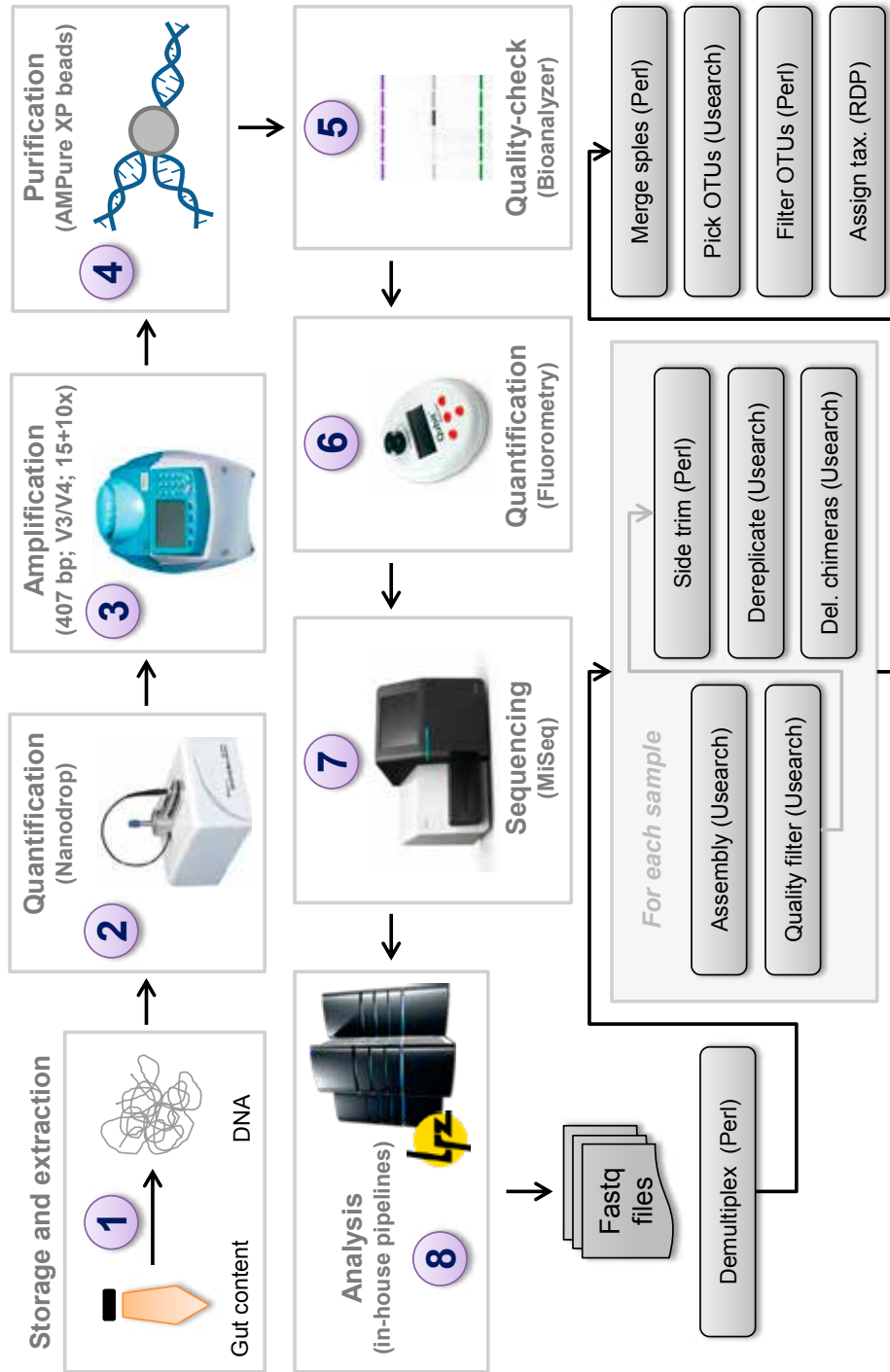


Figure 2: Workflow of the high-throughput 16S rRNA gene sequencing pipeline. Frozen samples in DNA stabilization solution are extracted by mechanical lysis and purified either by precipitation or using columns (see below). 16S rRNA genes are amplified with primers 341F-785R⁵⁴ using a 2-steps procedure to limit artifacts.⁵⁵ After purification and quantification, sample pools (≤ 300) are sequenced in paired-end modus using the Illumina technology. For analysis, raw files are demultiplexed (max. 2 error/bc) and each sample is processed following UPARSE.⁵⁶ Paired reads with expected error > 3 are discarded. Sequences are de-replicated and checked for chimeras with UCHIME.⁵⁷ Operational taxonomic units (OTUs) are picked at a threshold of 97 % similarity, and those with a rel. abundance > 0.5 % tot. seq. in at least 1 sample are kept. RDP classifier is used to assign taxonomy (80 % confidence).⁵⁸



Reproducibility is one main concern when using approaches that consist of obtaining a proxy of communities by reducing sample diversity to sets of millions of 16S rRNA gene fragments. Indeed, these approaches are based on protocols that include many steps, each having a relatively high risk to introduce biases. Moreover, beyond issues regarding sample collection and storage that will not be discussed here, DNA extraction strategies can have major influences on the output of analysis. We developed two main extraction protocols based either on DNA purification using columns, which guarantees rapidity and purity, or based on precipitation using solvents, which ensures higher yields of extraction and DNA integrity (less fragmentation). In both cases, we observed that variation between triplicate samples is low when compared with inter-individual differences (**Figure 3**). Moreover, the influence of DNA purification was substantial, yet still minor when compared with sample specificity.

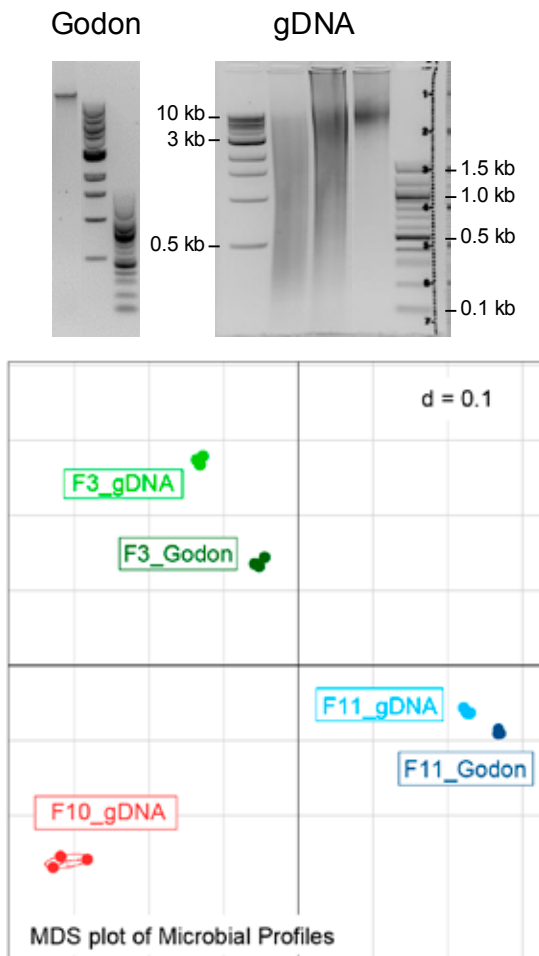


Figure 3: Variations in 16S-based diversity due to technical replication and DNA extraction procedure. Three aliquots of each three human fecal samples were processed in parallel either using an in-house developed protocol based on DNA columns (NucleoSpin® gDNA, Macherey-Nagel), or following the procedure by Godon *et al.* based on DNA precipitation.⁵⁹ In both cases, microbial cells were lysed mechanically by beadbeating. Representative agarose gels in the upper panel show that a sharp DNA band >10 kb is obtained following the Godon protocol, whereas a very wide span of DNA fragments is obtained after column purification. Yields of extraction are higher with the Godon protocol, yet purity (260/280 and 260/230 ratios) is higher with the gDNA protocol (data not shown). In the present experiment, 16S libraries for fecal sample #10 extracted after Godon could not be obtained, likely due to inhibition of the PCR reaction, no matter which dilution of the DNA sample was used as template. Samples were sequenced and analyzed as shown above in Fig. 2. The multi-dimensional scaling (MDS) plot based on generalized UniFrac distances shows the following ranking of differences in bacterial diversity: individual > extraction > replicates.

The protocol presented above (Fig. 2) for high-throughput 16S rRNA gene sequence analysis has been already used for the purpose of collaborative studies in mice about the influence of maternal inflammation on cecal microbiota and gut pathology in the offspring (**PAPER 7**), and about the impact of immune cells on the development of hepatic cancer (**PAPER 8**). Additionally, own work partly based on 16S rRNA gene analysis is detailed below in section 2 (**PAPER 13**) and section 3 (**PAPER 15**). We are now using the sequencing platform for large-scale analysis of fecal samples from the KORA study, which reflects my interest in studying the gut microbiome in the context of metabolic disorders. The KORA study has been examining the health of thousands of citizens in and around the city of Augsburg over the last 20 years to survey the development of chronic diseases, especially myocardial infarction and diabetes mellitus (<http://www.helmholtz-muenchen.de/kora>). The primary asset of this project is that it is based on the analysis of a state-of-the-art study cohort including individuals who have been very well genotyped and phenotyped over time. Based on the analysis of 2,500 fecal samples by high-throughput sequencing (16S and metagenomics), we intend to generate novel hypotheses on the role of gut bacteria in metabolic disorders by identifying bacterial phylotypes and functions that are associated with disease onset and specific dietary habits, in a prospective manner.

Importantly, my interest in the molecular analysis of microbial ecosystems is not limited to the study of 16S rRNA gene sequences for diversity and composition analysis, but extends to the assessment of ecosystem's functions via *omics* approaches. For instance, based on high-throughput analysis of the cecal ecosystem in mice at the metaproteomic and metabolomic level, we provided the first comparative metaproteomic analysis of the mouse gut microbiota in response to diet. These results will be detailed below in section 3 (p34). As a short summary, we demonstrated that (i) diet can alter the biochemical composition of the gut microbiota either by shifting phylotype composition or shifting activity of bacterial cells, (ii) changes in bacterial metaproteome after HF feeding are most pronounced for pathways of amino acid metabolism, and (iii) cecal metabolic pathways affected by HF feeding include eicosanoid, steroid hormone, macrolide, bile acid and bilirubin metabolism. These findings showed that a HF diet has a major impact on the mouse cecal microbiota that extends beyond compositional changes to major alterations in bacterial physiology and metabolite landscape.

Besides the absence of consensus on standards to be followed for molecular analysis of bacterial communities, the field also suffers from the lack of tools for global assessment of the pool of knowledge accumulated in databases. The majority of published papers indeed reports findings obtained in the course of single studies, even though latest papers include ever increasing number of samples. Dataset submission to up-to-date repositories should become a must and the field would greatly benefit from the implementation of novel approaches for rapid, wide-ranging and high-quality analysis of microbial communities from various ecosystems based on all sequence-based information available. Hence, there is an urgent need for the sustainment of expertise to disseminate state-of-the-art procedures and tools meeting high-quality standards. Following the observation that the field of microbial ecology would greatly benefit from new approaches for global assessment of metagenomes on the basis of the entire pool of knowledge available in existing repositories, my group has initiated an inter-disciplinary project in collaboration with the faculty of informatics to exploit the accumulated knowledge on 16S rRNA gene diversity available in the public resource SRA (Sequence Read Archive). This work relies on the establishment of in-house pipelines for extraction and processing of sequencing data into organized databases under a unifying scheme. One example of the use of this pipeline to assess the prevalence of bacterial isolates from the mouse gut has been already shown above in section 1.1 (p21). Given the number of possible applications of this approach, we are currently working on the development of a web front (imNGS) to share benefits with the research community. Based on this experience in organizing, automatically analyzing and building resources from massive amounts of data from public repositories, we propose to create similar pipelines for global assessment of metagenomic profiles in the near future.

As an overall conclusion of this first section on microbiota diversity, molecular and culture-based analysis of gut microbial communities are complementary and should be considered as such. Each approach has advantages and flaws and their use must be adapted to the question that is addressed. Molecular studies generally have higher throughput, capture more diversity (although the snap-shot views that are obtained are biased too) and are very helpful to generate hypotheses on the relevance of specific microbial groups or functions thereof under specific environmental or host-specific conditions. Culture is cheap, capture sub-dominant diversity and most of all allow downstream functional analysis and thus proof-of-concept studies. Hence, the study of bacterial diversity as described in this first section can serve the purpose of projects relevant to the two other research topics detailed below in section 2 (nutrition and microbiome) and section 3 (microbe-host interactions). For instance, high-throughput analysis of fecal microbial profile in participants of the KORA study as mentioned above represent a unique chance to determine specific associations between gut microbiota and dietary profiles in relation to prospective analysis of metabolic diseases onset.

2 Nutrition and microbiome

Among the trillions of bacterial cells present in the human or mouse intestine, strictly anaerobic species are dominant and carry out important metabolic functions such as the conversion of host-derived substrates (e.g. mucin and bile salts), but also indigestible components and micronutrients from the food (e.g. polysaccharides, polyphenols), thereby producing short-chain fatty acids and bioactive metabolites. In the present section, I present major outputs of my work on the interaction between dietary compounds and intestinal bacteria. I first give some background information and highlight results related to my long-lasting interest in studying the metabolism of phytoestrogens, primarily lignans and isoflavones, by gut bacteria.⁶⁰ In the last part of this section, I summarize data on the use of mouse models to study the effects of diet composition on gut bacterial communities.

My recognition in this field of phenolics bioavailability led to the recent publication of one book chapter that summarizes knowledge from the literature and all major own findings on relationships between the microbiome and dietary phenolic substrates (**PAPER 12**). Beyond investigation of the role of gut bacteria in modifying the structure of plant phenolics, I was also involved in the study of biological activities of caffeic acid derivatives, where we pointed at structure-function relationships and dissected molecular pathways underlying anti-inflammatory effects (**PAPER 9**). Also, besides the work on lignans described in details below, I have been very interested in searching for bacterial species able to produce the isoflavone equol. This led to the isolation and description of one active species of the novel genus *Enterorhabdus*, but we also found that another species of this genus was inactive (**PAPER 2**), indicating that equol production by the gut microbiome is a very specific function.

The production of enterolignans from plant substrates in the diet is a paradigm example of bioactive metabolites of bacterial origin in the gut.⁶¹ Enterodiol (ED) and enterolactone (EL) were first detected in primates in 1980 and were thought to be new steroids,⁶² underlining that lignans share structural features with endogenous hormones and are thus considered as phytoestrogens. Two years later, the same authors reported that urinary lignans originate from plant substrates.⁶³ The conversion of plant lignans by gut bacteria was studied more in detail shortly

thereafter.⁶⁴ Due to their structural similarity with estrogens as well as possible anti-oxidant properties and the modulation of host enzyme activities, enterolignans have been extensively studied in terms of health-promoting effects.⁶⁵ Flaxseeds and the lignans they contain are proposed to be of benefit for the treatment or prevention of metabolic and cardiovascular diseases as well as breast and prostate cancer.⁶⁶⁻⁶⁹ However, although evidence in culture systems and experimental models is good, there is urgent need for state-of-the-art randomized clinical trials. Nevertheless, no matter what health effects lignans have, intestinal bacteria are essential for their activation from plant substrates.

Despite the discovery of the bacterial activation of lignans as early as the 1980's, lignan-converting strains were first isolated from fecal samples 15 years later.⁷⁰ From the work I performed during my PhD thesis, we learnt that the production of enterolignans from secoisolariciresinol diglucoside (SDG), the most abundant lignan in flaxseeds, results from the activity of phylogenetically and metabolically diverse bacteria that catalyze sequential activation via deglycosylation, demethylation, dehydroxylation, and dehydrogenation.^{61, 71-73} Deglycosylation and demethylation seem not to be limiting steps thanks to functional redundancy between different species and the ability of one strain to metabolize different substrates. Moreover, the main species catalyzing dehydroxylation, *i.e.*, *Eggerthella lenta*, belongs to the core gut microbiome in humans and is thus dominant and prevalent in the intestine. In contrast, we showed that enterolactone-producing communities belong to sub-dominant populations and only one enterolactone-producing species has been isolated and characterized to date. My PhD ended with the establishment of a consortium of 4 bacterial strains capable of activating SDG *in vitro*.⁷⁴ The logical consequence of this work was to test the relevance of our findings *in vivo*. On the basis of this minimal consortium of bacteria, experiments in rats were performed to show that production of enterolignans occurs only in animals that were successfully colonized by the four strains, when compared to germfree controls (**PAPER 10**). One subsequent paper also published in collaboration showed that colonization of rats with the consortium combined with feeding of a diet enriched with 5 % ground flaxseeds triggered a reduction of chemically-induced breast tumor numbers and size (**PAPER 11**).

From the work detailed above, it is obvious that *in vitro* work and experimental studies in mice can deliver valuable data with respect to the importance of gut bacteria for phytoestrogens metabolism and bioactivities. Because ED and EL have been described as being more biologically active than plant substrates, it is sound to hypothesize that gut microbial profile influence enterolignan production phenotypes with possible ensuing consequences on physiological effects. However, in spite of published *in vitro* studies based on fermentation experiments using human fecal slurries,^{75, 76} there is to the best of our knowledge no data available in humans on the interaction between gut bacterial profiles and enterolignan production phenotypes in response to dietary intake of plant substrates. Therefore, in collaboration with the Clinical Nutritional Medicine Unit at TUM, I initiated, designed and conducted a pilot intervention study in healthy male adult subjects, in order to address the question to what extent taxonomic composition of gut bacterial communities is associated with concentrations of enterolignans. The work is ongoing and I will therefore not detail yet unpublished data here. In brief, based on the analysis of 27 samples overtime from 9 participants, we observed no major shifts in dominant fecal bacterial communities following ingestion of ca. 30 g flaxseeds per day for a week. This tends to challenge the recent consensus that the gut microbiome is highly dependent on diet,²³ but agrees with the former notion that dominant bacterial populations in distal parts of the intestine are relatively stable over a timespan of months without major alterations in diet or medication.^{16, 77} However, we observed a marked increase of enterolignan concentrations in blood after intervention, and correlations networks pointed at associations between specific members of the *Firmicutes* and the amounts of lignans detected in blood (data not shown). An overview of my accomplishments in the field of lignan research is shown below in **Figure 4**.

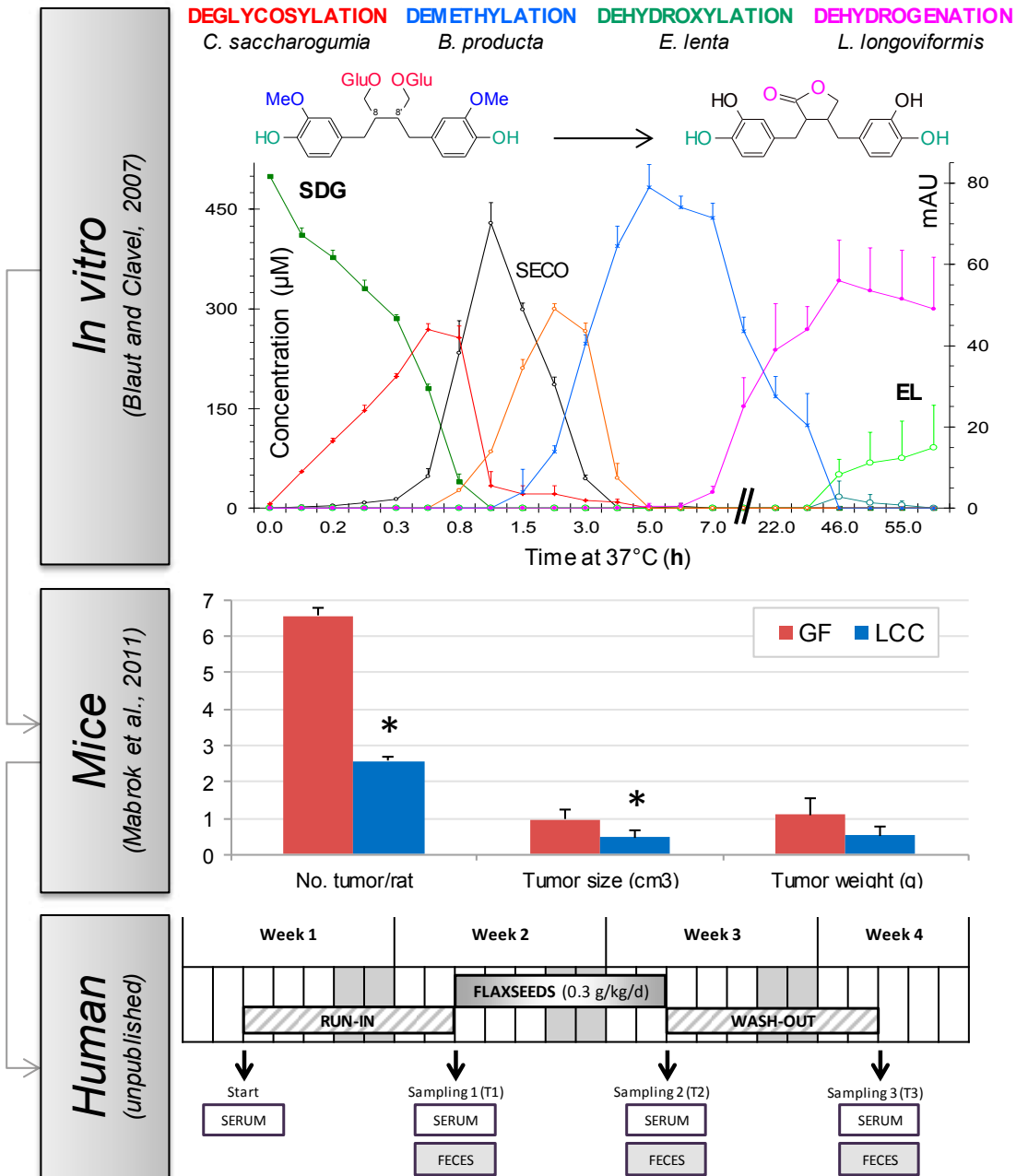


Figure 4: Interactions between dietary lignans and the gut microbiota – from bench to bed.

My search for bacteria capable of activating the dietary lignan SDG led to the identification of a consortium of 4 strains (top panel) that converted SDG to EL *in vitro* via production of intermediate substrates.⁷⁴ Follow-up work demonstrated that colonization of germfree rat with this consortium triggers production of enterolignans *in vivo*,⁷⁸ which showed the potential to lower tumor burden in chemically-induced breast cancer (mid panel).⁷⁹ Currently, we are performing a pilot trial in healthy male human subjects including a 1-week intervention with flaxseeds to identify fecal bacterial profiles associated with high production of enterolignans (lower panel). Abbreviations: EL, enterolactone; GF, germfree; LCC, lignan-converting consortium of 4 bacteria; SECO, secoisolariciresinol; SDG, secoisolariciresinol diglucoside.

My interest in the field of nutrition and the microbiome is of course not limited to the study of polyphenols, but extends also to the impact of diet in general on bacterial communities. Ongoing work based on the use of next-generation sequencing to characterize relationships between dietary patterns and fecal microbiota profiles in the context of the state-of-the-art prospective KORA cohort has been already introduced above in section 1 (p25). The following paragraphs focus on findings in experimental models, which are summarized in **PAPER 13**. For instance, collaborators at the Nutritional Physiology Unit showed that a Western-style diet causing obesity via the offered choice of several palatable food items is more detrimental in causing liver pathologies than a classical high-fat diet, which contains more fat but less simple sugars.^{80, 81} Based on fluorescence *in situ* hybridisation, I could show that the Western-style and high-fat diets had also distinct effects on cecal bacterial composition: Mice fed the Western-style diet had 3-fold decreased proportions of *Bacteroidales* and increased proportions of the *Clostridium leptum* subgroup. Hence, bacterial proportions were mostly affected by the cafeteria diet, supporting the notion that changes in mouse gut microbiota depend more strongly upon diet composition than obesity per se.⁸² In relation to these findings, ongoing work in collaboration with the Molecular Nutritional Medicine Unit aims at deciphering the impact of fat source (animal- or plant-derived fat) on metabolic parameters and the gut microbiome.

Most importantly, using standard carbohydrate diets provided either as a powder or in pellet form, we found that diet-dependent effects on gut bacterial communities not only relate to composition, but also to texture. The powder diet substantially decreased phylotype richness, and β -diversity analysis showed a clear clustering between mice fed the powder vs. pellet diet (**PAPER 13**). Taxonomic assignment of sequences revealed a marked decrease in the abundance of *Firmicutes*, mainly due to lower sequence proportions of *Lachnospiraceae* and *Ruminococcaceae*. This was accompanied by a bloom of sequences assigned to the genus *Akkermansia*, a member of the phylum *Verrucomicrobia* shown to decrease in abundance under high-fat diet feeding and proposed to be negatively associated with fat mass or weight gain, adipose tissue inflammation, endotoxemia, and insulin resistance.^{41, 83}

As a take-home message of this section 2 on Nutrition & Microbiome, one can say that gut bacteria play an important role in regulating the bioavailability of dietary components. It is also clear that diet influences gut microbiota, but that differences at the functional level matters more than variations in composition, which can arise partly from experimental flaws. Interpreting descriptive data on bacterial diversity and composition that were obtained in the course of mouse experiments where results largely depend upon experimental conditions, especially feeding protocols, can be misleading. Detailed information on diet composition and texture should be obligatory for publishing and effort in standardization is urgently needed. Nevertheless, microbial community analysis in both humans and mice allows the generation of hypotheses on metabolically important bacterial groups, the relevance of which in metabolic processes can be tested in experimental models. This requires that target bacterial strains are made available, underlining the urgent need to culture bacteria, characterize them properly, and ensure long-term storage, transparent archiving and availability. Moreover, besides collecting descriptive 16S-based data, it is also crucial to analyze bacterial genes or proteins expression and metabolites production in order to generate hypothesis-driven approaches with clear functional targets. In the next section dedicated to the study of microbe-host interactions, I will detail our work on the functional analysis of bacterial communities in diet-induced obesity and present ongoing work on the role of *Coriobacteriaceae* in hepatic steatosis.

3 Microbe-host interaction: The gut-liver axis

The use of bacteria to beneficially influence health has long been a matter of interest, for instance through pioneering work on lactic acid bacteria by Ilya Metchnikoff more than a century ago.³¹ Thanks to technological breakthrough in gnotobiology in the 1960's, researchers studied in details the protective effect of endogenous gut microorganisms on for instance resistance towards infection. Nowadays, the impact of the gut microbiome on human health, and the onset and maintenance of chronic immune-mediated or metabolic diseases is undeniable.⁹ However, emphasis has been hitherto rather on global description of changes affecting the ecosystem in a wide spectrum of diseases, and more effort is now required for the discovery of specific ways of interactions between the host and its microbiomes. In **PAPER 14**, we reviewed the literature on the importance of the gut and its resident microbial communities on the development of the immune system, with emphasis on allergies. We and others have also underlined the importance of the gut microbiome in metabolic disorders.^{84, 85} Despite the advances made and the knowledge accumulated, the *status quo* is that functional studies proving the causal role of commensal microbes in diseases and investigating detailed molecular mechanisms beyond broad description of the cross-talk between microbiota and their host species are urgently needed. In this last section of chapter 2, I will highlight some of our main findings in diet-induced mouse models and present the rationale for studying specific bacterial groups of interest.

One principal contribution I made to the field of molecular microbial ecology in the last years relates to the study of mouse gut bacterial functions in the context of high-fat diet-feeding (**PAPER 15**). In the frame of this work, I designed experimental workflows for high-throughput analysis of the caecal ecosystem in mice at the metaproteomic and metabolomic level, thereby providing the first comparative metaproteomic analysis of the mouse gut microbiota in response to diet. First, it should be noted that annotation of mass spectra remains challenging as < 5% of acquired spectra can usually be matched to protein sequences or metabolite masses, which hampers comprehensive analysis and functional interpretation. Nonetheless, changes in functional categories of differently detected proteins inferred

that the mouse cecal microbiota under high-fat feeding is subject to substrate deprivation characterized by low levels of protein synthesis relative to preformed ribosomal proteins. We also found signs of shift toward utilization of amino acids and simple sugars and adaptation to an environment with altered redox potential, which is in line with findings from shotgun DNA-based analysis of mouse and human intestinal microbiota.⁸⁶⁻⁸⁹ Diet-induced alterations of the metaproteome were accompanied by clear-cut changes in cecal metabolite profiles in mice fed the control or high-fat diet. In particular, prostaglandins, thromboxanes and several steroids and conjugates thereof were absent in cecal contents from mice fed the high-fat diet, which is in agreement with low cholesterol levels in intestinal and hepatic tissues despite plasma hypercholesterolemia in mice fed the high-fat diet, likely due to an increased cholesterol demand for chylomicron building and proper lipid absorption.⁸⁰ Prostaglandins and steroids can influence bile acids composition and bile secretion.^{90, 91} In our study, high-fat feeding diet led to lower intensity of spectra annotated as 3,7,12 α ,26-tetrahydroxy-5 β -cholestane. Altogether, these findings emphasize the importance of investigating bacterial metabolism of cholesterol and its derivatives in the gut, especially steroids and bile salts produced by the host.

Although many of the most abundant gut bacterial species as detected by 16S rRNA gene sequencing have nowadays representative strains in culture, some core species and many bacteria at the borderline of dominance possibly expressing important metabolic functions are still yet uncultured or are understudied.⁴⁵ There is accumulating evidence that cultivable and dominant commensal anaerobes such as *Akkermansia muciniphila* and *Faecalibacterium prausnitzii* may be beneficial to the host with respect to metabolic health and inflammatory processes,^{41, 42} but specific mechanisms must be identified. Based on the molecular work aforementioned (**PAPER 15**) and evidence from the literature, I propose that molecular mechanisms underlying the conversion of steroids and bile acids by specific gut bacteria is of particular importance for the onset of metabolic disorders. In **PAPER 16**, we summarized current knowledge on the diversity, taxonomy and properties of one specific family of gut bacteria that most likely play important roles in the metabolic processes mentioned above: the *Coriobacteriaceae*. Members of this family belong to dominant gut communities in mammals but have been so far understudied, although they catalyze the dehydrogenation and dehydroxylation of bile acids and

steroids. Bile acid metabolism by bacteria is considered as an important factor that influences host lipid metabolism and chronic intestinal inflammation, yet experimental evidence is sparse [11, 12]. Moreover, despite the apparent biological implication for the host of bacterial rearrangement of hormonal networks in the gut, related functional studies in experimental models have also not yet been performed. Hence, one of my primary interests at the moment is the use of minimal bacterial consortia to study the role of cholesterol-derived substrates in inflammatory processes underlying metabolic dysfunctions, using the *Coriobacteriaceae* as model organisms.

The term “pathobiont” is used to describe opportunistic but otherwise harmless bacteria that contribute to disease under specific environmental conditions.⁹² Bacteria of the family *Coriobacteriaceae* within the phylum *Actinobacteria* can be seen as paradigm pathobionts. They belong to dominant commensal communities in humans and mice, e.g., *Collinsella aerofaciens* is a member of the human gut core microbiome as highlighted by both 16S rRNA gene and metagenomic analysis,^{10, 14} and *Eggerthella lenta* has for long been cultivated from human feces⁹³ and is detectable in most individuals by molecular techniques.^{94, 95} However, several members have also been implicated in various pathologies such as inflammatory bowel diseases, colon cancer, periodontitis and bacteremia.⁹⁶ It is striking that all 30 species of the family have been recovered only from body habitats in mammals and insects, suggesting that strong evolutionary forces shaped colonization processes and *Coriobacteriaceae*-host interactions.

The occurrence of 16S rRNA gene sequences assigned to the genus *Eggerthella* and *Enterorhabdus* within the *Coriobacteriaceae* in feces correlated positively with intrahepatic levels triacylglycerol concentrations and non-HDL plasma concentrations in mice or hamsters.⁹⁷⁻⁹⁹ Moreover, the recent metagenomic study by Qin *et al.* based on high-throughput analysis of 350 human fecal samples from Chinese diabetic and control participants identified *Eggerthella lenta* as one of the molecular species linked to the occurrence of type-2 diabetes.⁹⁵ On the other hand, another recent metagenomic study in 145 European women with diabetes, impaired or normal glucose tolerance reported depletion of metagenomic clusters assigned to *Coriobacteriaceae* in fecal samples from diabetic individuals.¹⁰⁰

Various strains of *Eggerthella lenta* and *Collinsella aerofaciens* possess hydroxysteroid dehydrogenases (HSDH) responsible for stereospecific oxidation and epimerization of bile acids, thereby generating stable oxo-bile acid intermediates.¹⁰¹ However, the impact of bacterial HSDH activities on bile acid metabolism and host functions in vivo is undefined. Moreover, *Eggerthella lenta* is also able to transform corticoids such as deoxycorticosterone to progesterone via 21-dehydroxylase activity.¹⁰² This species also carries a corticoid-converting 16 α -dehydroxylase¹⁰³ and a 3 α -HSDH.¹⁰⁴ Although these findings relate to possible changes in the host hormonal status, functional studies in experimental animal models have not yet been performed. Taken together, evidence from the literature strongly suggests that *Coriobacteriaceae* are important constituents of gut microbiomes affecting host physiology. To test this, I have initiated a multi-center project funded by the German Research Foundation to study whether and how *Coriobacteriaceae* influence lipid metabolism and the development of hepatic steatosis and insulin resistance. This current work on the use of a *Coriobacteriaceae* consortium to study bile acids metabolism and steatosis could take a new dimension considering the recent collaborative work with Mathias Heikenwalder (**PAPER 8**). This work demonstrated the involvement of specific immune cells in the onset of hepatocellular carcinoma following dietary challenge in mice. One promising perspective is to assess the impact of specific gut bacterial communities on these processes, *i.e.*, study their involvement in immune cell activation and hepatic lipid accumulation using gnotobiotic models.

Chapter 3 - Conclusion

Research on the mammalian gut microbiota in health and diseases witnessed a bloom in the number of publications and has gained an unprecedented attention over the last ten years. Molecular tools for assessment of microbiomes opened new avenues of research that revolutionized our view of the complexity and dynamism of microbial ecosystems and their interaction host species. However, most of the work published has been explorative, *i.e.*, it delivered tremendous amounts of descriptive data that are often difficult to compare, and many of those exploratory data have misleadingly been use to make conclusive statements. There is urgent need for process standardization in the field of metagenomics and also for dissemination of news approaches for global assessment of diversity and functions of microbial communities. I am convinced that the return to classic microbiological techniques will rapidly be of benefit to the field in coming years. Having bacteria in hands is very useful for description of new diversity and for implementation of existing databases. Here too however, standardization effort is required to avoid for instance bottlenecks created by the use of in-house repositories of microbes that hamper dissemination and reproducibility of results. The main asset of culture-based approaches is that they are the fundament of experimental studies to dissect mechanisms underlying microbe-microbe and microbe-host interactions and to identify specific microbial molecules and study their bioactivities, as exemplified in chapter 2.3 with the *Coriobacteriaceae* and their possible role in metabolic disorders. Culture approaches, possibly combined with molecular engineering, can also form the basis of interventional strategies in clinical settings. We currently experience a turning point in the field of gut microbiome research. The potential lying in this ecosystem with respect to diagnostics and interventional approaches to regulate human health is very encouraging. However, it is time to sharpen our tools and increase the resolution of analysis, so as to bring light to many aspects of this research on an ecosystem that still remains a black box, especially with respect to targeted intervention strategies and interactions with the host.

Cited literature

(own publications appear in bold letters)

1. Hoehler TM, Jorgensen BB (2013) Microbial life under extreme energy limitation. *Nat Rev Microbiol* 11:83.
2. Price PB (2007) Microbial life in glacial ice and implications for a cold origin of life. *FEMS Microbiol Ecol* 59:217.
3. Cordero OX, Polz MF (2014) Explaining microbial genomic diversity in light of evolutionary ecology. *Nat Rev Microbiol* 12:263.
4. Stecher B, Maier L, Hardt WD (2013) 'Blooming' in the gut: how dysbiosis might contribute to pathogen evolution. *Nat Rev Microbiol* 11:277.
5. Newton AC, Fitt BD, Atkins SD, Walters DR, Daniell TJ (2010) Pathogenesis, parasitism and mutualism in the trophic space of microbe-plant interactions. *Trends Microbiol* 18:365.
6. Raoult D, Fournier PE, Drancourt M (2004) What does the future hold for clinical microbiology? *Nat Rev Microbiol* 2:151.
7. HMP (2012) A framework for human microbiome research. *Nature* 486:215.
8. Hormannsperger G, Clavel T, Haller D (2012) Gut matters: microbe-host interactions in allergic diseases. *J Allergy Clin Immunol* 129:1452.
9. Kau AL, Ahern PP, Griffin NW, Goodman AL, Gordon JI (2011) Human nutrition, the gut microbiome and the immune system. *Nature* 474:327.
10. Qin J, Li R, Raes J, Arumugam M, Burgdorf KS, Manichanh C, Nielsen T, Pons N, Levenez F, Yamada T, Mende DR, Li J, Xu J, Li S, Li D, Cao J, Wang B, Liang H, Zheng H, Xie Y, Tap J, Lepage P, Bertalan M, Batto JM, Hansen T, Le Paslier D, Linneberg A, Nielsen HB, Pelletier E, Renault P, Sicheritz-Ponten T, Turner K, Zhu H, Yu C, Jian M, Zhou Y, Li Y, Zhang X, Qin N, Yang H, Wang J, Brunak S, Dore J, Guarner F, Kristiansen K, Pedersen O, Parkhill J, Weissenbach J, Bork P, Ehrlich SD (2010) A human gut microbial gene catalogue established by metagenomic sequencing. *Nature* 464:59.
11. Aidy SE, van den Bogert B, Kleerebezem M (2014) The small intestine microbiota, nutritional modulation and relevance for health. *Curr Opin Biotechnol* 32C:14.
12. Nigro G, Rossi R, Commere PH, Jay P, Sansonetti PJ (2014) The cytosolic bacterial peptidoglycan sensor Nod2 affords stem cell protection and links microbes to gut epithelial regeneration. *Cell Host Microbe* 15:792.
13. Mahowald MA, Rey FE, Seedorf H, Turnbaugh PJ, Fulton RS, Wollam A, Shah N, Wang C, Magrini V, Wilson RK, Cantarel BL, Coutinho PM, Henrissat B, Crock LW, Russell A, Verberkmoes NC, Hettich RL, Gordon JI (2009) Characterizing a model human gut microbiota composed of members of its two dominant bacterial phyla. *Proc Natl Acad Sci U S A* 106:5859.
14. Tap J, Mondot S, Levenez F, Pelletier E, Caron C, Furet JP, Ugarte E, Munoz-Tamayo R, Paslier DL, Nalin R, Dore J, Leclerc M (2009) Towards the human intestinal microbiota phylogenetic core. *Environ Microbiol* doi:10.1111/j.1462-2920.2009.01982.x:
15. **Clavel T, Fallani M, Lepage P, Levenez F, Mathey J, Rochet V, Serezat M, Sutren M, Henderson G, Bennetau-Pelissero C, Tondou F, Blaut M, Dore J, Coxam V (2005) Isoflavones and functional foods alter the dominant intestinal microbiota in postmenopausal women. *J Nutr* 135:2786.**
16. Zoetendal EG, Akkermans AD, De Vos WM (1998) Temperature gradient gel electrophoresis analysis of 16S rRNA from human fecal samples reveals stable and host-specific communities of active bacteria. *Appl Environ Microbiol* 64:3854.
17. Palmer C, Bik EM, DiGiulio DB, Relman DA, Brown PO (2007) Development of the human infant intestinal microbiota. *PLoS Biol* 5:e177.

18. Fallani M, Amarri S, Uusijarvi A, Adam R, Khanna S, Aguilera M, Gil A, Vieites JM, Norin E, Young D, Scott JA, Dore J, Edwards CA (2011) Determinants of the human infant intestinal microbiota after the introduction of first complementary foods in infant samples from five European centres. *Microbiology* 157:1385.
19. Penders J, Vink C, Driessen C, London N, Thijs C, Stobberingh EE (2005) Quantification of *Bifidobacterium* spp., *Escherichia coli* and *Clostridium difficile* in faecal samples of breast-fed and formula-fed infants by real-time PCR. *FEMS Microbiol Lett* 243:141.
20. Koenig JE, Spor A, Scalfone N, Fricker AD, Stombaugh J, Knight R, Angenent LT, Ley RE (2011) Succession of microbial consortia in the developing infant gut microbiome. *Proc Natl Acad Sci U S A* 108 Suppl 1:4578.
21. Vanhoutte T, Huys G, Brandt E, Swings J (2004) Temporal stability analysis of the microbiota in human feces by denaturing gradient gel electrophoresis using universal and group-specific 16S rRNA gene primers. *FEMS Microbiol Ecol* 48:437.
22. Wu GD, Chen J, Hoffmann C, Bittinger K, Chen YY, Keilbaugh SA, Bewtra M, Knights D, Walters WA, Knight R, Sinha R, Gilroy E, Gupta K, Baldassano R, Nessel L, Li H, Bushman FD, Lewis JD (2011) Linking long-term dietary patterns with gut microbial enterotypes. *Science* 334:105.
23. David LA, Maurice CF, Carmody RN, Gootenberg DB, Button JE, Wolfe BE, Ling AV, Devlin AS, Varma Y, Fischbach MA, Biddinger SB, Dutton RJ, Turnbaugh PJ (2014) Diet rapidly and reproducibly alters the human gut microbiome. *Nature* 505:559.
24. McNulty NP, Yatsunenkov T, Hsiao A, Faith JJ, Muegge BD, Goodman AL, Henrissat B, Oozeer R, Cools-Portier S, Gobert G, Chervaux C, Knights D, Lozupone CA, Knight R, Duncan AE, Bain JR, Muehlbauer MJ, Newgard CB, Heath AC, Gordon JI (2011) The impact of a consortium of fermented milk strains on the gut microbiome of gnotobiotic mice and monozygotic twins. *Sci Transl Med* 3:106ra106.
25. Veiga P, Pons N, Agrawal A, Oozeer R, Guyonnet D, Brazeilles R, Faurie JM, van Hylckama Vlieg JE, Houghton LA, Whorwell PJ, Ehrlich SD, Kennedy SP (2014) Changes of the human gut microbiome induced by a fermented milk product. *Sci Rep* 4:6328.
26. Guarner F, Bourdet-Sicard R, Brandtzaeg P, Gill HS, McGuirk P, van Eden W, Versalovic J, Weinstock JV, Rook GA (2006) Mechanisms of disease: the hygiene hypothesis revisited. *Nat Clin Pract Gastroenterol Hepatol* 3:275.
27. von Mutius E, Vercelli D (2010) Farm living: effects on childhood asthma and allergy. *Nat Rev Immunol* 10:861.
28. Dominguez-Bello MG, Costello EK, Contreras M, Magris M, Hidalgo G, Fierer N, Knight R (2010) Delivery mode shapes the acquisition and structure of the initial microbiota across multiple body habitats in newborns. *Proc Natl Acad Sci U S A* 107:11971.
29. Thavagnanam S, Fleming J, Bromley A, Shields MD, Cardwell CR (2008) A meta-analysis of the association between Caesarean section and childhood asthma. *Clin Exp Allergy* 38:629.
30. Willing BP, Russell SL, Finlay BB (2011) Shifting the balance: antibiotic effects on host-microbiota mutualism. *Nat Rev Microbiol* 9:233.
31. Mackowiak PA (2013) Recycling metchnikoff: probiotics, the intestinal microbiome and the quest for long life. *Front Public Health* 1:52.
32. Holdeman LV, Moore WE (1972) Roll-tube techniques for anaerobic bacteria. *Am J Clin Nutr* 25:1314.
33. Hungate RE, Smith W, Clarke RT (1966) Suitability of butyl rubber stoppers for closing anaerobic roll culture tubes. *J Bacteriol* 91:908.
34. Savage DC, McAllister JS, Davis CP (1971) Anaerobic bacteria on the mucosal epithelium of the murine large bowel. *Infect Immun* 4:492.
35. Schaedler RW, Dubos R, Costello R (1965) The Development of the Bacterial Flora in the Gastrointestinal Tract of Mice. *J Exp Med* 122:59.
36. Vrieze A, Van Nood E, Holleman F, Salojarvi J, Kootte RS, Bartelsman JF, Dallinga-Thie GM, Ackermans MT, Serlie MJ, Oozeer R, Derrien M, Druesne A, Van Hylckama Vlieg JE, Bloks VW,

- Groen AK, Heilig HG, Zoetendal EG, Stroes ES, de Vos WM, Hoekstra JB, Nieuwdorp M (2012) Transfer of intestinal microbiota from lean donors increases insulin sensitivity in individuals with metabolic syndrome. *Gastroenterology* 143:913.
37. Samuel BS, Shaito A, Motoike T, Rey FE, Backhed F, Manchester JK, Hammer RE, Williams SC, Crowley J, Yanagisawa M, Gordon JI (2008) Effects of the gut microbiota on host adiposity are modulated by the short-chain fatty-acid binding G protein-coupled receptor, Gpr41. *Proc Natl Acad Sci U S A* 105:16767.
38. Mazmanian SK, Liu CH, Tzianabos AO, Kasper DL (2005) An immunomodulatory molecule of symbiotic bacteria directs maturation of the host immune system. *Cell* 122:107.
39. Ivanov, II, Atarashi K, Manel N, Brodie EL, Shima T, Karaoz U, Wei D, Goldfarb KC, Santee CA, Lynch SV, Tanoue T, Imaoka A, Itoh K, Takeda K, Umesaki Y, Honda K, Littman DR (2009) Induction of intestinal Th17 cells by segmented filamentous bacteria. *Cell* 139:485.
40. Atarashi K, Tanoue T, Oshima K, Suda W, Nagano Y, Nishikawa H, Fukuda S, Saito T, Narushima S, Hase K, Kim S, Fritz JV, Wilmes P, Ueha S, Matsushima K, Ohno H, Olle B, Sakaguchi S, Taniguchi T, Morita H, Hattori M, Honda K (2013) Treg induction by a rationally selected mixture of Clostridia strains from the human microbiota. *Nature* 500:232.
41. Everard A, Belzer C, Geurts L, Ouwerkerk JP, Druart C, Bindels LB, Guiot Y, Derrien M, Muccioli GG, Delzenne NM, de Vos WM, Cani PD (2013) Cross-talk between *Akkermansia muciniphila* and intestinal epithelium controls diet-induced obesity. *Proc Natl Acad Sci U S A* 110:9066.
42. Sokol H, Pigneur B, Watterlot L, Lakhdari O, Bermudez-Humaran LG, Gratadoux JJ, Blugeon S, Bridonneau C, Furet JP, Corthier G, Grangette C, Vasquez N, Pochart P, Trugnan G, Thomas G, Blottiere HM, Dore J, Marteau P, Seksik P, Langella P (2008) *Faecalibacterium prausnitzii* is an anti-inflammatory commensal bacterium identified by gut microbiota analysis of Crohn disease patients. *Proc Natl Acad Sci U S A* 105:16731.
43. Goodman AL, Kallstrom G, Faith JJ, Reyes A, Moore A, Dantas G, Gordon JI (2011) Extensive personal human gut microbiota culture collections characterized and manipulated in gnotobiotic mice. *Proc Natl Acad Sci U S A* 108:6252.
44. Lagier JC, Armougom F, Million M, Hugon P, Pagnier I, Robert C, Bittar F, Fournous G, Gimenez G, Maraninchi M, Trape JF, Koonin EV, La Scola B, Raoult D (2012) Microbial culturomics: paradigm shift in the human gut microbiome study. *Clin Microbiol Infect* 18:1185.
45. Walker AW, Duncan SH, Louis P, Flint HJ (2014) Phylogeny, culturing, and metagenomics of the human gut microbiota. *Trends Microbiol* 22:267.
46. Chung H, Pamp SJ, Hill JA, Surana NK, Edelman SM, Troy EB, Reading NC, Villablanca EJ, Wang S, Mora JR, Umesaki Y, Mathis D, Benoist C, Relman DA, Kasper DL (2012) Gut immune maturation depends on colonization with a host-specific microbiota. *Cell* 149:1578.
47. Frese SA, Benson AK, Tannock GW, Loach DM, Kim J, Zhang M, Oh PL, Heng NC, Patil PB, Juge N, Mackenzie DA, Pearson BM, Lapidus A, Dalin E, Tice H, Goltsman E, Land M, Hauser L, Ivanova N, Kyrpides NC, Walter J (2011) The evolution of host specialization in the vertebrate gut symbiont *Lactobacillus reuteri*. *PLoS Genet* 7:e1001314.
- 48. Perez-Munoz ME, Bergstrom K, Peng V, Schmaltz R, Jimenez-Cardona R, Marsteller N, McGee S, Clavel T, Ley R, Fu J, Xia L, Peterson DA (2014) Discordance between changes in the gut microbiota and pathogenicity in a mouse model of spontaneous colitis. *Gut Microbes* 5:286.**
49. Dewhirst FE, Chien CC, Paster BJ, Ericson RL, Orcutt RP, Schauer DB, Fox JG (1999) Phylogeny of the defined murine microbiota: altered Schaedler flora. *Appl Environ Microbiol* 65:3287.
50. Becker N, Kunath J, Loh G, Blaut M (2011) Human intestinal microbiota: characterization of a simplified and stable gnotobiotic rat model. *Gut Microbes* 2:25.
51. Lagkouvardos I, Weinmaier T, Lauro FM, Cavicchioli R, Rattei T, Horn M (2014) Integrating metagenomic and amplicon databases to resolve the phylogenetic and ecological diversity of the Chlamydiae. *ISME J* 8:115.

52. Morgan XC, Huttenhower C (2014) Meta'omic analytic techniques for studying the intestinal microbiome. *Gastroenterology* 146:1437.
53. Noller HF, Woese CR (1981) Secondary structure of 16S ribosomal RNA. *Science* 212:403.
54. Klindworth A, Pruesse E, Schweer T, Peplies J, Quast C, Horn M, Glockner FO (2013) Evaluation of general 16S ribosomal RNA gene PCR primers for classical and next-generation sequencing-based diversity studies. *Nucleic Acids Res* 41:e1.
55. Berry D, Ben Mahfoudh K, Wagner M, Loy A (2011) Barcoded primers used in multiplex amplicon pyrosequencing bias amplification. *Appl Environ Microbiol* 77:7846.
56. Edgar RC (2013) UPARSE: highly accurate OTU sequences from microbial amplicon reads. *Nat Methods* 10:996.
57. Edgar RC, Haas BJ, Clemente JC, Quince C, Knight R (2011) UCHIME improves sensitivity and speed of chimera detection. *Bioinformatics* 27:2194.
58. Cole JR, Wang Q, Fish JA, Chai B, McGarrell DM, Sun Y, Brown CT, Porras-Alfaro A, Kuske CR, Tiedje JM (2014) Ribosomal Database Project: data and tools for high throughput rRNA analysis. *Nucleic Acids Res* 42:D633.
59. Godon JJ, Zumstein E, Dabert P, Habouzit F, Moletta R (1997) Molecular microbial diversity of an anaerobic digester as determined by small-subunit rDNA sequence analysis. *Appl Environ Microbiol* 63:2802.
- 60. Clavel T, Mapesa JO. Phenolics in human nutrition: importance of the intestinal microbiome for isoflavone and lignan bioavailability. In: Ramawat KG, Merillon J-M, eds. Handbook of Natural Products: Springer, 2013.**
- 61. Clavel T, Dore J, Blaut M (2006) Bioavailability of lignans in human subjects. *Nutr Res Rev* 19:187.**
62. Setchell KD, Bull R, Adlercreutz H (1980) Steroid excretion during the reproductive cycle and in pregnancy of the vervet monkey (*Cercopithecus aethiopus pygerythrus*). *J Steroid Biochem* 12:375.
63. Axelson M, Sjovall J, Gustafsson BE, Setchell KD (1982) Origin of lignans in mammals and identification of a precursor from plants. *Nature* 298:659.
64. Borriello SP, Setchell KD, Axelson M, Lawson AM (1985) Production and metabolism of lignans by the human faecal flora. *J Appl Bacteriol* 58:37.
65. Adlercreutz H (2007) Lignans and human health. *Crit Rev Clin Lab Sci* 44:483.
66. Bassett CM, Rodriguez-Leyva D, Pierce GN (2009) Experimental and clinical research findings on the cardiovascular benefits of consuming flaxseed. *Appl Physiol Nutr Metab* 34:965.
67. Demark-Wahnefried W, Polascik TJ, George SL, Switzer BR, Madden JF, Ruffin MTt, Snyder DC, Owzar K, Hars V, Albala DM, Walther PJ, Robertson CN, Moul JW, Dunn BK, Brenner D, Minasian L, Stella P, Vollmer RT (2008) Flaxseed supplementation (not dietary fat restriction) reduces prostate cancer proliferation rates in men presurgery. *Cancer Epidemiol Biomarkers Prev* 17:3577.
68. Sun Q, Wedick NM, Pan A, Townsend MK, Cassidy A, Franke AA, Rimm EB, Hu FB, van Dam RM (2014) Gut microbiota metabolites of dietary lignans and risk of type 2 diabetes: a prospective investigation in two cohorts of U.S. women. *Diabetes Care* 37:1287.
69. Thompson LU (1998) Experimental studies on lignans and cancer. *Baillieres Clin Endocrinol Metab* 12:691.
70. Wang LQ, Meselhy MR, Li Y, Qin GW, Hattori M (2000) Human intestinal bacteria capable of transforming secoisolariciresinol diglucoside to mammalian lignans, enterodiol and enterolactone. *Chem Pharm Bull (Tokyo)* 48:1606.
- 71. Clavel T, Henderson G, Alpert CA, Philippe C, Rigottier-Gois L, Dore J, Blaut M (2005) Intestinal bacterial communities that produce active estrogen-like compounds enterodiol and enterolactone in humans. *Appl Environ Microbiol* 71:6077.**

72. Clavel T, Henderson G, Engst W, Dore J, Blaut M (2006) Phylogeny of human intestinal bacteria that activate the dietary lignan secoisolariciresinol diglucoside. *FEMS Microbiol Ecol* 55:471.
73. Clavel T, Lippman R, Gavini F, Dore J, Blaut M (2007) *Clostridium saccharogumia* sp. nov. and *Lactonifactor longoviformis* gen. nov., sp. nov., two novel human faecal bacteria involved in the conversion of the dietary phytoestrogen secoisolariciresinol diglucoside. *Syst Appl Microbiol* 30:16.
74. Blaut M, Clavel T (2007) Metabolic diversity of the intestinal microbiota: implications for health and disease. *J Nutr* 137:751S.
75. Aura AM, Oikarinen S, Mutanen M, Heinonen SM, Adlercreutz HC, Virtanen H, Poutanen KS (2006) Suitability of a batch in vitro fermentation model using human faecal microbiota for prediction of conversion of flaxseed lignans to enterolactone with reference to an in vivo rat model. *Eur J Nutr* 45:45.
76. Bolca S, Wyns C, Possemiers S, Depypere H, De Keukeleire D, Bracke M, Verstraete W, Heyerick A (2009) Cosupplementation of isoflavones, prenylflavonoids, and lignans alters human exposure to phytoestrogen-derived 17beta-estradiol equivalents. *J Nutr* 139:2293.
77. Martinez I, Muller CE, Walter J (2013) Long-term temporal analysis of the human fecal microbiota revealed a stable core of dominant bacterial species. *PLoS One* 8:e69621.
78. Woting A, Clavel T, Loh G, Blaut M (2010) Bacterial transformation of dietary lignans in gnotobiotic rats. *FEMS Microbiol Ecol* 72:507.
79. Mabrok HB, Klopfleisch R, Ghanem KZ, Clavel T, Blaut M, Loh G (2012) Lignan transformation by gut bacteria lowers tumor burden in a gnotobiotic rat model of breast cancer. *Carcinogenesis* 33:203.
80. Desmarchelier C, Dahlhoff C, Keller S, Sailer M, Jahreis G, Daniel H (2012) C57Bl/6 N mice on a western diet display reduced intestinal and hepatic cholesterol levels despite a plasma hypercholesterolemia. *BMC Genomics* 13:84.
81. Desmarchelier C, Ludwig T, Scheundel R, Rink N, Bader BL, Klingenspor M, Daniel H (2013) Diet-induced obesity in ad libitum-fed mice: food texture overrides the effect of macronutrient composition. *Br J Nutr* 109:1518.
82. Hildebrandt MA, Hoffman C, Sherrill-Mix SA, Keilbaugh SA, Hamady M, Chen YY, Knight R, Ahima RS, Bushman F, Wu GD (2009) High fat diet determines the composition of the murine gut microbiome independently of obesity. *Gastroenterology*
83. Shin NR, Lee JC, Lee HY, Kim MS, Whon TW, Lee MS, Bae JW (2013) An increase in the *Akkermansia* spp. population induced by metformin treatment improves glucose homeostasis in diet-induced obese mice. *Gut*
84. Clavel T, Desmarchelier C, Haller D, Gerard P, Rohn S, Lepage P, Daniel H (2014) Intestinal microbiota in metabolic diseases: From bacterial community structure and functions to species of pathophysiological relevance. *Gut Microbes* 5:544.
85. Delzenne NM, Neyrinck AM, Backhed F, Cani PD (2011) Targeting gut microbiota in obesity: effects of prebiotics and probiotics. *Nat Rev Endocrinol* 7:639.
86. Turnbaugh P, Ridaura V, Faith J, Rey F, Knight R, Gordon J (2009) The effect of diet on the human gut microbiome: a metagenomic analysis in humanized gnotobiotic mice. *Science Translational Medicine* 1:
87. Turnbaugh PJ, Backhed F, Fulton L, Gordon JI (2008) Diet-induced obesity is linked to marked but reversible alterations in the mouse distal gut microbiome. *Cell Host Microbe* 3:213.
88. Xiao Y, Cui J, Shi YH, Sun J, Wang ZP, Le GW (2010) Effects of duodenal redox status on calcium absorption and related genes expression in high-fat diet-fed mice. *Nutrition* 26:1188.
89. Yatsunenkov T, Rey FE, Manary MJ, Trehan I, Dominguez-Bello MG, Contreras M, Magris M, Hidalgo G, Baldassano RN, Anokhin AP, Heath AC, Warner B, Reeder J, Kuczynski J, Caporaso JG, Lozupone CA, Lauber C, Clemente JC, Knights D, Knight R, Gordon JI (2012) Human gut microbiome viewed across age and geography. *Nature* 486:222.

90. Beckh K, Kneip S, Arnold R (1994) Direct regulation of bile secretion by prostaglandins in perfused rat liver. *Hepatology* 19:1208.
91. Everson GT, Fennessey P, Kern F, Jr. (1988) Contraceptive steroids alter the steady-state kinetics of bile acids. *J Lipid Res* 29:68.
92. Chow J, Tang H, Mazmanian SK (2011) Pathobionts of the gastrointestinal microbiota and inflammatory disease. *Curr Opin Immunol* 23:473.
93. Eggerth AH (1935) The Gram-positive Non-spore-bearing Anaerobic Bacilli of Human Feces. *J Bacteriol* 30:277.
94. Kageyama A, Benno Y (2001) Rapid detection of human fecal *Eubacterium* species and related genera by nested PCR method. *Microbiol Immunol* 45:315.
95. Qin J, Li Y, Cai Z, Li S, Zhu J, Zhang F, Liang S, Zhang W, Guan Y, Shen D, Peng Y, Zhang D, Jie Z, Wu W, Qin Y, Xue W, Li J, Han L, Lu D, Wu P, Dai Y, Sun X, Li Z, Tang A, Zhong S, Li X, Chen W, Xu R, Wang M, Feng Q, Gong M, Yu J, Zhang Y, Zhang M, Hansen T, Sanchez G, Raes J, Falony G, Okuda S, Almeida M, LeChatelier E, Renault P, Pons N, Batto JM, Zhang Z, Chen H, Yang R, Zheng W, Yang H, Wang J, Ehrlich SD, Nielsen R, Pedersen O, Kristiansen K (2012) A metagenome-wide association study of gut microbiota in type 2 diabetes. *Nature* 490:55.
- 96. Clavel T, Lepage P, Charrier C. Family *Coriobacteriaceae*. In: Rosenberg E, DeLong E, Thompson F, Lory S, Stackebrand E, eds. *The prokaryotes*: Springer, 2013.**
97. Claus SP, Ellero SL, Berger B, Krause L, Bruttin A, Molina J, Paris A, Want EJ, de Waziers I, Cloarec O, Richards SE, Wang Y, Dumas ME, Ross A, Rezzi S, Kochhar S, Van Bladeren P, Lindon JC, Holmes E, Nicholson JK (2011) Colonization-induced host-gut microbial metabolic interaction. *MBio* 2:e00271.
98. Martinez I, Lattimer JM, Hubach KL, Case JA, Yang J, Weber CG, Louk JA, Rose DJ, Kyureghian G, Peterson DA, Haub MD, Walter J (2013) Gut microbiome composition is linked to whole grain-induced immunological improvements. *ISME J* 7:269.
99. Martinez I, Perdicaro DJ, Brown AW, Hammons S, Carden TJ, Carr TP, Eskridge KM, Walter J (2013) Diet-induced alterations of host cholesterol metabolism are likely to affect the gut microbiota composition in hamsters. *Appl Environ Microbiol* 79:516.
100. Karlsson FH, Tremaroli V, Nookaew I, Bergstrom G, Behre CJ, Fagerberg B, Nielsen J, Backhed F (2013) Gut metagenome in European women with normal, impaired and diabetic glucose control. *Nature* 498:99.
101. Ridlon JM, Kang DJ, Hylemon PB (2006) Bile salt biotransformations by human intestinal bacteria. *J Lipid Res* 47:241.
102. Bokkenheuser VD, Winter J, Dehazya P, Kelly WG (1977) Isolation and characterization of human fecal bacteria capable of 21-dehydroxylating corticoids. *Appl Environ Microbiol* 34:571.
103. Bokkenheuser VD, Winter J, O'Rourke S, Ritchie AE (1980) Isolation and characterization of fecal bacteria capable of 16 *alpha*-dehydroxylating corticoids. *Appl Environ Microbiol* 40:803.
104. Bokkenheuser VD, Winter J, Finegold SM, Sutter VL, Ritchie AE, Moore WE, Holdeman LV (1979) New markers for *Eubacterium lentum*. *Appl Environ Microbiol* 37:1001.

PART II

Selected publications

Paper 1-8 Microbiota diversity

The following selected publications refer to research topic 1 (see detailed description above on p16-27). They reflect my interest in describing the diversity of bacterial communities in the mammalian gut using both culture-based and molecular techniques.

1. T Clavel,* A Saalfrank, C Charrier, D Haller (2010) Isolation of bacteria from mouse cecal samples and description of *Bacteroides sartorii* sp. nov., *Arch Microbiol* 192:427; *corresponding author
2. T Clavel,* W Duck, C Charrier, C Elson, D Haller (2010) *Enterorhabdus caecimuris* sp. nov., a novel member of the family *Coriobacteriaceae* isolated from a mouse model of spontaneous colitis, *Int J Syst Evol Microbiol* 60:1527; *corresponding author
3. N Pfeiffer, C Desmarchelier, M Blaut, H Daniel, D Haller, T Clavel (2012) *Acetatifactor muris* gen. nov., sp. nov., a novel acetate- and butyrate-producing bacterium isolated from the intestine of an obese mouse, *Arch Microbiol* 194:901
4. T Clavel,* C Charrier, M Wenning, D Haller (2013) *Parvibacter caecicola* gen. nov., sp. nov., a new bacterium of the family *Coriobacteriaceae* isolated from the caecum of a mouse, *Int J Syst Evol Microbiol* 63:2642; *corresponding author
5. T Clavel,* C Charrier, D Haller (2013) *Streptococcus danieliae* sp. nov., a novel bacterium from the caecum of a mouse, *Arch Microbiol* 195:43; *corresponding author
6. K Kläring, L Hanske, N Bui, C Charrier, M Blaut, D Haller, CM Plugge, T Clavel (2013) *Intestinimonas butyriciproducens* gen. nov., sp. nov., a novel butyrate-producing bacterium from the mouse intestine, *Int J Syst Evol Microbiol* 63:4606

Paper 1 to 6 testify to my long-lasting interest in isolating and characterizing novel bacteria from gut environments. The description of new bacteria is an essential step not only for performing functional studies in experimental models in order to assess molecular mechanisms underlying host-microbe interactions, but also for the implementation of genomic databases for the sake of metagenomic studies. Isolated strains so far include novel butyrate producers within the *Firmicutes*, a new species of the genus *Bacteroides* which has been used already for the study of experimental colitis,⁴⁸ and new members of the family *Coriobacteriaceae* of relevance for the study of hepatic steatosis in section three. All these papers form the basis of my current work on the establishment of the first state-of-the-art collection of gut bacterial strains from the mouse intestine.

7. J Hemmerling, K Heller, G Hörmannspenger, M Bazanella, T Clavel, G Kollias, D Haller (2014) Fetal exposure to maternal inflammation does not affect postnatal development of genetically driven ileitis and colitis, *PLoSone* 9(5):e98237

8. M Wolf, A Adili, K Piotrowitz, Z Abdullah, Y Boege, K Stemmer, M Ringelhan, N Simonavicius, M Sigg, D Wohlleber, A Lorentzen, C Einer, S Schulz, T Clavel, U Protzer, C Thiele, H Zischka, H Moch, M Tschöp, AV Tumanov, D Haller, K Unger, M Karin, M Kopf, P Knolle, A Weber, M Heikenwalder (2014) Metabolic activation of intrahepatic CD8+ and NKT-cells causes nonalcoholic steatohepatitis and hepatocellular carcinoma via cross-talk with hepatocytes, *Cancer Cell*, in press

Paper 7 and 8 are examples of collaborative work that took advantage of descriptive analysis of gut bacterial communities based on the high-throughput 16S rRNA gene sequencing platform I established at TUM. Paper 7 is a work of my mentor Dirk Haller where we showed that maternal inflammation in mice has no real impact on the diversity and composition of cecal bacterial communities. Paper 8 is a work by Mathias Heikenwälder demonstrating for the first time the involvement of immune cells (CD8+ and NKT cells) in the development of hepatocellular carcinoma. We could show that disappearance of the phenotype in RAG-deficient mice is independent of changes in fecal bacterial diversity. Paper 13 and 15 (below) also fall into this category of manuscripts that integrate 16S-based datasets. However, taking into account that the main messages convey in these two own pieces of work relate to nutrition and metabolic disorders, they appear below in section 2 and 3, respectively.

PAPER 1

Isolation of bacteria from mouse caecal samples and description of *Bacteroides sartorii* sp. nov

Thomas Clavel · Anja Saalfrank · Cédric Charrier · Dirk Haller

Received: 11 August 2009 / Revised: 2 February 2010 / Accepted: 17 March 2010 / Published online: 6 April 2010
© Springer-Verlag 2010

Abstract Caecal samples from wild-type and TNF^{deltaARE} mice were cultured on selective media containing bile salts, amino acids or casein macro-peptides. Twenty-two strains were isolated and identified by 16S rRNA gene sequencing. Twenty-one strains showed >98% similarity to known bacteria (*Blautia* spp., *Clostridium innocuum*, *Enterococcus* spp., *Escherichia coli*, *Lactobacillus murinus*, *Parabacteroides goldsteinii* and *Shigella dysenteriae*). One additional isolate, strain A-C2-0, was a new bacterium. The closest relatives were *Bacteroides massiliensis*, *Bacteroides dorei* and *Bacteroides vulgatus* ($\leq 94\%$ similarity). Strain A-C2-0 is a Gram-negative rod that does not form spores and has a G + C content of DNA of 41.5%. Its major cellular fatty acid is C_{15:0} ANTEISO, and its major respiratory quinone is MK-9. Cells are aerotolerant but grow only under strict anoxic conditions. They are resistant to cefotaxime and tobramycin. When compared with related *Bacteroides* spp., the new bacterium was positive for α -arabinosidase, negative for glutamyl glutamic acid arylamidase and did not metabolise galactose, glucose, fructose, mannose, raffinose and sucrose. Strain A-C2-0 therefore merits recognition as a member of a novel species within the genus *Bacteroides*,

for which the name *Bacteroides sartorii* is proposed. The type strain is A-C2-0^T (= DSM 21941^T = CCUG 57211^T).

Keywords Mouse caecum · Bacterial diversity · *Bacteroidetes* · *Bacteroides sartorii* · TNF^{deltaARE} mice · Chronic intestinal inflammation

Introduction

Intestinal microbes are crucial for human health. They play important roles in barrier functions (Lievin-Le Moal and Servin 2006), maturation of the immune system (Rothkotter and Pabst 1989), energy balance (Backhed et al. 2004) and production of bioactive metabolites (Clavel et al. 2005). However, under certain circumstances, intestinal microbes contribute to the development of diseases.

The involvement of bacteria in the onset and maintenance of inflammatory bowel diseases (IBD) has been demonstrated using germ-free animals and faecal stream diversion in IBD patients (Onderdonk et al. 1981; Rutgeerts et al. 1991). Although the occurrence of *Mycobacterium* spp. and *Chlamydia pneumoniae* may be associated with inflammation, a causative role in IBD remains to be proven (Muller et al. 2006; Mendoza et al. 2009). Molecular techniques have allowed in-depth assessment of intestinal microbiota in IBD (Manichanh et al. 2006; Sokol et al. 2006). Under chronic inflammation, intestinal microbiota seem to be characterised by global changes that affect commensal bacterial communities, including loss of functional groups and changes in spatial distribution (Clavel and Haller 2007). According to early studies comparing fluorescence and viable counts, not yet isolated and characterised bacteria may account for >60% of total intestinal bacteria (Langendijk et al. 1995). Thus, the main advantage of

Communicated by Erko Stackebrandt.

The GenBank accession number for the 16S rRNA and gyrase B gene sequences of strain A-C2-0 is GQ456204 and GQ409831, respectively.

T. Clavel (✉) · A. Saalfrank · D. Haller
Biofunctionality, ZIEL, Research Center for Nutrition and Food Science, Technische Universität München (TUM), Gregor-Mendel-Str. 2, 85350 Freising Weihenstephan, Germany
e-mail: thomas.clavel@wzw.tum.de

C. Charrier
NovaBiotics Ltd., Aberdeen AB21 9TR, UK

molecular-based techniques relies on the possibility to assess both cultured and uncultured bacterial taxonomic units. However, uncultured bacteria can also be considered as a pool of functions that remain to be characterised in vitro, and the isolation of novel commensal bacteria may give the opportunity to study in detail some of these functions, including modulation of host cell stress responses. The challenge is to gain access to novel bacteria out of highly diverse consortia of microorganisms.

The human distal intestinal tract harbours very dense and complex communities of mostly anaerobic bacteria. At the phylum level, the *Firmicutes* and *Bacteroidetes* account for more than 95% of total intestinal bacterial diversity (Tap et al. 2009). However, at the species and strain level, bacterial populations are highly diverse, resulting in inter-individual differences in gut bacterial composition. Despite this high diversity, the notion of a core microbiome has emerged, referring to bacteria and underlying functions found in most healthy individuals. Members of the order *Bacteroidales*, including bacteria related to the species *Bacteroides fragilis*, *Bacteroides massiliensis*, *Bacteroides ovatus*, *Bacteroides thetaiotaomicron*, *Bacteroides vulgatus* and *Parabacteroides distasonis*, are dominant and prevalent bacteria in the intestine (Finegold et al. 1983; Rigottier-Gois et al. 2003; Tap et al. 2009). They carry functions of importance for gut homeostasis, including conversion of oligosaccharides and regulation of immune responses (Hooper et al. 1999; Mazmanian et al. 2005; Martens et al. 2009; Reichardt et al. 2009). However, they are also involved in bacterial infections (Brook 1989). In IBD patients, increased counts of *Bacteroides* in mucosal samples have been observed (Lucke et al. 2006). In a gnotobiotic HLA-B27 rat model of intestinal inflammation, *B. ovatus* led to more severe inflammation than that induced by *Escherichia coli* (Rath et al. 1999). To date, there is still little data available on bacterial diversity in the mouse intestine when compared with data in human subjects and most of the recent studies used molecular-based approaches (Salzman et al. 2002; Lupp et al. 2007; Ley et al. 2008).

Our aim was to isolate caecal bacteria from wild-type (WT) and TNF^{deltaARE} mice. Adult TNF^{deltaARE} mice develop chronic inflammation in the distal ileum (Kontoyiannis et al. 1999; Hormannsperger et al. 2009). Additionally, we focused on the genotypic and phenotypic description of strain A-C2-0, a new member of the genus *Bacteroides*.

Materials and methods

Sample collection

Male WT and heterozygous TNF^{deltaARE} C57BL/6 mice (n = 3 each) fed a standard diet (Ssniff, Soest, Germany,

cat. no. V1534-000 R/M-H) were killed by neck dislocation at the age of 5 weeks. Animal use was approved by the local institution in charge (Regierung von Oberbayern, approval no. 55.2-1-54-2531-74-06). Caecal contents were collected into 2-ml tubes and kept on ice for a maximum of 40 min prior to isolation. Wet weights were determined by weighing tubes before and after collection using a TB-215D precision balance (Denver Instrument). For histological analysis, 5-mm-long distal ileal segments adjacent to the caecum were fixed in formalin and embedded in paraffin. Sections were stained with haematoxylin and eosin. Histological scores, from 0 (not inflamed) to 12 (highly inflamed), were determined by assigning points to pathological criteria, as described previously (Katakura et al. 2005). There was no sign of inflammation in the 5-week-old TNF^{deltaARE} mice (mean histological score: 1.0 ± 0.3 and 0.7 ± 0.4 for TNF^{deltaARE} and WT mice, respectively).

Media

The basal solid medium (BM) contained: 4.2 g/l NaHCO₃, 720 mg/l Na₂HPO₄·H₂O, 415 mg/l PdCl₂ (Sigma, cat. no. 520657), 400 mg/l KH₂PO₄, 300 mg/l NaCl, 124 mg/l MgSO₄·7H₂O, 2.5 mg/l phenosafranine, 1.5% (w/v) agar and 1% (v/v) rumen fluid. After autoclaving (121°C, 15 min), BM was allowed to cool down (55°C) in a water bath and was supplemented with filter-sterilised solutions of L-cysteine and DTT to a final concentration of 0.025% (w/v) and 0.02%, respectively. The following compounds were added to BM to obtain the selective medium containing amino acids (A), bile salts (BS) or casein macro-peptides (CMP): 0.25% (w/v) each L-arginine (Sigma, cat. no. A8094) and glycine (AppliChem, cat. no. A1067), 0.25% bile salts (Fluka, cat. no. 48305) or 0.2% casein macro-peptides (LACRODAN[®] CGMP-10, Arla Foods Ingredients amba). The pH of the medium prior to autoclaving was set to: 6.5 (BS), 7.2 (BM and CMP) or 8.5 (A).

Isolation

All steps were carried out in a VA500 workstation (Don Whitley Scientific) containing 85% (v/v) N₂, 10% CO₂ and 5% H₂. The atmosphere was kept at 37°C and 75% humidity. It was tested for anaerobic conditions using Anaerostest[®] (Merck, cat. no. 1.15112.0001). All materials, including agar media, were brought into the workstation 24 h prior to isolation. According to caecal weight measurement, tenfold dilutions (w/v) were prepared by adding appropriate volumes of filter-sterilised phosphate-buffered saline solution (per litre dH₂O: 8.60 g NaCl, 0.87 g Na₂HPO₄, 0.40 g KH₂PO₄, pH 7.2) supplemented with 0.02% (w/v) peptone from meat and 0.05% L-cysteine. Samples were homogenised by vortexing using sterile

glass beads and left to stand for 3 min to sediment debris. Undiluted, ten- and hundredfold diluted cell suspensions (100 µl each) were spread onto the agar media using sterile glass beads. All colony morphology types observed after 6 days of growth were streaked onto blood agar plates (Biomérieux) to support better growth and ensure purity. After 4 days of growth, cells were transferred into GYBHc broth (Clavel et al. 2009) prepared using anaerobic culture techniques (N₂ gas phase) (Attebery and Finegold 1969). Culture purity was examined by observing cell morphology after Gram-staining and colony morphology. Cryo-stocks (100 µl) were prepared by mixing bacterial suspensions with equal volumes of Tris-buffered aqueous solution (60 mM) containing 40% glycerol. Cryo-stocks were stored at –80°C after snap-freezing in liquid nitrogen.

Phylogenetic analysis and DNA base composition

Washed bacterial cell pellets were boiled in 0.02% (w/v) SDS (95°C, 5 min) and used as template for PCR reactions. If necessary, DNA was extracted from bacterial cell pellets using the innuPREP Bacteria DNA Kit (Analytik Jena). The 16S rRNA genes were amplified using primer 27F 5'-AGA GTT TGA TCC TGG CTC AG and 1492R 5'-GGT TAC CTT GTT ACG ACT T (Kageyama et al. 1999). The annealing temperature was 56°C. Amplicons were purified using agarose gel electrophoresis and the Wizard SV Gel and PCR Clean-Up System (Promega) and sequenced with primer 27F using the Qiagen Genomic Services. The 16S rRNA gene of strain A-C2-0 was further sequenced using primers 338F 5'-ACT CCT ACG GGA GGC AGC and 1492R. The gyrase B genes of strain A-C2-0, *Bacteroides uniformis* and *B. vulgatus* were amplified as described previously using primer gyrBBNDN1 (5' ccgtcc acgtcggrtcngycat) and gyrBBAUP2 (5' gcggaagcggcng snatgta) (Santos and Ochman 2004). Amplicons (approximately 1,500 bp) were purified as described above and sequenced using the aforementioned primers. Sequences of organisms closely related to the isolated strains were obtained using the BLAST function of the NCBI server (Altschul et al. 1990), the Ribosomal Database Project (Cole et al. 2003) and The All-Species Living Tree Project (Yarza et al. 2008). Ribosomal sequences were checked for anomalies using the program Pintail (Ashelford et al. 2005). All sequences were aligned using the Bioedit software, version 7.0.5.3 (Hall 1999). Percentages of similarity were calculated after unambiguous alignment of each isolated sequence with those of the most closely related species, using the DNA Distance Matrix function. The G + C content of DNA of strain A-C2-0 was determined at the German Collection of Microorganisms and Cell Cultures (DSMZ) according to standard methods (Cashion et al.

1977; Tamaoka and Komagata 1984; Mesbah et al. 1989; Visuvanathan et al. 1989).

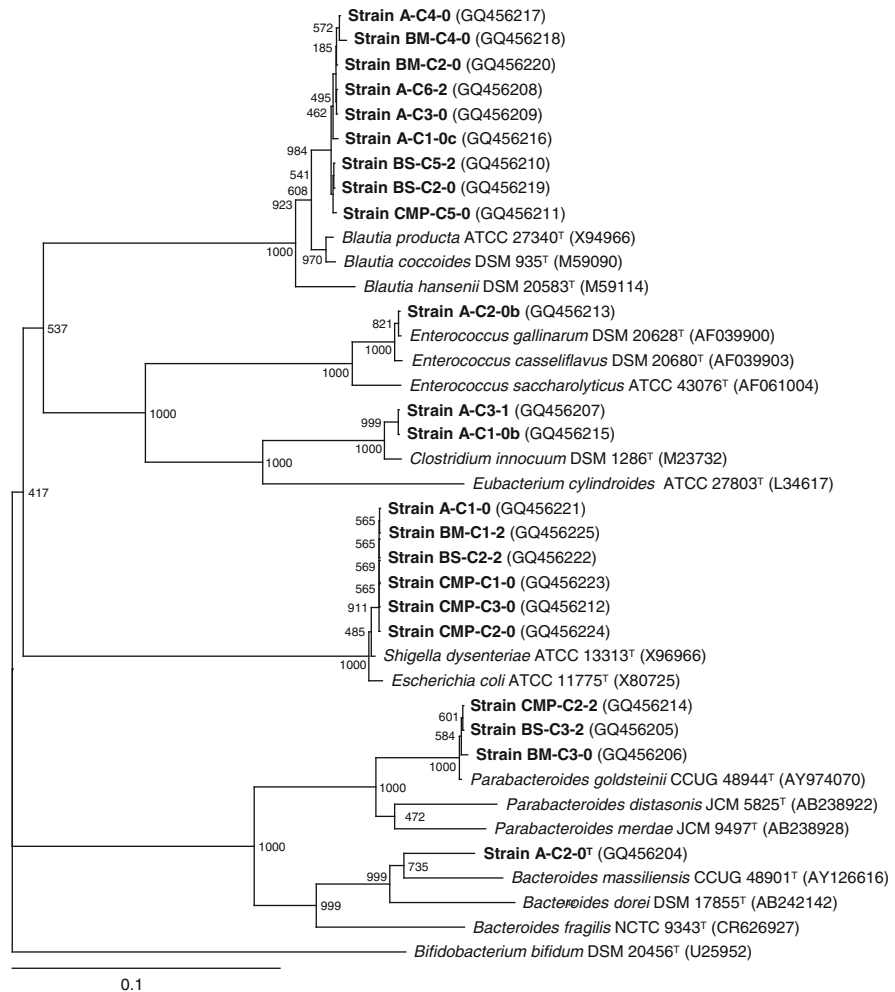
Phenotypic characterisation

All tests were performed as described previously (Clavel et al. 2009). Bacteria were grown in anoxic WCA broth (Oxoid). Quinone, peptidoglycan, polar lipid, whole cell sugar and API 50 CHL analyses were done at the Identification Service of the DSMZ (Braunschweig, Germany) according to standard procedures (Rhuland et al. 1955; Staneck and Roberts 1974; Whiton et al. 1985). Cellular fatty acids were analysed at the Culture Collection University of Göteborg (CCUG, Sweden). Bacteria were grown anaerobically at 37°C on Chocolate-agar (medium no. C376). Conditions for preparation of cell extracts and gas chromatography analysis are detailed in MIDI Technical Note #101 (Microbial ID Inc., Newark, Delaware, USA). Detailed experimental information is available online (<http://www.ccug.se>). Comparison analysis with reference strains was performed as described previously (Eerola and Lehtonen 1988).

Results and discussion

Twenty-two bacterial strains were isolated on four selective agar media from caecal contents obtained from six 5-week-old male WT and heterozygous TNF^{deltaARE} C57BL/6 mice. Figure 1 shows the phylogenetic position and the origin of the isolated strains. The fact that several strains of the same species were obtained from different mice, in spite of the relatively low number of colonies analysed, implies that the identified species belong to common bacterial communities in the mouse caecum. This is in agreement with previously published work, for instance with respect to the occurrence of *Blautia* spp. and *Clostridium innocuum* (Lee et al. 1991; Wang et al. 1996). Limited data are available on the isolation and quantification of members of the genus *Parabacteroides* from mouse intestinal samples (Wang et al. 1996; Dewhirst et al. 1999). However, recent investigations using molecular tools have provided a multitude of cloned sequences similar to the sequence of the *Parabacteroides goldsteinii* strains isolated in the present study, suggesting that this taxon, originally recovered from clinical infections of human intestinal origin, is indeed common in the mouse intestine (Salzman et al. 2002; Stecher et al. 2007; Garner et al. 2009). Finally, although cultivation methods have been used for long to enumerate enterococci and *Enterobacteriaceae* from mouse intestinal samples (Tannock and Savage 1974) and the latter taxonomic group seems to be associated with inflammatory conditions (Lupp et al. 2007; Wohlgemuth et al. 2009), only a few mouse intestinal

Fig. 1 Phylogenetic position of the isolated strains among closely related species. The GenBank accession numbers of the 16S rRNA gene sequences (5'-end, 548 bp) used to construct the tree are indicated in brackets. The strains isolated in the present study are written in *bold letters*. Strain numbers indicate the medium used for isolation (A, BM, BS, or CMP), the mouse caecum number (C1 to 6; mouse 1, 2 and 4 were TNF^{deltaARE} mice) and the dilution plated (10^{-x}). Sequences were aligned using the Bioedit Software, and the tree was constructed with Clustal X 1.8 using the neighbour-joining method with bootstrap values calculated from 1,000 trees. Major groupings were confirmed using the maximum parsimony method. *Bifidobacterium bifidum*, a member of the family *Actinobacteria*, was used as outgroup to root the tree. The *bar* represents 10 nucleotide changes per 100 nucleotides



isolates are available (Berg 1980; Kim et al. 2005; Clavel et al. 2009; Wohlgemuth et al. 2009).

From the data obtained, it was determined that one of the twenty-two isolates, strain A-C2-0, was a novel bacterium isolated from the caecum of a TNF^{deltaARE} mouse on the selective medium containing amino acids. It was identified as a new member of the phylum *Bacteroidetes*. The partial 16S rRNA gene sequence of strain A-C2-0 (1,327 bp) (GQ456204) was: (1) 99% similar to the as yet not described isolate *Bacteroides* sp. TP-5 (AB499846), originating from the intestine of TCR-beta and p53 double-knockout mice, and to cloned sequences from monkey, mouse and rat intestinal samples (Turnbaugh et al. 2006; Ley et al. 2008); (2) $\leq 94\%$ similar to sequences of described species: *B. massiliensis* (94.0%), isolated from blood culture of a newborn (Fenner et al. 2005), *Bacteroides dorei* (93.7%) (Bakir et al. 2006) and *B. vulgatus*

(93.0%) (Eggerth and Gagnon 1933), which are both members of human gut microbiota. Detailed phylogenetic analysis, including all representative members of the order *Bacteroidales*, for which 16S rRNA gene sequences are available, showed that strain A-C2-0 belongs to the genus *Bacteroides* (Fig. 2). Since strain A-C2-0 clustered together with numerous cloned sequences obtained in the course of several studies on mammalian gut bacteria, we hypothesise that strain A-C2-0 is a dominant taxon in the intestine of mammals. Additional work on quantitative analysis of strain A-C2-0 and related strains is needed to test this hypothesis. Based on partial sequence analysis of gyrase B genes (1,337 bp), strain A-C2-0 (GQ409831) was 70.4% similar to *B. vulgatus* (GQ409833), 69.2% to *B. fragilis* (CR626927), the type species of the genus, and 69.1% to *B. uniformis* (GQ409832). These data confirm that strain A-C2-0 differs from previously described species of the

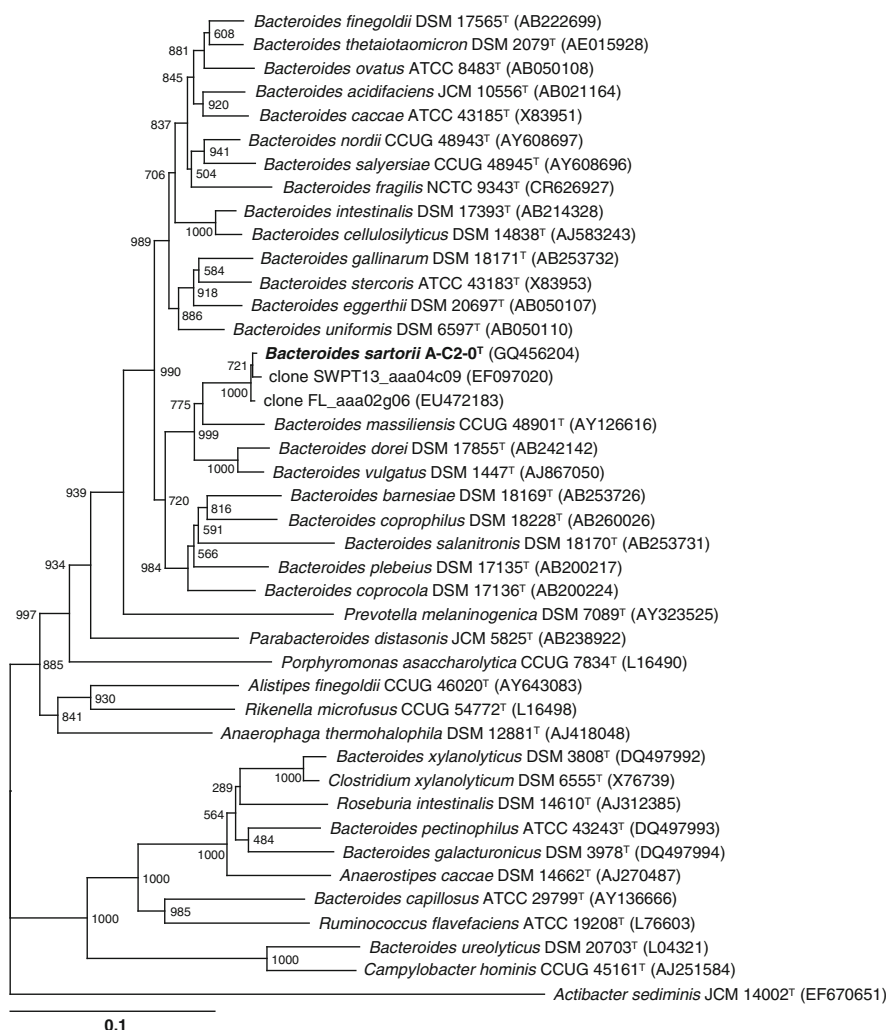


Fig. 2 Phylogenetic position of strain A-C2-0 among members of the order *Bacteroidales*. The tree was constructed as described in Fig. 1. Sequence length was 1,327 bp. *Actibacter sediminis*, a member of the

class *Flavobacteria* within the phylum *Bacteroidetes*, was used as outgroup to root the tree

genus *Bacteroides*. The isolate's G + C content of DNA (41.5 mol%) is in the range of G + C contents reported in the literature for members of the genus *Bacteroides*, e.g., 41–44 mol% for *B. fragilis* and 40–42 mol% for *B. vulgatus* (Holdeman et al. 1984).

Cellular fatty acid analysis showed that strain A-C2-0 has a unique fatty acid profile within the genus. The major fatty acid was C_{15:0} ANTEISO (43.6% of total fatty acids). As expected for a member of the genus *Bacteroides*, the diamino acid in the peptidoglycan of strain A-C2-0 was identified as *meso*-diaminopimelic acid. Galactose, glucose and ribose were detected as whole cell sugars. The polar lipid pattern of strain A-C2-0 is shown in Fig. 3. The

presence of phosphatidylethanolamine as the sole major diacylglycerol-based phospholipid confirmed that the isolate belongs to the phylum *Bacteroidetes*. The major menaquinone of strain A-C2-0 was MK-9 (100%). With the exception of *Bacteroides gingivalis*, *Bacteroides levii* and *Bacteroides splanchnicus*, the respiratory quinones of most *Bacteroides* spp., including *B. vulgatus* and the type species *B. fragilis*, are MK-10 to -13 (Shah and Collins 1983). Microscopic observation of strain A-C2-0 revealed single straight rod-shaped cells (Fig. 4) that stained Gram-negative. Cells grew in WCA broth in the presence of 0.5% (v/v) bile salts (Fluka, cat. no. 48305). *B. uniformis* and *Enterorhabdus mucosicola* were used as a positive

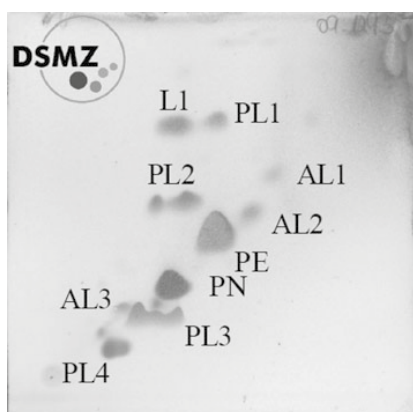


Fig. 3 Two-dimensional thin-layer chromatogram of the polar lipids of strain A-C2-0. Batch cultures (1.5 l) of strain A-C2-0 grown under anoxic conditions for 48 h in WCA broth supplemented with 0.05% (w/v) cysteine were centrifuged ($5,525 \times g$, 10 min, RT) in 500-ml-containers using a 4K15C centrifuge (Sigma). Pellets were re-suspended in sterile PBS, pooled in 50-ml-FALCON tubes and bacterial suspensions were centrifuged ($5,525 \times g$, 15 min, RT). Supernatants were discarded, cell pellets were frozen at -80°C and dried by lyophilisation for 24 h (Alpha 1-4 LDplus, Christ) prior to shipping. Polar lipid analysis was done by the Identification Service of the DSMZ and Dr. B.J. Tindall (Braunschweig, Germany). AL, unidentified aminolipid (AL1 stains orange); L, lipid; PE, phosphatidylethanolamine; PL, phospholipid; PN, aminophospholipid

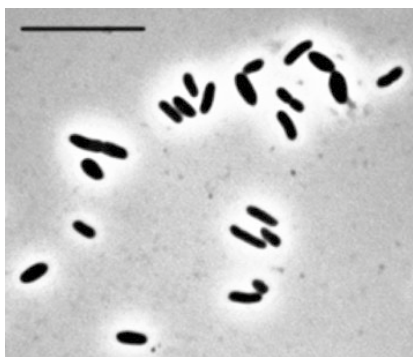


Fig. 4 Phase contrast microscopic picture showing the cell morphology of strain A-C2-0. The bar represents 10 μm

and negative control, respectively. Enzymatic tests using rapid ID 32 A and API 50 CHL strips (Biomérieux) showed that strain A-C2-0 was positive for α - and β -galactosidase, α -glucosidase, α -arabinosidase, N-acetyl- β -glucosaminidase, mannose and raffinose fermentation, glutamic acid decarboxylase, α -fucosidase, alkaline phosphatase, arginine, leucyl glycine, leucine and alanine arylamidase as well as lactose, maltose and melibiose

metabolism. Parameters that distinguish the isolate from phylogenetically closely related species are given in Table 1. The sensitivity of strain A-C2-0 was tested towards ten antimicrobial agents as described previously (Clavel et al. 2009). Each antibiotic was tested in duplicate in three independent experiments and the MIC breakpoint was expressed as the average of those six replicates. MIC breakpoints were ($\mu\text{g/ml}$): cefotaxime (3rd generation cephalosporin), >32 ; ciprofloxacin, 3.000 ± 0.967 ; clarithromycin, 0.006 ± 0.010 ; clindamycin, <0.016 ; erythromycin, 0.151 ± 0.032 ; metronidazole, 0.110 ± 0.036 ; oxacillin (class penicillin), 8.500 ± 1.708 ; tetracycline, 0.089 ± 0.014 ; tobramycin, >256 ; vancomycin, 4.667 ± 0.615 . Thus, strain A-C2-0 is resistant to the broad spectrum β -lactam antibiotic cefotaxime and to the aminoglycoside tobramycin. Most of the other antimicrobial agents tested, with the exception of oxacillin, a narrow-spectrum β -lactam antibiotic, and vancomycin demonstrated high susceptibility of strain A-C2-0. With respect to cefotetan (2nd generation cephalosporin), clindamycin, metronidazole and vancomycin, *B. massiliensis* showed a similar pattern of antibiotic resistance (Fenner et al. 2005).

In conclusion, the work has led to the isolation and identification of six cultivable species from the mouse caecum, including one novel bacterium. Ongoing investigations aim at characterising the prevalence and functions of the new species with respect to host cellular responses in the gut.

Description of *Bacteroides sartorii* sp. nov

Bacteroides sartorii (sar.to'ri.i. N.L. gen. n. *sartorii*, in honour of Balfour Sartor, Professor of Medicine, Microbiology and Immunology at the University of North Carolina in Chapel Hill, for his outstanding contribution to the understanding of microbial ecology in IBD).

The species has the features of the genus. It is phylogenetically related to *Bacteroides massiliensis*. Cells are approximately $1.0\text{--}1.5 \times 2.0\text{--}4.0 \mu\text{m}$, are aerotolerant but grow only under strict anoxic conditions. They grow well at pH values between 6.0 and 9.0, in the temperature range from 25 to 40°C and in the presence of 0.5% (v/v) bile salts. Slight turbidity is observed at pH values between 4.5 and 6.0. After 48 h of growth at 37°C on blood agar, colonies are circular, entire, raised, grey and non-haemolytic. The species is positive for α -arabinosidase, negative for glutamyl glutamic acid arylamidase and does not metabolise galactose, glucose, fructose, mannose, raffinose and sucrose. Its major menaquinone is MK-9 and its major fatty acid is $\text{C}_{15:0}$ ANTEISO. The G + C content of DNA is 41.5 mol%. Resistance to cefotaxime and tobramycin has been shown.

Table 1 Characteristics of strain A-C2-0 and of phylogenetically closely related species of the genus *Bacteroides* (Symbols: +, positive reaction; –, negative reaction; ±, ambiguous reaction (Fenner et al. 2005; Bakir et al. 2006); ND not determined)

	1	2	3	4
Origin	Mouse caecum	Newborn blood	Human faeces	Human faeces
G + C content of DNA (mol%)	41.5	49	40–42	43
α -Arabinosidase [†]	+	–	+	+
β -glucuronidase [†]	–	–	+	+
Glutamic acid decarboxylase [†]	+	±	+	+
Glutamyl glutamic acid arylamidase [†]	–	±	+	+
Leucine arylamidase [†]	+	+	–	+
Galactose*	–	+	ND	ND
Glucose*	–	+	+	+
Fructose*	–	+	+	ND
Lactose*	+	+	+	+
Maltose*	+	+	+	+
Mannose*	–	+	+	+
Melibiose*	+	+	ND	ND
Raffinose*	–	+	+	+
Sucrose*	–	+	+	+
Respiratory quinones	MK-9	ND	MK-10, -11	ND
Cellular fatty acids [§]				
13:0	–	–	0.9	–
13:0 ISO	0.5	0.7	0.6	–
13:0 ANTEISO	1.0	1.2	1.7	0.7
14:0	0.6	0.3	1.1	0.4
14:0 ISO	–	–	3.2	1.2
14:0 aldehyde	–	–	–	0.5
15:0	12.9	7.7	26.2	12.5
15:0 ISO	7.3	9.6	6.3	7.0
15:0 ANTEISO	43.6	31.1	28.4	35.2
15:0 ISO aldehyde	3.9	9.7	1.5	7.8
15:0 3OH	–	–	4.1	2.0
16:0	4.3	2.9	3.3	3.4
16:0 ISO	0.5	0.4	–	–
16:0 3OH	1.9	0.0	4.2	2.3
16:0 ISO 3OH	–	–	1.1	0.6
16:1 w7c	0.0	0.4	0.3	–
17:0 ISO	0.5	0.7	–	–
17:0 ANTEISO	0.8	0.8	–	0.4
17:0 2OH	–	–	1.2	1.9
17:0 3OH	–	–	2.9	2.0
17:0 ISO 3OH	11.6	21.3	5.2	11.8
17:1 w9c ANTEISO	0.8	1.2	–	–
18:0	1.0	1.1	0.6	1.2
18:0 ANTE	4.7	6.1	3.3	4.4
18:1 w9c	3.1	3.7	2.5	2.7
Unidentified	–	1.1	1.3	2.1

Taxa: 1, *Bacteroides sartorii* sp. nov. (strain A-C2-0^T); 2, *B. massiliensis* (Fenner et al. 2005); 3, *B. vulgatus* (Holdeman et al. 1984); 4, *B. dorei* (Bakir et al. 2006)

[†], * Analysed using the rapid ID 32 A and the API 20 A identification system, respectively

[§] Strains were *B. sartorii* CCUG 57211^T, *B. massiliensis* CCUG 48901^T, *B. vulgatus* CCUG 12546 and *B. dorei* CCUG 53892^T

The type strain, A-C2-0^T (= DSM 21941^T = CCUG 57211^T), was isolated from the caecum of a 5-week-old male heterozygous TNF^{deltaARE} C57BL/6 mouse.

Acknowledgments The heterozygous TNF^{deltaARE} mouse model of ileitis was a generous gift from Dr. George Kollias (Biomedical Sciences Research Center Alexander Fleming, Vari, Greece). We thank Prof. J.P. Euzeby (Ecole Nationale Vétérinaire, Toulouse, France) for his support in creating Latin names, Dr. Sigrid Kisting (TUM, BFLM) for histological analysis, Dr. Herbert Seiler (TUM, Microbiology) for microscopic analysis and co-workers of the DSMZ and of the Culture Collection University of Göteborg (CCUG) for contributing to the description of strain A-C2-0.

References

- Altschul SF, Gish W, Miller W, Myers EW, Lipman DJ (1990) Basic local alignment search tool. *J Mol Biol* 215:403–410
- Ashelford KE, Chuzhanova NA, Fry JC, Jones AJ, Weightman AJ (2005) At least 1 in 20 16S rRNA sequence records currently held in public repositories is estimated to contain substantial anomalies. *Appl Environ Microbiol* 71:7724–7736
- Attebery HR, Finegold SM (1969) Combined screw-cap and rubber-stopper closure for Hungate tubes (pre-reduced anaerobically sterilized roll tubes and liquid media). *Appl Microbiol* 18:558–561
- Backhed F, Ding H, Wang T, Hooper LV, Koh GY, Nagy A, Semenkovich CF, Gordon JI (2004) The gut microbiota as an environmental factor that regulates fat storage. *Proc Natl Acad Sci USA* 101:15718–15723
- Bakir MA, Sakamoto M, Kitahara M, Matsumoto M, Benno Y (2006) *Bacteroides dorei* sp. nov., isolated from human faeces. *Int J Syst Evol Microbiol* 56:1639–1643
- Berg RD (1980) Inhibition of *Escherichia coli* translocation from the gastrointestinal tract by normal cecal flora in gnotobiotic or antibiotic-decontaminated mice. *Infect Immun* 29:1073–1081
- Brook I (1989) Pathogenicity of the *Bacteroides fragilis* group. *Ann Clin Lab Sci* 19:360–376
- Cashion P, Holder-Franklin MA, McCully J, Franklin M (1977) A rapid method for the base ratio determination of bacterial DNA. *Anal Biochem* 81:461–466
- Clavel T, Haller D (2007) Molecular interactions between bacteria, the epithelium, and the mucosal immune system in the intestinal tract: implications for chronic inflammation. *Curr Issues Intest Microbiol* 8:25–43
- Clavel T, Henderson G, Alpert CA, Philippe C, Rigottier-Gois L, Dore J, Blaut M (2005) Intestinal bacterial communities that produce active estrogen-like compounds enterodiol and enterolactone in humans. *Appl Environ Microbiol* 71:6077–6085
- Clavel T, Charrier C, Braune A, Wenning M, Blaut M, Haller D (2009) Isolation of bacteria from the ileal mucosa of TNF^{deltaARE} mice and description of *Enterorhabdus mucosicola* gen. nov., sp. nov. *Int J Syst Evol Microbiol* 59:1805–1812
- Cole JR, Chai B, Marsh TL, Farris RJ, Wang Q, Kulam SA, Chandra S, McGarrell DM, Schmidt TM, Garrity GM, Tiedje JM (2003) The Ribosomal Database Project (RDP-II): previewing a new autoaligner that allows regular updates and the new prokaryotic taxonomy. *Nucleic Acids Res* 31:442–443
- Dewhirst FE, Chien CC, Paster BJ, Ericson RL, Orcutt RP, Schauer DB, Fox JG (1999) Phylogeny of the defined murine microbiota: altered Schaedler flora. *Appl Environ Microbiol* 65:3287–3292
- Eerola E, Lehtonen OP (1988) Optimal data processing procedure for automatic bacterial identification by gas-liquid chromatography of cellular fatty acids. *J Clin Microbiol* 26:1745–1753
- Eggerth AH, Gagnon BH (1933) The *Bacteroides* of human feces. *J Bacteriol* 25:389–413
- Fenner L, Roux V, Mallet MN, Raoult D (2005) *Bacteroides massiliensis* sp. nov., isolated from blood culture of a newborn. *Int J Syst Evol Microbiol* 55:1335–1337
- Finegold SM, Sutter VL, Mathisen GE (1983) Normal indigenous intestinal flora. In: Henteges DJ (ed) Human intestinal microflora in health and disease. Academic Press, New York, pp 3–31
- Garner CD, Antonopoulos DA, Wagner B, Duhamel GE, Keresztes I, Ross DA, Young VB, Altier C (2009) Perturbation of the small intestine microbial ecology by streptomycin alters pathology in a *Salmonella enterica* serovar typhimurium murine model of infection. *Infect Immun* 77:2691–2702
- Hall TA (1999) Bioedit: a user-friendly biological sequence alignment editor and analysis program for Windows 95/98/NT. *Nuc Acids Symp Ser* 41:95–98
- Holdeman LV, Kelley RW, Moore WEC (1984) Genus I. *Bacteroides*. In: Holt GJ (ed) Bergey's manual systematic bacteriology. Williams & Wilkins, Baltimore, pp 610–613
- Hooper LV, Xu J, Falk PG, Midtvedt T, Gordon JI (1999) A molecular sensor that allows a gut commensal to control its nutrient foundation in a competitive ecosystem. *Proc Natl Acad Sci USA* 96:9833–9838
- Hormansperger G, Clavel T, Hoffmann M, Reiff C, Kelly D, Loh G, Blaut M, Holzwimmer G, Laschinger M, Haller D (2009) Post-translational inhibition of IP-10 secretion in IEC by probiotic bacteria: impact on chronic inflammation. *PLoS One* 4:e4365
- Kageyama A, Benno Y, Nakase T (1999) Phylogenetic evidence for the transfer of *Eubacterium lentum* to the genus *Eggerthella* as *Eggerthella lenta* gen. nov., comb. nov. *Int J Syst Bacteriol* 49:1725–1732
- Katakura K, Lee J, Rachmilewitz D, Li G, Eckmann L, Raz E (2005) Toll-like receptor 9-induced type I IFN protects mice from experimental colitis. *J Clin Invest* 115:695–702
- Kim SC, Tonkonogy SL, Albright CA, Tsang J, Balish EJ, Braun J, Huycke MM, Sartor RB (2005) Variable phenotypes of enterocolitis in interleukin 10-deficient mice monoassociated with two different commensal bacteria. *Gastroenterology* 128:891–906
- Kontoyiannis D, Pasparakis M, Pizarro TT, Cominelli F, Kollias G (1999) Impaired on/off regulation of TNF biosynthesis in mice lacking TNF AU-rich elements: implications for joint and gut-associated immunopathologies. *Immunity* 10:387–398
- Langendijk PS, Schut F, Jansen GJ, Raangs GC, Kamphuis GR, Wilkinson MH, Welling GW (1995) Quantitative fluorescence in situ hybridization of *Bifidobacterium* spp. with genus-specific 16S rRNA-targeted probes and its application in fecal samples. *Appl Environ Microbiol* 61:3069–3075
- Lee WK, Fujisawa T, Kawamura S, Itoh K, Mitsuoka T (1991) Isolation and identification of clostridia from the intestine of laboratory animals. *Lab Anim* 25:9–15
- Ley RE, Hamady M, Lozupone C, Turnbaugh PJ, Ramey RR, Birchler JS, Schlegel ML, Tucker TA, Schrenzel MD, Knight R, Gordon JI (2008) Evolution of mammals and their gut microbes. *Science* 320:1647–1651
- Lievin-Le Moal V, Servin AL (2006) The front line of enteric host defense against unwelcome intrusion of harmful microorganisms: mucins, antimicrobial peptides, and microbiota. *Clin Microbiol Rev* 19:315–337
- Lucke K, Miehle S, Jacobs E, Schuppler M (2006) Prevalence of *Bacteroides* and *Prevotella* spp. in ulcerative colitis. *J Med Microbiol* 55:617–624
- Lupp C, Robertson ML, Wickham ME, Sekirov I, Champion OL, Gaynor EC, Finlay BB (2007) Host-mediated inflammation disrupts the intestinal microbiota and promotes the overgrowth of *Enterobacteriaceae*. *Cell Host Microbe* 2:204

- Manichanh C, Rigottier-Gois L, Bonnaud E, Gloux K, Pelletier E, Frangeul L, Nalin R, Jarrin C, Chardon P, Marteau P, Roca J, Dore J (2006) Reduced diversity of faecal microbiota in Crohn's disease revealed by a metagenomic approach. *Gut* 55:205–211
- Martens EC, Koropatkin NM, Smith TJ, Gordon JI (2009) Complex glycan catabolism by the human gut microbiota: the *Bacteroides* Sus-like paradigm. *J Biol Chem* 284:24673–24677
- Mazmanian SK, Liu CH, Tzianabos AO, Kasper DL (2005) An immunomodulatory molecule of symbiotic bacteria directs maturation of the host immune system. *Cell* 122:107–118
- Mendoza JL, Lana R, Diaz-Rubio M (2009) *Mycobacterium avium* subspecies *paratuberculosis* and its relationship with Crohn's disease. *World J Gastroenterol* 15:417–422
- Mesbah M, Premachandran U, Whitman W (1989) Precise measurement of the G + C content of deoxyribonucleic acid by high performance liquid chromatography. *Int J Syst Bact* 39:159–167
- Muller S, Arni S, Varga L, Balsiger B, Hersberger M, Maly F, Seibold F (2006) Serological and DNA-based evaluation of *Chlamydia pneumoniae* infection in inflammatory bowel disease. *Eur J Gastroenterol Hepatol* 18:889–894
- Onderdonk AB, Franklin ML, Cisneros RL (1981) Production of experimental ulcerative colitis in gnotobiotic guinea pigs with simplified microflora. *Infect Immun* 32:225–231
- Rath HC, Wilson KH, Sartor RB (1999) Differential induction of colitis and gastritis in HLA-B27 transgenic rats selectively colonized with *Bacteroides vulgatus* or *Escherichia coli*. *Infect Immun* 67:2969–2974
- Reichardt N, Gniechwitz D, Steinhart H, Bunzel M, Blaut M (2009) Characterization of high molecular weight coffee fractions and their fermentation by human intestinal microbiota. *Mol Nutr Food Res* 53:287–299
- Rhuland L, Work E, Denman R, Hoare D (1955) The behavior of the isomers of alpha, epsilon-diaminopimelic acid on paper chromatograms. *J Am Chem Soc* 77:4844–4846
- Rigottier-Gois L, Rochet V, Garrec N, Suau A, Dore J (2003) Enumeration of *Bacteroides* species in human faeces by fluorescent in situ hybridisation combined with flow cytometry using 16S rRNA probes. *Syst Appl Microbiol* 26:110–118
- Rothkotter HJ, Pabst R (1989) Lymphocyte subsets in jejunal and ileal Peyer's patches of normal and gnotobiotic minipigs. *Immunology* 67:103–108
- Rutgeerts P, Goboos K, Peeters M, Hiele M, Penninckx F, Aerts R, Kerremans R, Vantrappen G (1991) Effect of faecal stream diversion on recurrence of Crohn's disease in the neoterminal ileum. *Lancet* 338:771–774
- Salzman NH, de Jong H, Paterson Y, Harmsen HJ, Welling GW, Bos NA (2002) Analysis of 16S libraries of mouse gastrointestinal microflora reveals a large new group of mouse intestinal bacteria. *Microbiology* 148:3651–3660
- Santos SR, Ochman H (2004) Identification and phylogenetic sorting of bacterial lineages with universally conserved genes and proteins. *Environ Microbiol* 6:754–759
- Shah HN, Collins MD (1983) Genus *Bacteroides*. A chemotaxonomical perspective. *J Appl Bacteriol* 55:403–416
- Sokol H, Lepage P, Seksik P, Dore J, Marteau P (2006) Temperature gradient gel electrophoresis of fecal 16S rRNA reveals active *Escherichia coli* in the microbiota of patients with ulcerative colitis. *J Clin Microbiol* 44:3172–3177
- Staneck JL, Roberts GD (1974) Simplified approach to identification of aerobic *Actinomycetes* by thin-layer chromatography. *Appl Microbiol* 28:226–231
- Stecher B, Robbiani R, Walker AW, Westendorf AM, Barthel M, Kremer M, Chaffron S, Macpherson AJ, Buer J, Parkhill J, Dougan G, von Mering C, Hardt WD (2007) *Salmonella enterica* serovar *typhimurium* exploits inflammation to compete with the intestinal microbiota. *PLoS Biol* 5:2177–2189
- Tamaoka J, Komagata K (1984) Determination of DNA base composition by reversed-phase high-performance liquid chromatography. *FEMS Microbiol Lett* 25:125–128
- Tannock GW, Savage DC (1974) Influences of dietary and environmental stress on microbial populations in the murine gastrointestinal tract. *Infect Immun* 9:591–598
- Tap J, Mondot S, Levenez F, Pelletier E, Caron C, Furet JP, Ugarte E, Munoz-Tamayo R, Paslier DL, Nalin R, Dore J, Leclerc M (2009) Towards the human intestinal microbiota phylogenetic core. *Environ Microbiol* 11:2574–2584
- Turnbaugh PJ, Ley RE, Mahowald MA, Magrini V, Mardis ER, Gordon JI (2006) An obesity-associated gut microbiome with increased capacity for energy harvest. *Nature* 444:1027–1031
- Visuvanathan S, Moss M, Standord J, Hermon-Taylor J, McFadden J (1989) Simple enzymatic method for isolation of DNA from diverse bacteria. *J Microbiol Methods* 10:59–64
- Wang RF, Cao WW, Cerniglia CE (1996) PCR detection and quantitation of predominant anaerobic bacteria in human and animal fecal samples. *Appl Environ Microbiol* 62:1242–1247
- Whiton RS, Lau P, Morgan SL, Gilbert J, Fox A (1985) Modifications in the alditol acetate method for analysis of muramic acid and other neutral and amino sugars by capillary gas chromatography-mass spectrometry with selected ion monitoring. *J Chromatogr* 347:109–120
- Wohlgemuth S, Haller D, Blaut M, Loh G (2009) Reduced microbial diversity and high numbers of one single *Escherichia coli* strain in the intestine of colitic mice. *Environ Microbiol* 11:1562–1571
- Yarza P, Richter M, Peplies J, Euzéby J, Amann R, Schleifer KH, Ludwig W, Glockner FO, Rossello-Mora R (2008) The all-species living tree project: a 16S rRNA-based phylogenetic tree of all sequenced type strains. *Syst Appl Microbiol* 31:241–250

PAPER 2

Enterorhabdus caecimuris sp. nov., a member of the family *Coriobacteriaceae* isolated from a mouse model of spontaneous colitis, and emended description of the genus *Enterorhabdus* Clavel *et al.* 2009

Thomas Clavel,¹ Wayne Duck,² Cédric Charrier,³ Mareike Wenning,⁴ Charles Elson² and Dirk Haller¹

Correspondence

Thomas Clavel
thomas.clavel@wzw.tum.de

¹Biofunctionality, ZIEL – Research Center for Nutrition and Food Science, Technische Universität München (TUM), 85350 Freising Weihenstephan, Germany

²Division of Gastroenterology and Hepatology, Department of Medicine, University of Alabama at Birmingham, Birmingham, AL, USA

³NovaBiotics Ltd, Aberdeen, AB21 9TR, UK

⁴Microbiology, ZIEL – Research Center for Nutrition and Food Science, TUM, 85350 Freising Weihenstephan, Germany

The C3H/HeJBir mouse model of intestinal inflammation was used for isolation of a Gram-positive, rod-shaped, non-spore-forming bacterium (B7^T) from caecal suspensions. On the basis of partial 16S rRNA gene sequence analysis, strain B7^T was a member of the class *Actinobacteria*, family *Coriobacteriaceae*, and was related closely to *Enterorhabdus mucosicola* Mt1B8^T (97.6%). The major fatty acid of strain B7^T was C_{16:0} (19.1%) and the respiratory quinones were mono- and dimethylated. Cells were aerotolerant, but grew only under anoxic conditions. Strain B7^T did not convert the isoflavone daidzein and was resistant to cefotaxime. The results of DNA–DNA hybridization experiments and additional physiological and biochemical tests allowed the genotypic and phenotypic differentiation of strain B7^T from the type strain of *E. mucosicola*. Therefore, strain B7^T represents a novel species, for which the name *Enterorhabdus caecimuris* sp. nov. is proposed. The type strain is B7^T (=DSM 21839^T =CCUG 56815^T).

The family *Coriobacteriaceae* currently comprises 13 genera, four of which have been described recently, and includes *Adlercreutzia equolifaciens* (Maruo *et al.*, 2008), the type species of which was isolated from human faeces; *Asaccharobacter celatus* (Minamida *et al.*, 2008), isolated from a rat caecum; *Enterorhabdus mucosicola* (Clavel *et al.*, 2009), isolated from the inflamed ileal mucosa of a mouse; and *Gordonibacter pamelaiae* (Würdemann *et al.*, 2009), isolated from a patient with Crohn's disease.

During the course of experiments focused on flagellated bacteria and their implication in intestinal inflammation (Duck *et al.*, 2007), strain B7^T was isolated from the

caecum of a C3H/HeJBir mouse, a mouse substrain prone to spontaneous colitis (Sundberg *et al.*, 1994), after 3 days growth at 37 °C on ATCC medium 602 E. Additional information on strain isolation and 16S rRNA gene sequencing has been published elsewhere (Duck *et al.*, 2007). Unless otherwise stated, all experiments for the description of strain B7^T were carried out as described previously (Clavel *et al.*, 2009). *Bacteroides vulgatus* was used as a positive control for the determination of growth with bile salts (no. 48305; Fluka). Cellular fatty acids, respiratory quinones, peptidoglycan and whole-cell sugars were analysed by the DSMZ, Braunschweig, Germany, according to standard procedures (Sasser, 1990; Cashion *et al.*, 1977; De Ley *et al.*, 1970; Huß *et al.*, 1983; Mesbah *et al.*, 1989; Rhuland *et al.*, 1955; Staneck & Roberts, 1974; Tamaoka & Komagata, 1984; Visuvanathan *et al.*, 1989; Whiton *et al.*, 1985).

16S rRNA gene sequences from strain B7^T (determined as described previously; Duck *et al.*, 2007) and GenBank were aligned using BioEdit version 7.0.5.3 (Hall, 1999) and a

Abbreviation: FT-IRS, Fourier-transform infrared spectroscopy.

The GenBank/EMBL/DDBJ accession numbers for the 16S rRNA and gyrase B gene sequences of strain B7^T are DQ789120 and GQ409830, respectively.

Supplementary figures showing the polar lipid compositions and daidzein conversion abilities of strain B7^T and the type strain of *Enterorhabdus mucosicola* are available with the online version of this paper.

rooted tree was constructed using the neighbour-joining method with CLUSTAL X version 1.8. Bootstrap values were calculated on the basis of 1000 resamplings. The maximum-parsimony method was used to confirm the topology of the phylogeny. Fig. 1 gives a current phylogenetic overview of the family *Coriobacteriaceae* and the position of strain B7^T. Sequence similarity values were obtained with the DNA distance matrix function in the BioEdit software. The 16S rRNA gene sequence of strain B7^T (1336 bp) was related most closely (>99%) to sequences originating from as-yet-uncultured mouse intestinal bacteria (Ley *et al.*, 2005, 2006) and *E. mucosicola* Mt1B8^T (97.6%). Lower similarities were found to sequences from *Asaccharobacter celatus* do03^T (93.4%), *Adlercreutzia equolifaciens* FJC-B9^T (93.3%) and two *Eggerthella* strains (<90%). The resolution of 16S rRNA gene sequence analysis does not allow the identification of closely related species. However, it consistently depicts phylogenetic relationships from the level of domains to moderately related species (Stackebrandt & Goebel, 1994). It has been proposed that a genus could be defined as containing species that have 95% 16S rRNA gene sequence similarity to each other (Rossello-Mora & Amann, 2001). We suggest that strain B7^T does not belong to either of the genera *Adlercreutzia* or *Asaccharobacter*, as the strain has

16S rRNA gene sequence similarity values with members of these genera of <94%.

The gyrase B gene of strain B7^T was amplified as described previously (Santos & Ochman, 2004). Amplicons (1500 bp) were purified using agarose gel electrophoresis and the Wizard SV Gel and PCR Clean-Up System (Promega). Purified products were sequenced using the primers *gyrBBNDN1* (5'-CCGTCCACGTCGGCRTCNG-YCAT-3') and *gyrBBAUP2* (5'-GCGGAAGCGGCCNGSN-ATGTA-3'). The gyrase B gene sequence of strain B7^T shared 95.7 and 79.3% similarity with sequences from *E. mucosicola* Mt1B8^T (GenBank accession no. EU594341) and *Eggerthella lenta* DSM 2243^T (EU594342; 524 bp), respectively. Strain B7^T exhibited low DNA-DNA relatedness to *E. mucosicola* DSM 19490^T (28.0 ± 2.0%, two experiments), which supported the fact that these two bacteria belong to different species. The DNA G+C content of strain B7^T (64.5 mol%) was comparable to those reported in the literature for its phylogenetic neighbours.

The results of phenotypic and chemotaxonomic analyses are given in the species description and in Table 1. The fatty acid profile of strain B7^T was similar to that of *E. mucosicola* DSM 19490^T. The diamino acid in the peptidoglycan was identified as *meso*-diaminopimelic acid,

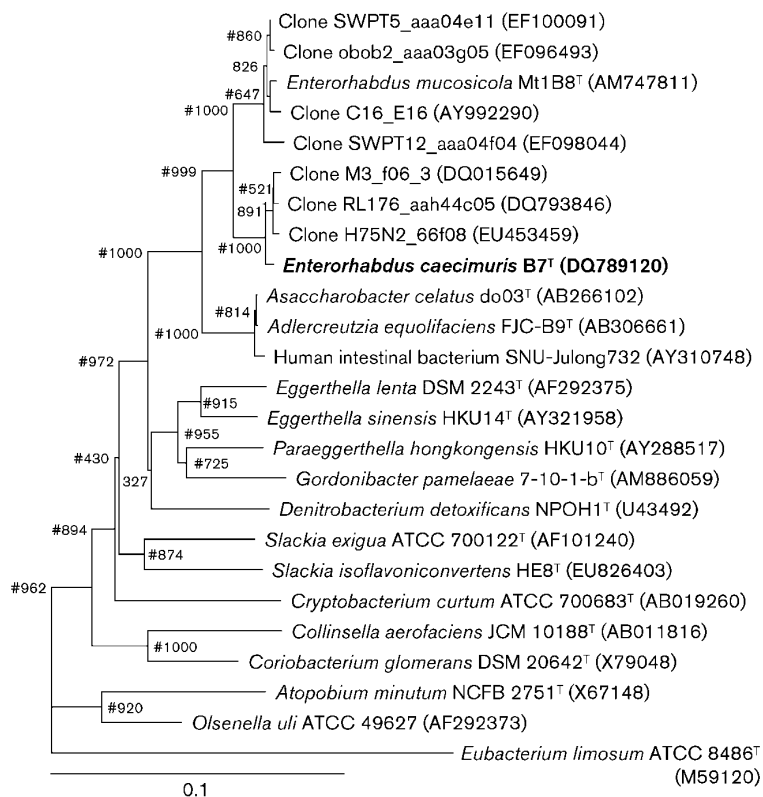


Fig. 1. Phylogenetic position of strain B7^T within the family *Coriobacteriaceae*, based on a neighbour-joining analysis of 16S rRNA gene sequences (1338 bp). Bootstrap values based on 1000 resamplings are shown at branch nodes. Hash signs indicate that the corresponding nodes were also recovered in the tree generated using the maximum-parsimony method. *Eubacterium limosum* ATCC 8486^T, a member of the phylum *Firmicutes*, was used as an outgroup. Bar, 10 substitutions per 100 nucleotide positions.

Table 1. Characteristics that differentiate strain B7^T and *E. mucosicola* DSM 19490^T

Strains: 1, B7^T; 2, *E. mucosicola* DSM 19490^T. Data were taken from this study. DMA, Dimethylacetal; DMMK, dimethylmenaquinone; MMK, monomethylmenaquinone; R, resistant (MIC >32 µg ml⁻¹); ND, not determined.

Characteristic	1	2
Diaminopimelic acid	<i>meso</i>	LL
Major menaquinones (%)		
MMK-6	60	100
DMMK-6	40	0
Whole-cell sugars		
Glucose	+	-
Enzyme activities*		
Aminopeptidase	-	+
Glutamic acid decarboxylase	+	-
Isoflavone conversion		
Daidzein	-	+
Genistein	ND	+
Antibiotic MIC (µg ml ⁻¹)†		
Cefotaxime	R (>32)	1.250 ± 0.112
Ciprofloxacin	0.305 ± 0.035	R (>32)
Clarithromycin	<0.016	<0.016
Clindamycin	0.105 ± 0.010	<0.016
Erythromycin	<0.016	0.048 ± 0.007
Metronidazole	0.016 ± 0.000	0.034 ± 0.004
Oxacillin	R (36.000 ± 5.750)	4.667 ± 0.667
Tetracycline	0.120 ± 0.005	0.115 ± 0.007
Tobramycin	4.333 ± 0.558	2.667 ± 0.211
Vancomycin	1.500 ± 0.129	1.333 ± 0.105
Cellular fatty acids		
iso-C _{12:0}	0.36	0.50
C _{12:0}	1.21	0.72
iso-C _{13:0}	-	0.15
anteiso-C _{13:0}	0.43	0.49
C _{13:1} c12	0.29	0.17
iso-C _{14:0}	3.83	2.48
C _{14:0}	15.08	12.11
C _{14:0} DMA	0.68	0.41
iso-C _{15:0}	1.20	1.60
anteiso-C _{15:0}	2.82	2.29
C _{15:0}	1.77	1.60
C _{15:0} DMA	0.40	0.42
C _{16:0} ALDE	2.28	2.31
C _{16:0}	19.14	18.06
iso-C _{16:0}	0.52	0.42
C _{16:0} DMA	9.62	11.56
C _{16:1} c9	0.94	0.93
anteiso-C _{17:0}	0.82	0.75
anteiso-C _{17:0} DMA	-	0.19
C _{17:0}	0.87	-
C _{17:0} DMA	-	0.20
C _{17:1} c8	1.16	0.52
C _{17:1} c9	-	0.41
C _{18:0} DMA	2.40	3.73
C _{18:0}	7.99	9.35

Table 1. cont.

Characteristic	1	2
C _{18:1} c9	15.25	16.68
C _{18:1} c9 DMA	4.94	4.75
C _{18:1} c11 DMA	0.59	0.56
C _{18:1} c11/t9/t6	4.16	3.83
C _{18:2} c9,12	1.24	1.30

*Data obtained with Rapid ID32A identification system for anaerobes (bioMérieux).

†Values are expressed as mean ± SD of six replicates (three independent experiments with duplicates).

which so far has been reported only for the peptidoglycan type A1γ and three variations of peptidoglycan type A4γ. The quinones were monomethylmenaquinone-6 (60%) and dimethylmenaquinone-6 (40%).

For polar lipid analysis, batch cultures (1.5 l) of strain B7^T and *E. mucosicola* DSM 19490^T were grown under anoxic conditions for 48 h in GYBHIc [brain–heart infusion broth (no. 211059; BD) supplemented with (l⁻¹) 4 g glucose, 4 g yeast extract and 0.05% (w/v) cysteine] and harvested by centrifugation [5525 g for 10 min at room temperature in 500 ml containers using a 4K15C centrifuge (Sigma)]. Pellets were resuspended in filter-sterilized PBS [(1 distilled water)⁻¹: 8.60 g NaCl, 0.87 g Na₂HPO₄, 0.40 g KH₂PO₄; pH 7.2] and supernatants were centrifuged again as above. Resuspended pellets were pooled in 50 ml Falcon tubes and centrifuged as above for 15 min. Supernatants were discarded first by inverting the tubes and subsequently pipetting the remaining liquid after the tubes had been left to stand for 30 s. Samples were stored at -80 °C prior to shipping on dry ice. Polar lipid analysis was done by the Identification Service of the DSMZ and Dr B. J. Tindall (Braunschweig, Germany). The polar lipid pattern of strain B7^T differed from that of *E. mucosicola* DSM 19490^T (Supplementary Fig. S1, available in IJSEM Online). The major polar lipids were diphosphatidylglycerol, phosphatidylglycerol, one unknown phospholipid, two unknown glycolipids and one unidentified lipid.

Fourier-transform infrared spectroscopy (FT-IRS) was used to further differentiate strain B7^T and *E. mucosicola* DSM 19490^T. FT-IRS relies on the absorption of infrared radiation by cell components and results in fingerprint-like spectra that reflect the cellular chemical composition and allow the identification of closely related bacteria (Kirschner *et al.*, 2001; Wenning *et al.*, 2008). Clusters were calculated using Ward's algorithm and vector-normalized first derivatives of the spectra (Savitzky–Golay algorithm) in the ranges 3000–2800 and 1800–700 cm⁻¹ (Fig. 2). Measurements of duplicate cultures of *E. mucosicola* DSM 19490^T at two time points clustered together and demonstrated the reproducibility of the technique. For each strain, spectra from independent cultures were more similar to one another than to those

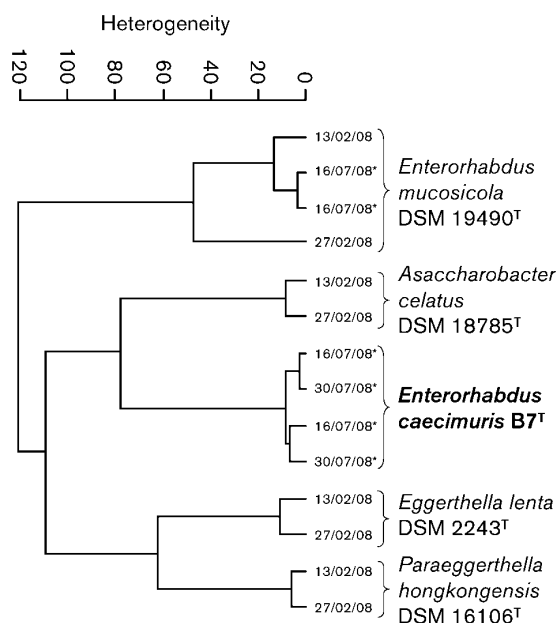


Fig. 2. Cluster analysis of FT-IRS spectra of strain B7^T and closely related strains. Data were taken from this study and Clavel *et al.* (2009). Dates indicate date of measurement. Asterisks indicate results from this study.

from other species and attested to the robustness of the observed spectral variations between taxa. Interestingly, the spectra from strain B7^T were less closely related to those from *E. mucosicola* DSM 19490^T than to those from more distant phylogenetic neighbours, providing evidence at the whole-cell biochemical level that there were differences between these two organisms. Thus, although it is not useful for taxonomic purposes, FT-IRS can be used for the rapid identification of members of the family *Coriobacteriaceae* if the dataset is extended to other members of the family.

The sensitivity of strain B7^T was tested towards ten antimicrobial agents as described previously (Clavel *et al.*, 2009). The MICs are presented in Table 1. Strain B7^T was resistant to cefotaxime, a broad-spectrum antibiotic interfering with cell-wall synthesis, and oxacillin, a narrow-spectrum β -lactam antibiotic, but highly sensitive to clarithromycin, erythromycin and metronidazole. Strain B7^T grew in the presence of 2% (w/v) NaCl and at pH 6.0–9.0, but not in the presence of 0.5% (w/v) bile salts. At pH 6.9, cysteine was not required for growth. In contrast to *E. mucosicola* DSM 19490^T, strain B7^T did not convert a variety of amino acid derivatives and was positive for glutamic acid decarboxylase (Rapid ID32A; bioMérieux). Strain B7^T was also positive for arginine dihydrolase.

Because *E. mucosicola* DSM 19490^T produces equol from the isoflavone daidzein (Matthies *et al.*, 2008), we investigated

daidzein conversion in strain B7^T. Stock solutions (20 mM) of daidzein (no. D7802; Sigma-Aldrich) and (*R,S*)-equol (no. ALX-385-032; Axxora) were prepared in DMSO and stored at -20°C . The daidzein stock solution was filter-sterilized prior to storage (Millex-LG PTFE membrane, 0.22 μm ; Millipore). *E. mucosicola* DSM 19490^T was used as a positive control; separate negative controls for daidzein and bacteria were included. Each bacterium was tested in duplicate at 37°C under anoxic conditions (100% N₂) in GYBHc. The initial concentration of daidzein was approximately 120 μM . Samples were taken over time with a syringe and stored at -20°C . Supernatants (14 000 g for 5 min; 200 μl) were diluted fivefold in a mixture of the eluents (30%, v/v, B in A; see below) and 50 μl samples were used for reversed-phase HPLC analysis using an Agilent HPLC 1100 Series and a ProntoSIL 120-5-C18 ace-EPS 5.0 μm column (250 mm \times 4.6 mm; Bischoff). The mobile phase was water/acetonitrile/formic acid (94.9:5:0.1, v/v; A) and water/acetonitrile/formic acid (5:94.9:0.1, v/v; B) in a gradient mode (from 10 to 100% B within 32 min, then 100% B for 8 min). The flow rate was 1.0 ml min⁻¹ and compounds were detected with a diode array detector at 300 nm. Retention times for daidzein and equol were 19.5 and 23.5 min, respectively. Calibration used two independent dilution series of daidzein that included the following concentrations: 0.1, 1, 10, 25, 50, 100 and 200 μM . Growing cells of strain B7^T were not capable of converting daidzein under the experimental conditions used (Supplementary Fig. S2, available in IJSEM Online).

On the basis of the phylogenetic, chemotaxonomic and phenotypic analyses presented above, strain B7^T can be distinguished from the type strain of *E. mucosicola* and thus represents a novel species, for which the name *Enterorhabdus caecimuris* sp. nov. is proposed.

Emended description of the genus *Enterorhabdus* Clavel *et al.* 2009

The description is as given previously (Clavel *et al.*, 2009) with the following modifications. Members of the genus are aerotolerant anaerobes. No growth occurs in the presence of 0.5% (w/v) bile salts. Do not possess glycosidases. Cysteine is not required for growth. The diamino acid in the peptidoglycan is *meso*- or *LL*-diaminopimelic acid. The main cellular fatty acid is C_{16:0} (approx. 20% of total fatty acids). Major polar lipids are diphosphatidylglycerol and two glycolipids. Whole-cell sugars include galactose and ribose. Respiratory menaquinones are mainly monomethylated ($\geq 60\%$ total lipokinones). The G + C content is 64.2–64.5 mol%.

Description of *Enterorhabdus caecimuris* sp. nov.

Enterorhabdus caecimuris (ca.e.ci.mu'ris. L. n. caecum caecum; L. n. *mus muris* mouse; N.L. gen. n. *caecimuris* of the caecum of a mouse).

Gram-positive, non-motile, non-spore-forming rods (0.5 \times 2.0 μm) growing as single cells under strictly anoxic

conditions. Colonies are small (pinpoint), circular, entire and non-haemolytic after 48 h at 37 °C on Columbia blood agar. Grows in the presence of 2% (w/v) NaCl and at 27–40 °C. Major fatty acids are C_{14:0}, C_{16:0} and C_{18:1} c9. Whole-cell sugars are galactose, glucose and ribose. Quinones are mono- and dimethylated. Produces glutamate decarboxylase and arginine dihydrolase but not aminopeptidase. The type strain is resistant to cefotaxime and does not convert daidzein to equol. The DNA G+C content of the type strain is 64.5 mol%.

The type strain is B7^T (=DSM 21839^T =CCUG 56815^T), isolated from the caecum of a C3H/HeJ mouse.

Acknowledgements

We are grateful to Professor J. P. Euzéby (Ecole Nationale Vétérinaire, Toulouse, France) for his help with Latin etymology, to Benjamin Tiemann for technical assistance and to members of the Culture Collection University of Göteborg (CCUG), especially Dr Enevold Falsen. This research was supported in part by National Institutes of Health grants DK071176 and DK64400.

References

- Cashion, P., Holder-Franklin, M. A., McCully, J. & Franklin, M. (1977). A rapid method for the base ratio determination of bacterial DNA. *Anal Biochem* **81**, 461–466.
- Clavel, T., Charrier, C., Braune, A., Wenning, M., Blaut, M. & Haller, D. (2009). Isolation of bacteria from the ileal mucosa of TNFdeltaARE mice and description of *Enterorhabdus mucosicola* gen. nov., sp. nov. *Int J Syst Evol Microbiol* **59**, 1805–1812.
- De Ley, J., Cattoir, H. & Reynaerts, A. (1970). The quantitative measurement of DNA hybridization from renaturation rates. *Eur J Biochem* **12**, 133–142.
- Duck, L. W., Walter, M. R., Novak, J., Kelly, D., Tomasi, M., Cong, Y. & Elson, C. O. (2007). Isolation of flagellated bacteria implicated in Crohn's disease. *Inflamm Bowel Dis* **13**, 1191–1201.
- Hall, T. A. (1999). BioEdit: a user-friendly biological sequence alignment editor and analysis program for Windows 95/98/NT. *Nucleic Acids Symp Ser* **41**, 95–98.
- HuB, V. A. R., Festl, H. & Schleifer, K. H. (1983). Studies on the spectrophotometric determination of DNA hybridization from renaturation rates. *Syst Appl Microbiol* **4**, 184–192.
- Kirschner, C., Maquelin, K., Pina, P., Ngo Thi, N. A., Choo-Smith, L. P., Sockalingum, G. D., Sandt, C., Ami, D., Orsini, F. & other authors (2001). Classification and identification of enterococci: a comparative phenotypic, genotypic, and vibrational spectroscopic study. *J Clin Microbiol* **39**, 1763–1770.
- Ley, R. E., Backhed, F., Turnbaugh, P., Lozupone, C. A., Knight, R. D. & Gordon, J. I. (2005). Obesity alters gut microbial ecology. *Proc Natl Acad Sci U S A* **102**, 11070–11075.
- Ley, R. E., Turnbaugh, P. J., Klein, S. & Gordon, J. I. (2006). Microbial ecology: human gut microbes associated with obesity. *Nature* **444**, 1022–1023.
- Maruo, T., Sakamoto, M., Ito, C., Toda, T. & Benno, Y. (2008). *Adlercreutzia equolificiens* gen. nov., sp. nov., an equol-producing bacterium isolated from human faeces, and emended description of the genus *Eggerthella*. *Int J Syst Evol Microbiol* **58**, 1221–1227.
- Matthies, A., Clavel, T., Gutschow, M., Engst, W., Haller, D., Blaut, M. & Braune, A. (2008). Conversion of daidzein and genistein by an anaerobic bacterium newly isolated from the mouse intestine. *Appl Environ Microbiol* **74**, 4847–4852.
- Mesbah, M., Premachandran, U. & Whitman, W. (1989). Precise measurement of the G+C content of deoxyribonucleic acid by high performance liquid chromatography. *Int J Syst Bacteriol* **39**, 159–167.
- Minamida, K., Ota, K., Nishimukai, M., Tanaka, M., Abe, A., Sone, T., Tomita, F., Hara, H. & Asano, K. (2008). *Asaccharobacter celatus* gen. nov., sp. nov., isolated from rat caecum. *Int J Syst Evol Microbiol* **58**, 1238–1240.
- Rhuland, L. E., Work, E., Denman, R. F. & Hoare, D. S. (1955). The behavior of the isomers of α,ϵ -diaminopimelic acid on paper chromatograms. *J Am Chem Soc* **77**, 4844–4846.
- Rossello-Mora, R. & Amann, R. (2001). The species concept for prokaryotes. *FEMS Microbiol Rev* **25**, 39–67.
- Santos, S. R. & Ochman, H. (2004). Identification and phylogenetic sorting of bacterial lineages with universally conserved genes and proteins. *Environ Microbiol* **6**, 754–759.
- Sasser, M. (1990). *Identification of bacteria by gas chromatography of cellular fatty acids*, MIDI Technical Note 101. Newark, DE: MIDI Inc.
- Stackebrandt, E. & Goebel, B. M. (1994). Taxonomic note: a place for DNA-DNA reassociation and 16S rRNA sequence analysis in the present species definition in bacteriology. *Int J Syst Bacteriol* **44**, 846–849.
- Staneck, J. L. & Roberts, G. D. (1974). Simplified approach to identification of aerobic actinomycetes by thin-layer chromatography. *Appl Microbiol* **28**, 226–231.
- Sundberg, J. P., Elson, C. O., Bedigian, H. & Birkenmeier, E. H. (1994). Spontaneous, heritable colitis in a new substrain of C3H/HeJ mice. *Gastroenterology* **107**, 1726–1735.
- Tamaoka, J. & Komagata, K. (1984). Determination of DNA base composition by reversed-phase high-performance liquid chromatography. *FEMS Microbiol Lett* **25**, 125–128.
- Visuvanathan, S., Moss, M. T., Standord, J. L., Hermon-Taylor, J. & McFadden, J. J. (1989). Simple enzymatic method for isolation of DNA from diverse bacteria. *J Microbiol Methods* **10**, 59–64.
- Wenning, M., Scherer, S. & Naumann, D. (2008). Infrared spectroscopy in the identification of microorganisms. In *Vibrational Spectroscopy for Medical Diagnosis*, pp. 71–96. Edited by M. Diem, P. R. Griffith & J. M. Chalmers. Chichester, UK: Wiley.
- Whiton, R. S., Lau, P., Morgan, S. L., Gilbert, J. & Fox, A. (1985). Modifications in the alditol acetate method for analysis of muramic acid and other neutral and amino sugars by capillary gas chromatography-mass spectrometry with selected ion monitoring. *J Chromatogr* **347**, 109–120.
- Würdemann, D., Tindall, B. J., Pukall, R., Lünsdorf, H., Strömpl, C., Namuth, T., Nahrstedt, H., Wos-Oxley, M., Ott, S., Schreiber, S., Timmis, K. N. & Oxley, A. P. A. (2009). *Gordonibacter pamelaee* gen. nov., sp. nov., a new member of the *Coriobacteriaceae* isolated from a patient with Crohn's disease and reclassification of *Eggerthella hongkongensis* Lau et al. 2006 as *Paraeggerthella hongkongensis* gen. nov., comb. nov. *Int J Syst Evol Microbiol* **59**, 1405–1415.

PAPER 3

Acetatifactor muris gen. nov., sp. nov., a novel bacterium isolated from the intestine of an obese mouse

Nora Pfeiffer · Charles Desmarchelier ·
Michael Blaut · Hannelore Daniel · Dirk Haller ·
Thomas Clavel

Received: 10 March 2012 / Revised: 10 May 2012 / Accepted: 11 May 2012 / Published online: 4 June 2012
© Springer-Verlag 2012

Abstract We used selective agar media for culturing bacteria from the caecum of mice fed a high calorie diet. In addition to the isolation of *Enterobacteriaceae* growing on a medium containing cholesterol and bile salts, we focused on the characterization of strain CT-m2^T, which, based on 16S rDNA analysis, did not appear to correspond to any currently described organisms. The isolate belongs to the *Clostridium* cluster XIV and is most closely related to members of the *Lachnospiraceae*, including the genera *Anaerostipes*, *Blautia*, *Butyrivibrio*, *Clostridium*, *Coprococcus*, *Eubacterium*, *Robinsoniella*, *Roseburia*, *Ruminococcus* and *Syntrophococcus* ($\leq 90\%$ similarity). Strain CT-m2^T is a non-motile Gram-positive rod that does not form spores and has a G + C content of DNA of 48.5%. Cells grow under strictly anoxic conditions (100% N₂) and

produce acetate and butyrate after growth in reduced WCA broth. In contrast to related species, the new bacterium does not metabolize glucose and is positive for phenylalanine arylamidase, and its major cellular fatty acid is C_{14:0}. Based on phylogenetic and phenotypic studies, the isolate merits recognition as a member of a novel genus and species, for which the name *Acetatifactor muris* is proposed. The type strain is CT-m2^T (= DSM 23669^T = ATCC BAA-2170^T).

Keywords Mouse intestinal microbiota · Diet-induced obesity · *Firmicutes* · *Clostridia* · *Acetatifactor muris*

Introduction

The mammalian gut microbiota is dominated by over 1,000 species of strictly anaerobic bacteria, predominantly Gram-positive type cells belonging to the phylum *Firmicutes* (Ley et al. 2008). The study of such highly diverse ecosystems is partly hampered by the fact that most gut bacteria (>60%) have no representative strains yet in culture (Goodman et al. 2011), highlighting the importance of isolating novel bacterial species for further in vitro

Communicated by Erko Stackebrandt.

The GenBank accession number of the 16S rRNA gene sequence of strain CT-m2^T is HM989805.

Electronic supplementary material The online version of this article (doi:10.1007/s00203-012-0822-1) contains supplementary material, which is available to authorized users.

N. Pfeiffer · M. Blaut
Gastrointestinal Microbiology, German Institute of Human
Nutrition Potsdam-Rehbrücke, Nuthetal, Germany

C. Desmarchelier · H. Daniel
Molecular Nutrition Unit, ZIEL, Research Centre for Nutrition
and Food Sciences, Technische Universität München,
Freising-Weihenstephan, Germany

Present Address:

C. Desmarchelier
Faculté de Médecine, INSERM, UMR 1062 « Nutrition, Obesity
and Risk of Thrombosis »/INRA, UMR1260/Université
d'Aix-Marseille, Marseille, France

D. Haller · T. Clavel
Biofunctionality, ZIEL, Research Centre for Nutrition and Food
Sciences, Technische Universität München,
Freising-Weihenstephan, Germany

T. Clavel (✉)
Young Research Group Intestinal Microbiome, TU München,
ZIEL, BFLM, Gregor-Mendel-Str. 2,
85350 Freising-Weihenstephan, Germany
e-mail: thomas.clavel@tum.de

characterization of functions of interest, including metabolic features and regulation of host cell stress responses (Alain and Querellou 2009). Ultimately, the isolation of new bacteria is also essential for refining taxonomic definitions of complex and heterogeneous groups of bacteria, such as the *Clostridia*. Several members of the *Firmicutes* encode functions of relevance to host health, including production of the short-chain fatty acid butyrate or conversion of dietary components such as polyphenols (Clavel et al. 2006; Louis and Flint 2009). Moreover, it has been recently shown that the occurrence of *Firmicutes*, especially members of the family *Erysipelotrichaceae*, is markedly increased in mouse models of diet-induced obesity (Turnbaugh et al. 2009; Fleissner et al. 2010). In that context, we aimed at isolating bacteria from the caecum of obese mice and focused on the description of one novel bacterial genus within the *Firmicutes*.

Materials and methods

Sampling

Male C57BL/6Ncr1 mice were fed a standard (STD) or a cafeteria (CT) diet ($n = 5$ mice/group). The feeding protocol and the diets are given in the Electronic Supplementary Material. All procedures were conducted according to the German guidelines for animal care and approved by the state ethics committee (ref. no. 209.1/211-2531-41/03). After 81 days on the experimental diets, mice were killed by cervical dislocation. Caecal contents were collected, weighed using a precision balance (TB-215D, Denver Instrument) and immediately used for culturing.

Media

Two agar media were used for isolation, referred to as CBS and CT agar hereafter. The cholesterol and bile salts (CBS) agar is described in the Electronic Supplementary Material. The selective CT medium was used to mimic dietary intake in mice fed the CT diet. It was prepared using 10.4 g pellets of cocoa-flavoured, 7.4 g coconut-flavoured and 2.2 g peanut-flavoured diet (Suppl. Table S1), which were ground and solved in distilled water (1 l) by mixing for 30 min at 50 °C. After addition of 2 % (w/v) agar, the medium was autoclaved (121 °C, 15 min). The sterile medium (55 °C) was supplemented with the following filter-sterilized solutions prior to pouring into Petri dishes (final concentrations in CT agar are given in brackets): DTT (0.02 %), cysteine (0.05 %), taurine (15 mM) (Sigma, cat. no. T0625), ammonium iron citrate (0.05 %) (Sigma, cat. no. 09713), erythromycin (10 µg/ml) (Sigma, cat. no. 45673) and polymyxin B (50 µg/ml) (AppliChem, cat. no. A0890). Antibiotics were used to select

for anaerobic Gram-positive bacteria other than streptococci, staphylococci and bacilli.

Isolation of bacteria

Anaerobic work was carried out in a VA500 workstation (Don Whitley Scientific) containing 90 % (v/v) N₂ and 10 % H₂. The atmosphere was kept at 37 °C and 75 % humidity. It was tested for anaerobic conditions using Anaerotest[®] (Merck, cat. no. 1.15112.0001). All materials, including agar media and buffered solutions, were brought into the workstation approximately 24 h prior to the sample preparation. Immediately after the collection and weight determination, caecal samples were brought into the anaerobic workstation and suspended in filter-sterilized phosphate-buffered saline (PBS) solution (per litre dH₂O: NaCl, 8.60 g; Na₂HPO₄, 0.86 g; KH₂PO₄, 0.40 g, pH 7.2) supplemented with 0.02 % peptone from meat (Roth, cat. no. 2366) and 0.05 % L-cysteine (PBS/PC). Tenfold serial dilutions were prepared for each sample. Bacterial suspensions (100 µl) were spread on CBS and CT agar using sterile glass beads. Counts were determined after 6 days of incubation. Only plates with 10–200 colonies per plate were taken into account for cell density determination. Weighted means were calculated if two successive dilutions gave rise to appropriate numbers of colonies. Results were expressed as mean ± SD of colony-forming units (CFU) per gram of wet caecal content or as logarithmic values thereof. Data were analysed statistically (*t* test) using the SigmaStat software, version 3.10 (Systat Software Inc.). All single-colony morphology types observed after 6 days of growth were streaked onto CBS or CT agar to ensure purity. Thereafter, the non-selective medium used for sub-culturing isolates was reduced WCA, that is, Wilkins-Chalgren-Anaerobe bouillon (Oxoid, cat. no. CM0643) supplemented with cysteine and DTT and prepared using strictly anaerobic techniques (100 % N₂) (Attebery and Finegold 1969). Culture purity was examined by observing cell morphology after Gram-staining and colony morphology. Cryo-stocks (100 µl) were stored at –80 °C after mixing bacterial suspensions with equal volumes of Tris-buffered aqueous solution (60 mM) containing 40 % glycerol.

Phylogenetic and DNA-based analyses

DNA was extracted from washed bacterial cell pellets using the DNeasy Blood & Tissue kit (Qiagen), following the instructions for pretreatment of Gram-positive bacteria. The 16S rRNA genes were amplified using primer 27F 5'-AGA GTT TGA TCC TGG CTC AG and 1492R 5'-GGT TAC CTT GTT ACG ACT T (Kageyama et al. 1999). The annealing temperature was 56 °C. Amplicons were purified using the Wizard SV Gel and PCR Clean-Up System

(Promega) and sequenced with primer 27F using the Qiagen Genomic Services. The 16S rRNA gene of strain CT-m2^T was further sequenced using primer 1492R. Sequences of organisms closely related to the isolated strains were obtained using the BLAST function of the NCBI server (Altschul et al. 1990) and The All-Species Living Tree project (Yarza et al. 2008). Ribosomal sequences were checked for anomalies using the greengenes web application (DeSantis et al. 2006a, b). All sequences were aligned using the BioEdit software, version 7.0.5.3 (Hall 1999). Percentages of similarity were calculated after unambiguous alignment of each isolated sequence with those of the most closely related species, using the DNA Distance Matrix function of the BioEdit software. The G + C content of DNA of strain CT-m2^T was determined at the German Collection of Microorganisms and Cell Cultures by using high-performance liquid chromatography (www.dsmz.de).

Phenotypic characterization

Strain CT-m2^T was characterized as described previously (Clavel et al. 2009; Clavel et al. 2010). For all tests, bacteria were grown in reduced WCA medium. Peptidoglycan, whole-cell sugars, polar lipids and cellular fatty acids were analysed by the Identification Service of the DSMZ (Braunschweig, Germany) according to the standard procedures. For these analyses, cell mass was obtained as follows: batch cultures (1.5 l) grown under anoxic conditions for 3 days in reduced WCA broth were centrifuged (5525 ×g, 20 min, RT) in 500-ml containers using a 4K15C centrifuge (Sigma). Pellets were re-suspended in sterile PBS, and supernatants were centrifuged again as above. The pellets were pooled with the first ones in 50-ml Falcon tubes, and bacterial suspensions were centrifuged (5525 ×g, 15 min, RT). Supernatants were discarded by inverting the tubes. Cell pellets were stored at −80 °C and dried by lyophilization overnight (Alpha 1–4 LDplus, Christ) prior to shipment. To determine enzymatic features, bacterial suspensions were analysed with the rapid ID 32A test and with ANI cards using the VITEK[®] system following the manufacturer's instructions (Biomérieux, Marcy-l'Étoile, France). For both tests, two cell suspensions in PBS (>Mc Farland Standard no. 3) were prepared from two independent batch cultures grown for 48 h. Data obtained with the rapid ID 32A were compared using apiweb (<https://apiweb.biomerieux.com>). For VITEK[®] analysis, ANI cards were inoculated automatically using the VITEK filling module and were incubated aerobically for 4 h at 37 °C. The cards were read manually against a comparator template provided by the manufacturer. Data were analysed using the VITEK program. To measure the production of short-chain fatty acids, cells were grown for 72 h in reduced WCA broth. Acetate, butyrate, propionate,

valerate and isovalerate were measured with an HP 5890 series II gas chromatograph (Hewlett-Packard, Waldbronn, Germany) equipped with an HP-20 M column and a flame ionization detector. Supernatants (200 µl) collected at 0, 24, 48 and 72 h after inoculation were mixed with 23.6 µl of isobutyric acid (12 mM), 270 µl of NaOH (1 M) and 280 µl of HClO₄ (0.36 M). Freeze-dried mixtures were re-suspended in 400 µl of acetone and 100 µl of formic acid (5 M). After centrifugation, supernatants (1 µl) were injected twice into the chromatograph.

Results and discussion

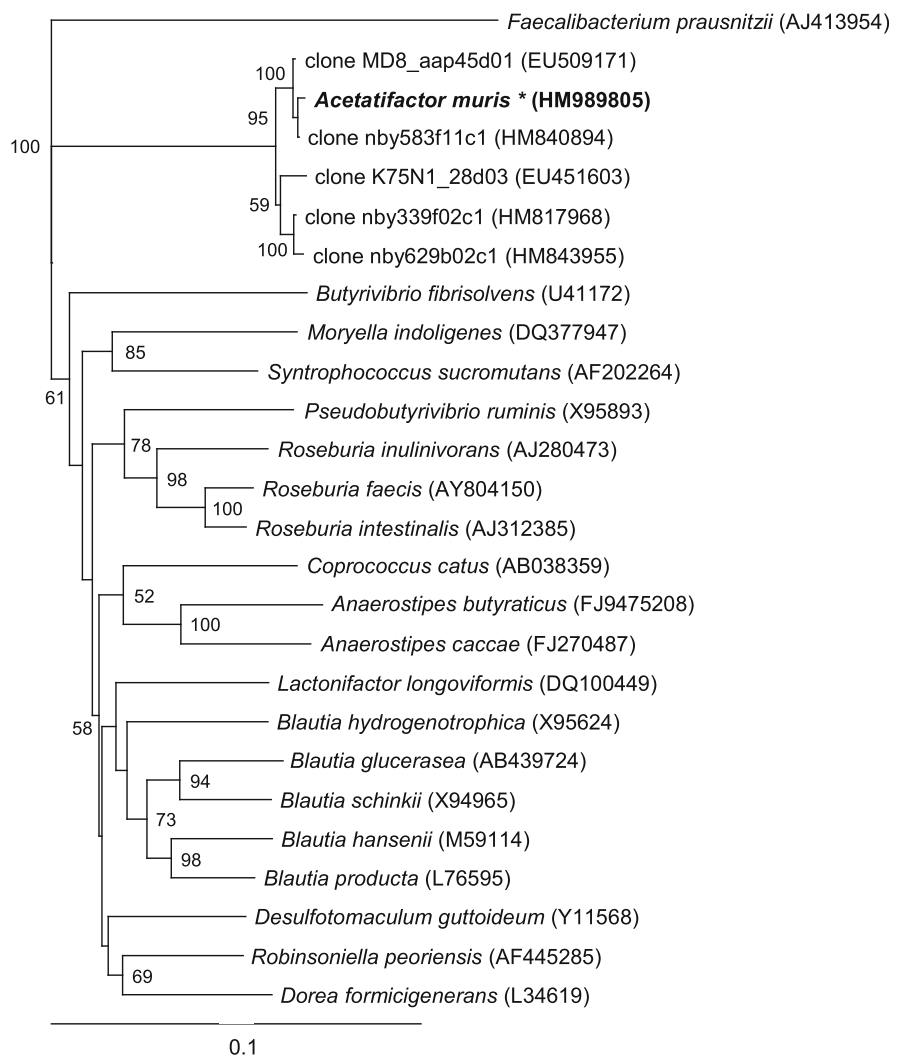
Isolation and identification of bacterial isolates

The density of caecal bacteria able to grow on CBS agar containing cholesterol and bile salts tended to be higher in mice fed the CT diet. Counts were 5.4 ± 1.0 versus $4.0 \pm 1.0 \log_{10}$ (CFU/g wet weight) for the CT and STD group, respectively ($p = 0.098$). Further description of CBS isolates is given in the Electronic Supplementary Material. On the selective CT agar, the number of colonies was too low (<10 per plate) to provide reliable counts. Representatives of each of the four types of colonies observed were picked and isolates ($n = 7$) were identified by 16S rRNA gene sequencing. Apart from members of the genera *Proteus* and *Enterococcus* and the species *Parabacteroides gordonii*, we found that one bacterium, strain CT-m2^T, isolated from CT diet-fed mouse no. 2, belonged to a novel taxon, based on phylogenetic and phenotypic evidence.

Genotypic characterization of strain CT-m2^T

Phylogenetic analysis based on partial 16S rRNA gene sequencing showed that the new isolate is a member of the order *Clostridiales* (Fig. 1 and Suppl. Fig. S1). Indeed, strain CT-m2^T was very distantly related to bacteria from classes other than *Clostridia* within the *Firmicutes*, namely *Bacilli* (e.g. enterococci and lactobacilli), *Erysipelotrichi* (*Clostridium cylindroides*, *Clostridium ramosum* and related species), *Negativicutes* (e.g. *Clostridium quercicolum* and *Veillonella parvula*) and *Thermolithobacteria* (e.g. *Thermolithobacter ferrireducens*). Moreover, the new strain fell into the *Clostridium* cluster XIV, as defined by Collins et al. (Collins et al. 1994), the members of which belong almost exclusively to the family *Clostridiaceae*, *Eubacteriaceae*, *Lachnospiraceae* and *Ruminococcaceae* within the *Clostridiales* (Rainey 2009a, b). According to BLAST analysis, the partial 16S rRNA gene sequence of strain CT-m2^T (1 376 bp) (HM989805) was ≥ 98 % similar to already published sequences of uncultured bacteria obtained from the mouse caecum, including lean mice

Fig. 1 Phylogenetic tree showing the position of strain CT-m2^T within members of the *Lachnospiraceae*. The GenBank accession numbers of the 16S rRNA gene sequences used to construct the tree are indicated in brackets. Sequences were aligned using the BioEdit software, and the rooted tree was constructed with Clustal X 2.0 using the neighbour-joining method with bootstrap values calculated from 1,000 trees. *Faecalibacterium prausnitzii*, a member of the family *Ruminococcaceae* within the *Clostridium* cluster IV, was used as outgroup to root the tree



(EU509171 and EU451603) (Wen et al. 2008) and from mouse skin samples (HM817968, HM840894 and HM843955) (Grice et al. 2010). The closest relatives of strain CT-m2^T (percentages of similarity between 88 and 90 %) with validly published names included *Anaerostipes caccae* (AB243985), *Bacteroides pectinophilus* (DQ497993), *Blautia producta* (X94966), *Butyrivibrio fibrisolvens* (U77341), *Clostridium aldenense* (DQ279736), *Clostridium celerecrescens* (X71848), *Clostridium sphenoides* (AB075772), *Coprococcus catus* (EU266552), *Dorea longicatena* (HQ259728), *Eubacterium plexicaudatum* (AF157058), *Desulfotomaculum guttoideum* (NR_026409), *Roseburia intestinalis* (AJ312386), *Ruminococcus gnavus* (X94967) and *Syntrophococcus sucromutans* (AF202264). Furthermore, local BLAST search against a set of 16 528

16S rRNA gene sequences (300–500 bp) from the caecum of five wild-type C57BL/6 mice (Werner et al. 2011) suggests that the novel bacterium is a subdominant member of mouse caecal microbiota, that is, we did not find any full-length hit corresponding to the sequence of strain CT-m2^T. The isolate's G + C content of DNA is 48.5 mol %, which differs substantially from the G + C content of some members of phylogenetically related genera, including *Blautia* spp. (37–47 mol %), *Butyrivibrio fibrisolvens* (42 mol %), *Clostridium butyricum* (28 mol %), *Clostridium celerecrescens* (38 mol %), *Coprococcus catus* (39 to 41 mol %), *Desulfotomaculum guttoideum* (54 mol %), *Dorea* spp. (40–46 mol %), *Eubacterium ramulus* (39 mol %), *Roseburia intestinalis* (29–31 mol %) and *Ruminococcus hansenii* (38 mol %).

Phenotypic characterization of strain CT-m2^T

Strain CT-m2^T formed long and thin straight rods occurring as single cells, in pairs or small chains. Cells stained Gram-variable, yet the KOH test was negative, which is consistent with a Gram-positive cell wall. Taking into account that strain CT-m2^T belongs to the *Firmicutes*, the presence of *meso*-diaminopimelic acid as a diagnostic component of the peptidoglycan suggested that strain CT-m2^T is characterized by the peptidoglycan type A1 γ . Enzymatic tests using the rapid ID 32 A and VITEK[®] system showed that strain CT-m2^T was positive for α -arabinosidase, α -fucosidase, α - and β -galactosidase, α -glucosidase, N-acetyl-glucosaminidase, phenylalanine arylamidase as well as arabinose and xylose metabolism. Whole-cell sugars were glucose, ribose, galactose and traces of xylose. Polar lipids in strain CT-m2^T included diphosphatidylglycerol, phosphatidylglycerol, phosphatidylethanolamine, phosphoglycolipid and one each aminolipid and aminoglycolipid (Suppl. Fig. S2). The cellular fatty acid composition of cells grown for 72 h in reduced WCA under anaerobic conditions was (% total fatty acids): C_{10:0} (2.4 %), C_{11:0 DMA} (2.3 %), C_{12:0} (2.6 %), C_{14:0} (48.7 %), C_{14:0 DMA} (14.6 %), C_{16:0} (8.8 %), C_{17:0 DMA} (2.5 %), C_{18:0} (5.2 %), C_{18:1 w9c} (5.2 %), C_{18:1 w9c DMA} (4.5 %) and unidentified CFA (3.3 %). Strain CT-m2^T grew best at 30–37 °C between pH 7.0 and 8.0 in reduced WCA broth under anaerobic conditions (100 % N₂). Growth was

not inhibited by erythromycin up to ca. 200 μ g/ml. Spores have not been observed, and cells did not survive heat treatment under anoxic conditions (60 °C, 20 min and 70 °C, 10 min). After 72 h of growth in reduced WCA, strain CT-m2^T produced acetate (1 370 \pm 290 μ mol/l medium), butyrate (530 \pm 30 μ mol/l) and trace amounts of propionate (<70 \pm 50 μ mol/l) (n = 2 independent cultures). Valerate and isovalerate were not detected. So far, approximately 20 butyrate-producing bacteria have been isolated from gut samples and many of them belong to the *Clostridium* cluster XIV (Duncan et al. 2004; Louis and Flint 2009; Eeckhaut et al. 2010). The fact that most of these bacteria produce high concentrations of butyrate (>10 mM) when compared with strain CT-m2^T is likely due to the slow growth rate of our isolate or to the absence of intermediate substrates (*e.g.* acetate or lactate) in the reduced WCA broth originally used to assess butyrate production (Pacaud et al. 1986; Duncan et al. 2004). Addition of arabinose (4 mM), xylose (10 mM), lithium lactate (10 mM) and sodium acetate (10 mM) to the medium did not markedly increase turbidity and butyrate production (680 \pm 30 μ mol/l) after 72 h of growth.

Based on these phenotypic and genotypic data, it is proposed that strain CT-m2^T be designated the type species of a novel bacterial genus, namely *Acetatifactor muris*, and that it belongs to the *Lachnospiraceae* within the *Clostridiales* (Rainey 2009a). Parameters that distinguish the isolate from related taxa are given in Table 1.

Table 1 Characteristics of strain CT-m2^T and phylogenetically related species

	1	2	3	4	5	6	7	8
Origin	Mouse caecum	Dog faeces	Cow rumen	Cow manure	Human faeces	Swine manure	Human faeces	Human faeces
Gram type	Positive	Positive	Negative	Positive	Positive	Positive	Positive	Positive
Motility	–	–	+	+	–	–	+	–
Spore formation	–	+	–	+	n.r.	+	–	–
Major CFA	C _{14:0}	C _{16:0 DMA}	C _{16:0}	n.r.	n.r.	C _{16:0}	n.r.	C _{16:0}
α -arabinosidase	+	n.r.	–	n.r.	n.r.	+	n.r.	n.r.
α -glucosidase	+	–	n.r.	n.r.	n.r.	+	n.r.	n.r.
Phe arylamidase	+	n.r.	–	n.r.	n.r.	–	–	n.r.
Arabinose	+	+	+	+	–	+	+	+
Glucose	–	+	+	+	+	+	+	+
Raffinose	–	+	–	+	–	+	+	+
Xylose	+	+	+	+	–	+	+	+
Butyrate	+	–	+	+	+	–	+	–
G + C (mol %)	48.5	40.7	42.1	38.0	39–41	48.7	29–31	43

Taxa: 1, *Acetatifactor muris*; 2, *Blautia glucerasea* (Furuya et al. 2010); 3, *Butyrivibrio fibrisolvans* (Kopečný et al. 2003); 4, *Clostridium celerecrescens* (Palop et al. 1989); 5, *Coprococcus catus* (Holdeman and Moore 1974); 6, *Robinsoniella peoriensis* (Cotta et al. 2009); 7, *Roseburia intestinalis* (Duncan et al. 2002); 8, *Ruminococcus gnavus* (Moore et al. 1976)

Symbols and abbreviations: +, positive reaction; –, negative reaction; CFA cellular fatty acid; n.r. not reported, Phe phenylalanine. Carbohydrate utilization by strain CT-m2^T was tested using the rapid ID 32A test and with ANI cards using the VITEK[®] system following the manufacturer's instructions (Biomérieux, Marcy-l'Étoile, France)

Description of *Acetatifactor* gen. nov.

(A.ce.ta.ti.fac'tor. N.L. n. *acetas -atis*, acetate; L. masc. n. *factor*, a maker; N.L. masc. n. *Acetatifactor*, acetate-maker).

Bacteria of the genus *Acetatifactor* are strictly anaerobic Gram-positive rods that grow best in a gas phase of 100 % N₂ and produce acetate and butyrate in a ratio of approximately 3:1. Cultures in the stationary growth phase are characterized by a very low turbidity in reduced WCA broth (<0.5 McFarland standard). Spore formation and motility have not been observed. Major cellular fatty acids are C_{14:0} and C_{14:0} DMA. Galactose, glucose, ribose and traces of xylose are detected as whole-cell sugars. The diamino acid in the peptidoglycan is *meso*-diaminopimelic acid. Major polar lipids are diphosphatidylglycerol, phosphatidylglycerol, phosphatidylethanolamine, phosphoglycolipid and one each aminolipid and aminoglycolipid. Within the *Clostridiales*, members of the genus *Acetatifactor* are distantly related to bacteria belonging to the *Clostridium* cluster XIV, namely members of the genera *Anaerostipes*, *Blautia*, *Butyrivibrio*, *Clostridium*, *Coproccoccus*, *Dorea*, *Eubacterium*, *Lactonifactor*, *Robinsoniella*, *Roseburia*, *Ruminococcus* and *Syntrophococcus* (≤90 % similarity based on partial 16S rRNA gene sequence analysis). The type species is *Acetatifactor muris*.

Description of *Acetatifactor muris* gen. nov., sp. nov.

(mu'ris. L. gen. n. *muris*, of a mouse).

The species has the features of the genus. Cells are approximately 1.0 μm wide and 2.0 to 5.0 μm long. They grow best in the temperature range from 30 to 37 °C and give rise to pinpoint translucent colonies after 6 days of growth on CT agar. The species is positive for α-arabinosidase, α-fucosidase, α- and β-galactosidase, α-glucosidase, N-acetyl-glucosaminidase, phenylalanine arylamidase as well as arabinose and xylose fermentation. It is negative for β-fucosidase, β-glucosidase, β-glucuronidase, β-lactosidase, alanine, arginine, glutamic acid, glycine, histidine, leucyl glycine, lysine, proline, serine, tryptophan and tyrosine arylamidase, urea hydrolysis as well as glucose, mannose, raffinose and trehalose fermentation. Its G + C content of DNA is 48.5 mol %. The type strain (CT-m2^T = DSM 23669^T = ATCC BAA-2170^T) is resistant to erythromycin and was isolated from the caecal content of a 20-week-old male C57BL/6NcrJ mouse fed a high calorie diet.

Acknowledgments We are grateful to Nico Gebhardt, Melanie Klein, Katharina Rank (TU München) and Sabine Schmidt (DIfE) for excellent technical assistance, to Jean P. Euzéby (Ecole Nationale Vétérinaire, Toulouse, France) for helping with Latin bacterial names and to staff members of the DSMZ for carrying out descriptive

analysis of the isolate. C.D. was financed by the EU FP6 project Nutrient Sensing in Satiety Control and Obesity (NuSISCO, Grant no. MEST-CT-2005-020494).

References

- Alain K, Querellou J (2009) Cultivating the uncultured: limits, advances and future challenges. *Extremophiles* 13:583–594
- Altschul SF, Gish W, Miller W, Myers EW, Lipman DJ (1990) Basic local alignment search tool. *J Mol Biol* 215:403–410
- Attebery HR, Finegold SM (1969) Combined screw-cap and rubber-stopper closure for Hungate tubes (pre-reduced anaerobically sterilized roll tubes and liquid media). *Appl Microbiol* 18:558–561
- Clavel T, Henderson G, Engst W, Dore J, Blaut M (2006) Phylogeny of human intestinal bacteria that activate the dietary lignan secoisolariciresinol diglucoside. *FEMS Microbiol Ecol* 55:471–478
- Clavel T, Charrier C, Braune A, Wenning M, Blaut M, Haller D (2009) Isolation of bacteria from the ileal mucosa of TNF^{delta}ARE mice and description of *Enterorhabdus mucosicola* gen. nov., sp. nov. *Int J Syst Evol Microbiol* 59:1805–1812
- Clavel T, Saalfrank A, Charrier C, Haller D (2010) Isolation of bacteria from mouse caecal samples and description of *Bacteroides sartorii* sp. nov. *Arch Microbiol* 192:427–435
- Collins MD, Lawson PA, Willems A, Cordoba JJ, Fernandez-Garayzabal J, Garcia P, Cai J, Hippe H, Farrow JA (1994) The phylogeny of the genus *Clostridium*: proposal of five new genera and eleven new species combinations. *Int J Syst Bacteriol* 44:812–826
- Cotta MA, Whitehead TR, Falsen E, Moore E, Lawson PA (2009) *Robinsoniella peoriensis* gen. nov., sp. nov., isolated from a swine-manure storage pit and a human clinical source. *Int J Syst Evol Microbiol* 59:150–155
- DeSantis TZ, Hugenholtz P, Larsen N, Rojas M, Brodie EL, Keller K, Huber T, Dalevi D, Hu P, Andersen GL (2006a) Greengenes, a chimera-checked 16S rRNA gene database and workbench compatible with ARB. *Appl Environ Microbiol* 72:5069–5072
- DeSantis TZ Jr, Hugenholtz P, Keller K, Brodie EL, Larsen N, Piceno YM, Phan R, Andersen GL (2006b) NAST: a multiple sequence alignment server for comparative analysis of 16S rRNA genes. *Nucleic Acids Res* 34:W394–W399
- Duncan SH, Hold GL, Barcenilla A, Stewart CS, Flint HJ (2002) *Roseburia intestinalis* sp. nov., a novel saccharolytic, butyrate-producing bacterium from human faeces. *Int J Syst Evol Microbiol* 52:1615–1620
- Duncan SH, Louis P, Flint HJ (2004) Lactate-utilizing bacteria, isolated from human feces, that produce butyrate as a major fermentation product. *Appl Environ Microbiol* 70:5810–5817
- Eeckhaut V, Van Immerseel F, Pasmans F, De Brandt E, Haesebrouck F, Ducatelle R, Vandamme P (2010) *Anaerostipes butyraticus* sp. nov., an anaerobic, butyrate-producing bacterium from *Clostridium* cluster XIVa isolated from broiler chicken caecal content, and emended description of the genus *Anaerostipes*. *Int J Syst Evol Microbiol* 60:1108–1112
- Fleissner CK, Huebel N, Abd El-Bary MM, Loh G, Klaus S, Blaut M (2010) Absence of intestinal microbiota does not protect mice from diet-induced obesity. *Br J Nutr* 104:919–929
- Furuya H, Ide Y, Hamamoto M, Asanuma N, Hino T (2010) Isolation of a novel bacterium, *Blautia glucerasesi* sp. nov., hydrolyzing plant glucosylceramide to ceramide. *Arch Microbiol* 192:365–372
- Goodman AL, Kallstrom G, Faith JJ, Reyes A, Moore A, Dantas G, Gordon JI (2011) Extensive personal human gut microbiota

- culture collections characterized and manipulated in gnotobiotic mice. *Proc Natl Acad Sci USA* 108:6252–6257
- Grice EA, Snitkin ES, Yockey LJ, Bermudez DM, Liechty KW, Segre JA (2010) Longitudinal shift in diabetic wound microbiota correlates with prolonged skin defense response. *Proc Natl Acad Sci USA* 107:14799–14804
- Hall TA (1999) Bioedit: a user-friendly biological sequence alignment editor and analysis program for Windows 95/98/NT. *Nuc Acids Symp Ser* 41:95–98
- Holdeman LV, Moore WEC (1974) New genus, *Coprococcus*, twelve new species, and emended descriptions of four previously described species of bacteria from human feces. *Int J Syst Bacteriol* 24:260–277
- Kageyama A, Benno Y, Nakase T (1999) Phylogenetic evidence for the transfer of *Eubacterium lentum* to the genus *Eggerthella* as *Eggerthella lenta* gen. nov., comb. nov. *Int J Syst Bacteriol* 49:1725–1732
- Kopecny J, Zorec M, Mrazek J, Kobayashi Y, Marinsek-Logar R (2003) *Butyrivibrio hungatei* sp. nov. and *Pseudobutyrvibrio xylanivorans* sp. nov., butyrate-producing bacteria from the rumen. *Int J Syst Evol Microbiol* 53:201–209
- Ley RE, Hamady M, Lozupone C, Turnbaugh PJ, Ramey RR, Birchler JS, Schlegel ML, Tucker TA, Schrenzel MD, Knight R, Gordon JI (2008) Evolution of mammals and their gut microbes. *Science* 320:1647–1651
- Louis P, Flint HJ (2009) Diversity, metabolism and microbial ecology of butyrate-producing bacteria from the human large intestine. *FEMS Microbiol Lett* 294:1–8
- Moore WEC, Johnson JL, Holdeman LV (1976) Emendation of *Bacteroidaceae* and *Butyrivibrio* and descriptions of *Desulfomonas* gen. nov. and ten new species in the genera *Desulfomonas*, *Butyrivibrio*, *Eubacterium*, *Clostridium* and *Ruminococcus*. *Int J Syst Bacteriol* 26:238–252
- Pacaud S, Loubiere P, Goma G, Lindley ND (1986) Organic acid production during methylotrophic growth of *Eubacterium limosum* B 2: displacement towards increased butyric acid yields by supplementing with acetate. *Appl Microbiol Biotechnol* 23:330–335
- Palop M, Valles S, Pinaga F, Flors A (1989) Isolation and characterization of an anaerobic, cellulolytic bacterium, *Clostridium celerecrescens* sp. nov. *Int J Syst Bacteriol* 39:68–71
- Rainey FA (2009a) Family V. *Lachnospiraceae* fam. nov. In: De Vos P, Garrity G, Jones D, Krieg NR, Ludwig W, Rainey FA, Schleifer K-H, Whitman WB (eds) *Bergey's manual of systematic bacteriology*, 2nd edn. Springer, New York, p 921
- Rainey FA (2009b) Family VIII. *Ruminococcaceae* fam. nov. In: De Vos P, Garrity G, Jones D, Krieg NR, Ludwig W, Rainey FA, Schleifer K-H, Whitman WB (eds) *Bergey's manual of systematic bacteriology*, 2nd edn. Springer, New York, p 1016
- Turnbaugh P, Ridaura V, Faith J, Rey F, Knight R, Gordon J (2009) The effect of diet on the human gut microbiome: a metagenomic analysis in humanized gnotobiotic mice. *Sci Trans Med* 1:6ra14
- Wen L, Ley RE, Volchkov PY, Stranges PB, Avanesyan L, Stonebraker AC, Hu C, Wong FS, Szot GL, Bluestone JA, Gordon JI, Chervonsky AV (2008) Innate immunity and intestinal microbiota in the development of Type 1 diabetes. *Nature* 455:1109–1113
- Werner T, Wagner SJ, Martinez I, Walter J, Chang JS, Clavel T, Kislung S, Schuemann K, Haller D (2011) Depletion of luminal iron alters the gut microbiota and prevents Crohn's disease-like ileitis. *Gut* 60:325–333
- Yarza P, Richter M, Peplies J, Euzéby J, Amann R, Schleifer KH, Ludwig W, Glockner FO, Rossello-Mora R (2008) The all-species living tree project: a 16S rRNA-based phylogenetic tree of all sequenced type strains. *Syst Appl Microbiol* 31:241–250

PAPER 4

Parvibacter caecicola gen. nov., sp. nov., a bacterium of the family *Coriobacteriaceae* isolated from the caecum of a mouse

Thomas Clavel,¹ Cédric Charrier,² Mareike Wenning³ and Dirk Haller¹

Correspondence

Thomas Clavel
thomas.clavel@tum.de

¹Biofunctionality Unit, ZIEL - Research Center for Nutrition and Food Sciences, TU München, Freising-Weihenstephan, Germany

²NovaBiotics Ltd, Aberdeen, AB21 9TR, United Kingdom

³Microbiology Unit, ZIEL - Research Center for Nutrition and Food Sciences, TU München, Freising-Weihenstephan, Germany

A single strain, NR06^T, was isolated from the intestine of a TNF^{deltaARE} mouse. Based on phylogenetic analysis of partial 16S rRNA gene sequences, strain NR06^T belongs in the family *Coriobacteriaceae* within the *Actinobacteria*. The most closely related species with validly published names are members of the genera *Adlercreutzia*, *Asaccharobacter* and *Enterorhabdus* (<96% sequence similarity). Strain NR06^T was characterized by a high prevalence of monomethylmenaquinone-6 (MMK-6; 76%) and the presence of *meso*-diaminopimelic acid in the cell wall. One of the major cellular fatty acids of strain NR06^T was C_{15:0} ISO. Glucose was detected as a whole cell sugar. Strain NR06^T was resistant to the antibiotic colistin and was positive for arginine and leucine arylamidase activity. Based on these characteristics, strain NR06^T differed from related described bacteria. Therefore, the name *Parvibacter caecicola* gen. nov., sp. nov. is proposed to accommodate the novel bacterium. The type strain of the type species is NR06^T (=DSM 22242^T=CCUG 57646^T).

The intestinal tract of mammals is host to one of the densest and most diverse microbial ecosystems on earth (Bäckhed *et al.*, 2005). Gut microbial ecosystems consist of fungi, protozoa, viruses, archaea and a tremendous variety of mostly anaerobic bacteria. Whereas diversity is limited at high taxonomic levels (only two bacterial phyla, the *Firmicutes* and the *Bacteroidetes*, usually cover >95% of total 16S rRNA gene sequence diversity in distal parts of the gut), the number of different species exceeds 1000 per host (Qin *et al.*, 2010). Until recently, one major drawback of bacteriological studies of intestinal ecosystems was the difficulty in culturing most bacterial species in laboratories. Over the last twenty years, advances in molecular approaches have brought light into this so-called uncultured majority (Lepage *et al.*, 2013). However, the rush on using new molecular tools in gut microbiology has led to the misleading assumption that culturing bacteria is not worth the effort. Goodman *et al.* recently reported that >60% of gut bacteria can actually be cultured *in vitro*

(Goodman *et al.*, 2011). The isolation of new bacteria is essential in as much as it allows further characterization of functions of interest (Alain & Querellou, 2009). Nevertheless, from an ecological point of view, it is clear that a pool of functions identified from cultivable strains is merely a proxy for community functions in the original environment (Ritz, 2007). In addition to *Firmicutes* and *Bacteroidetes*, a substantial number of mammalian gut bacteria belong to the *Proteobacteria* and *Actinobacteria*. The family *Coriobacteriaceae* within the *Actinobacteria* includes Gram-positive type cells of strictly anaerobic bacteria. At the time of writing, this family comprises only 29 species belonging to 13 genera; four of the genera have been described recently: *Adlercreutzia* (Maruo *et al.*, 2008), the type species of which was isolated from human faeces; *Asaccharobacter* (Minamida *et al.*, 2008), from a rat caecum; *Enterorhabdus* (Clavel *et al.*, 2009), from the inflamed ileal mucosa of a mouse; and *Gordonibacter* (Würdemann *et al.*, 2009), from the colon of a patient with Crohn's disease. With the exception of species of the genera *Atopobium*, *Collinsella*, *Eggerthella* and *Slackia*, members of the family *Coriobacteriaceae* seem to belong to subdominant populations in the intestinal tract of most human subjects and rodents. However, *Coriobacteriaceae* carry out functions of importance to their host such as polyphenol conversion (Maruo *et al.*, 2008; Clavel *et al.*, 2009; Matthies

Abbreviation: FT-IR, Fourier transform infrared.

The GenBank/EMBL/DDBJ accession numbers for the partial 16S rRNA and *gyrB* gene sequences of strain NR06^T are GQ456228 and GQ456226, respectively.

Four supplementary figures are available with the online version of this paper.

et al., 2012) as well as bile acid and hepatic lipid metabolism (Ridlon *et al.*, 2006; Claus *et al.*, 2011). Moreover, the occurrence of *Coriobacteriaceae* in the gut has been shown to depend upon host genotype (Benson *et al.*, 2010) and certain members have been described in the context of bacterial infections and intestinal inflammation (Lau *et al.*, 2004; Clavel *et al.*, 2009; Würdemann *et al.*, 2009; Clavel *et al.*, 2010). In that context, this study deals with the characterization of one bacterium isolated from the intestine of a mouse, which is proposed to belong to a novel genus within the family *Coriobacteriaceae*.

A caecal sample was collected from one male heterozygous TNF^{deltaARE} C57BL/6 mouse fed a standard chow diet (animal use was approved by the local institution in charge: animal welfare authorization 32-568, Freising District Office). The working area and dissection set were cleaned and the mouse was copiously sprayed with 70 % (v/v) ethanol prior to dissection. Bacteria were cultured using Wilkins-Chalgren Anaerobe (WCA) agar (Oxoid). After autoclaving, the medium was allowed to cool in a water bath (55 °C) and was supplemented with autoclaved rumen fluid and filter-sterilized aqueous solutions of cysteine and DTT to a final concentration of 1 % (v/v), 0.05 % and 0.02 % (w/v), respectively. All steps were carried out in a VA500 workstation (Don Whitley Scientific) containing 85 % (v/v) N₂, 10 % CO₂ and 5 % H₂. The atmosphere was kept at 37 °C and 75 % humidity and was tested for anaerobic conditions using Anaerotest (Merck, cat. no. 1.15112.0001). All materials, including agar media, were brought into the workstation 24 h prior to isolation. Dilution series of the caecal sample (100 µl) were plated onto WCA using sterile glass beads. All single colony morphology types observed after six days of growth at 37 °C were streaked onto WCA to ensure purity. Cells were then transferred into WCA broth prepared using strictly anaerobic culture techniques (100 % N₂) (Attebery & Finegold, 1969). Culture purity was examined by observing cell morphology after Gram-staining and colony morphology. DNA was extracted from washed bacterial cell pellets using the DNeasy Blood & Tissue kit (Qiagen), following the instructions for pre-treatment of Gram-positive bacteria. The 16S rRNA genes were amplified using primer 27F 5'-AGAGTTTGATCCTGGCTCAG-3' and 1492R 5'-GGTTACCTTGTACGACTT-3' (Kageyama *et al.*, 1999). The annealing temperature was 56 °C. Amplicons were purified using agarose gel electrophoresis and the Wizard SV Gel and PCR Clean-Up System (Promega) and sequenced at GATC Biotech AG (Konstanz, Germany) using primer 27F, 338F 5'-ACTCCTACGGGAGGAGCAGC-3', 609F 5'-GGATTAGATACCCBDGTA-3', 907F 5'-AAACTYAAA-KGAATTGACGG-3', 907R and 1492R. Sequences of organisms closely related to the isolated strains were obtained using the BLAST function of the NCBI server (Altschul *et al.*, 1990) and The All-Species Living Tree Project (Yarza *et al.*, 2008). All sequences were aligned using the BioEdit software, version 7.0.5.3 (Hall, 1999) and the greengenes web application (DeSantis *et al.*, 2006b; DeSantis *et al.*, 2006a). Percentages of similarity were calculated after unambiguous

alignment of each isolated sequence with those of the most closely related species, using the DNA Distance Matrix function of the BioEdit software.

The partial 16S rRNA gene sequence obtained from one of the isolates, strain NR06^T, did not appear to correspond to any currently described organism. Detailed phylogenetic analysis revealed that this strain belonged to the family *Coriobacteriaceae* (Fig. 1). Sequences were aligned using the BioEdit software and the rooted tree was constructed using the Neighbour-Joining method (Saitou & Nei, 1987) in MEGA5 (Tamura *et al.*, 2011). All major groupings were confirmed using the maximum-parsimony (Fig. S1, available in IJSEM Online) and the maximum-likelihood (Fig. S2) methods. The 16S rRNA gene sequence of strain NR06^T (1442 bp) (GenBank accession no. GQ456228) was characterized by the following percentages of similarity when compared with sequences available in public databases: >99 %, uncultured bacteria from the human and mouse intestine (GenBank accession no. EF099602; AM276097) (Turnbaugh *et al.*, 2006; Kassinen *et al.*, 2007); <96 %, *Adlercreutzia equolifaciens* DSM 19450^T (AB306661), *Asaccharobacter celatus* DSM 18785^T (AB266102), *Enterorhabdus caecimuris* DSM 21839^T (DQ789120) and *Enterorhabdus mucosicola* DSM 19490^T (AM747811); <93 %, *Eggerthella lenta* DSM 2243^T (AF292375) and *Eggerthella sinensis* DSM 16107^T (AY321958). Thus, considering genus-specific phylogenetic distances (Fig. 1) and similarity values of approximately 95 % (Rosselló-Mora & Amann, 2001), it was assumed that strain NR06^T did not belong to the genera *Adlercreutzia*, *Asaccharobacter*, *Eggerthella* and *Enterorhabdus*. Local BLAST analysis against partial 16S rRNA gene sequences (V1–V3 region) previously obtained from the caecum of five wild-type ($n=16\,528$ sequences) and five heterozygous TNF^{deltaARE} ($n=18\,379$ sequences) C57BL/6 mice (Werner *et al.*, 2011) suggested that strain NR06^T is a subdominant member of mouse caecal microbiota, i.e. no sequences matching that of strain NR06^T were found. Nevertheless, we cannot exclude that strain NR06^T and relatives belong to dominant communities in specific niches in the gut. The phylogenetic distances described above were confirmed by sequencing *gyrB* genes. These genes were amplified as described previously (Santos & Ochman, 2004). Amplicons (approx. 1500 bp) were purified as described above for 16S rRNA genes and sequenced using primer *gyrBBNDN1* 5'-CCGTCCACGTCGGCRTCNGYCAT-3' and *gyrBBAUP2* 5'-GCGGAAGCGCCNGSNATGTA-3'. Based on the analysis of 524 bp, the *gyrB* gene sequence of strain NR06^T (GenBank accession no. GQ456226) was ≤80 % similar to that of *Eggerthella lenta* DSM 2243^T (EU594342), *Enterorhabdus caecimuris* DSM 21839^T (GQ409830) and *Enterorhabdus mucosicola* DSM 19490^T (EU594341). The phylogenetic position of strain NR06^T amongst members of the family *Coriobacteriaceae*, for which *GyrB* amino acid sequences are available, is shown in Fig. S3.

In order to assess differences between strain NR06^T and its closest relatives at the whole cell biochemical level, cell suspensions were analysed using Fourier transform infrared

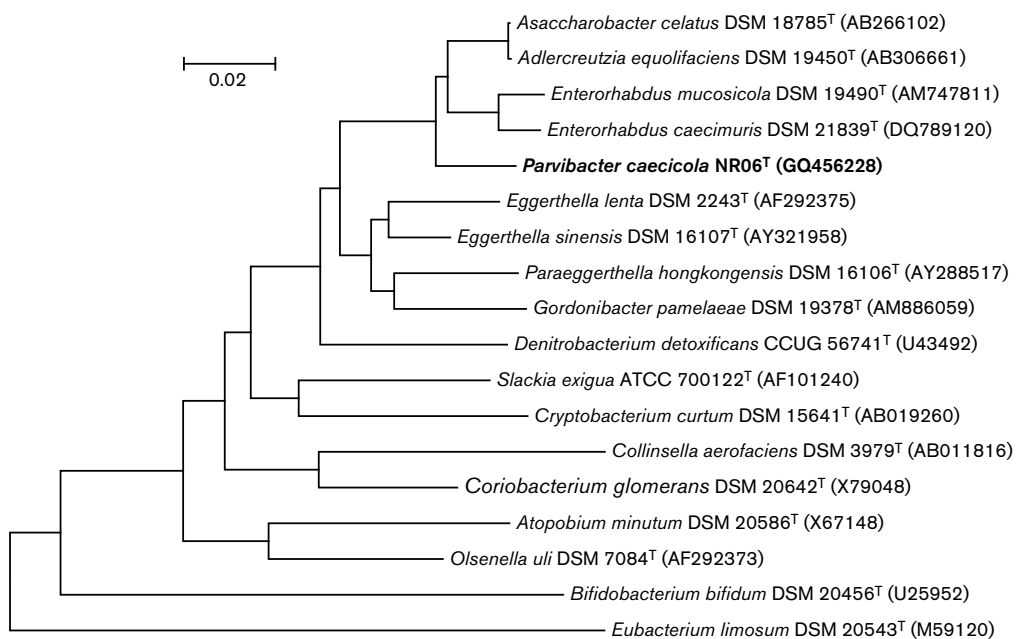


Fig. 1. Phylogenetic position of strain NR06^T within the family *Coriobacteriaceae*. The accession numbers of the 16S rRNA gene sequences (1442 bp) used to construct the tree are indicated in parentheses. *Eubacterium limosum* DSM 20543^T, a member of the phylum *Firmicutes*, was used to root the tree. Bar, 2 nt changes per 100 nt.

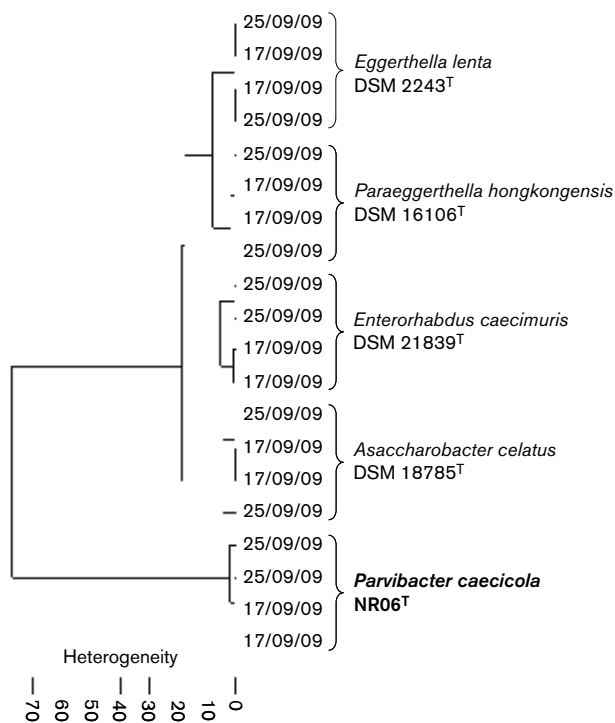


Fig. 2. Chemotaxonomic position of strain NR06^T according to cluster analysis of FT-IR spectra. For each strain, spectra from independent cultures measured at different time points were more similar to one another than to spectra from other species, attesting to the robustness of the observed spectral variations between taxa.

Table 1. Antimicrobial resistance and cellular fatty acid pattern of strain NR06^T and closely related members of the family *Coriobacteriaceae*

Strain: 1, NR06^T; 2, *Enterorhabdus caecimuris* DSM 21839^T; 3, *Enterorhabdus mucosicola* DSM 19490^T; 4, *Adlercreutzia equolifaciens* DSM 18785^T; 5, *Asaccharobacter celatus* DSM 19450^T. Major discriminative features of strain NR06^T are in bold type. ND, Not determined; R, resistant; –, not detected.

Character	1	2	3	4	5
Antibiotic* (MIC, µg ml⁻¹)					
Cefotaxime	4.167 (±0.654)	>32 (R)	1.250 (±0.112)	ND	ND
Ciprofloxacin	0.061 (±0.008)	0.305 (±0.035)	>32 (R)	ND	ND
Clarithromycin	<0.016	<0.016	<0.016	ND	ND
Clindamycin	<0.016	0.105 (±0.010)	<0.016	ND	ND
Colistin	>256 (R)	ND	>256 (R)	ND	ND
Erythromycin	<0.016	<0.016	0.048 (±0.007)	ND	ND
Metronidazole	0.069 (±0.017)	0.016 (±0.000)	0.034 (±0.004)	ND	ND
Oxacillin	6.000 (±1.000)	36.000 (±5.750)	4.667 (±0.667)	ND	ND
Tetracycline	0.069 (±0.005)	0.120 (±0.005)	0.115 (±0.007)	ND	ND
Tobramycin	0.600 (±0.056)	4.333 (±0.558)	2.667 (±0.211)	ND	ND
Vancomycin	0.585 (±0.076)	1.500 (±0.129)	1.333 (±0.105)	ND	ND
Cellular fatty acids†					
12:0	0.25	1.21	0.72	–	–
12:0 ISO	–	0.36	0.50	–	–
13:0 ISO	0.35	–	0.15	–	–
13:0 ANTEISO	0.23	0.43	0.49	–	–
13:1 CIS 12	–	0.29	0.17	–	–
14:0	6.70	15.08	12.11	–	–
14:0 ISO	0.78	3.83	2.48	2.8	–
14:0 DMA	0.36	0.68	0.41	–	–
15:0	2.06	1.77	1.60	–	–
15:0 ISO	10.67	1.20	1.16	–	–
15:0 ANTEISO	2.46	2.82	2.29	3.8	–
15:0 DMA	0.23	0.40	0.42	–	–
15:0 ISO DMA	0.24	–	–	–	–
16:0 ALDE	1.16	2.28	2.31	2.8	–
16:0	25.53	19.14	18.06	11.4	8.4
16:0 ISO	0.22	0.52	0.42	–	–
16:0 DMA	6.78	9.62	11.56	11.4	–
16:1 CIS 9	0.46	0.94	0.93	–	–
17:0 ANTEISO	0.52	0.82	0.75	–	–
17:0	2.01	0.87	–	–	–
17:0 ISO	1.58	–	–	–	–
17:0 DMA	0.31	–	0.20	–	–
17:0 ANTEISO DMA	–	–	0.19	–	–
17:1 CIS 8	–	1.16	0.52	–	–
17:1 CIS 9	–	–	0.41	–	–
17:2	0.83	–	–	–	–
18:0	8.57	7.99	9.35	11.4	11.7
18:0 ALDE	–	–	1.16	3.6	–
18:0 DMA	3.77	2.40	3.73	18.5	–
18:1 CIS 9	10.17	15.25	16.68	24.1	54.0
18:1 CIS 9 DMA	4.06	4.94	4.75	7.8	–
18:1 CIS 11 DMA	–	0.59	0.56	–	–
18:1c11/t9/t6	1.68	4.16	3.83	–	–
18:1 t11	7.05	–	0.80	–	–
18:2 CIS 9,12	0.97	1.24	1.30	–	–

*The MIC breakpoint is expressed as mean ± standard error (n=6).

†The CFA pattern of strain NR06^T, *Enterorhabdus caecimuris* DSM 21839^T and *Enterorhabdus mucosicola* DSM 19490^T were determined at the DSMZ. Peaks were analysed using the BHIBLA method. Cell biomass was obtained after batch culture (1.5 l) under anoxic conditions for 48 h in reduced WCA broth. The CFA pattern of *Enterorhabdus caecimuris* DSM 18785^T and *Enterorhabdus mucosicola* DSM 19450^T are as published elsewhere (Maruo *et al.*, 2008; Minamida *et al.*, 2008).

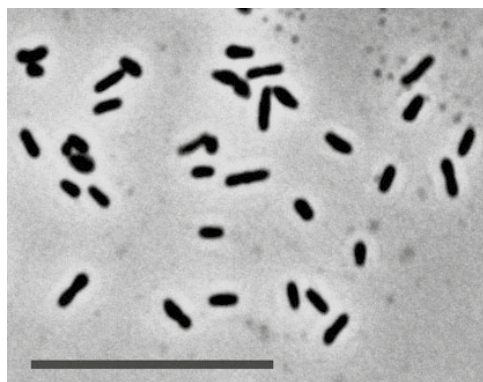


Fig. 3. Phase-contrast micrograph of strain NR06^T grown for 24 h in reduced WCA broth. Bar, 10 μ m.

(FT-IR) spectroscopy. FT-IR spectroscopy relies on the absorption of IR radiation by cell components, which results in fingerprint-like spectra that reflect chemical cellular composition, allowing identification of closely related bacteria (Wenning *et al.*, 2008). Pure cultures were prepared as previously described (Clavel *et al.*, 2009). Suspensions were pipetted onto a zinc/selenide 96-well-plate, allowed to dry (20 min, 45 °C) and analysed by transmission using a TENSOR 27 spectrometer coupled with a HTS-XT high throughput device (Bruker Optics). The spectrum of each sample was computed from 32 scans. Spectral similarities were assessed by hierarchical cluster analysis using the OPUS software version 6.5 (Bruker). Clusters were calculated using the Ward's algorithm and vector normalized first derivatives (Savitzky-Golay algorithm) of the spectra in the range from 3000 to 2800 cm^{-1} and 1800 to 700 cm^{-1} . FT-IR spectra of

strain NR06^T differed markedly from that of members of related genera, including *Asaccharobacter* and *Enterorhabdus*, indicating substantial differences in the overall chemical make-up of cells (Fig. 2). Additional chemotaxonomic analysis of strain NR06^T included analysis of the peptidoglycan, menaquinones, cellular fatty acids, whole cell sugars and polar lipids. These analyses were performed at the Identification Service of the German Collection of Microorganisms and Cell Cultures (DSMZ, Braunschweig, Germany). Biomass for these analyses was obtained after batch culture (1.5 l) under anoxic conditions for 48 h in reduced WCA broth. Cells were washed once in PBS (5525 g, 15 min, RT) and stored at -20 °C prior to shipment. In contrast to *Adlercreutzia equolifaciens* DSM 18785^T or *Asaccharobacter celatus* DSM 19450^T, the main respiratory quinone in strain NR06^T was monomethylmenaquinone-6 (MMK-6; 76 %) and not dimethylmenaquinone-6 (DMMK-6; 24 %) or an unidentified quinone. The cellular fatty acid composition of strain NR06^T is shown in Table 1. In contrast to members of closely related genera (*Enterorhabdus*, *Asaccharobacter* and *Adlercreutzia*), the main cellular fatty acids in strain were C_{16:0} (26 % total fatty acids) and C_{15:0} ISO (11 %). The polar lipid pattern of strain NR06^T also differed substantially from that of members of the genus *Enterorhabdus* (Fig. S4). Lipids were extracted from freeze-dried cells using a chloroform : methanol : 0.3 % aqueous NaCl mixture modified after Bligh & Dyer (1959) and analysed by 2-dimensional thin layer chromatography (Tindall *et al.*, 2007). Polar lipids in strain NR06^T were phosphatidylglycerol, diphosphatidylglycerol, three phospholipids, four glycolipids and one unidentified lipid. Taking into account that strain NR06^T belongs to the family *Coriobacteriaceae*, the presence of *meso*-diaminopimelic acid as a diagnostic component of the peptidoglycan suggested that strain NR06^T is characterized by the peptidoglycan type A1 γ (the variations of peptidoglycan type A4 γ based on *meso*-diaminopimelic acid have been found

Table 2. Traits that differentiate strain NR06^T from related members of the family *Coriobacteriaceae*

Strain: 1, NR06^T; 2, *Enterorhabdus caecimuris* DSM 21839^T; 3, *Enterorhabdus mucosicola* DSM 19490^T; 4, *Asaccharobacter celatus* DSM 18785^T; 5, *Adlercreutzia equolifaciens* DSM 19450^T. +, Positive; -, negative; ND, not determined.

Characteristic	1	2	3	4	5
Source of isolation	Mouse caecum	Mouse caecum	Mouse ileal mucosa	Rat caecum	Human faeces
Diaminopimelic acid*	<i>meso</i>	<i>meso</i>	LL	<i>meso</i>	<i>meso</i>
Major menaquinones*	MMK-6 (76 %), DMMK-6 (24 %)	MMK-6 (60 %), DMMK-6 (40 %)	MMK-6 (100 %)	unknown	MMK-6 (1–29 %), DMMK-6 (70–96 %)
Whole cell sugars*					
Glucose	+	+	-	ND	ND
Rapid ID 32 A tests:					
Arginine arylamidase	+	-	-	ND	+
Leucine arylamidase	+	-	+	-	+
Glutamic acid decarboxylase	-	+	-	ND	ND
Major cellular fatty acids*	C _{16:0} , C _{15:0} ISO, C _{18:1} CIS 9	C _{16:0} , C _{14:0} , C _{18:1} CIS 9	C _{16:0} , C _{14:0} , C _{18:1} CIS 9	C _{18:1} CIS 9	C _{18:1} CIS 9, C _{18:0} DMA, C _{16:0}

*Analysed by the Identification Service of the DSMZ (Braunschweig, Germany).

so far exclusively in members of the genera *Brachy bacterium* and *Dermabacter*). Ribose, galactose and glucose were detected as whole cell sugars in cells of strain NR06^T.

For phenotypic characterization, all tests were performed as described previously, e.g. growth characteristics, motility, spore formation, antibiotic resistance and enzymic tests (Clavel *et al.*, 2007; Clavel *et al.*, 2009). Microscopic observation revealed that strain NR06^T grew as single small straight rods (Fig. 3). Results of the rapid ID 32 A, API 20A and Biolog tests are listed in the species description. The susceptibility of the isolate towards eleven antimicrobial substances was tested. Each antibiotic was tested in duplicate in three independent experiments and MIC breakpoints ($\mu\text{g ml}^{-1}$) were expressed as means \pm standard errors of those six replicates. Results are summarized in Table 1. Strain NR06^T was resistant to colistin. The G + C content of DNA of strain NR06^T was 62.5 mol%, as determined by HPLC at the DSMZ according to standard methods (Cashion *et al.*, 1977; Tamaoka & Komagata 1984; Mesbah *et al.*, 1989). This is in the range of values usually reported in the literature for closely related members of the family *Coriobacteriaceae* (56–67 mol%).

Based on these chemotaxonomic, genotypic and phenotypic analyses, strain NR06^T represents a novel species in a new genus of the family *Coriobacteriaceae*, for which the name *Parvibacter caecicola* gen. nov., sp. nov. is proposed. Traits that distinguish strain NR06^T from related species are given in Table 2.

Description of *Parvibacter* gen. nov.

Parvibacter (Par.vi.bac^{ter}. L. adj. *parvus* small; N.L. masc. n. *bacter* rod; N.L. masc. n. *Parvibacter* small rod).

Cells are aerotolerant Gram-positive rods that grow only under strictly anoxic conditions. Cultures in the stationary phase of growth are characterized by a typically low turbidity (≤ 0.5 McFarland standard). Spore formation and motility have not been observed. Major cellular fatty acids are C_{16:0} and C_{15:0} ISO. Galactose, glucose and ribose are detected as whole cell sugars. The principal respiratory quinone is MMK-6. The diamino acid in the peptidoglycan is *meso*-diaminopimelic acid. The major polar lipids are diphosphatidylglycerol, phosphatidylglycerol, three phospholipids, four glycolipids and one unidentified lipid. The genus *Parvibacter* belongs to the family *Coriobacteriaceae* and is distantly related to the genera *Adlercreutzia*, *Asaccharobacter* and *Enterorhabdus* ($\leq 95\%$ similarity based on partial 16S rRNA gene sequence analysis). The type species is *Parvibacter caecicola*.

Description of *Parvibacter caecicola* sp. nov.

Parvibacter caecicola [ca.e.ci^{co}.la. N.L. n. *caecum* (from *L. caecum intestinum* caecum) caecum; L. suff. *-cola* (from *L. n. incola* dweller, inhabitant; N.L. n. *caecicola* caecum-dweller].

The species shows the following characteristics in addition to the aforementioned features of the genus. Cells are approximately $0.5 \times 1.5 \mu\text{m}$. Grows well in the temperature range of 25–37 °C. After 48 h of growth at 37 °C on WCA agar under anoxic conditions, colonies are circular, entire, pinpoint and grey. In the rapid ID 32 A test, positive result only for hydrolysis of the amino acid derivatives proline, phenylalanine, leucine, tyrosine, alanine, glycine and serine arylamidase. Negative result for urease activity, arginine dihydrolase, α - and β -galactosidase, α - and β -glucosidase, α -arabinosidase, β -glucuronidase, β -*N*-acetylglucosamine, mannose and raffinose fermentation, glutamic acid decarboxylase, α -fucosidase, nitrate reduction, indole production, alkaline phosphatase, as well as arginine, leucylglycine, pyroglutamic acid, histidine and glutamyl glutamic acid arylamidase. In the Biolog test, positive result for L-fucose, palatinose, α -hydroxybutyric acid, DL-lactic acid, D-lactic acid methyl ester, D-malic acid, pyruvic acid, pyruvic acid methyl ester, m-tartaric acid, L-methionine, L-phenylalanine and L-valine. Negative result for all additional substrates in the Biolog plate and for all reactions in the API 20A test. The type strain (NR06^T) is resistant to colistin.

The type strain, NR06^T (=DSM 22242^T =CCUG 57646^T), was isolated from the caecal content of a 25-week-old male heterozygous TNF^{deltaARE} C57BL/6 mouse suffering from ileitis. The DNA G + C content of the type strain is 62.5 %.

Acknowledgements

The heterozygous TNF^{deltaARE} mouse model of ileitis was a generous gift from Dr George Kollias (Biomedical Sciences Research Center Alexander Fleming, Vari, Greece). We are grateful to Nico Gebhardt, Melanie Klein, Silvia Pitariu and Caroline Ziegler (TUM, BFLM) for excellent technical assistance, Professor Euzéby (Ecole Nationale Vétérinaire, Toulouse, France) for suggesting the Latin bacterial names, Dr Herbert Seiler (TUM, Microbiology) for microscopic analysis and staff members of the DSMZ and the Culture Collection University of Göteborg (CCUG) for contributing to the description of strain NR06^T.

References

- Alain, K. & Querellou, J. (2009). Cultivating the uncultured: limits, advances and future challenges. *Extremophiles* **13**, 583–594.
- Altschul, S. F., Gish, W., Miller, W., Myers, E. W. & Lipman, D. J. (1990). Basic local alignment search tool. *J Mol Biol* **215**, 403–410.
- Attebery, H. R. & Finegold, S. M. (1969). Combined screw-cap and rubber-stopper closure for Hungate tubes (pre-reduced anaerobically sterilized roll tubes and liquid media). *Appl Microbiol* **18**, 558–561.
- Bäckhed, F., Ley, R. E., Sonnenburg, J. L., Peterson, D. A. & Gordon, J. I. (2005). Host-bacterial mutualism in the human intestine. *Science* **307**, 1915–1920.
- Benson, A. K., Kelly, S. A., Legge, R., Ma, F., Low, S. J., Kim, J., Zhang, M., Oh, P. L., Nehrenberg, D. & other authors (2010). Individuality in gut microbiota composition is a complex polygenic trait shaped by multiple environmental and host genetic factors. *Proc Natl Acad Sci U S A* **107**, 18933–18938.
- Bligh, E. G. & Dyer, W. J. (1959). A rapid method of total lipid extraction and purification. *Can J Biochem Physiol* **37**, 911–917.

- Cashion, P., Holder-Franklin, M. A., McCully, J. & Franklin, M. (1977). A rapid method for the base ratio determination of bacterial DNA. *Anal Biochem* **81**, 461–466.
- Claus, S. P., Ellero, S. L., Berger, B., Krause, L., Bruttin, A., Molina, J., Paris, A., Want, E. J., de Waziers, I. & other authors (2011). Colonization-induced host-gut microbial metabolic interaction. *mBio* **2**, e00271–10.
- Clavel, T., Lippman, R., Gavini, F., Doré, J. & Blaut, M. (2007). *Clostridium saccharogumia* sp. nov. and *Lactonifactor longoviformis* gen. nov., sp. nov., two novel human faecal bacteria involved in the conversion of the dietary phytoestrogen secoisolariciresinol diglucoside. *Syst Appl Microbiol* **30**, 16–26.
- Clavel, T., Charrier, C., Braune, A., Wenning, M., Blaut, M. & Haller, D. (2009). Isolation of bacteria from the ileal mucosa of TNFdeltaARE mice and description of *Enterorhabdus mucosicola* gen. nov., sp. nov. *Int J Syst Evol Microbiol* **59**, 1805–1812.
- Clavel, T., Duck, W., Charrier, C., Wenning, M., Elson, C. & Haller, D. (2010). *Enterorhabdus caecimuris* sp. nov., a member of the family *Coriobacteriaceae* isolated from a mouse model of spontaneous colitis, and emended description of the genus *Enterorhabdus* Clavel et al. 2009. *Int J Syst Evol Microbiol* **60**, 1527–1531.
- DeSantis, T. Z., Hugenholtz, P., Larsen, N., Rojas, M., Brodie, E. L., Keller, K., Huber, T., Dalevi, D., Hu, P. & Andersen, G. L. (2006a). Greengenes, a chimera-checked 16S rRNA gene database and workbench compatible with ARB. *Appl Environ Microbiol* **72**, 5069–5072.
- DeSantis, T. Z., Jr, Hugenholtz, P., Keller, K., Brodie, E. L., Larsen, N., Piceno, Y. M., Phan, R. & Andersen, G. L. (2006b). NAST: a multiple sequence alignment server for comparative analysis of 16S rRNA genes. *Nucleic Acids Res* **34** (Web Server issue,), W394–W399.
- Goodman, A. L., Kallstrom, G., Faith, J. J., Reyes, A., Moore, A., Dantas, G. & Gordon, J. I. (2011). Extensive personal human gut microbiota culture collections characterized and manipulated in gnotobiotic mice. *Proc Natl Acad Sci U S A* **108**, 6252–6257.
- Hall, T. A. (1999). BioEdit: a user-friendly biological sequence alignment editor and analysis program for Windows 95/98/NT. *Nucleic Acids Symp Ser* **41**, 95–98.
- Kageyama, A., Benno, Y. & Nakase, T. (1999). Phylogenetic evidence for the transfer of *Eubacterium lentum* to the genus *Eggerthella* as *Eggerthella lenta* gen. nov., comb. nov. *Int J Syst Bacteriol* **49**, 1725–1732.
- Kassinen, A., Krogius-Kurikka, L., Mäkivuokko, H., Rintilä, T., Paulin, L., Corander, J., Malinen, E., Apajalahti, J. & Palva, A. (2007). The fecal microbiota of irritable bowel syndrome patients differs significantly from that of healthy subjects. *Gastroenterology* **133**, 24–33.
- Lau, S. K., Woo, P. C., Woo, G. K., Fung, A. M., Wong, M. K., Chan, K. M., Tam, D. M. & Yuen, K. Y. (2004). *Eggerthella hongkongensis* sp. nov. and *Eggerthella sinensis* sp. nov., two novel *Eggerthella* species, account for half of the cases of *Eggerthella* bacteremia. *Diagn Microbiol Infect Dis* **49**, 255–263.
- Lepage, P., Leclerc, M. C., Joossens, M., Mondot, S., Blottiere, H. M., Raes, J., Ehrlich, D. & Dore, J. (2013). A metagenomic insight into our gut's microbiome. *Gut* **62**, 146–158.
- Maruo, T., Sakamoto, M., Ito, C., Toda, T. & Benno, Y. (2008). *Adlercreutzia equolifaciens* gen. nov., sp. nov., an equol-producing bacterium isolated from human faeces, and emended description of the genus *Eggerthella*. *Int J Syst Evol Microbiol* **58**, 1221–1227.
- Matthies, A., Loh, G., Blaut, M. & Braune, A. (2012). Daidzein and genistein are converted to equol and 5-hydroxy-equol by human intestinal *Slackia isoflavoniconvertens* in gnotobiotic rats. *J Nutr* **142**, 40–46.
- Mesbah, M., Premachandran, U. & Whitman, W. (1989). Precise measurement of the G+C content of deoxyribonucleic acid by high performance liquid chromatography. *Int J Syst Bacteriol* **39**, 159–167.
- Minamida, K., Ota, K., Nishimukai, M., Tanaka, M., Abe, A., Sone, T., Tomita, F., Hara, H. & Asano, K. (2008). *Asaccharobacter celatus* gen. nov., sp. nov., isolated from rat caecum. *Int J Syst Evol Microbiol* **58**, 1238–1240.
- Qin, J., Li, R., Raes, J., Arumugam, M., Burgdorf, K. S., Manichanh, C., Nielsen, T., Pons, N., Levenez, F. & other authors (2010). A human gut microbial gene catalogue established by metagenomic sequencing. *Nature* **464**, 59–65.
- Ridlon, J. M., Kang, D. J. & Hylemon, P. B. (2006). Bile salt biotransformations by human intestinal bacteria. *J Lipid Res* **47**, 241–259.
- Ritz, K. (2007). The plate debate: cultivable communities have no utility in contemporary environmental microbial ecology. *FEMS Microbiol Ecol* **60**, 358–362.
- Rosselló-Mora, R. & Amann, R. (2001). The species concept for prokaryotes. *FEMS Microbiol Rev* **25**, 39–67.
- Saitou, N. & Nei, M. (1987). The neighbor-joining method: a new method for reconstructing phylogenetic trees. *Mol Biol Evol* **4**, 406–425.
- Santos, S. R. & Ochman, H. (2004). Identification and phylogenetic sorting of bacterial lineages with universally conserved genes and proteins. *Environ Microbiol* **6**, 754–759.
- Tamaoka, J. & Komagata, K. (1984). Determination of DNA base composition by reversed-phase high-performance liquid chromatography. *FEMS Microbiol Lett* **25**, 125–128.
- Tamura, K., Peterson, D., Peterson, N., Stecher, G., Nei, M. & Kumar, S. (2011). MEGA5: molecular evolutionary genetics analysis using maximum likelihood, evolutionary distance, and maximum parsimony methods. *Mol Biol Evol* **28**, 2731–2739.
- Tindall, B. J., Sikorski, J., Smibert, R. M. & Krieg, N. R. (2007). Phenotypic characterization and the principles of comparative systematics. In *Methods for General and Molecular Microbiology*, pp. 330–393. Edited by C. A. Reddy, T. J. Beveridge, J. A. Breznak, G. Marzluf, T. M. Schmidt & L. R. Snyder. Washington D.C.: American Society for Microbiology.
- Turnbaugh, P. J., Ley, R. E., Mahowald, M. A., Magrini, V., Mardis, E. R. & Gordon, J. I. (2006). An obesity-associated gut microbiome with increased capacity for energy harvest. *Nature* **444**, 1027–1031.
- Wenning, M., Scherer, S. & Naumann, D. (2008). Infrared spectroscopy in the identification of microorganisms. In *Vibrational spectroscopy for medical diagnosis*, pp. 71–96. Edited by M. Diem, P. R. Griffith & J. M. Chalmers. Chichester: John Wiley & Sons, Ltd.
- Werner, T., Wagner, S. J., Martínez, I., Walter, J., Chang, J. S., Clavel, T., Kising, S., Schuemann, K. & Haller, D. (2011). Depletion of luminal iron alters the gut microbiota and prevents Crohn's disease-like ileitis. *Gut* **60**, 325–333.
- Würdemann, D., Tindall, B. J., Pukall, R., Lünsdorf, H., Strömpl, C., Namuth, T., Nahrstedt, H., Wos-Oxley, M., Ott, S. & other authors (2009). *Gordonibacter pamelaee* gen. nov., sp. nov., a new member of the *Coriobacteriaceae* isolated from a patient with Crohn's disease, and reclassification of *Eggerthella hongkongensis* Lau et al. 2006 as *Paraeggerthella hongkongensis* gen. nov., comb. nov. *Int J Syst Evol Microbiol* **59**, 1405–1415.
- Yarza, P., Richter, M., Peplies, J., Euzéby, J., Amann, R., Schleifer, K. H., Ludwig, W., Glöckner, F. O. & Rosselló-Móra, R. (2008). The All-Species Living Tree project: a 16S rRNA-based phylogenetic tree of all sequenced type strains. *Syst Appl Microbiol* **31**, 241–250.

PAPER 5

Streptococcus danieliae sp. nov., a novel bacterium isolated from the caecum of a mouse

Thomas Clavel · Cédric Charrier · Dirk Haller

Received: 13 June 2012 / Revised: 22 August 2012 / Accepted: 25 September 2012
© Springer-Verlag Berlin Heidelberg 2012

Abstract We report the characterization of one novel bacterium, strain ERD01G^T, isolated from the caecum of a TNF^{deltaARE} mouse. The strain was found to belong to the genus *Streptococcus* based on phylogenetic analysis of partial 16S rRNA gene sequences. The bacterial species with standing name in nomenclature that was most closely related to our isolate was *Streptococcus alactolyticus* (97 %). The two bacteria were characterized by a DNA–DNA hybridization similarity value of 35 %, demonstrating that they belong to different species. The new isolate was negative for acetoin production, esculin hydrolysis, urease, α -galactosidase and β -glucosidase, was able to produce acid from starch and trehalose, grew as beta-hemolytic coccobacilli on blood agar, did not grow at >40 °C, did not survive heat treatment at 60 °C for 20 min and showed negative agglutination in Lancefield tests. On the basis of these characteristics, strain ERD01G^T differed from the most closely related species *S. alactolyticus*, *Streptococcus gordonii*, *Streptococcus intermedius* and *Streptococcus sanguinis*. Thus, based on genotypic and phenotypic evidence, we propose that the isolate belongs to

a novel bacterial taxon within the genus *Streptococcus*, for which the name *Streptococcus danieliae* is proposed. The type strain is ERD01G^T (= DSM 22233^T = CCUG 57647^T).

Keywords TNF^{deltaARE} mice · Crohn's disease-like ileitis · Intestinal microbiota · Bacterial culture · *Streptococcus*

Introduction

Intestinal microorganisms play a crucial role in the regulation of host health and the development of chronic inflammatory disorders such as allergies and inflammatory bowel diseases (IBD) (Clavel and Haller 2007; Hörmann-sperger et al. 2012). The density and diversity of microorganisms hosted in the gastrointestinal (GI) tract of mammals is very high, yet most of these microorganisms, mainly bacteria of the phylum *Firmicutes* and *Bacteroidetes*, have not yet representative members in culture (Goodman et al. 2011). Within the *Firmicutes*, streptococci are Gram-positive lactic acid-producing coccoid bacteria that are common inhabitants of humans and other mammals, for example, they colonize the skin as well as the respiratory, GI and urogenital tract (Wilson 2005). Streptococci are one of the first bacteria isolated during the advent of microbiology at the end of the nineteenth century. Many of them have been originally isolated before 1950, and the first reports of *Streptococcus pyogenes* and *Streptococcus pneumoniae* by Rosenbach and Klein are dated from 1884. Hence, the taxonomic classification of streptococci has for long been driven by the study of clinically relevant isolates and associated phenotypic features. However, advances in molecular approaches like the analysis of 16S ribosomal gene sequences, G + C content

The GenBank accession number of the partial 16S ribosomal RNA and gyrase B gene sequence of strain ERD01G^T is GQ456229 and GQ456227, respectively.

Communicated by Erko Stackebrandt.

T. Clavel (✉) · D. Haller
Biofunctionality Unit, ZIEL—Research Center for Nutrition and Food Sciences, Technische Universität München,
Gregor-Mendel-Strasse 2, 85350 Freising-Weihenstephan,
Germany
e-mail: thomas.clavel@tum.de

C. Charrier
NovaBiotics Ltd, Aberdeen AB21 9TR, UK

of DNA and DNA–DNA relatedness have led to profound changes in the taxonomy of streptococci, for example, the classification of more than 20 *Streptococcus* spp. has been or still is a matter of debate (www.bacterio.cict.fr). To date, some of the gold-standard parameters that help distinguishing streptococci from each other and from phylogenetically related bacteria such as *Enterococcaceae* and *Lactococcus* spp. are hemolysis and surface antigen phenotypes, the inability to grow in the presence of 6.5 % NaCl, leucine arylamidase activity as well as esculin hydrolysis and acetoin production. Streptococci are functionally versatile and include pathogenic members expressing virulence factors, for example, *S. pneumoniae*, *S. pyogenes* and *Streptococcus suis*, as well as species generally recognized as safe that are widely used for production of food products, for example, *Streptococcus thermophilus*. Streptococci belong to dominant populations in the mouth, where certain species such as *Streptococcus mutans* contribute to the development of caries. *Streptococcus* spp. are also endogenous members of the gastric microbiota (Bik et al. 2006). However, their cell density decreases in distal parts of the GI tract, although some species may preferentially grow in microenvironments near the mucosal surface (Qin et al. 2010; Hong et al. 2011; Zoetendal et al. 2012) with possible detrimental effects in genetically susceptible hosts, for example, in IBD patients (Cartun et al. 1993; Conte et al. 2006; Fyderek et al. 2009). In the present paper, we focused our effort on the characterization of a novel bacterium of the genus *Streptococcus* isolated from the intestine of a mouse.

Materials and methods

Isolation

A male heterozygous TNF^{deltaARE} C57BL/6 mouse fed a standard diet (Ssniff, Soest, Germany, cat. no. V1534-000 R/M-H) was killed by cervical dislocation at the age of 25 weeks. Animal use was approved by the local institution in charge (animal welfare authorization 32-568, Freising District Office). The working area and dissection set were cleaned, and the mouse was copiously sprayed with 70 % (v/v) ethanol prior to dissection. The cecal content was collected into a 2-ml tube by squeezing and kept on ice for a maximum of 30 min prior to isolation. Wet weight of the cecal sample was determined by weighing tubes before and after collection using a TB-215D precision balance (Denver Instrument). Serial dilutions of the cecal content in phosphate-buffered saline solution were spread onto blood agar (Biomérieux) using sterile glass beads. Plates were incubated under aerobic conditions (5 % CO₂) for 6 days at 37 °C. Culture purity of single colonies was assured by

streaking twice onto blood agar and was examined by observing cell morphology after Gram-staining and colony morphology.

Phylogenetic and DNA-based analyses

DNA was extracted from washed bacterial cell pellets using the DNeasy Blood & Tissue kit (Qiagen), following the instructions for pretreatment of Gram-positive bacteria. The 16S rRNA genes were amplified using primer 27F 5'-AGA GTT TGA TCC TGG CTC AG and 1492R 5'-GGT TAC CTT GTT ACG ACT T (Kageyama et al. 1999). The annealing temperature was 56 °C. Amplicons were purified using agarose gel electrophoresis and the Wizard SV Gel and PCR Clean-Up System (Promega) and sequenced with primer 27F, 338F 5'-ACT CCT ACG GGA GGC AGC and 1492R using the Qiagen Genomic Services.

The gyrase B gene was amplified as described previously (Santos and Ochman 2004). Amplicons (approximately 1,500 bp) were purified as described above and sequenced using primer gyrBBNDN1 (5'-CCG TCC ACG TCG GCR TCN GYC AT) and gyrBBAUP2 (5'-GCG GAA GCG GCC NGS NAT GTA).

Sequences of closely related organisms were obtained using the BLAST function of the NCBI server (Altschul et al. 1990) and The All-Species Living Tree Project (Yarza et al. 2010). Ribosomal sequences were checked for anomalies using the program Pintail (Ashelford et al. 2005). All sequences were aligned using the BioEdit software, version 7.0.5.3 (Hall 1999) and the greengenes web application (DeSantis et al. 2006a, b). Percentages of similarity were calculated after unambiguous alignment of each isolated sequence with those of the most closely related species, using the DNA Distance Matrix function of the BioEdit software.

DNA–DNA hybridization experiments (De Ley et al. 1970; Huss et al. 1983; Visuvanathan et al. 1989) and determination of the G + C content of DNA by HPLC (Cashion et al. 1977; Tamaoka and Komagata 1984; Mesbah et al. 1989) were performed at the German Collection of Microorganisms and Cell Cultures (DSMZ) according to standard methods.

Phenotypic characterization

All tests were performed as described previously, for example, growth characteristics, motility, spore formation, antibiotic resistance and enzymatic tests (Clavel et al. 2007, 2009). Strain ERD01G^T and *Streptococcus alactolyticus* DSM 20728^T were analyzed in duplicate using the api[®] 20 STREP test following the manufacturer's instructions (Biomérieux). Carbohydrate antigens were analyzed using the Streptococcal Grouping Kit (Oxoid, cat. no. DR0585).

Results and discussion

DNA-based analysis of strain ERD01G^T

The partial 16S rRNA gene sequence of one pure culture obtained from a blood agar plate inoculated with the 10-fold-diluted (w/v) mouse cecal suspension did not appear to correspond to any currently described organism.

Phylogenetic analysis suggested that strain ERD01G^T (accession no. GQ456229) belongs to a new species within the viridans streptococci (Fig. 1). The closest relatives of strain ERD01G^T with a validly published name were *Streptococcus alactolyticus* (97.0 % similarity), *Streptococcus gordonii* (96.7 %), *Streptococcus sanguinis* (96.6 %) and *Streptococcus intermedius* (96.1 %). The partial 16S rRNA gene sequence of *S. pyogenes*, the type species of the genus *Streptococcus*, was 94 % similar to that of strain ERD01G^T.

Hybridization of DNA from strain ERD01G^T with DNA from *S. alactolyticus* DSM 20728^T revealed a relatedness value of 34.8 ± 3.9 % ($n = 2$ experiments). This value showed that strain ERD01G^T and *S. alactolyticus* belong to different taxa, indicating that strain ERD01G^T represents a novel bacterial species (Wayne et al. 1987).

Further phylogenetic analysis confirmed that the novel species is distantly related to any so far described streptococci (Fig. 2). Based on partial *gyrB* gene sequence analysis (458 bp), the closest relatives of strain ERD01G^T (GQ456227) were *Streptococcus suis* (EU003812) and *Streptococcus mitis* (EU003731) (64 % similarity) (Glazunova et al. 2009). Sequence similarity with *S. alactolyticus* (EU003787), *S. gordonii* (EU003750), *S. intermedius* (EU003777), *S. sanguinis* (EU003779) and *S. pyogenes* (EU003756) was <61 %.

Local BLAST analysis against partial 16S rRNA gene sequences (V1–V3 region) previously obtained from the

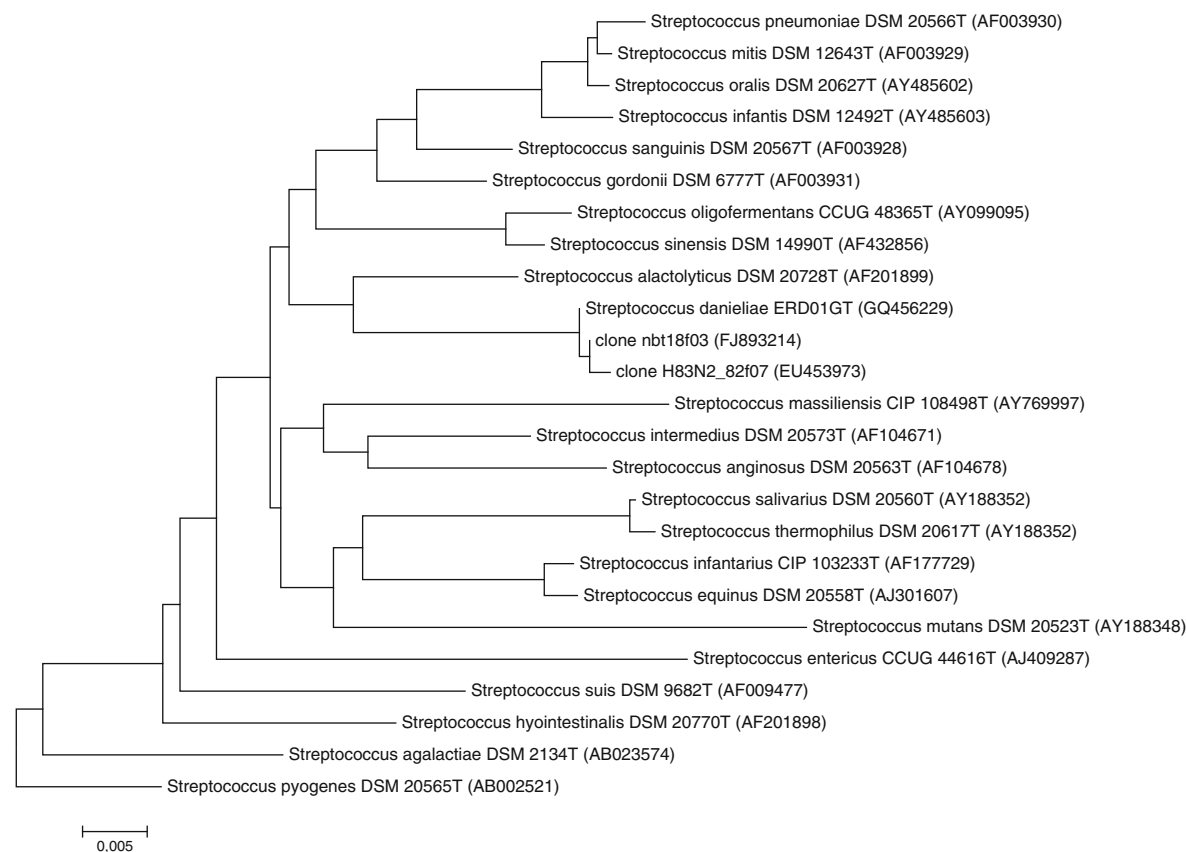


Fig. 1 Phylogenetic position of strain ERD01G^T within the genus *Streptococcus* based on partial sequence analysis of 16S rRNA genes (1,265 bp). The accession numbers of the 16S rRNA gene sequences used to construct the tree are indicated in brackets. NAST-aligned sequences (DeSantis et al. 2006) were used to construct the tree using

the neighbor-joining method (Saitou and Nei 1987) in MEGA5 (Tamura et al. 2011). Groupings were confirmed using the maximum parsimony method. *S. pyogenes*, the type species of the genus, was used to root the tree. The bar below the tree represents 5 nucleotide changes per 1,000 nucleotides

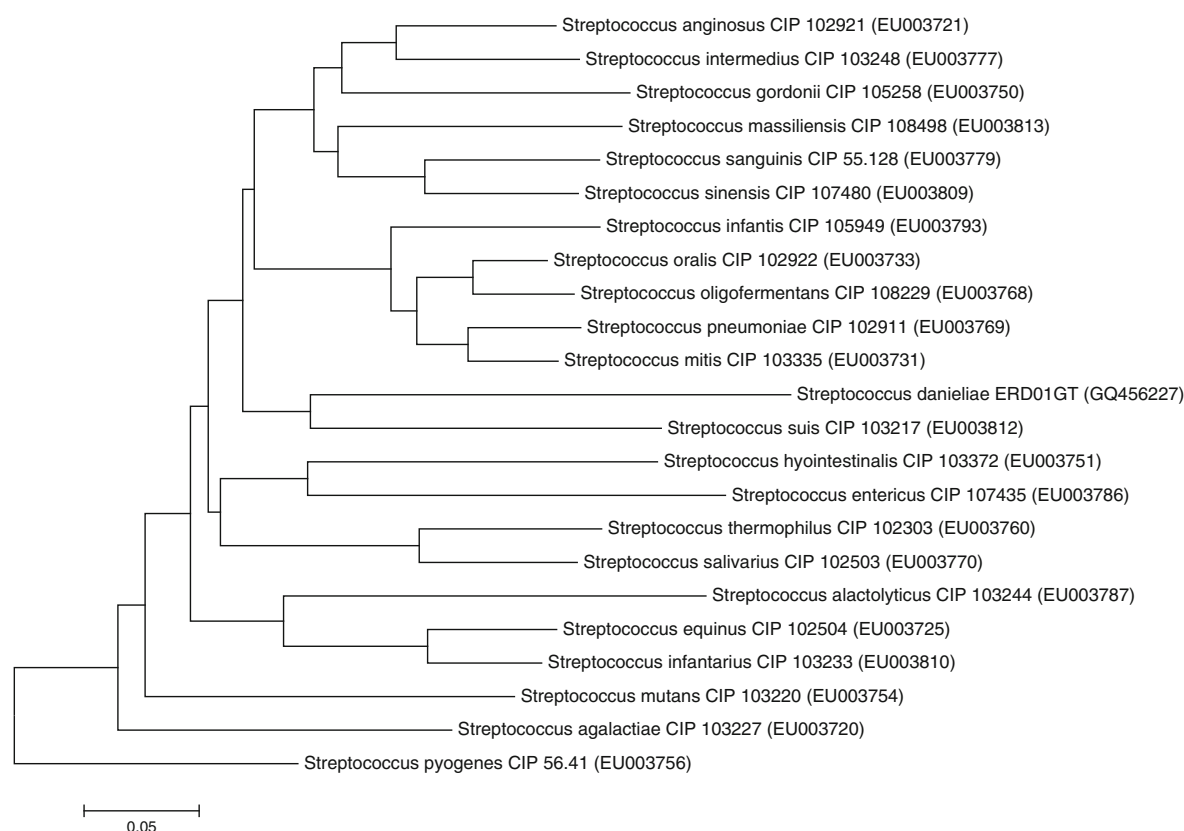


Fig. 2 Phylogenetic position of strain ERD01G^T within the genus *Streptococcus* based on partial sequence analysis of *gyrB* genes (458 bp). The tree was computed and formatted as in Fig. 1 using sequences aligned by ClustalW. The paper by Glazunova et al. (2009)

was used as reference to obtain *gyrB* gene sequences and accession numbers. The bar below the tree represents 5 nucleotide changes per 100 nucleotides

cecum of five wild-type ($n = 16,528$ sequences) and five heterozygous TNF^{deltaARE} ($n = 18,379$ sequences) C57BL/6 mice (Werner et al. 2011) revealed that strain ERD01G^T is a subdominant member of mouse cecal microbiota, *that is*, we found only one (in wild-type mice) and four (in TNF^{deltaARE} mice) full-length hits corresponding to the sequence of strain ERD01G^T. This fits with the observation that the common habitat of streptococci in mammals is the mouth and upper respiratory tract (Hardie and Whiley 2006).

The G + C content of DNA of strain ERD01G^T was 45.1 mol%, as measured by HPLC. This is in the upper range of values reported in the literature for most closely related *Streptococcus* spp. (37–46 mol%).

Phenotypic characterization of strain ERD01G^T

After 24 h of growth at 37 °C on blood agar under aerobic conditions (5 % CO₂), strain ERD01G^T occurred as round, flat, greenish to yellowish, β -hemolytic colonies characterized

by the presence of a darkened circular center (Fig. 3a). Colonies of strain ERD01G^T adhered to the agar after 24 h of growth so that it was difficult to remove them with a loop. Cells grew as chains of Gram-positive coccobacilli each measuring 1.0–3.0 μ m in length (Fig. 3b). They did not grow on blood agar containing 6.5 % (w/v) NaCl but grew on blood agar supplemented with 10 mg/l colistin sulfate and 5 mg/l oxolinic acid (*Streptococcus* selective supplement; Oxoid, cat. no. SR0126). Strain ERD01G^T did not survive heat treatment at 60 °C for 20 min and did not give positive results with any of the Lancefield reagents. In contrast, *S. alactolyticus* DSM 20729^T reacted with Group-D-specific antibodies, as reported previously for other strains (Vandamme et al. 1999). The susceptibility of strain ERD01G^T was tested toward eleven antimicrobial substances. MIC break-points (μ g/ml) were ($n = 6$) the following: cefotaxime, 0.242 ± 0.030 ; ciprofloxacin, 0.232 ± 0.031 ; clarithromycin, <0.016 ; clindamycin, <0.016 ; colistin, 8.000 ± 0.894 ; erythromycin, <0.016 ; metronidazole, >256 ; oxacilin, 2.333 ± 0.333 ; tetracycline, 1.229 ± 0.275 ; tobramycin,

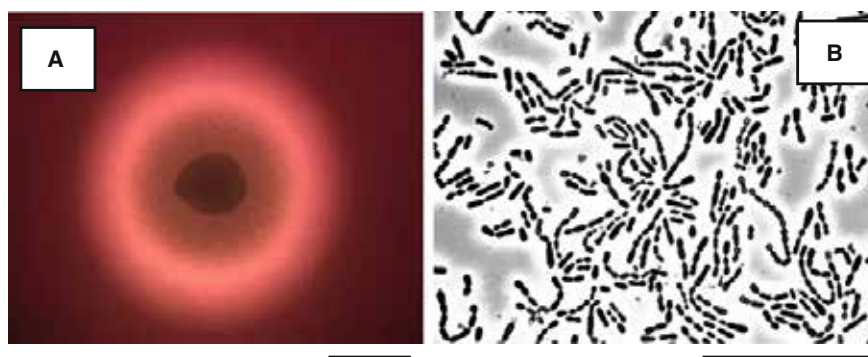


Fig. 3 Phase contrast microscopic picture showing the colony and cell morphology of strain ERD01G^T. **a** β-hemolytic colony of strain ERD01G^T grown on blood agar (Biomérieux) for 24 h at 37 °C under

aerobic conditions (5 % CO₂). The bar represents 1 mm. **b** Cell morphology of strain ERD01G^T grown on blood agar. The bar represents 10 μm

0.542 ± 0.042; vancomycin, 1.125 ± 0.125. Results of enzymatic tests are listed below in the species description and in Table 1.

In summary, comparative analysis of strain ERD01G^T and related species is shown in Table 1. Based on these findings, we propose that strain ERD01G^T merits recognition as member of a novel species within the genus *Streptococcus*, for which the name *Streptococcus danieliae* is proposed.

Description of *S. danieliae* sp. nov

Streptococcus danieliae (da.ni.e.li'ae. N.L. gen. fem. n. *danieliae*, of Daniel, named after Prof. Hannelore Daniel, in recognition of her research achievements in the field of gut physiology).

The species has the features of the genus. It is phylogenetically related to *Streptococcus alactolyticus*, *Streptococcus gordonii*, *Streptococcus sanguinis* and *Streptococcus*

Table 1 Traits that differentiate strain ERD01G^T from related bacteria

	1	2	3	4	5
Cell morphology	Cocccobacilli	Cocci	Cocci	Cocci	Cocci
Lancefield test	Not detected	Group D	Usually group H	Ungroupable	Usually group H
Hemolysis	<i>Beta</i>	<i>Alpha</i>	<i>Alpha</i>	<i>Alpha</i> or <i>gamma</i>	Usually <i>alpha</i>
Growth at >40 °C	–	+	NR	NR	NR
Acetoin production (VP)	–	+	–	+	–
Alkaline phosphatase ^a	–/+	–	+	+	–
Esculin hydrolysis	–	+	+	+	+/-
Urease	–	+	–	–	–
Acid from inulin	–	–	+	–	–/+
Acid from mannitol	–	+	–	–	–
Acid from raffinose ^a	–/+	+	–/+	–	+/-
Acid from starch	+	–	–	NR	–
Acid from trehalose	+	–	+	+	+
<i>Alpha</i> -galactosidase	–	+	–/+	–	+/-
<i>Beta</i> -glucosidase	–	+/-	+	–/+	+
Leucine arylamidase	+	+	+	+	+
Pyroglutonyl arylamidase	–	–	NR	–	NR
G + C content of DNA	45	39–41	38–43	37–38	40–46
16S rRNA gene similarity (%)	100	97.0	96.7	96.1	96.6

Strain: 1, ERD01G^T; 2, *Streptococcus alactolyticus* (Vandamme et al. 1999); 3, *Streptococcus gordonii* (Kilian et al. 1989; Hardie and Whiley 2006); 4, *Streptococcus intermedius* (Whiley and Beighton 1991; Hardie and Whiley 2006); 5, *Streptococcus sanguinis* (Kilian et al. 1989; Hardie and Whiley 2006); NR not reported

^a Results varied for strain ERD01G^T depending on the enzymatic test used (rapid ID 32 A or api[®] 20 STREP, Biomérieux). For each test, duplicate cultures of strain ERD01G^T and *S. alactolyticus* DSM 20728^T were tested in parallel

intermedius. Cells are approximately 1.0 µm wide, 1.0 to 3.0 µm long and occur mostly in chains of coccobacilli. They grow well under aerobic conditions (both under atmospheric conditions and in the presence of 5 % CO₂) in the temperature range from 25 to 37 °C. After 24 h of growth at 37 °C on blood agar, colonies are round, flat, greenish to yellowish, β-hemolytic and are characterized by the presence of a darkened circular center. Spore formation and motility have not been observed. Based on the use of the rapid ID 32A and api[®] 20 STREP tests (Biomérieux), the species is positive for mannose and raffinose fermentation, acid production from trehalose and starch, alkaline phosphatase (api[®] 20 STREP) leucine aminopeptidase as well as for arginine, leucine and tyrosine arylamidase. It is negative for urease activity, acetoin production from sodium pyruvate, hydrolysis of hippuric acid and esculin, arginine dehydrolase, α- and β-galactosidase, α- and β-glucosidase, α-arabinosidase, β-glucuronidase, β-N-acetyl glucosamine, glutamic acid decarboxylase, α-fucosidase, acid production from arabinose, glycogen, inulin, lactose, mannitol, raffinose (api[®] 20 STREP), ribose and sorbitol, nitrate reduction, indole production, alkaline phosphatase (rapid ID 32 A), arginine dihydrolase and proline, leucylglycine, phenylalanine, pyroglutamic acid, pyrrolidonyl, alanine, glycine histidine, glutamyl glutamic acid and serine arylamidase. The species did not give positive results with any of the Lancefield reagents. Its G + C content of DNA is 45.1 mol%. The type strain (ERD01G^T = DSM 22233^T = CCUG 57647^T) is resistant to metronidazole. It was isolated from the cecal content of a 25-week-old male heterozygous TNF^{deltaARE} C57BL/6 mouse suffering from ileitis.

Acknowledgments The heterozygous TNF^{deltaARE} mouse model of ileitis was a generous gift from Dr. George Kollias (Biomedical Sciences Research Center Alexander Fleming, Vari, Greece). We are grateful to Nico Gebhardt, Melanie Klein and Silvia Pitariu (TUM, BFLM) for excellent technical assistance, to Prof. Euzéby (Ecole Nationale Vétérinaire, Toulouse, France) for suggesting the Latin bacterial name, to Dr. Herbert Seiler (TUM, Microbiology) for microscopic analysis and to staff members of the DSMZ and the Culture Collection University of Göteborg (CCUG) for contributing to the description of strain ERD01G^T.

References

- Altschul SF, Gish W, Miller W, Myers EW, Lipman DJ (1990) Basic local alignment search tool. *J Mol Biol* 215:403–410
- Ashelford KE, Chuzhanova NA, Fry JC, Jones AJ, Weightman AJ (2005) At least 1 in 20 16S rRNA sequence records currently held in public repositories is estimated to contain substantial anomalies. *Appl Environ Microbiol* 71:7724–7736
- Bik EM, Eckburg PB, Gill SR, Nelson KE, Purdom EA, Francois F, Perez-Perez G, Blaser MJ, Relman DA (2006) Molecular analysis of the bacterial microbiota in the human stomach. *Proc Natl Acad Sci USA* 103:732–737
- Cartun RW, Van Kruiningen HJ, Pedersen CA, Berman MM (1993) An immunocytochemical search for infectious agents in Crohn's disease. *Mod Pathol* 6:212–219
- Cashion P, Holder-Franklin MA, McCully J, Franklin M (1977) A rapid method for the base ratio determination of bacterial DNA. *Anal Biochem* 81:461–466
- Clavel T, Haller D (2007) Bacteria- and host-derived mechanisms to control intestinal epithelial cell homeostasis: implications for chronic inflammation. *Inflamm Bowel Dis* 13:1153–1164
- Clavel T, Lippman R, Gavini F, Dore J, Blaut M (2007) *Clostridium saccharogumia* sp. nov. and *Lactonifactor longoviformis* gen. nov., sp. nov., two novel human faecal bacteria involved in the conversion of the dietary phytoestrogen secoisolariciresinol diglucoside. *Syst Appl Microbiol* 30:16–26
- Clavel T, Charrier C, Braune A, Wenning M, Blaut M, Haller D (2009) Isolation of bacteria from the ileal mucosa of TNF^{deltaARE} mice and description of *Enterorhabdus mucosicola* gen. nov., sp. nov. *Int J Syst Evol Microbiol* 59:1805–1812
- Conte MP, Schippa S, Zamboni I, Penta M, Chiarini F, Seganti L, Osborn J, Falconieri P, Borrelli O, Cucchiara S (2006) Gut-associated bacterial microbiota in paediatric patients with inflammatory bowel disease. *Gut* 55:1760–1767
- De Ley J, Cattoir H, Reynaerts A (1970) The quantitative measurement of DNA hybridization from renaturation rates. *Eur J Biochem* 12:133–142
- DeSantis TZ, Hugenholtz P, Larsen N, Rojas M, Brodie EL, Keller K, Huber T, Dalevi D, Hu P, Andersen GL (2006a) Greengenes, a chimera-checked 16S rRNA gene database and workbench compatible with ARB. *Appl Environ Microbiol* 72:5069–5072
- DeSantis TZ Jr, Hugenholtz P, Keller K, Brodie EL, Larsen N, Piceno YM, Phan R, Andersen GL (2006b) NAST: a multiple sequence alignment server for comparative analysis of 16S rRNA genes. *Nucleic Acids Res* 34:W394–W399
- Fyderek K, Strus M, Kowalska-Duplaga K, Gosiewski T, Wedrychowicz A, Jedynak-Wasowicz U, Sladek M, Pieczarkowski S, Adamski P, Kochan P, Heczko PB (2009) Mucosal bacterial microflora and mucus layer thickness in adolescents with inflammatory bowel disease. *World J Gastroenterol* 15:5287–5294
- Glazunova OO, Raoult D, Roux V (2009) Partial sequence comparison of the rpoB, sodA, groEL and gyrB genes within the genus *Streptococcus*. *Int J Syst Evol Microbiol* 59:2317–2322
- Goodman AL, Kallstrom G, Faith JJ, Reyes A, Moore A, Dantas G, Gordon JI (2011) Extensive personal human gut microbiota culture collections characterized and manipulated in gnotobiotic mice. *Proc Natl Acad Sci U S A* 108:6252–6257
- Hall TA (1999) Bioedit: a user-friendly biological sequence alignment editor and analysis program for Windows 95/98/NT. *Nuc Acids Symp Ser* 41:95–98
- Hardie J, Whiley RA (2006) The genus *Streptococcus*—Oral. In: Dworkin M, Flakow S, Rosenberg E, Schleifer KH, Stackebrandt E (eds) *Prokaryotes*. Springer, Berlin, pp 76–107
- Hong PY, Croix JA, Greenberg E, Gaskins HR, Mackie RI (2011) Pyrosequencing-based analysis of the mucosal microbiota in healthy individuals reveals ubiquitous bacterial groups and micro-heterogeneity. *PLoS ONE* 6:e25042
- Hörmannspurger G, Clavel T, Haller D (2012) Gut matters: microbe-host interactions in allergic diseases. *J Allergy Clin Immunol* 159:1452–1459
- Huss VAR, Festl H, Schleifer KH (1983) Studies on the spectrometric determination of DNA hybridization from renaturation rates. *Syst Appl Microbiol* 4:184–192
- Kageyama A, Benno Y, Nakase T (1999) Phylogenetic evidence for the transfer of *Eubacterium lentum* to the genus *Eggerthella* as *Eggerthella lenta* gen. nov., comb. nov. *Int J Syst Bacteriol* 49:1725–1732

- Kilian M, Mikkelsen L, Henrichsen J (1989) Taxonomic study of viridans streptococci: description of *Streptococcus gordonii* sp. nov. and emended descriptions of *Streptococcus sanguis* (White and Niven 1946), *Streptococcus oralis* (Bridge and Sneath 1982), and *Streptococcus mitis* (Andrewes and Horder 1906). Int J Syst Bact 39:471–484
- Mesbah M, Premachandran U, Whitman W (1989) Precise measurement of the G + C content of deoxyribonucleic acid by high performance liquid chromatography. Int J Syst Bact 39:159–167
- Qin J, Li R, Raes J, Arumugam M, Burgdorf KS, Manichanh C, Nielsen T, Pons N, Levenez F, Yamada T, Mende DR, Li J, Xu J, Li S, Li D, Cao J, Wang B, Liang H, Zheng H, Xie Y, Tap J, Lepage P, Bertalan M, Batto JM, Hansen T, Le Paslier D, Linneberg A, Nielsen HB, Pelletier E, Renault P, Sicheritz-Ponten T, Turner K, Zhu H, Yu C, Jian M, Zhou Y, Li Y, Zhang X, Qin N, Yang H, Wang J, Brunak S, Dore J, Guarner F, Kristiansen K, Pedersen O, Parkhill J, Weissenbach J, Bork P, Ehrlich SD (2010) A human gut microbial gene catalogue established by metagenomic sequencing. Nature 464:59–65
- Saitou N, Nei M (1987) The neighbor-joining method: a new method for reconstructing phylogenetic trees. Mol Biol Evol 4:406–425
- Santos SR, Ochman H (2004) Identification and phylogenetic sorting of bacterial lineages with universally conserved genes and proteins. Environ Microbiol 6:754–759
- Tamaoka J, Komagata K (1984) Determination of DNA base composition by reversed-phase high-performance liquid chromatography. FEMS Microbiol Lett 25:125–128
- Tamura K, Peterson D, Peterson N, Stecher G, Nei M, Kumar S (2011) MEGA5: molecular evolutionary genetics analysis using maximum likelihood, evolutionary distance, and maximum parsimony methods. Mol Biol Evol 28:2731–2739
- Vandamme P, Devriese LA, Haesebrouck F, Kersters K (1999) *Streptococcus intestinalis* Robinson et al. 1988 and *Streptococcus alactolyticus* Farrow et al. 1984 are phenotypically indistinguishable. Int J Syst Bacteriol 49 Pt 2:737–741
- Visuvanathan S, Moss M, Standord J, Hermon-Taylor J, McFadden J (1989) Simple enzymatic method for isolation of DNA from diverse bacteria. J Microbiol Methods 10:59–64
- Wayne LG, Brenner DJ, Colwell RR, Grimont PAD, Kandler O, Krichevsky MI, Moore LH, Moore WEC, Murray RGE, Stackebrandt E, Starr MP, Trüper HG (1987) Report of the ad hoc committee on reconciliation of approaches to bacterial systematics. Int J Syst Bact 37:463–464
- Werner T, Wagner SJ, Martinez I, Walter J, Chang JS, Clavel T, Kislung S, Schuemann K, Haller D (2011) Depletion of luminal iron alters the gut microbiota and prevents Crohn's disease-like ileitis. Gut 60:325–333
- Whiley RA, Beighton D (1991) Emended descriptions and recognition of *Streptococcus constellatus*, *Streptococcus intermedius*, and *Streptococcus anginosus* as distinct species. Int J Syst Bacteriol 41:1–5
- Wilson M (2005) Microbial inhabitants of humans: their ecology and role in health and disease. Cambridge University Press, New York
- Yarza P, Ludwig W, Euzéby J, Amann R, Schleifer KH, Glockner FO, Rossello-Mora R (2010) Update of the all-species living tree project based on 16S and 23S rRNA sequence analyses. Syst Appl Microbiol 33:291–299
- Zoetendal EG, Raes J, van den Bogert B, Arumugam M, Booijink CC, Troost FJ, Bork P, Wels M, de Vos WM, Kleerebezem M (2012) The human small intestinal microbiota is driven by rapid uptake and conversion of simple carbohydrates. ISME J 6:1415–1426

PAPER 6

Intestinimonas butyriciproducens gen. nov., sp. nov., a butyrate-producing bacterium from the mouse intestine

Karoline Kläring,^{1,2†} Laura Hanske,^{2†} Nam Bui,^{3†} Cédric Charrier,⁴
Michael Blaut,² Dirk Haller,⁵ Caroline M. Plugge³ and Thomas Clavel^{1,5‡}

Correspondence

Thomas Clavel
thomas.clavel@tum.de

¹ZIEL-Research Center for Nutrition and Food Sciences, Junior Research Group Intestinal Microbiome, Biofunctionality Unit, Technische Universität München (TUM), Freising, Germany

²Department of Gastrointestinal Microbiology, German Institute of Human Nutrition Potsdam-Rehbrücke (DIfE), Nuthetal, Germany

³Laboratory of Microbiology, Wageningen University, The Netherlands

⁴NovaBiotics Ltd, Aberdeen, UK

⁵Chair of Nutrition and Immunology, Technische Universität München, Freising, Germany

A Gram-positive, spore-forming, non-motile, strictly anaerobic rod-shaped bacterium was isolated from the caecal content of a TNF^{deltaARE} mouse. The isolate, referred to as strain SRB-521-5-I^T, was originally cultured on a reduced agar medium containing yeast extract, rumen fluid and lactic acid as main energy and carbon sources. Phylogenetic analysis of partial 16S rRNA genes revealed that the species most closely related to strain SRB-521-5-I^T were *Flavonifractor plautii* and *Pseudoflavonifractor capillosus* (<95% sequence similarity; 1436 bp). In contrast to *F. plautii* and *P. capillosus*, strain SRB-521-5-I^T contained a substantial amount of C_{18:0} dimethylacetal. Additional major fatty acids were C_{14:0} methyl ester, C_{16:0} dimethylacetal and C_{18:0} aldehyde. Strain SRB-521-5-I^T differed in its enzyme profile from *F. plautii* and *P. capillosus* by being positive for dextrin, maltotriose, turanose, DL-lactic acid and D-lactic acid methyl ester but negative for D-fructose. In reduced Wilkins-Chalgren-Anaerobe broth, strain SRB-521-5-I^T produced approximately 8 mM butyrate and 4 mM acetate. In contrast to *F. plautii*, the strain did not metabolize flavonoids. It showed intermediate resistance towards the antibiotics ciprofloxacin, colistin and tetracycline. Based on genotypic and phenotypic characteristics, we propose the name *Intestinimonas butyriciproducens* gen. nov., sp. nov. to accommodate strain SRB-521-5-I^T (=DSM 26588^T=CCUG 63529^T) as the type strain.

The mammalian gut harbours a remarkable density and variety of bacterial species (Qin *et al.*, 2010). These bacteria contribute to functions of importance for the mammalian host, e.g. the maturation of immune responses (Hörmannspurger *et al.*, 2012), the regulation of energy homeostasis (Bäckhed *et al.*, 2004), and the conversion of host-derived substrates such as mucin, bile acids and steroids (Bokkenheuser *et al.*, 1977; Derrien *et al.*, 2004; Ridlon *et al.*, 2006) as well as dietary

compounds such as indigestible carbohydrates and polyphenols (Clavel *et al.*, 2006a; Roberfroid, 2007). Among important food components converted by gut bacteria, polyphenols have drawn much attention because of their possible beneficial health effects (Manach *et al.*, 2005). To date, several gut bacteria able to convert polyphenols such as lignans (e.g. secoisolariciresinol), isoflavones (e.g. daidzein), flavonols (e.g. quercetin) and prenylflavonoids (e.g. xanthohumol) have been studied (Schneider *et al.*, 1999; Clavel *et al.*, 2006b, 2009; Hanske *et al.*, 2010). One of these polyphenol-converting bacteria, *Flavonifractor plautii*, is well known for its ability to metabolize the flavonoids quercetin, apigenin and luteolin (Schoefer *et al.*, 2003). *F. plautii* is a butyrate-producing, strictly anaerobic bacterium originally described as [*Clostridium orbiscindens*] (Winter *et al.*, 1991). The species was reclassified as *F. plautii* after Carlier *et al.* (2010) isolated several strains from clinical samples (blood, pus and infected

†These authors contributed equally to the work and share first authorship.

‡Present address: TU München, ZIEL-NFG Intestinal Microbiome, Gregor-Mendel-Strasse 2, 85350 Freising-Weihenstephan, Germany.

Abbreviation: CFA, cellular fatty acid.

The GenBank/EMBL/DBJ accession number for the 16S rRNA gene sequence of strain SRB-521-5-I^T is KC311367.

Six supplementary figures are available with the online version of this paper.

tissue) and demonstrated that [*C. orbiscindens*] and [*Eubacterium plautii*] were very similar based on genotypic and phenotypic characteristics. The only differences observed by Carlier *et al.* (2010) were the inability of [*E. plautii*] DSM 4000^T to produce spores and the motility of [*C. orbiscindens*] DSM 6740^T. The same authors also proposed the name *Pseudoflavonifractor capillosus* to accommodate the misclassified species of the genus *Bacteroides*, [*Bacteroides capillosus*], a non-motile, Gram-negative, non-spore-forming bacillus originally isolated from faeces of human infants and referred to as [*Bacillus capillosus*] (Tissier 1908). The present work deals with the description of a novel mouse intestinal bacterium related to *F. plautii* and *P. capillosus*.

A caecal sample was collected from one 17-week-old female heterozygous TNF^{deltaARE} C57BL/6 mouse (Kontoyiannis *et al.*, 1999) fed a standard experimental diet (cat. no. S5745-E7020; ssniff GmbH). Animal use was approved by the local institution in charge (animal welfare authorization 32-568, Freising District Office). Mouse dissection, bacterial isolation and cultivation procedures were as described previously (Clavel *et al.*, 2010; Pfeiffer *et al.*, 2012). Strictly anaerobic techniques were used (unless otherwise stated, the gas atmosphere was N₂/H₂, 90 : 10 for isolation in a Whitley H85 workstation and 100% N₂ for subculturing in Hungate tubes). The selective agar medium used for isolation, based on the formulation by Postgate for the isolation of sulphate-reducing bacteria (Postgate 1963), contained (per litre): 11.3 g M9 minimal salts (M6030; Sigma-Aldrich), 1.5 g Na₂SO₄, 500 mg FeSO₄ · 7H₂O, 100 mg yeast extract, 100 mg CaCl₂, 100 mg MgSO₄ · 4H₂O, 50 mg PdCl₂, 2.5 mg phenosafranin and 5 ml autoclaved rumen fluid which had been stored at 4 °C for 6 months. After autoclaving (121 °C, 15 min), the medium was allowed to cool in a water bath (55 °C). Filter-sterilized cysteine, DTT and DL-lactic acid sodium salt solution (A1831; Applichem) were added to a final concentration of 0.05% (w/v), 0.02% (w/v) and 1% (v/v), respectively. Bacteria from 10-fold serial dilutions of the

caecal content were allowed to grow for 18 days. The purity of isolates was ensured by streaking twice onto selective agar plates. Purity was examined by observing cell morphology after Gram-staining and colony morphology. Wilkins-Chalgren-Anaerobe (WCA) broth (Oxoid) supplemented with 0.05% (w/v) cysteine and 0.02% DTT was used for subculturing. The genomic DNA of isolates was extracted and 16S rRNA gene sequences were analysed using primers 27F and 1492R as described previously (Pfeiffer *et al.*, 2012). Primers 338F (5'-ACTCCTACGGGAGGCAGC), 609F (5'-GGATTAGATACCCBDGTA), 907F (5'-AAACTYAAAKGATTGACGG) and 907R were also used for sequencing isolates of interest. The search-based approach DECIPHER was used to test for the presence of chimeras (Wright *et al.*, 2012).

Analysis using the BLAST program (Altschul *et al.*, 1990) revealed that one of the isolated strains (SRB-521-5-I^T) was related only distantly to any known recognized species. Unambiguous alignment of partial 16S rRNA gene sequences (1475 bp) showed that the sequence of strain SRB-521-5-I^T was: (i) 100% similar to cloned sequences from pig (GenBank accession no. AF371948) (Leser *et al.*, 2002) and human intestine (nos. HQ785725, HQ783112, HQ770450 and FJ366757) (Turnbaugh *et al.*, 2009; Li *et al.*, 2012); (ii) 100% similar to two hitherto unclassified cultured strains isolated from the human gut (nos. JX101685 and JX273469) as well as one mucin-degrading and butyrate-producing bacterium from swine intestine (no. JX629258) (Levine *et al.*, 2013); and (iii) ≤94.5% similar to *P. capillosus* CCUG 15402^T and *F. plautii* DSM 4000^T. A phylogenetic tree based on the neighbour-joining method showed that strain SRB-521-5-I^T and the three as yet unclassified strains mentioned in (ii) above formed one cluster separated from the genera *Pseudoflavonifractor* and *Flavonifractor* (Fig. 1). This grouping was confirmed using the maximum-likelihood method (Fig. S1 available in IJSEM Online). A total of 261 full-length 16S rRNA gene sequences in the GenBank database matched the sequence

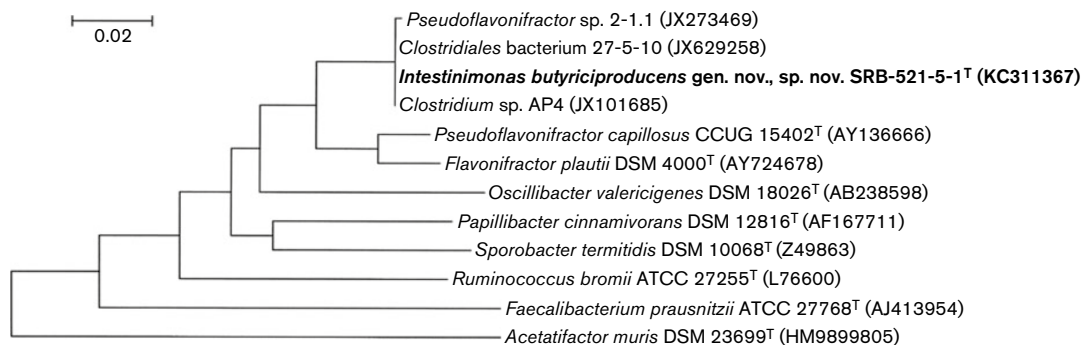


Fig. 1. Phylogenetic tree of strain SRB-521-5-I^T and related species based on partial 16S rRNA gene sequencing. Accession numbers of the 16S rRNA gene sequences (1436 bp) used to reconstruct the tree are indicated in parentheses. Sequences were aligned using Greengenes and the tree was reconstructed using the neighbour-joining method (Saitou & Nei 1987) in MEGA5 (Tamura *et al.*, 2011). Bar, 2 nt changes per 100 nt.

of strain SRB-521-5-I^T with a similarity >95%. A majority of these sequences originated from intestinal samples in various species (human, mouse, chicken, zebra, cow, etc.), suggesting that this bacterial group within *Clostridium* cluster IV has been repeatedly found in gut ecosystems. However, local BLAST analysis against 85 949 chimera-checked and quality-filtered partial 16S rRNA gene sequences (V1–V3 region) from the caecum of conventional mice (Werner *et al.*, 2011) revealed that only eight sequences matched that of strain SRB-521-5-I^T at a similarity >95%. This indicates that these bacteria are subdominant in the mouse gut, although their numbers probably depend on environmental factors such as diet and hygiene standards. Genotypic analysis of strain SRB-521-5-I^T also included determination of the DNA G + C content by HPLC at the German Collection of Microorganisms and Cell Culture (DSMZ). The isolate had a DNA G + C content of 58.4 mol%, which is in the range of those of its most closely related species (*F. plautii*, 58–61.6 mol%; *P. capillosus*, 60 mol%).

Strain SRB-521-5-I^T was analysed further using chemotaxonomic methods. Cell biomass was produced by cultivation at 37 °C in reduced WCA broth. Incubation time was 24 h (in 300 ml) for cellular fatty acid (CFA) analysis and 72 h (in 1.5 litres) for polar lipid and quinone analysis. Cells were pelleted by centrifugation (5500 g, 10 min), washed once in filter-sterilized PBS, and stored at –80 °C prior to freeze-drying overnight and shipment at room temperature. Samples were measured by the Identification Service of the DSMZ. Details on the experimental procedures are available online (www.dsmz.de/services/services-microorganisms/identification). The CFA pattern of strain SRB-521-5-I^T is shown in Table 1. As in *F. plautii* and *P. capillosus*, major fatty acids were saturated (>90% of the total fatty acids) and included C_{14:0} methyl ester, C_{14:0} dimethyl acetal and C_{16:0} dimethyl acetal. However, the new isolate showed a markedly lower proportion of C_{16:0} aldehyde, C_{16:0} methyl ester and C_{16:0} dimethyl acetal, as well as a higher proportion of C_{12:0} methyl ester, C_{18:0} aldehyde and C_{18:0} dimethyl acetal compared with the two other species (Table 1). Concerning polar lipids, strain SRB-521-5-I^T was characterized by the presence of diphosphatidylglycerol, eight glycolipids, six phosphoglycolipids, six phospholipids and three unidentified lipids (Fig. S2). No respiratory quinones were detected in cells of strain SRB-521-5-I^T.

Classical phenotypic characterization, e.g. growth features, motility, enzyme tests and spore formation, was performed as described previously (Clavel *et al.*, 2007, 2009). Based on microscopic observation after Gram-staining, the isolate stained Gram-negative. The KOH test was positive (formation of mucoid string), which also indicates that cells of strain SRB-521-5-I^T are Gram-negative. However, a Gram-negative-type cell-wall structure was not clearly visible in electron micrographs (Fig. 2). The cells seem to be characterized by the presence of an exocellular slime layer that possibly hampers proper staining. For transmission electron microscopy, cells of strain SRB-521-5-I^T were

grown for 48 h in Reinforced Clostridial Medium (Difco) and fixed with 2.5% (w/v) glutaraldehyde in 0.1 M sodium cacodylate buffer (pH 7.2) at 4 °C. After rinsing with cacodylate buffer (0.1 M), post-fixation was done in 1% (w/v) OsO₄ and 1% (w/v) potassium ferricyanide for 1 h at room temperature. Cells were embedded in 5% (w/v) gelatin that was then solidified at 0 °C. After dehydration in a graded ethanol series, cells were infiltrated with

Table 1. Cellular fatty acid pattern of strain SRB-521-5-I^T and related species

Strains: 1, SRB-521-5-I^T; 2, *F. plautii* DSM 6740^T; 3, *P. capillosus* CCUG 15402A^T. Data were obtained in the present study. The three strains were grown and analysed under identical conditions. Details for cell biomass production are given in the text. CFAs were analysed at the DSMZ using the BHIBLA method (www.dsmz.de/services/services-microorganisms/identification). Values are percentages of total fatty acids. Bold type indicates fatty acids for which substantial quantitative differences between strain SRB-521-5-I^T and the two related species were observed. ai, anteiso; ALDE, aldehyde; DMA, dimethylacetal; FAME, fatty acid methyl ester; i, iso; ND, not detected.

Fatty acid	1	2	3
10:0 FAME	0.2	ND	0.2
i-12:0 FAME	ND	ND	0.2
12:0 FAME	4.8	0.2	2.8
11:0 DMA	1.9	0.2	0.2
ai-13:0 FAME	ND	ND	0.1
13:0 FAME	0.2	ND	0.3
i-14:0 FAME	0.2	0.1	2.5
14:1 CIS 9 FAME	0.9	0.2	ND
14:0 FAME	33.1	28.3	33.3
14:0 DMA	4.0	9.1	3.0
i-15:0 FAME	0.2	0.8	ND
ai-15:0 FAME	0.1	0.1	0.1
16:0 ALDE	1.7	5.2	7.4
15:0 FAME	ND	0.5	0.4
i-15:0 DMA	ND	ND	0.1
i-16:0 FAME	ND	ND	0.3
16:1 CIS 9 FAME	0.9	0.2	0.2
16:1 CIS 11 FAME	ND	0.2	ND
16:0 FAME	1.9	12.2	7.4
16:1 CIS 9 DMA	0.2	ND	ND
16:0 DMA	9.1	27.9	38.2
18:0 ALDE	7.8	2.7	0.3
17:0 DMA	0.2	ND	0.1
18:2 CIS 9,12 FAME	0.3	ND	ND
18:1 CIS 9 FAME	2.8	0.9	0.5
18:0 FAME	1.8	0.9	0.3
18:1 CIS 9 DMA	1.5	0.4	0.2
18:1 CIS 11 DMA	0.4	ND	ND
18:0 DMA	23.0	8.1	0.6
19:0 FAME	1.4	0.7	ND
20:0 FAME	0.3	ND	ND
Unidentified	1.4	2.2	1.4

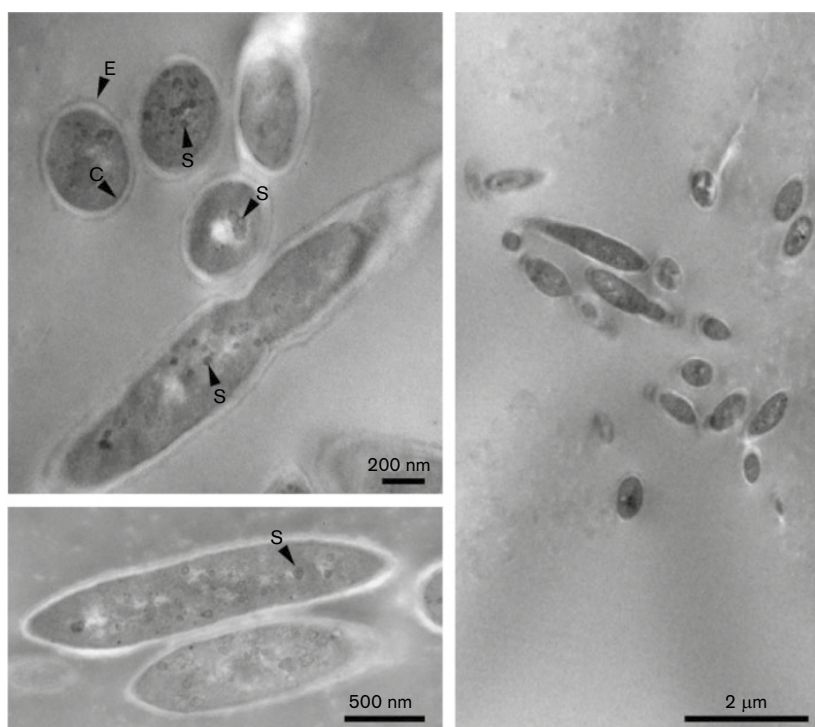


Fig. 2. Cell morphology of strain SRB-521-5-1^T. Cells were analysed using transmission electron microscopy as explained in the text. Arrowheads indicate the presence of exocellular polymeric substances (E), a cytoplasmic membrane (C) and storage granules (S).

modified Spurr resin mixture (Serva) and sectioned on an ultramicrotome (Ultracut S; Reichert). Micrographs were taken with a JEOL JEM 1011 transmission electron microscope. In contrast to *P. capillosus*, strain SRB-521-5-1^T and *F. plautii* were able to grow in reduced WCA broth after heat treatment (60 °C/20 min and 80 °C/10 min under aerobic conditions; tested in three independent experiments). Using light microscopy, small terminal and subterminal endospores were detected after 7 days of growth (Fig. S3). In addition, the isolate was tested for the presence of the sporulation gene *spo0A* by PCR, as described by Brill & Wiegel (1997). In contrast to *F. plautii* and *P. capillosus*, the *spo0A* gene was not amplified from genomic DNA of strain SRB-521-5-1^T (Fig. S4). The production of short chain fatty acids was determined in batch culture supernatants by means of GC (Pfeiffer *et al.*, 2012). Cells were grown in reduced WCA broth with a gas phase of N₂/CO₂ (80:20). After 48 h, strain SRB-521-5-1^T produced 3.6 mM acetate and 8.1 mM butyrate (two experiments). Minor amounts of lactate, isovalerate and valerate were also detected (<0.5 mM). In contrast, *P. capillosus* produced acetate (3.0 mM) but no butyrate (<0.1 mM). *F. plautii* produced 3.6 mM acetate and 7.1 mM butyrate. Biolog enzyme profiles (determined in

duplicate for each strain) were obtained as per the manufacturer's instructions. Fresh 24 h cultures in reduced WCA broth were used as inoculum. Cells were collected by centrifugation (5000 g, 5 min) under anaerobic conditions. After addition of Biolog-AN inoculating fluid (OD₆₀₀ of about 0.3) and inoculation under aerobic conditions, the plates were incubated at 37 °C for 24 h in a jar containing an Anaerogen sachet (Oxoid). Reactions were read visually and by measuring the OD at 590 nm. Substrates in wells characterized by a visible violet stain and an OD₅₉₀ of >0.05 after background subtraction (negative water control) were considered positive. The results for strain SRB-521-5-1^T are given in the species description. Comparative enzyme patterns are shown in Fig. S5. Discriminative features are listed in Table 2.

The susceptibility of the isolate towards 11 antimicrobial substances was tested using Etest strips (Bio-Stat Diagnostics), according to CLSI standard M11-A8 (<http://www.clsi.org/>). Briefly, a sterile swab was dipped into the inoculum suspension (fresh culture in reduced WCA broth) and the excess liquid was removed by turning the swab against the inside of the tube. The surface of reduced WCA agar plates was spread evenly with the swab. Plates were allowed to air-dry for 10–15 min and, using sterile forceps, Etest strips were applied to the inoculated agar surface. Two

Table 2. Differential characteristics between strain SRB-521-5-I^T and its closest relatives

Strains: 1, SRB-521-5-I^T; 2, *F. plautii* DSM 6740^T; 3, *P. capillosus* CCUG 15402A^T. CFA, cellular fatty acid; ND, not determined; R, resistant; S, sensitive; V, variable.

Characteristic	1	2	3
Cell-wall type	Gram-positive	V	Gram-negative
Motility	–	V	–
Spore formation*	+	V	–
<i>spo0A</i> (sporulation gene)	–	+	+
Heat treatment (80 °C, 10 min)	R	R	S
Butyrate production	+	+	–
Growth at 45 °C	+	Slow	+
Flavonoids			
Apigenin	–	+	ND
Eriodictyol	–	+	ND
Luteolin	–	+	ND
Naringenin	–	+	ND
Quercetin	–	+	–
Taxifolin	–	+	ND
Enzyme test (Biolog)			
<i>N</i> -Acetyl-D-glucosamine	+	–	+
Dextrin	+	–	–
Dulcitol	–	+	–
D-Fructose	–	+	+
L-Fucose	–	–	+
D-Galactose	+	–	+
D-Galacturonic acid	–	–	+
Gentiobiose	–	–	+
α -D-Glucose	+	+	–
Glucose 1-phosphate	–	–	+
Lactulose	–	–	+
Maltose	–	–	+
Maltotriose	+	–	–
D-Mannitol	–	+	–
Palatinose	–	–	+
D-Sorbitol	+	+	–
Turanose	+	–	–
β -Hydroxybutyric acid	+	+	–
α -Ketobutyric acid	–	+	–
α -Ketovaleric acid	–	+	–
DL-Lactic acid	+	–	–
D-Lactic acid methyl ester	+	–	–
Alaninamide	–	+	–
L-Alanine	–	+	–
L-Asparagine	–	+	–
Glycyl L-methionine	–	–	+
Inosine	+	+	–
Thymidine	+	+	–
Thymidine 5'-monophosphate	+	+	–
Uridine 5'-monophosphate	+	+	–
Teicoplanin (MIC, $\mu\text{g ml}^{-1}$)	0.029 \pm 0.007	0.25–0.5	0.25–0.5
Vancomycin (MIC, $\mu\text{g ml}^{-1}$)	0.482 \pm 0.059	4–8	4–8
Major CFA beside 14:0 FAME	18:0 DMA	16:0 DMA	16:0 DMA

*Strain SRB-521-5-I^T was analysed by microscopic observation after Schaeffer-Fulton staining.

Etest strips were used per plate (with antimicrobial gradients in opposing directions) and bacteria were left to grow. The MIC values were read directly from the strips after 48 h of

incubation in a Don Whitley miniMACS anaerobic workstation (N₂/H₂/CO₂ 80:10:10). The range of concentrations tested was 0.016–256 $\mu\text{g ml}^{-1}$ for all antibiotics except

ciprofloxacin (0.002–32 µg ml⁻¹). Three independent repeats of duplicate experiments were carried out for each antibiotic. MIC breakpoints (µg ml⁻¹) were expressed as means ± SEM (*n*=6): cefotaxime, 0.029 ± 0.009; ciprofloxacin, 22.667 ± 4.341; clindamycin, 0.022 ± 0.005; colistin, 30.667 ± 4.341; erythromycin, 0.099 ± 0.015; metronidazole, <0.016; oxacillin, 0.750 ± 0.091; teicoplanin, 0.029 ± 0.007; tetracycline, 6.167 ± 0.910; tobramycin, 1.417 ± 0.369; vancomycin, 0.482 ± 0.059. Thus, the cationic cyclic polypeptide colistin, which interacts with the cytoplasmic membrane of Gram-negative bacteria, failed to inhibit the growth of strain SRB-521-5-I^T at concentrations <30 µg ml⁻¹. Ciprofloxacin, a broad-spectrum quinolone antibiotic that inhibits bacterial cell division, also showed a relatively high MIC. The broad-spectrum antibiotic tetracycline, which inhibits protein synthesis by binding to the 30S subunit of ribosomes, showed an intermediate resistance profile according to the CLSI standard M100-S22 (<4 µg ml⁻¹, sensitive; 8 µg ml⁻¹, intermediate). Similarly to its closest phylogenetically related species (Carlier *et al.*, 2010), strain SRB-521-5-I^T was susceptible to the glycopeptide teicoplanin. However, the isolate appeared to be more sensitive to the glycopeptide vancomycin than *F. plautii* and *P. capillosus* (0.5 versus 4–8 µg ml⁻¹), which is common for most Gram-positive bacteria.

Finally, because *F. plautii* is known as a flavonoid-converting bacterium (Schoefer *et al.*, 2003; Carlier *et al.*, 2010), we tested the ability of strain SRB-521-5-I^T to metabolize 16 flavonoid compounds (apigenin, apigenin-7-glucoside, daidzein, eriodictyol, genistein, luteolin, luteolin-3-, 5- and 7-glucoside, naringenin, naringenin-7-neohesperosid, phloretin, phloridzin, quercetin, rutin and taxifolin) by means of batch culture fermentation followed by liquid chromatography analysis, as described previously (Schoefer *et al.*, 2003). In contrast to *F. plautii*, the new isolate was not able to convert any of the flavonoids tested. Template chromatograms showing the conversion of eriodictyol and luteolin by *F. plautii* compared with strain SRB-521-5-I^T are provided in Fig. S6.

Based on the aforementioned genotypic and phenotypic traits, we propose that strain SRB-521-5-I^T represents a novel species of a new bacterial genus, for which the name *Intestinimonas butyriciproducens* gen. nov., sp. nov. is proposed. Transmission electron microscopy did not show a typical Gram-negative structure of the cell wall in cells of strain SRB-521-5-I^T. Taken together with the ability to form spores and the sensitivity towards vancomycin, the strain appears to be Gram-positive, although cells stain Gram-negative. Features that help distinguishing strain SRB-521-5-I^T from related species are summarized in Table 2.

Description of *Intestinimonas* gen. nov.

Intestinimonas [In.tes.ti.ni.mo'nas. L. n. *intestinum* gut, intestine; L. fem. n. *monas* a monad, unit; N.L. fem. n. *Intestinimonas* a unit (bacterium) isolated from the intestine].

Phylogenetically related to members of the genera *Flavonifractor* and *Pseudoflavonifractor* within the order

Clostridiales, phylum *Firmicutes*. Gram-positive, strictly anaerobic, grow well at 25–45 °C and form terminal or subterminal endospores. Motility is not observed. Major fermentation products in WCA broth are butyrate and acetate. CFAs are mostly saturated (91.9%), including C_{14:0} methyl ester and C_{18:0} dimethyl acetal as the two major fatty acids. Respiratory quinones are not detected. The type species is *Intestinimonas butyriciproducens*.

Description of *Intestinimonas butyriciproducens* gen. nov., sp. nov.

Intestinimonas butyriciproducens (bu.ty.ri.ci.pro.du'cens. N.L. n. *acidum butyricum* butyric acid; L. part. adj. *producens* producing; N.L. part. adj. *butyriciproducens* producing butyric acid).

Has the following characteristics in addition to those given for the genus. After 48 h of growth on reduced WCA agar, colonies are pinpoint to 1 mm in diameter, circular, entire, opaque, white, shiny and convex. Cells are straight fusiform rods (0.5 × 2–5 µm) that may be elongated and curved after 7 days of growth at 45 °C. They occur mostly singly or sometimes in pairs. Positive for *N*-acetyl-D-glucosamine, dextrin, D-galactose, α-D-glucose, glucose 6-phosphate, maltotriose, 3-methyl D-glucose, D-sorbitol, turanose, β-hydroxybutyric acid, DL-lactic acid, D-lactic acid methyl ester, pyruvic acid, pyruvic acid methyl ester, L-serine, L-threonine, 2'-deoxyadenosine, inosine, thymidine, uridine, thymidine 5'-monophosphate and uridine 5'-monophosphate. Negative for all other substrates in the Biolog AN plate. Does not metabolize flavonoids. Contains diphosphatidylglycerol, eight glycolipids, six phosphoglycolipids, six phospholipids and three unidentified lipids. Shows intermediate resistance towards the antibiotics ciprofloxacin, colistin and tetracycline.

The type strain, SRB-521-5-I^T (=DSM 26588^T=CCUG 63529^T), was isolated from the caecal content of a 17-week-old female heterozygous TNF^{deltaARE} C57BL/6 mouse. The DNA G + C content of the type strain is 58.4 mol%.

Acknowledgements

The heterozygous TNF^{deltaARE} mouse model of ileitis was a generous gift from Dr George Kollias (Biomedical Sciences Research Centre Alexander Fleming, Vari, Greece). We are grateful to: Professor J. P. Euzéby (Ecole Nationale Vétérinaire, Toulouse, France) for his help with etymology; Sabine Schmidt and Bärbel Gruhl (DIFE), Caroline Ziegler and Simone Daxauer (TUM) for technical assistance; co-workers of the DSMZ for contributing to the phenotypic characterization of strain SRB-521-5-I^T; and Tiny Franssen-Verheijen (Laboratory of Virology, Wageningen University, The Netherlands) for transmission electron microscopy. This research has been financially supported by ERC grant 250172 – Microbes Inside. We thank Willem M. deVos for valuable advice.

References

Altschul, S. F., Gish, W., Miller, W., Myers, E. W. & Lipman, D. J. (1990). Basic local alignment search tool. *J Mol Biol* 215, 403–410.

- Bäckhed, F., Ding, H., Wang, T., Hooper, L. V., Koh, G. Y., Nagy, A., Semenkovich, C. F. & Gordon, J. I. (2004). The gut microbiota as an environmental factor that regulates fat storage. *Proc Natl Acad Sci U S A* **101**, 15718–15723.
- Bokkenheuser, V. D., Winter, J., Dehazya, P. & Kelly, W. G. (1977). Isolation and characterization of human fecal bacteria capable of 21-dehydroxylating corticoids. *Appl Environ Microbiol* **34**, 571–575.
- Brill, J. A. & Wiegel, J. (1997). Differentiation between spore-forming and asporogenic bacteria using a PCR and Southern hybridization based method. *J Microbiol Methods* **31**, 29–36.
- Carlier, J. P., Bedora-Faure, M., K'ouas, G., Alauzet, C. & Mory, F. (2010). Proposal to unify *Clostridium orbiscindens* Winter *et al.* 1991 and *Eubacterium plautii* (Séguin 1928) Hofstad and Aasjord 1982, with description of *Flavonifractor plautii* gen. nov., comb. nov., and reassignment of *Bacteroides capillosus* to *Pseudoflavonifractor capillosus* gen. nov., comb. nov. *Int J Syst Evol Microbiol* **60**, 585–590.
- Clavel, T., Doré, J. & Blaut, M. (2006a). Bioavailability of lignans in human subjects. *Nutr Res Rev* **19**, 187–196.
- Clavel, T., Henderson, G., Engst, W., Doré, J. & Blaut, M. (2006b). Phylogeny of human intestinal bacteria that activate the dietary lignan secoisolariciresinol diglucoside. *FEMS Microbiol Ecol* **55**, 471–478.
- Clavel, T., Lippman, R., Gavini, F., Doré, J. & Blaut, M. (2007). *Clostridium saccharogumia* sp. nov. and *Lactonifactor longoviformis* gen. nov., sp. nov., two novel human faecal bacteria involved in the conversion of the dietary phytoestrogen secoisolariciresinol diglucoside. *Syst Appl Microbiol* **30**, 16–26.
- Clavel, T., Charrier, C., Braune, A., Wenning, M., Blaut, M. & Haller, D. (2009). Isolation of bacteria from the ileal mucosa of TNF^{deltaARE} mice and description of *Enterorhabdus mucosicola* gen. nov., sp. nov. *Int J Syst Evol Microbiol* **59**, 1805–1812.
- Clavel, T., Saalfrank, A., Charrier, C. & Haller, D. (2010). Isolation of bacteria from mouse caecal samples and description of *Bacteroides sartorii* sp. nov. *Arch Microbiol* **192**, 427–435.
- Derrien, M., Vaughan, E. E., Plugge, C. M. & de Vos, W. M. (2004). *Akkermansia muciniphila* gen. nov., sp. nov., a human intestinal mucin-degrading bacterium. *Int J Syst Evol Microbiol* **54**, 1469–1476.
- Hanske, L., Loh, G., Sczesny, S., Blaut, M. & Braune, A. (2010). Recovery and metabolism of xanthohumol in germ-free and human microbiota-associated rats. *Mol Nutr Food Res* **54**, 1405–1413.
- Hörmannspenger, G., Clavel, T. & Haller, D. (2012). Gut matters: microbe–host interactions in allergic diseases. *J Allergy Clin Immunol* **129**, 1452–1459.
- Kontoyiannis, D., Pasparakis, M., Pizarro, T. T., Cominelli, F. & Kollias, G. (1999). Impaired on/off regulation of TNF biosynthesis in mice lacking TNF AU-rich elements: implications for joint and gut-associated immunopathologies. *Immunity* **10**, 387–398.
- Leser, T. D., Amenuvor, J. Z., Jensen, T. K., Lindecrona, R. H., Boye, M. & Møller, K. (2002). Culture-independent analysis of gut bacteria: the pig gastrointestinal tract microbiota revisited. *Appl Environ Microbiol* **68**, 673–690.
- Levine, U. Y., Looft, T., Allen, H. K. & Stanton, T. B. (2013). Butyrate-producing bacteria, including mucin degraders, from the swine intestinal tract. *Appl Environ Microbiol* **79**, 3879–3881.
- Li, E., Hamm, C. M., Gulati, A. S., Sartor, R. B., Chen, H., Wu, X., Zhang, T., Rohlf, F. J., Zhu, W. & other authors (2012). Inflammatory bowel diseases phenotype, *C. difficile* and NOD2 genotype are associated with shifts in human ileum associated microbial composition. *PLoS ONE* **7**, e26284.
- Manach, C., Williamson, G., Morand, C., Scalbert, A. & Rémésy, C. (2005). Bioavailability and bioefficacy of polyphenols in humans. I. Review of 97 bioavailability studies. *Am J Clin Nutr* **81** (Suppl), 230S–242S.
- Pfeiffer, N., Desmarchelier, C., Blaut, M., Daniel, H., Haller, D. & Clavel, T. (2012). *Acetatifactor muris* gen. nov., sp. nov., a novel bacterium isolated from the intestine of an obese mouse. *Arch Microbiol* **194**, 901–907.
- Postgate, J. R. (1963). Versatile medium for the enumeration of sulfate-reducing bacteria. *Appl Microbiol* **11**, 265–267.
- Qin, J., Li, R., Raes, J., Arumugam, M., Burgdorf, K. S., Manichanh, C., Nielsen, T., Pons, N., Levenez, F. & other authors (2010). A human gut microbial gene catalogue established by metagenomic sequencing. *Nature* **464**, 59–65.
- Ridlon, J. M., Kang, D. J. & Hylemon, P. B. (2006). Bile salt biotransformations by human intestinal bacteria. *J Lipid Res* **47**, 241–259.
- Roberfroid, M. (2007). Prebiotics: the concept revisited. *J Nutr* **137** (Suppl 2), 830S–837S.
- Saitou, N. & Nei, M. (1987). The neighbor-joining method: a new method for reconstructing phylogenetic trees. *Mol Biol Evol* **4**, 406–425.
- Schneider, H., Schwartz, A., Collins, M. D. & Blaut, M. (1999). Anaerobic transformation of quercetin-3-glucoside by bacteria from the human intestinal tract. *Arch Microbiol* **171**, 81–91.
- Schoefer, L., Mohan, R., Schwartz, A., Braune, A. & Blaut, M. (2003). Anaerobic degradation of flavonoids by *Clostridium orbiscindens*. *Appl Environ Microbiol* **69**, 5849–5854.
- Tamura, K., Peterson, D., Peterson, N., Stecher, G., Nei, M. & Kumar, S. (2011). MEGA5: molecular evolutionary genetics analysis using maximum likelihood, evolutionary distance, and maximum parsimony methods. *Mol Biol Evol* **28**, 2731–2739.
- Tissier, H. (1908). Recherches sur la flore intestinale normale des enfants âgés d'un an à cinq ans. *Ann Inst Pasteur (Paris)* **22**, 189–208.
- Turnbaugh, P. J., Hamady, M., Yatsunenko, T., Cantarel, B. L., Duncan, A., Ley, R. E., Sogin, M. L., Jones, W. J., Roe, B. A. & other authors (2009). A core gut microbiome in obese and lean twins. *Nature* **457**, 480–484.
- Werner, T., Wagner, S. J., Martínez, I., Walter, J., Chang, J. S., Clavel, T., Kisting, S., Schuermann, K. & Haller, D. (2011). Depletion of luminal iron alters the gut microbiota and prevents Crohn's disease-like ileitis. *Gut* **60**, 325–333.
- Winter, J., Popoff, M. R., Grimont, P. & Bokkenheuser, V. D. (1991). *Clostridium orbiscindens* sp. nov., a human intestinal bacterium capable of cleaving the flavonoid C-ring. *Int J Syst Bacteriol* **41**, 355–357.
- Wright, E. S., Yilmaz, L. S. & Noguera, D. R. (2012). DECIPHER, a search-based approach to chimera identification for 16S rRNA sequences. *Appl Environ Microbiol* **78**, 717–725.

PAPER 7

Fetal Exposure to Maternal Inflammation Does Not Affect Postnatal Development of Genetically-Driven Ileitis and Colitis

Jana Hemmerling^{1,2}, Katharina Heller^{1,2}, Gabriele Hörmannspurger^{1,2}, Monika Bazanella^{1,2}, Thomas Clavel^{1,2}, George Kollias³, Dirk Haller^{1,2*}

1 Chair of Nutrition and Immunology, Technische Universität München, Freising- Weihenstephan, Bavaria, Germany, **2**ZIEL - Research Center for Nutrition and Food Sciences, Freising-Weihenstephan, Bavaria, Germany, **3**Biomedical Sciences Research Centre, Institute for Immunology, Alexander Fleming, Vari, Athens, Greece

Abstract

Background: Chronic inflammatory disorders have been increasing in incidence over the past decades following geographical patterns of industrialization. Fetal exposure to maternal inflammation may alter organ functions and the offspring's disease risk. We studied the development of genetically-driven ileitis and colitis in response to maternal inflammation using mouse models.

Methods: Disease susceptible ($Tnf^{AARE/+}$ and $IL10^{-/-}$) and disease-free ($Tnf^{+/+}$ and $IL10^{-/+}$) offspring were raised in inflamed and non-inflamed dams. Ileal, caecal and colonic pathology was evaluated in the offspring at 8 or 12 weeks of age. Ly6G-positive cells in inflamed sections from the distal ileum and distal colon were analysed by immunofluorescence microscopy. Gene expression of pro-inflammatory cytokines was measured in whole tissue specimens by quantitative PCR. Microarray analyses were performed on laser microdissected intestinal epithelium. Caecal bacterial communities were assessed by Illumina sequencing of 16S rRNA amplicons.

Results: Disease severity, the number of infiltrated neutrophils as well as *Tnf* and *Il12p40* mRNA expression were independent of maternal inflammation in the offspring of mouse models for ileitis ($Tnf^{AARE/+}$) and colitis ($IL10^{-/-}$). Although TNF-driven maternal inflammation regulated 2,174 (wild type) and 3,345 ($Tnf^{AARE/+}$) genes in the fetal epithelium, prenatal gene expression patterns were completely overwritten after birth. In addition, co-housing experiments revealed no change in phylogenetic diversity of the offspring's caecal microbiota in response to maternal inflammation. This is independent of the offspring's genotype before and after the onset of tissue pathology.

Conclusions: Disease risk and activity in mouse models of chronic ileitis and colitis was independent of the fetal exposure to maternal inflammation. Likewise, maternal inflammation did not alter the diversity and composition of offspring's caecal microbiota, clearly demonstrating that changes of the gene expression program in the fetal gut epithelium were not relevant for the development of chronic inflammatory disorders in the gut.

Citation: Hemmerling J, Heller K, Hörmannspurger G, Bazanella M, Clavel T, et al. (2014) Fetal Exposure to Maternal Inflammation Does Not Affect Postnatal Development of Genetically-Driven Ileitis and Colitis. PLoS ONE 9(5): e98237. doi:10.1371/journal.pone.0098237

Editor: Mathias Chamaillard, INSERM, France

Received: December 28, 2013; **Accepted:** April 29, 2014; **Published:** May 21, 2014

Copyright: © 2014 Hemmerling et al. This is an open-access article distributed under the terms of the Creative Commons Attribution License, which permits unrestricted use, distribution, and reproduction in any medium, provided the original author and source are credited.

Funding: This work was supported by the 'Nutritional Adaptation and Epigenetic Mechanisms' program of ZIEL - Research Center for Nutrition and Food Sciences. The funders had no role in study design, data collection and analysis, decision to publish, or preparation of the manuscript.

Competing Interests: The authors have declared that no competing interests exist.

* E-mail: Dirk.Haller@tum.de.

Introduction

Lifestyle changes in industrialized countries are associated with a sharp increase in the incidence of immune-mediated chronic pathologies such as inflammatory bowel diseases (IBD), multiple sclerosis or type-1 diabetes. Th1-driven inflammatory processes are key mechanisms in the pathogenesis of these chronic pathologies[1]. IBD are spontaneously relapsing, immunologically mediated disorders of the gastrointestinal tract[2]. Although the pathogenesis of these multifactorial diseases is still not fully understood, the combination of genetic predisposition[3] and environmental factors (microbiota, diet and lifestyle)[4] drives disease development. Apart from the major impact of IBD on life quality of the affected patients, epidemiological studies link

Crohn's disease (CD) activity during pregnancy to adverse outcomes such as preterm birth, spontaneous abortion and labor complications[5,6]. This is not clear in the context of ulcerative colitis.

Despite the fact that alterations of the cytokine milieu during CD-associated pregnancy lead to peri- and postnatal complications[6–8], the transmission of maternal inflammation to the offspring with consequences for later disease susceptibility, severity or phenotype is completely unknown. A potential impact of inflammatory processes during pregnancy on fetal organ functions was recently shown for endotoxin-induced chorioamnionitis[9]. In this context, the maturation of the fetal gut barrier was prevented [10]. Furthermore, maternal exposure to high-fat diet was recently

reported to induce intestinal inflammation in fetal sheep, suggesting that even low grade maternal inflammation might affect intestinal functions and IBD susceptibility in the offspring[11]. Maternally transmitted compositional changes of the microbiota might be an important factor that contributes to this influence on disease susceptibility in the offspring [12].

In this context, we asked the question whether chronic maternal inflammation is a risk factor for postnatal disease susceptibility in the normal and genetically susceptible host. We applied sophisticated breeding systems with heterozygous $Tnf^{ARE/+}$ and homozygous $IL10^{-/-}$ mice to generate genetically-driven inflammatory disease environments *in utero* in two well-established models of chronic ileitis and colitis, enabling us to study the role of maternal inflammation on postnatal disease onset. Exemplarily, we took also advantage of the $Tnf^{ARE/+}$ model with ileitis to assess transcriptional profiling of fetal and postnatal intestinal epithelial cells (IEC) obtained by laser microdissection in order to provide high resolution of cellular specificity at this disease relevant interface. This second objective fits with the hypothesis that the pathogenesis of CD is characterized by a failure of innate immune mechanisms to recognize microbial triggers at the early stage of disease development[4]. Selective overexpression of TNF in the intestinal epithelium seems to be sufficient to trigger CD-like ileitis[13], suggesting an important role of the epithelium in the pathogenesis of chronic intestinal inflammation in $Tnf^{ARE/+}$ mice[14].

Thus, the aim of the present study was to characterize the role of genetically-driven maternal inflammation in programming the fetal epithelium towards postnatal development of intestinal inflammation.

Materials and Methods

Ethics Statement

Mouse experiments were performed between 2009 and 2011 in accordance to the German guidelines for animal care (Regierung von Oberbayern, Bavaria, Germany). No animal approval was obtained, because no intervention was performed with living mice. All mice were reported as mice “sacrificed for research purposes” at the Regierung von Oberbayern.

Animals and Experimental Design

All mice were conventionally housed in groups of 3–5 mice per cage at a 12 h light/dark cycle at 24–26°C. They received fresh tap water and breeding diet (Ssniff Chow) ad libitum and were sacrificed by neck dislocation. $Tnf^{ARE/+}$ (ARE) dams were bred with $Tnf^{+/+}$ wildtype (WT) sires (C57BL/6N genetic background) and vice versa (n = 5–10 breeding pairs), generating offspring from healthy WT dams (WT and ARE) and inflamed ARE dams (iWT and iARE) (Figure 1A) (n = 5 each). The period of conception was set from 8–12 weeks in order to avoid suffering in genetically susceptible ARE dams. Dams were sacrificed at an average age of 13 weeks \pm 5 d (WT dams) and 11 weeks \pm 1 d (ARE dams) for the prenatal time point and at 17 weeks \pm 1 d (WT dams) and 14 weeks \pm 3 d (ARE dams) for the weaning time point (3 weeks after giving birth). Offspring were sacrificed at the age of 17.5 days post conception (dpc), 3 (weaning) and 8 weeks by neck dislocation. Morphological criteria of fetuses at 17.5 dpc were evaluated according to Theiler stage 25 (TS25) based on the onset of skin wrinkling, whiskers and eyelid closure. Placentas and offspring's gut were embedded in Optimal Cutting Temperature (O.C.T.) matrix (Sakura Finetek, Torrance, USA) and stored at -80°C until laser microdissection of intestinal epithelial cells and subsequent microarray experiments.

For co-housing experiments, ARE and WT dams were kept together in one cage to generate mixed beddings from the age of 4 weeks. From week 8 on, dams were mated with WT males overnight only until pregnancy was observed. During the day, dams were co-housed again. After giving birth, beddings of ARE and WT dams and litters were exchanged to create a synchronized environment independent of the dam's genotype, so as to be able to analyse only the effect of inflammation *in utero* on shaping gut bacterial colonization. Dams and offspring were sacrificed before weaning, *i.e.*, 3 weeks after birth.

Female $IL10^{-/-}$ were bred with male $IL10^{+/+}$ (both on the 129Sv/Ev genetic background) and vice versa (n = 5–6 each), generating offspring (n = 5–15 each) from healthy $IL10^{+/+}$ dams ($IL10^{+/+}$, $IL10^{-/-}$) or inflamed $IL10^{-/-}$ dams (i $IL10^{+/+}$, i $IL10^{-/-}$) (Figure 1B). The breeding period was set between 15–21 weeks. Dams were sacrificed at weaning at an average age of 25 \pm 2 weeks ($IL10^{-/-}$ dams) and 27 \pm 4 weeks ($IL10^{+/+}$ dams). $IL10^{-/-}$ dams showing a total colitis score of at least 2 (0–12) (Figure 1 D) were considered as inflamed and the offspring was included in the analysis. Offspring were sacrificed at the age of 12 weeks by neck dislocation in order to blindly determine histological colitis scores.

Histopathology

Scoring was performed on 10% formalin-fixed paraffin-embedded or cryo-fixed tissue for the postnatal or prenatal time point, respectively. The histological score was ascertained in a blinded fashion on H&E-stained transversal sections of the terminal ileum (WT, iWT, ARE, iARE) or of the cecum tip, proximal colon and distal colon ($IL10^{+/+}$, $IL10^{-/-}$, i $IL10^{+/+}$, i $IL10^{-/-}$), resulting in a score from 0 (non-inflamed) to 12 (highly inflamed) per section as previously described[15]. The total colitis score per mouse was determined by calculating the mean of all three colonic compartments.

Plasma Measurements of Maternal Tumor Necrosis Factor

Plasma TNF was measured using Mouse TNF alpha ELISA Ready -SET-Go! ELISA, according to the manufacturer's instructions (eBioscience, San Diego, USA). A volume of 100 μl total plasma was incubated on a pre-coated plate for 2 h at RT (room temperature), followed by incubation of anti-TNF detection antibody linked with Avidin/Biotin. HRP-conjugated antibody was incubated for 30 min and substrate conversion was stopped after 15 min with 2N H_2SO_4 . The product absorbance of standard dilutions and plasma sample was measured at 405 nm to the reference wavelength of 570 nm. Quantification was performed using the linear equation of the standard dilutions.

Immunofluorescence Staining of Ly6G and REG3B in the Intestine

Transversal sections (5 μm thick) were cut from either formalin-fixed paraffin embedded (FFPE) or from frozen distal ileum or colon and transferred onto Superfrost Plus slides (Thermo Scientific, Braunschweig, Germany). After deparaffinization of FFPE tissue (Leica ST5020 Multistainer system), antigen demasking was performed by boiling in 1 \times sodium citrate buffer (pH 6, 900 W, 23 min). After cool down to RT, slides were washed 3 times in dH₂O for 5 min, followed by 5 min in PBS. Frozen sections were equilibrated to room temperature (30 min), fixed in ice cold acetone (-20°C) for 10 min, followed by 30 min air drying at RT and 3 times 5 min washing in PBS. Sections were blocked with 50 μl blocking buffer raised against the species of the secondary antibody for 60 min at RT in a humidified chamber.

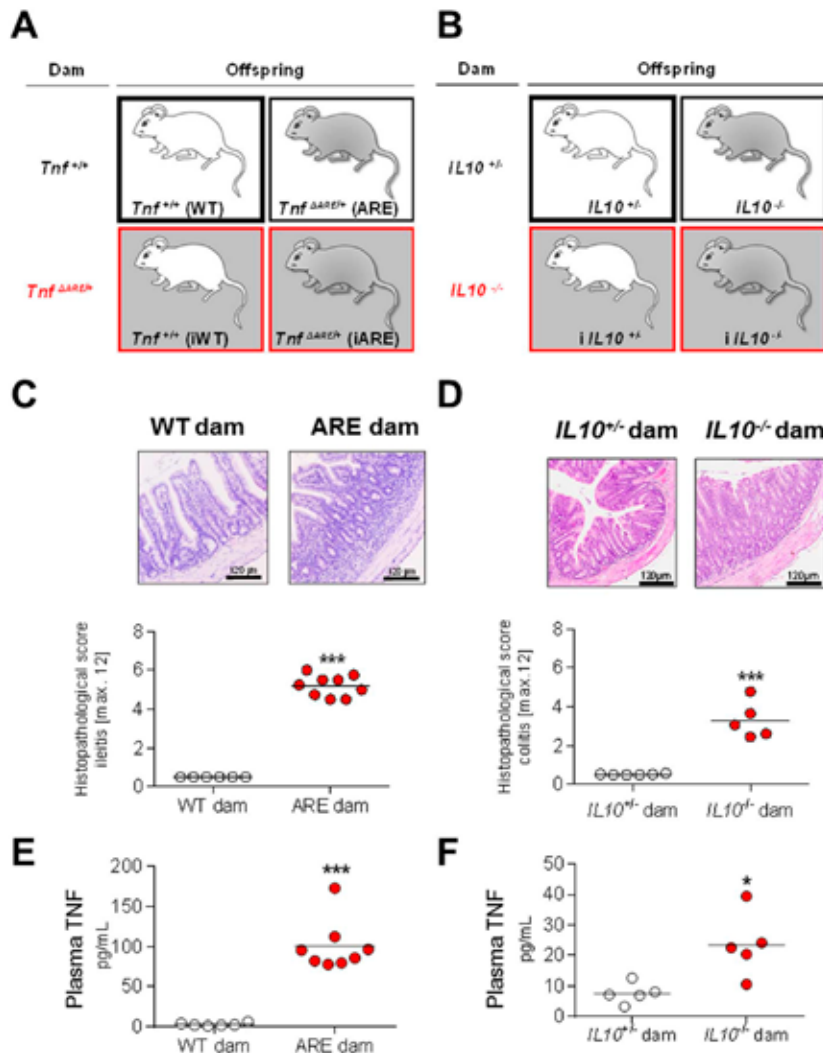


Figure 1. Breeding schemes and the maternal inflammatory environment. Breeding schemes of TNF- (A) and IL10-driven (B) maternal inflammation. Offspring developed under non inflamed conditions (white background: white mouse = WT or *IL10*^{+/-}; grey mouse = ARE or *IL10*^{-/-}) and under maternal inflammation (grey background: white mouse = iWT or *IL10*^{+/-}; grey mouse = iARE or *IL10*^{-/-}). (C) Representative H&E-stained transversal sections of the distal ileum and individual plots of ileitis score in WT (n = 6) and ARE (n = 8) dams. (D) Total colitis score in *IL10*^{+/-} (n = 8) and *IL10*^{-/-} dams (n = 8) and representative H&E-stained sections of distal colon from non-inflamed *IL10*^{+/-} and inflamed *IL10*^{-/-} dams. Scores [0, not inflamed, to 12, highly inflamed] were determined using tissue sections from dams sacrificed 3 weeks after giving birth. TNF in maternal plasma indicates that the inflammation is also systemically relevant in both the ileitis (E) and colitis (F) models. Individual data and means are shown; t-test, **p* < 0.05, ****p* < 0.001.

doi:10.1371/journal.pone.0098237.g001

Primary antibody against Ly6G (rat-anti-Ly6G, BD Pharmingen, 1:500) was incubated overnight at 4°C. Primary antibody against REG3B (sheep- anti-REG3B, R&D Systems, 1:100 dilution) was incubated at RT for 1–3 hours in a humidified chamber. Fluorochrome-conjugated secondary antibodies, namely goat anti-rat IgG (H+L) Alexa Fluor 546 (Invitrogen) or donkey anti-sheep IgG (H+L) DyLight 488 (Jackson ImmunoResearch), were diluted 1:200 and incubated for 1 h at RT. Nuclei were counterstained using DAPI (1:2000) in secondary antibody solution. Sections were visualized using a confocal microscope (Olympus Fluoview 1000 using the FV10-ASW software). The

amount of Ly6G positive cells per area was counted using the Volocity 5.51 software (Perkin Elmer) defining the lamina propria as region of interest. For each individual mouse, 3 microscopic fields at a 600-fold magnification were quantified for mean Ly6G-positive cells per mm². Immunofluorescence intensity of REG3B was quantified with Volocity Demo 5.5 software (Perkin Elmer) defining epithelial cells as region of interest. For each individual mouse 3 different areas were quantified as mean intensity of the fluorescence signal per μm².

Gene Expression Analysis of Whole Gut Tissue and Laser Microdissected IEC

RNA from cryosections of distal ileum (3 sections of 10 μm each) and colonic swiss rolls (2 sections of 10 μm each) was isolated using the RNA isolation kit according to the manufacturer's instructions (Macherey & Nagel). Reverse transcription was performed using SuperScript III Reverse Transcriptase (Invitrogen). RNA of laser microdissected IEC (10 ng) was preamplified with the QuantiTect Whole Transcriptome Kit (Qiagen, Hilden, Germany) according to the manufacturer's instructions. Gene-specific nucleotide sequences and accession numbers were obtained from the National Center for Biotechnology Information (NCBI) website (<http://www.ncbi.nlm.nih.gov/gene>). Primer pairs (Table 1) were designed using the Universal ProbeLibrary (UPL) design center (Roche Diagnostics, Mannheim, Germany). Quantitative real-time PCR was performed on 10 ng cDNA using the LightCycler 480 System (Roche Diagnostics, Mannheim, Germany). Crossing points (Cp) were determined using the second derivative maximum method by the LightCycler 480 software release 1.5.0. Data were normalized to the Cp mean of reference genes (*Gapdh* for whole gut tissue and *18s*, *Rpl13a* and *Gapdh* for pre-amplified cDNA of IEC) and expressed as $2^{-\Delta\text{Ct}}$ values in order to compare expression levels among all groups.

Laser Microdissection (LMD) Microscopy of Intestinal Epithelial Cells

Ileal cryo-sections (Microm, Walldorf, Germany) were generated at -20°C . PET frame slides (MicroDissect, Herborn, Germany) were treated with RNase ZAP (Sigma-Aldrich, Steinheim, Germany) before use and dried at RT. Transversal sections (10 μm) were mounted on slides, air-dried and stored at -80°C for short periods of time (<7 d) until use. Each slide was stained directly before LMD microscopy. Briefly, after equilibration to RT (2 min), slides were fixed for 1 min with 70%(v/v) EtOH, rinsed with Diethylpyrocarbonate (DEPC) water for 30 sec, stained with Harris hematoxylin for 1 min and rinsed with DEPC water for 30 sec. After bluing with 0.1% (v/v) NH_4OH for 30 sec, slides were counterstained with 2.5% Eosin for 2 min. Finally, sections were dehydrated in ascending EtOH series (96%, 100%) for 30 sec each and air dried at RT for 5 min. Ileal IEC were cut at a magnification of 630 \times using the UV laser-cutting system LMD 6000 and the Leica Application Suite software (Leica, Wetzlar, Germany). Lysis buffer (100 μl) supplied in the AllPrep DNA/RNA Micro Kit (Qiagen, Hilden, Germany) was added to epithelial pieces directly after dissection. Samples were kept frozen at -80°C until DNA/RNA isolation. In total, a

mean area of $1.330\pm 0.024\times 10^6 \mu\text{m}^2$ IECs was collected per sample (Figure S1).

RNA Isolation and Quality Control

Total RNA was isolated using the column-based AllPrep DNA/RNA Micro Kit (Qiagen, Hilden, Germany). RNA concentration was measured using the Quant-iT RiboGreen RNA Assay Kit (Invitrogen, Eugene, USA). RNA integrity was determined using the RNA 6000 Pico Kit and the Bioanalyzer 2100 (Agilent, Waldbronn, Germany). An amount of 50 ng total RNA (3 μl sample volume adjusted by vacuum centrifugation) was used for microarray analysis.

Microarray-based Gene Expression Analysis

Microarray analysis was performed with ileal IEC from 17.5 *dpc* and 8-week-old mice ($n = 20$ in total). All samples from one time point were run together. RNA preparation, reverse-transcription, amplification and biotin labeling were performed using the GeneChip 3' IVT Express kit (Affymetrix, Santa Clara, USA). Hybridization, washing and staining were performed using the GeneChip Hybridization, Wash and Stain (Affymetrix) and the GeneChip Fluidics Station 450 (Affymetrix). Labeled RNA samples were hybridized to customized murine genome Nu-GO_Mm1a520177 microarrays containing 23,865 probe sets (covering 15,313 genes, Affymetrix). Gene chips were visually inspected for irregularities and scanned with GeneChip Scanner 3000. Data were analyzed using the Affymetrix GCOS Manager software and the R- and Bioconductor-based MADMAX interface (Management and Analysis Database for Multi-platform micro-Array eXperiments, <https://madmax.bioinformatics.nl>), including R version 2.11.1, Bioconductor version 2.6 and AnnotationDbi version 1.10.2. Data were normalized using the gc Robust Multichip Average (slow) algorithm. Probe sets were annotated to the transcripts with Custom Chip Definition files version 13.0.0. (nugomm1a520177mmentrezg.cdf). No previous filtering was applied to the datasets. MADMAX calculated Fold Changes (FCs), p -values, FDR-values and q -values to the study groups with the LIMMA procedure. The LIMMA (log₂ based) FCs were calculated comparing iWT, ARE and iARE groups to the WT control group ($n = 5$ each). Genes were considered to be significantly regulated according to the raw p -value of LIMMA with $p < 0.05$ and a threshold FC of ± 1.5 . Heatmaps were generated using the MultiExperiment Viewer (TigrMEV) software. Gene Ontology (GO) terms were computed using the GeneRanker program (Genomatix, München, Germany). Over-representation of biological terms were calculated and listed in the output together with respective p -values.

Table 1. Primer sequences and UPL probe IDs for qPCR analysis.

Gene	Forward primer	Reverse primer	Probe	Amplicon
<i>Gapdh</i>	5'-tcc act cat ggc aaa ttc aa	5'-ttt gat gtt agt ggg gtc tcg	#9	108 nt
<i>Rpl13a</i>	5'-atc cct cca ccc tat gac aa	5'-gcc cca ggt aag caa act t	#108	97 nt
<i>18s</i>	5'-aaa tca gtt atg gtt cct ttg gtc	5'-gct cta gaa tta cca cag tta tcc aa	#55	67 nt
<i>C3</i>	5'-acc tta cct cgg caa gtt tct	5'-ttg tag agc tgc tgg tca gg	#76	75 nt
<i>Il12p40</i>	5'-atc gtt ttg ctg gtg tct cc	5'-gga gtc gac tcc acc tct aca	#78	80 nt
<i>Tnf</i>	5'-tgc cta tgt ctg agc ctg ttc	5'-gag gcc att tgg gaa ctt ct	#49	117 nt

Housekeeping genes are underlined.
doi:10.1371/journal.pone.0098237.t001

Illumina Sequencing of 16S rRNA Gene Amplicons from Caecal Contents

Bacterial DNA was obtained after bead beating and ethanol precipitation [16] from directly frozen caecal contents (co-housing experiment) or from caecal contents embedded in O.C.T. Amplicons of the V4 region of 16S rRNA genes were obtained after 25 PCR cycles as described previously [17]. They were sequenced in paired-end modus (PE200) using the MiSeq system (Illumina Inc., San Diego, USA). Sequences were analyzed using in-house developed pipelines partly based on UPARSE [18], the open source software package QIIME [19] and the Ribosomal Database Project [20]. Sequences were filtered at a base call accuracy of 99%. Sequences containing any ambiguous nucleotide (N character) were discarded. The presence of chimeras was checked after dereplication using UCHIME [21]. Operational taxonomic units (OTUs) were picked at a threshold of 97%. Only those OTUs occurring in at least one sample at abundances >0.5% total sequences were included in the analysis. Sequence proportions of bacterial taxa were analyzed for significant differences using F-Test followed by Benjamini-Hochberg correction for multiple testing in the R programming environment (2008, ISBN 3-900051-07-0).

Statistics

Statistical analyses were performed with SigmaPlot 11.0 using unpaired t-test, Kruskal-Wallis test followed by Dunn's multiple comparison or ANOVA followed by pairwise comparisons testing (Holm-Sidak test). Data were expressed as mean \pm SD. Differences between groups were considered significantly if p -values were <0.05 (*), <0.01 (**), <0.001 (***). Graphics were created using GraphPad Prism version 5.00 (GraphPad software, San Diego, USA).

Results

Maternal Inflammation does not Influence Postnatal Development of Intestinal Inflammation

Conventionally raised $Tnf^{ARE/+}$ (ARE) and $IL10^{-/-}$ mice were used to study the impact of maternal inflammation on the intestine in healthy and genetically susceptible offspring. As expected, all ARE dams were affected by moderate inflammation in the distal ileum (score 5.2 ± 0.5) (Figure 1C). $IL10^{-/-}$ dams showed a more heterogeneous inflammation in the large intestine and an inflammation score of 2 was set as minimal value to discriminate inflamed dams, resulting in a mean inflammatory score of 3.3 ± 0.8 for the dams that were included in the study (Figure 1D). The local inflammation in the intestine of dams was reflected systemically by significantly elevated TNF levels in the plasma of both inflamed $Tnf^{ARE/+}$ (2.9 ± 1.9 pg/mL vs. 100.0 ± 31.6 pg/mL) and $IL10^{-/-}$ mice (7.6 ± 3.3 pg/mL vs. 23.5 ± 10.4 pg/mL) (Figures 1E and F). The abundance of plasma TNF significantly correlated with the inflammation grade in the intestine (data not shown). The intestinal inflammation of healthy and genetically susceptible offspring was found to be unaffected by maternal inflammation in both models at the age of 8 weeks (ileitis) and 12 weeks (colitis) (Figure 2A and B). Both, ARE and iARE mice developed moderate ileitis with comparable histological scores (4.4 ± 0.9 and 4.0 ± 0.7). Likewise, $IL10^{-/-}$ and $iIL10^{-/-}$ offspring showed similar histological grades of colitis (3.0 ± 1.1 and 2.7 ± 1.1). There was no correlation between maternal and offspring's intestinal inflammation (data not shown). Additionally, the number of infiltrated Ly6G-positive cells into inflamed tissue of the distal ileum of $Tnf^{ARE/+}$ offspring or the distal colon of $IL10^{-/-}$ offspring was unaffected by maternal inflammation (ARE

vs. iARE: 473 ± 262 cells/mm² vs. 621 ± 434 cells/mm²; $IL10^{-/-}$ vs. $iIL10^{-/-}$: 521 ± 454 cells/mm² vs. 497 ± 441 cells/mm²) (Figures 2C and D). The variation of neutrophil numbers in the distal colon of $IL10^{-/-}$ was strongly associated ($r=0.82$, $p<0.0001$) with histological scores in the distal colon, which showed high heterogeneity (total colitis score from 0.6 to 8.8). The fact that histological scores were not affected by maternal inflammation was supported by unchanged mRNA expression of pro-inflammatory cytokines in whole gut sections from the distal ileum ($Tnf^{ARE/+}$) and colonic swiss rolls ($IL10^{-/-}$) between the different offspring groups (Figures 2E and F). In other words, Tnf and $Il12p40$ mRNA levels were not altered between ARE and iARE or $IL10^{-/-}$ and $iIL10^{-/-}$, but were significantly increased between WT and ARE or $IL10^{+/-}$ and $IL10^{-/-}$ offspring. All these data consistently show that maternal inflammation does not impact genetically-driven disease phenotypes in both mouse models of intestinal inflammation. In addition, these results raised the question of whether there is any early transcriptional programming effect on the offspring's epithelium that is induced by maternal inflammation.

Transcriptional Fingerprints of the Fetal Epithelium in Response to Maternal Inflammation do not Persist in Grownup Mice

Selective overexpression of TNF in the intestinal epithelium is sufficient to trigger CD-like ileitis [13], suggesting an important role of the epithelium in the pathogenesis of chronic intestinal inflammation in $Tnf^{ARE/+}$ mice. Furthermore, TNF plays a pivotal role in the development of CD, which has been effectively treated with anti-TNF agents [22]. To further characterize the role of maternal inflammation on the offspring's intestinal homeostasis, we focused on the impact of maternal inflammation on IEC. Since $IL10^{-/-}$ dams and offspring showed variable degrees of disease severity along the large intestine, we focused on offspring from $Tnf^{ARE/+}$ and $Tnf^{+/+}$ mice to perform this more detailed cell-specific analysis. Therefore, we measured gene expression profiles in IEC at pre- (17.5 *dpc*) and postnatal (8 weeks) time points using laser dissected ileal epithelium. Randomly selected fetuses of different stages (15–19 *dpc*) are shown in Figure 3A. At 17.5 *dpc*, fetuses had comparable sizes, but body weight was decreased in iARE compared to ARE fetuses (Figure 3B). Equivalent surface areas of laser microdissected IEC were collected in all groups (Figure S1A). RNA integrity numbers (RIN) were 5.0 ± 0.8 and 5.5 ± 1.2 for fetal and postnatal RNA, respectively.

Gene expression profiles showed two distinct patterns according to maternal and postnatal inflammation (GEO data base accession number GSE44433). In fetal IEC, gene expression was highly influenced by maternal inflammation with 2,174 and 3,345 significantly regulated genes in iWT and iARE progeny, respectively (Figure 3C). Heatmap comparisons showed similar patterns in iWT and iARE, indicating that similar genes were regulated under conditions of maternal inflammation (1,614 common genes) (Figure 3D, Table 2). The 5 most up- and down-regulated genes at pre- and postnatal time points are shown in Table 3. *Reg3b* (regenerating islet-derived 3 beta) and *Fabp6* (fatty acid binding protein 6) were identified among the top-regulated genes under maternal inflammation. The fetal ARE genotype was apparently not relevant at this early gut developmental stage (only 117 regulated genes). In contrast to the fetal stage, gene expression profiles in postnatal IEC were highly influenced by the ARE genotype with 1,154 and 1,197 significantly regulated genes under ARE and iARE conditions, respectively (Figure 3A). Only 229 genes were significantly regulated in iWT compared to WT mice, indicating that the postnatal environment and the disease

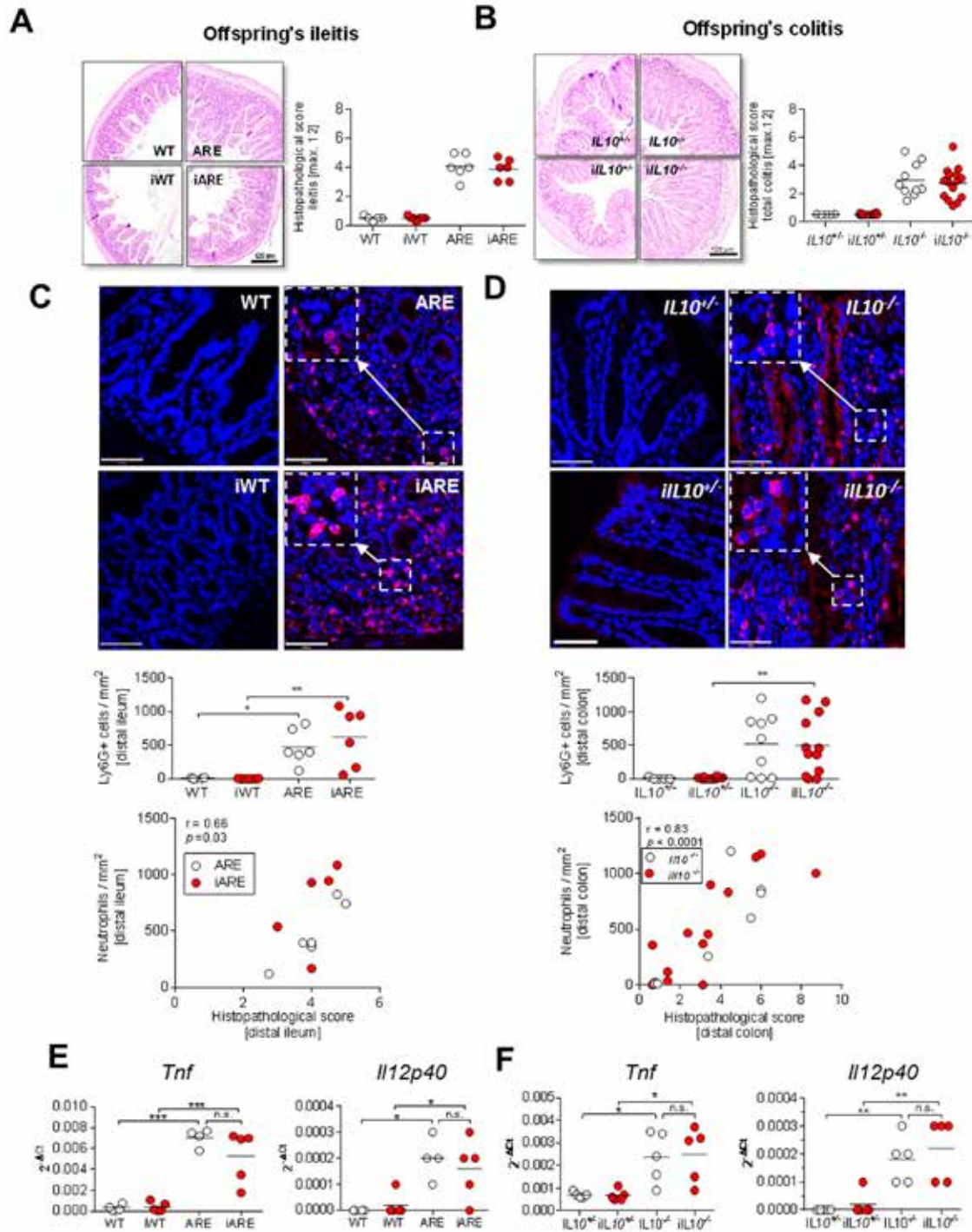


Figure 2. Postnatal tissue inflammation in *Tnf*^{ARE/+} and *IL10*^{-/-} mice is not affected by maternal inflammation. (A) Ileitis scores from WT, iWT, ARE and iARE (each n = 5–7) offspring sacrificed at 8 weeks of age with representative H&E stained sections of the distal ileum. (B) Total colitis scores from *IL10*^{-/-}, *IL10*^{+/+}, *IL10*^{-/-} and *IL10*^{+/+} offspring at 12 weeks of age (n = 5–15) with representative H&E-stained sections of the distal colon. Individual data and means are shown, *p < 0.05, *** p < 0.001 Kruskal-Wallis Test with Dunn's multiple comparisons. (C+D) Representative microscopic pictures (600× magnification) of confocal laser microscopy for Ly6G-immunofluorescence (red) from distal ileum in WT, iWT, ARE and iARE offspring and from distal colon in *IL10*^{-/-}, *IL10*^{+/+}, *IL10*^{-/-} and *IL10*^{+/+} offspring. Nuclei are counterstained with DAPI (blue). Three pictures per mouse were analyzed. Lamina propria and submucosa were defined as regions of interest. The numbers of Ly6G-positive cells per mm² from all 3

pictures per mouse were counted. Individual data and means are shown (Two-Way ANOVA, * $p < 0.05$, ** $p < 0.01$). Correlation analysis in $Tnf^{iARE/+}$ and $IL10^{-/-}$ offspring indicated strong associations between histopathological scores and infiltration of Ly6G-positive neutrophils. (E-F) Whole tissue specimens were analyzed for *Tnf* and *Il12p40* gene expression in offspring from ileitis and colitis mouse models as described in the method section. RNA was isolated from distal ileal cryosections ($3 \times 10 \mu\text{m}$) of WT, iWT, ARE and iARE offspring and from colonic swiss rolls of $IL10^{+/+}$, $IL10^{+/-}$, $IL10^{-/-}$ and $iIL10^{-/-}$ offspring ($n = 5$ each). Single values and means are indicated as $2^{-\Delta Ct}$. Two Way ANOVA, * $p < 0.05$, ** $p < 0.001$, *** $p < 0.0001$. doi:10.1371/journal.pone.0098237.g002

susceptible genotype of the offspring almost completely overwrote the gene expression program in the fetal gut. Heatmap analysis confirmed these different patterns and showed that postnatal tissue inflammation (ARE and iARE) most strikingly triggered *C3* and *S100a8* gene expression. The majority of regulated genes were shared according to postnatal tissue inflammation (830 commonly regulated genes between ARE and iARE mice).

The two distinct gene expression patterns (pre- and postnatal) were reflected as well in the Gene Ontology (GO) terms for 'biological processes' (GO_BP) (Figure 3F). 'Metabolic' (GO:0008152) and 'cellular processes' (GO:0009987) were predominantly overrepresented according to maternal inflammation in the prenatal state and according to postnatal inflammation in adult mice, respectively. For example, among 'metabolic processes', 989 (iWT) and 1,501 (iARE) genes were significantly regulated in the fetal stage. *Fabp6* was highly up-regulated due to maternal inflammation and is part of both 'metabolic' and 'cellular processes'. In the absence of maternal inflammation, fetal IEC from ARE mice were characterized by only 47 significant genes involved in 'metabolic processes' (Figure 3F, red bars). In contrast, the transcriptional profile of postnatal IEC revealed a lower significance of association ($\log_{10} p$ -value) for 'biological processes', highly influenced by postnatal but not maternal inflammation. In ARE mice, 507 and 695 genes were significantly regulated in 'metabolic' and 'cellular processes', respectively, whereas in iWT mice only 105 and 124 genes were responsible for overrepresentation (Figure 3F, grey bars). At this postnatal stage, *C3* encoding complement component 3 had the strongest impact on 'metabolic' and 'cellular processes' in ARE and iARE groups, but not in iWT mice.

Microarray Validation of *Tnf* and *C3* mRNA Expression by qPCR

In order to validate the microarray data, we performed targeted gene expression analysis of two candidate genes via qPCR. Our first target was *Tnf* mRNA, which is stabilized in the genetically engineered $Tnf^{iARE/+}$ mouse model and therefore served as control. We observed a very high correlation between microarray fluorescence data and $2^{-\Delta Ct}$ values (Figure 3E). In the prenatal stage, *Tnf* was not expressed and not regulated in both microarrays and qPCR. At 8 weeks of age, when the inflammation in the offspring was fully established, *Tnf* was highly up-regulated in $Tnf^{iARE/+}$ mice in both datasets. These data mirror the increased *Tnf* transcript levels in whole distal ileal tissues from $Tnf^{iARE/+}$ offspring seen in Figure 2E. We further analyzed *complement component 3* (*C3*), which was identified by microarray analysis as the top up-regulated gene between WT and ARE offspring (FC 39.04). We again observed a high correlation between the microarray fluorescence intensities and qPCR results (Figure 3E). *Reg3b* was identified as the strongest induced gene under maternal inflammation at 17.5 *dpc*, albeit at low gene expression levels (GEO data base accession number GSE44433). In essence, the success of microarray validation is fragile as many factors can influence both methodologies [23]. For instance, low array spot intensities for *Reg3b* ranged from ~ 10 –300 (prenatal stage) and might have resulted in a discrepancy of results indicated by a low correlation between microarray fluorescence intensities and $2^{-\Delta Ct}$

values ($r = 0.51$, $p = 0.0007$). Therefore, we investigated the intestinal expression of REG3B at the level of proteins.

Maternal Inflammation Influences REG3B Protein Expression in Adult WT Offspring, but has no Influence on the Intestinal Inflammation in $Tnf^{iARE/+}$ Offspring

Immunofluorescence analysis of REG3B expression overtime was performed in ileal gut sections from WT and $Tnf^{iARE/+}$ offspring at 17.5 *dpc*, 3 and 8 weeks of age. In all groups, REG3B protein was not detectable in the prenatal gut, but protein expression was clearly detectable in the epithelium of 8-week-old mice (Figure 4A–C). REG3B protein expression appeared earliest in the ileal epithelium at weaning (3 weeks of age) and further increased at 8 weeks. Quantification of REG3B proteins in IEC of 8-week-old mice revealed significant reduction in iWT mice compared to WT control ($p = 0.008$), suggesting that maternal inflammation slightly affects postnatal protein expression in the absence of any tissue pathology. But, under intestinal inflammation, both ARE and iARE mice showed almost a complete loss of REG3B protein expression when compared with WT ($p < 0.0001$). The loss of REG3B protein suggests that postnatal tissue inflammation profoundly impacts the expression of REG3B protein (Figure 4C and D). Tissue pathology of the distal ileum in Tnf^{iARE7+} offspring was not detectable in the pre- and perinatal period (until 3 weeks of age), but was moderate in 8-week-old-offspring, the age where an inflammation-driven loss of epithelial REG3B occurs. With the finding that maternal and postnatal inflammation was associated with decreased REG3B expression in the epithelium, we measured REG3B in aqueous and bacterial fractions of caecal contents from 8-week-old mice in order to evaluate an alteration in luminal secreted REG3B. Representative blots revealed the presence of REG3B in bacterial fractions (Figure 4E). Large amounts of REG3B were detected in bacterial fractions of WT mice, whereas moderate and low amounts were found in WT and inflamed ARE/iARE mice, respectively.

Caecal Bacterial Communities are not Altered in Response to Maternal Inflammation

Down-regulation of REG3B expression in healthy WT offspring suggested that maternal inflammation has a priming effect on the offspring's gut bacterial ecosystem. We were preferentially interested in early development of the microbiota due to maternal inflammation independently of postnatal inflammation and REG3B regulation. Therefore, we analyzed 16S-based diversity and composition in the caecal content from offspring at 3 weeks of age (pre-weaning). At this stage, we circumvented possible effects of postnatal diet on gut bacteria. We followed two different breeding strategies. Our first strategy was to co-house WT and Tnf^{iARE7+} dams in order to synchronize the dam's microbiota prior to colonization of the pups at birth. We obtained a total of 1,755,593 quality-checked sequences (28,633 to 86,232 per sample) representing a total of 263 OTUs with an average of 122 ± 33 molecular species per sample. Members of the phyla *Firmicutes*, *Bacteroidetes* and *Proteobacteria* were dominant, with abundances of 70.9%, 21.3% and 4.6% total sequences, respectively. *Lachnospiraceae* (59.3%) and *Porphyromonadaceae* (8%) were the most abundant families. We observed no effect of maternal

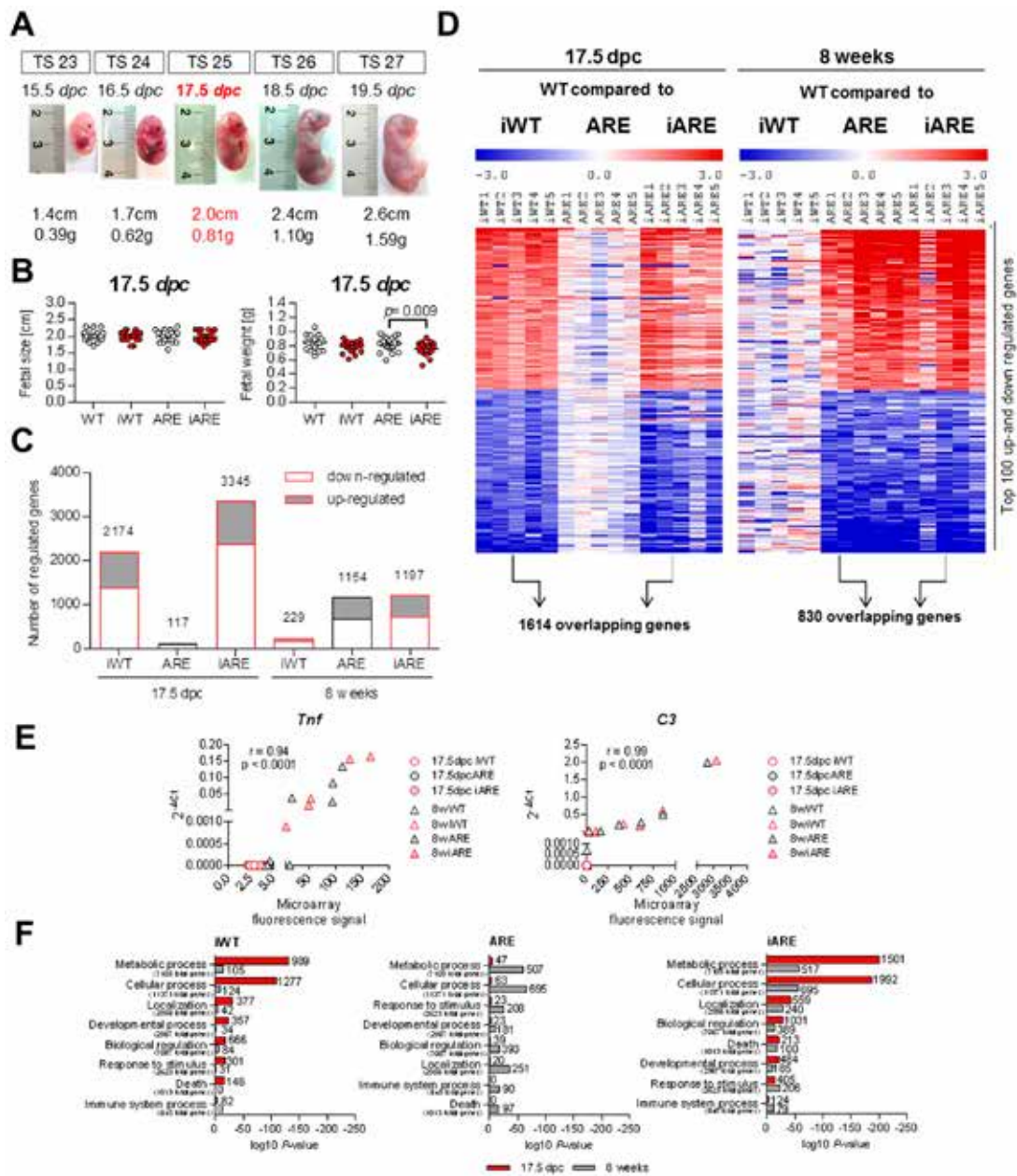


Figure 3. Fetal gene expression profiles in the ileal epithelium are overwritten by postnatal inflammation. (A) Randomly selected fetuses of the last 5 Theiler stages (TS) (15–19 dpc). (B) 17.5 dpc fetus genotypes plotted against fetal size and weight (total of 98 fetuses); Two-Way ANOVA followed by Holm-Sidak test, $*p < 0.05$, $***p < 0.001$. (C) Number of regulated genes in iWT, ARE and iARE mice at 17.5 dpc and 8 weeks of age when compared to WT considering a threshold fold change of ± 1.5 , $p < 0.05$ (each group and time point $n = 5$). (D) Heat map of top-100 up- and down-regulated genes in iWT, ARE and iARE mice plotted as signal log ratios from -3 to 3 . Two distinct gene clusters are shown between maternal (fetal iWT and iARE) and postnatal inflammation (ARE and iARE). Data are based on corresponding WT control mice according to MADMAX statistical analysis. (E) Microarray validation of the *Tnf* and *C3* genes by plotting individual microarray fluorescence intensities against $2^{-\Delta Ct}$ values obtained by qPCR from both prenatal and postnatal mice. Correlation coefficient (r) and significance levels are indicated in the respective plots. (F) Significantly overrepresented GO_BP of prenatal (red bars) and postnatal (grey bars) iWT, ARE and iARE mice. Numbers below the GO terms indicate total genes for the particular process. Numbers next to the bars indicate observed numbers of significantly regulated genes belonging to the respective process. doi:10.1371/journal.pone.0098237.g003

Table 2. Top 10 up- and down-regulated overlapping genes between prenatal WT/iWT and WT/iARE gene expression patterns (effect of maternal inflammation) and between postnatal WT/ARE and WT/iARE gene expression patterns (effect of offspring genotype/disease).

Overlapping genes between WT/iWT and WT/iARE at 17.5 dpc				Overlapping genes between WT/ARE and WT/iARE at 8 weeks			
ID	Gene	FC iWT	FC iARE	ID	Gene	FC ARE	FC iARE
18489	<i>Reg3b</i>	22.45	15.53	12266	<i>C3</i>	39.04	37.53
16204	<i>Fabp6</i>	15.61	30.29	20201	<i>S100a8</i>	38.08	21.38
58861	<i>Cysltr1</i>	6.69	4.20	17105	<i>Lyz2</i>	25.47	21.82
319636	<i>Fsd1l</i>	6.66	8.17	68891	<i>Cd177</i>	18.34	16.52
17967	<i>Ncam1</i>	5.58	4.72	17388	<i>Mmp15</i>	16.11	16.31
12843	<i>Col1a2</i>	5.29	3.04	70045	<i>2610528A11Rik</i>	15.46	14.98
12660	<i>Chka</i>	5.17	5.74	20202	<i>S100a9</i>	15.46	8.83
12552	<i>Cdh11</i>	4.82	2.04	22418	<i>Wnt5a</i>	14.78	15.00
77700	<i>9130208D14Rik</i>	4.68	3.47	14990	<i>H2-M2</i>	14.42	17.06
19876	<i>Robo1</i>	4.54	4.22	13419	<i>Dnase1</i>	11.42	16.73
208677	<i>Cretb3b</i>	-4.44	-1.66	105387	<i>Akr1c14</i>	-8.71	-12.00
18605	<i>Enpp1</i>	-5.13	-5.35	70564	<i>5730469M10Rik</i>	-8.82	-5.89
68979	<i>Nol11</i>	-5.54	-8.16	13487	<i>Slc26a3</i>	-8.96	-7.01
381259	<i>Als2cr4</i>	-5.62	-4.79	14344	<i>Fut2</i>	-9.18	-8.35
667373	<i>Gm14446</i>	-5.81	-2.39	109731	<i>Maob</i>	-9.59	-8.39
100647	<i>Upk3b</i>	-6.01	-7.90	17161	<i>Maoa</i>	-12.93	-15.73
66350	<i>Plazg12a</i>	-7.53	-6.07	170752	<i>Bco2</i>	-16.1	-19.65
19336	<i>Rab24</i>	-8.62	-6.47	432720	<i>Akr1c19</i>	-17.17	-10.11
107272	<i>Psat1</i>	-9.03	-11.71	12116	<i>Bhmt</i>	-22.04	-23.73
12696	<i>Cirbp</i>	-10.18	-7.56	16173	<i>Ilf8</i>	-25.04	-24.48

FC = log₂ based fold change, $p < 0.05$.
doi:10.1371/journal.pone.0098237.t002

Table 3. Top 5 up- and down-regulated genes in iWT, ARE and iARE mice pre- and postnatally.

		8 weeks					
5 most up- and down-regulated genes							
		17.5 dpc					
ID	Gene	Description	FC	ID	Gene	Description	FC
iWT	18489	Reg3b	regenerating islet-derived 3 beta	14170	Fgf15	fibroblast growth factor 15	4.50
	16204	Fabp6	fatty acid binding protein 6, ileal (gastrotropin)	56485	Slc2a5	solute carrier family 2, member 5	4.15
	58861	Cyslr1	cysteinyl leukotriene receptor 1	224093	Fam43a	family with sequence similarity 43, member A	2.87
	319636	Fsd11	fibronectin type III and SPRY domain containing 1-like	64452	Slc5a4a	solute carrier family 5, member 4a	2.73
	17967	Ncam1	neural cell adhesion molecule 1	17388	Mmp15	matrix metalloproteinase 15	2.48
	12696	Cirbp	cold inducible RNA binding protein	20753	Spr1a	small proline-rich protein 1A	-3.88
	107272	Psat1	phosphoserine aminotransferase 1	14583	Gfpt1	glutamine fructose-6-phosphate transaminase 1	-3.03
	19336	Rab24	RAB24, member RAS oncogene family	625599	Gml	GPI anchored molecule like protein	-2.97
	66350	Plazg12a	phospholipase A2, group XIIA	71578	Syal1	seminal vesicle antigen-like 1	-2.80
	14607	Gip	gastric inhibitory polypeptide	20210	Saa3	serum amyloid A 3	-2.73
ARE	18489	Reg3b	regenerating islet-derived 3 beta	12266	C3	complement component 3	39.04
	69814	Prss32	protease, serine, 32	20201	S100a8	S100 calcium binding protein A8 (calgranulin A)	38.08
	16204	Fabp6	fatty acid binding protein 6, ileal (gastrotropin)	17105	Ly22	lysozyme 2	25.47
	19662	Rbp4	retinol binding protein 4, plasma	68891	Cd177	CD177 antigen	18.34
	56312	Nupr1	nuclear protein 1	17388	Mmp15	matrix metalloproteinase 15	16.11
	259301	Leap2	liver-expressed antimicrobial peptide 2	16173	Il18	interleukin 18	-25.04
	56012	Pgam2	phosphoglycerate mutase 2	12116	Bhmt	betaine-homocysteine methyltransferase	-22.04
	106861	Abhd3	abhydrolase domain containing 3	432720	Akr1c19	aldo-keto reductase family 1, member C19	-17.17
	23958	Nr2e3	nuclear receptor subfamily 2, group E, member 3	170752	Bco2	beta-carotene oxygenase 2	-16.10
	14058	F10	coagulation factor X	17161	Maoa	monoamine oxidase A	-12.93
iARE	16204	Fabp6	fatty acid binding protein 6, ileal (gastrotropin)	12266	C3	complement component 3	37.53
	14963	H2-BI	histocompatibility 2, blastocyst	17105	Ly22	lysozyme 2	21.82
	18489	Reg3b	regenerating islet-derived 3 beta	20201	S100a8	S100 calcium binding protein A8 (calgranulin A)	21.38
	67092	Gatm	glycine amidinotransferase	14990	H2-M2	histocompatibility 2, M region locus 2	17.06
	319636	Fsd11	fibronectin type III and SPRY domain containing 1-like	13419	Dnase1	deoxyribonuclease 1	16.73
	545369	Gm5835	predicted gene 5835	16173	Il18	interleukin 18	-24.48
	107272	Psat1	phosphoserine aminotransferase 1	12116	Bhmt	betaine-homocysteine methyltransferase	-23.73
	665146	Gm7517	predicted gene 7517	170752	Bco2	beta-carotene oxygenase 2	-19.65
	68979	Nol11	nucleolar protein 11	17161	Maoa	monoamine oxidase A	-15.73
	12466	Cct6a	chaperonin containing Tcp1, subunit 6a (zeta)	105387	Akr1c14	aldo-keto reductase family 1, member C14	-12.00

Fold changes refer to WT control mice according to MADMAX statistical analysis (n = 5 per group, $p < 0.05$; FC = log 2 based fold change).
doi:10.1371/journal.pone.0098237.t003

inflammation on the phylogenetic make-up of caecal bacterial communities between WT and iWT offspring at the age of 3 weeks, *i.e.*, there was no clustering of samples according to dam genotypes based on the analysis of weighted UniFrac distances (Figure 4F). Our second strategy was to assess whether there is a general effect of $Tnf^{ARE/+}$ dams on the offspring's microbiota compared to WT dams. Therefore, we performed a second breeding of WT and $Tnf^{ARE/+}$ dams that were housed separately. We obtained in this case a total of 1,940,009 quality-checked sequences (16,865 to 61,102 per sample) representing a total of 286 OTUs. Again, we found no influence of the maternal $Tnf^{ARE/+}$ genotype on the phylogenetic make-up of bacterial communities in caecal contents in both WT and $Tnf^{ARE/+}$

offspring ($n = 4$ to 6 mice per group) (Figure 4G). The number of phylotypes was also not influenced by maternal inflammation and offspring's genotype (Table S1). These data demonstrate that overall bacterial diversity is not affected by maternal inflammation or offspring's genotype before the onset of postnatal inflammation. Interestingly, analysis of the caecal microbiota at 8 weeks of age, when inflammation of the distal ileum is established ($n = 4$ to 6 mice per group), revealed that REG3B does not affect bacterial diversity and composition of Chow diet-fed offspring (Figure S2). Taxonomic assignment revealed no statistically significant differences in sequence abundances due to maternal or postnatal inflammation after adjustment for multiple testing (Tables S2A and S2B). However, feeding offspring a well-defined semisynthetic

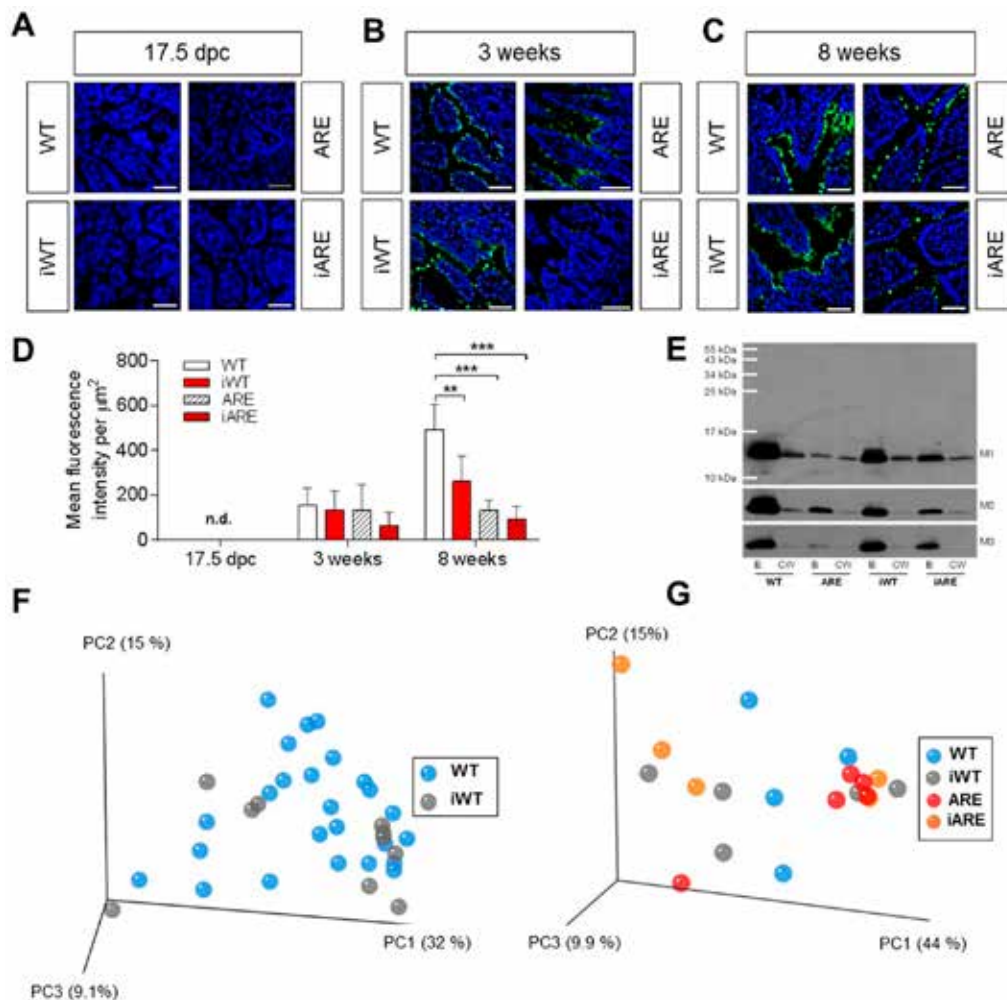


Figure 4. Pre- and postnatal REG3B protein expression in the distal ileum and offspring's caecal bacterial diversity are unaffected by maternal inflammation. (A–C) Immunofluorescence analysis overtime (17.5 dpc, 3 and 8 weeks) of REG3B (green) from distal ileal sections of WT, iWT, ARE, iARE mice. Nuclei were counterstained with DAPI (blue). (D) Data represent mean fluorescence intensity of REG3B signal per $\mu\text{m}^2 \pm$ SD from 5 mice per group (3 regions per mouse were evaluated). Significant differences in comparison to WT mice were assessed by Two-Way ANOVA followed by Holm-Sidak method; ** $p < 0.01$, *** $p < 0.001$, n.d. = not detectable. (E) Western blot analysis of REG3B in caecal content (B = bacterial fraction, CW = cecal water fraction, M1–M3 = 3 individual mice of each group). (F+G) PCoA analysis of weighted UniFrac distances indicated no change in phylogenetic diversity at 3 weeks of age after cohousing (F) of WT and $Tnf^{ARE/+}$ dams and litters ($n = 10$ –25 offspring per group) (left panel; even sampling of 28,633 sequences) or without co-housing (G) ($n = 4$ –6 offspring per group) (right panel; even sampling of 16,865 sequences). 16S ribosomal RNA gene amplicons of the V4 region (233 bp) in caecal contents were sequenced using a MiSeq platform and analyzed as described in the methods section.
doi:10.1371/journal.pone.0098237.g004

experimental diet revealed clear differences in bacterial diversity according to the offspring's genotype, i.e., PCoA analysis indicated a change in beta-diversity between WT and *Tnf^{ARE/+}* offspring (n = 4–5 mice each). Statistical analysis on mean phylogenetic distances between groups (inter-group distances) clearly indicated significance (Figure S2). Besides inflammation-associated alterations driven by the offspring genotype, we did not observe any shifts in diversity in response to maternal inflammation (Fig S2D and S2F). When comparing chow-fed mice at the age of 3 and 8 weeks, we observed age-dependent shifts in *beta*-diversity independently of dam and offspring genotype (Figure S3A). Major age-dependent effects on bacterial taxa included an increase in members of the *Lactobacillaceae*, and *Prevotellaceae* as well as decreased proportions of *Lachnospiraceae* and *Deferribacteriaceae* (Figure S3B and Table S3).

Discussion

In the present work, we provide clear experimental evidence that maternal inflammation has no impact on the offspring's risk to develop genetically-driven ileitis and colitis, despite the fact that TNF-driven maternal ileitis extensively modulates transcriptional responses in the fetal epithelium. This clearly suggests that effects of maternal inflammation are overwritten in genetically-driven models for intestinal inflammation, indicating that the disease end point might be independent of fetal exposure to inflammation[24].

CD-associated pregnancy in humans is characterized by alterations of the cytokine milieu leading to peri- and postnatal complications including preterm labor and low birth weights [6,7]. Most importantly, we showed that 8-week-old ARE and iARE mice developed similar levels of ileal inflammation. This effect was confirmed in a second mouse model for colitis, clearly supporting the hypothesis that maternal inflammation does not affect the onset or severity of disease in the genetically susceptible offspring. Nevertheless, our experiments demonstrate for the first time that TNF-driven maternal inflammation substantially modulates the transcriptional profile in the fetal intestinal epithelium, supporting the hypothesis that not only infection-driven acute but also chronic maternal inflammation impacts on the progeny[25,26]. We identified two clearly distinct clusters of genes that were strongly associated with fetal exposure to maternal inflammation (1,614 genes) or postnatal development of TNF-mediated tissue pathology (830 genes). In fetuses, similar patterns were observed in iWT and iARE with 1,614 common genes in both groups (around 70% overlap). The fetal ARE genotype however seemed not to be relevant at the early developmental stage (117 regulated genes), suggesting that the disease-susceptible genotype does not have a major influence on fetal gut programming. In contrast, gene expression profiles in postnatal IEC were highly influenced by the genetically-driven disease phenotype with 1,154 and 1,197 significantly regulated genes under ARE and iARE conditions, respectively. Heat map analysis confirmed the substantial overlap of similarly regulated genes (around 70%; 830 genes) in these two groups of ARE mice, implying that transcriptional fingerprints in the fetal gut were completely overwritten by signals derived from the postnatal environment independently of the disease-susceptible genotype. These findings may suggest that genetically-driven ileitis in mice is largely induced by the postnatal environment.

Gene ontology analysis identified 'metabolic and cellular' processes as being significantly linked to maternal inflammation to a higher extent in the fetal than in the postnatal stage. Consistent with the over representation of 'metabolic processes', *Fabp6* was strongly up-regulated in the fetal gut in response to maternal inflammation. FABP6 facilitates efficient transepithelial

transport of both bile and fatty acids [27]. Although other biological processes such as 'localization' and 'death' were not influenced to the same extent as 'metabolic and cellular processes', they included top-regulated genes such as *C3*, *S100a8* and *Lyz2* in both ARE and iARE offspring. This reflects a disease-associated inflammatory program[28,29] as well as bacterial defense mechanisms[30,31]. Additionally, the strong down-regulation of *Il18* by approximately 25-fold, hints at the relevance of missing immune tolerance in the *Tnf^{ARE/+}* model for CD[32].

Both the fetal and postnatal stage revealed a significant changes within the GO category 'response to stimulus', albeit with lower number of observed genes when compared with top-categories like 'metabolic and cellular processes'. Interestingly, this category comprises *Reg3b* as top-regulated gene under maternal inflammation at 17.5dpc. The *Reg3* gene family belongs to a group of C-type lectins, based on their carbohydrate recognition domains[33]. Interestingly, REG3B protein was not detectable in the prenatal gut, but was clearly visible in the epithelium of mice at 8 weeks of age. Immunofluorescence analysis of REG3B expression over time showed appearance earliest at weaning (3 weeks). This observation is consistent with a previously published *Reg3g* expression analysis from Matsumoto *et al.*[34]. The closely related lectin REG3G is known to drive host-bacterial segregation[35], preferentially targeting Gram-positive bacteria[36]. Thus, loss of REG3B seems to be associated with inflammatory signals at postnatal stages and may contribute to the development of genetically-driven ileitis through mechanisms that involve the intestinal microbiota of *Tnf^{ARE/+}* mice[16,37]. Quantification of REG3B protein levels in IEC of 8-week-old mice revealed significant reduction in iWT, suggesting that maternal inflammation can slightly affect postnatal protein expression. However, ARE and iARE mice almost completely lost REG3B, suggesting that postnatal tissue inflammation profoundly impacts REG3B expression independently of earlier gene transcriptional up-regulation by maternal inflammation. This is supported by the fact that, fetal epithelial programming is completely overwritten in adult offspring, clearly suggesting that postnatal disease-relevant signals initialize genetically-driven ileal pathogenesis.

Interestingly, loss of REG3B in the epithelium was linked to lower REG3B levels preferably bound to bacterial fractions in the caecal content, clearly suggests that the postnatal microbiota harbors disease-relevant signals that show stronger potential to initialize the genetically-driven ileal pathogenesis compared to maternal stimuli. This is supported by the fact that maternally-induced changes in the fetal epithelium did not cause any shifts in diversity and composition of caecal bacterial communities at 3 weeks of age before weaning. This was shown in two different breeding strategies, with and without co-housing of WT and *Tnf^{ARE/+}* dams. However, at 8 weeks of age, we observed an inflammation-driven loss of REG3B in IEC and bacterial fractions of the caecal content that is not additionally affected by maternal inflammation. The fact that the microbial composition and diversity was not affected by maternal or offspring's inflammation indicates that REG3B expression in the epithelium has no influence on the overall phylogenetic make-up of caecal bacterial communities in the *Tnf^{ARE/+}* mouse model. We cannot fully explain this absence of any major signs of maternal or inflammation-driven dysbiosis in the offspring's microbiota despite changes in REG3B expression. Diet might be one main confounding factor, since wheat-based Ssniff Chow diets are characterized by highly varying quality due to heterogeneity of raw products used during production. This suggestion was supported by clear inflammation-driven shifts in *beta*-diversity

between WT and ARE mice when fed a well-defined semisynthetic experimental diet based on corn starch.

Taking all these findings together, we summarize that neither maternal nor genetically-driven inflammation impact the overall phylogenetic diversity of caecal bacterial communities in the offspring under conventional conditions. The observation of age-dependent shifts in bacterial diversity and composition between 3 and 8 weeks of age goes in line with a previously published work by Garrett et al. [12]. But, unlike their findings that a colitogenic microbiota is transmitted from mothers to offspring under SPF conditions, we could not observe any changes through maternal inflammation in our experiments. Altogether, we conclude from our studies that maternal inflammation impacts the ileal transcriptome in fetuses, but these effects do not persist in grownup mice and are therefore not relevant for the modulation of intestinal inflammation in the genetically susceptible *Tnf^{ΔARE/+}* mouse. Consistent with these findings is the occurrence of age- and diet- but not maternal-dependent shifts in bacterial diversity and composition, indicating that postnatal factors largely overwrite a possible maternal influence on the offspring's microbial ecosystem in both non-disease and disease susceptible offspring. This is also in line with the fact that the host immune response at the site of inflammation is consistently unaffected by maternal inflammation in two different mouse models for genetically-driven ileitis and colitis inflammation. Consequently, maternal inflammation during gestation in mouse models did not alter the genetically-driven risk to develop chronic inflammation in the intestine.

Supporting Information

Figure S1 Fetal environment and laser microdissection of fetal intestinal epithelial cells. **(A)** Randomly selected fetuses of the last 5 Theiler stages (TS) (15–19 *dpc*). **(B)** Macroscopic view of a 17.5 *dpc* gut and subsequent laser microdissection procedure of fetal ileal epithelium. Epithelial areas of $1.33 \pm 0.024 \times 10^6 \mu\text{m}^2$ (mean \pm SD) were cut for microarray analysis. (TIF)

Figure S2 Experimental diet clearly influences changes in caecal bacterial diversity in response to postnatal but not maternal inflammation. Histological scores of terminal ileum from WT, iWT, ARE and iARE offspring on **(A)** chow diet (experiment from Figure 2A, $n = 5-7$ mice each), or **(B)** experimental diet ($n = 6-16$ mice each). With both diets, there was no difference in inflammatory scores relative to maternal inflammation. **(C+E)** Analysis of phylogenetic distances indicated no significant change in *beta*-diversity between offspring fed the Ssniff chow diet. Comparisons of mean phylogenetic distances (weighted UniFrac) between individual mice (WT, iWT, ARE, iARE) within groups (intra-group distances, e.g. all WT) and between mice from different groups (inter-group distances, e.g. WT vs. iWT) revealed no significant differences related to the offspring's genotype or maternal inflammation. **(D+F)** PCoA analysis indicated an inflammation-driven change in *beta*-diversity between 8-week-old

References

1. Renz H, von Mutius E, Brandtzaeg P, Cookson WO, Autenrieth IB, et al. (2011) Gene-environment interactions in chronic inflammatory disease. *Nature immunology* 12: 273–7.
2. Khor B, Gardet A, Xavier RJ (2011) Genetics and pathogenesis of inflammatory bowel disease. *Nature* 474: 307–17.
3. Franke A, McGovern DP, Barrett JC, Wang K, Radford-Smith GL, et al. (2010) Genome-wide meta-analysis increases to 71 the number of confirmed Crohn's disease susceptibility loci. *Nature genetics* 42: 1118–25.
4. Kaser A, Zeissig S, Blumberg RS (2010) Inflammatory bowel disease. *Annual review of immunology* 28: 573–621.

WT and *Tnf^{ΔARE/+}* offspring fed an experimental diet ($n = 4-5$ mice each). Statistical comparisons of phylogenetic distances indicated significant separation between WT and ARE or iWT and iARE but not between WT and iWT or ARE and iARE (Two-Way ANOVA, $***p > 0.0001$). (TIF)

Figure S3 Age-dependent shifts in bacterial diversity and composition. **(A)** PCoA analysis indicated a change in diversity between mice at the age of 3 and 8 weeks ($n = 18-19$). **(B)** Major bacterial taxa that were characterized by significantly different sequence proportions at 3 and 8 weeks of age are shown in box plots (F-test followed by Benjamini-Hochberg adjustment). Individual data for all taxa are given in Table S3. (TIF)

Table S1 Observed phylotype numbers in caecal contents of WT, iWT, ARE and iARE offspring at 3 and 8 weeks of age. Indicated are means \pm SD ($n = 4-5$ per group). Three Way ANOVA. (XLSX)

Table S2 Sequence proportions of bacterial taxa in caecal contents from offspring ($n = 4-5$) at **(A)** 3 or **(B)** 8 weeks of age. OTUs occurring in less than 2 mice and $<0.05\%$ total sequences per sample were excluded from the analysis. Sequence proportions were analyzed for significant differences using F-Test followed by Benjamini-Hochberg correction for multiple testing in the R programming environment after adjustment for multiple testing. (XLSX)

Table S3 Sequence proportions of bacterial taxa in caecal contents from 3- and 8-week old offspring ($n = 4-6$) show age differences. OTUs occurring in less than 2 mice and $<0.05\%$ total sequences per sample were excluded from the analysis. Sequence proportions were analyzed for significant age-differences using F-Test followed by Benjamini-Hochberg correction for multiple testing in the R programming environment after adjustment for multiple testing. (XLSX)

Acknowledgments

We thank Melanie Manyet for helping with immunofluorescence analysis. None of the material has been published or is under consideration elsewhere, including the internet. The animal experiments were performed according to the German guidelines for animal care. Raw microarray data are available on the GEO database (<http://www.ncbi.nlm.nih.gov/geo/query/acc.cgi?token=hrqhlcmccoishc&acc=GSE44433>).

Author Contributions

Conceived and designed the experiments: DH. Performed the experiments: JH KH GH MB. Analyzed the data: JH KH TC. Wrote the paper: JH DH. Provided the *TNF^{ΔARE/+}* mouse: GK. Critically revised the manuscript: TC GH.

9. Wolfs TG, Buurman WA, Zoer B, Moonen RM, Derikx JP, et al. (2009) Endotoxin induced chorioamnionitis prevents intestinal development during gestation in fetal sheep. *PLoS one* 4:e5837.
10. Renz H, Brandtzaeg P, Hornef M (2012) The impact of perinatal immune development on mucosal homeostasis and chronic inflammation. *Nat Rev Immunol* 12: 9–23.
11. Yan X, Huang Y, Wang H, Du M, Hess BW, et al. (2011) Maternal obesity induces sustained inflammation in both fetal and offspring large intestine of sheep. *Inflamm Bowel Dis* 17: 1513–22.
12. Garrett WS, Gallini CA, Yatsunenko T, Michaud M, DuBois A, et al. (2010) Enterobacteriaceae act in concert with the gut microbiota to induce spontaneous and maternally transmitted colitis. *Cell host & microbe* 8: 292–300.
13. Roulis M, Armaka M, Manoloukos M, Apostolaki M, Kollias G (2011) Intestinal epithelial cells as producers but not targets of chronic TNF suffice to cause murine Crohn-like pathology. *Proceedings of the National Academy of Sciences of the United States of America* 108: 5396–401.
14. Swamy M, Jamora C, Havran W, Hayday A (2010) Epithelial decision makers: in search of the 'epimunome'. *Nature immunology* 11: 656–65.
15. Katakura K, Lee J, Rachmilewitz D, Li G, Eckmann L, et al. (2005) Toll-like receptor 9-induced type I IFN protects mice from experimental colitis. *J Clin Invest* 115: 695–702.
16. Werner T, Wagner SJ, Martinez I, Walter J, Chang JS, et al. (2011) Depletion of luminal iron alters the gut microbiota and prevents Crohn's disease-like ileitis. *Gut* 60: 325–33.
17. Caporaso JG, Lauber CL, Walters WA, Berg-Lyons D, Lozupone CA, et al. (2011) Global patterns of 16S rRNA diversity at a depth of millions of sequences per sample. *Proceedings of the National Academy of Sciences of the United States of America* 108 Suppl 1: 4516–22.
18. Edgar RC (2013) UPARSE: highly accurate OTU sequences from microbial amplicon reads. *Nature methods* 10: 996–8.
19. Caporaso JG, Kuczynski J, Stombaugh J, Bittinger K, Bushman FD, et al. (2010) QIIME allows analysis of high-throughput community sequencing data. *Nature methods* 7: 335–6.
20. Cole JR, Chai B, Marsh TL, Farris RJ, Wang Q, et al. (2003) The Ribosomal Database Project (RDP-II): previewing a new autoaligner that allows regular updates and the new prokaryotic taxonomy. *Nucleic acids research* 31: 442–3.
21. Edgar RC, Haas BJ, Clemente JC, Quince C, Knight R (2011) UCHIME improves sensitivity and speed of chimera detection. *Bioinformatics* 27: 2194–200.
22. Behm BW, Bickston SJ (2008) Tumor necrosis factor-alpha antibody for maintenance of remission in Crohn's disease. *The Cochrane database of systematic reviews*:CD006893.
23. Morey JS, Ryan JC, Van Dolah FM (2006) Microarray validation: factors influencing correlation between oligonucleotide microarrays and real-time PCR. *Biological procedures online* 8: 175–93.
24. Wagner SJ, Schmidt A, Effenberger MJ, Gruber L, Daner J, et al. (2013) Semisynthetic diet ameliorates Crohn's disease-like ileitis in TNFDeltaARE/WT mice through antigen-independent mechanisms of gluten. *Inflamm Bowel Dis* 19: 1285–94.
25. Cardenas I, Mulla MJ, Myrtolli K, Stakianaki AK, Norwitz ER, et al. (2011) Nod1 activation by bacterial iE-DAP induces maternal-fetal inflammation and preterm labor. *J Immunol* 187: 980–6.
26. Urakubo A, Jarskog LF, Lieberman JA, Gilmore JH (2001) Prenatal exposure to maternal infection alters cytokine expression in the placenta, amniotic fluid, and fetal brain. *Schizophrenia research* 47: 27–36.
27. Labonte ED, Li Q, Kay CM, Agellon LB (2003) The relative ligand binding preference of the murine ileal lipid binding protein. *Protein expression and purification* 28: 25–33.
28. Yuan Y, Ren J, Cao S, Zhang W, Li J (2012) Exogenous C3 protein enhances the adaptive immune response to polymicrobial sepsis through down-regulation of regulatory T cells. *International immunopharmacology* 12: 271–7.
29. Vogl T, Gharibyan AL, Morozova-Roche LA (2012) Pro-Inflammatory S100A8 and S100A9 Proteins: Self-Assembly into Multifunctional Native and Amyloid Complexes. *International journal of molecular sciences* 13: 2893–917.
30. Salzman NH, Hung K, Haribhai D, Chu H, Karlsson-Sjoberg J, et al. (2010) Enteric defensins are essential regulators of intestinal microbial ecology. *Nature immunology* 11: 76–83.
31. Cadwell K, Liu JY, Brown SL, Miyoshi H, Loh J, et al. (2008) A key role for autophagy and the autophagy gene Atg16l1 in mouse and human intestinal Paneth cells. *Nature* 456: 259–63.
32. Oertli M, Sundquist M, Hitzler I, Engler DB, Arnold IC, et al. (2012) DC-derived IL-18 drives Treg differentiation, murine Helicobacter pylori-specific immune tolerance, and asthma protection. *J Clin Invest* 122: 1082–96.
33. Gallo RL, Hooper LV (2012) Epithelial antimicrobial defence of the skin and intestine. *Nat Rev Immunol* 12: 503–16.
34. Matsumoto S, Konishi H, Maeda R, Kiryu-Seo S, Kiyama H (2012) Expression analysis of the regenerating gene (Reg) family members Reg-IIIbeta and Reg-IIIgamma in the mouse during development. *The Journal of comparative neurology* 520: 479–94.
35. Vaishnava S, Yamamoto M, Severson KM, Ruhn KA, Yu X, et al. (2011) The antibacterial lectin RegIIIgamma promotes the spatial segregation of microbiota and host in the intestine. *Science* 334: 255–8.
36. Cash HL, Whitham CV, Behrendt CL, Hooper LV (2006) Symbiotic bacteria direct expression of an intestinal bactericidal lectin. *Science* 313: 1126–30.
37. von Schillde MA, Hormannspenger G, Weiher M, Alpert CA, Hahne H, et al. (2012) Lactocepain secreted by Lactobacillus exerts anti-inflammatory effects by selectively degrading proinflammatory chemokines. *Cell host & microbe* 11: 387–96.

PAPER 8

Metabolic Activation of Intrahepatic CD8⁺ T Cells and NKT Cells Causes Nonalcoholic Steatohepatitis and Liver Cancer via Cross-Talk with Hepatocytes

Monika Julia Wolf,¹ Arlind Adili,² Kira Piotrowitz,³ Zeinab Abdullah,⁴ Yannick Boege,¹ Kerstin Stemmer,⁵ Marc Ringelhan,^{2,6} Nicole Simonavicius,² Michèle Egger,¹ Dirk Wohlleber,⁷ Anna Lorentzen,² Claudia Einer,⁸ Sabine Schulz,⁸ Thomas Clavel,^{9,10} Ulrike Protzer,² Christoph Thiele,³ Hans Zischka,⁸ Holger Moch,¹ Matthias Tschöp,⁵ Alexei V. Tumanov,¹¹ Dirk Haller,¹⁰ Kristian Unger,¹² Michael Karin,¹³ Manfred Kopf,¹⁴ Percy Knolle,^{4,7,15} Achim Weber,^{1,15,*} and Mathias Heikenwalder^{2,15,*}

¹Institute of Surgical Pathology, University Hospital Zurich, Zurich 8091, Switzerland

²Institute of Virology, Technische Universität München and Helmholtz Zentrum München, Munich 81675, Germany

³LIMES Life and Medical Sciences Institute, University of Bonn, Bonn 53125, Germany

⁴Institutes of Molecular Medicine and Experimental Immunology, University of Bonn, Bonn 53105, Germany

⁵Institute for Diabetes and Obesity, Helmholtz Diabetes Center, Helmholtz Zentrum München & Division of Metabolic Diseases, Technische Universität München, Munich 81657, Germany

⁶Second Medical Department, Klinikum Rechts der Isar, Technische Universität München, Munich 81657, Germany

⁷Institute of Molecular Immunology, Technische Universität München, Munich 81675, Germany

⁸Institute of Molecular Toxicology and Pharmacology, Helmholtz Center Munich, German Research Center for Environmental Health, Neuherberg 85764, Germany

⁹Junior Group Intestinal Microbiome

¹⁰Chair of Nutrition and Immunology, ZIEL—Research Center for Nutrition and Food Sciences, Biofunctionality Unit Technische Universität München, Freising-Weihenstephan 85350, Germany

¹¹Trudeau Institute, Saranac Lake, New York, NY 12983, USA

¹²Research Unit of Radiation Cytogenetics, Helmholtz Zentrum München, German Research Center for Environmental Health, Neuherberg 85764, Germany

¹³Laboratory of Gene Regulation and Signal Transduction, Departments of Pharmacology and Pathology, University of California, San Diego, School of Medicine, San Diego, CA 92093, USA

¹⁴Molecular Biomedicine, Institute of Molecular Health Sciences, ETH Zurich, Zurich 8093, Switzerland

¹⁵Co-senior author

*Correspondence: achim.weber@usz.ch (A.W.), heikenwalder@helmholtz-muenchen.de (M.H.)

<http://dx.doi.org/10.1016/j.ccell.2014.09.003>

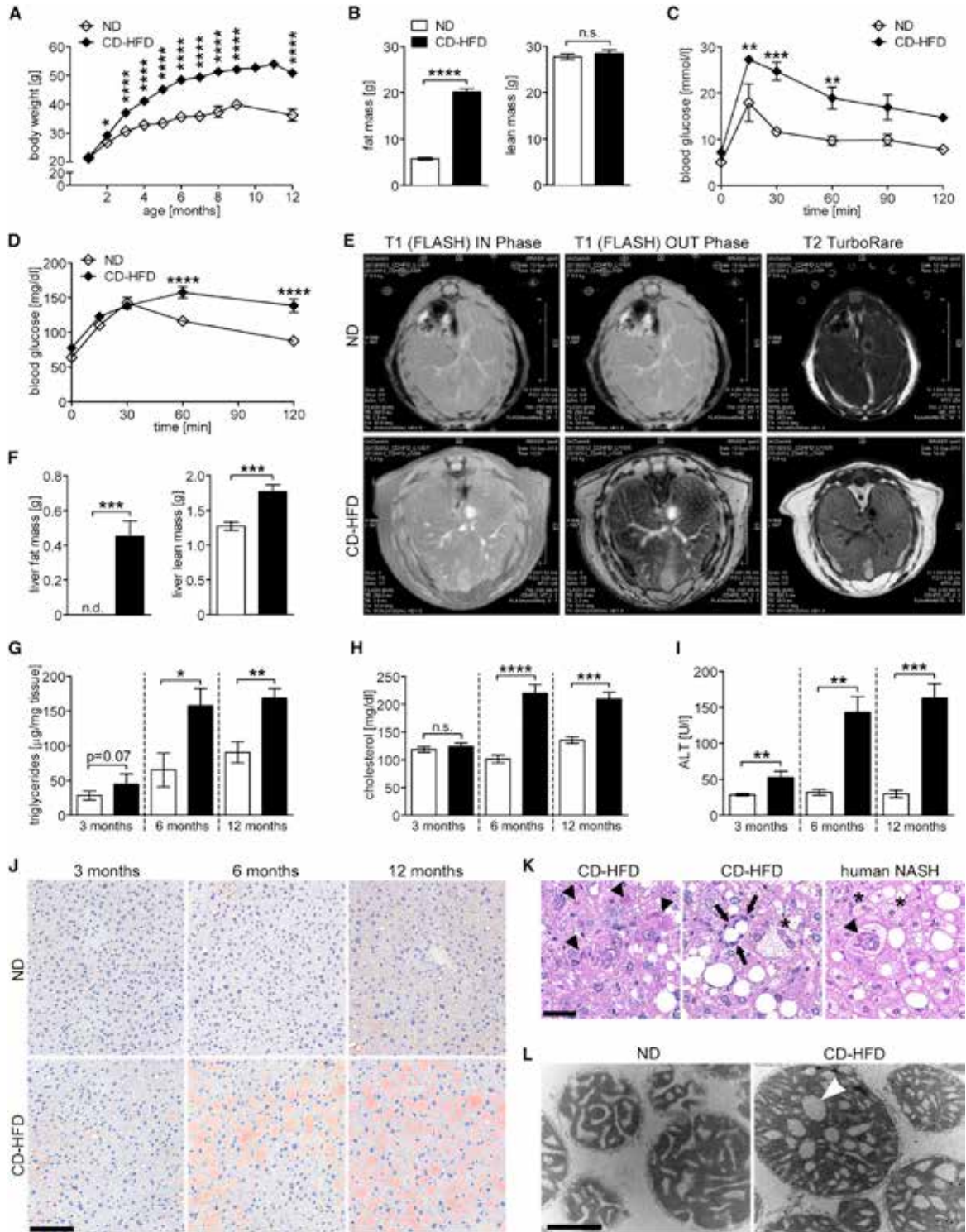
SUMMARY

Hepatocellular carcinoma (HCC), the fastest rising cancer in the United States and increasing in Europe, often occurs with nonalcoholic steatohepatitis (NASH). Mechanisms underlying NASH and NASH-induced HCC are largely unknown. We developed a mouse model recapitulating key features of human metabolic syndrome, NASH, and HCC by long-term feeding of a choline-deficient high-fat diet. This induced activated intrahepatic CD8⁺ T cells, NKT cells, and inflammatory cytokines, similar to NASH patients. CD8⁺ T cells and NKT cells but not myeloid cells promote NASH and HCC through interactions with hepatocytes. NKT cells primarily cause steatosis via secreted LIGHT, while CD8⁺ and NKT cells cooperatively induce liver damage. Hepatocellular LTβR and canonical NF-κB signaling facilitate NASH-to-HCC transition, demonstrating that distinct molecular mechanisms determine NASH and HCC development.

Significance

NASH resulting from hypercaloric nutrition is rapidly increasing worldwide and can cause HCC, but the underlying mechanisms have remained elusive. In a mouse model of long-term choline-deficient high-fat diet (CD-HFD), we recapitulate NASH and NASH-driven HCC in humans. Activation of CD8⁺ T cells and NKT cells during CD-HFD by hepatocytes (metabolic activation) initiates release of soluble mediators such as LIGHT and lymphotoxin that determine steatosis/NASH and NASH-to-HCC transition, respectively. The vicious cycle of lymphocyte-driven steatohepatitis during hypercaloric nutrition identifies an important function of the adaptive immune system in NASH and HCC pathogenesis. Interference with localization of lymphocytes to the liver or blocking hepatocyte-lymphocyte cross-talk is a promising strategy to treat NASH and prevent NASH-driven HCC.





(legend on next page)

INTRODUCTION

Hepatocellular carcinoma (HCC) is the most common primary liver malignancy and the third most common cause of cancer-related death worldwide, with a rising incidence in developing and industrialized countries (Jemal et al., 2011). The most prevalent risk factors for HCC development are chronic hepatitis due to hepatitis B virus or hepatitis C virus (HCV) infection or chronic alcohol consumption (El-Serag, 2011).

A strong link between obesity and cancer is well-established, and a body mass index (BMI) > 25 kg/m² increases the risk for cancer (Calle and Kaaks, 2004). A dramatic rise in cancer incidence is expected due to high caloric intake, smoking and sedentary lifestyle, doubling within the next two decades (Stewart and Wild, 2014). A modest rise in BMI significantly elevates the risk for HCC and other cancers (e.g., pancreatic carcinoma and gastrointestinal [GI] cancer) (Calle and Kaaks, 2004). In recent years, obesity leading to metabolic syndrome, steatosis, and steatohepatitis has attracted increased attention because of increased HCC incidence in Western countries (White et al., 2012). In line, HCC is the most rapidly increasing cancer type in the United States, with 19,160 new cases and 16,780 deaths in 2007 (American Cancer Society, 2007).

Enhanced fat uptake by hepatocytes leads to nonalcoholic fatty liver disease (NAFLD), comprising a spectrum of liver disorders ranging from fatty liver (steatosis) to nonalcoholic steatohepatitis (NASH), which can proceed to fibrosis, cirrhosis, and HCC (Anstee and Day, 2013). Thus, increased fat uptake, hepatic lipid accumulation, and NASH represent incremental risk factors for HCC. At the same time, there is no established pharmacological treatment for NASH, and therapy for HCC is limited (Michelotti et al., 2013).

A “two-hit hypothesis” has been proposed for NASH progression from simple liver steatosis. Lipid accumulation in hepatocytes is considered the first step in NASH development; however, a second hit promoting oxidative stress, inflammation, DNA damage, hepatocyte cell death, or fibrosis is needed (Caballero et al., 2009).

In C57BL/6 mice, NASH-like liver pathology can be induced by a methionine-choline deficient diet (MCD) or a choline-deficient diet (CD) but not by a high-fat diet (HFD). However, C57BL/6 mice fed an MCD or a CD do not develop obesity or metabolic

syndrome but rather develop weight loss or cachexia (Hebbard and George, 2011). Thus, this approach does not recapitulate NASH and its consequences in humans. Choline deficiency is known to exacerbate NAFLD and NASH (Corbin and Zeisel, 2012; Guerrero et al., 2012). Moreover, humans with inadequate choline uptake have defects in hepatic lipoprotein secretion, oxidative damage caused by mitochondrial dysfunction, and endoplasmic reticulum (ER) stress (Corbin and Zeisel, 2012). Choline deprivation leads to fatty liver development (Zeisel and da Costa, 2009). At least 90% of the US population does not meet the recommended intake for choline (Zeisel and Caudill, 2010).

The precise mechanisms leading to dietary-induced HCC are unknown, and appropriate mouse models for studying NAFLD-induced HCC development are lacking. Concomitant injection of a chemical carcinogen (e.g., diethyl-nitrosamine [DEN]) and HFD was studied in comparison with DEN-induced liver carcinogenesis under a normal diet (ND) (Park et al., 2010). This study revealed increased HCC, linking the inflammation-promoting cytokines IL1 β , IL6, and TNF to HFD-induced obesity. An HFD led to enhanced tumorigenesis in a liver cancer model (NEMO^{Δhep} mice) (Wunderlich et al., 2008) and caused progression of chronic ER stress to oxidative stress, finally resulting in HCC (Nakagawa et al., 2014).

On the basis of the clinical observations of choline deficiency in NASH patients (Corbin and Zeisel, 2012; Guerrero et al., 2012), we combined choline deficiency with an HFD (CD-HFD) to investigate hepatic steatosis, NASH, and HCC development.

RESULTS

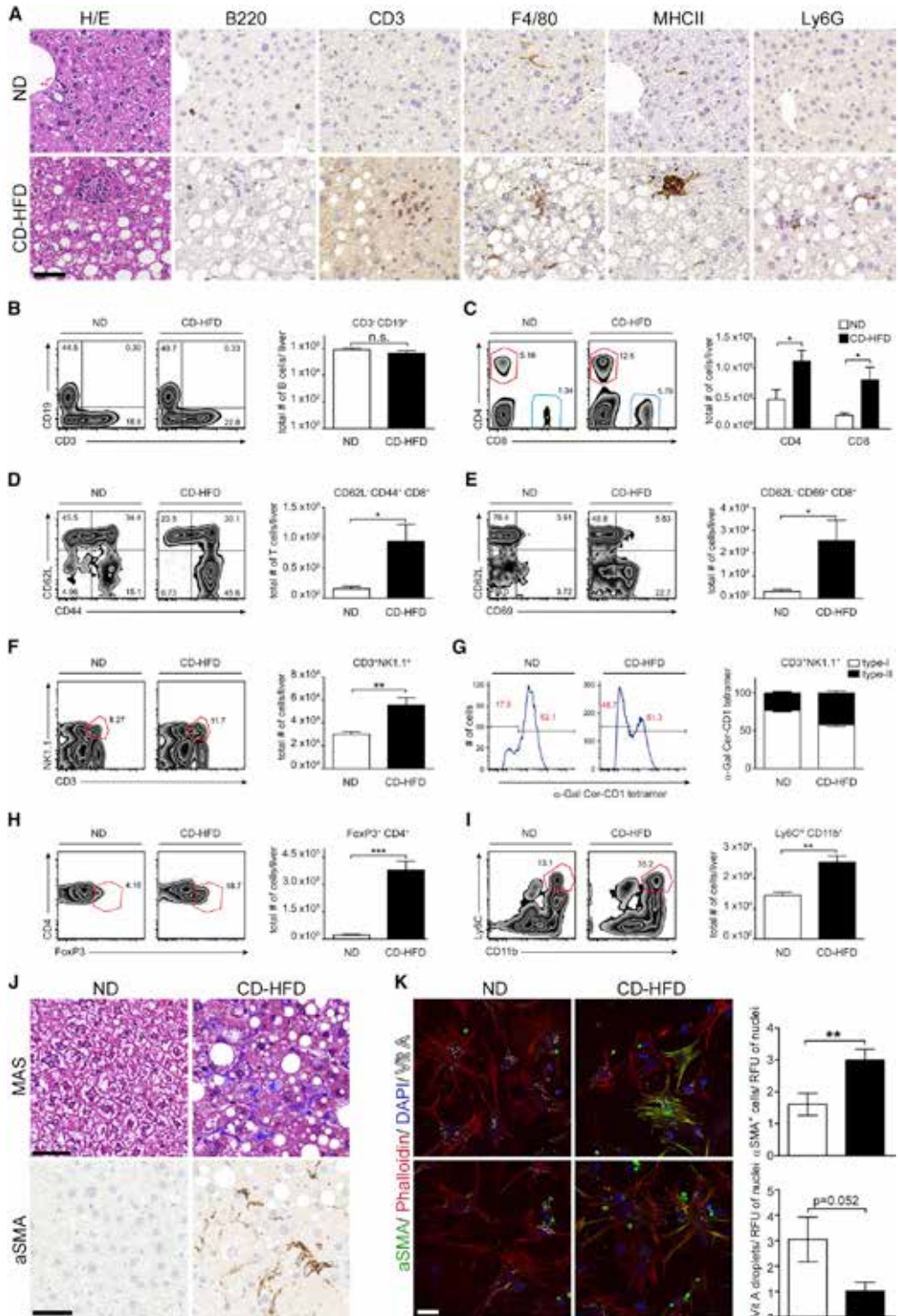
Long-Term CD-HFD Causes Features of Metabolic Syndrome, Liver Damage, and NASH in C57BL/6 Mice

We first studied the effects of long-term CD-HFD feeding on body weight, glucose metabolism, and liver integrity in C57BL/6 mice. A constant rise in body weight was observed in male and female mice (Figure 1A; Figure S1A available online) compared with ND mice. Long-term HFD resulted in similar body weight gain over time (Figure S1B). Total food intake was similar between groups (Figure S1C). Whole-body echo magnetic resonance imaging (MRI) revealed significantly increased body fat mass in male and female CD-HFD mice compared

Figure 1. Long-Term CD-HFD Leads to Metabolic Syndrome in C57BL/6 Mice

- (A) Weight development in male ND and CD-HFD C57BL/6 mice.
 (B) Quantitative analysis of the body composition by MRI. Fat (left) and lean mass (right) from 10-month-old male ND and CD-HFD C57BL/6 mice (n = 5 each).
 (C) IPGTT performed with 6-month-old male ND and CD-HFD C57BL/6 mice (n = 3 each).
 (D) Pyruvate tolerance test performed with 10-month-old male C57BL/6 mice (ND, n = 9; CD-HFD, n = 10).
 (E) MRI analyses on livers of 6-month-old ND and CD-HFD C57BL/6 mice. T1 (fast low-angle shot [FLASH]) OUT phase: dark color indicative of steatosis. T2 TurboRare visualizes increase in subcutaneous and abdominal fat and hepatic lipid accumulation (bright regions) in CD-HFD mice.
 (F) Quantitative analysis of liver composition by MRI. Fat (left) and lean mass (right) from 10- to 11-month-old ND and CD-HFD C57BL/6 mice (n = 5 each).
 (G) Quantification of liver triglyceride content in 3-, 6-, and 12-month-old ND and CD-HFD C57BL/6 mice (n ≥ 8 each).
 (H) Quantification of serum cholesterol (n ≥ 8 each).
 (I) Quantification of serum ALT in male C57BL/6 mice (n ≥ 8 each).
 (J) Representative Sudan red staining illustrating fat accumulation in livers of ND and CD-HFD C57BL/6 mice. The scale bar represents 100 μ m.
 (K) Representative H&E staining of 12-month-old CD-HFD C57BL/6 mice illustrating NASH. Accumulation of MDB (arrowhead), ballooned hepatocytes (asterisk), and satellitosis (arrow) similar to human NASH pathology (right image). The scale bar represents 50 μ m.
 (L) Electron microscopic images of mitochondria isolated from 6-month-old ND and CD-HFD C57BL/6 mice. Arrowhead: widened and rounded cristae. The scale bar represents 500 nm.

All data are presented as mean \pm SEM. See also Figure S1.



(legend on next page)

with ND mice. In contrast, only mild alterations in body lean mass could be observed (Figure 1B; Figure S1D). Metabolic analyses with an intraperitoneal glucose tolerance test (IPGTT) revealed an impaired glucose response in CD-HFD and HFD mice (Figure 1C; Figures S1E and S1F). Mice on a CD-HFD produced significantly more glucose upon pyruvate injection (Figure 1D; Figure S1E), indicating aberrant gluconeogenesis in CD-HFD mice.

MRI analysis revealed liver steatosis and subcutaneous and abdominal fat accumulation in CD-HFD but not ND mice (Figure 1E). In line, quantitation of MRI analysis showed a strong increase in fat mass, as well as an increase in lean mass in the livers of CD-HFD mice (Figure 1F; Figure S1G). This was consistent with strongly increased triglyceride deposition in the livers of CD-HFD mice (Figure 1G). Serum analyses revealed rising cholesterol levels, especially of low-density lipoprotein, but unaltered triglyceride levels (Figure 1H; Figure S1H; data not shown). CD-HFD and HFD mice displayed increased cholesterol levels (Figure S1I). In line, liver cholesterol levels were significantly elevated upon CD-HFD (Figure S1J). Liver steatosis was accompanied by progressive liver damage, reflected by increased serum alanine transaminase (ALT) and aspartate transaminase (AST) levels (Figure 1I; Figures S1K and S1L). In contrast, HFD mice lacked liver damage at 6 months (data not shown). No significant alterations in serum bilirubin or alkaline phosphatase levels were found, indicating that long-term CD-HFD does not cause significant biliary damage. However, a modest increase in bile acid levels was measured in serum (Figure S1M). Hematoxylin and eosin (H&E) and Sudan red staining of liver sections further illustrated the progression from mild to severe steatosis over time. Quantification of the Sudan red⁺ area and the sizes of lipid droplets revealed a strong increase of large fatty droplets culminating in macrovesicular steatosis (Figure 1J; Figures S1N and S1O).

In addition to severe steatosis, the livers of CD-HFD mice displayed ballooned hepatocytes, immune cell infiltration, satellitosis, Mallory-Denk body (MDB) formation, and glycogenated nuclei, all features reminiscent of human NASH (Figure 1K). Furthermore, signs of oxidative stress were observed in the livers of CD-HFD mice (Figure S1P). Screening analyses of mRNA revealed significant downregulation of several genes involved in lipid metabolism in CD-HFD compared with ND mice (Figure S1Q). Genes such as hepatic lipase or lipoprotein lipase, regulated by inflammatory cells and their secreted factors (e.g., cytokines, chemokines; Lo et al., 2007) and genes involved in cholesterol biosynthesis were significantly deregulated.

Mitochondrial alterations found in the hepatocytes of NASH patients (Pirola et al., 2013), such as mitochondrial structural def-

icits, were also observed in CD-HFD mice. Mitochondrial cristae were shortened, more rounded, and partially enlarged in size, with a balloon-like appearance (Figure 1L). Moreover, mitochondria displayed reduced ATP production and increased vulnerability to extracellular calcium (Figures S1R and S1S).

Infiltration and Activation of Immune Cells in Livers of CD-HFD C57BL/6 Mice

We next investigated whether CD-HFD feeding affects the homeostasis of hepatic immune cells, similar to what has been postulated for NASH patients (Caballero et al., 2012; De Vito et al., 2012). Intrahepatic immune cells comprised CD3⁺ T cells, F4/80⁺ macrophages, MHCII⁺ cells, and Ly6G⁺ neutrophils in CD-HFD but not in ND or HFD mice (Figure 2A; Figure S2A). Whereas numbers of CD3⁻CD19⁺ B cells remained unchanged (Figure 2B), strong increases in CD4⁺ and CD8⁺ T cells were observed in CD-HFD compared with ND mice (Figure 2C). Furthermore, CD8⁺ and CD4⁺ T cells expressed more CD44 and CD69, indicating local T cell activation (Figures 2D and 2E; Figures S2B and S2C). Enhanced secretion of TNF by CD8⁺ T cells and IL-17 by CD4⁺ T cells was observed (Figures S2D and S2E). Moreover, significant increases in hepatic NKT cells (CD3⁺NK1.1⁺), especially in α -GalCer-CD1d negative type II NKT cells, and regulatory T cells were found in CD-HFD mice (Figures 2F–2H). Elevated T cells were accompanied by increased proinflammatory Ly6C^{hi} monocytes, Ly6G⁺ granulocytes, and F4/80⁺ Kupffer cells (Figure 2I; Figures S2F and S2G). Splenic immune cells displayed a similar phenotype, suggesting systemic activation of immune cells upon CD-HFD (Figure S2H). In addition, TNF superfamily (TNFSF) cytokines and *Tgfb*, *Ifn* γ , and *Il1* β were upregulated in hepatic lymphocytes from CD-HFD mice (Figure S2I). In particular, LT β R ligands (*Light*, *Lta*, and *Ltb*) were strongly upregulated.

Long-term CD-HFD caused mild pericellular fibrosis accompanied by elevated α SMA⁺ cells indicative of hepatic stellate cell (HSC) activation (Figure 2J). In line, expression of genes indicative of fibrosis or liver tissue remodeling was enhanced (Figure S2J). Splenocytes from CD-HFD mice sufficed to activate isolated HSCs in vitro, reflected by an increase in α SMA⁺ expression and a loss of vitamin A droplets, whereas ND splenocytes did not (Figure 2K). These data suggest a contribution of activated immune cells to liver tissue remodeling in the CD-HFD model.

Long-Term CD-HFD Causes HCC in C57BL/6 Mice

Mice were sacrificed at 12 months, and livers were analyzed macro- and microscopically. HFD and CD-HFD mice showed enlarged, pale yellow livers indicative of steatosis. One of 40 HFD mice (incidence ~2.5%) displayed a tumor. In contrast,

Figure 2. CD-HFD Induces Enhanced Presence and Activation of Hepatic Lymphocytes and Mild Fibrosis

(A) Representative histology and IHC on liver sections of 6-month-old ND (upper row) and CD-HFD (lower row) C57BL/6 mice. From left to right: H&E, B220, CD3, F4/80, MHCII, and Ly6G. The scale bar represents 50 μ m.

(B–I) Representative zebra plots and quantification of flow cytometric analyses comparing 6-month-old ND and CD-HFD C57BL/6 mice ($n \geq 4$). CD19⁺CD3⁻ B cells (B), CD4⁺ and CD8⁺ T cells (C), CD44⁺CD8⁺CD62L⁻ T cells (D), CD69⁺CD8⁺CD62L⁻ T cells (E), CD19⁻CD3⁺NK1.1⁺ NKT cells (F), α -Gal Cer CD1-tetramer staining of CD3⁺NK1.1⁺ NKT cells to quantify numbers of type I and type II NKT cells (G), Foxp3⁺CD4⁺ regulatory T cells (H), and CD11b⁺Ly6C⁺ inflammatory monocytes (I) are shown.

(J) Masson's trichrome staining (MAS) and α SMA IHC on liver sections of 12-month-old ND and CD-HFD C57BL/6 mice. The scale bar represents 50 μ m.

(K) Immunofluorescence staining on primary HSC co-cultured with ND and CD-HFD splenocytes. The scale bar represents 25 μ m. α SMA⁺ cells and vitamin A⁺ droplets are quantified.

All data are presented as mean \pm SEM. See also Figure S2.

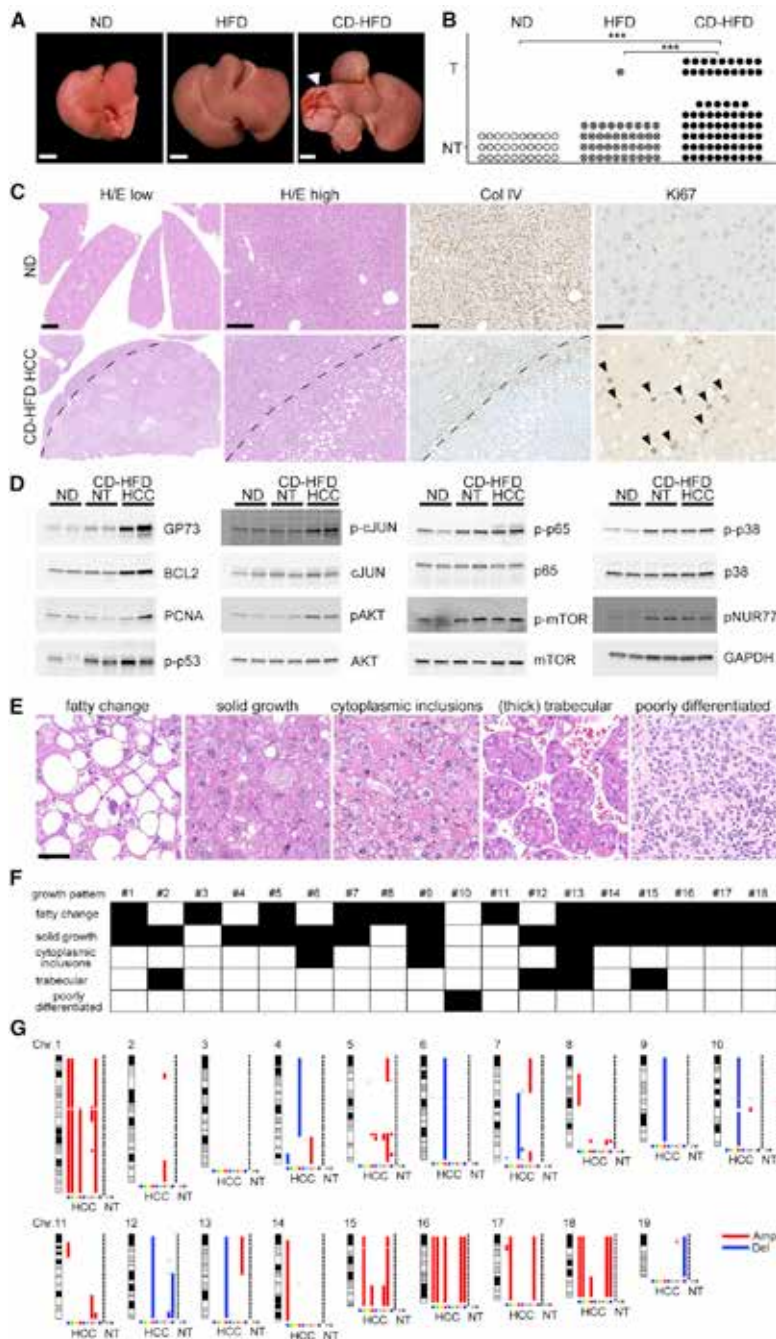


Figure 3. Long-Term CD-HFD Leads to HCC Development in C57BL/6 Mice

(A) Macroscopy of livers from 12-month-old ND, HFD, or CD-HFD C57BL/6 mice, with arrowhead pointing toward HCC. The scale bar represents 5 mm.

(B) Graph summarizing C57BL/6 mice without tumor (NT) and with tumor (T) on ND, HFD, and CD-HFD. Symbols depict individual mice.

(C) Histology and IHC of livers derived from 12-month-old C57BL/6 mice on ND (upper row) and CD-HFD with HCC (lower row). Dashed lines depict HCC border. The scale bars represent H&E: 2 mm (low) and 200 μ m (high); collagen IV: 200 μ m; Ki67: 100 μ m (depicted by arrowheads).

(D) Immunoblot analyses of liver homogenates from ND and CD-HFD C57BL/6 mice with or without HCC (NT).

(E) H&E stains of HCC of various growth patterns. The scale bar represents 50 μ m.

(F) Distribution of the growth patterns per HCC analyzed. Each column represents one individual mouse.

(G) Karyoplot of an aCGH analysis on nine HCCs from CD-HFD C57BL/6 mice and two samples of livers without HCC (NT). The q-arm of each chromosome is shown, and dark horizontal bars within the symbolized chromosomes represent G bands. See also Figure S3 and Table S1.

cords, and Ki67⁺ proliferating tumor cells were observed within the tumor lesions, thus tumors resembled human HCC (Figure 3C; Figure S3C). In addition, HCCs from CD-HFD and HFD mice were positive for the tumor markers GP73, α -fetoprotein, and the oval cell marker A6 but negative for glutamine synthetase (Figure S3D).

Immunoblot analysis of HCC confirmed enhanced expression of GP73, the antiapoptotic protein BCL2, and the proliferation marker proliferating cell nuclear antigen when compared with ND or CD-HFD livers without tumors (NT). Several signaling pathways (including NF- κ B, AKT, cJUN, mTOR, and p38) are associated with liver cancer (Moeini et al., 2012). Indeed, phosphorylation of AKT, cJUN, and p53 was found within HCC (Figure 3D). CD-HFD induced phosphorylation of p65, p38, mTOR, and NUR77 not only within HCC nodules but also in NT tissue. In contrast, HFD did not activate p38, mTOR, or NUR77 (Figure S3E).

Accordingly, IHC revealed enhanced nuclear p65 translocation in immune cells and hepatocytes of CD-HFD livers but not in ND or HFD livers (Figure S3F). Moreover, CD-HFD and HFD livers displayed an increase in Ki67⁺ hepatocytes compared with ND, indicative of compensatory proliferation (Figure S3F). In addition, sequencing of *Tp53* exons revealed missense mutations in 4 of

19 of 75 CD-HFD mice displayed at least one liver tumor, with male and female mice being affected at similar rates (incidence ~25%) (Figures 3A and 3B; Figures S3A and S3B). ND livers lacked tumors.

Tumors were further analyzed by immunohistochemistry (IHC). Loss of collagen IV networks, broadening of liver cell

Cancer Cell

CD8⁺ and NKT Cells Promote NASH and NASH-Induced HCC

12 HCCs, which most likely accounts for p53 activation (Figure S3G).

CD-HFD-Induced HCCs Are Heterogeneous in Growth, Genomic Alterations, and Gene Expression Patterns

Histological analysis of CD-HFD-induced HCC revealed different growth patterns, with predominantly fatty change and solid growth, sometimes with cytoplasmic inclusions or (thick) trabecular growth, and poor differentiation in one case (Figures 3E and 3F; Figure S3H). Thus, CD-HFD-induced HCC are heterogeneous. For molecular characterization, HCC were microdissected and analyzed by array comparative genomic hybridization analysis (aCGH), revealing chromosomal aberrations in all HCCs but not in control tissue. NT livers did not display chromosomal aberrations. Hence, CD-HFD does not directly induce chromosomal alterations in the liver (Figure 3G). Although amplifications on chromosomes 1, 15, 16, and 18 were found in 4 of the 9 HCCs (Figure S3I), no clear recurrent pattern was found ($p = 0.35$). Synteny analyses revealed that most of the genes found to be altered in copy number in CD-HFD livers were congruent with loci found to be changed in human cryptogenic HCC (Schlaeger et al., 2008) (Figure S3J and Table S1). Moreover, clonality of individual HCC nodules spreading within one liver was found (Figure S3K).

Application of an expression signature to distinguish proliferative and aggressive from differentiated and less aggressive hepatoblastoma or HCC (Cairo et al., 2008) confirmed that CD-HFD-induced HCC are heterogeneous, ranging from HCC with increased expression of differentiation genes to HCC with high expression of proliferation genes (Figure S3L). Moreover, we assessed the expression pattern of selected oncogenes and tumor suppressors deregulated in HCC (Zender et al., 2010). Of 78 genes tested, we identified significant deregulation of several genes involved in the regulation of transcription, cell cycle, and proliferation and apoptosis (Figures S3M and N), including the tumor suppressor genes *Tp53*, *Apc*, and *Axin1*.

Lymphocytes, LT β R, and NF- κ B Signaling in Hepatocytes Facilitate CD-HFD-Induced Liver Cancer

Both protective and procarcinogenic roles have been attributed to immune cells in liver cancer, depending on the type of model and the study performed (Vucur et al., 2010). Therefore, *Rag1*^{-/-} mice, lacking mature B, T, and NKT cells and unable to mount adaptive immune responses and *Ccr2*^{-/-} mice, which have reduced numbers of proinflammatory monocytes and myeloid-derived suppressor cells, were fed with CD-HFD and analyzed for liver carcinogenesis.

Because CD-HFD led to p65 activation and expression of LT β R ligands in the livers of C57BL/6 mice, we analyzed mice with hepatocyte-specific deficiencies in canonical NF- κ B (*Ikk β* ^{Δhep} mice) and LT β R signaling (*Lt β* ^{Δhep} mice) (Figure S4A).

Importantly, CD-HFD *Rag1*^{-/-} mice lacked HCC, whereas *Ccr2*^{-/-} mice displayed a similar HCC incidence as C57BL/6 mice. Moreover, CD-HFD *Lt β* ^{Δhep} and *Ikk β* ^{Δhep} mice displayed a significant reduction or trend toward reduction in HCC incidence (Figures 4A and 4B). IHC further confirmed HCCs in *Ccr2*^{-/-}, *Lt β* ^{Δhep}, and *Ikk β* ^{Δhep} mice, which were similar to HCCs in CD-HFD C57BL/6 mice, as well as the absence of liver tumorigenesis in *Rag1*^{-/-} mice (Figures 4C; Figure S4B). Real-time PCR for HCC-associated genes, aCGH, and histological

analyses showed that HCC from CD-HFD *Ccr2*^{-/-}, *Lt β* ^{Δhep}, and *Ikk β* ^{Δhep} mice were qualitatively similar to those from CD-HFD C57BL/6 mice (Figures S4C–S4F).

Analysis and quantification of hepatic lipid accumulation illustrated severe steatosis in *Ccr2*^{-/-} and *Ikk β* ^{Δhep} mice, a reduction in *Lt β* ^{Δhep} mice, as well as an absence in CD-HFD *Rag1*^{-/-} mice (Figures 4D and 4E). Notably, triglyceride levels were unchanged in CD-HFD *Rag1*^{-/-} and *Lt β* ^{Δhep} livers compared with ND C57BL/6 livers. In contrast, triglyceride accumulation in CD-HFD *Ccr2*^{-/-} and *Ikk β* ^{Δhep} livers was similar to CD-HFD C57BL/6 livers (Figure 4F). CD-HFD *Ccr2*^{-/-}, *Ikk β* ^{Δhep}, and *Lt β* ^{Δhep} mice displayed elevated serum cholesterol and ALT levels similar to CD-HFD C57BL/6 mice (Figure S4G). In line, CD-HFD *Lt β* ^{Δhep} mice showed similar body weights to CD-HFD C57BL/6 mice (Figure S4H).

Moreover, histological features of NASH, such as severe steatosis, ballooning hepatocytes, satellitosis, and MDB, were absent in *Rag1*^{-/-} livers but present in *Lt β* ^{Δhep}, *Ccr2*^{-/-}, and *Ikk β* ^{Δhep} livers (Figure S4I). Fibrosis was observed in *Lt β* ^{Δhep}, *Ccr2*^{-/-}, and *Ikk β* ^{Δhep} livers but not *Rag1*^{-/-} livers (Figure S4I). IHC and flow cytometric analyses of *Lt β* ^{Δhep} mice revealed the presence of activated CD8⁺ and NKT cells (Figures S4J and S4K). Also, the deregulation of lipid metabolism genes in CD-HFD C57BL/6 livers described above was partially prevented in CD-HFD *Lt β* ^{Δhep} livers (Figure S4L). Despite the presence of activated immune cells, NASH, and overt liver damage in CD-HFD *Lt β* ^{Δhep} mice, they showed a strongly reduced HCC incidence, suggesting a direct influence of LT β R signaling on liver carcinogenesis.

Our data demonstrate that lymphocytes directly contribute to liver steatosis, NASH, and carcinogenesis in the CD-HFD model and that LT β R and canonical NF- κ B signaling in hepatocytes interfere with the transition from NASH to HCC.

Role of Lymphocytes in Liver Damage and Steatosis

Consistent with histological data, MRI analyses confirmed the lack of steatosis in CD-HFD *Rag1*^{-/-} livers without significant changes in liver lean mass compared with C57BL/6. However, subcutaneous and abdominal fat was present (Figures 5A and 5B).

Serum analysis showed no increase in cholesterol, ALT, or AST levels in CD-HFD *Rag1*^{-/-} mice compared with ND C57BL/6 mice (Figures 5C; Figure S5A). ALT, AST, cholesterol, and liver triglycerides were not significantly changed in ND *Rag1*^{-/-} mice compared with ND C57BL/6 mice (data not shown).

Alterations in lipid metabolism or uptake might be a reason for the absence of fat accumulation in livers and reduced serum cholesterol in CD-HFD *Rag1*^{-/-} mice. Immunoblot analysis revealed that CD-HFD *Rag1*^{-/-} mice lacked phosphorylation of p65, mTOR, and NUR77 (Figure 5D). Moreover, transcriptional analyses demonstrated that the deregulation of several genes involved in lipid metabolism observed in CD-HFD C57BL/6 mice was partially prevented in CD-HFD *Rag1*^{-/-} mice (Figure 5E).

To investigate whether *Rag1*^{-/-} mice display a reduced capacity to take up fatty acids (FAs) from the circulation or the GI tract, we intravenously or orally administered traceable FAs to ND C57BL/6 and *Rag1*^{-/-} mice. No difference in FA uptake into C57BL/6 and *Rag1*^{-/-} livers was observed with either administration route (Figures S5B and S5C). Hepatocytes isolated from C57BL/6 or *Rag1*^{-/-} mice also showed no difference

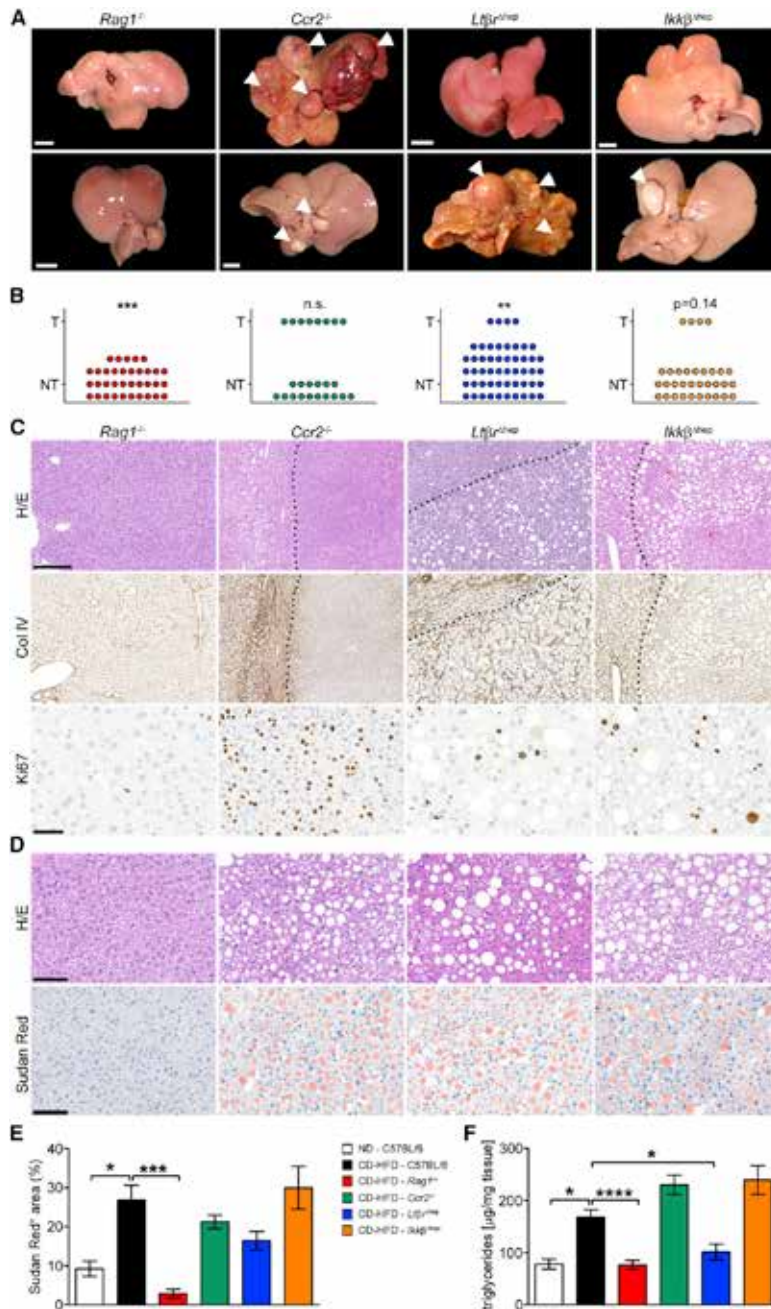


Figure 4. HCC Depends on the Presence of Lymphocytes, LTβR, and Canonical NF-κB Signaling

(A) Macroscopy of livers from 12-month-old CD-HFD *Rag1*^{-/-}, *Ccr2*^{-/-}, *Ltβr*^{Δhep}, and *Ikkβ*^{Δhep} mice with (arrowheads) or without HCC. The scale bar represents 5 mm.

(B) Graph representing numbers of mice without tumor (NT) and with tumor (T). Each symbol depicts one individual mouse; statistical significance compared with CD-HFD C57BL/6 mice is shown.

(C) Histological analysis of livers derived from 12-month-old CD-HFD *Rag1*^{-/-}, *Ccr2*^{-/-}, *Ltβr*^{Δhep}, and *Ikkβ*^{Δhep} mice (from left to right). H&E stains are shown, with dashed line depicting HCC borders, collagen IV staining (both scale bars represent 200 μm), and Ki67 staining (the scale bar represents 100 μm).

(D) H&E and Sudan red staining for fat accumulation in livers of 12-month-old CD-HFD *Rag1*^{-/-}, *Ccr2*^{-/-}, *Ltβr*^{Δhep}, and *Ikkβ*^{Δhep} mice (from left to right; the scale bar represents 100 μm).

(E) Quantification of total Sudan red⁺ area (n ≥ 6 per genotype).

(F) Quantification of liver triglycerides (n ≥ 12 each).

All data are presented as mean ± SEM. See also Figure S4.

ure S5G). These data demonstrate that the phenotype of *Rag1*^{-/-} mice is due not to an altered FA uptake but rather to the lack of lymphocytes.

We next addressed whether differences in CD-HFD *Rag1*^{-/-} and C57BL/6 mice could be due to changes in the barrier function of the GI tract or the intestinal microbiota diversity. Oral administration of FITC-dextran revealed no differences in GI barrier function. Additionally, IHC for E-cadherin suggested intact GI barrier structures in both genotypes (Figures S5H and S5I). Co-housing of CD-HFD C57BL/6 and *Rag1*^{-/-} mice did not alter the CD-HFD-related phenotypes in either genotype. In particular, no elevation of serum cholesterol, ALT, AST, or liver triglyceride levels was observed in CD-HFD *Rag1*^{-/-} mice co-housed with C57BL/6 (Figure S5J). Moreover, high-throughput sequencing of partial 16S rRNA genes (V4 region) amplified from fecal DNA collected from the co-housed CD-HFD C57BL/6 and *Rag1*^{-/-} mice showed no difference in phylogenetic makeup between these genotypes (Figure S5K). In addition, analysis of the amount of endotoxin in the portal vein did not reveal differences between CD-HFD C57BL/6 and *Rag1*^{-/-} mice (Figure S5L). These data indicate that a leaky gut barrier or differences in microbiota are unlikely to cause the phenotypes observed in CD-HFD *Rag1*^{-/-} and C57BL/6 mice.

in their capacity to take up FA in vitro (Figure S5D). In line, CD-HFD *Rag1*^{-/-} mice showed an increase in body weight similar to C57BL/6 (Figure S5E). However, analysis of liver-to-body weight ratios confirmed the absence of liver fat accumulation (Figure S5F) despite body weight gain in *Rag1*^{-/-} mice. In addition, IPGTT revealed that CD-HFD *Rag1*^{-/-} mice showed impaired glucose tolerance, similar to C57BL/6 mice (Fig-

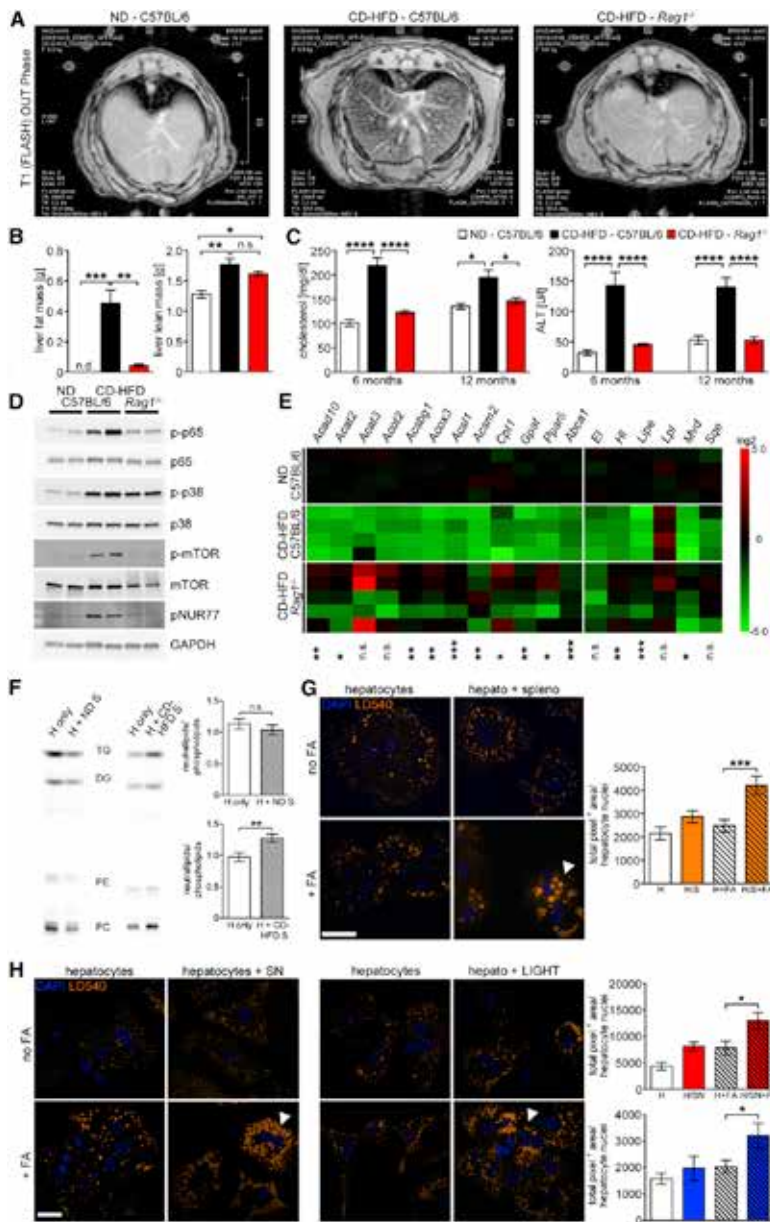


Figure 5. Interaction with Activated Immune Cells Triggers Hepatic Lipid Uptake

(A) MRI analyses on livers of 6-month-old ND and CD-HFD C57BL/6 and *Rag1*^{-/-} mice. T1-weighted FLASH OUT phase indicated lack of steatosis in CD-HFD *Rag1*^{-/-} mice.

(B) Quantitative analysis of liver composition by MRI. Lean (left) and fat mass (right) from 10-month-old ND and CD-HFD C57BL/6 and *Rag1*^{-/-} mice (n = 5 each).

(C) Quantification of serum cholesterol (left) and ALT (right) (n ≥ 8 each).

(D) Immunoblot analysis of 12-month-old ND and CD-HFD C57BL/6 and *Rag1*^{-/-} mice.

(E) Real-time PCR analysis for lipid metabolism genes on mRNA isolated from ND and CD-HFD C57BL/6 and *Rag1*^{-/-} livers.

(F) Thin-layer chromatography to visualize FA uptake by hepatocytes (H) upon co-cultivation with splenocytes (S) from 6-month-old ND (left) or CD-HFD C57BL/6 mice (right) and quantification of the neutrallipid:phospholipid ratio.

(G) Staining with LD540 (orange) and DAPI (blue) to visualize lipid droplet accumulation (arrowhead) in hepatocytes co-cultured with CD-HFD splenocytes and addition of FAs. The scale bar represents 20 μm. Quantification of the LD540⁺ area.

(H) Staining with and quantification of LD540 to visualize lipid droplet accumulation in hepatocytes cultured with conditioned medium from CD-HFD splenocytes or recombinant LIGHT. The scale bar represents 20 μm.

All data are presented as mean ± SEM. See also Figure S5.

We next investigated whether lymphocytes could trigger enhanced FA uptake into hepatocytes by co-culturing with splenocytes from ND C57BL/6 mice. However, no differences in FA uptake into hepatocytes with or without splenocytes were observed (Figure 5F). Notably, co-culture with activated splenocytes (from CD-HFD mice) led to significantly enhanced FA uptake by hepatocytes, independent of the concentration of FAs or the hepatocyte/splenocyte ratio (Figure 5F; Figures S5M and S5N). Quantification of LD540 staining revealed that co-culturing of hepatocytes with splenocytes from CD-HFD C57BL/6 mice led to

increased lipid accumulation and macrovesicular steatosis (Figure 5G).

Next, we investigated whether direct cell contact with splenocytes or whether immune-cell-derived soluble factors mediate hepatic lipid uptake. Thus, primary hepatocytes were cultured with CD-HFD splenocyte conditioned in the absence or presence of FA. Conditioned medium sufficed to mediate lipid uptake into hepatocytes (Figure 5H). Our analyses from isolated splenocytes, intrahepatic lymphocytes, and protein analyses of their supernatant indicated that members of the TNFSF (e.g., *Light* and *Ltαβ*) were strongly upregulated (Figure S2; data not shown). Therefore, we added recombinant LIGHT to primary hepatocytes. Indeed, the addition of LIGHT sufficed to induce hepatic lipid uptake (Figure 5H).

increased lipid accumulation and macrovesicular steatosis (Figure 5G).

CD8⁺ T Cells and NKT Cells Control NASH and NASH-Induced HCC

Increased numbers and enhanced activation of CD8⁺ and NKT cells were observed in CD-HFD C57BL/6 livers. Thus, *β2m*^{-/-} mice, which display strongly reduced CD8⁺ and NKT cells, were fed with CD-HFD and analyzed at 6 and 12 months. Flow cytometric analysis verified significant reductions in CD8⁺ T cells

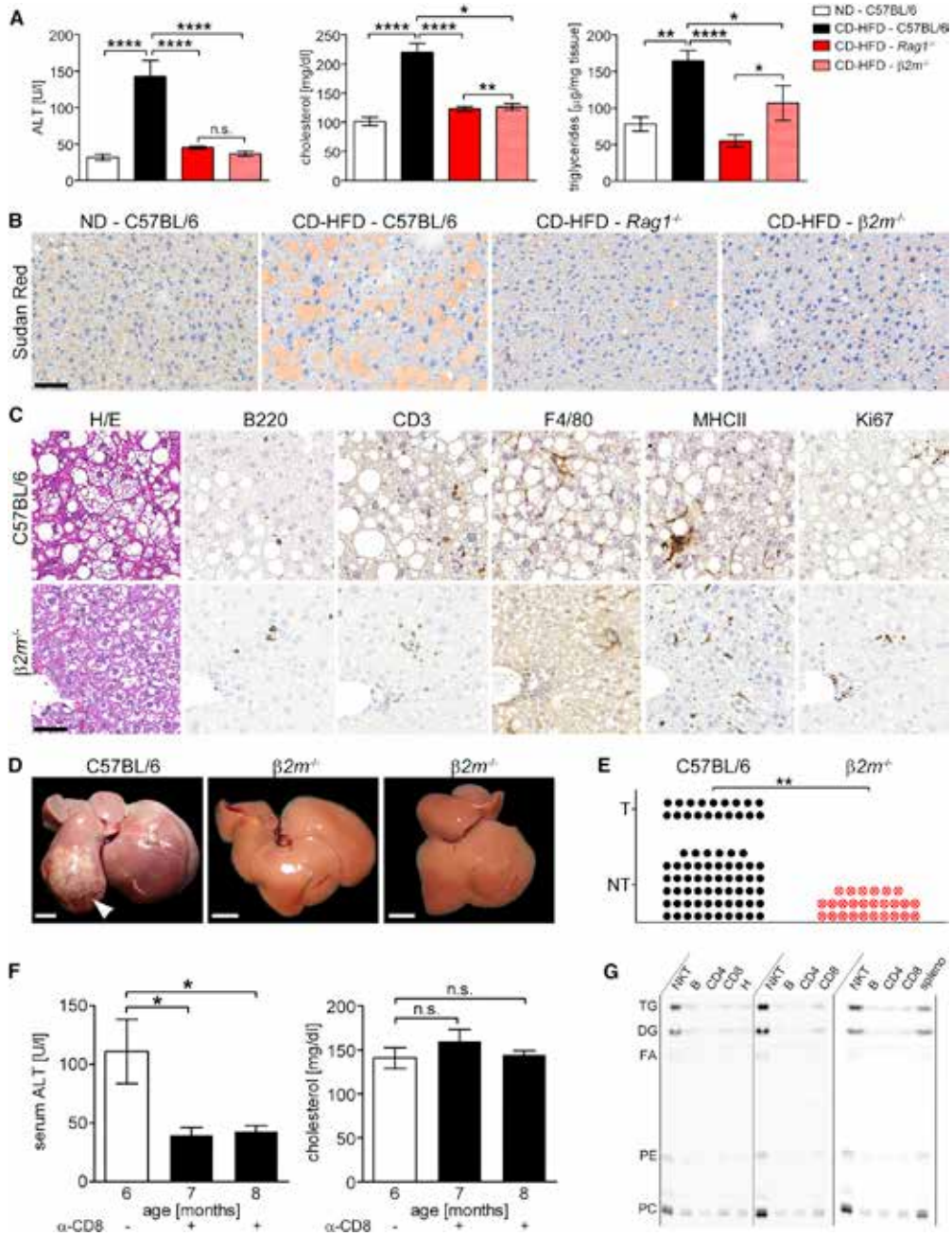


Figure 6. CD8⁺ T Cells and NKT Cells Control Liver Damage, NASH, and HCC in a Nonredundant Manner

(A) Quantification of serum ALT and cholesterol in 6-month-old CD-HFD C57BL/6 and *β2m*^{-/-} mice ($n \geq 8$ each) and liver triglycerides in 12-month-old mice ($n \geq 11$ each).

(B) Sudan red staining of liver sections (12-month-old, indicated genotypes).

(C) Representative histology and IHC on liver sections of 12-month-old CD-HFD C57BL/6 and *β2m*^{-/-} mice. From left to right: H&E, B220, CD3, F4/80, MHCII, and Ly6G. The scale bar represents 50 μ m.

(D) Macroscopy of livers derived from 12-month-old CD-HFD C57BL/6 and *β2m*^{-/-} mice. The scale bar represents 5 mm; arrowhead depicts HCC.

(E) Graph summarizing CD-HFD C57BL/6 and *β2m*^{-/-} mice without tumor (NT) and with tumor (T). Symbols depict individual mice.

(legend continued on next page)

Cancer Cell

CD8⁺ and NKT Cells Promote NASH and NASH-Induced HCC

and α -Gal Cer⁺ NKT cells in CD-HFD $\beta 2m^{-/-}$ livers compared with CD-HFD C57BL/6 livers (Figure S6A). Aged CD-HFD $\beta 2m^{-/-}$ mice showed a similar increase in body weight as CD-HFD C57BL/6 and a trend toward reduction in liver-to-body weight ratio (Figure S6B). Importantly, $\beta 2m^{-/-}$ mice were protected from CD-HFD-induced liver damage similar to *Rag1*^{-/-} mice (Figure 6A). In line, $\beta 2m^{-/-}$ mice displayed significant reductions in serum cholesterol and liver triglyceride levels compared with CD-HFD C57BL/6 mice (Figure 6A). This was confirmed by Sudan red staining (Figure 6B). All CD-HFD $\beta 2m^{-/-}$ mice lacked overt NASH and fibrosis (Figure S6C). In 2 of 23 mice, we observed moderate steatosis, hepatocyte ballooning, and occasional hepatic inflammatory cells (Figure 6C), histological changes that could be considered borderline NASH.

Strikingly, CD-HFD $\beta 2m^{-/-}$ mice lacked HCC (Figures 6D and 6E). Immunoblot analysis revealed that $\beta 2m^{-/-}$ livers lacked or had strongly reduced p65 and NUR77 phosphorylation. Phosphorylation of mTOR was observed in some $\beta 2m^{-/-}$ mice upon CD-HFD feeding (Figure S6D). Moreover, deregulation of genes involved in lipid metabolism in CD-HFD C57BL/6 livers was partially prevented in $\beta 2m^{-/-}$ mice (Figures S6E and S6F).

We next investigated whether CD8⁺ and NKT cells exert non-redundant functions in CD-HFD-induced liver disease. To assess the role of CD8⁺ T cells, antibody-mediated cell depletion was performed in CD-HFD C57BL/6 mice with established pathology. Efficacy of CD8⁺ T cell depletion was confirmed by flow cytometry (Figure S6G). After 4 and 8 weeks of anti-CD8 treatment and continuous CD-HFD feeding, liver damage was rescued (Figure 6F). Notably, serum cholesterol values remained unchanged, suggesting that CD8⁺ T cells trigger CD-HFD-induced liver damage but do not affect lipid metabolism.

Because CD8⁺ T cells did not appear to strongly influence lipid metabolism, we addressed whether NKT cells could influence hepatic lipid metabolism. Sorted CD19⁺ B, CD4⁺/CD8⁺ T, or NKT cells from CD-HFD C57BL/6 spleens were co-cultured with hepatocytes, and their capacity to mediate FA uptake was assessed (Figures 6G; Figure S6H). Only NKT cells appeared to efficiently enhance FA uptake by hepatocytes, which was as effective as incubation of hepatocytes with total splenocytes.

Having observed that CD-HFD splenocytes activate HSC in vitro, we next investigated whether CD8⁺ or NKT cells can activate HSCs in the CD-HFD model. Notably, HSC activation was strongly induced by CD-HFD NKT cells but only to a minor extent by CD8⁺ T cells (Figure S6I).

These data highlight the importance of CD8⁺ and NKT cells in HCC development. Moreover, CD8⁺ T cells do not mediate FA uptake or HSC activation as efficiently as NKT cells but rather contribute to CD-HFD-induced liver damage.

NKT Cell-Derived LIGHT Exacerbates Liver Damage, NASH, and HCC Development

The LT β R ligand LIGHT (TNFSF14), one the most strongly upregulated cytokines in lymphocytes from CD-HFD C57BL/6 mice,

has been reported to be involved in the regulation of lipid homeostasis (Lo et al., 2007) and to control FA uptake of hepatocytes in vitro. Therefore, we asked whether LIGHT deficiency would interfere with steatosis and NASH development and reduce HCC incidence upon CD-HFD feeding. To this end, aged CD-HFD *Light*^{-/-} mice were analyzed for HCC. Macroscopic and histological analyses of livers showed that CD-HFD *Light*^{-/-} mice lacked HCC (Figure 7A; Figure S7A). Serum analysis revealed lower ALT and cholesterol levels in CD-HFD *Light*^{-/-} mice compared with C57BL/6 (Figure 7B). Sudan red staining and quantification, as well as liver triglyceride measurements, revealed reduced steatosis in *Light*^{-/-} livers (Figure 7C). Immunoblot analysis revealed absent or strongly reduced p65 and NUR77 phosphorylation in CD-HFD *Light*^{-/-} livers; however, absence of LIGHT did not attenuate phosphorylation of mTOR upon CD-HFD feeding (Figure S7B). Moreover, analysis of lipid metabolism genes in CD-HFD *Light*^{-/-} livers indicated that deregulation found in CD-HFD C57BL/6 mice was almost completely restored, resulting in expression levels similar to ND and HFD C57BL/6 mice (Figures S7C and D). IHC revealed a lack of NASH despite infiltrating immune cells in livers of CD-HFD *Light*^{-/-} mice similar to CD-HFD C57BL/6 mice (Figure 7D; Figure S7E). Further analyses of intrahepatic T cell populations by flow cytometry showed no difference in the number or activation status of CD8⁺ T cells between CD-HFD C57BL/6 and *Light*^{-/-} mice. Similar to ND C57BL/6 mice, CD-HFD *Light*^{-/-} mice lacked any increase in intrahepatic NKT cells (Figure 7E). Thus, LIGHT expression and the presence of NKT cells play an important role in CD-HFD-induced steatosis, NASH, and HCC development.

To investigate whether lack of LIGHT signaling in CD8⁺ T cells could account for the observed reduction in liver damage in *Light*^{-/-} mice, we blocked LT β R signaling in CD-HFD C57BL/6 mice using LT β R-Ig. Systemic administration of LT β R-Ig did not alter CD-HFD-induced liver damage, suggesting that the reduced liver damage seen in *Light*^{-/-} mice was due not to the lack of LIGHT expression on activated CD8⁺ T cell but rather primarily to the reduction of hepatic NKT cells (Figure S7F). These data, together with the CD8⁺ T cell depletion experiments, suggest that CD8⁺ and NKT cells cooperate to promote liver damage.

To confirm that NKT cell-derived LIGHT is essential for hepatocyte lipid uptake, we blocked LT β R signaling in vitro in a hepatocyte-splenocyte co-culture. LT β R-Ig reduced the splenocyte-mediated ability to enhance FA uptake (Figure S7G). Thus, in line with data from *Lt β ^{Δhep}* mice, hepatic LT β R signaling (i.e., through NKT cell-derived LIGHT) enhanced lipid uptake.

Increase of LIGHT-Expressing CD8⁺ T Cells and NKT Cells in Livers of Patients with NASH and NASH-Related HCC

We next asked whether the T cell populations and cytokines identified in CD-HFD mice are also found in human liver diseases

(F) Quantification of serum ALT and cholesterol in CD-HFD C57BL/6 mice. Six-month-old mice were injected with anti-CD8 antibody and serum was analyzed every 4 weeks (n = 5).

(G) Thin-layer chromatography visualizing FA uptake of hepatocytes co-cultured with NKT, B, CD4⁺, or CD8⁺ T cells isolated from spleens of 6-month-old CD-HFD C57BL/6 mice. Data from 3 individual mice are shown.

All data are presented as mean \pm SEM. See also Figure S6.

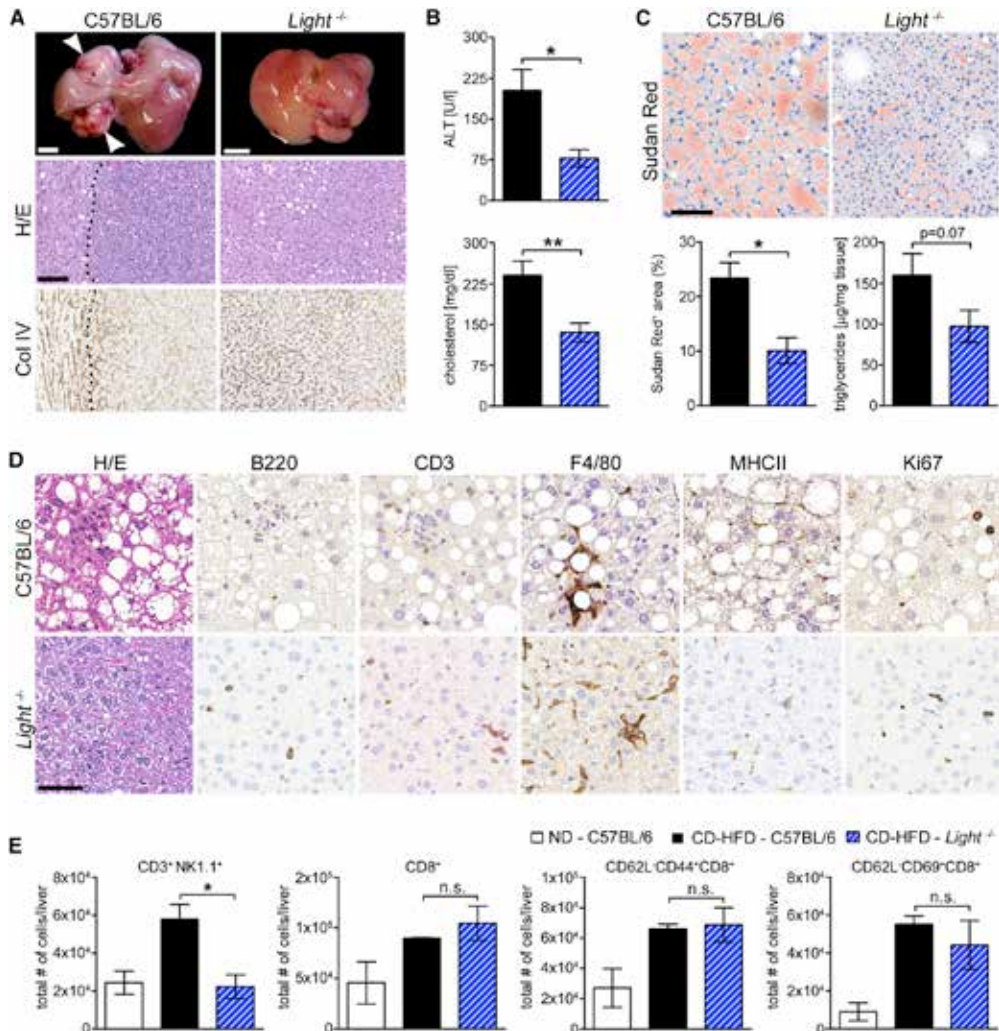


Figure 7. Lack of LIGHT Expression Protects from Liver Damage, NASH, and HCC

(A) Macroscopy of livers of 12-month-old CD-HFD C57BL/6 and *Light*^{-/-} mice (the scale bar represents 5 mm) and H&E and collagen IV stains (the scale bar represents 100 μm).

(B) Quantification of serum ALT and cholesterol in 12-month-old mice (n = 10).

(C) Sudan red staining and quantification on liver sections of 12-month-old CD-HFD C57BL/6 and *Light*^{-/-} mice; quantification of liver triglyceride levels (n = 10).

(D) Histology and IHC on liver sections of 12-month-old CD-HFD C57BL/6 and *Light*^{-/-} mice. From left to right: H&E, B220, CD3, F4/80, MHCII, and Ki67. The scale bar represents 50 μm.

(E) Quantification of flow cytometry analyses for NKT cells and activation of CD8⁺ T cells on hepatic lymphocytes from 6-month-old ND and CD-HFD C57BL/6 and *Light*^{-/-} mice (n = 3).

All data are presented as mean ± SEM. See also Figure S7.

involving steatosis (i.e., NASH, alcoholic steatohepatitis [ASH], and chronic HCV [genotype 3] infection). Moreover, we analyzed NASH- and HCV-related HCC (Table S2). Livers of NASH patients revealed significantly increased numbers of CD8⁺ T cells compared with non-diseased livers (Figures 8A and 8B), as did the livers of patients with ASH, chronic HCV infection, and NASH-induced HCC (Figure S8A). A significantly increased number of CD57⁺CD3⁺ NKT cells was found in the livers of patients

with NASH and chronic HCV infection (Figures 8A and 8B) but not in ASH or HCC (Figure S8A). Samples of ASH and HCC patients lacked increased numbers of LTβ⁺ cells, whereas NASH displayed only a trend and HCV samples a significantly increased number (Figures 8A and 8B; Figure S8A). Of note, *LIGHT* mRNA expression was significantly enhanced in NASH livers, but not in ASH, chronic HCV infection, or HCC (Figure 8B; Figure S8A). Furthermore, co-immuno reactivity was found for

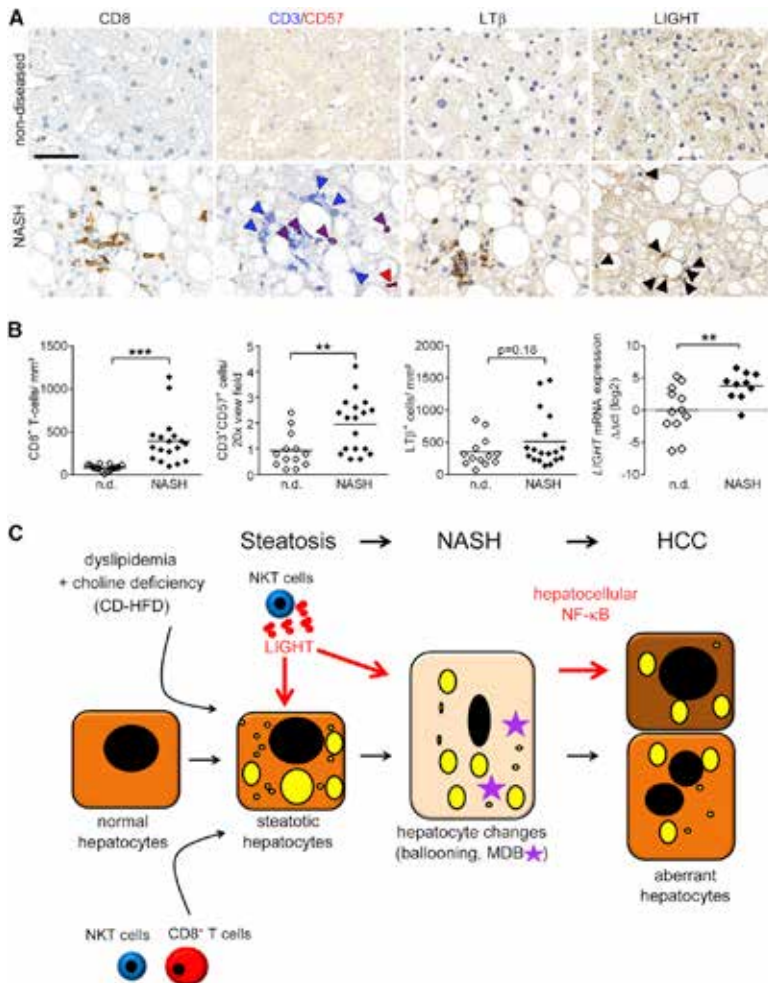


Figure 8. Increased LIGHT⁺ NKT Cells in Livers of NASH Patients

(A) Representative IHC of human non-diseased control livers (n = 13) and livers of NASH patients (n = 18) for CD8⁺ T cells, CD3⁺CD57⁺ NKT cells, LTβ, and LIGHT expression with arrowheads indicating positive cells (the scale bar represents 50 μm).

(B) Quantification of stained cells per area and LIGHT mRNA expression.

(C) In a state of hypernutrition and concomitant choline deficiency, activated intrahepatic NKT cells enhance hepatocyte lipid uptake via secreted LIGHT leading to steatosis. CD8⁺ T cells, NKT cells, and associated inflammatory cytokines cooperatively cause liver damage and contribute to hepatocellular canonical and noncanonical NF-κB signaling facilitating NASH-to-HCC transition. Yellow symbols: lipid droplets.

All data are presented as mean ± SEM. See also Figure S8 and Table S2.

LIGHT and CD57 or CD8, suggesting that CD8⁺ T cells and CD57⁺CD3⁺ NKT cells are the major source of LIGHT (Figure S8B). Thus, as seen in CD-HFD mice, CD8⁺ T cells and NKT cells are found in steatosis-related human liver diseases. Notably, significantly enhanced LIGHT expression was only found in the liver tissue of NASH patients and only to a minor degree in ASH and HCV infection.

DISCUSSION

The exact contribution of immune cells to steatosis, NASH, and HCC development is unclear. Moreover, the underlying signaling pathways activated in parenchymal and non-parenchymal liver cells promoting NASH and facilitating the transition from NASH to HCC remain poorly understood.

Recently, it was reported that immune cells (e.g., NKT cells) suppress NAFLD in short-term experiments with HFD or high-sugar diet (Martin-Murphy et al., 2014) and prevent obesity and metabolic disorder (Lynch et al., 2012). In contrast, immune cells were also reported to promote obesity, tissue inflammation (Sa-

toh et al., 2012) or NAFLD upon short-term HFD or high-fructose diet (Bhattacharjee et al., 2014). This discrepancy in results might be due to an influence of the mouse genetic background, as, for example, Balb/c mice are resistant to diet-induced obesity, the specific composition of diets leading to differences in the activation of immune cells, and the presence or absence of hepatocyte damage, creating an environment that attracts NKT cells. Long-term CD-HFD, in contrast to HFD, induced oxidative stress and mitochondrial damage as well as activation of various signaling pathways and chronic liver damage, preconditioning the liver microenvironment. Moreover, short-term choline-deficient amino acid-defined diet (CDA) causes activation of inflammatory monocytes and Kupffer cell depletion ameliorated steatohepatitis (Miura et al., 2012). In addition, a combination of CDA and HFD caused severe fibrosis in NASH (Matsumoto et al., 2013).

Few of these regimens cause features of a chronic metabolic syndrome concomitant with NASH. By applying long-term CD-HFD, we recapitulate the process of a chronic metabolic disorder and NASH (Figure 8C; Figures S8C–S8G). This caused hepatic infiltration and activation of immune cells, in particular CD8⁺ T cells and NKT cells. In addition, activated lymphocytes were also observed in the spleen, indicating a diet-induced systemic immune activation or dissemination of T cells activated in the liver. However, the exact mechanisms of immune cell activation and which antigens generated during hypercaloric nutrition trigger CD8⁺ T cell and NKT cell activation will require further investigation.

NASH patients displayed significantly increased amounts of hepatic CD8⁺ T cells and NKT cells compared with non-diseased controls. However, an increase of CD8⁺ T cells and/or NKT cells

was also found in patients with ASH, chronic HCV infection, and NASH-related HCC. Taking into account that ASH and NASH are not always clinically distinguishable and also share partially overlapping pathophysiologies (Cope et al., 2000; Petrasek et al., 2013), and that steatosis (and occasionally steatohepatitis) is a hallmark of HCV genotype 3 infection (Rubbia-Brandt et al., 2000), it cannot be expected that the hepatic immune response we describe is exclusively found in NASH. *LIGHT* expression, however, was significantly upregulated in the livers of NASH patients, but not in the livers of patients with ASH or chronic HCV infection. Consistently, costaining indicates that CD8⁺ T cells and CD57⁺CD3⁺ cells in the liver are the major source of *LIGHT*.

Despite weight gain and decreased glucose tolerance, CD-HFD *Rag1*^{-/-} showed a reduced liver-to-body weight ratio, implicating lymphocytes as drivers of liver pathology. The rescued liver phenotype in CD-HFD *Rag1*^{-/-} mice was not due to a deficit in FA uptake, increased hepatic endotoxin, or a change in the GI barrier. The gut microbiota has been reported to exacerbate hepatic steatosis and inflammation, as well as exacerbate chemical hepatocarcinogenesis (Henao-Mejia et al., 2012; Yoshimoto et al., 2013). However, mixing and virtually equalizing the gut microbiota between *Rag1*^{-/-} versus C57BL/6 mice via co-housing experiments did not affect liver damage and NASH development.

Similar to the situation in obese humans with NASH, long-term CD-HFD caused NASH and NASH-to-HCC transition. Our data rather suggest the requirement for “multiple hits,” in line with other reports (Caballero et al., 2009), comprising the presence of reactive oxygen species, influx of activated CD8⁺ T cells and NKT cells, and activation of distinct signaling cascades driving NAFLD to NASH and subsequently to HCC.

We provide evidence that LTβR and canonical NF-κB signaling in hepatocytes are crucial for the transition from NASH to HCC: *Ikkβ*^{Δhep} and *Ltβ*^{Δhep} mice displayed a reduced HCC incidence despite having developed overt NASH, liver damage, and elevated serum cholesterol levels (Figure S8G). *Ikkβ*^{Δhep} mice showed high triglyceride levels, whereas *Ltβ*^{Δhep} mice had reduced liver triglycerides, consistent with reports that immune cell-initiated LTβR activation on hepatocytes affects liver lipid homeostasis (Lo et al., 2007). Thus, similar to other models of inflammation-induced liver cancer (Haybaeck et al., 2009; Pikarsky et al., 2004), canonical NF-κB and LTβR signaling are critical, hepatocyte-intrinsic modulators of NASH to HCC transition but have distinct functions with regard to hepatic lipid uptake. Although hepatocyte-specific deletion of NF-κB or LTβR signaling strongly reduced HCC incidence, deletion of neither of the two pathways sufficed to fully prevent NASH-promoted HCC, suggesting a partial contribution of other pathways.

We detected *Tp53* mutations in one-third of CD-HFD-driven HCC, indicating that a well-known tumor suppressor gene is altered in this model. It is conceivable that the relatively low tumor incidence found in CD-HFD C57BL/6 mice could be increased by feeding *Tp53*^{-/-} mice or other strains lacking HCC-relevant tumor suppressor genes such as *Apc* or *Axin1* (Zender et al., 2010).

Co-culturing primary hepatocytes with distinct immune cell populations revealed that lymphocyte activation (as observed in CD-HFD mice) or supernatant from activated splenocytes strongly induces hepatocellular lipid accumulation, leading to

macrovesicular steatosis. Thus, immune cell/hepatocyte cross-talk, most likely through immune cell-derived cytokines, is critically involved.

Data from CD-HFD *Rag1*^{-/-} mice, flow cytometry, and IHC analyses suggested a link between particular T cell populations, NASH, and HCC development. We reasoned that CD8⁺ T cells or CD1d-restricted NKT cells might be causally linked to NASH and subsequent HCC development. CD1d is an antigen-presenting molecule with the capacity to bind self and foreign lipids and glycolipids (Godfrey et al., 2010), thus enabling metabolic immunity via NKT cells. Indeed, *β2m*^{-/-} mice, which lack both CD1 and MHC1 molecules, displayed strongly reduced liver damage, had no overt NASH, and lacked HCC, suggesting a crucial role of CD8⁺ and NKT cells in NASH and HCC development.

Depletion of CD8⁺ T cells in CD-HFD C57BL/6 mice reversed liver damage but left cholesterol levels unchanged, indicating that CD8⁺ T cells are involved in CD-HFD-induced liver damage rather than in modulating lipid metabolism. Moreover, LTβR inhibition in CD-HFD C57BL/6 mice did not reduce liver damage, arguing against a role of LTβR signaling in the direct control of liver damage in this model. In line, CD-HFD *Ltβ*^{Δhep} mice developed liver damage and NASH. Thus, CD8⁺ T cells are causally linked to liver damage in an LTβR-independent manner.

Intriguingly, coculture of distinct lymphocyte populations with primary hepatocytes showed that NKT cells, but neither CD8⁺ and CD4⁺ T cells nor CD19⁺ B cells, induce efficient FA uptake. Thus, CD8⁺ T cells (with or without NKT cells) induce liver damage in an LTβR-independent manner, whereas NKT cells promote hepatocyte FA uptake and thereby initiate steatosis (Figure S8E). Notably, addition of *LIGHT* to primary hepatocytes sufficed to induce a strong hepatocellular lipid uptake in the presence of FAs, whereas LTβR-Ig blocked lipid uptake by primary hepatocytes cocultivated with splenocytes from CD-HFD mice. Thus, *LIGHT* signaling positively regulates hepatic lipid uptake.

As *LIGHT* signaling has been implicated in the regulation of lipid metabolism (Lo et al., 2007) and as we have observed *LIGHT* and other members of the TNFSF to be upregulated on intrahepatic lymphocytes and splenocytes in CD-HFD C57BL/6 mice, we reasoned that CD-HFD *Light*^{-/-} mice might display reduced NASH and HCC incidence. We found that altered expression of genes involved in lipid metabolism we had observed in CD-HFD C57BL/6 mice was restored in CD-HFD *Light*^{-/-} livers. Surprisingly, *LIGHT* deficiency prevented liver damage and NASH and HCC development and led to a strong reduction in hepatic NKT cells, leaving CD8⁺ T cell numbers unaffected. Thus, the rescued phenotype in *Light*^{-/-} mice could be either directly attributed to the lack of *LIGHT* or might be the result of reduced intrahepatic NKT cells. Notably, liver damage was prevented despite activated hepatic CD8⁺ T cells in *Light*^{-/-} mice, suggesting that CD8⁺ T cells alone were not sufficient to cause liver damage in the absence of NKT cells. Therefore, both CD8⁺ and NKT cells contribute to the induction of liver damage in CD-HFD (Figure S8F).

Our study reveals a cross-talk of CD8⁺ T cells, NKT cells, and their secreted cytokines with hepatocytes in NASH development and the subsequent transition to HCC. Our results indicate that NASH and HCC development is not merely the consequence

of chronic liver damage but is triggered by defined signaling pathways. CD8⁺ T cells and NKT cells enhance steatosis, NASH development, and transition to HCC, adding knowledge of how the immune system contributes to NASH-driven liver damage and HCC. Our data suggest that efficient reduction in the numbers of hepatic CD8⁺ and/or NKT cells or prevention of their cross-talk with hepatocytes by targeting particular signaling pathways has the potential to minimize the risk for developing liver damage, dietary-induced NASH, and HCC.

EXPERIMENTAL PROCEDURES

Human Material

Formalin-fixed, paraffin-embedded normal or tumor tissue was retrieved from the archives and biobank of the Institute of Surgical Pathology, University Hospital Zurich, for IHC and molecular analysis. This study was approved by the local ethics committee of the Canton of Zurich (Kantonale Ethikkommission [KEK] Zurich: KEK-StV 26-2005 and KEK-ZH-Nr. 2013-0382). In line with the regulation of KEK, individual informed consent from all patients was not required for this kind of retrospective analysis on patients' material.

Mice

Animals were maintained under specific pathogen-free conditions, and experiments were conducted in accordance with the guidelines of the Swiss Animal Protection Law and were approved by the Veterinary Office of the Canton of Zurich (licenses 63/2011 and 136/2014). C57BL/6J mice were purchased from Harlan or obtained from own breedings. *Ikkβ^{Δhep}* mice (Maeda et al., 2005), *Ccr2^{-/-}* mice (Kuziel et al., 1997), *Light^{-/-}* mice (Scheu et al., 2002), and *Ltβ^{Δhep}* mice (generated by crossing of *Ltβ^{loxP/loxP}* [Wang et al., 2010] with Alb-Cre mice [Haybaeck et al., 2009]) were bred in house, and *Rag1^{-/-}* and *β2m^{-/-}* mice were purchased from Jackson Laboratories and bred in house. Four- to 5-week-old mice were fed with ND (Provimi Kliba), HFD (Research Diets; D12451), or CD-HFD (Research Diets; D05010402). For co-housing experiments, mice were housed in the same cage after weaning.

In Vitro FA Uptake

Primary hepatocytes were isolated and in dishes with or without splenocytes (5:1 ratio unless otherwise indicated) isolated from 6-month-old ND or CD-HFD C57BL/6 mice for 2 hr in Williams E medium. FAs (alkyne-oleate [66 μM] and alkyne-palmitate [33 μM]) were added for 10 min. After washing, lipids were extracted in chloroform-methanol.

Flow Cytometry

Livers were minced and hepatic lymphocytes were purified using a Ficoll gradient. A FACSCanto II or Fortessa (BD Biosciences) and FlowJo software (TreeStar) were used for acquisition and data analysis.

Statistical Analysis

Statistical analysis was performed using GraphPad Prism software version 5.0 (GraphPad Software) or SPSS (SPSS, Inc.). All data were analyzed by analysis of variance with the post hoc Bonferroni multiple comparison test. Analysis of two samples was performed with Student's t test, and statistics for HCC incidence were calculated using Fisher's exact test. Statistical significance is indicated as follows: ****p < 0.0001, ***p < 0.001, **p < 0.01, and *p < 0.05; "n.s." indicates not significant.

ACCESSION NUMBER

Comparative genomic hybridization (CGH) data are available at ArrayExpress (accession number E-MTAB-2469).

SUPPLEMENTAL INFORMATION

Supplemental Information includes Supplemental Experimental Procedures, eight figures, and two tables and can be found with this article online at <http://dx.doi.org/10.1016/j.ccell.2014.09.003>.

AUTHOR CONTRIBUTIONS

M.J.W., A.A., K.P., Z.A., and Y.B. performed most of the experiments and analyses together with M.R., N.S., A.L., K.S., M.E., D.W., C.E., S.S., T.C., A.W., and M.H. H.Z., H.M., U.P., C.T., and A.V.T. contributed to specific experiments. M.H. conceived the project. M.J.W., P.K., A.W., and M.H. designed the experiments and wrote the paper together with M.K. and M.K. Unpublished reagents or reagents and advice, design, and supervision of experiments were provided by H.Z., H.M., A.V.T., M.T., D.H., K.U., C.T., M.K., and P.K.

ACKNOWLEDGMENTS

We thank R. Maire, D. Kull, R. Hillermann, O. Seelbach, C. Leitzinger, M. Bawohl, R. Reimann, V. Schüppel, E. Koroleva, B. Höchst, F. Böhm, L. Lei, and R. Meyer for excellent technical support; T. Longerich for CGH data; T. O'Connor for critically reading the manuscript; and J. Browning for discussions. Research was supported by the Helmholtz Association, the Foundation for Experimental Biomedicine Zurich (Hofschneider Foundation), the European Research Council (LiverCancerMech), the GRK482, the Helmholtz Alliance Pre-clinical Comprehensive Cancer Center, and SFB-TR36 (to M.H.), grants from Krebsliga Schweiz (Oncosuisse), Promedica Stiftung, Julius Müller Stiftung, Kurt and Senta Herrmann Stiftung (to A.W.), the Crohn's and Colitis Foundation of America (to A.V.T.), Deutsche Forschungsgemeinschaft grant RU742/6-1 (to H.Z.), SFB-704, SFB-TR57, SFB-TR36, Excellence Cluster ImmunoSensation (to P.K.), and the Virtual Liver Network (to K.P., P.K., and C.T.).

Received: March 21, 2014

Revised: July 28, 2014

Accepted: September 17, 2014

Published: October 13, 2014

REFERENCES

- American Cancer Society (2007). Cancer Facts & Figures. (American Cancer Society). <http://www.cancer.org/research/cancerfactsstatistics/cancerfactsfigures2007/index>.
- Anstee, Q.M., and Day, C.P. (2013). The genetics of NAFLD. *Nat. Rev. Gastroenterol. Hepatol.* 10, 645–655.
- Bhattacharjee, J., Kumar, J.M., Arindkar, S., Das, B., Pramod, U., Juyal, R.C., Majumdar, S.S., and Nagarajan, P. (2014). Role of immunodeficient animal models in the development of fructose induced NAFLD. *J. Nutr. Biochem.* 25, 219–226.
- Caballero, F., Fernández, A., De Lacy, A.M., Fernández-Checa, J.C., Caballería, J., and García-Ruiz, C. (2009). Enhanced free cholesterol, SREBP-2 and StAR expression in human NASH. *J. Hepatol.* 50, 789–796.
- Caballero, T., Gila, A., Sánchez-Salgado, G., Muñoz de Rueda, P., León, J., Delgado, S., Muñoz, J.A., Caba-Molina, M., Carazo, A., Ruiz-Extremuera, A., and Salmerón, J. (2012). Histological and immunohistochemical assessment of liver biopsies in morbidly obese patients. *Histol. Histopathol.* 27, 459–466.
- Cairo, S., Armengol, C., De Reyniès, A., Wei, Y., Thomas, E., Renard, C.A., Goga, A., Balakrishnan, A., Semeraro, M., Gresh, L., et al. (2008). Hepatic stem-like phenotype and interplay of Wnt/beta-catenin and Myc signaling in aggressive childhood liver cancer. *Cancer Cell* 14, 471–484.
- Calle, E.E., and Kaaks, R. (2004). Overweight, obesity and cancer: epidemiological evidence and proposed mechanisms. *Nat. Rev. Cancer* 4, 579–591.
- Cope, K., Risby, T., and Diehl, A.M. (2000). Increased gastrointestinal ethanol production in obese mice: implications for fatty liver disease pathogenesis. *Gastroenterology* 119, 1340–1347.
- Corbin, K.D., and Zeisel, S.H. (2012). Choline metabolism provides novel insights into nonalcoholic fatty liver disease and its progression. *Curr. Opin. Gastroenterol.* 28, 159–165.
- De Vito, R., Alisi, A., Masotti, A., Ceccarelli, S., Panera, N., Citti, A., Salata, M., Valenti, L., Feldstein, A.E., and Nobili, V. (2012). Markers of activated inflammatory cells correlate with severity of liver damage in children with nonalcoholic fatty liver disease. *Int. J. Mol. Med.* 30, 49–56.

- El-Serag, H.B. (2011). Hepatocellular carcinoma. *N. Engl. J. Med.* **365**, 1118–1127.
- Godfrey, D.I., Pellicci, D.G., Patel, O., Kjer-Nielsen, L., McCluskey, J., and Rossjohn, J. (2010). Antigen recognition by CD1d-restricted NKT T cell receptors. *Semin. Immunol.* **22**, 61–67.
- Guerrero, A.L., Colvin, R.M., Schwartz, A.K., Molleston, J.P., Murray, K.F., Diehl, A., Mohan, P., Schwimmer, J.B., Lavine, J.E., Torbenson, M.S., and Scheimann, A.O. (2012). Choline intake in a large cohort of patients with nonalcoholic fatty liver disease. *Am. J. Clin. Nutr.* **95**, 892–900.
- Haybaeck, J., Zeller, N., Wolf, M.J., Weber, A., Wagner, U., Kurrer, M.O., Bremer, J., Izzi, G., Graf, R., Clavien, P.A., et al. (2009). A lymphotoxin-driven pathway to hepatocellular carcinoma. *Cancer Cell* **16**, 295–308.
- Hebbard, L., and George, J. (2011). Animal models of nonalcoholic fatty liver disease. *Nat. Rev. Gastroenterol. Hepatol.* **8**, 35–44.
- Henaoui-Mejia, J., Elinav, E., Jin, C., Hao, L., Mehal, W.Z., Strowig, T., Thaiss, C.A., Kau, A.L., Eisenbarth, S.C., Jurczak, M.J., et al. (2012). Inflammation-mediated dysbiosis regulates progression of NAFLD and obesity. *Nature* **482**, 179–185.
- Jemal, A., Bray, F., Center, M.M., Ferlay, J., Ward, E., and Forman, D. (2011). Global cancer statistics. *CA Cancer J. Clin.* **61**, 69–90.
- Kuziel, W.A., Morgan, S.J., Dawson, T.C., Griffin, S., Smithies, O., Ley, K., and Maeda, N. (1997). Severe reduction in leukocyte adhesion and monocyte extravasation in mice deficient in CC chemokine receptor 2. *Proc. Natl. Acad. Sci. U S A* **94**, 12053–12058.
- Lo, J.C., Wang, Y., Tumanov, A.V., Bamji, M., Yao, Z., Reardon, C.A., Getz, G.S., and Fu, Y.X. (2007). Lymphotoxin beta receptor-dependent control of lipid homeostasis. *Science* **316**, 285–288.
- Lynch, L., Nowak, M., Varghese, B., Clark, J., Hogan, A.E., Toxavidis, V., Balk, S.P., O'Shea, D., O'Farrelly, C., and Exley, M.A. (2012). Adipose tissue invariant NKT cells protect against diet-induced obesity and metabolic disorder through regulatory cytokine production. *Immunity* **37**, 574–587.
- Maeda, S., Kamata, H., Luo, J.L., Leffert, H., and Karin, M. (2005). IKKbeta couples hepatocyte death to cytokine-driven compensatory proliferation that promotes chemical hepatocarcinogenesis. *Cell* **121**, 977–990.
- Martin-Murphy, B.V., You, Q., Wang, H., De La Houssey, B.A., Reilly, T.P., Friedman, J.E., and Ju, C. (2014). Mice lacking natural killer T cells are more susceptible to metabolic alterations following high fat diet feeding. *PLoS ONE* **9**, e80949.
- Matsumoto, M., Hada, N., Sakamaki, Y., Uno, A., Shiga, T., Tanaka, C., Ito, T., Katsume, A., and Sudoh, M. (2013). An improved mouse model that rapidly develops fibrosis in non-alcoholic steatohepatitis. *Int. J. Exp. Pathol.* **94**, 93–103.
- Michelotti, G.A., Machado, M.V., and Diehl, A.M. (2013). NAFLD, NASH and liver cancer. *Nat. Rev. Gastroenterol. Hepatol.* **10**, 656–665.
- Miura, K., Yang, L., van Rooijen, N., Ohnishi, H., and Seki, E. (2012). Hepatic recruitment of macrophages promotes nonalcoholic steatohepatitis through CCR2. *Am. J. Physiol. Gastrointest. Liver Physiol.* **302**, G1310–G1321.
- Moieni, A., Cornellà, H., and Villanueva, A. (2012). Emerging signaling pathways in hepatocellular carcinoma. *Liver Cancer* **1**, 83–93.
- Nakagawa, H., Umemura, A., Taniguchi, K., Font-Burgada, J., Dhar, D., Ogata, H., Zhong, Z., Valasek, M.A., Seki, E., Hidalgo, J., et al. (2014). ER stress cooperates with hypernutrition to trigger TNF-dependent spontaneous HCC development. *Cancer Cell* **26**, 331–343.
- Park, E.J., Lee, J.H., Yu, G.Y., He, G., Ali, S.R., Holzer, R.G., Osterreicher, C.H., Takahashi, H., and Karin, M. (2010). Dietary and genetic obesity promote liver inflammation and tumorigenesis by enhancing IL-6 and TNF expression. *Cell* **140**, 197–208.
- Petrasek, J., Csak, T., Ganz, M., and Szabo, G. (2013). Differences in innate immune signaling between alcoholic and non-alcoholic steatohepatitis. *J. Gastroenterol. Hepatol.* **28** (Suppl 1), 93–98.
- Pikarsky, E., Porat, R.M., Stein, I., Abramovitch, R., Amit, S., Kasem, S., Gukovich-Pyest, E., Urieli-Shoval, S., Galun, E., and Ben-Neriah, Y. (2004). NF-kappaB functions as a tumour promoter in inflammation-associated cancer. *Nature* **431**, 461–466.
- Pirola, C.J., Gianotti, T.F., Burgueño, A.L., Rey-Funes, M., Loidl, C.F., Mallardi, P., Martino, J.S., Castaño, G.O., and Sookoian, S. (2013). Epigenetic modification of liver mitochondrial DNA is associated with histological severity of nonalcoholic fatty liver disease. *Gut* **62**, 1356–1363.
- Rubbia-Brandt, L., Quadri, R., Abid, K., Giostra, E., Malé, P.J., Mentha, G., Spahr, L., Zarski, J.P., Borisch, B., Hadengue, A., and Negro, F. (2000). Hepatocyte steatosis is a cytopathic effect of hepatitis C virus genotype 3. *J. Hepatol.* **33**, 106–115.
- Satoh, M., Andoh, Y., Clingan, C.S., Ogura, H., Fujii, S., Eshima, K., Nakayama, T., Taniguchi, M., Hirata, N., Ishimori, N., et al. (2012). Type II NKT cells stimulate diet-induced obesity by mediating adipose tissue inflammation, steatohepatitis and insulin resistance. *PLoS ONE* **7**, e30568.
- Scheu, S., Alferink, J., Pözl, T., Barchet, W., Kalinke, U., and Pfeffer, K. (2002). Targeted disruption of LIGHT causes defects in costimulatory T cell activation and reveals cooperation with lymphotoxin beta in mesenteric lymph node genesis. *J. Exp. Med.* **195**, 1613–1624.
- Schlaeger, C., Longerich, T., Schiller, C., Bewerunge, P., Mehrabi, A., Toedt, G., Kleff, J., Ehemann, V., Eils, R., Lichter, P., et al. (2008). Etiology-dependent molecular mechanisms in human hepatocarcinogenesis. *Hepatology* **47**, 511–520.
- Stewart, B.W., and Wild, C.P. (2014). *World Cancer Report 2014*. (Geneva, Switzerland: WHO Press).
- Vucur, M., Roderburg, C., Bettermann, K., Tacke, F., Heikenwalder, M., Trautwein, C., and Luedde, T. (2010). Mouse models of hepatocarcinogenesis: what can we learn for the prevention of human hepatocellular carcinoma? *Oncotarget* **1**, 373–378.
- Wang, Y., Koroleva, E.P., Kuprash, D.V., Nedospasov, S.A., Fu, Y.X., and Tumanov, A.V. (2010). Lymphotoxin beta receptor signaling in intestinal epithelial cells orchestrates innate immune responses against mucosal bacterial infection. *Immunity* **32**, 403–413.
- White, D.L., Kanwal, F., and El-Serag, H.B. (2012). Association between nonalcoholic fatty liver disease and risk for hepatocellular cancer, based on systematic review. *Clin. Gastroenterol. Hepatol.* **10**, 1342–1359.e2.
- Wunderlich, F.T., Luedde, T., Singer, S., Schmidt-Suppran, M., Baumgartl, J., Schirmacher, P., Pasparakis, M., and Brünig, J.C. (2008). Hepatic NF-kappa B essential modulator deficiency prevents obesity-induced insulin resistance but synergizes with high-fat feeding in tumorigenesis. *Proc. Natl. Acad. Sci. U S A* **105**, 1297–1302.
- Yoshimoto, S., Loo, T.M., Atarashi, K., Kanda, H., Sato, S., Oyadomari, S., Iwakura, Y., Oshima, K., Morita, H., Hattori, M., et al. (2013). Obesity-induced gut microbial metabolite promotes liver cancer through senescence secretome. *Nature* **499**, 97–101.
- Zeisel, S.H., and Caudill, M.A. (2010). Choline. *Adv. Nutr.* **1**, 46–48.
- Zeisel, S.H., and da Costa, K.A. (2009). Choline: an essential nutrient for public health. *Nutr. Rev.* **67**, 615–623.
- Zender, L., Villanueva, A., Tovar, V., Sia, D., Chiang, D.Y., and Llovet, J.M. (2010). Cancer gene discovery in hepatocellular carcinoma. *J. Hepatol.* **52**, 921–929.

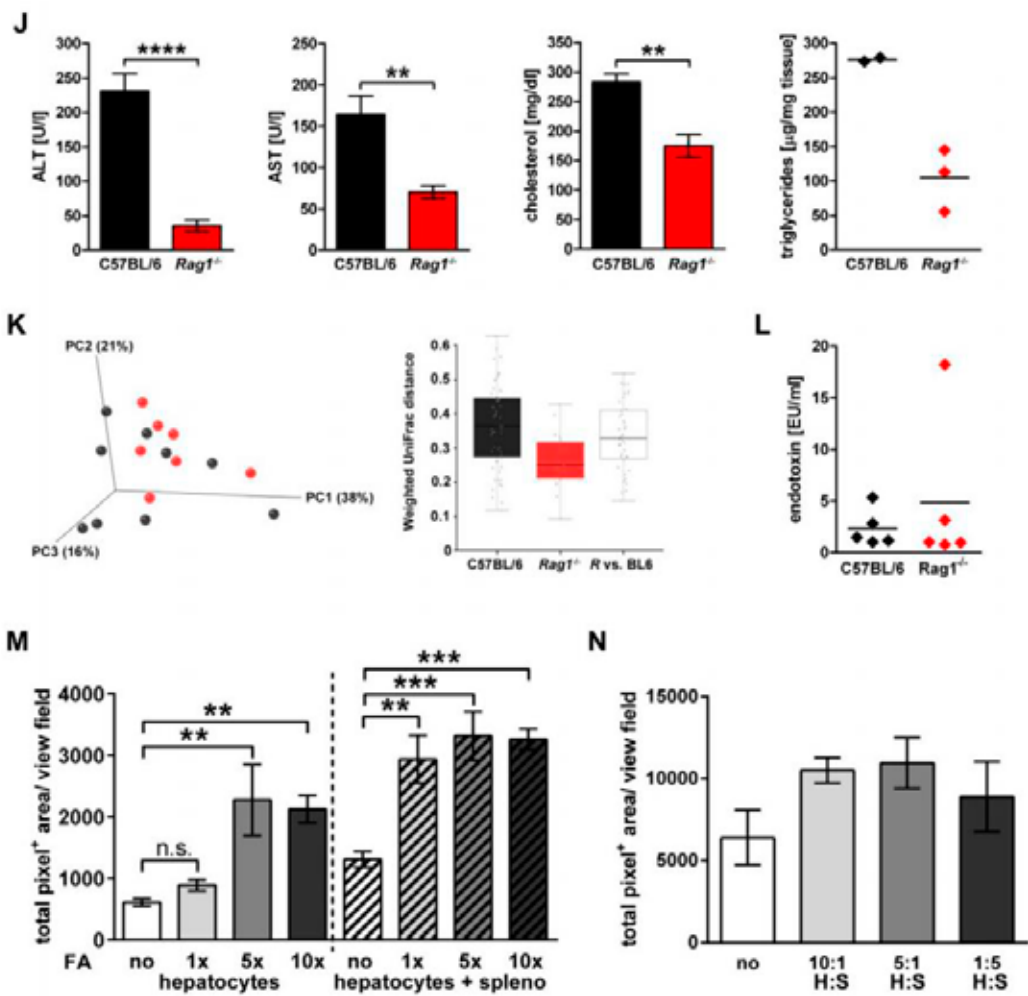


Figure S5: (J) Quantification of serum ALT, AST and cholesterol levels of 6- and 9-month-old co-housed C57BL/6 and Rag1^{-/-} mice. Liver triglycerides were measured in 10-month-old mice of both genotypes. (K) Output of Principal Coordinate Analysis (PCoA) of phylogenetic distances (weighted UniFrac) at an even sampling of 16000 sequences derived from 16S sequencing by Illumina (233bp) using feces of co-housed, CD-HFD fed C57BL/6 and Rag1^{-/-} mice. Dots are color-coded according the genotype of the mice. There were substantial inter-individual differences, especially within C57BL/6, and sample did not cluster according to the mouse genotype (left panel). The right panel supports the non-clustering observed in PCoA since mean distances between groups were not significantly higher than distances within respective groups. (L) Measurement of the endotoxin concentration in serum taken from the portal vein of co-housed 10-month-old CD-HFD fed C57BL/6 and Rag1^{-/-} mice. (M) Quantification of LD540+ area in hepatocytes or hepatocytes co-cultured with splenocytes (5:1 ratio) and incubated with various concentrations of FA for 6 h. (N) Quantification of LD540+ area in hepatocytes or hepatocytes co-cultured with splenocytes derived from CD-HFD fed C57BL/6 mice in various cell ratios incubated with 1 x FA overnight. No significant differences were observed.

Paper 9-13

Nutrition and microbiome

The following selected publications refer to research topic 2 (see detailed description above on p28-33). Most of these papers (9-12) reflect my interest in studying the activation of dietary polyphenols by gut bacteria and their biological properties. Work in this section also refers to the study of gut microbiota in the context of dietary interventions, especially using diets characterized by high-energy content.

9. J Mapesa, N Waldschmitt, I Schmoeller, C Blume, T Hofmann, S Mahungu, T Clavel, D Haller (2011) Catechols in caffeic acid phenethyl ester are essential for inhibition of TNF-mediated IP-10 expression through NF- κ B-dependent but HO-1- and p38-independent mechanisms in mouse intestinal epithelial cells, *Mol Nutr Food Res* 55:1850

Besides its scientific content (related to my interest in studying biological effects of polyphenols), this publication is the best testimony to the importance of human relationships in science (see acknowledgements). Paper 9 is the result of co-supervision efforts to accompany one outstanding graduate student from Kenya on his scientific journey. The paper highlights structure-function relationships behind anti-inflammatory properties of caffeic acid phenethyl ester in intestinal epithelial cells.

10. A Woting, T Clavel, G Loh, M Blaut (2010) Bacterial transformation of dietary lignans in gnotobiotic rats, *FEMS Microbiol Ecol* 72:507

11. H Mabrok, R Klopfleisch, K Ghanem, T Clavel, M Blaut, G Loh (2011) Lignan transformation by gut bacteria lowers tumor burden in a gnotobiotic rat model of breast cancer, *Carcinogenesis* 33:203

Paper 10 and 11 correspond to collaborative studies based on my former *in vitro* work on the identification of human gut bacteria capable of activating dietary lignans. They prove the *in vivo* relevance of our findings using gnotobiology.

12. T Clavel, JO Mapesa (2013) Phenolics in human nutrition: importance of the intestinal microbiome for isoflavone and lignan bioavailability, In Handbook of Natural Products, KG Ramawat, JM Merillon (Eds), Elsevier, ISBN 978-3-642-221-43-9/44-6

This publication symbolizes my recognition in the field of polyphenol research. It is an invited contribution, which highlights the importance of the gut microbiota for the bioavailability of two major families of phytoestrogens: the isoflavones and the lignans.

13. T Clavel,* C. Desmarchelier, D Haller, P Gérard, S Rohn, P Lepage, H Daniel (2014) Intestinal microbiota in metabolic diseases: from bacterial community structure and functions to species of pathophysiological relevance, *Gut Microbes* 5:544; *corresponding author

Paper 13 presents data on the impact of diet composition and texture on gut bacterial diversity and composition in mice. It has been published as an addendum of paper 15 (see section 3 below). Thus, Paper 13 presents also issues related to the impact of gut microbiota on metabolic disorders as well as the usefulness and limitations of experimental studies in mouse models of obesity.

PAPER 9

RESEARCH ARTICLE

Catechols in caffeic acid phenethyl ester are essential for inhibition of TNF-mediated IP-10 expression through NF- κ B-dependent but HO-1- and p38-independent mechanisms in mouse intestinal epithelial cells

Job O. Mapesa^{1,2}, Nadine Waldschmitt¹, Ingrid Schmoeller¹, Carolin Blume¹, Thomas Hofmann³, Symon Mahungu², Thomas Clavel¹ and Dirk Haller¹

¹Chair for Biofunctionality, ZIEL – Research Center for Nutrition and Food Sciences, CDD – Center for Diet and Disease, Technische Universität München, Freising-Weihenstephan, Germany

²Dairy and Food Science Department, Egerton University, Njoro, Kenya

³Food Chemistry and Molecular Sensory Science, ZIEL – Research Center for Nutrition and Food Sciences, Technische Universität München, Freising-Weihenstephan, Germany

Scope: Caffeic acid phenethyl ester (CAPE) is an active constituent of honeybee propolis inhibiting nuclear factor (NF)- κ B. The aims of our study were to provide new data on the functional relevance and mechanisms underlying the role of CAPE in regulating inflammatory processes at the epithelial interface in the gut and to determine the structure/activity relationship of CAPE.

Methods and results: CAPE significantly inhibited TNF-induced IP-10 expression in intestinal epithelial cells. Using various analogues, we demonstrated that substitution of catechol hydroxyl groups and addition of one extra hydroxyl group on ring B reversed the functional activity of CAPE to inhibit IP-10 production. The anti-inflammatory potential of CAPE was confirmed in ileal tissue explants and embryonic fibroblasts derived from TNF^{ΔARE/+} mice. Interestingly, CAPE inhibited both TNF- and LPS-induced IP-10 production in a dose-dependent manner, independently of p38 MAPK, HO-1 and Nrf2 signaling pathways. We found that CAPE did not inhibit TNF-induced I κ B phosphorylation/degradation or nuclear translocation of RelA/p65, but targeted downstream signaling events at the level of transcription factor recruitment to the gene promoter.

Conclusion: This study reveals the structure–activity effects and anti-inflammatory potential of CAPE in the intestinal epithelium.

Keywords:

Caffeic acid phenethyl ester / Inflammatory bowel diseases / Intestinal epithelium / Nuclear factor κ B / Polyphenols

1 Introduction

Caffeic acid phenethyl ester (CAPE) is proposed to have a wide range of biological activities via modulation of cellular

processes such as immune responses, cell division and apoptosis [1, 2]. Recent publications illustrate the promising

Abbreviations: CAPE, caffeic acid phenethyl ester; CAPEA, caffeic acid phenethyl amine; ChIP, chromatin immunoprecipitation; HO-1, heme oxygenase-1; IEC, intestinal epithelial cells; I κ B, inhibitor of κ B; IKK, I κ B kinase; IP-10, interferon- γ inducible 10 kDa protein; MAPK, mitogen-activated protein kinase; MEF, mouse embryonic fibroblasts; MIP-2, macrophage inflammatory protein 2; NAC, N-acetylcysteine; NF- κ B, nuclear factor κ B; Nrf2, nuclear factor-erythroid 2 p45-related factor 2; PDC, phenethyl dimethyl caffeate; SEAP, secreted alkaline phosphatase; TNF, tumor necrosis factor; WT, wild type

Correspondence: Professor Dirk Haller, Chair for Biofunctionality, ZIEL – Research Center for Nutrition and Food Sciences, Technische Universität München, Gregor-Mendel Str. 2, 85350 Freising-Weihenstephan, Germany

E-mail: haller@wzw.tum.de

Fax: +49-8161-71-2824

Received: February 18, 2011

Revised: August 10, 2011

Accepted: August 22, 2011



role of CAPE as a potential prophylactic and therapeutic agent with emphasis on anti-inflammatory effects [3–5]. CAPE was first isolated as an active phenolic constituent of honeybee propolis possessing cytotoxic and antitumor activities [6]. In subsequent experiments, CAPE potently inhibited activation of the nuclear factor (NF)- κ B signaling pathway [7]. However, the molecular mechanisms underlying NF- κ B inhibition by CAPE are largely unknown. Previously, we assessed the functional diversity of various polyphenols with respect to the modulation of NF- κ B, interferon regulatory factor and Akt activation that shape inflammatory responses involved in cytokine induction [8, 9]. Although our understanding of how most of these non-nutritive polyphenols modulate cellular functions *in vitro* has improved, the structural features responsible for mechanistic effects remain unclear. The limited structural complexity of CAPE makes it a good model compound for structure function analysis. However, most studies on CAPE do not show evidence for the specific pharmacophore (a set of structural features with biological activity that is recognized at receptor sites of target proteins) responsible for anti-oxidative and/or anti-inflammatory properties [10–12].

Interferon- γ inducible 10 kDa protein (IP-10) has been described as a chemoattractant, which binds to the chemokine (C-X-C motif) receptor 3 (CXCR3) receptors on monocytes and activated Th1 lymphocytes upon challenge with tumor necrosis factor (TNF) or LPS [13]. Recently, we have shown that IP-10 protein expression by intestinal epithelial cells (IEC) is up-regulated in the TNF ^{Δ ARE/+} mouse model of experimental ileitis [14]. One of the most important signaling mediators related to inflammatory processes is NF- κ B, which plays a key role in coordinating the transcriptional induction of several cytokines such as TNF- α and IL-1 and chemokines such as IL-8 and IP-10. The critical process of NF- κ B activation has been comprehensively

described [15, 16]. Typically, NF- κ B binds to DNA as homodimers or heterodimers of five possible subunits, including RelA (p65), c-Rel, RelB, p100/p52 and p105/p50, where p52 and p50 are truncated forms of p100 and p105, respectively. These dimeric complexes bind at NF- κ B-binding sites in target genes with distinct preferences, distinguishable affinity and specificity, whereby different combinations of these heterodimers act as transcriptional activators or repressors. Regulation of NF- κ B is mediated by the inhibitor of κ B (I κ B). In activated cells, I κ B α is phosphorylated by the activated I κ B kinase (IKK) complex followed by ubiquitylation and degradation by the 26S proteasome. Liberated NF- κ B translocates to the nucleus where it binds to NF- κ B-specific DNA sequences resulting in transcription of many pro-inflammatory cytokines [17, 18]. NF- κ B activation or suppression in epithelial cells seems to be critical for tissue homeostasis in the gut mucosa, as observed in various experimental conditions [19–21].

The first aim of the present study was to identify structural features of CAPE that are essential for anti-inflammatory properties, as measured by production of IP-10 in the IEC line Mode-K. In addition, we aimed at providing new insights into the mechanistic significance of CAPE in the regulation of NF- κ B activity. Finally, we tested the physiological relevance of our *in vitro* findings using samples from TNF ^{Δ ARE/+} mice.

2 Materials and methods

2.1 Chemicals

The structures of the compounds used in the present study are shown in Fig. 1. CAPE, phenethyl 3-methyl caffeate (P3MC) and phenethyl dimethyl caffeate (PDC) were

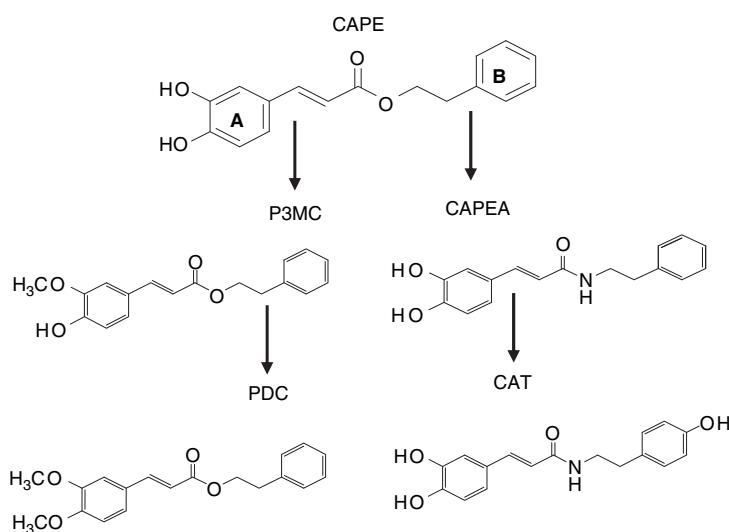


Figure 1. Chemical structures of CAPE and analogues. Phenethyl 3-methyl caffeate (P3MC) was substituted with one methoxyl, while phenethyl dimethyl caffeate (PDC) had two substitutions on the hydroxyl groups of the catechol ring (A). Caffeic acid phenethyl amine (CAPEA) was prepared by substituting the ester with an amide, while Caffeic acid tyramine (CAT) was prepared by adding one extra hydroxyl on the benzene ring (B) of CAPEA.

purchased from LKT Laboratories (St. Paul, MN, USA). Caffeic acid phenethyl amine (CAPEA) and caffeic acid tyramine (CAT) were synthesized at the Food Chemistry and Molecular Sensory Science department (TU München) using standard protocols. TNF was purchased from Invitrogen. LPS, SB203580 and BAY11-7082 were purchased from Sigma-Aldrich. For all treatments, TNF and LPS were used at a final concentration of 10 and 100 ng/mL, respectively.

2.2 Cell culture

The small IEC line Mode-K (passage 13–25) [22] was cultivated in high glucose DMEM medium (Invitrogen) containing 10% v/v FBS, 1% Antibiotic/Antimycotic (PAA) and 2 mM of L-Glutamine (Invitrogen). Cells were grown at 37°C in tissue culture plates (Cell Star, Greiner bio-one) in a humidified atmosphere containing 5% CO₂. They were split every third day and grown to 80% confluency before stimulation.

2.3 Mouse embryonic fibroblasts (MEF)

For preparation of embryonic fibroblasts, C57BL/6 wild type (WT) and TNF^{ΔARE/+} mice were killed by cervical dislocation at day 13.5 of pregnancy. Embryos were taken out, placed in separate wells and killed by decapitation. Heart and liver were removed. Embryonic tissues were rinsed with pre-warmed PBS, transferred into 3 mL of 0.25% Trypsin/EDTA (supplemented with 2% chicken serum), and minced into small pieces. After incubation time of 15 min at 37°C, 10 mL of MEF medium was added [DMEM medium supplemented with 10% FBS, 1% Antibiotic/Antimycotic (PAA), 2 mmol/L L-Glutamine, 100 μM non-essential amino acids (PAA) and 1 mM sodium pyruvate (Sigma)]. The suspensions were transferred into 15 mL falcon tubes leaving cell debris to settle. Supernatants were transferred and centrifuged (430 × g, 5 min, RT). Pellets were re-suspended in 7 mL MEF medium. Cells from each embryo were seeded separately in T25 flasks and incubated at 37°C, 5% CO₂. The medium was changed after 24 h and cells were incubated for additional 24 h. Following genotyping, MEF were pooled together (passage 1) in MEF freezing medium (70% MEF medium supplemented with 20% FBS and 10% DMSO) and stored in cryo-vials at –180°C until use. Stimulation experiments were carried out using MEF between passages 1–7. Nrf2^{+/+} and Nrf2^{-/-} MEF (a generous gift from Dr. Albena Dinkova-Kostova and Prof. Masayuki Yamamoto) were maintained in culture as described previously [23].

2.4 Tissue explants

Ileal tissues obtained from 12-wk-old WT and TNF^{ΔARE/+} mice were flushed with PBS and cut open into 4-mm-long tissue pieces, which were placed onto Netwell inserts in

Mode-K medium with the serosal side touching the transwell membrane (Corning Life Sciences). After incubation with or without CAPE (20 μM) for 24 h, supernatants were collected while the tissue was mashed in lysis buffer containing 1% Triton X-100, 150 mM NaCl, 10 mM Tris pH 7.4, 1 mM EDTA, 1 mM EGTA as well as complete Mini (protease) and Phos-Stop (phosphatase) inhibitors (Roche). Tissue homogenates were centrifuged (16 000 × g, 4°C, 10 min) and protein-containing supernatants were used for immunoblotting.

2.5 Cell viability and cytotoxicity

Cells were grown to 80% confluency in 96-well plates followed by pre-incubation with test substances for 24 h. Proliferation and cytotoxicity assays were performed using the cell counting kit-8 (Dojindo) according to manufacturer's instructions. The absorbance was measured at 450 nm using a Multiskan spectrophotometer (Thermo scientific).

2.6 ELISA analysis

Mode-K cells and TNF^{ΔARE/+} MEF were pre-incubated with test compounds (10 μM) for the indicated times followed by stimulation with or without TNF or LPS for additional 24 h. Secreted IP-10, TNF and MIP-2 proteins in the supernatants were measured using mouse-specific DuoSet ELISA kits, according to manufacturer's instructions (R&D Systems). All experiments were performed in triplicate and repeated at least three times.

2.7 Reporter (SEAP) gene assay for NF-κB transcriptional activity

The secreted alkaline phosphatase (SEAP) gene is under the control of an NF-κB inducible endothelial leukocyte adhesion molecule 1 (ELAM1) composite promoter, which drives the expression of a reporter gene that is induced in the presence of NF-κB or repressed in its absence. The SEAP gene reporter assay was carried out as described previously [9]. Briefly, *pNifly-SEAP* transfected Mode-K cells were pre-incubated with CAPE and its analogues for 1 h before TNF stimulation for 24 h. Subsequent assays were carried out according to manufacturer's recommendations (InvivoGen). Samples were measured at 405 nm in a Multiskan spectrophotometer (Thermo scientific).

2.8 Chromatin immunoprecipitation (ChIP)

ChIP was performed using the ChIP kit (Cell Signaling; #9003) as described by the manufacturer. Briefly, Mode-K cells were pretreated for 4 h with CAPE before addition of TNF. After 30 min, cells were fixed in 1% formaldehyde

(10 min, RT). The chromatin digest was normalized according to the purified DNA concentration and immunoprecipitated against anti-phospho-RelA^{ser536}, anti- α H3, anti-acetyl CBP/p300 (all from Cell signaling) and NF- κ B p50 (D-17) (Santa Cruz) antibodies. H3 and normal rabbit IgG antibodies (Cell Signaling) were used as positive and negative controls, respectively. Immunoprecipitated DNA, together with purified DNA as input control (2% of the total chromatin extract) was used as template for PCR amplification using the following promoter-specific primers: IP-10, F-5'-aaggagcacaagagggg, R-5'-attgctgacttggag; SimpleChip mouse RPL30 (Cell Signaling). PCR products were resolved by electrophoresis on 1% agarose gels.

2.9 RT-PCR

Total RNA was extracted from cells using the Isol-RNA-Lysis according to manufacturer's instructions (5-Prime). Nucleotide concentrations were determined using the Nanodrop spectrophotometer (Peqlab). Complementary DNA (cDNA) was obtained from 1 μ g RNA by reverse transcription using random primers (Invitrogen) and M-MLV reverse transcriptase (Invitrogen). Real-time qPCR was performed using the UPL master mix and primer sets designed by the Universal Probe Library on the LightCycler 480 (Roche). Crossing point (Ct) values were obtained using the Second Derivative Maximum method. Coefficients of regulation between treated and control samples were calculated from triplicate samples according to the $\Delta\Delta$ Ct method [24]. Primer pairs (mouse UPL, Roche) were: GAPDH, F-5'-tccactcatggcaaatca, R-5'-ttgatgttagtgggtctcg (probe no. 9); IP-10, F-5'-gctgccgtcatttctgc, R-5'-tctactggcccgtcatc (probe no. 3); TNF, F-5'-tgctatgtctcagcctctc, R-5'-gaggccattgggaactctt (probe no. 49); MIP-2, F-5'-cctggtcaga-aatcatcca-3', R-5'-cttccgttgaggacagc-3' (probe no. 63); NF- κ B RelA, F-5'-cccagaccgagatcct-3', R-5'-ttctgctctggacc-3' (probe no. 47); NF- κ B p105, F-5'-cactgctcaggtccactgtc-3', R-5'-actgaggccctatcactgtc-3' (probe no. 69); NF- κ B p100, F-5'-tggaacagcaaacagc-3', R-5'-tacctcaaacggctcac (probe no. 76); NF- κ B RelB, F-5'-gtgacctctctcctgtcact-3', R-5'-aaccttagtagctgtatgt-3' (probe no. 80).

2.10 Western blotting

Cells were lysed in SDS-PAGE sample buffer and 10 μ g proteins resolved on a 10 or 15% SDS-polyacrylamide gel. Antibodies against phospho-RelA (Ser536), phospho-p38 MAPK, p38 MAPK, phospho-I κ B α , I κ B α , phospho-ERK, ERK, phospho-SAPK/JNK, SAPK/JNK, phospho-AMPK, AMPK (Cell Signaling), p65/RelA (Santa Cruz), IP-10 (R&D systems), heme oxygenase-1 (HO-1) (Stressgen) and β -actin (MP Biomedicals) were used and the protein bands were detected with the Amersham ECL detection kit (GE Healthcare).

2.11 Immunofluorescence and confocal microscopy

Cells were grown on cover-slips in 6-well plates to 80% confluency, treated with CAPE for 1 h followed by TNF for 20 min and fixation with 4% formaldehyde in PBS (15 min, RT). Cover-slips were rinsed three times in PBS (5 min each) before blocking (1 h) in 5% normal goat serum supplemented with 0.5% Triton X-100. After overnight incubation at 4°C in anti-RelA primary antibody [1:100 dilution; sc-372, (Santa Cruz)], cover-slips were rinsed three times as above and Alexa-Fluor 488 goat-anti-rabbit secondary antibody (Invitrogen) was added. After 2 h at room temperature in the dark, rinsed slides were covered in VectaShield HardSet mounting medium with DAPI (Vector Laboratories). Cellular localization of RelA was determined using a Leica SP2 confocal laser scanning microscope (Leica Microsystems).

2.12 Feeding experiment in TNF^{ARE/+} mice

The animal use protocol was approved by the Bavarian Animal Care and Use Committee (No. 55.2-1-54-2531-88-09). Twelve-week-old heterozygous TNF^{ARE/+} (kindly provided by Dr. George Kollias) and WT C57BL/6 mice ($n = 5$ per treatment/genotype group) were fed gelatin pellets (15% w/v gelatin and 20% sucrose) with or without CAPE (10 mg/kg body weight) three times a wk for six wks in addition to their usual diet [8]. Mice were killed by cervical dislocation at the age of 18 weeks and samples were prepared for histological scoring and IEC isolation as previously described [8].

2.13 Statistical analysis

Values were expressed as mean \pm SD of triplicate measurements representative of at least two independent experiments. Statistical analyses were performed using the SigmaPlot 11 (Systat Software). Mean values were compared by ANOVA (data were tested for normal distribution and equality of variances). The Holm–Sidak test was used for pairwise comparisons. For all tests, the bilateral α risk was $\alpha = 0.05$.

3 Results

3.1 CAPE inhibits IP-10 expression in a dose- and time-dependent manner

CAPE inhibited IP-10 induction in Mode-K cells in a dose-dependent manner, i.e. both intracellular (Fig. 2A) and secreted IP-10 protein levels (Supporting Information Fig. S1A) were reduced in the presence of CAPE. Since we obtained a marked and reproducible inhibition using 10 μ M and the test compounds were less cytotoxic at this concentration (80% viability after 24 h) (Supporting Information Fig. S1B), 10 μ M

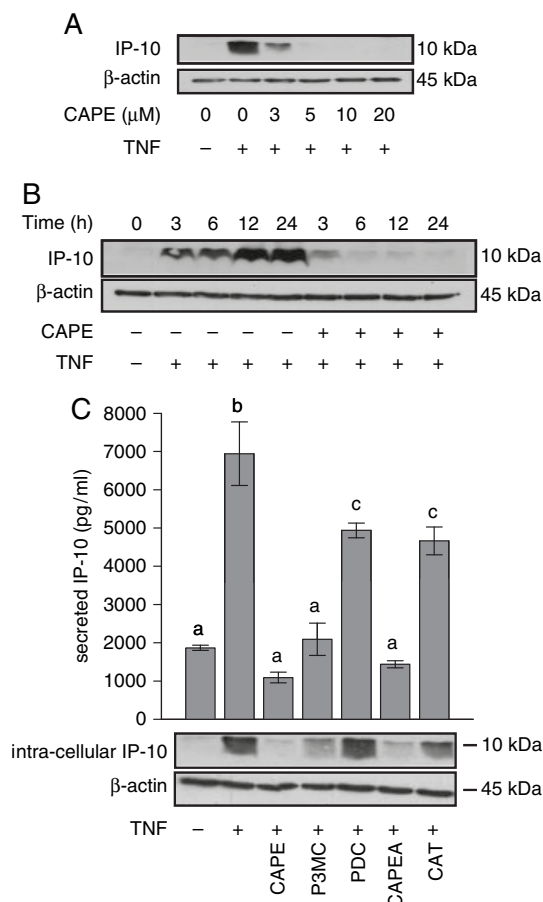


Figure 2. CAPE inhibits IP-10 in a dose-, time- and structure-dependent manner. (A) Cells were pre-incubated with the indicated concentrations of CAPE for 1 h before TNF (10 ng/mL) for additional 24 h. (B) Cells were pre-incubated with CAPE for 1 h followed by TNF for the indicated time. (C) Cells were pre-incubated with 10 μ M of test compounds followed by TNF for additional 24 h. The results are mean \pm SD from triplicate measurements representative of three independent experiments; means without a common letter differ, $p < 0.05$.

was used as the concentration of reference in all subsequent experiments, unless otherwise stated. To determine how long CAPE sustained inhibition of TNF-induced IP-10 production, we performed time-course experiments. CAPE abolished IP-10 expression from 3 to 24 h of TNF stimulation, indicating that CAPE-mediated inhibitory functions occurred at early time points and persisted over time (Fig. 2B).

3.2 Hydroxyl groups determine the anti-inflammatory effects of CAPE

To investigate the structure/activity relationship of CAPE, we used a variety of CAPE analogues (Fig. 1) and examined

Table 1. The half maximal inhibitory concentration 50 (IC_{50}) of CAPE and its analogs for cell cytotoxicity and IP-10 inhibition in Mode-K cells

Compound	Cytotoxicity (μ M)	IP-10 inhibition (μ M)
CAPE	61.0	0.85
P3MC	76.8	1.78
PDC	> 100.00	> 100.00
CAPEA	85.2	0.98
CAT	90.2	27.91

IC_{50} values were generated from three independent experiments (CAPE concentrations in the range of 0–200 μ M) using the Four Parameter Logistic Equation in SigmaPlot 11 (Systat Software).

their activity via measurement of cell viability and TNF-induced IP-10 expression in Mode-K cells. Both ELISA and Western blot analyses revealed that CAPE, P3MC and CAPEA significantly reduced IP-10 expression ($p < 0.05$), while PDC and CAT were significantly less active (Fig. 2C). These observations prompted us to determine the half maximal inhibitory concentrations 50 (IC_{50}) of all five compounds. The IC_{50} values were in the micromolar (cytotoxicity) and nanomolar (IP-10 inhibition) range and showed that CAPE was most potent (Table 1). The gradual decrease in cytotoxic IC_{50} CAPE > P3MC > PDC suggested that the catechol hydroxylic groups in ring A define functional effects, i.e. the presence of one hydroxyl group retains activity while substitution of both hydroxyl groups in ring A leads to a loss of activity. Also, substitution of the ester functional group with an amide group (CAPEA) revealed only limited functional consequences, i.e. led only to a slight decrease in IC_{50} . However, further modification of CAPEA to CAT by addition of a hydroxyl group to ring B markedly reduced the IC_{50} (Table 1). Importantly, we found that the effect of CAPE treatment on Mode-K cells was specific. CAPE, as well as P3MC and CAPEA, did not affect the expression of another TNF-induced chemokine of the CXC family, namely macrophage inflammatory protein 2 (MIP-2), to the same extent as IP-10, i.e. return to basal levels as in the absence of TNF (Supporting Information Fig. S2).

3.3 CAPE inhibits NF- κ B by attenuating transcription factor recruitment to the gene promoter

To elucidate anti-inflammatory mechanisms underlying IP-10 inhibition, we investigated the influence on NF- κ B activity. Therefore, we examined the effect of CAPE and analogues on promoter activity using the SEAP reporter assay. Compared with control samples, SEAP expression was up-regulated after TNF administration. However, it was significantly reduced after treatment with CAPE and CAPEA, but not P3MC, PDC and CAT (Fig. 3A). Importantly, CAPE completely abolished NF- κ B transactivation revealing that the catechol hydroxylic groups are essential

for its bioactivity. The influence of CAPE on gene transcription was confirmed by measurement of IP-10 mRNA levels. CAPE completely blocked IP-10 mRNA (Fig. 3A) and protein (Fig. 2C) synthesis indicating that it most likely targets the de novo synthesis of IP-10 mRNA and protein via the NF- κ B pathway [17]. The most important mechanism that prevents spontaneous NF- κ B activation is the cytoplasmic retention via I κ B α . I κ B α phosphorylation, ubiquitination and subsequent proteasomal degradation is essential for full NF- κ B activation. To further investigate molecular mechanisms of CAPE-mediated inhibition of the NF- κ B pathway, we checked for TNF-induced I κ B α degradation and RelA phosphorylation. CAPE neither inhibited I κ B α degradation nor RelA phosphorylation (Fig. 3B). Even at increasing concentrations, CAPE did not reverse the I κ B α degradation process after 30 min of TNF stimulation (Fig. 3C). We also compared CAPE and BAY-11-7082 with respect to their ability to inhibit NF- κ B activity. BAY-11-7082 selectively inhibits NF- κ B activation by blocking TNF-induced degradation of I κ B α without affecting constitutive

I κ B α phosphorylation. The results confirmed that CAPE does not inhibit I κ B α degradation (Supporting Information Fig. S3A). It has been shown that I κ B α expression is induced by NF- κ B providing a negative feedback that terminates NF- κ B activation [25]. However, NF- κ B activation is known to be biphasic following TNF stimulation (the initial phase lasts one hour followed by a persistent second phase that depends on the input stimuli concentration), and some genes require persistent TNF stimulation to be fully activated [25]. To investigate the influence of CAPE on prolonged TNF stimulation, we monitored I κ B α phosphorylation and degradation leading to NF- κ B activation over eight hours. The results showed that CAPE neither altered the extent of TNF-induced RelA phosphorylation nor I κ B α phosphorylation/degradation (Supporting Information Fig. S3B). In addition, we investigated the influence of CAPE on RelB, p100, p105 and p65 mRNA expression. The results indicated that, in combination with TNF, CAPE induced the expression of relB and p105, a p50 precursor (Supporting Information Fig. S3C). We next investigated

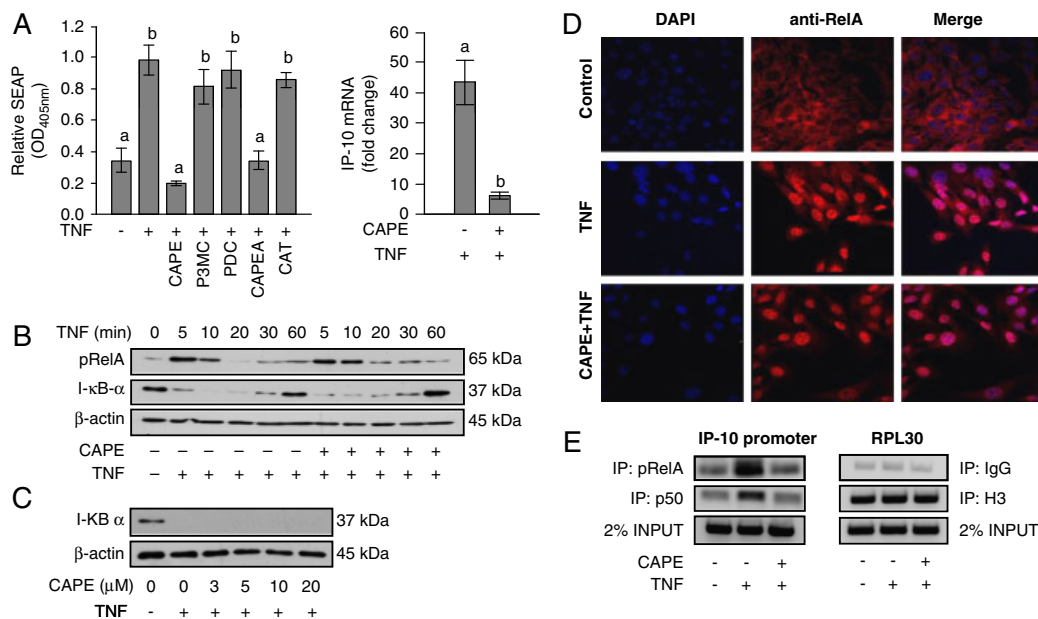


Figure 3. CAPE attenuates NF- κ B activity at the promoters of target genes. (A) CAPE targets the NF- κ B site of the ELAM1 promoter. Mode-K cells were stably transfected with a pNifty plasmid expressing the SEAP gene under the control of an NF- κ B-inducible ELAM1 composite promoter. Transfectants were pre-incubated for 1 h with 10 μ M of indicated compounds before TNF stimulation for additional 24 h. In addition, CAPE inhibited IP-10 mRNA expression (Mode-K cells were pre-incubated with 10 μ M CAPE for 1 h before TNF stimulation for 4 h). The results are mean \pm SD of triplicate measurements representative of three independent experiments; means without a common letter differ, $p < 0.05$. (B to D) CAPE neither inhibited TNF-induced I κ B α degradation nor RelA phosphorylation and subsequent nuclear translocation. (B) Time course for Mode-K cells treated with or without CAPE for 1 h followed by TNF induction. (C) Dose dependence for Mode-K cells treated with or without CAPE for 1 h followed by TNF for 30 min. (D) Confocal immunofluorescence images (400 \times) of cells labeled with anti-RelA (red) showing cytoplasmic staining (control) and nuclear translocation (TNF-stimulated) and DAPI (blue) signals were generated from Mode K cells treated with or without CAPE for 1 h followed by TNF for 20 min. The results are representative of two independent experiments. (E) CAPE reduces recruitment of p50/RelA heterodimer to the IP-10 promoter. Cells were pre-incubated with CAPE for 4 h before TNF stimulation for 30 min followed by RelA, p50, H3 and IgG antibody immunoprecipitation of the enriched chromatin; H3 and IgG were included as positive and negative controls against the ribosomal protein L30 (RPL30) gene.

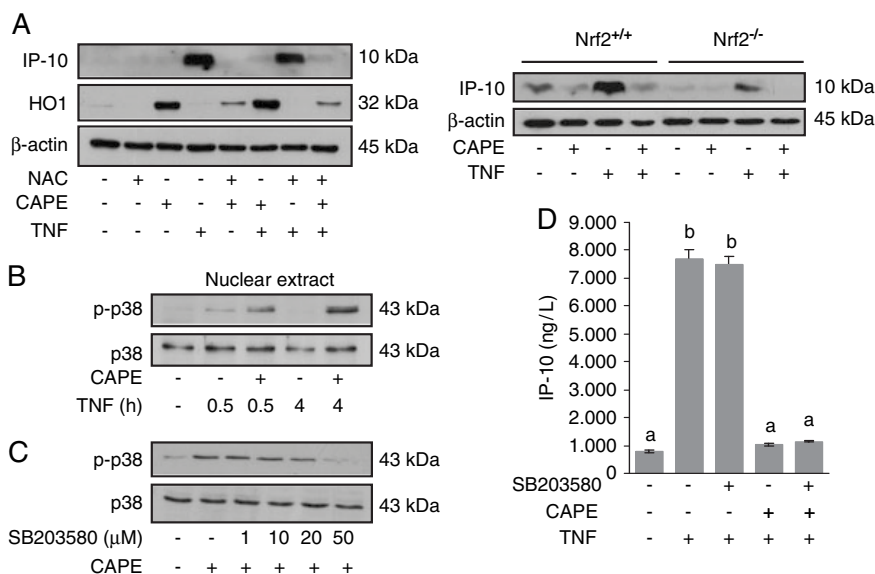


Figure 4. Accumulation of HO-1 and phospho-p38 MAPK had no influence on CAPE-mediated IP-10 inhibition. (A) Co-treatment of Mode-K cells with NAC (HO-1 inhibitor) (20 mM) for 16 h did not reverse CAPE mediated IP-10 inhibition. CAPE also abolished IP-10 expression in Nrf2^{-/-} MEF (a generous gift from Dr. Albena Dinkova-Kostova and Prof. Masayuki Yamamoto). Nrf2^{+/+} and Nrf2^{-/-} MEF cells were pre-incubated with 10 μM CAPE for 1 h before TNF stimulation for 24 h. (B) CAPE increases phosphorylation of p38 MAPK in a time-dependent manner. Mode-K cells were pre-incubated with or without CAPE for 1 h followed by TNF for the indicated time. (C) Mode-K cells were pre-incubated with indicated amounts of SB203580 for 30 min prior to CAPE treatment for 4 h. (D) Inhibition of p38 MAPK phosphorylation does not reverse CAPE-mediated IP-10 inhibition. Cells were incubated with or without SB203580 (50 μM) then CAPE for 1 h followed by TNF for 24 h.

whether CAPE targets nuclear translocation of RelA. In comparison to non-treated cells, CAPE treatment had no effect on RelA translocation as demonstrated by immunofluorescence analysis (Fig. 3D). Indeed, RelA was localized in the cytoplasm in non-treated cells and quickly shifted into the nucleus following TNF stimulation, even when cells were pre-incubated with CAPE. These observations pointed at a process in which NF-κB activity is controlled at the level of transcription factor binding to the gene promoter and chromatin remodeling. To investigate this assumption, we analyzed IP-10 promoter regions for NF-κB binding using ChIP analysis, with emphasis on the functional specificity of the p50/RelA heterodimer. CAPE reduced TNF-induced IP-10 promoter occupancy of both p50 and phospho-RelA NF-κB subunits (Fig. 3E), suggesting that both subunits are essential for IP-10 expression.

3.4 CAPE-mediated IP-10 inhibition is independent of HO-1, Nrf2 and p38 MAPK signaling pathways

Several polyphenols exhibit a strong anti-oxidative capacity. Since HO-1 is a key player in response to oxidative stress, we assessed the role of HO-1 activation and underlying nuclear factor-erythroid 2 p45-related factor 2 (Nrf2) signaling pathway in CAPE-mediated inhibition of IP-10 production. As shown in Fig. 4A, CAPE (10 μM) strongly induced HO-1

protein expression, yet inhibition of CAPE-induced HO-1 protein levels using N-acetylcysteine (NAC) did not affect inhibition of IP-10 production. By using Nrf2-knockout MEF, we also showed that CAPE-induced IP-10 inhibition seems not to be dependent upon Nrf2 signaling (Fig. 4A). Activation of mitogen-activated protein kinases (MAPKs), like p38, has also been associated with anti-inflammatory effects of polyphenols. Interestingly, the levels of phospho-p38 MAPK increased markedly in the nucleus within 4 h of CAPE treatment (Fig. 4B). To determine whether the p38 MAPK pathway activation is required for the observed inhibitory effects, Mode-K cells were co-treated with CAPE and increasing amounts of SB203580, a p38 MAPK inhibitor (Fig. 4C). Interestingly, SB203580 did not reverse the inhibitory effect of CAPE on IP-10 expression (Fig. 4D), suggesting that the accumulation of phospho-p38 MAPK in the nucleus does not play a direct role in CAPE-mediated IP-10 inhibition. Additionally, CAPE was not able to activate ERK but phosphorylated SAPK/JNK and AMPK in a time-dependent manner (Supporting Information Fig. S4).

3.5 CAPE suppressed IP-10 and TNF expression *ex vivo* but failed to reduce ileitis in TNF^{ARE/+} mice

To bring to the test the relevance of our *in vitro* experiments in TNF-stimulated Mode-K cells, we generated embryonic

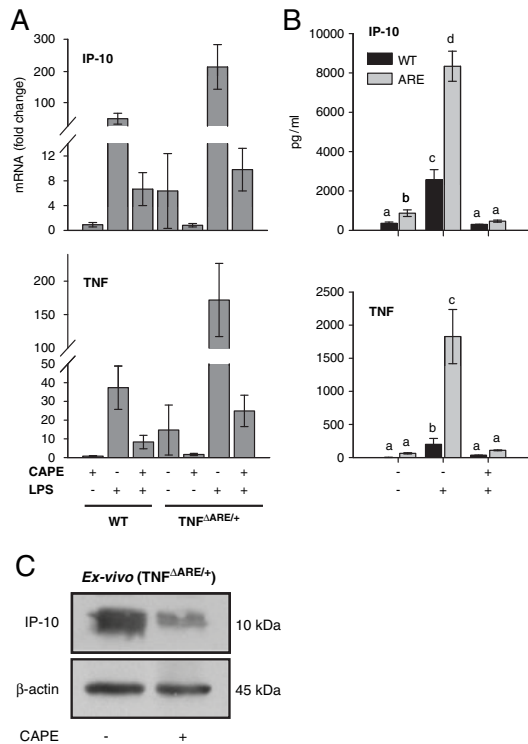


Figure 5. CAPE suppresses IP-10 and TNF mRNA and protein expression ex vivo. WT and $TNF^{\Delta ARE/+}$ MEF were pre-incubated with or without CAPE for 1 h followed by LPS stimulation for 4 h (A) (mRNA expression) or 24 h (B) (protein concentrations in culture supernatant). The results are mean \pm SD of triplicate measurements representative of three separate experiments; means without a common letter differ, $p < 0.05$. (C) IP-10 inhibition in ileum tissue explants. Washed ileal tissues from WT and $TNF^{\Delta ARE/+}$ mice placed onto Netwell inserts were incubated with or without CAPE (20 μ M) for 24 h. Tissue were mashed in lysis buffer, centrifuged and used for Western blotting.

fibroblasts using the $TNF^{\Delta ARE/+}$ mouse model of experimental ileitis. It is here worthwhile to note that $TNF^{\Delta ARE/+}$ mice produce excessive amounts of TNF, a hallmark for chronic inflammation in the gastrointestinal tract. Both transcriptional (Fig. 5A) and post-transcriptional (Fig. 5B) analysis confirmed that CAPE significantly inhibited IP-10 as well as TNF gene and protein expression. It also showed that CAPE not only targeted TNF signaling, but also the LPS-induced TLR4 signaling pathway. To determine the expression of IP-10 in the ileum, we performed ex vivo experiments using explant tissues from 12-week-old mice. The results clearly showed that CAPE suppressed intracellular expression of IP-10 (Fig. 5C). We then tested the efficacy of CAPE in the $TNF^{\Delta ARE/+}$ mouse model of ileitis. After six weeks of feeding, CAPE did not antagonize the development of Crohn's disease-like ileitis (Supporting Information Fig. S5A). When compared with sham-fed control mice, $TNF^{\Delta ARE/+}$ mice were characterized by similar

levels of leukocyte infiltration in the mucosa and submucosa (Supporting Information Fig. S5B).

4 Discussion

In the present study, we demonstrate anti-inflammatory effects of CAPE on IP-10 expression by providing novel data on structure/activity relationship and molecular mechanisms underlying NF- κ B pathway inhibition. We focused on the chemokine IP-10 as endpoint target because IP-10 has been described as a master effector molecule of inflammatory responses [13, 26, 27].

We observed a time- and concentration-dependent inhibition of TNF-induced IP-10 expression by CAPE in intestinal epithelial Mode-K cells. By comparing the activity of several analogous compounds obtained by synthetic modification, we found that catecholic hydroxyls are more reactive in comparison to methoxyl groups. Substitution of one of the hydroxyl in ring A (P3MC) resulted in reduced activity and methoxylation of both hydroxyls (PDC) rendered the compound inactive. The ability of P3MC to inhibit IP-10 expression but not SEAP activity when compared with CAPE can be attributed to methoxylation of the reactive hydroxyl group in ring A lowering the potency to reduce NF- κ B-induced gene expression. Inhibition of TNF-induced IP-10 production by P3MC and CAPE depends on downstream events within the NF- κ B signaling pathway as influenced by different NF- κ B dimer combinations, whereas the SEAP assay is primarily under the control of κ B-binding repeats. Of course, we also cannot exclude the fact that signaling pathways other than NF- κ B play a substantial role in the inhibition of IP-10 production by P3MC. These observations in Mode-K cells are in agreement with a recent study showing that methylation of the hydroxyl residues in polyphenols resulted in a loss in potency against human leukemia cells [28]. In addition, Wang et al. [29] and Lee et al. [30] have also shown very recently that methoxy derivatives of CAPE are characterized by impaired or diminished cytoprotective and NF- κ B inhibitory functions, respectively. In our experiments, the importance of hydroxyl groups in mediating anti-inflammatory mechanisms was also supported by the fact that CAPE retained most of its biological activity after the ester was replaced with an amide (CAPEA), suggesting that the more stable amides are as active as the corresponding structurally flexible (less rigid and more volatile) esters. However, modification of CAPEA to CAT by further addition of a hydroxyl group to ring B resulting in the formation of a phenol ring led to a total loss of activity. One possible explanation is that the proximity of hydroxyl residues of the catechol structure facilitates formation of sterically important reactive intermediates [31, 32]. The subtle structural differences between PDC and CAT may account for loss of activity as a result of: (i) increased polarity and, as a consequence, reduced cell membrane permeability; (ii) disturbed hydrophobic interactions in

target protein binding sites. These results confirm the recent findings by Wang et al. and Lee et al. showing that the phenethyl moiety of CAPE determines activity, i.e. caffeic acid or *n*-alkyl derivatives were characterized by loss of cytoprotection and anti-inflammatory activity [29, 30]. Taken together, our molecular similarity analyses revealed that the reactivity of the catecholic hydroxyl groups control the potency of CAPE, that is, its ability to interact with target proteins.

We next aimed at providing novel insights into the molecular mechanisms underlying CAPE activity, focusing primarily on the functional effects of the p50/RelA heterodimer, which has been shown to transactivate many inflammatory genes [33–35]. The major regulatory step that prevents spontaneous NF- κ B activity is the retention of the NF- κ B/I κ B α complex in the cytoplasm. Dissociation of this complex results in I κ B α degradation and NF- κ B liberation to the nucleus. While others reported inhibitory effects of CAPE on the IKK complex and I κ B α phosphorylation in human CD4⁺ T cells and the gastric epithelium [36, 37], we could show that phosphorylation of NF- κ B and I κ B α , degradation of I κ B α and RelA nuclear translocation were unchanged in Mode-K cells after CAPE treatment, suggesting that effects are cell/tissue type-specific. However, our results are in agreement with two previous reports which demonstrated that CAPE has no effect on I κ B α degradation in osteoclasts [38] and U937 cells [7]. Concentrations also likely influence effects. For instance, Lee et al. also obtained results that contradict ours, i.e. partial prevention of I κ B α degradation by CAPE, but using higher concentrations (>25 μ M) in HCT116 cells [30]. The non-canonical NF- κ B signaling pathway is a result of p100 to p52 processing by the proteasome. The liberated p52 forms active p52/RelB complexes that induce transcriptional process responses differing from the I κ B α -dependent canonical pathway. Processing of p100 and I κ B α degradation regulate different NF- κ B dimers and as a consequence non-canonical and canonical pathways regulate distinct NF- κ B target genes that are stimuli specific. In our experiments, CAPE did not alter p100 mRNA expression, yet induced transcripts of the p50 precursor p105. Consistent with a previous report that polyphenols affect recruitment of transcription factors to gene promoter regions [8], we found that CAPE inhibits NF- κ B (p50/RelA heterodimer) binding to the IP-10 promoter. This is also in line with a genetic analysis study by Hoffmann et al., who found that both p50 and RelA subunits are essential for IP-10 expression [17]. Whereas CAPE inhibited p50 and RelA binding onto the IP-10 promoter, its failure to inhibit the coordinated degradation and re-synthesis of I κ B α may be attributed to selective gene activation in the I κ B α promoter [39]. Importantly, Hoffmann et al. also showed that, whereas most regulatory genes are RelA subunit-dependent, the p50 subunit is dispensable for some of these genes including the neutrophils chemokine MIP-2 that controls mucosal lymphocyte migration in IEC [40]. MIP-2 can be induced by many of the

RelA-containing dimeric complexes including p50/RelA, p52/RelA and RelA/RelA. Recently, it was shown that NF- κ B and AP-1 activation is required for MIP-2 up-regulation and silencing of NF- κ B alone may not be sufficient to reduce inflammation in acute pancreatitis [41]. Data from the literature have also demonstrated that CAPE does not affect AP-1 promoter activity [7]. Taken together, we propose that CAPE targets NF- κ B DNA-binding sites of the p50/RelA heterodimer without compromising other essential NF- κ B functions. This suggests that although CAPE targets activity within the core of NF- κ B binding in the promoter regions, it may in fact have selective effects, for instance, inhibition of IP-10 pro-inflammatory signals without completely blocking MIP-2, an acute phase response gene.

Since CAPE exhibits a strong radical scavenging activity [42] and HO-1 and Nrf2 have been shown to interact with inflammatory pathways [43, 44], we determined whether the combined effect of reduced NF- κ B activity and increased anti-oxidative stress responses was a prerequisite for the anti-inflammatory effect of CAPE. We could demonstrate a strong induction of HO-1 after CAPE treatment. Using NAC to inhibit CAPE-induced HO-1 induction, we found that IP-10 inhibition occurred independently of the presence or absence of HO-1 proteins. Because induction of HO-1 is mediated by the transcription factor Nrf2 [45], we also aimed at analyzing the impact of Nrf2 signaling on CAPE-induced IP-10 expression. Using Nrf2 knockout MEF, we found that Nrf2 is not required for inhibition of IP-10 protein expression by CAPE. Via knockdown of Nrf2 using shRNA in HCT116 cells, Lee et al. had previously proposed that CAPE-mediated Nrf2 activation is associated with inhibition of the NF- κ B pathways [30]. However, differences observed after specific knockdown were marginal at concentrations below 25 μ M and related only to NF- κ B reporter gene activity, whereas our data refer to the endpoint readout of interest IP-10. Also, our data goes along the line of the work on interaction between anti-inflammatory and -oxidative properties by Liu et al. [46], who found that a variety of phase 2 inducers, i.e. chemicals inducing for instance NQO1, were capable of inhibiting NO production by mouse peritoneal macrophages, independently of macrophage origin (WT or Nrf2^{-/-} mice). Another important result of the present study is that CAPE potentiates phosphorylation and accumulation of p38 MAPK in the nucleus. Phosphorylation of p38 MAPK under conditions of oxidative/electrophilic stress has been shown to be synergistic to NF- κ B activity via phosphorylation of RelA by MSK1, a p38 MAPK substrate [47]. However, based on our findings using the p38 MAPK inhibitor SB203580, we propose that NF- κ B-dependent IP-10 inhibition is not related to the p38 MAPK pathway activation. As for the effect of CAPE on p-AMPK and JNK activation, further work is needed to draw conclusion on their impact on IP-10 inhibition.

Epithelial cells are in direct contact with the gut luminal content including bacteria and their metabolites and other chemical stimuli that trigger chemokine production in a

dysregulated gut homeostasis. Experimental evidence has demonstrated up-regulation of the chemokine IP-10 in ileitis [14], brain ischemia [48] and adipocyte maturation [49]. In the present study, we have shown that CAPE abolishes expression of both TNF- and LPS-induced IP-10 expression in embryonic fibroblasts from TNF^{AARE/+} mice. Furthermore, IP-10 production was also inhibited in ileum tissue explants from TNF^{AARE/+} mice after CAPE treatment. Nevertheless, we found that oral treatment with CAPE had no influence on ileitis in TNF^{AARE/+} mice under the experimental conditions used. In inflammation, many chemokines are expressed at different times following cell stimulation, thus failure of CAPE to inhibit MIP-2 gives a hint into the complexity of signals that are involved in leukocyte trafficking under inflammatory conditions. Hence, we should not expect blockade of a single chemokine secreted by the epithelium to be sufficient to suppress disease progression. Furthermore, a prerequisite for in vivo activity is that active compounds must reach target cells (distal epithelial cells in the present study). Whereas CAPE permeated IEC membranes at micromolar concentrations in the in vitro assays, this was most likely not the case in vivo, possibly due to rapid absorption in the upper GI tract and subsequent excretion or degradation by intestinal microorganisms [50]. Contrary to our findings, it has been previously reported that CAPE attenuates peptidoglycan-polysaccharide-induced colitis in rats [51]. However, the authors used an acute model of inflammation and daily intraperitoneal injection of CAPE (30 mg/kg body weight) for one week, which contrasts to our dietary treatment (10 mg/kg, three times a week over six weeks) in a chronic inflammatory model of ileitis.

In summary, we showed that CAPE has a strong inhibitory effect on TNF-induced IP-10 expression in IECs. We provided evidence that the catechol moiety controls CAPE potency. In addition, we showed that CAPE exhibits its anti-inflammatory effects by disrupting the p50/RelA NF- κ B heterodimer binding to the IP-10 promoter. Although feeding experiments in TNF^{AARE/+} mice failed to prevent TNF-driven Crohn's disease ileitis, the anti-inflammatory potential of CAPE was confirmed in ileal tissue explants and embryonic fibroblasts derived from TNF^{AARE/+} mice.

The authors thank Gabriele Hörmannspurger and Emmanuel Berger for helpful discussions, Tilo Wuensch for confocal microscopy and Nico Gebhardt for excellent technical assistance. They are grateful to Dr. Albenka Dinkova-Kostova (Biomedical Research Institute, University of Dundee, UK) and Prof. Masayuki Yamamoto (Tohoku University Graduate School of Medicine, Sendai, Japan) for providing Nrf2-knockout mouse embryonic fibroblasts, and Dr. George Kollias (Biomedical Sciences Research Center Alexander Fleming, Vari, Greece) for providing the TNF^{AARE/+} mouse model. J. O. M was funded by the Deutscher Akademischer Austausch Dienst (DAAD). J. O. M., N. W., I. S., T. H., S. M. and D. H. designed research; J. O. M., C. B. and N. W. conducted research; T. H. and D. H.

provided essential materials; J. O. M., C. B., I. S. and T. C. analyzed and interpreted data; J. O. M., N. W., T. C. and D. H. wrote paper; J. O. M. and D. H. had primary responsibility for final content.

The authors have declared no conflict of interest.

5 References

- [1] Xia, Y. F., Ye, B. Q., Li, Y. D., Wang, J. G. et al., Andrographolide attenuates inflammation by inhibition of NF-kappa B activation through covalent modification of reduced cysteine 62 of p50. *J. Immunol.* 2004, **173**, 4207–4217.
- [2] Kart, A., Cigremis, Y., Ozen, H., Dogan, O., Caffeic acid phenethyl ester prevents ovary ischemia/reperfusion injury in rabbits. *Food Chem. Toxicol.* 2009, **47**, 1980–1984.
- [3] Toyoda, T., Tsukamoto, T., Takasu, S., Shi, L. et al., Anti-inflammatory effects of caffeic acid phenethyl ester (CAPE), a nuclear factor-kappaB inhibitor, on *Helicobacter pylori*-induced gastritis in Mongolian gerbils. *Int. J. Cancer* 2009, **125**, 1786–1795.
- [4] Jin, U. H., Song, K. H., Motomura, M., Suzuki, I. et al., Caffeic acid phenethyl ester induces mitochondria-mediated apoptosis in human myeloid leukemia U937 cells. *Mol. Cell. Biochem.* 2008, **310**, 43–48.
- [5] Demestre, M., Messerli, S. M., Celli, N., Shahhossini, M. et al., CAPE (caffeic acid phenethyl ester)-based propolis extract (Bio 30) suppresses the growth of human neurofibromatosis (NF) tumor xenografts in mice. *Phytother. Res.* 2009, **23**, 226–230.
- [6] Grunberger, D., Banerjee, R., Eisinger, K., Oltz, E. M. et al., Preferential cytotoxicity on tumor cells by caffeic acid phenethyl ester isolated from propolis. *Experientia* 1988, **44**, 230–232.
- [7] Natarajan, K., Singh, S., Burke, T. R., Jr., Grunberger, D. et al., Caffeic acid phenethyl ester is a potent and specific inhibitor of activation of nuclear transcription factor NF-kappa B. *Proc. Natl. Acad. Sci. USA* 1996, **93**, 9090–9095.
- [8] Ruiz, P. A., Braune, A., Holzlwimmer, G., Quintanilla-Fend, L. et al., Quercetin inhibits TNF-induced NF-kappaB transcription factor recruitment to proinflammatory gene promoters in murine intestinal epithelial cells. *J. Nutr.* 2007, **137**, 1208–1215.
- [9] Ruiz, P. A., Haller, D., Functional diversity of flavonoids in the inhibition of the proinflammatory NF-kappaB, IRF, and Akt signaling pathways in murine intestinal epithelial cells. *J. Nutr.* 2006, **136**, 664–671.
- [10] Ahn, M. R., Kunimasa, K., Kumazawa, S., Nakayama, T. et al., Correlation between antiangiogenic activity and antioxidant activity of various components from propolis. *Mol. Nutr. Food Res.* 2009, **53**, 643–651.
- [11] Chen, M. F., Keng, P. C., Lin, P. Y., Yang, C. T. et al., Caffeic acid phenethyl ester decreases acute pneumonitis after irradiation in vitro and in vivo. *BMC Cancer* 2005, **5**, 158.

- [12] Coban, S., Yildiz, F., Terzi, A., Al, B. et al., The effect of caffeic acid phenethyl ester (CAPE) against cholestatic liver injury in rats. *J. Surg. Res.* 2008.
- [13] Dufour, J. H., Dziejman, M., Liu, M. T., Leung, J. H. et al., IFN-gamma-inducible protein 10 (IP-10; CXCL10)-deficient mice reveal a role for IP-10 in effector T cell generation and trafficking. *J. Immunol.* 2002, *168*, 3195–3204.
- [14] Hoermannsperger, G., Clavel, T., Hoffmann, M., Reiff, C. et al., Post-translational inhibition of IP-10 secretion in IEC by probiotic bacteria: impact on chronic inflammation. *PLoS One* 2009, *4*, e4365.
- [15] Gilmore, T. D., The Rel/NF-kappaB signal transduction pathway: introduction. *Oncogene* 1999, *18*, 6842–6844.
- [16] Hayden, M. S., Ghosh, S., Shared principles in NF-kappaB signaling. *Cell* 2008, *132*, 344–362.
- [17] Hoffmann, A., Leung, T. H., Baltimore, D., Genetic analysis of NF-kappaB/Rel transcription factors defines functional specificities. *EMBO J.* 2003, *22*, 5530–5539.
- [18] Karin, M., Ben-Neriah, Y., Phosphorylation meets ubiquitination: the control of NF-[kappa]B activity. *Annu. Rev. Immunol.* 2000, *18*, 621–663.
- [19] Andresen, L., Jorgensen, V. L., Perner, A., Hansen, A. et al., Activation of nuclear factor kappaB in colonic mucosa from patients with collagenous and ulcerative colitis. *Gut* 2005, *54*, 503–509.
- [20] Schreiber, S., Nikolaus, S., Hampe, J., Activation of nuclear factor kappa B inflammatory bowel disease. *Gut* 1998, *42*, 477–484.
- [21] La Ferla, K., Seeger, D., Schreiber, S., Activation of NF-kappaB in intestinal epithelial cells by *E. coli* strains isolated from the colonic mucosa of IBD patients. *Int. J. Colorectal Dis.* 2004, *19*, 334–342.
- [22] Vidal, K., Grosjean, I., evillard, J. P., Gespach, C. et al., Immortalization of mouse intestinal epithelial cells by the SV40-large T gene. Phenotypic and immune characterization of the MODE-K cell line. *J. Immunol. Methods* 1993, *166*, 63–73.
- [23] Wakabayashi, N., Dinkova-Kostova, A. T., Holtzclaw, W. D., Kang, M. I. et al., Protection against electrophile and oxidant stress by induction of the phase 2 response: fate of cysteines of the Keap1 sensor modified by inducers. *Proc. Natl. Acad. Sci. USA* 2004, *101*, 2040–2045.
- [24] Pfaffl, M. W., A new mathematical model for relative quantification in real-time RT-PCR. *Nucleic Acids Res.* 2001, *29*, e45.
- [25] Nelson, D. E., Ihekwa, A. E., Elliott, M., Johnson, J. R. et al., Oscillations in NF-kappaB signaling control the dynamics of gene expression. *Science* 2004, *306*, 704–708.
- [26] Ugucioni, M., Gionchetti, P., Robbiani, D. F., Rizzello, F. et al., Increased expression of IP-10, IL-8, MCP-1, and MCP-3 in ulcerative colitis. *Am. J. Pathol.* 1999, *155*, 331–336.
- [27] Dwinell, M. B., Luger, N., Eckmann, L., Kagnoff, M. F., Regulated production of interferon-inducible T-cell chemoattractants by human intestinal epithelial cells. *Gastroenterology* 2001, *120*, 49–59.
- [28] Landis-Piwowar, K. R., Milacic, V., Dou, Q. P., Relationship between the methylation status of dietary flavonoids and their growth-inhibitory and apoptosis-inducing activities in human cancer cells. *J. Cell Biochem.* 2008, *105*, 514–523.
- [29] Wang, X., Stavchansky, S., Kerwin, S. M., Bowman, P. D., Structure–activity relationships in the cytoprotective effect of caffeic acid phenethyl ester (CAPE) and fluorinated derivatives: effects on heme oxygenase-1 induction and antioxidant activities. *Eur. J. Pharmacol.* 2010, *635*, 16–22.
- [30] Lee, Y., Shin, D. H., Kim, J. H., Hong, S. et al., Caffeic acid phenethyl ester-mediated Nrf2 activation and I kappa B kinase inhibition are involved in NFkappaB inhibitory effect: structural analysis for NFkappaB inhibition. *Eur. J. Pharmacol.* 2010, *643*, 21–28.
- [31] Rice-Evans, C., Spencer, J. P., Schroeter, H., Rechner, A. R., Bioavailability of flavonoids and potential bioactive forms in vivo. *Drug Metabol. Drug Interact.* 2000, *17*, 291–310.
- [32] Rice-Evans, C. A., Miller, N. J., Paganga, G., Structure–antioxidant activity relationships of flavonoids and phenolic acids. *Free Radic. Biol. Med.* 1996, *20*, 933–956.
- [33] Hayden, M. S., West, A. P., Ghosh, S., NF-kappaB and the immune response. *Oncogene* 2006, *25*, 6758–6780.
- [34] Curran, C. L., Blackwell, T. S., Christman, J. W., NF-kappaB: a therapeutic target in inflammatory diseases. *Expert Opin. Ther. Targets* 2001, *5*, 197–204.
- [35] Tak, P. P., Firestein, G. S., NF-kappaB: a key role in inflammatory diseases. *J. Clin. Invest.* 2001, *107*, 7–11.
- [36] Abdel-Latif, M. M., Windle, H. J., Homasany, B. S., Sabra, K. et al., Caffeic acid phenethyl ester modulates *Helicobacter pylori*-induced nuclear factor-kappa B and activator protein-1 expression in gastric epithelial cells. *Br. J. Pharmacol.* 2005, *146*, 1139–1147.
- [37] Wang, L. C., Chu, K. H., Liang, Y. C., Lin, Y. L. et al., Caffeic acid phenethyl ester inhibits nuclear factor-kappaB and protein kinase B signalling pathways and induces caspase-3 expression in primary human CD4+ T cells. *Clin. Exp. Immunol.* 2010, *160*, 223–232.
- [38] Ha, J., Choi, H. S., Lee, Y., Lee, Z. H. et al., Caffeic acid phenethyl ester inhibits osteoclastogenesis by suppressing NF kappaB and downregulating NFATc1 and c-Fos. *Int. Immunopharmacol.* 2009, *9*, 774–780.
- [39] Hoffmann, A., Levchenko, A., Scott, M. L., Baltimore, D., The I kappa B-NF-kappaB signaling module: temporal control and selective gene activation. *Science* 2002, *298*, 1241–1245.
- [40] Ohtsuka, Y., Lee, J., Stamm, D. S., Sanderson, I. R., MIP-2 secreted by epithelial cells increases neutrophil and lymphocyte recruitment in the mouse intestine. *Gut* 2001, *49*, 526–533.
- [41] Orlichenko, L. S., Behari, J., Yeh, T. H., Liu, S. et al., Transcriptional regulation of CXC-ELR chemokines KC and MIP-2 in mouse pancreatic acini. *Am. J. Physiol. Gastrointest. Liver Physiol.* 2010, *299*, G867–G876.
- [42] Izuta, H., Narahara, Y., Shimazawa, M., Mishima, S. et al., 1,1-Diphenyl-2-picrylhydrazyl radical scavenging activity of bee products and their constituents determined by ESR. *Biol. Pharm. Bull.* 2009, *32*, 1947–1951.

- [43] Dinkova-Kostova, A. T., Liby, K. T., Stephenson, K. K., Holtzclaw, W. D. et al., Extremely potent triterpenoid inducers of the phase 2 response: correlations of protection against oxidant and inflammatory stress. *Proc. Natl. Acad. Sci. USA* 2005, *102*, 4584–4589.
- [44] Pae, H. O., Chung, H. T., Heme oxygenase-1: its therapeutic roles in inflammatory diseases. *Immune Netw.* 2009, *9*, 12–19.
- [45] Alam, J., Stewart, D., Touchard, C., Boinapally, S. et al., Nrf2, a Cap'n'Collar transcription factor, regulates induction of the heme oxygenase-1 gene. *J. Biol. Chem.* 1999, *274*, 26071–26078.
- [46] Liu, H., Dinkova-Kostova, A. T., Talalay, P., Coordinate regulation of enzyme markers for inflammation and for protection against oxidants and electrophiles. *Proc. Natl. Acad. Sci. USA* 2008, *105*, 15926–15931.
- [47] Kefaloyianni, E., Gaitanaki, C., Beis, I., ERK1/2 and p38-MAPK signalling pathways, through MSK1, are involved in NF-kappaB transactivation during oxidative stress in skeletal myoblasts. *Cell Signal.* 2006, *18*, 2238–2251.
- [48] Wang, X., Ellison, J. A., Siren, A. L., Lysko, P. G. et al., Prolonged expression of interferon-inducible protein-10 in ischemic cortex after permanent occlusion of the middle cerebral artery in rat. *J. Neurochem.* 1998, *71*, 1194–1204.
- [49] Krinninger, P., Brunner, C., Ruiz, P. A., Schneider, E. et al., Role of the adipocyte-specific NF(kappa)B activity in the regulation of IP-10 and T cell migration. *Am. J. Physiol. Endocrinol. Metab.* 2011, *300*, E304–E311.
- [50] Gonthier, M. P., Remesy, C., Scalbert, A., Cheynier, V. et al., Microbial metabolism of caffeic acid and its esters chlorogenic and caftaric acids by human faecal microbiota in vitro. *Biomed. Pharmacother.* 2006, *60*, 536–540.
- [51] Fitzpatrick, L. R., Wang, J., Le, T., Caffeic acid phenethyl ester, an inhibitor of nuclear factor-kappaB, attenuates bacterial peptidoglycan polysaccharide-induced colitis in rats. *J. Pharmacol. Exp. Ther.* 2001, *299*, 915–920.

PAPER 10

Bacterial transformation of dietary lignans in gnotobiotic rats

 Anni Woting¹, Thomas Clavel², Gunnar Loh¹ & Michael Blaut¹
¹Department of Gastrointestinal Microbiology, German Institute of Human Nutrition Potsdam-Rehbruecke (DIfE), Nuthetal, Germany; and ²Department of Biofunctionality, ZIEL – Research Center for Nutrition and Food Science, Technische Universität München (TUM), Weihenstephan, Germany

Correspondence: Michael Blaut, Department of Gastrointestinal Microbiology, German Institute of Human Nutrition Potsdam-Rehbruecke (DIfE), Arthur-Scheunert-Allee 114-116, 14558 Nuthetal, Germany. Tel.: +49 332 00 88 470; fax: +49 332 00 88 407; e-mail: blaut@dife.de

Received 21 December 2009; revised 22 February 2010; accepted 23 February 2010. Final version published online 29 March 2010.

DOI:10.1111/j.1574-6941.2010.00863.x

Editor: Julian Marchesi

Keywords

lignan; intestinal bacteria; *Clostridium saccharogumia*; *Eggerthella lenta*; *Blautia producta*; *Lactonifactor longoviformis*.

Abstract

The bioactivity of lignans depends on their transformation by gut bacteria. The intestinal bacteria *Clostridium saccharogumia*, *Eggerthella lenta*, *Blautia producta* and *Lactonifactor longoviformis* convert the plant lignan secoisolariciresinol diglucoside via secoisolariciresinol (SECO) into the bioactive enterolignans enterodiol (ED) and enterolactone (EL). While the *in vitro* conversion of lignans by these bacteria has already been demonstrated, it is unclear whether this defined community is also capable of catalysing lignan transformation *in vivo*. We therefore associated germ-free rats with these four species. Germ-free rats served as a control. All animals were fed a diet containing 5% ground flaxseed. The caecal contents of rats associated with the four lignan-activating bacteria (ALB rats) contained SECO, ED and EL. The maximal EL formation rate from lignans in the pooled caecal contents of ALB rats was 7.52 nmol min⁻¹ g⁻¹ dry matter. The ALB rats excreted EL, but no SECO and ED, in their urine. The caecal contents of germ-free rats contained SECO, but no ED and EL. Their urine was devoid of lignans. Hence, the presence of enterolignans in the ALB rats, but not in the germ-free rats, demonstrates that this defined microbial community is capable of transforming plant lignans into EL *in vivo*.

Introduction

Lignans are diphenolic compounds likely acting as phytoalexins in plants (Ayres & Loike, 1990). The lignan secoisolariciresinol diglucoside (SDG) is one of the most abundant dietary lignans and flaxseed is one of the best sources of SDG, with contents varying from approximately 1–26 mg g⁻¹ flaxseed (Milder *et al.*, 2005; Muir, 2006). Dietary lignans are proposed to prevent breast (Thompson *et al.*, 1996; Wang *et al.*, 2005), colon (Serraino & Thompson, 1992; Jenab & Thompson, 1996; Bommarreddy *et al.*, 2006, 2009) and prostate cancer (Lin *et al.*, 2002; Demark-Wahnefried *et al.*, 2008), atherosclerosis (Prasad, 1999, 2005, 2008, 2009) and diabetes (Prasad, 2001; Pan *et al.*, 2007; Zhang *et al.*, 2008). However, the reported beneficial effects of lignans depend on their conversion into the enterolignans enterodiol (ED) and enterolactone (EL) by human intestinal bacteria. *In vitro* data indicated that SDG is stable in the upper part of the gastrointestinal tract (Clavel *et al.*, 2006a). However, it is still unknown to what extent enzymes of the intestinal brush border contribute to the

deglycosylation of SDG, as shown for flavonoids (Day *et al.*, 1998; Lambert *et al.*, 1999; Németh *et al.*, 2003). ED is produced by dominant members of the gut microbial community, while subdominant species produce EL (Clavel *et al.*, 2006b). The first step leading to the production of EL is the deglycosylation of SDG to secoisolariciresinol (SECO) (Wang *et al.*, 2000; Clavel *et al.*, 2006b). Many bacterial species are capable of catalysing this reaction (Clavel *et al.*, 2006b), which is probably not a rate-limiting step in the production of enterolignans in the human gut (Clavel *et al.*, 2006a). Although *Bacteroides* species play an important role in the deglycosylation of SDG in the gut (Clavel *et al.*, 2006b), *Clostridium* species are also capable of deglycosylating SDG. The recently isolated species *Clostridium saccharogumia*, a subdominant member of the human gut microbiota, showed the highest initial conversion rate of SDG to SECO compared with the other bacterial species tested (Clavel *et al.*, 2006a). The second step in the transformation of SDG to EL is the demethylation of SECO to the intermediate 2,3-bis-(3,4-dihydroxy-benzyl)butane-1,4-diol. Several bacterial species, including *Eubacterium*

limosum and *Blautia producta*, catalyse this reaction (Wang *et al.*, 2000; Clavel *et al.*, 2006b). Subsequently, 2,3-bis-(3,4-dihydroxy-benzyl)butane-1,4-diol is dehydroxylated to ED. *Eggerthella lenta* catalyses this reaction enantioselectively (Jin *et al.*, 2007). Co-incubation of *B. producta* and *E. lenta* in SECO-containing media results in the formation of ED. *E. lenta* alone does not show any dehydroxylating activity on SECO, but is able to reduce the plant lignans pinoresinol and lariciresinol (Clavel *et al.*, 2006a). The last step in the transformation of SDG to EL is the dehydrogenation of ED to EL. A recently isolated bacterial species, *Lactonifactor longoviformis*, a subdominant member of the human intestinal microbiota, catalyses the formation of EL (Clavel *et al.*, 2006b). These results show that more than one species is capable of catalysing the first three steps of lignan activation. In contrast, so far, only one species, namely *L. longoviformis*, is known to dehydrogenate ED to EL. This does not exclude the possibility that intestinal species other than *L. longoviformis* catalyse the latter reaction as well.

The bioactivation of the plant lignan SDG requires the interaction of different bacterial species. To investigate this interaction, we chose four bacterial species known to be involved in lignan activation: *C. saccharogumia* (*O*-deglycosylation), *E. lenta* (*O*-demethylation), *B. producta* (dehydroxylation) and *L. longoviformis* (dehydrogenation). A previous *in vitro* study demonstrated that the coincubation of these four bacterial species with SDG results in the formation of EL from SDG (Blaut & Clavel, 2007). To determine whether this bacterial consortium is also capable of activating lignans under *in vivo* conditions, we associated germ-free rats with these four species. We determined the concentrations of enterolignans in urine, faeces and gut contents of the animals in response to feeding a 5% flaxseed diet.

Materials and methods

Chemicals

SDG was a generous gift from Peter Winterhalter (Technical University of Braunschweig), who isolated SDG from flaxseed as described previously (Degenhardt *et al.*, 2002). SECO and EL were purchased from Sigma-Aldrich (Taufkirchen, Germany), ED from the VTT Technical Research Centre of Finland (Espoo, Finland). All lignans were racemic. Stock solutions of SDG (100 mM) were prepared in water. Stock solutions of SECO (100 mM), ED (50 mM) and EL (50 mM) were prepared in methanol.

Bacterial strains and culture conditions

Cryostocks of *C. saccharogumia* DSM 17460^T, *Blautia producta* DSM 3507, *E. lenta* DSM 2243^T and *L. longoviformis* DSM 17459^T were obtained from the collection of the

German Institute of Human Nutrition Potsdam-Rehbruecke. The organisms were cultured at 37 °C under strictly anoxic conditions (Hungate, 1969; Bryant, 1972) in Brain Heart Infusion Broth (Roth, Karlsruhe, Germany) supplemented with 5 g L⁻¹ yeast extract (Roth) and 5 mg L⁻¹ haemin (Sigma-Aldrich) (YH-BHI). The strains were subcultured every 2 weeks and stored at 4 °C. Purity was checked by inspecting the colony morphology after anaerobic growth on YH-BHI agar (Oxoid, Basingstoke, UK) and the cell morphology after Gram staining. All strains were streaked on YH-BHI agar and incubated aerobically to detect any aerobic contaminants.

Animals and experimental design

Ten eight-week-old male germ-free Sprague–Dawley rats were purchased from Charles River (Wiga, France). They were kept in positive-pressure isolators (Metall & Plastik, Radolfzell, Germany) under a 12-h light cycle, constant temperature and air humidity. The rats had free access to autoclaved distilled water and a diet sterilized by gamma irradiation (25 kGy; Gamma Service Produktbestrahlung GmbH, Radeberg, Germany). The experiments and the maintenance of the rats were approved by the local animal welfare committee (approval no. 23-2347-8-16-2008). After five days on a standard diet (1314, Altromin, Lage, Germany), the rats were assigned either to the experimental or to the control group (*n* = 5 per group). The rats of the experimental group were associated on 2 consecutive days with the lignan-activating bacteria *C. saccharogumia*, *B. producta*, *E. lenta* and *L. longoviformis*, hereafter referred to as ALB rats. The inoculum was freshly prepared by growing each bacterial species in YH-BHI. The cell densities were determined using a counting chamber and the liquid cultures were subsequently combined. The final inoculum (500 µL) containing 10⁸ cells of each species was applied intragastrically to each rat. The control rats remained germ free. Three days after the first colonization, both groups were switched from the standard diet to a diet containing 5% ground flaxseed, 58% wheat starch, 20% casein, 5% sunflower oil, 5% cellulose, 5% mineral mixture and 2% vitamin mixture. The rats were fed the experimental diet for 12 days. Over the last 48 h, all rats were kept in metabolic cages and faeces and urine were collected. Finally, the rats were anaesthetized with isofluran (Sigma-Aldrich) and decapitated. Faeces as well as caecal and colonic contents were freeze-dried (freeze-drying system alpha 1–4, Christ, Osterode, Germany) and stored at 4 °C until analysis.

FISH and quantification of bacterial cells

The successful colonization and the relative proportions of the four lignan-activating bacteria were evaluated using species-specific oligonucleotide probes (Table 1).

Table 1. Cy3-labelled oligonucleotide probes used for fluorescence *in situ* hybridization to quantify bacteria

Probe	Sequence (5'-3')	Target organism	Hybridization temperature (°C)	Reference
S-S-Csac-0067-a-A-20	CTC GGA CAT TAC TGC CCG CG	<i>Clostridium saccharogumia</i>	46	Clavel <i>et al.</i> (2006a)
S-*-ProCo-1264-a-A-23	TTG GGA TTC GCT CAA CAT CGC TG	<i>Blautia producta</i>	35	Clavel <i>et al.</i> (2005)
S-*-Ato-0291-a-A-17	GGT CGG TCT CTC AAC CC	<i>Eggerthella lenta</i>	54	Harmsen <i>et al.</i> (2000)
S-S-Llong-0831-a-A-20	GGA CGC CTT TGG CGC CCG AC	<i>Lactonifactor longoviformis</i>	46	This paper

The probes were validated for their species specificity within the consortium. They were labelled with the fluorescent dye Cy3 at their 5'-end. FISH was performed as described previously (Thiel & Blaut, 2005) with the following modifications: the fixed samples were sonicated (10 s, 0.5 cycles, 20% amplitude) in addition to homogenization with a Uniprep-Gyrator (UniEquip, Martinsried, Germany). The concentration of each oligonucleotide probe was 10 µM in hybridization buffer. Then, 1 µL was applied to each well. Hybridization buffer containing 30% (v/v) formamide was used for the probe ProCo-1264. After an overnight hybridization in a moist chamber, the slides were washed with hybridization buffer for 20 min at 2 °C above the hybridization temperature. Bacterial cells were counted with fluorescence microscopy as described previously (Reichardt *et al.*, 2009).

Measurement of SDG in ground flaxseed, experimental diet, caecal contents and faeces

The lignan-containing samples (100 mg) were defatted for 2 h with *n*-hexane and extracted for 17 h with 3 mL methanol/water (70/30, v/v). After centrifugation (3000 g, 10 min), the supernatants were collected and the pellets were washed twice with methanol/water (70/30, v/v). The supernatants of the wash steps were pooled. Methanol was evaporated (speed vac RC 10-22, Jouan, Dreieich, Germany) and residual water was removed by lyophilization (Christ). The lyophilisates were dissolved in 0.5 mL 1 M NaOH for 3 h, neutralized with HCl and freeze-dried again. The lyophilisates were suspended in 75–80 µL methanol/water (70/30, v/v) and analysed by high-performance liquid chromatography (HPLC).

Measurement of SECO, ED and EL in caecal and colonic contents

Free lignans were determined as described above with the following modifications: approximately 100 mg of gut contents were extracted with 0.6 mL methanol/water (70/30, v/v) by shaking for 10 min. Lyophilisates were suspended in 50 µL methanol/water (70/30, v/v) and analysed by HPLC. In case of the conjugated lignans, only caecal contents provided sufficient material to determine glucuronidated and sulphated fractions. Caecal contents (100 mg) were

suspended in 600 µL water and mixed with 534 µL sodium acetate buffer (0.29 M, pH 5) and 144 µL of a β-glucuronidase/sulphatase preparation (type HP-2; 102 000/ ≤ 7500 U mL⁻¹; Sigma-Aldrich). The samples were incubated for 16 h at 37 °C, followed by extraction and lyophilization as described above. The lyophilisates were suspended in 65 µL methanol/water (70/30, v/v) and analysed by HPLC.

In vitro formation rates of the free lignans SECO, ED and EL in pooled caecal contents

Freshly collected caecal contents were stored on ice and kept under anoxic conditions (AnaeroGen Compact, Oxoid, Basingstoke, UK). The five samples from each group were separately pooled in an anoxic workstation (MAKS MG, Meintrup DWS, Laehden, Germany). The pooled samples were aliquoted in tubes (0.5 g each) and incubated at 37 °C under anoxic conditions (N₂/CO₂/H₂, 80/10/10, v/v/v). At 0, 1, 2, 4 and 8 h, the incubation was stopped by freezing the tubes in liquid nitrogen. The samples were freeze-dried (Christ) and subsequently extracted with methanol/water (70/30, v/v) as described above. The lyophilisates were suspended in 100 µL methanol/water (70/30, v/v) and analysed by HPLC.

Measurement of ED and EL in urine

Urine was thawed, centrifuged (1000 g, 15 min, 4 °C) and the supernatants were filtered (0.45 µm, Roth). Lignans were extracted from 0.2 mL of the supernatants with 0.6 mL ethyl acetate by shaking for 10 min. After centrifugation (3000 g, 10 min), the upper ethyl acetate phase containing the lignans was collected. These steps were repeated two times and the ethyl acetate phases combined. Samples were evaporated (Jouan), the residues were dissolved in 33 µL methanol/water (70/30, v/v) and analysed by HPLC.

Glucuronidated/sulphated lignans were deconjugated within 16 h of incubation with hydrolytic enzymes at 37 °C. Urine (200 µL) was mixed with 178 µL sodium acetate buffer (0.29 M, pH 5) and 48 µL β-glucuronidase/sulphatase (type HP-2, Sigma-Aldrich). The lignans were extracted as described above.

Detection of lignans by HPLC

Samples were centrifuged (13 000 g, 3 min) and the supernatants were analysed. Lignans were measured using an HPLC system with a diode array detector (Gynkotec, Germering, Germany). The HPLC system was equipped with a pump Model 480, degasser DG-503, autosampler GINA 50, a column oven, a UV/Vis diode array detector UVD-320 and a reversed-phase C₁₈ column (LiChroCart 250-4 LiChrospher 100 RP-18, 250 × 4 mm, 5 µm; Merck, Darmstadt, Germany) protected with a guard RP-18 column (4 × 4 mm, 5 µm). The column temperature was maintained at 37 °C. The flow rate was 0.3 mL min⁻¹ and the injection volume was 20 µL. Lignans were detected at 285 nm. For data acquisition, the software Chromeleon version 6.40 (Dionex, Idstein, Germany) was used.

The mobile phase was a mixture of 50 mM sodium acetate (pH 5)/methanol (80/20, v/v) (solvent A), as well as 50 mM sodium acetate/methanol/acetonitrile (40/40/20, v/v/v) (solvent B). The gradient was 20–80% B within 10 min, 80–100% B within 14 min, 100% B for 11 min and back to 20% B within 1 min. The lignans were quantified using calibration curves ranging from 10 to 1500 µM. The retention times of the standard lignans were: SDG, 20.4 min; SECO, 25.8 min; ED, 29.2 min; and EL, 32.9 min. Lignans were identified by comparison with the retention times and spectra of the standard lignans.

Recovery of lignans in the analysed materials

Freeze-dried faeces (100 mg) of a germ-free rat containing no lignans were spiked with 90 µL of each SDG, SECO and ED solution (100 µM) and 35 µL of an EL solution (250 µM). The faeces were extracted with methanol/water (70/30, v/v) as described above and analysed by HPLC. For each lignan, the recovery was determined using three independent spiked faecal samples. Recoveries were as follows: 91.8 ± 6.95% for SDG, 52.8 ± 1.71% for SECO, 62.1 ± 0.80% for ED and 47.5 ± 0.95% for EL.

The recovery of lignans in urine was determined by spiking 200 µL urine of a germ-free rat containing no lignans with 15 µL of each SDG, SECO, ED and EL solution (1.5 µM). The lignans were extracted with ethyl acetate as described above and analysed by HPLC. The recovery of each lignan was determined using three independent spiked urine samples. Recoveries were as follows: 84.2 ± 6.96% for SECO, 97.2 ± 1.97% for ED and 100 ± 6.05% for EL. SDG was not recovered after ethyl acetate extraction.

Statistical analysis

The statistical package for the social sciences for Windows version 14.0 (SPSS Inc., Chicago, IL) was used to conduct the statistical analysis. Values were tested for normal

distribution using the Kolmogorov–Smirnov test. Differences in the caecal and faecal lignan concentrations between ALB and germ-free rats were checked for significance using an unpaired *t*-test. Data are presented as their mean ± SD.

Results and discussion

The lignan-activating bacteria *C. saccharogumia*, *E. lenta*, *B. producta* and *L. longoviformis* activate the plant lignan SDG under *in vitro* conditions (Clavel *et al.*, 2006b). To investigate their ability to activate SDG *in vivo*, these four species were introduced into the gastrointestinal tract of germ-free rats (ALB rats). Germ-free animals were used as a control. All rats were fed a diet containing 5% ground flaxseed.

The four lignan-converting bacteria colonized the intestinal tract of the rats

Because the establishment of the lignan-activating consortium was a prerequisite for successfully conducting the study, bacteria were enumerated in caecal and colonic samples using FISH. Data analysis revealed the presence of the four lignan-activating bacterial species in the caecal and colonic contents of the ALB rats, demonstrating their ability to establish and persist in the rat intestinal tract. Bacterial cell numbers are given in Table 2. The bacterial proportions did not differ significantly between the caecum and the colon of the ALB rats. *Blautia producta* accounted for approximately 58% of the total bacteria in both the caecum and the colon, while *C. saccharogumia* accounted for 26% in the caecum and 23% in the colon. The proportion of *E. lenta* was 11% in the caecum and 14% in the colon, while *L. longoviformis* amounted to approximately 5% in both gut sections.

SDG concentrations in flaxseed and in the faeces of gnotobiotic rats

Before starting the *in vivo* experiment, we determined the SDG content in ground flaxseed and in the experimental

Table 2. Proportions of lignan-activating bacteria in the caecal and colonic contents of the rats associated with these four species; cells were enumerated by fluorescence microscopy

Species	Count (cells g ⁻¹ DM)	
	Caecum	Colon
<i>Clostridium saccharogumia</i>	3.39 × 10 ¹⁰ ± 1.17 × 10 ¹⁰	5.21 × 10 ¹⁰ ± 1.74 × 10 ¹⁰
<i>Blautia producta</i>	7.44 × 10 ¹⁰ ± 2.56 × 10 ¹⁰	1.31 × 10 ¹¹ ± 7.22 × 10 ¹⁰
<i>Eggerthella lenta</i>	1.47 × 10 ¹⁰ ± 4.04 × 10 ⁹	3.25 × 10 ¹⁰ ± 1.35 × 10 ¹⁰
<i>Lactonifactor longoviformis</i>	7.13 × 10 ⁹ ± 1.64 × 10 ⁹	1.10 × 10 ¹⁰ ± 2.70 × 10 ⁹

Values are means ± SD, *n* = 5.

diet. Because SDG in flaxseed is incorporated into a lignan macromolecule, we decided to cleave the ester bonds by alkaline hydrolysis, thereby releasing the SDG from macromolecules, as reported previously (Struijs, 2008). The SDG content in the ground flaxseed was $3.09 \pm 0.19 \mu\text{mol g}^{-1}$, which is in the lower range of SDG contents reported for flaxseed (Muir, 2006). Accordingly, the SDG content of the diet was $0.15 \pm 0.02 \mu\text{mol g}^{-1}$.

After 10 days on the flaxseed diet, all rats were transferred to metabolic cages. Faeces were collected for 48 h and analysed for SDG. Faeces of the ALB rats contained $0.29 \pm 0.09 \mu\text{mol SDG g}^{-1}$ dry matter (DM), while the faeces of germ-free rats contained $1.39 \pm 0.39 \mu\text{mol SDG g}^{-1}$ DM ($P \leq 0.01$). Significantly lower faecal concentrations of SDG in the ALB rats compared with the germ-free rats were the first indication that the microbial community in the ALB rats converted the dietary lignan SDG.

Levels of SDG and the metabolites SECO, ED and EL in caecal and colonic contents

After 48 h in metabolic cages, the rats were killed and their caecal and colonic contents were analysed for SDG and the metabolites thereof. The caecal contents of the ALB rats contained significantly lower SDG concentrations than those of the germ-free rats ($P \leq 0.001$; Table 3). The material collected from the colon was insufficient to determine the SDG concentrations. Caecal and colonic contents were also analysed for the unconjugated lignan metabolites

Table 3. Caecal concentrations of free and conjugated lignans in germ-free rats and rats associated with ALB

Lignan	Concentration ($\mu\text{mol g}^{-1}$ DM)	
	ALB rats	Germ-free rats
SDG	$0.52 \pm 0.07^{***}$	1.89 ± 0.15
SECO		
Free	BD*	BD*
Conjugated	0.41 ± 0.08	0.35 ± 0.11
ED		
Free	BD*	BD*
Conjugated	0.05 ± 0.01	BD [†]
EL		
Free	0.37 ± 0.12	BD*
Conjugated	0.58 ± 0.17	BD [†]

Free SDG was determined after alkaline hydrolysis to release it from the lignan macromolecule. Free SECO, ED and EL were determined without any treatment. Conjugated lignans were determined after treatment with β -glucuronidase/sulphatase.

Values are means \pm SD, $n = 5$; data are normally distributed (Kolmogorov–Smirnov test); significance was checked using an unpaired t -test.

***Value was significantly different from that of the germ-free rats ($P \leq 0.001$).

*Below the detection limit (BD) $< 5.0 \text{ nmol g}^{-1}$ DM.

[†]BD $< 6.5 \text{ nmol g}^{-1}$ DM.

SECO, ED and EL. Caecal contents were in addition examined for lignan conjugates. Free SECO was neither detected in the caecal and colonic contents of germ-free rats nor of ALB rats. After β -glucuronidase/sulphatase treatment of the caecal contents, the caecal SECO concentrations did not differ significantly between ALB rats and germ-free rats (Table 3). The presence of SECO in the germ-free rats may be explained as follows: (i) brushborder enzymes of the epithelium possibly deglycosylated SDG to SECO as reported for other phenols (Day *et al.*, 1998). In this case, host enzymes would catalyse the first step of the SDG activation and *C. saccharogumia* would not be required. (ii) The β -glucuronidase/sulphatase preparation used for the deconjugation of SECO might have had some deglycosylating activity, as it stems from *Helix pomatia*, which may contain traces of β -glucosidase (Robinson, 1956). However, based on *in vitro* experiments, we can exclude that the deglycosylation of SDG to SECO was due to hydrolysis in the upper part of the gastrointestinal tract (Clavel *et al.*, 2006a; Eeckhaut *et al.*, 2008).

Free ED was detected in the gut contents of neither the ALB rats nor the germ-free rats. Following deconjugation treatment, ED was detected in the caecal contents of the ALB rats, but not of the germ-free rats (Table 3). EL is the final metabolite formed during bacterial lignan transformation. EL was found in the caecal and colonic contents of the ALB rats. β -glucuronidase/sulphatase treatment of the caecal contents revealed the presence of conjugated EL in the ALB rats, while neither form of EL was detectable in the caecal or the colonic contents of the germ-free rats (Table 3). While 61% of the total caecal EL concentration of the ALB rats was glucuronidated or sulphated, 39% was unconjugated. The occurrence of ED and EL in the ALB rats, but not in the germ-free rats provides evidence that ED and EL were of bacterial origin. It may be concluded that the bacterial species *B. producta*, *E. lenta* and *L. longoviformis* catalysed *O*-demethylation, dehydroxylation and dehydrogenation to produce EL from SECO in the rat intestinal tract. The low concentration of ED in the gut contents, which we observed in our study, is in contrast to a study by Adlercreutz *et al.* (1995), who reported that faeces of Finnish women contained more ED than EL. The EL-producing *L. longoviformis* is one of the subdominant members of the human intestinal microbiota and, therefore, the dehydrogenation of ED to EL is probably the rate-limiting step in the conversion, at least in humans (Clavel *et al.*, 2006b). However, even though the concentration of *L. longoviformis* was lower than that of the other species of the defined bacterial community in the gut of the ALB rats, this species obviously catalysed the dehydrogenation reaction very effectively.

The detection of SECO, ED and EL after β -glucuronidase/sulphatase treatment of the caecal contents demonstrates that these lignans are preferentially present as glucuronides

or sulphates and that they undergo enterohepatic circulation. We were unable to distinguish between enterolignan glucuronides and sulphates, but it is known that conventional rats excrete biliary ED and EL mainly as glucuronides and only traces of lignan sulphates are formed (< 1%) (Axelson & Setchell, 1981).

Flaxseed also contains small amounts of the plant lignans matairesinol and pinoresinol (Meagher *et al.*, 1999), which can also be metabolized to ED and EL (Heinonen *et al.*, 2001). Because *E. lenta* is also able to reduce pinoresinol and laricresinol, it is likely that these plant lignans contributed to the enterolignan formation in the ALB rats.

Anaerobic *in vitro* formation of EL by pooled caecal samples

Pooled caecal contents collected from the ALB rats were examined for their ability to form the free lignan metabolites SECO, ED and EL *in vitro* from the lignans contained in the caecal material. SECO and ED were not detected in any of the samples after 0, 1, 2, 4 and 8 h of incubation. The starting concentration (0 h) of free EL in these samples was $0.58 \pm 0.10 \mu\text{mol g}^{-1} \text{DM}$. Within 2 h of incubation, the EL concentration reached $1.06 \pm 0.02 \mu\text{mol g}^{-1} \text{DM}$ (Fig. 1). The maximal *in vitro* EL formation rate of $7.52 \text{ nmol min}^{-1} \text{g}^{-1} \text{DM}$ was observed between 1 and 2 h after the start of the incubation, demonstrating the efficient interaction of the lignan-activating bacteria. The pooled caecal contents of germ-free rats did not produce any free lignans. The material of the ALB rats and the germ-free rats was too scarce to determine the SDG concentrations.

Lignan metabolites in the urine of gnotobiotic rats

Urine samples of ALB rats and germ-free rats were analysed for lignan metabolites to investigate their urinary excretion.

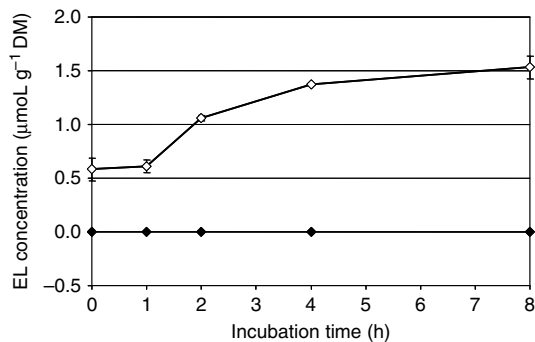


Fig. 1. Formation of unconjugated EL by pooled caecal contents of rats associated with lignan-activating bacteria (◇) and of germ-free rats (◆) under anaerobic conditions ($\text{N}_2/\text{CO}_2/\text{H}_2$, 80/10/10, v/v/v) at 37 °C. Values are means \pm SD, $n = 2$. DM, dry matter.

No lignans were observed in the urine of the germ-free rats. In contrast, we detected free and glucuronidated/sulphated EL (2.61 ± 3.23 and $16.3 \pm 12.9 \text{ nmol mL}^{-1}$, respectively) in the urine of ALB rats, while SECO and ED were not found in any form. The proportion of free lignans in the ALB rats (10.4%) was considerably higher than reported in previous studies for human and rat urine (0.3–1%) (Axelson & Setchell, 1981; Adlercreutz *et al.*, 1991). Over 48 h, the ALB rats excreted $340 \pm 226 \text{ nmol}$ of EL in the urine. Previous publications reported a higher urinary enterolignan excretion in rats. The urine of rats fed 5% flaxseed reached enterolignan concentrations of up to $2663 \pm 294 \text{ nmol}$ within 24 h (Jenab & Thompson, 1996; Thompson *et al.*, 1996). This difference is probably due to the fact that we used gnotobiotic rats associated with only four bacterial species, while previous researchers used conventional rats with a complex microbiota. The gnotobiotic animal model used in this study is an artificial system that does not take into account the influence of the other members of the gut microbial community. In addition, the microbial status influences the metabolism of the host as evident from considerable metabolic differences between germ-free and conventional rats (Hooper *et al.*, 1999, 2003). In particular, the expression of xenobiotic-metabolizing host enzymes depends on the microbial status of the rats (Meinl *et al.*, 2009).

In conclusion, we demonstrated for the first time the *in vivo* transformation of plant lignans by a defined bacterial community. By determining the maximal *in vitro* formation rate of EL in the rat caecal samples, we demonstrated the efficient interaction of the bacterial species involved in the transformation of lignans, particularly SDG. Our results also show that the metabolites arising from plant lignans undergo hepatic circulation and are excreted in the urine.

Acknowledgements

We are grateful to Prof. Peter Winterhalter from the Institute of Food Chemistry at the Technical University of Braunschweig for providing the SDG; Ines Grüner, Ute Lehmann, Anke Gühler, Sabine Schmidt for technical assistance; and Anastasia Matthies and Natalie Becker for helpful advice.

References

- Adlercreutz H, Fotsis T, Bannwart C, Wähälä K, Brunow G & Hase T (1991) Isotope dilution gas chromatographic-mass spectrometric method for the determination of lignans and isoflavonoids in human urine, including identification of genistein. *Clin Chim Acta* **199**: 263–278.
- Adlercreutz H, van der Wildt J, Kinzel J, Attalla H, Wähälä K, Mäkelä T, Hase T & Fotsis T (1995) Lignan and isoflavonoid

- conjugates in human urine. *J Steroid Biochem Mol Biol* **52**: 97–103.
- Axelsson M & Setchell KD (1981) The excretion of lignans in rats – evidence for an intestinal bacterial source for this new group of compounds. *FEBS Lett* **123**: 337–342.
- Ayres DC & Loike JD (1990) *Chemistry and Pharmacology of Natural Products. Lignans: Chemical, Biological and Clinical Properties*. Cambridge University Press, Cambridge.
- Blaut M & Clavel T (2007) Metabolic diversity of the intestinal microbiota: implications for health and disease. *J Nutr* **137**: 751S–755S.
- Bommareddy A, Arasada BL, Mathees DP & Dwivedi C (2006) Chemopreventive effects of dietary flaxseed on colon tumor development. *Nutr Cancer* **54**: 216–222.
- Bommareddy A, Zhang X, Schrader D, Kaushik RS, Zeman D, Mathees DP & Dwivedi C (2009) Effects of dietary flaxseed on intestinal tumorigenesis in Apc(Min) mouse. *Nutr Cancer* **61**: 276–283.
- Bryant MP (1972) Commentary on the Hungate technique for culture of anaerobic bacteria. *Am J Clin Nutr* **25**: 1324–1328.
- Clavel T, Henderson G, Alpert CA, Philippe C, Rigottier-Gois L, Doré J & Blaut M (2005) Intestinal bacterial communities that produce active estrogen-like compounds enterodiol and enterolactone in humans. *Appl Environ Microbiol* **71**: 6077–6085.
- Clavel T, Borrmann D, Braune A, Doré J & Blaut M (2006a) Occurrence and activity of human intestinal bacteria involved in the conversion of dietary lignans. *Anaerobe* **12**: 140–147.
- Clavel T, Doré J & Blaut M (2006b) Bioavailability of lignans in human subjects. *Nutr Res Rev* **19**: 187–196.
- Day AJ, DuPont MS, Ridley S, Rhodes M, Rhodes MJ, Morgan MR & Williamson G (1998) Deglycosylation of flavonoid and isoflavonoid glycosides by human small intestine and liver beta-glucosidase activity. *FEBS Lett* **436**: 71–75.
- Degenhardt A, Habben S & Winterhalter P (2002) Isolation of the lignan secoisolariciresinol diglucoside from flaxseed (*Linum usitatissimum* L.) by high-speed counter-current chromatography. *J Chromatogr A* **943**: 299–302.
- Demark-Wahnefried W, Polascik TJ, George SL *et al.* (2008) Flaxseed supplementation (not dietary fat restriction) reduces prostate cancer proliferation rates in men presurgery. *Cancer Epidem Biomar* **17**: 3577–3587.
- Eeckhaut E, Struijs K, Possemiers S, Vincken JP, Keukeleire DD & Verstraete W (2008) Metabolism of the lignan macromolecule into enterolignans in the gastrointestinal lumen as determined in the simulator of the human intestinal microbial ecosystem. *J Agr Food Chem* **56**: 4806–4812.
- Harmsen HJ, Gibson GR, Elfferich P, Raangs GC, Wildeboer-Veloo AC, Argaz A, Roberfroid MB & Welling GW (2000) Comparison of viable cell counts and fluorescence *in situ* hybridization using specific rRNA-based probes for the quantification of human fecal bacteria. *FEMS Microbiol Lett* **183**: 125–129.
- Heinonen S, Nurmi T, Liukkonen K, Poutanen K, Wähälä K, Deyama T, Nishibe S & Adlercreutz H (2001) *In vitro* metabolism of plant lignans: new precursors of mammalian lignans enterolactone and enterodiol. *J Agr Food Chem* **49**: 3178–3186.
- Hooper LV, Xu J, Falk PG, Midtvedt T & Gordon JI (1999) A molecular sensor that allows a gut commensal to control its nutrient foundation in a competitive ecosystem. *P Natl Acad Sci USA* **96**: 9833–9838.
- Hooper LV, Stappenbeck TS, Hong CV & Gordon JI (2003) Angiogenins: a new class of microbicidal proteins involved in innate immunity. *Nat Immunol* **4**: 269–273.
- Hungate RE (1969) A roll tube method for cultivation of strict anaerobes. *Methods Microbiol* **3**: 117–132.
- Jenab M & Thompson LU (1996) The influence of flaxseed and lignans on colon carcinogenesis and beta-glucuronidase activity. *Carcinogenesis* **17**: 1343–1348.
- Jin JS, Zhao YF, Nakamura N, Akao T, Kakiuchi N, Min BS & Hattori M (2007) Enantioselective dehydroxylation of enterodiol and enterolactone precursors by human intestinal bacteria. *Biol Pharm Bull* **30**: 2113–2119.
- Lambert N, Kroon PA, Faulds CB, Plumb GW, McLauchlan WR, Day AJ & Williamson G (1999) Purification of cytosolic beta-glucosidase from pig liver and its reactivity towards flavonoid glycosides. *Biochim Biophys Acta* **1435**: 110–116.
- Lin X, Gingrich JR, Bao W, Li J, Haroon ZA & Demark-Wahnefried W (2002) Effect of flaxseed supplementation on prostatic carcinoma in transgenic mice. *Urology* **60**: 919–924.
- Meagher LP, Beecher GR, Flanagan VP & Li BW (1999) Isolation and characterization of the lignans, isolariciresinol and pinoresinol, in flaxseed meal. *J Agr Food Chem* **47**: 3173–3180.
- Meinl W, Sczesny S, Brigelius-Flohé R, Blaut M & Glatt H (2009) Impact of gut microbiota on intestinal and hepatic levels of phase 2 xenobiotic-metabolizing enzymes in the rat. *Drug Metab Dispos* **37**: 1179–1186.
- Milder IE, Feskens EJ, Arts IC, Bueno de Mesquita HB, Hollman PC & Kromhout D (2005) Intake of the plant lignans secoisolariciresinol, matairesinol, lariciresinol, and pinoresinol in Dutch men and women. *J Nutr* **135**: 1202–1207.
- Muir AD (2006) Flax lignans – analytical methods and how they influence our understanding of biological activity. *J AOAC Int* **89**: 1147–1157.
- Németh K, Plumb GW, Berrin JG, Juge N, Jacob R, Naim HY, Williamson G, Swallow DM & Kroon PA (2003) Deglycosylation by small intestinal epithelial cell beta-glucosidases is a critical step in the absorption and metabolism of dietary flavonoid glycosides in humans. *Eur J Nutr* **42**: 29–42.
- Pan A, Sun J & Chen Y (2007) Effects of a flaxseed-derived lignan supplement in type 2 diabetic patients: a randomized, double-blind, cross-over trial. *PLoS One* **2**: e1148.
- Prasad K (1999) Reduction of serum cholesterol and hypercholesterolemic atherosclerosis in rabbits by secoisolariciresinol diglucoside isolated from flaxseed. *Circulation* **99**: 1355–1362.

PAPER 11

Lignan transformation by gut bacteria lowers tumor burden in a gnotobiotic rat model of breast cancer

Hoda B.Mabrok^{1,2}, Robert Klopffleisch³,
Kadry Z.Ghanem², Thomas Clavel⁴, Michael Blaut¹ and
Gunnar Loh¹

¹Department of Gastrointestinal Microbiology, German Institute of Human Nutrition Potsdam-Rehbruecke, D-14558 Nuthetal, Germany, ²Department of Food Science and Nutrition, National Research Center, 12311 Cairo, Egypt, ³Institute of Veterinary Pathology, Free University Berlin, D-14163 Berlin, Germany and ⁴ZIEL—Research Center for Nutrition and Food Sciences, Young Research Group Intestinal Microbiome, TU München, D-85350 Freising-Weihenstephan, Germany

*To whom correspondence should be addressed. Tel: +49 33 20 08 83 18;
Fax: +49 33 20 08 84 07;
Email: loh@dife.de

High dietary lignan exposure is implicated in a reduced breast cancer risk in women. The bacterial transformation of plant lignans to enterolignans is thought to be essential for this effect. To provide evidence for this assumption, gnotobiotic rats were colonized with the lignan-converting bacteria *Clostridium saccharogumia*, *Eggerthella lenta*, *Blautia producta* and *Lactonifactor longoviformis* (LCC rats). Germ-free rats were used as the control. All animals were fed a lignan-rich flaxseed diet and breast cancer was induced with 7,12-dimethylbenz(a)anthracene. The lignan secoisolariciresinol diglucoside was converted into the enterolignans enterodiols and enterolactone in the LCC but not in the germ-free rats. This transformation did not influence cancer incidence at the end of the 13 weeks experimental period but significantly decreased tumor numbers per tumor-bearing rat, tumor size, tumor cell proliferation and increased tumor cell apoptosis in LCC rats. No differences between LCC and control rats were observed in the expression of the genes encoding the estrogen receptors (ERs) α , ER β and G-coupled protein 30. The same was true for IGF-1 and EGFR involved in tumor growth. The activity of selected enzymes involved in the degradation of oxidants in plasma and liver was significantly increased in the LCC rats. However, plasma and liver concentrations of reduced glutathione and malondialdehyde, considered as oxidative stress markers, did not differ between the groups. In conclusion, our results show that the bacterial conversion of plant lignans to enterolignans beneficially influences their anticancer effects.

Introduction

Breast cancer is the most commonly diagnosed cancer and the leading cause of cancer death in women worldwide (1). Since high circulating estrogen levels have been considered as a risk factor of breast cancer (2), dietary interventions that modulate the tumor-promoting estrogen effects may be effective in breast cancer prevention. Proposed dietary interventions include a high consumption of lignan-rich food because lignans belong to the non-nutritive plant compounds with estrogenic and/or anti-estrogenic properties (3). The majority of lignans is taken up with whole grain cereals, vegetables and fruits but flaxseed is one of the richest sources of the lignan secoisolariciresinol diglucoside, SDG (4).

Abbreviations: CAT, catalase; DMBA, 7,12-dimethylbenz(a)anthracene; ED, enterodiols; EGFR, epidermal growth factor receptor; EL, enterolactone; ER, estrogen receptor; GPR30, G-coupled protein 30; GSH, glutathione; GST, glutathione-S-transferase; HPLC, high-performance liquid chromatography; IGF-1, insulin-like growth factor 1; MDA, malondialdehyde; PCR, polymerase chain reaction; SCFA, short-chain fatty acid; SDG, secoisolariciresinol diglucoside; SECO, secoisolariciresinol; SOD, superoxide dismutase.

In chemically induced animal models of breast cancer, flaxseed feeding reduces the incidence, number and growth of tumors at the initiation, promotion and progression stages of carcinogenesis (5,6). Similar effects were observed when SDG was applied to chemically induced or xenograph animal models, suggesting that the observed effects largely depend on the SDG content of the flaxseed (7,8).

Intestinal bacteria are capable of converting plant lignans into enterolignans. The transformation of SDG includes the deglycosylation to secoisolariciresinol (SECO) followed by the demethylation and dehydroxylation of SECO to enterodiols (ED). Finally, ED is converted to enterolactone (EL) by dehydrogenation (9). It has been concluded from epidemiologic and experimental studies that the products of bacterial SDG transformation, ED and EL, are the bioactive compounds (4). Women with high EL serum levels and high urinary EL excretion have a significantly reduced breast cancer risk (10,11). In addition, pure ED and EL inhibit breast tumor growth in a mouse cancer model (12). However, the essential role of bacterial transformation in the gut for the lignan anticancer effects has so far not been demonstrated *in vivo*.

In previous studies, we demonstrated that a consortium consisting of the commensal gut bacteria *Clostridium saccharogumia* (O-deglycosylation), *Blautia producta* (O-demethylation), *Eggerthella lenta* (dehydroxylation) and *Lactonifactor longoviformis* (dehydrogenation) is capable of forming ED and EL from SDG under *in vitro* conditions and in rats colonized exclusively with these four bacterial species (13,14). We took advantage of this gnotobiotic animal model to investigate the role of bacterial lignan transformation in breast cancer formation and selected cancer-associated parameters in a 7,12-dimethylbenz(a)anthracene (DMBA)-induced cancer model. We compared the effects of lignan feeding on breast cancer formation in germ-free rats and in rats colonized exclusively with lignan-transforming bacteria to clarify whether the bacterial activation of SDG to ED and EL is really crucial for the cancer-preventing effects of dietary lignans.

Materials and methods

Bacterial strains and culture conditions

The lignan-converting bacteria *C.saccharogumia* DSM17460^T, *B.producta* DSM3507, *E.lenta* DSM2243^T and *L.longoviformis* DSM17459^T were cultured anaerobically at 37°C in Brain Heart Infusion Broth (Roth, Karlsruhe, Germany) supplemented with 5 g/l yeast extract and 5 mg/l hemin (Sigma-Aldrich, Taufkirchen, Germany). Purity of the cultures was checked by inspecting the colony morphology after anaerobic growth on respective agar plates and the cell morphology after gram staining.

Animal experiment

Three week old female germ-free Sprague Dawley rats were randomly assigned to one of the study groups ($n = 10$, each). Animals were housed in Trexler-type plastic film isolators under controlled housing conditions (20°C \pm 2°C, 55 \pm 10% air humidity, 12 h light/dark cycle). All diets and the drinking water were sterilized by gamma irradiation (50 kGy) and autoclaving, respectively. Before dietary intervention, animals were fed a standard chow (Diet 1314, Altromin, Lage, Germany). A 300 μ l inoculum containing 10⁸ cells of each bacterial species was intragastrically applied to each rat of one of the animal groups (LCC rats). The rats in the other group received growth medium as a vehicle control. Fecal samples were collected throughout the study in order to confirm the microbial status of the animals. We prepared a flaxseed-rich diet composed of 58% wheat starch, 20% casein, 5% ground flaxseed, 5% sunflower oil, 5% cellulose, 5% mineral mixture and 2% vitamin mixture. This diet contained 0.34 g/kg SDG as determined by high-performance liquid chromatography (HPLC) (see below). Two weeks after association, the rats were switched from the chow to this experimental diet. All animals were fed from one single batch to avoid batch-to-batch variability in the dietary SDG content. Breast cancer was induced in all animals with a single oral dose of 25 mg DMBA (Sigma-Aldrich) diluted in corn oil 2 weeks after diet switch. Body

weight and the development of palpable tumors were monitored weekly. Thirteen weeks after DMBA application, animals were kept in metabolic cages for 24 h to quantitatively collect feces and urine. Subsequently, the animals (now 20 weeks of age) were removed from the isolators and blood from the retrobulbar venous plexus was sampled under anesthesia. Plasma and serum were prepared and stored at -20°C until further analysis. After killing of the animals, breast tumors were removed and number of tumors per animal, tumor weight and size were determined. The liver was frozen in liquid N_2 and stored at -80°C until further analysis. Representative parts of the tumors were fixed in 10% neutral buffered formalin and prepared for histology and immunohistochemistry. The remaining tumor material was frozen in liquid N_2 and stored at -80°C for later RNA extraction. Colonic and cecal contents were used for microbial examination and the remaining material was freeze-dried and stored at 4°C until analysis. The experimental protocol was approved by the local animal welfare committee (approval no. 23-2347-8-16-2008).

Intestinal colonization status and short-chain fatty acid determination

The germ-free state of the control rats was confirmed throughout the complete study by microscopic inspection of gram-stained fecal material and incubation of feces in complex growth media at 37°C . The colonization of the LCC rats by the four lignan-converting species was checked by fluorescent *in situ* hybridization using fecal material and intestinal contents. Fixation of bacterial cells and the fluorescent *in situ* hybridization procedure were performed as described earlier (14) using species-specific 16S ribosomal RNA targeted 5'-Cy3-labeled oligonucleotide probes (*C.saccharogumia*: S-S-Csac-0067-a-A-20; *B.producta*: S*-ProCo-1264-a-A-23; *E.lenta*: S*-Ato-0291-a-A-17; *L.longoviformis*: S-S-Llong-0831-a-A-20). Bacterial cells were counted with a fluorescence microscope and bacterial cell numbers were calculated as \log_{10} /g dry weight. Concentrations of short-chain fatty acids (SCFA) in cecal and colonic sample material were measured as described elsewhere (15). Briefly, SCFAs were extracted and sample material (1 μl) was injected into a gas chromatograph (Hewlett-Packard, Waldbronn, Germany). The chromatograph was equipped with an HP-FFAP capillary column (30 m \times 0.53 mm inner diameter, 1 μm film thickness) and helium (1 ml/min) was used as the carrier gas.

Lignan determination

Lignan extraction was performed as described elsewhere (14) with minor modifications. Briefly, sample material (100 mg) was defatted with *n*-hexane. SDG was extracted for 3 h at 55°C and subsequently overnight at room temperature using an aqueous methanol solution (70%). After centrifugation, the supernatants were collected and the pellets were washed twice. The SDG-containing extracts were combined, methanol was evaporated and the residues were lyophilized. The lyophilisates were dissolved in 1 M NaOH for 3 h at 50°C , neutralized with HCl, freeze-dried, resuspended in aqueous methanol solution (70%) and subsequently subjected to HPLC analysis. In order to extract total SECO, ED and EL, feces and gut contents (100 mg) were mixed with sodium acetate buffer (0.1 M, pH 5) containing 1000 U of a β -glucuronidase/sulfatase preparation (type HP-2; Sigma-Aldrich). The samples were incubated overnight at 37°C , followed by an extraction with diethyl ether. After centrifugation, the upper lignan-containing diethyl ether phase was collected and the pellets were washed twice. The supernatants obtained during the washing steps were pooled and the diethyl ether was evaporated. The residues were dissolved in 70% aqueous methanol solution and analyzed by HPLC. Urine samples were thawed and centrifuged at 1000g for 15 min, 4°C . The supernatants were filtered (0.22 μm) and the filtrate (200 μl) was mixed with sodium acetate buffer (0.10 M, pH 5) containing 300 U of the β -glucuronidase/sulfatase preparation. After 16 h of incubation at 37°C with the enzyme preparation, lignans were extracted as described above. Lignans were quantified with an HPLC system equipped with a UV/Vis diode array detector as described earlier (14). Peak identification was based on the retention time and UV spectra of reference compounds and quantification of lignans was performed using calibration curves generated with the standard lignans SDG, SECO, ED and EL (Sigma-Aldrich).

Immunohistochemistry and detection of apoptosis

Ki-67, active caspase-3 and the estrogen receptor (ER) status of the tumors were analyzed immunohistochemically using 5 μm tumor sections. The primary antibodies applied were MIB-5 (Dianova, Hamburg, Germany) diluted 1:100 in Tris-buffered saline (50 mM, pH 7.6) for Ki-67, Asp175 (Cell Signaling, Beverly, MA) diluted 1:200 for cleaved caspase-3 and EI629C01 (DCS, Hamburg, Germany) diluted 1:400 for ER. After blocking non-specific antigens, samples were incubated overnight with the respective antibodies followed by incubation with biotinylated goat anti-rabbit immunoglobulin G as the secondary antibody. Subsequently, samples were treated with avidin and biotinylated horseradish peroxidase macromolecular complexes (Vector Laboratories, Burlingame, CA). Diaminobenzidine tetrahydrochloride (Sigma-Aldrich) was used as chromogen and slides were counterstained with hematoxylin.

The *in situ* terminal deoxynucleotidyl transferase-mediated nick end-labeling assay was performed with the TACS.XL-DAB *in situ* apoptosis detection kit (Trivigen, Gaithersburg, MD). The relative proportion of Ki-67-positive and negative cells (Ki-67 labeling index) was taken as an indicator for tumor cell proliferation. Cells detected in the active caspase-3 and the transferase-mediated nick end-labeling assay were counted as apoptotic cells per square millimeter. The ER status of the tumor cells was evaluated using the Allred score.

Quantitative real-time polymerase chain reaction

The relative expression of the genes encoding the ERs α (ER α), β (ER β), the G-coupled protein 30 (GPR30), the epidermal growth factor receptor (EGFR) and the insulin-like growth factor 1 (IGF-1) in breast tumors was determined by quantitative real-time polymerase chain reaction (PCR). Therefore, RNA was extracted from tumor tissue using the RNasy Mini kit (Qiagen, Hilden, Germany). One microgram of RNA was reverse transcribed to single-stranded complementary DNA with the RevertAid[®] H Minus First Strand complementary DNA Synthesis Kit (Fermentas, St Leon-Rot, Germany). Real-time PCR was performed with the Stratagene's Mx3005P QPCR system (Agilent Technologies, Boblingen, Germany). The real-time-PCR mix (25 μl) contained the template DNA, the QuantiFastTMSYBR Green PCR master mix (Qiagen) and the respective primer pairs. The primer pairs used were as follows: ER α -for (5'-GCA TGA TGA AAG GCG GGA TAC GA-3') and ER α -rev (5'-AAA GGT TGG CAG CTC TCA TGT CTC-3'), ER β -for (5'-TGG TCT GGG TGA TTG CGA AGA G-3') and ER β -rev (5'-ATG CCC TTG TTA CTG ATG TGC C-3'), GPR30-for (5'-CGA GGT GTT CAA CCT GGA CGA-3') and GPR30-rev (5'-GGC AAA GCA GAA GCA GGC CT-3'), EGFR-for (5'-TGC CCA CTA TGT TGA TGG TCC C-3') and EGFR-rev (5'-GCC CAG CAC ATC CAT AGG TAC AG-3'), and IGF-1-for (5'-AAG ACT CAG AAG TCC CAG CCC-3') and IGF-1-rev (5'-GGT CTT GTT TCC TGC ACT TCC T-3'). Relative expression levels of the target genes were calculated with the relative standard curve method after normalizing the target gene expression to the expression of the house-keeping gene encoding glyceraldehyde 3-phosphate dehydrogenase. The expression of the latter was measured with the primers glyceraldehyde 3-phosphate dehydrogenase-for (5'-CAA GGT CAT CCA TGA CAA CTT TG-3') and glyceraldehyde 3-phosphate dehydrogenase-rev (5'-GTC CAC CAC CCT GTT GCT GTA G-3').

Selected plasma and liver enzyme activities and serum estradiol determination

The specific activities of selected enzymes in the plasma and in liver homogenates were measured using standard procedures. In brief, catalase (CAT) activity was determined as H_2O_2 consumption concluded from the decrease in absorbance at 240 nm (16). Superoxide dismutase (SOD) activity was assessed by the nitro blue tetrazolium reduction method (17) and glutathione-S-transferase (GST) activity was measured using 1-chloro-2,4-dinitrobenzene (18). Reduced glutathione (GSH) and malondialdehyde (MDA) were determined according to Ellman (19) and Mihara and Uchiyama (20), respectively. Total protein was quantified according to Bradford (21). Serum 17 β -estradiol concentrations were measured with the Estradiol EIA Kit (Cayman Chemical, Ann Arbor, MI) according to the manufacturer's specifications.

Statistical analysis

Statistical analyses were conducted with SPSS 14.0 (IBM). Values were tested for normal distribution with the Kolmogorov-Smirnov test. Depending on data distribution, the two-tailed Student's *t*-test or the Mann-Whitney test was used. Normally distributed values are expressed as means with standard error. Differences were considered significant at $P \leq 0.05$.

Results

Bacterial numbers and SCFA concentrations in intestinal samples

Successful establishment of the lignan-converting consortium in the intestine of LCC rats was the prerequisite for conducting the study. Therefore, cell numbers of each member of the selected strains were determined before and during the dietary intervention phase and at the end of the study. Fluorescent *in situ* hybridization analysis using fecal material confirmed the presence of all four consortium members in the intestine throughout the complete study period (data not shown). At the end of the study, *C.saccharogumia* was detected at $\log 10.03 \pm 0.04$ cells/g dry weight in the cecum and $\log 10.20 \pm 0.02$ cells/g dry matter (DM) in the colon of LCC rats. Numbers for *B.producta* were $\log 10.27 \pm 0.03$ and $\log 10.48 \pm 0.03$ cells/g DM in the cecum and colon, respectively. *E.lenta* was detected at $\log 9.60 \pm 0.03$ cells/g DM in the colon and $\log 9.99 \pm 0.03$ cells/g DM in the cecum. Lowest

numbers were determined for *L.longoviformis* with log 9.07 ± 0.06 cells/g DM in the colon and log 9.05 ± 0.07 cells/g DM in the cecum. Direct microscopic inspection and anaerobic and aerobic cultivation of fecal and intestinal sample material confirmed the germ-free status of the control rats throughout and at the end of the animal experiment, respectively.

SCFA concentrations in cecal and colonic sample material were measured as marker for bacterial metabolism. Cecal acetate concentrations were 40.24 ± 5.20 μmol and 43.60 ± 8.61 $\mu\text{mol/g DM}$ in associated and germ-free rats, respectively. Concentrations in the colon were 16.27 ± 75 μmol in the associated rats and 26.78 ± 4.53 $\mu\text{mol/g DM}$ in the germ-free rats. Propionate concentrations were below 0.7 μmol and butyrate concentrations were ~ 0.1 $\mu\text{mol/g DM}$ in all samples.

Lignan concentrations in intestinal, fecal and urine sample materials
 Since we hypothesized that the conversion of lignans by gut bacteria influences their effects on breast cancer development, we quantified SDG in cecal and fecal sample material. SECO, ED and EL were determined in cecal and colonic material, in feces and in urine. Cecal SDG concentrations were significantly lower in LCC than in germ-free rats (1.47 ± 0.17 $\mu\text{mol/g DM}$ versus 5.22 ± 0.52 $\mu\text{mol/g DM}$, $P < 0.0001$) and fecal SDG excretion was significantly higher in germ-free rats than in LCC rats (2.58 ± 0.24 versus 0.81 ± 0.07 $\mu\text{mol/g DM}$, $P < 0.0001$). SECO was detected in gut contents and feces from both LCC and germ-free rats (Table I). However, concentrations were significantly higher in the LCC rats than in the germ-free animals. ED and EL were detected exclusively in gut contents and feces of the LCC rats but ED was only detected in cecal samples. In contrast, EL was found in all samples analyzed. No urinary lignan excretion was observed for the germ-free rats. The LCC rats but not the germ-free rats excreted both ED and EL in the urine. The concentration of the latter was significantly higher ($P < 0.0001$) than that of the former.

Animal health status

Breast cancer induction with one single oral application of DMBA resulted in weight loss and/or growth retardation of the juvenile animals. Because of severe body weight loss, one LCC rat was killed in this phase for ethical reasons. All the remaining animals recovered completely and did not differ in body weight gain during the remaining experimental phase (data not shown). There was no significant difference between the LCC and the germ-free group in the latency

Table I. Lignan concentrations in intestinal, fecal ($\mu\text{mol/g DM}$) and urine sample ($\mu\text{mol/24h}$ urine excretion) material obtained from LCC ($n = 9$) and germ-free rats ($n = 10$)

	Germ-free rats	LCC rats
Lignans		
Cecum		
Total SECO	0.268 ± 0.12	$0.512 \pm 0.05^{**}$
Total ED	Not detected	0.134 ± 0.04
Total EL	Not detected	1.364 ± 0.44
Colon		
Total SECO	0.268 ± 0.12	$0.438 \pm 0.05^{**}$
Total ED	Not detected	Not detected
Total EL	Not detected	0.469 ± 0.07
Feces		
Total SECO	0.161 ± 0.03	0.187 ± 0.02
Total ED	Not detected	Not detected
Total EL	Not detected	0.409 ± 0.047
Urine		
Total SECO	Not detected	Not detected
Total ED	Not detected	0.204 ± 0.03
Total EL	Not detected	1.792 ± 0.298

Significance of differences between the animal groups is indicated (** $P \leq 0.01$).

period until the first tumors were palpable (9.5 ± 0.50 and 8.0 ± 0.82 weeks, respectively) or in total tumor incidence (Table II). However, the number of tumors per tumor-bearing rat was lower for the LCC than for the germ-free animals ($P = 0.049$) and the total number of tumors observed in the LCC group was reduced by 40% ($P = 0.037$) at the end of the animal experiment. Mean tumor size and weight were $\sim 50\%$ lower in the LCC rats but only differences in tumor size were statistically significant ($P = 0.036$). Results from the serum estradiol measurements did not differ between the animals (33.65 ± 1.70 and 34.44 ± 2.77 pg/ml , respectively).

Histological and immunohistochemical tumor phenotypes and ER gene expression

Histological examination revealed that all tumors analyzed were moderately differentiated tubulopapillary adenocarcinomas with rare areas of solid growth. They were well circumscribed with no evidence of invasive growth into the surrounding connective tissue or invasion into adjacent vessels. Tumor cells were moderately pleomorphic and anisokaryotic with an average of three mitotic figures per microscopic field. No differences in the ER status scores were observed between the tumors from LCC (4.20 ± 0.19) and germ-free rats (4.29 ± 0.13). A $>50\%$ lower Ki-67 labeling index indicated a lower tumor cell proliferation rate in the LCC rats ($P < 0.0001$) than in the germ-free controls (Figure 1A). In addition, the number of apoptotic tumor cells was significantly higher ($P = 0.038$) in LCC rats than germ-free rats (Figure 1B). The messenger RNA expression of the ER genes *ER α* , *ER β* and *GPR30* and of the cell growth-associated genes *IGF-1* and *EGFR* was slightly lower in the tumor tissue obtained from LCC rats. However, differences did not reach statistical significance (data not shown).

Liver and plasma antioxidant enzyme activities

To address possible effects of bacterial lignan transformation on the oxidative status of the rats, we determined the specific activity of CAT, SOD and GST in liver homogenates and in plasma samples. In addition, we measured GSH and MDA concentrations, which are considered as oxidative stress markers. The activities of CAT, SOD and GST in liver and plasma were significantly higher in LCC than in germ-free rats (Table III). In contrast, no significant differences between the two groups in liver and plasma MDA and GSH concentrations were observed.

Discussion

Several epidemiological studies indicate that a high dietary lignan intake might be protective against breast cancer (22,23) but other studies do not support this association (24,25). The heterogeneity of study groups with respect to age, dietary lignan exposure, breast cancer subtypes and genetic factors have been proposed to be responsible for these discrepancies (26). Differences in intestinal microbiota composition might be an additional factor that influences the outcome of such studies since the bacterial conversion to enterolignans is thought to be important for the health effects of lignans. This notion

Table II. Tumor incidence, tumor quantity, tumor size and tumor weight in LCC ($n = 9$) and germ-free control rats ($n = 10$)

	Germ-free rats	LCC rats
No. of rats with tumors	7	7
No. of tumors per group	45^*	18
No. of tumors per tumor-bearing rat	$6.57 \pm 0.20^*$	2.57 ± 0.11
No. of tumor per No. of rats in group	$4.50 \pm 0.13^{**}$	0.57 ± 0.02
Mean tumor size (cm^3)	$0.97 \pm 0.28^*$	0.47 ± 0.18
Mean tumor weight (g)	1.09 ± 0.46	0.52 ± 0.24

Significance of differences between the animal groups is indicated (* $P \leq 0.05$, ** $P \leq 0.01$).



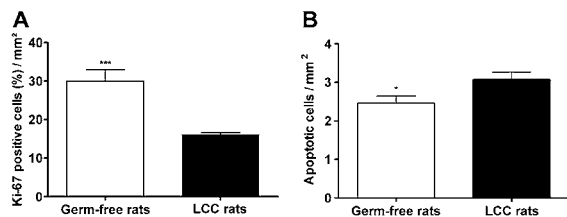


Fig. 1. Effect of bacterial lignan conversion on breast cancer cell proliferation (percentage of Ki-67-positive tumor cells per square millimeter tumor tissue) (A) and apoptosis (apoptotic cells per square millimeter tumor tissue). (B) Significance of differences between the animal groups is indicated (* $P < 0.05$, ** $P \leq 0.01$).

Table III. Selected enzyme activities and concentrations of reduced GSH and MDA in LCC ($n = 9$) and germ-free rats ($n = 10$)

	Germ-free rats	LCC rats
Liver		
CAT ^a	39.37 ± 2.19**	50.65 ± 3.08
SOD ^b	2.04 ± 0.14*	2.63 ± 0.17
GST ^c	0.57 ± 0.05***	1.25 ± 0.14
Reduced GSH ^d	85.87 ± 4.64	100.84 ± 9.32
MDA ^e	0.27 ± 0.05	0.21 ± 0.02
Plasma		
CAT ^f	0.92 ± 0.13**	1.52 ± 0.14
SOD ^g	39.27 ± 3.67*	51.66 ± 2.52
GST ^h	1.60 ± 0.32**	3.70 ± 0.65
Reduced GSH ⁱ	0.26 ± 0.02	0.30 ± 0.02
MDA ^j	3.24 ± 0.10	3.05 ± 0.16

Significance of differences between the animal groups is indicated (* $P \leq 0.05$, ** $P \leq 0.01$, *** $P \leq 0.001$).

^aμmol H₂O₂ consumed/min/(mg protein).

^bUnits/mg protein.

^cUnits/mg protein.

^dμmol GSH utilized/mg protein.

^enmol MDA produced/mg protein.

^fμmol H₂O₂ consumed/min/ml.

^gUnit/ml.

^hUnit/l.

ⁱmmol/l.

^jnmol/ml.

is supported by the fact that the occurrence of lignan-converting gut bacteria in human study subjects may differ (13). However, whether the bacterial conversion of the plant lignans to the enterolignans is a prerequisite for their health-promoting effects has not yet been demonstrated *in vivo*. We therefore colonized rats with a lignan-converting bacterial consortium, fed these animals a lignan-rich diet and chemically induced breast cancer. Effects of lignan feeding in this model were compared with those in identically treated germ-free rats.

All bacteria of the consortium successfully colonized the intestine of the LCC rats and enterolignans were produced from SDG in the LCC but not in the germ-free rats. These findings, and also the presence of SECO in germ-free animals, are in agreement with previous observations in this model (14). Fecal EL excretion by LCC rats was comparable with concentrations in premenopausal women (27). In these women but not in our experimental animals, fecal excretion of ED was observed. We therefore conclude that the conversion of ED to EL by *L.longoviformis* was very efficient under our experimental conditions. Urinary ED and EL excretion, indicative of their bioavailability, was comparable with conventionally colonized rats (5) and to healthy humans subjected to a single dose of SDG (28).

Bacterial lignan transformation did not influence tumor incidence in our model but significantly lowered the number of tumors per tumor-bearing animal and the tumor size. These results are in line

with findings in a DMBA rat model treated with EL (29) and with the plant lignan lariciresinol, which is also converted by gut bacteria to ED and EL (30). We concluded from the Ki-67 index and the transferase-mediated nick end-labeling assay that the reduced tumor growth in LCC rats resulted from a lower proliferation in conjunction with a higher apoptotic rate of the tumor cells. Such anti-proliferative and pro-apoptotic effects of ED and EL have been demonstrated previously in human breast cancer-derived cell cultures (31). In addition, an increased tumor cell apoptosis was observed in an SDG-treated mouse model for breast cancer (30) and a decreased Ki-67 index was reported for hyperplastic breast tissue obtained from SDG-treated women (32).

The mechanisms possibly involved in the protective role of lignans in cancer development include anti-angiogenic, pro-apoptotic, anti-estrogenic and antioxidant mechanisms (33). To study the effect of bacterial lignan transformation on the latter two mechanisms, we compared the serum estrogen levels and the relative expression of estrogen-sensitive genes and genes involved in tumor cell growth. In addition, the oxidative stress of the animals was addressed by measuring the activity of enzymes involved in the breakdown of oxidants and of selected markers for oxidative stress in liver homogenates and in the plasma.

We did not observe any differences between the study groups in circulating estrogen concentrations and only minor differences in the expression of the estrogen-sensitive genes *ERα*, *ERβ* and *GPR30*. In addition, no significant changes in the expression of *EGFR* and *IGF-1* were detected. In contrast to our findings, feeding an SDG-rich diet (1 g/kg) or a 10% flaxseed diet has been reported to influence the expression of *ERα* and *ERβ* in an athymic ovariectomized mouse model for breast cancer (34,35). Since the ER expression in our animals was not corrected for estrogen cycling, this discrepancy might be explained by the constant low levels of circulating estrogen concentrations in these mice. A higher amount of dietary SDG might also be responsible for the observed differences because our experimental diet contained only 5% flaxseed or 0.34 g SDG/kg of diet. The fact that EL exerts dose-dependent effects on *ERα* and *ERβ* expression in cultured cancer cells (36) supports the assumption that the lignan content in our diet was too low to influence the ER expression. This explanation might also be valid for missing effects of lignan transformation on *EGFR* and *IGF-1* expression. Reduced expression of these genes was reported in mouse models for breast cancer fed a diet containing 0.1% SDG or 10% flaxseed but no effects were observed when a 5% flaxseed diet was used (35,37,38). Taken together, our study results do not support an estrogen-dependent mechanism after feeding a 5% flaxseed diet.

To study potential effects of lignans on enzyme systems involved in the degradation of oxidants, we measured the specific activities of GST, SOD and CAT in liver homogenates and in the plasma of LCC and germ-free rats. GSH and MDA were used as markers for oxidative stress in these compartments. Compared with the germ-free rats, LCC rats displayed higher GST, SOD and CAT activities in liver and plasma suggesting a higher capacity to diminish the concentration of oxidants. However, we found no indication for a protective effect of the increased activities of these enzymes: both GSH and MDA concentrations were similar in experimental and control rats. Thus, it may be speculated that even though the enterolignans enhanced the activity of antioxidant enzymes, they did not reduce the systemic oxidative burden. A reduction of oxidative stress by radical scavenging in response to lignan treatment has been demonstrated in cell culture experiments (39–41). In addition and in contrast to our results, short-term feeding of a 10% flaxseed diet or equivalent amounts of SDG to healthy rats did not change hepatic activities of enzymes involved in oxidant breakdown but the direct antioxidant activity of the lignans was proposed to be responsible for beneficial effects (42). Further studies are necessary to finally clarify how the antioxidant properties of enterolignans are brought about and whether such mechanisms are indeed involved in their protective effects against breast cancer.

We cannot completely rule out that bacterial factors other than the transformation of lignans have been involved in the observed effects

of flaxseed feeding in our animal model. For instance, SCFA and especially butyrate mainly produced from indigestible carbohydrates have the potential to reduce cell growth and to promote apoptosis in colorectal tumors (43) and findings in human cell lines implicate that SCFA might also exert beneficial effects in breast cancer (44). However, we did not find differences in cecal and colonic SCFA concentrations between the associated and the germ-free rats. In addition, the SCFA concentrations in our experimental animals were much lower than reported for conventional rats and for rats that were colonized with a limited number of dominant gut bacteria and fed comparable purified diets (15,45). Thus, it is not very likely that bacterial SCFA production had any influence on tumor development in our experimental animals.

In summary, our results are not in favor of an estrogen-dependent mechanism as an explanation for the protective effects of enterolignans observed under our experimental conditions. The increased activity of oxidant-degrading enzyme systems in response to enterolignans did not result in a decrease of oxidative stress markers in liver and plasma. We therefore conclude that the bacterial transformation of flaxseed-derived lignans is the prerequisite for their beneficial effects in a rat model of breast cancer and that the underlying mechanisms require further investigation.

Funding

The German Academic Exchange Service; The Ministry of Higher Education and Scientific Research of the Arab Republic of Egypt (German Egyptian Research Long-Term Scholarship A/09/92542).

Acknowledgements

We thank Ines Grüner and Ute Lehmann for excellent animal care and Marion Urbich for technical assistance.

Conflict of Interest Statement: None declared.

References

- Jemal,A. *et al.* (2011) Global cancer statistics. *CA Cancer J. Clin.*, **61**, 69–90.
- Key,T. *et al.* (2002) Endogenous sex hormones and breast cancer in postmenopausal women: reanalysis of nine prospective studies. *J. Natl Cancer Inst.*, **94**, 606–616.
- Adlercreutz,H. (2002) Phyto-oestrogens and cancer. *Lancet Oncol.*, **3**, 364–373.
- Adlercreutz,H. (2007) Lignans and human health. *Crit. Rev. Clin. Lab. Sci.*, **44**, 483–525.
- Thompson,L.U. *et al.* (1996) Flaxseed and its lignan and oil components reduce mammary tumor growth at a late stage of carcinogenesis. *Carcinogenesis*, **17**, 1373–1376.
- Serrano,M. *et al.* (1992) Flaxseed supplementation and early markers of colon carcinogenesis. *Cancer Lett.*, **63**, 159–165.
- Thompson,L.U. *et al.* (1996) Antitumorigenic effect of a mammalian lignan precursor from flaxseed. *Nutr. Cancer*, **26**, 159–165.
- Rickard,S.E. *et al.* (1999) Dose effects of flaxseed and its lignan on N-methyl-N-nitrosourea-induced mammary tumorigenesis in rats. *Nutr. Cancer*, **35**, 50–57.
- Clavel,T. *et al.* (2006) Bioavailability of lignans in human subjects. *Nutr. Res. Rev.*, **19**, 187–196.
- Pietinen,P. *et al.* (2001) Serum enterolactone and risk of breast cancer: a case-control study in eastern Finland. *Cancer Epidemiol. Biomarkers Prev.*, **10**, 339–344.
- Ingram,D. *et al.* (1997) Case-control study of phyto-oestrogens and breast cancer. *Lancet*, **350**, 990–994.
- Power,K.A. *et al.* (2006) Mammalian lignans enterolactone and enterodiol, alone and in combination with the isoflavone genistein, do not promote the growth of MCF-7 xenografts in ovariectomized athymic nude mice. *Int. J. Cancer*, **118**, 1316–1320.
- Clavel,T. *et al.* (2006) Occurrence and activity of human intestinal bacteria involved in the conversion of dietary lignans. *Anaerobe*, **12**, 140–147.
- Woting,A. *et al.* (2010) Bacterial transformation of dietary lignans in gnotobiotic rats. *FEMS Microbiol. Ecol.*, **72**, 507–514.
- Becker,N. *et al.* (2011) Human intestinal microbiota: characterization of a simplified and stable gnotobiotic rat model. *Gut Microbes*, **2**, 25–33.
- Aebi,H. (1984) Catalase *in vitro*. *Methods Enzymol.*, **105**, 121–126.
- Beauchamp,C. *et al.* (1971) Superoxide dismutase: improved assays and an assay applicable to acrylamide gels. *Anal. Biochem.*, **44**, 276–287.
- Mannervik,B. *et al.* (1981) Glutathione transferase (human placenta). *Methods Enzymol.*, **77**, 231–235.
- Ellman,G.L. (1959) Tissue sulfhydryl groups. *Arch. Biochem. Biophys.*, **82**, 70–77.
- Mihara,M. *et al.* (1978) Determination of malonaldehyde precursor in tissues by thiobarbituric acid test. *Anal. Biochem.*, **86**, 271–278.
- Bradford,M.M. (1976) A rapid and sensitive method for the quantitation of microgram quantities of protein utilizing the principle of protein-dye binding. *Anal. Biochem.*, **72**, 248–254.
- Velentzis,L.S. *et al.* (2009) Lignans and breast cancer risk in pre- and postmenopausal women: meta-analyses of observational studies. *Br. J. Cancer*, **100**, 1492–1498.
- McCann,S.E. *et al.* (2010) Dietary lignan intakes in relation to survival among women with breast cancer: the Western New York Exposures and Breast Cancer (WEB) Study. *Breast Cancer Res. Treat.*, **122**, 229–235.
- Ward,H.A. *et al.* (2010) Breast, colorectal, and prostate cancer risk in the European Prospective Investigation into Cancer and Nutrition-Norfolk in relation to phytoestrogen intake derived from an improved database. *Am. J. Clin. Nutr.*, **91**, 440–448.
- Hedelin,M. *et al.* (2008) Dietary phytoestrogens are not associated with risk of overall breast cancer but diets rich in coumestrol are inversely associated with risk of estrogen receptor and progesterone receptor negative breast tumors in Swedish women. *J. Nutr.*, **138**, 938–945.
- Sonested,E. *et al.* (2010) Enterolactone and breast cancer: methodological issues may contribute to conflicting results in observational studies. *Nutr. Res.*, **30**, 667–677.
- Kurzer,M.S. *et al.* (1995) Fecal lignan and isoflavonoid excretion in premenopausal women consuming flaxseed powder. *Cancer Epidemiol. Biomarkers Prev.*, **4**, 353–358.
- Kuijsten,A. *et al.* (2005) Pharmacokinetics of enterolignans in healthy men and women consuming a single dose of secoisolariciresinol diglycoside. *J. Nutr.*, **135**, 795–801.
- Saarinen,N.M. *et al.* (2000) Hydroxymatairesinol, a novel enterolactone precursor with antitumor properties from coniferous tree (*Picea abies*). *Nutr. Cancer*, **36**, 207–216.
- Saarinen,N.M. *et al.* (2008) Dietary lariciresinol attenuates mammary tumor growth and reduces blood vessel density in human MCF-7 breast cancer xenografts and carcinogen-induced mammary tumors in rats. *Int. J. Cancer*, **123**, 1196–1204.
- Schultze-Mosgau,M.H. *et al.* (1998) Regulation of c-fos transcription by chemopreventive isoflavonoids and lignans in MDA-MB-468 breast cancer cells. *Eur. J. Cancer*, **34**, 1425–1431.
- Fabian,C.J. *et al.* (2010) Reduction in Ki-67 in benign breast tissue of high-risk women with the lignan secoisolariciresinol diglycoside. *Cancer Prev. Res. (Phila)*, **3**, 1342–1350.
- Webb,A.L. *et al.* (2005) Dietary lignans: potential role in cancer prevention. *Nutr. Cancer*, **51**, 117–131.
- Saggari,K.K. *et al.* (2010) The effect of secoisolariciresinol diglycoside and flaxseed oil, alone and in combination, on MCF-7 tumor growth and signaling pathways. *Nutr. Cancer*, **62**, 533–542.
- Chen,J. *et al.* (2009) Flaxseed and pure secoisolariciresinol diglycoside, but not flaxseed hull, reduce human breast tumor growth (MCF-7) in athymic mice. *J. Nutr.*, **139**, 2061–2066.
- Penttinen,P. *et al.* (2007) Diet-derived polyphenol metabolite enterolactone is a tissue-specific estrogen receptor activator. *Endocrinology*, **148**, 4875–4886.
- Chen,J. *et al.* (2007) Flaxseed alone or in combination with tamoxifen inhibits MCF-7 breast tumor growth in ovariectomized athymic mice with high circulating levels of estrogen. *Exp. Biol. Med. (Maywood)*, **232**, 1071–1080.
- Chen,J. *et al.* (2007) Dietary flaxseed interaction with tamoxifen induced tumor regression in athymic mice with MCF-7 xenografts by downregulating the expression of estrogen related gene products and signal transduction pathways. *Nutr. Cancer*, **58**, 162–170.
- Kitts,D.D. *et al.* (1999) Antioxidant activity of the flaxseed lignan secoisolariciresinol diglycoside and its mammalian lignan metabolites enterodiol and enterolactone. *Mol. Cell Biochem.*, **202**, 91–100.
- Prasad,K. (1997) Hydroxyl radical-scavenging property of secoisolariciresinol diglycoside (SDG) isolated from flax-seed. *Mol. Cell Biochem.*, **168**, 117–123.
- Prasad,K. (2000) Antioxidant activity of secoisolariciresinol diglycoside-derived metabolites, secoisolariciresinol, enterodiol, and enterolactone. *Int. J. Angiol.*, **9**, 220–225.

42. Yuan, Y.V. *et al.* (1999) Short-term feeding of flaxseed or its lignan has minor influence on *in vivo* hepatic antioxidant status in young rats. *Nutr. Res.*, **19**, 1233–1243.
43. Scharlau, D. *et al.* (2009) Mechanisms of primary cancer prevention by butyrate and other products formed during gut flora-mediated fermentation of dietary fibre. *Mutat. Res.*, **682**, 39–53.
44. Yonezawa, T. *et al.* (2007) Short-chain fatty acids induce acute phosphorylation of the p38 mitogen-activated protein kinase/heat shock protein 27 pathway via GPR43 in the MCF-7 human breast cancer cell line. *Cell. Signal.*, **19**, 185–193.
45. Kleessen, B. *et al.* (1997) Feeding resistant starch affects fecal and cecal microflora and short-chain fatty acids in rats. *J. Anim. Sci.*, **75**, 2453–2462.

Received August 23, 2011; revised October 26, 2011; accepted November 5, 2011

PAPER 12

Phenolics in Human Nutrition: Importance of the Intestinal Microbiome for Isoflavone and Lignan Bioavailability

78

Thomas Clavel and Job O. Mapesa

Contents

1	Introduction	2434
2	Phenolics in Human Nutrition	2435
3	Bioavailability: Importance of the Intestinal Microbiota	2439
4	Microbial Diversity: Relevance for Phenolic Conversion	2441
5	The Gut Microbiota Influences Health Effects of Phenolics	2442
5.1	Core Bacterial Reactions and Conversion of Isoflavones and Lignans	2442
5.2	Health Effects of Isoflavones and the Bacterial Metabolite Equol	2446
5.3	Health Effects of Enterolignans	2449
6	Impact of Phenolics on Intestinal Microbiota	2451
7	Can We Potentiate Intestinal Microbial Metabolism?	2453
8	Conclusion	2455
	References	2456

Abstract

Depending on nutritional habits, our diet may contain a substantial load of phenolics, defined as plant secondary metabolites consisting of one to several phenol groups. Their bioavailability, in other words the active fraction of ingested amounts that reaches targeted cell types or tissues where biochemical

T. Clavel (✉)

Biofunctionality Unit – Junior Research Group Intestinal Microbiome, ZIEL – Research Center for Nutrition and Food Sciences, TU München, Freising-Weihenstephan, Germany

e-mail: thomas.clavel@tum.de

J.O. Mapesa

Biofunctionality Unit, ZIEL – Research Center for Nutrition and Food Sciences, TU München, Freising-Weihenstephan, Germany

Department of Dairy and Food Science and Technology, Egerton University, Egerton, Kenya

Agri-Food and Nutrition Innovations, Nairobi, Kenya

K.G. Ramawat, J.M. Mérillon (eds.), *Natural Products*,
DOI 10.1007/978-3-642-22144-6_94, © Springer-Verlag Berlin Heidelberg 2013

2433

properties can act, is markedly influenced by metabolism and absorption in the gastrointestinal tract. Indeed, our intestine is the primary metabolically active site of absorption of exogenous factors in our body and harbors trillions of microbial cells with a vast metabolic potential, referred to as the intestinal microbiota. The aim of the present book chapter is to give insights into the role of phenolic compounds in human health. We will focus our attention on two families of polyphenols of importance in human nutrition, namely, the isoflavones and lignans, and will discuss in detail the role of intestinal microorganisms in regulating their metabolism and thereby health effects.

Keywords

Bioavailability • enterolignans • equol • health • human nutrition • intestinal microbiota • isoflavones • lignans • microbiome • phenolics • phytoestrogens

Abbreviations

BMD	Bone mineral density
DNA	Deoxyribonucleic acid
<i>E. coli</i>	<i>Escherichia coli</i>
ED	Enterodiol
EFSA	European Food Safety Authority
EL	Enterolactone
ER	Estrogen receptor
FOS	Fructooligosaccharides
GI	Gastrointestinal
LDL	Low-density lipoprotein
PCR	Polymerase chain reaction
RCT	Randomized controlled trials
SDG	Secoisolariciresinol diglucoside

1 Introduction

Nutrition, in combination with other environmental factors such as climate shifts and changes in ecosystem structure, has played a key role in evolutionary processes that made us what we are: *Homo sapiens*. Our brain must be constantly fueled with energy in the form of glucose, and essential nutrients such as fatty acids are required for proper brain development. Thus, selectively advantageous eating behaviors have certainly favored essential nutrient supply, efficient energy harvest from food stuff and effective mechanisms of energy storage, contributing to nutritional stability and thereby to more rapid development of cognitive functions and the emergence of our species [1]. Beyond evolutionary issues, it is nowadays acknowledged that nutrition, along with physical activity, are important factors influencing human health. In westernized countries, the long-term deleterious health effects of diets rich in calories, simple sugars, saturated fat, and red meat with respect to the

development of cardiovascular diseases, colorectal cancer, and the metabolic syndrome are as much recognized as the virtue of eating enough portions of fruits and vegetables, although underlying mechanisms of actions remain to be described [2–4]. Positive effects of fruits and vegetables are usually attributed to high content of fiber, vitamins, and phenolic compounds (hereon defined as plant secondary metabolites with a backbone structure made of one or several phenol groups). Assuming that a substantial proportion of the dietary intake of common ancestor species consisted of plant materials, it is not surprising that, over millions of years of evolution, our body has inherited an efficient metabolic machinery to dispose of the large quantity of phenolic compounds that we still ingest daily as part of our omnivorous diet. Intestinal microorganisms are intrinsic parts of this metabolic machinery. Indeed, from an evolutionary perspective again, the human body can be considered as a supra-organism made of not only own eukaryotic cells, but also the hundred trillions of microorganisms that colonize various body sites such as the skin and the genital, respiratory and, most importantly with respect to nutrition, the gastrointestinal (GI) tract [5]. The intestinal microbiota is referred to as the assemblage of microbial communities and associated genomes (the metagenome) primarily colonizing the distal GI tract. Due to its highly diverse metabolic potential, the intestinal microbiota greatly alters the fate of phenolics in the human body by changing their structure and absorption rates in the gut, thereby influencing their biological effects.

In that context, the present chapter gives insights into the relevance of phenolic compounds in human nutrition. We will primarily discuss bioavailability and biological properties of isoflavones and lignans in the context of human health and disease, our main focus being the metabolic activities of intestinal bacteria.

2 Phenolics in Human Nutrition

Concoctions of plant products for the purpose of curing disease or sustaining health in human subjects have a long history of use, especially in traditional Chinese medicine. However, molecular mechanisms underlying positive effects have yet to be defined and traditional medicine therefore faces intense criticism [6]. Nevertheless, the emergence of systems biology approaches may help shedding light on host responses toward treatment with plant products that obviously contain a wealth of phenolic compounds [7–9]. Beyond these issues on the role of herbal treatment for improvement of human health, there is a plethora of epidemiological data highlighting beneficial effects associated with intake of food items rich in phenolic compounds. A well-known example of such food items is soy (or soy products) which contain elevated concentrations of the isoflavones daidzein and genistein as well as their glycosylated and methylated precursors (Fig. 78.1).

Biological properties of isoflavones were first coined in the 1940s, after infertility problems started to occur in female sheep grazing on clover pastures containing high amounts of isoflavones, and later in the 1980s in captive cheetahs fed a soy-based diet [10, 11]. These data already suggest that dietary phenolics or corresponding metabolites, such as equol, one of the two end metabolites produced

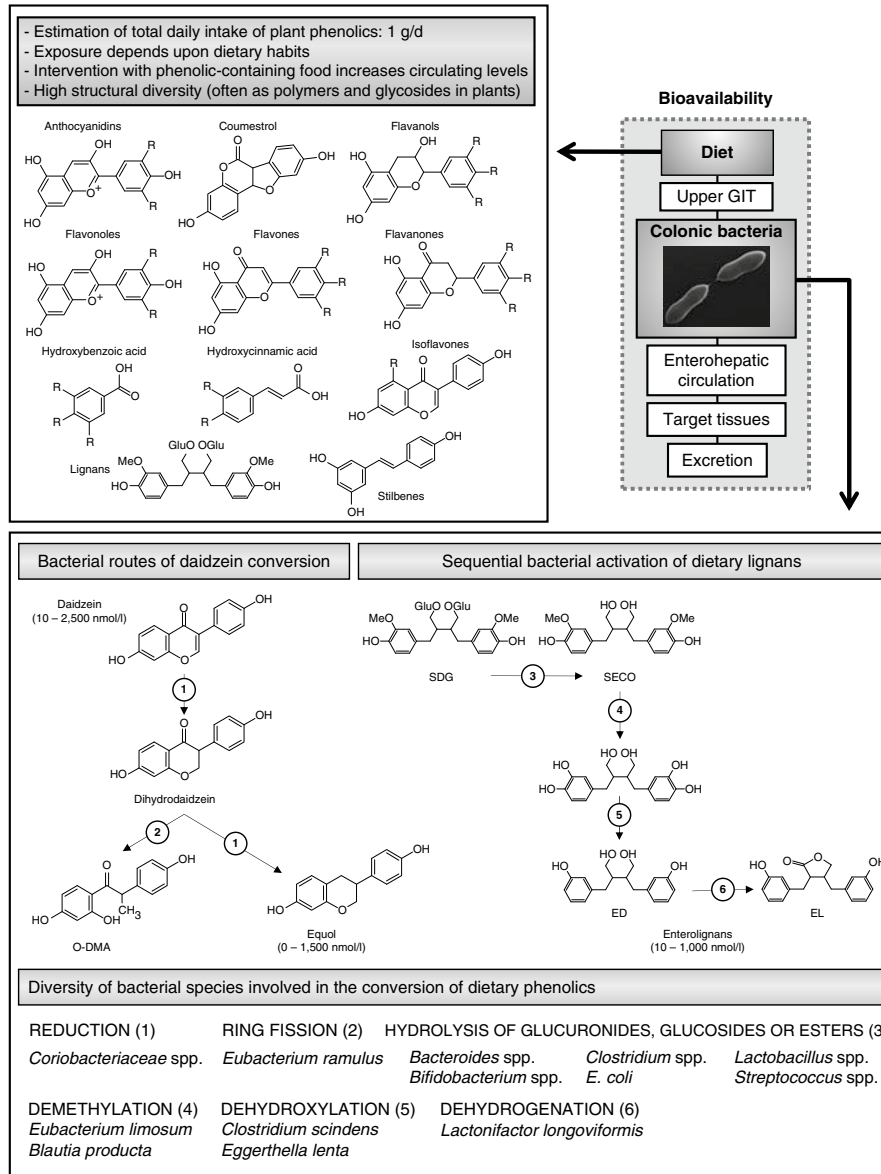


Fig. 78.1 Phenolics in human nutrition: A microbiological perspective. Bioavailability of dietary compounds depends on the sum of molecular mechanisms underlying liberation of the compounds from dietary matrices, absorption, distribution into body tissues via blood circulation, metabolism (in the GI tract or target tissues), and elimination from the body. The keypad shows parameters of relevance to phenolic bioavailability. The two enlarged windows illustrate the diversity of both phenolics in food and microbial functions involved in phenolic conversion, with a focus on isoflavones and lignans. Estimates of blood concentration of daidzein, equol, and enterolignans are

by bacteria from the plant isoflavone daidzein, have the potential to interfere with highly sensitive host hormonal pathways. Since then, numerous meta-analyses and epidemiological studies including Asian populations consuming soy products on a daily basis have reported positive effects of soy intake on the development of breast cancer, bone disorders, and cardiovascular diseases [12–14].

The lignans, a family of polyphenolic compounds with a dibenzylbutane structure (Fig. 78.1), are another example of major plant phenolics relevant to human nutrition. Dietary lignans are converted to the enterolignans enterodiol (ED) and enterolactone (EL) by bacteria in the GI tract [15]. In contrast to isoflavones that occur in high concentrations almost exclusively in soy, a vast variety of food items such as flaxseeds, sesame seeds, berries (blackberry and strawberry), cereals (rye and wheat), and beverages (coffee, tea, and wine) contain detectable concentrations of lignans, which are therefore of importance in westernized diets [16]. Importantly, lignans have also been shown to be dietary precursors of enterolignans [17]. Of note, researchers originally proposed in 1980 that enterolignans were new mammalian hormones after they detected them in urinary extracts from female primates and human adults via spectrometric measurement [18, 19]. This shows that lignans share structural features with steroid hormones and are, as isoflavones, also referred to as phytoestrogens. Two years later, in 1982, the same authors reported that urinary lignans originate from food precursors [20]. Thereafter, enterolignan production has been associated with positive effects on the incidence of heart diseases as well as breast and prostate cancer [21–23].

Besides isoflavones and lignans, human food contains a wealth of phenolic compounds (Fig. 78.1). Rapid improvement in the sensitivity of analytical tools, together with the development of specific databases such as Phenol-Explorer and the USDA Flavonoid Database, have substantially contributed to the understanding of human exposure to phenolics [24]. Table 78.1 provides a non-exhaustive list of major groups of dietary phenolics and representative food sources. Depending on dietary habits, total intake of phenolics in European populations can reach up to 1 g/day or higher [26, 28, 30]. By studying dietary intake in 4,942 French adults, Scalbert et al. showed that the most dominant dietary phenolics are hydroxycinnamic acids, flavonols, and anthocyanins [30]. However, there is a direct positive association between ingested amounts of specific food products and blood concentrations of corresponding metabolites, showing that one can easily and rapidly modulate exposure to specific phenolics by modulating dietary intake. In Asian populations for instance, isoflavones intake is nearing 100 mg/day due to high intake of soy products [35]. Nevertheless, health effects of dietary phenolics do not depend solely on ingested amounts, but rather on the concentration of active compounds that reaches target tissues. In that respect, what makes lignans and isoflavones outstanding is that plant precursors are usually less biologically

←
Fig. 78.1 (continued) given in brackets (large interindividual differences are observed due to various dietary habits and ability to metabolize polyphenols). Abbreviations: *ED* enterodiol, *EL* enterolactone, *GIT* gastrointestinal tract, *LARI* lariciresinol, *O-DMA* *O*-desmethylangolensin, *R* residues (–H, –OH, or –CH₃), *SECO* secoisolariciresinol, *SDG* secoisolariciresinol diglucoside

Table 78.1 Dietary intake and example food sources of phenolic compounds^a

Compound	Intake ^b	Food	Content ^c
<i>Phenolic acids</i>			
Hydroxybenzoic acids (e.g., gallic acid)	10–30	Blackberry	8–27
		Tea leaves	Up to 450
Hydroxycinnamic acids (e.g., caffeic and ferrulic acid)	25–800 (68 %)	Coffee	35–175
		Blueberry	Up to 200
<i>Flavonoids</i>			
Anthocyanidins (e.g., cyanidin, peonidin)	20–80	Blackberry	100–400
		Black currant	130–400
Flavanols (e.g., epicatechin)	10–20	Chocolate	45–60
		Apricot	10–25
Flavanones (e.g., naringenin, hesperitin)	25–50	Orange juice	22–69
		Grapefruit juice	10–65
Flavones (e.g., apigenin, luteolin)	5–30	Parsley	24–185
		Celery	2–14
Flavonols (e.g., quercetin, kaempferol)	10–20	Yellow onions	35–120
		Curly kale	30–60
Isoflavones (e.g., daidzein, genistein)	<1–60	Boiled soybean	20–90
	(0–82 %)	Soy milk	3–20
	(3–30 %)	Whole grain bread	0.3–0.8
<i>Lignans</i> ^d	0.5–2	Flaxseed	300
	(10 %)	Sesame seed	39
	(3 %)	Broccoli	1.3
	(16 %)	Strawberry	0.3
	(0.7 %)	Wheat bread (whole grain)	0.1
	(7.4 %)	Beer	0.03
	(3 %)	Coffee	0.02–0.03
	(11 %)		

^aCompiled using data from Phenol-Explorer (www.phenol-explorer.eu), the USDA Flavonoid Database (www.nal.usda.gov/fnic/foodcomp/Data/Flav/flav.html) and the following Refs. [16, 25–32]

^bGiven as ranges (in mg/day aglycone equivalent) for each of the listed families of phenolics (e.g., isoflavones). Ranges reflect fluctuations of mean dietary intake depending on population origin (Asia, Denmark, Finland, France, Germany, Holland, Italy, Spain, UK, or USA) and dietary habits. Values in brackets indicate mean contribution of some of the given food items to dietary intake in European populations

^cIn mg/100 g or 100 ml. Of note, concentration of phenolic compounds in food can be altered by food processing [33]. During production of tempeh for instance, a traditional soy product from Indonesia, isoflavone glycosides are hydrolyzed to aglycones [34]

^dRefers to lariciresinol, matairesinol, pinorensinol, and secoisolariciresinol

active so that enterolignans and equol can be seen as paradigm metabolites highlighting the relevance of bacterial activation of dietary components in the intestine. Hence, no matter which phenolics are of interest and what health effects they have, bioavailability and bacterial metabolism are matters of primary importance.

3 Bioavailability: Importance of the Intestinal Microbiota

Bioavailability refers to the proportion of absorbed doses of a molecule, and eventually metabolites thereof, which reaches sites of physiological activity. Our GI tract is of course at the front line of metabolic events regulating bioavailability due to its primary role in nutrient absorption and because oral intake is the major voluntary route of exchange with our environment (compared with passive exposure to exogenous factors via the skin and the respiratory tract). The liver and kidneys play a central role in bioavailability as well. Efficient conjugation of phenolics for the purpose of increasing water solubility, and eventually excretion, occurs in all three organs (gut, liver, kidneys) mainly via the activity of *O*-methyl transferases, UDP-glucuronosyltransferases, and sulfotransferases [26]. The bioavailability of dietary phenolics is thus tuned by the sum of molecular mechanisms underlying liberation from dietary matrices, absorption, metabolism (by both host and microbial cells), distribution, and excretion (Fig. 78.1).

In upper parts of the GI tract, there is a paucity of data on the fate and role of polyphenols. Their effects have been discussed in the context of oral cancer prevention [36]. Their fate in the stomach has not yet been systematically studied. Quercetin has been shown to be absorbed in the rat stomach, but only as aglycone [37]. Fast plasma appearance of anthocynins may also be explained by rapid absorption in the stomach [38]. Concerning lignans, we found that secoisolariciresinol diglucoside (SDG) (the main enterolignan precursor in flaxseed) is resistant to acid hydrolysis *in vitro* [39], which confirmed previous findings [40]. In the jejunum, there is good evidence that isoflavones and flavonols can be deglycosylated via lactase-phlorizin hydrolase activity and rapidly absorbed in the brush border membrane of enterocytes [41, 42]. Rat *in vitro* perfusion models have also been useful in demonstrating absorption of phenolic acids as well as quercetin and phloretin in the small intestine [43, 44]. However, the flavanol epigallocatechin-3-gallate can inhibit hydrolase activity *in vitro*, yet this inhibition is regulated by salivary proline-rich proteins [45]. This raises the question of the effect of chewing on polyphenol bioavailability via indirect or direct mechanisms such as salivary hydrolysis [46]. Plant phenolic substrates can be detected in blood and urine samples shortly after intake, which speaks in favor of rapid absorption, albeit, in low amounts. For instance, only about 2 % of the ingested dose of plant lignans was found in plasma of four individuals 1 h after intake of 50 g sesame seeds [47]. In some individuals however, plant lignans may occur in higher concentrations than enterolignans in blood samples [48]. This is also true for the isoflavone daidzein, which occurs at higher concentrations than its metabolite equol in blood samples [49], most likely because bacterial production of equol in the gut is a limiting reaction (see details in Sect. 5.1). Altogether, characterization of the metabolic network regulating phenolic bioavailability in the upper GI tract requires further investigation. In particular, very little is known about phenolic transport from gut lumen into blood stream. A recent pharmacokinetic study in human adults based on the use of equol isotopes revealed peak plasma concentrations 2–3 h after oral intake of the isotopes (350–500 ng/ml after

administration of a single bolus of 20 mg) [50]. One may interpret that transport mechanisms in the gut are not region-specific, since equol is supposed to be primarily produced in distal parts of the intestine. Absorption rates of phenolics and kinetics of appearance in blood vary greatly depending on chemical structure. For instance, glucosides of quercetin (but not rhamnoglucosides) are more efficiently absorbed than aglycones [51]. However, underlying molecular mechanisms of absorption are not known. So far, only monocarboxylic acid transporters and the plasma membrane carrier bilirubin translocase have been discussed for transport of phenolic acids and anthocyanins, respectively [52–55]. Independently of what exactly happens in the upper GI tract, it is acknowledged that a substantial proportion of ingested polyphenols can reach the colon, where lower transit time favors bacterial conversion.

The first piece of evidence demonstrating that distal parts of the GI tract are crucial for the metabolism of phenolics is the so-called second plasma peak observed after 6–8 h postprandial when measuring phenolic metabolites in plasma samples overtime after ingestion of plant substrates [56]. Indeed, a substantial proportion of absorbed phenolics is efficiently conjugated in enterocytes and later in the liver prior to secretion back into the small intestine via the bile (enterohepatic circulation) [57]. Enterohepatic circulation thereby contributes to bacterial “re-feeding” since the bulk of glucuronidated and sulfated phenolic metabolites released in the bile can be hydrolyzed by various bacterial species [58]. Bacterial hydrolysis thus allows reabsorption of otherwise lost conjugated phenolics to be excreted in feces and thereby to delayed appearance of phenolic metabolites in the blood (second plasma peak). Another piece of evidence showing that distal gut microorganisms are crucial for phenolic metabolism is the drop in plasma and urinary concentrations of phenolics associated with alteration of intestinal microbial communities following oral antibiotic treatment [56, 59, 60]. Finally, the use of germfree mice, that is, mice that are bred in isolators under sterile conditions and are thus deprived of any living microorganisms, has provided major insights into the important role of intestinal microbial communities in shaping host physiology, including the ability to metabolize food substrates such as phenolics. To some extent, one can consider germfree mice as knockout mice, in which a multifunctional set of genes (the microbiome) has been disrupted, leading to loss of functions. Indeed, besides alteration of immune cell development [61], the absence of microorganisms in germfree animals has major impacts on energy balance [62], nutrient supply via production of short-chain fatty acids, and degradation of mucin [63] as well as phytoestrogen conversion. Enterolignans and equol, for instance, are not detectable in the intestine and body fluids of germfree rats fed phenolic-rich diets, yet gnotobiotic rats colonized with fecal suspensions from phenolic-converting human donors or with isolated active bacterial consortia regain the ability to produce active metabolites [64–67]. Taking into account that the intestinal microbial ecosystem in mammals harbors a total of up to 10^{14} cells belonging to more than 1,000 different species per host, each bearing approximately a few thousands of genes, it is not surprising that the absence of such diverse microbial communities is linked to disturbances in metabolic functions. In the following two sections, we will highlight specific features of intestinal microbiota that are of importance for phenolic conversion.

4 Microbial Diversity: Relevance for Phenolic Conversion

As seen above in Sect. 2, a broad array of food items contain various phenolic compounds in a wide range of concentrations (from a few micrograms up to a few hundred milligrams per 100 g), which highlights the rationale for “eating a little of everything each day” to cover supplies yet avoid adverse effects due to long-term excessive intake of a limited number of food items. With respect to chemical structure, the variety of phenolics is also quite large and the amounts ingested are driven by dietary habits, which differ markedly between individuals (Fig. 78.1). Hence, the mixture of phenolics in the intestinal lumen is determined by multiple levels of complexity and is thus highly diverse and variable.

Diversity is also a major attribute of intestinal microbial communities in mammals. Indeed, although our intestinal microbiota consists dominantly of only four of the 30 known bacterial phyla (highest taxonomic level within the superkingdom *Bacteria*; www.ncbi.nlm.nih.gov/Taxonomy; www.bacterio.cict.fr), namely, the *Firmicutes*, *Bacteroidetes*, *Actinobacteria*, and *Proteobacteria*, the diversity at low taxonomic levels (\leq genus) is very high. Most recent molecular studies refer to a few thousands different bacterial species being present in the human gut, and accordingly even more individual strains [68]. Although bacteria make up the majority of intestinal microbial populations, our intestine harbors also *Archaea* (two dominant methane-producing species, *Methanobrevibacter smithii* and *Methanosphaera stadtmanae*, have been described to date), eukaryotic microorganisms, such as fungi and protozoa, as well as viruses. However, the role of these microorganisms in the metabolism of phenolics is unknown (bacteriophages may, for instance, influence phenolic conversion by regulating the density of specific active bacterial populations).

As often in biology, the efficacy of one complex system (the intestinal microbiota) is greater than the sum of its biologically active parts (bacterial strains). Indeed, one key asset of the high diversity of our intestinal microbiota is that several different bacterial species can carry out one given function, such as cleaving glucose moieties of phenolics. This is referred to as “functional redundancy” (one bacterium can take over the function of another if for some reason the latter disappears). This ensures flexibility and is crucial to achieve stability and ecosystem equilibrium over time upon influence of various environmental stimuli [69]. Hence, the high diversity of our intestinal microbiota helps us cope with the high diversity of exogenous chemical compounds that we ingest. Nevertheless, in spite of this high diversity, there are a few bacterial species (50–100), and by extension a few associated bacterial functions, that make up the so-called core microbiome [70], that is, the assemblage of species/functions that are dominant (occur in high numbers) and show a high prevalence (they are found in most individuals).

Despite the notion of a core microbiome and the stability of the gut microbial ecosystem over time without major changes in dietary habits, each individual person harbors their own characteristic intestinal microbiota (in the sense of a personalized fingerprint). Indeed, there are large interindividual differences in both intestinal bacterial composition (proportion of taxa) and diversity (qualitative pattern of

taxa); there is marked quantitative variation and low similarity indexes between gut samples from different individuals, even for dominant bacterial groups [68, 71, 72]. Individualized intestinal microbial patterns in adulthood are highly dependent upon a dynamic sequence of events affecting the ecosystem throughout life, especially in early life. At birth, the human body is colonized by microorganisms from the environment. Primary colonizers (aerobic or facultative anaerobic bacteria) help establish a reduced environment that is suitable for subsequent colonization by strictly anaerobic species, which largely dominate the ecosystem in adulthood. In infants below 1 to 2 years of age, the human intestinal microbiota is unstable and composition fluctuates greatly [73]. The infant gut microbiome seems not to be well equipped for efficient conversion of polyphenols. For example, equol is not detected in urine and blood samples from infants below the age of 12 months who are fed cow or breast milk [74, 75]. Delivery mode at birth (vaginal delivery vs. caesarian section) and breast versus formula milk feeding have been shown to influence microbial colonization patterns [76–79]. In early life, and very often thereafter, the intestinal ecosystem is challenged by infectious agents and antibiotic therapies. In most cases, the ecosystem shows resilience, thanks to its diversity, that is, it rapidly returns to its original state after a challenge. However, in some cases, and more likely and frequently during infancy where microbial populations are not yet fully stabilized, the ecosystem or at least specific community niches can be permanently affected [80]. Altogether, this variety of colonization and challenging events can partly explain why certain individuals harbor specific bacteria and others do not, and why the latter group therefore lacks the functions expressed by absent or subdominant bacterial species. For instance, it is well known that only about 30–50 % of human subjects produce equol from the isoflavone daidzein, meaning that one half to two thirds of human populations do not harbor equol-producing bacteria in their intestine, at least not in high enough densities [81, 82]. Likewise it has been shown that bacteria capable of catalyzing the production of enterolactone from plant lignans belong to subdominant populations, that is, they occur at densities below 10^8 cell/g content (compared to a total cell density of approximately 10^{12} cell/g) [83, 84].

In summary, our intestinal microbiome encodes numerous core functions of importance for the conversion of dietary phenolics, yet interindividual differences in the makeup of bacterial species that colonize our gut underlie interindividual differences in phenolic metabolism and thereby in possible health effects. In Sect. 5, we will give more details on active bacterial members and central metabolic reactions involved in phenolic conversion prior to focusing on health effects of isoflavones and lignans.

5 The Gut Microbiota Influences Health Effects of Phenolics

5.1 Core Bacterial Reactions and Conversion of Isoflavones and Lignans

Exceptions prove the rules: the functional diversity of intestinal microbiota implies that all plant phenolics that we ingest can be converted by microorganisms.

However, there are exceptions, such as the isoflavone irilone, which seems to be resistant to bacterial conversion [85]. Gut bacteria catalyze an array of dominant core reactions that play key roles in the metabolism of a large panel of phenolic compounds, including isoflavones and lignans: (I) hydrolysis of esterified and conjugated bounds, (II) deglycosylation (removal of sugar moieties), (III) demethylation (substitution of a methyl by a hydroxyl group), (IV) dehydroxylation (reduction of hydroxyl groups), (V) dehydrogenation, (VI) reduction. Figure 78.1 gives a brief overview of the so far identified bacterial species that catalyze these reactions [86, 87]. It is noteworthy that several species occur in proximal parts of the bowel (*Enterobacteriaceae*, lactobacilli, lactococci, and streptococci in the stomach and small intestine), showing that bacterial metabolism of phenolics may be crucial not only in the colon, but already before, for example, for hydrolysis of conjugated metabolites secreted in the bile. Most dietary phenolics occur as biologically inert polymers or glycosides, meaning that reaction type I and II are crucial for phenolic activation and influence downstream reactions such as demethylation. As a matter of fact, the production of one given active metabolite often results from sequential reactions involving several bacterial species. For instance, production of enterolignans from SDG requires four reactions, among which demethylation and dehydroxylation are catalyzed only if the substrate has been previously deglycosylated and demethylated, respectively [15, 88]. Reaction type III (demethylation) is also crucial with respect to biological activities since most plant phenolics are methylated and are less active than hydroxylated metabolites. This is obvious, for instance, in the case of caffeic acid phenyl ester (an active phenolic constituent of honeybee propolis), for which we found that methylation of catechols markedly reduces anti-inflammatory activities [89].

The physiological advantage for bacteria to convert phenolic compounds is easily understandable in the case of deglycosylation (active species can utilize released glucose moieties as carbon and energy sources) or demethylation (acetogenic bacteria, for instance, are capable of producing energy by incorporating methyl groups into the Wood-Ljungdahl pathway of acetogenesis). In contrast, it is more difficult to identify driving forces that led to the establishment of complex phenolic-converting metabolic chains involving various distantly related bacterial species. One simplistic way to assess such a complex system is to try gaining access to individual bacterial components of the metabolic chain by means of anaerobic cultivation for subsequent *in vitro* characterization. Indeed, the isolation of pure bacterial cultures, in combination with the use of biochemical techniques (high performance liquid chromatography and mass spectrometry), for the purpose of metabolite identification allows description of key bacterial players in phenolic metabolism, including subdominant bacterial populations [15, 90]. Microbiologists have been culturing microorganisms for a long time, rapidly leading to major breakthroughs in biomedical research such as the identification of *Mycobacterium tuberculosis* by Robert Koch in 1876 or the discovery of the antibiotic penicillin by Alexander Fleming in 1928. In contrast, it is only from the 1950s onwards that the development and use of anaerobic tools by pioneers such as René Dubos, Sydney Finegold, Lillian Holdeman, Robert Hungate, Edward Moore, and Russel Schaedler

Table 78.2 Cultivable bacteria capable of converting the isoflavone daidzein^a

Bacterial strain	End metabolite	Origin	References
<i>Adlercreutzia equolifaciens</i> FJC-B9 ^T	Equol	Human feces	Maruo et al. [96]
<i>Asaccharobacter celatus</i> do03 ^T	Equol	Rat cecum	Minamida et al. [97] Minamida et al. [98]
<i>Eggerthella</i> sp. YY7918	Equol	Human feces	Yokoyama et al. [99]
<i>Enterorhabdus mucosicola</i> Mt1-B8 ^{T a}	Equol	Mouse ileal mucosa	Matthies et al. [100] Clavel et al. [101]
<i>Eubacterium ramulus</i> wK1	<i>O</i> -desmethylangolensin	Human feces	Schoefer et al. [102]
<i>Lactococcus</i> sp. 20-92	Dihydrodaidzein	Human feces	Shimada et al. [103]
<i>Slackia equolifaciens</i> DZE ^{T a}	Equol	Human feces	Jin et al. [104] Jin et al. [105]
<i>Slackia isoflavoniconvertens</i> HE8 ^{T a}	Equol	Human feces	Matthies et al. [106]
<i>Slackia</i> sp. NATTS	Equol	Human feces	Tsuji et al. [107]
Strain D1 and D2	Equol	Pig feces	Yu et al. [108]
Strain HGH6	Dihydrodaidzein	Human feces	Hur et al. [109]
Strain HGH136	<i>O</i> -desmethylangolensin	Human feces	Hur et al. [110]
Strain Julong 732	Equol ^b	Human feces	Wang et al. [95]
Strain Niu-O16	Dihydrodaidzein	Bovine rumen	Wang et al. [111] Zhao et al. [112]
Strain SY8519	<i>O</i> -desmethylangolensin	Human feces	Yokoyama et al. [113]
Strain TM-40	Dihydrodaidzein	Human feces	Tamura et al. [114]

^aThese strains are also able to produce 5-hydroxy equol from the isoflavone genistein

^bFrom dihydrodaidzein only (this strain does not convert daidzein)

gave rise to extensive culture-based work dealing with commensal bacterial communities from human intestinal samples [91–93].

In 1985, Borriello et al. were the first to study the conversion of plant lignans by fecal slurries in detail [94], yet active bacterial strains were first isolated in 2000 [88]. In the case of phenolic acids, which as mentioned above are dominant phenolics in human diet, knowledge of bacterial conversion and involved species is scant. Hydroxycinnamates (e.g., *p*-coumaric, ferulic, and sinapic acid) as well as benzoic acids (e.g., gallic, syringic, and vanillic acids) are rapidly degraded by intestinal bacteria and a few members of the *Firmicutes* are known to demethylate a variety of phenolic acids [39, 86]. Actually, this is the case of isoflavones that rapidly drew most of the attention of microbiologists working in the field of polyphenols. Reasons for this are the low proportion of equol producers among humans (30–50 %) and the fact that equol is the most potent known isoflavone metabolite. Researchers have thus embarked on a microbial “Gold Rush” attempting to isolate and identify those rare equol-producing bacteria that colonize the human gut. The first evidence for microbial equol production was published in 1995 [81], however the first equol-producing bacterium, strain Julong 732, was isolated in 2005 (and so far this isolate is still not taxonomically classified) [95]. To date, a total of 16 daidzein-converting strains have been identified (Table 78.2).

From this listing, it is obvious that proper taxonomic description is needed, as some of the isolates could belong to the same species. It is also striking that all equol-producing bacteria with a validly published name are members of the family *Coriobacteriaceae*. This hints at functional specialization in the gut, maybe contributing to the better survival of this bacterial group in the competitive intestinal milieu. Interestingly, some *Coriobacteriaceae*, such as *Eggerthella* spp., are dominant intestinal bacteria and can convert steroid hormones and biliary acids [58]. This shows again that core functions such as dehydroxylation are relevant to various substrates and raises the question on the influence of host hormonal status on polyphenol metabolism [115].

A major advantage of culture-based approaches is that isolated strains can be used in vivo to assess physiological roles of phenolic-converting bacteria (in e.g., germfree mice) or in vitro for isolation and characterization of active enzymes. So far, very few corresponding data have been published. Crude enzyme extracts from *Asaccharobacter celatus* converts daidzein to dihydrodaidzein under anaerobic conditions and a dihydrodaidzein-producing reductase from lactococci has already been cloned (UniProtKB E1CIA4 and E7FL40/1) [103, 116]. However, culturing is per definition restricted to the study of microorganisms able to be isolated and to grow in the laboratory (most recent estimation refers to a proportion of 60 % cultivable bacteria in the mouse intestine) [62]. Again, it is important to remember that one given reaction can be catalyzed by several phylogenetically distantly related bacteria, which highlights the notion of functional bacterial groups and the importance of considering intestinal microbiota as a dynamic pool of functions rather than an assemblage of taxonomic entities. A more comprehensive way to assess the bacterial conversion of phenolics at the level of the entire ecosystem (the pool of microbial functions) than culturing is to use metagenomic techniques, i.e., molecular tools dedicated to the study of the metagenome (the sum of genomes originating from the thousands of bacterial species colonizing the intestine) [68, 117]. For instance, culture- or PCR-based screening of gut metagenomic clone libraries can give direct access to bacterial genomic information involved in conversion of phenolics, metagenomic libraries being defined as collections of >10,000 *Escherichia coli* clones where each clone expresses functions encoded on one large DNA fragment (commonly 40,000 bp) from the gut metagenome. As an example, metagenomic clones can be cultured on agar plates containing a glucosylated phenolic substrate as sole carbon and energy source, an approach that has been already used with other kinds of substrates such as β -glucans [118]. In such an assay, only clones capable of utilizing the substrate would grow and could be further analyzed by sequencing for determination of active gene sequences. Alternatively, colorimetric reactions may also be used for detection of for instance phenolic-demethylating clones [119].

One additional key issue in the field of bacterial enzymatic conversion of polyphenols is enantiospecificity. Many polyphenols, such as isoflavones and lignans, are optically active molecules that display several asymmetric carbon atoms. So far, only *S*-equol has been detected as a bacterial product of daidzein conversion [95, 120]. In the case of lignans, both (+)- and (-)-enantiomers occur in plants and

bacterial conversion in the gut seems to be enantiospecific and preserve absolute configuration [121]. There is strong evidence that biological activity depends upon chirality of equol [122, 123], stressing the need for stereochemical analysis of other phenolic metabolites produced by intestinal bacteria. This serves as further proof of the necessity to isolate phenolic-converting bacterial enzymes for potential biotechnological production of active metabolites [103]. Finally, the search for new bacterial metabolites (and determination of corresponding biological properties) is also of primary interest. Considering the diversity of both dietary phenolics and intestinal bacterial species, it is likely that the panel of intermediate and end metabolites produced by intestinal bacteria is much larger than hitherto observed. For instance, we have found that the lignan-dehydrogenating bacterium *Lactonifactor longoviformis* does not only produce enterolactone, but also the novel metabolite 2,3-bis(3,4-dihydroxybenzyl)butyrolactone, the occurrence of which in vivo along with biological activities is still to be determined [121].

In summary, the array of enzymatic reactions catalyzed by the gut microbiome alters the structure of ingested phenolics. In view of the notion of structure/activity relationship, we conclude that intestinal bacteria greatly influence the biological activities of dietary phenolics. In the case of the isoflavone daidzein the route of bacterial conversion (i.e., the production of equol or *O*-desmethylangolensin depending on gut bacterial composition), is key to downstream health effects (Fig. 78.1). In the following two sections, we will give detailed information on biological activities and potential health effects of isoflavones and lignans.

5.2 Health Effects of Isoflavones and the Bacterial Metabolite Equol

In recent reports, the European Food Safety Authority (EFSA) refuted claims about the role of isoflavones in body function effects (article 13.1) such as maintenance of normal blood LDL-cholesterol concentrations in the general population [124, 125]. This has two main implications (also true beyond the sole case of isoflavones): first, even when scientific rationale is sound and there is a substantial number of well-conducted studies showing an overall significant trend toward positive effects of a defined dietary compound, a major problem in nutrition research is that intake of definite food stuff may need to stretch over long life periods before one can observe significant effects, when compared, for example, with pharmacological products usually associated with instant target effects (even though long-term effects of pharmacological therapies are often also not determined, yet beneficial immediate effects indeed prevail). Thus, the preventive aspect of nutritional strategies implies to carry out studies at scales (both in terms of time and cohorts) virtually impossible to manage in order to substantiate beneficial effects. This very often hampers closing the gap between scientific evidence and clear recommendations for consumers. The second implication is that, whereas it is very difficult to corroborate

findings for the “general population,” it makes sense to look at health effects of isoflavones in sensitive target groups, like infants. For these reasons, this is not our intention to provide here an exhaustive review of possible health effects of isoflavones. Instead, we will focus our attention on osteoporosis affecting menopausal women and on the effect of early exposure to isoflavones, thereby highlighting the biological properties of the bacterial metabolite equol.

Infants make up a study population of particular interest for several reasons: (1) they have not yet necessarily acquired a fully functional phenolic-metabolizing machinery (at least from a microbiological perspective), (2) the use of soy-based infant formula has become a rather common feeding alternative in westernized countries, and (3) a growing human body may be particularly sensitive to the biological properties of isoflavones. There are several published papers showing that early exposure to isoflavones has the potential to influence hormone levels and organ differentiation in the offspring of various animal species [126–129]. For instance, male marmoset twin monkeys fed soy formula milk for 30–40 days from the age of 5 days were characterized by lower mean testosterone levels in blood samples [129]. However, long-term effects must be further investigated. Furthermore, caution must be taken when interpreting results obtained using doses higher than the estimated intake of 2–10 mg isoflavones per day per kilogram body weight in infants fed soy-based formula [130, 131]. Exposure of human infants to dietary isoflavones has drawn attention of researchers since the mid-1990s. Depending on studies, isoflavone concentrations in soy-based infant formula range from 30 to 280 mg/kg [131–133]. Setchell et al. found that mean plasma concentrations of both genistein and daidzein in seven infants fed soy-based formula were 979 ng/ml (approximately 4 $\mu\text{mol/l}$) [131]. This concentration was markedly higher than in infants fed either cow-milk formula (5.3 ng/ml) or human breast milk (4.2 ng/ml), and is also higher than in adults on their usual diet. Interestingly, infants can also be exposed to isoflavones via breast milk during lactation. In seven breastfeeding mothers, ingestion of 55 mg/day isoflavone glucosides for 2–4 days increased isoflavone concentrations significantly in breast milk (from ca. 5 to 70 nmol/l) and in infant urine (from ca. 30 to 110 nmol/mg creatinine) [134]. Hence, it is clear that infants can be exposed to relatively high isoflavone concentrations and experimental work shows some significant effects of early exposure to isoflavones in animals. However, there is an obvious lack of physiological evidence in humans, as underlined in recent review papers and human infant trials [135–139].

The rationale for considering possible health effects of dietary isoflavones in infants is substantiated by *in vitro* and *in vivo* work on their biological properties. Especially, the estrogenic-like properties of isoflavones have been studied as early as in the 1950s based on the mouse uterine weight method [140], 30 years before equol was first detected in human urine [141]. Among daidzin metabolites, equol has the strongest binding affinities to estrogen receptors (ER), especially for ER- β [122, 142, 143]. Nevertheless, 17 β -estradiol is 10–100 times more potent than equol. Interestingly, the *R*- and *S*-enantiomer of equol exhibit different binding affinities for ER- α (0.5 vs. 2 % of 17 β -estradiol binding, respectively) or ER- β (1 vs. 20 %) [122]. Beyond binding affinities, equol can also modulate ER

transcriptional activity [142, 144, 145]. Very recently, induction of estrogenic responses by equol has been demonstrated *in vivo* using the 3xERE-luciferase mouse model, which allows detection of estrogen activity by light production [146]. On the other hand, isoflavones have the potential to reduce estradiol bioavailability by increasing levels of circulating sex hormone-binding globulin [147, 148]. Obviously, the pro- or anti-estrogenic activities of equol depend on circulating concentrations of estradiol, which markedly vary during puberty, menstrual cycle, and menopause. Isoflavones concentrations in blood may reach up to a maximum of 10 $\mu\text{mol/l}$ after ingestion of phenolic-rich food, which exceeds blood concentration of estradiol by a factor of $> 10,000$ [149]. Interestingly, tissue accumulation of polyphenols (including isoflavones and lignans) has been reported, which likely contributes to modulation of biological properties in target tissues [150–153].

In spite of the aforementioned properties of equol, its direct contribution to health effects is unclear. From the complex metabolite mixtures found in blood and target tissues after soy intervention, it is impossible to relate effects to only one specific molecule. Still, discoveries from the last decade may form the basis of future research to assess the exact role of equol in mediating health effects. Indeed, the fact that single equol-producing bacterial strains are now available allows the design of gnotobiological experiments using animal model of diseases. In such experiments, germfree animals colonized with an equol-producing or non-producing bacterium (a closely related inactive species or a mutant strain in which active enzymes have been knocked-out) could be compared with respect to the development of, for instance, tumors in various tissues or bone disorders in response to ingestion of daidzein-rich diets. In addition, large-scale production of pure enantiomers of equol for use in experimental or even clinical studies will surely help in deciphering direct health effects and underlying molecular mechanisms (US Patent no. 7528267 and 6716424).

To follow up on phytoestrogenic activities of isoflavones *in vivo*, a number of studies have looked at the effect of soy consumption on fertility parameters in adults. Again, there is evidence in animal species [154, 155], but very few data in human [156]. Alteration of semen quality by soy food or isoflavones is questionable [157, 158] and a recent meta-analysis of 15 placebo-controlled studies concluded that soy or isoflavone consumption is not associated with changes in testosterone levels in healthy men [159]. In contrast, peri- and postmenopausal women represent a target population of particular relevance. We will here focus only on the effect of isoflavones on osteoporosis, which has been intensively studied in postmenopausal women and represent a major public health problem [160]. Readers interested in the effects of isoflavones on cardiovascular risks and breast cancer may refer to already published comprehensive papers [13, 14, 161–163]. Osteoporosis is characterized by low bone mass, deterioration of bone tissue, and disruption of bone microarchitecture resulting in compromised bone strength and increased fracture risk [160]. The diagnosis of osteoporosis is primarily established by measurement of bone mineral density (BMD) [164]. Of course, genetic factors determine peak bone mass. However, studies involving twins indicate that environmental factors, including dietary habits, play a substantial role in the pathogenesis of osteoporosis [165].

Again, the EFSA refuted claims related to the use of soy isoflavones for maintenance of BMD [125]. This highlights the difficulty to reach consistency in experimental setups required for drawing conclusion on definite intake of isoflavones associated with long-term health benefits. Nevertheless, there is a growing body of valid scientific data showing overall that beneficial effects of isoflavones on bone disorders in elderly women are promising [161]. In two recent meta-analyses [166, 167], Ma et al. selected randomized controlled trials (RCT) investigating the effects of soy isoflavones on BMD and markers of bone turnover in peri- and postmenopausal women. Based on a total of 19 RCT with an intervention period of 1–24 months and isoflavone intake of 4–150 mg/day, the authors concluded that isoflavone intervention significantly attenuates bone loss of the spine in menopausal women, inhibits bone resorption, and stimulates bone formation. These results were confirmed by even more recent meta-analyses [168, 169]. However, it must be acknowledged that most studies are not appropriate for assessment of soy isoflavone consumption for more than 1 year [12]. Thus, one major remaining challenge is to characterize long-term clinically relevant effects of isoflavones prior to making statements on their use in hormone replacement therapies [170]. In a very recent double-blind RCT, Tai et al. found that treatment with 300 mg/day isoflavones for 2 years did not prevent decline of BMD in lumbar spine and proximal femur in postmenopausal Taiwanese [171].

5.3 Health Effects of Enterolignans

As for isoflavones, there is a vast number of studies investigating various biological properties and potential health effects of lignans [115]. There is good experimental evidence that lignans are beneficial with respect to the development of cardiovascular diseases and breast cancer. It is obvious however that RCT in human subjects are lacking. Interventions based on the use of flaxseeds as main lignan source have revealed promising effects with respect to reduction of prostate cancer proliferation [172, 173], tumor growth in breast cancer patients [174–176], and low-density lipoprotein (LDL) cholesterol levels [22, 177]. In addition, recent data from the EPIC study (European Prospective Investigation into Cancer and Nutrition) suggested that lignan intake decreases colon cancer risk in women [178]. However, because flaxseeds contain substantial amounts of fibers and oil, it is not possible to distinguish between direct effects of lignans and confounding or synergistic effects of fibers and oil. We will thus focus hereafter only on studies assessing health effects that can be attributed to pure lignans converted *in vivo* to the enterolignans ED and EL by gut bacteria. Unfortunately, viewed from that perspective, the number of human intervention trials shrinks further away. We found only two different double-blind RCT, in which authors analyzed the effect of flaxseed extracts enriched in SDG (ca. 30 % dry mass). Hallund et al. found that an intervention with 500 mg/day SDG equivalent for 6 weeks in 22 healthy postmenopausal women marginally reduced C-reactive protein concentrations and had no effect on endothelial function and plasma lipid concentrations [179–181].

In another trial involving 78 subjects with benign prostatic hyperplasia, ingestion of a flaxseed lignan extract (>300 mg/day SDG equivalent) over a 4-month period significantly improved International Prostate Symptom and Quality of Life Scores [182]. It is thus again in laboratory animals that most of the beneficial effects of pure lignans have been reported. In rodents, Lilian Thompson and colleagues found that SDG reduces or delays mammary tumor growth [183–185], affects mammary gland structure [186, 187], reduces metastasis in the lung [188] as well as colon carcinogenesis (number of aberrant crypt foci after azoxymethane treatment) [189]. In contrast, matairesinol and secoisolariciresinol did not protect against intestinal tumor formation in Min mice [190]. More recently, lariciresinol was found to attenuate mammary tumor growth in xenograft- and carcinogen-induced rat models [191]. With respect to cardiovascular risks, SDG was found to reduce the incidence of atherosclerosis in rabbits and to induce neovascularization-mediated cardioprotection in rats [192–194].

Biological properties underlying the aforementioned protective effects of lignans are not well characterized, especially *in vivo*. As stated in Sect. 2, plant lignans are usually less active than enterolignans, which are thus seen as paradigm metabolites for the relevance of bacterial conversion. *In vitro* studies showed that EL has slightly higher binding affinity for the human pregnane X receptor, which mediates induction of enzymes involved in steroid metabolism and xenobiotic detoxification, than its precursor secoisolariciresinol [195]. Moreover, EL binds to estrogen receptors, with a preference for ER- α [142, 196], and can activate estrogen responsive elements [197]. Both ED and EL modulate ER- α mRNA and protein contents and compete dose dependently with estradiol and the unsaturated fatty acid arachidonic acid for binding site on rat and human α -fetoprotein, an estradiol-binding protein [198, 199]. However, binding affinities of enterolignans appear to be 10–10,000-fold lower than those of other phytoestrogens or sex hormones. Both enterolignans and plant lignans also bind to sex hormone-binding globulin, with possible consequences on circulating levels of the sex hormones testosterone and estradiol [200]. The estrogen-dependent properties of ED and EL include as well inhibition of aromatase, 5 α -reductase, and 17 β -hydroxysteroid dehydrogenase, three enzymes involved in the metabolism of growth-promoting steroid hormones [201–204]. Besides, EL was found to induce the expression of the estrogen-responsive protein pS2 in human breast cancer MCF-7 cells [205]. This and other *in vitro* studies showed that ED and EL alter cell proliferation of various breast, colon, and prostate cell lines, as well as endothelial cells derived from bovine brain capillaries [206–210]. *In vitro*, both ED and EL have also higher antioxidant activities than plant precursors [211, 212]. *In vivo*, short-term feeding of SDG to rats only led to minor changes in the antioxidant status of hepatic tissue [213].

To conclude on the last two sections on health effects, one can say that polyphenols are generally regarded as safe and there are only a few reports on possible toxic effects (yet not in the case of isoflavones and lignans in humans) [214–217]. However, polyphenols have the potential to interact with sensitive hormonal systems. Moreover, as implied above when discussing bioavailability, efficient conjugation and excretion mechanisms as well as relatively low phenolic concentrations in blood

(<200 nmol/l without intervention [51, 218, 219]), when compared with other molecules of dietary origin (sugars, amino acids, acetate, etc . . .), are hallmarks of efficient host metabolism dedicated to the elimination of exogenous molecules. Thus, one should not presume that biological properties of phenolics are solely synonyms of beneficial effects, for example, equol may trigger hyperplasia of rat uterine tissue [220] and lignans have been shown to affect pregnancy outcome, reproductive development, and estrous cycling in rats and women [221–223].

Isoflavones are promising with respect to improvement of osteoporosis in postmenopausal women, but long-term effects and dose/activity relationship must be further investigated. Regarding lignans, data obtained using animal models of cancer and cardiovascular disorders are promising too. However, there is a paucity of data in human subjects. In both cases (isoflavones and lignans), direct in vivo effects of bacterial metabolites is a future research area of particular interest.

6 Impact of Phenolics on Intestinal Microbiota

One fundament of intestinal ecosystems is the triad between dietary components, intestinal microorganisms, and the host. Over the last century, medical microbiology had been a dominant field of research and the focus was mainly placed on the study of bacteria-host interactions. However, over the last 20 years, the impact of nutrition on human health and the intestinal microbiome has gained a lot more attention in westernized countries [5]. This is mainly due to: (1) research-founded breakthroughs (molecular mechanisms underlying benefits or deleterious effects of specific dietary molecules are being described); (2) shifts in public health challenges and mentalities (while many bacterial infections are no major threat anymore, chronic disorders such as allergies, obesity, and inflammatory diseases in an ever-aging population represent an increasing social and economical burden; meanwhile, many people are concerned about self-improvement of well-being via nutrition); and (3) market-driven issues (global food companies are lured by profits associated with massive consumption of functional foods and nutraceuticals).

There is nowadays strong evidence that diet greatly influences the composition of intestinal microbiota. The most studied dietary components having striking effects on microbial diversity are fat and fibers [224, 225]. In contrast, the effect of dietary microcomponents like polyphenols on intestinal microbiota is much less known, in spite of various possible mechanisms of actions. First of all, the fact that the conversion of phenolics is under the control of bacterial metabolic chains means that any substrate affecting one chain link has the potential to alter the entire system. Secondly, there is good indication that phenolic extracts and pure phenolics have antimicrobial properties and may thereby alter the growth of intestinal bacteria like clostridia, bacilli, and members of the *Enterobacteriaceae* [226–229]. In addition, since gene expression of enzymes catalyzing, for instance, dehydroxylation can be induced by matching substrates [230], it is possible that polyphenols directly influence core gut microbial functions. At the same time, the growth of phenolic-metabolizing bacteria may be favored if conversion provides

a net energy input for the bacteria. This could lead in parallel to increased competitive advantage and thus indirect growth inhibition of other bacterial groups. Finally, certain polyphenols or metabolites thereof may interfere with quorum sensing, a molecular system that coordinates gene expression of, for instance, virulence factors according to bacterial cell density [226–229]. In spite of these mechanisms, which must still be substantiated by further investigations, there is to the best of our knowledge only 11 papers reporting effects of phenolic compounds on intestinal microbiota. In vitro experiments showed that incubation of fecal slurries with tea extracts prevented growth of clostridia [231]. Possemiers et al. showed that the hop prenylflavonoid isoxanthohumol increased the abundance of members of the *Clostridium* cluster XIV as well as bifidobacteria in a continuous culture system [232]. In rats, Hanske et al. found that xanthohumol does not affect the diversity of dominant fecal microbial communities, as analyzed by denaturing-gradient gel electrophoresis [233]. Smith et al. reported that a diet rich in proanthocyanidins increased the occurrence of *Enterobacteriaceae* and *Bacteroides* in rat feces [234]. The remaining papers relate to human intervention trials. Tea polyphenols increased viable counts of bifidobacteria and decreased counts of *Clostridium perfringens* in eight Japanese healthy adults [235], but had no major impact on fecal microbiota in six hypercholesterolemic volunteers [236]. We found in 2005 that a dietary treatment with 100 mg isoflavones per day for 1 month altered the bacterial diversity and composition in fecal samples from 39 postmenopausal women [71]. Very recently, Tzounis et al. found that a diet rich in cocoa-derived flavanols (494 mg/day) consumed for 4 weeks by 22 healthy human volunteers increased the proportion of lactic acid bacteria by a factor of two, as measured by in situ hybridization [237]. The same authors had previously reported that 150 mg/l of the flavanol monomers epicatechin and catechin stimulated growth of bifidobacteria, *E. coli* and members of the *Firmicutes* in vitro [238]. With respect to bacterial activities, Wiseman et al. found that soy consumption for 10 weeks increased beta-glucosidase activity in feces from 76 healthy young adults [239]. Finally, Hoey et al. reported two- to tenfold lower counts of bacteria in feces from ten infants (aged 4–12 months) fed a soya- versus milk-based formula [74]. However, the fecal concentration of total short chain fatty acids (ca. 45 $\mu\text{mol/g}$) as well as beta-glucosidase and glucuronidase activities (both ca. 10–25 $\mu\text{mol/h per g}$) were unchanged.

Bottom line is that the amount of data is too limited to draw firm conclusions on the impact of phenolics on intestinal microbiota. The task ahead is challenging due to the diversity of phenolics in food as well as interindividual intestinal microbial profiles. The use of next generation molecular approaches will be crucial for the identification of core responses to dietary phenolics at the level of the entire gut microbial ecosystem. High-throughput 16 S ribosomal RNA sequencing allows for instance in-depth characterization of changes in bacterial diversity. However, it will be essential to translate the meaning of such structural changes for host health development, since microbial functions are the driving force of bacteria-host interactions and changes in diversity are not necessarily linked to changes in ecosystem functions. Ecological approaches, such as metatranscriptomic

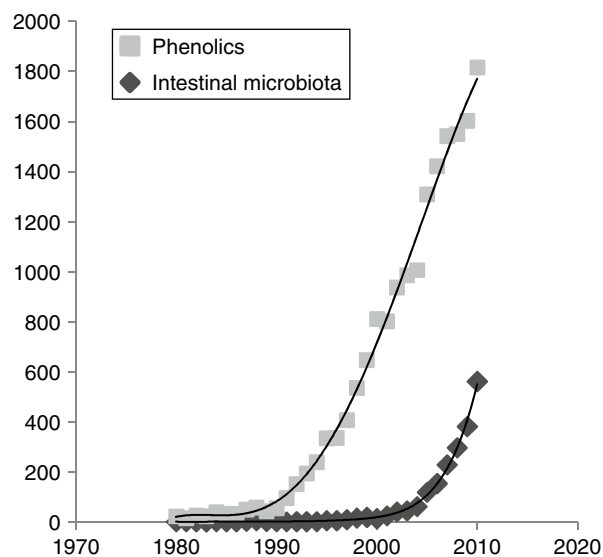
or metabolomic, for gene or metabolite expression profiling could be used for identification of core microbial functional markers under the influence of dietary phenolics [240].

7 Can We Potentiate Intestinal Microbial Metabolism?

The pace of research involving phenolic compounds has rapidly increased over the last two decades (Fig. 78.2). One obvious underlying reason is the wish to prevent or cure diseases by means of natural products. Since intestinal bacteria are essential for phenolic bioavailability and associated health effects, nutritional strategies favoring production of active metabolites via the microbiome look very attractive. As seen above, the use of antibiotics is the best proof-of-concept that influencing metabolite production by targeting intestinal microbial communities is promising [56, 60, 241–244]. However, there is to date no valid data substantiating the theory of diet-driven optimization of microbial phenolic conversion.

The link between intake of specific dietary components and phenolic metabolite production is unclear. Although increased excretion of equol has been associated with increased consumption of fat, meat, and fruits, for instance [82, 152, 245–247], and enterolignans excretion seems to correlate well with dietary intake of fibers [248–250], more work is needed to reach consensus in results. Nonetheless, it is clear that ingestion of isoflavone and lignan food substrates enhance production of equol and enterolignans [33, 251–253]. An intriguing question is however to know whether the activity or growth of phenolic-activating bacteria can be specifically induced, that is, in the case of equol, for example, whether non-equol producers on

Fig. 78.2 Publication output in the field of phenolic research and intestinal microbiota. The PubMed database of the National Center for Biotechnology Information (www.ncbi.nlm.nih.gov/pubmed) was searched for the number of articles per year (from 1980 until 2010) responding to the following queries: “intestinal microbiota” (*black diamonds*) and “phenolics OR phytoestrogens OR polyphenols” (*gray squares*)



their usual diet can become producers, thanks to ingestion of appropriate plant substrates. In 12 Caucasian postmenopausal women, Védrine et al. found that isoflavone intervention (100 mg/day) increased plasma equol concentrations from 0.31 to 0.99 $\mu\text{mol/l}$ in equol producers, but that the seven volunteers classified as non-equol producers did not acquire the ability to produce equol after 1 month exposure [251]. In contrast, another study in China revealed a higher proportion of equol producers among 200 healthy adults challenged with a soy-isoflavone supplement for 3 days (60 % equol producers after supplementation vs. 27 % at baseline) [254]. Here too, more work is needed to draw firm conclusions on equol phenotype changes and influence of demographic origin on phenolic bioavailability [245, 255, 256].

Probiotics are defined as live microorganisms that, when administered in adequate amounts, confer a health benefit to the host [257]. Their use has drawn quite some attention for improvement of phenolic activation in the gut based on the rationale that glucosidases from probiotic lactic acid bacteria (mainly lactobacilli and bifidobacteria) may enhance phenolic bioavailability by increasing concentrations of aglycones. However, the dominance of endogenous phenolic-deglycosylating *Bacteroides*, *Bifidobacterium*, and *Clostridium* spp. in the intestine suggests that deglycosylation is not a limiting step in the in vivo production of active metabolites. Moreover, while there are many reports on the fermentation of soy products by probiotic bacteria, all ten intervention trials based on soy and probiotic treatment in human subjects failed to demonstrate any positive effects of probiotic bacteria [258–267]. Concerning lignans, the only one study available also failed to show any beneficial probiotic effects [268]. More interestingly, researchers in the group of Willy Verstraete at Ghent University have successfully used phenolic-converting bacteria originating from the human intestine, such as *Eubacterium limosum* catalyzing demethylation, to enhance the activation of isoflavones and isoxanthohumol in continuous culture systems and in rats [269, 270].

Functional food products also include prebiotics like fructooligosaccharides (FOS) and inulin, which are nondigestible food ingredients that beneficially affect the host by selectively stimulating the growth and/or activity of one or a limited number of bacterial species already resident in the colon [271]. The prebiotic concept was first coined in 1995 by Glenn Gibson and the bifidogenic effect of FOS and inulin has since then been confirmed by many studies. In contrast, there are only a few reports on the influence of prebiotics on isoflavone bioavailability. Steer and colleagues showed in vitro that 10 g/l FOS in combination with soyabean isoflavones significantly prevented genistein breakdown in continuous culture system vessels [272]. Similar results were obtained by Piazza et al. using inulin in a randomized double-blind crossover study enrolling 12 healthy postmenopausal women [273]. The authors found increased plasma concentration of daidzein and genistein after inulin treatment (approximately 7 g/day) for 21 days. Possible synergistic effects of combined isoflavone and prebiotic intervention are of particular interest with respect to health parameters such as blood lipid profiles or bone density and calcium homeostasis [274–276].

8 Conclusion

The issue of phenolics in human nutrition bears resemblance to industrialized production factories, where input of raw materials is important, yet processing strategies determine the quality of final products. That is, the amount of phenolics that we eat makes of course a difference, but metabolism within the body determines their fate and health effects. Future prospects related to phenolic bioavailability (especially bacterial metabolism) that have been evoked throughout the chapter are summarized in [Table 78.3](#).

Intestinal microbial functions are essential for conversion of a vast majority of dietary phenolics, for example, isoflavone and lignan activation. The main future

Table 78.3 Take home messages and future challenges^a

Facts	Perspectives
Human diet contains a wealth of highly diverse phenolic compounds	Implementation of phenolic databases is crucial for good estimation of intake depending on dietary habits
Plant phenolics can be absorbed in the upper GI tract	Transport mechanisms and kinetic of appearance in blood must be characterized in detail, especially in relation to chemical structure
The intestinal microbiota is highly diverse and has a vast metabolic potential	Functional metagenomic screening is a promising approach for characterization of bacterial genes involved in phenolic conversion
Bacterial culture allows isolation of phenolic-converting bacteria	Identified strains can now be used for colonization of experimental animal models and for large-scale production of pure phenolics
Isoflavones may improve osteoporosis in postmenopausal women, and lignans can protect against tumor growth and atherosclerosis in animal models	More clinical data are needed; long-term effects must be defined Studies in gnotobionts or using pure substances are required for assessing direct health effects of equol and enterolignans in vivo
Health effects depend on the type of bacterial metabolites produced	Effort must be put into studying enantiospecificity of bacterial conversion
There are large interindividual differences in the ability to metabolize plant phenolics in the gut	High-throughput sequencing and metabolite analysis will allow dynamic characterization of the gut microbial ecosystem in human intervention trials
Intestinal microbiota is sensitive to dietary changes	Impact of phenolics on gut microbial diversity and activities must be further studied Use of pre- and probiotics to increase bacterial production of active metabolites is not yet scientifically founded
Infants can be exposed to substantial amounts of phenolics and colonization events determine the metabolic potential of intestinal microbiota	Epidemiological data on the impact of chronic early exposure to phenolics are warranted and effort should be put in characterizing the establishment of intestinal microbiota in large infant cohorts

challenge for microbiologists working in the field of phenolics and human nutrition is to characterize metabolic networks at the level of the entire intestinal ecosystem, in relation to host functions. New generation molecular techniques will certainly help taking on this challenge, although computer analysis of the colossal amounts of data generated by high-throughput methods is a high hurdle for most microbiologists. It would be valuable, for instance, if large-scale human intervention trials on phenolics were designed so as to include microbiological analysis of intestinal samples via, for instance, sequencing or spectrometry analysis to characterize bacterial diversity and identify core functions of relevance to phenolics. This could lead to the discovery of phenolic-specific enterotypes, as in the sense of specific clusters of microbial species associated with functional profiles of relevance [277], thereby allowing detailed characterization of interindividual differences. The long-term objective is the ability to generate personalized meta-metabolic profiling for development of individualized nutritional strategies [278].

In view of individualized nutritional strategies, we must also say that, even though the focus of the present chapter is the metabolic potential of intestinal microorganisms, host genotype strongly determine health effects of phenolics too. Thus, a challenging task is also to assess the role of host genotype in controlling phenolic health effects, either directly via differential expression of specific key genes (coding for ER or intestinal transporters for instance) or indirectly via alteration of microbiota [279].

Finally, it is important to remember that early life periods are critical for shaping the intestinal microbiome. More effort should be put into characterizing intestinal microbiota development in infants and the implication of early dietary exposure to phenolics for health homeostasis later in life. To date, it is also not possible to provide clear recommendations with respect to dietary intake of isoflavones or lignans for treatment or prevention of diseases. Nevertheless, good evidence has been accumulating regarding improvement of bone disorders in postmenopausal women by isoflavones and cardiovascular risks as well as breast cancer by lignans. More clinical and epidemiological data are mandatory and effort should be put into performing experiments in gnotobiotic animal models of disease to draw firm conclusions on the direct role of bacterial metabolites, such as equol and enterolignans, in host health.

Acknowledgments We are grateful to Prof. Hannelore Daniel (TU München, Molecular Nutrition Unit), Dr. Laura Hanske (German Institute of Human Nutrition Postdam-Rehbrücke, Department of Gastrointestinal Microbiology), Dr. Gemma Henderson (Grasslands Research Centre, AgResearch) and Dr. Augustin Scalbert (Clermont University, Department of Human Nutrition) for critically reading the manuscript and giving helpful recommendations.

References

1. Leonard WR, Snodgrass JJ, Robertson ML (2007) *Annu Rev Nutr* 27:311
2. Sluijs I, van der Schouw YT, van der AD, Spijkerman AM, Hu FB, Grobbee DE, Beulens JW (2011) *Am J Clin Nutr* 92:905
3. Gonzalez CA, Riboli E (2011) *Eur J Cancer* 46:2555
4. Crowe FL, Roddam AW, Key TJ et al (2011) *Eur Heart J* 32:1235

5. Kau AL, Ahern PP, Griffin NW, Goodman AL, Gordon JI (2011) *Nature* 474:327
6. Qiu J (2007) *Nature* 448:126
7. Fardet A, Llorach R, Martin JF, Besson C, Lyan B, Pujos-Guillot E, Scalbert A (2008) *J Proteome Res* 7:2388
8. van Wietmarschen H, Yuan K, Lu C et al (2009) *J Clin Rheumatol* 15:330
9. Ehrman TM, Barlow DJ, Hylands PJ (2007) *J Chem Inf Model* 47:2316
10. Messina M (2010) *J Nutr* 140:1350S
11. Setchell KD, Gosselin SJ, Welsh MB, Johnston JO, Balistreri WF, Kramer LW, Dresser BL, Tarr MJ (1987) *Gastroenterology* 93:225
12. Liu J, Ho SC, Su YX, Chen WQ, Zhang CX, Chen YM (2009) *Bone* 44:948
13. Anderson JW, Bush HM (2011) *J Am Coll Nutr* 30:79
14. Wu AH, Yu MC, Tseng CC, Stanczyk FZ, Pike MC (2009) *Am J Clin Nutr* 89:1145
15. Clavel T, Henderson G, Engst W, Dore J, Blaut M (2006) *FEMS Microbiol Ecol* 55:471
16. Milder IE, Arts IC, van de Putte B, Venema DP, Hollman PC (2005) *Br J Nutr* 93:393
17. Begum AN, Nicolle C, Mila I et al (2004) *J Nutr* 134:120
18. Setchell KD, Lawson AM, Mitchell FL, Adlercreutz H, Kirk DN, Axelson M (1980) *Nature* 287:740
19. Stitch SR, Toumba JK, Groen MB, Funke CW, Leemhuis J, Vink J, Woods GF (1980) *Nature* 287:738
20. Axelson M, Sjoval J, Gustafsson BE, Setchell KD (1982) *Nature* 298:659
21. McCann MJ, Gill CI, McGlynn H, Rowland IR (2005) *Nutr Cancer* 52:1
22. Pan A, Yu D, Demark-Wahnefried W, Franco OH, Lin X (2009) *Am J Clin Nutr* 90:288
23. Buck K, Zaineddin AK, Vrieling A, Linseisen J, Chang-Claude J (2010) *Am J Clin Nutr* 92:141
24. Scalbert A, Andres-Lacueva C, Arita M, Kroon P, Manach C, Urpi-Sarda M, Wishart D (2011) *J Agric Food Chem* 59:4331
25. Zamora-Ros R, Andres-Lacueva C, Lamuela-Raventos RM et al (2010) *J Am Diet Assoc* 110:390
26. Manach C, Scalbert A, Morand C, Remesy C, Jimenez L (2004) *Am J Clin Nutr* 79:727
27. Milder IE, Feskens EJ, Arts IC, Buenode Mesquita HB, Hollman PC, Kromhout D (2005) *J Nutr* 135:1202
28. Ovaskainen ML, Torronen R, Koponen JM, Sinkko H, Hellstrom J, Reinivuo H, Mattila P (2008) *J Nutr* 138:562
29. Perez-Jimenez J, Neveu V, Vos F, Scalbert A (2010) *J Agric Food Chem* 58:4959
30. Perez-Jimenez J, Fezeu L, Touvier M, Arnault N, Manach C, Hercberg S, Galan P, Scalbert A (2011) *Am J Clin Nutr* 93:1220
31. Ritchie MR, Cummings JH, Morton MS, Michael Steel C, Bolton-Smith C, Riches AC (2006) *Br J Nutr* 95:204
32. Chun OK, Chung SJ, Song WO (2007) *J Nutr* 137:1244
33. Kuijsten A, Arts IC, van't Veer P, Hollman PC (2005) *J Nutr* 135:2812
34. Cassidy A, Brown JE, Hawdon A, Faughnan MS, King LJ, Millward J, Zimmer-Nechemias L, Wolfe B, Setchell KD (2006) *J Nutr* 136:45
35. Kimira M, Arai Y, Shimoi K, Watanabe S (1998) *J Epidemiol* 8:168
36. Petti S, Scully C (2009) *J Dent* 37:413
37. Crespy V, Morand C, Besson C, Manach C, Demigne C, Remesy C (2002) *J Agric Food Chem* 50:618
38. Passamonti S, Vrhovsek U, Vanzo A, Mattivi F (2003) *FEBS Lett* 544:210
39. Clavel T, Borrmann D, Braune A, Dore J, Blaut M (2006) *Anaerobe* 12:140
40. Mazur W, Fotsis T, Wahala K, Ojala S, Salakka A, Adlercreutz H (1996) *Anal Biochem* 233:169
41. Nemeth K, Plumb GW, Berrin JG, Juge N, Jacob R, Naim HY, Williamson G, Swallow DM, Kroon PA (2003) *Eur J Nutr* 42:29
42. Day AJ, Canada FJ, Diaz JC, Kroon PA, McLauchlan R, Faulds CB, Plumb GW, Morgan MR, Williamson G (2000) *FEBS Lett* 468:166
43. Crespy V, Morand C, Besson C, Manach C, Demigne C, Remesy C (2001) *J Nutr* 131:2109

44. Lafay S, Morand C, Manach C, Besson C, Scalbert A (2006) *Br J Nutr* 96:39
45. Naz S, Siddiqi R, Dew TP, Williamson G (2011) *J Agric Food Chem* 59:2734
46. Walle T, Browning AM, Steed LL, Reed SG, Walle UK (2005) *J Nutr* 135:48
47. Penalvo JL, Nurmi T, Haajanen K, Al-Maharik N, Botting N, Adlercreutz H (2004) *Anal Biochem* 332:384
48. Smeds AI, Hakala K, Hurmerinta TT, Kortela L, Saarinen NM, Makela SI (2006) *J Pharm Biomed Anal* 41:898
49. Mathey J, Lamothe V, Coxam V, Potier M, Sauviant P, Bennetau-Pelissero C (2006) *J Pharm Biomed Anal* 41:957
50. Setchell KD, Zhao X, Jha P, Heubi JE, Brown NM (2009) *Am J Clin Nutr* 90:1029
51. Manach C, Williamson G, Morand C, Scalbert A, Remesy C (2005) *Am J Clin Nutr* 81:230S
52. Konishi Y, Kobayashi S, Shimizu M (2003) *J Agric Food Chem* 51:7296
53. Nicolin V, Grill V, Micali F, Narducci P, Passamonti S (2005) *J Mol Histol* 36:45
54. Vanzo A, Terdoslavich M, Brandoni A, Torres AM, Vrhovsek U, Passamonti S (2008) *Mol Nutr Food Res* 52:1106
55. Watanabe H, Yashiro T, Tohjo Y, Konishi Y (2006) *Biosci Biotechnol Biochem* 70:1928
56. Franke AA, Custer LJ, Hundahl SA (2004) *Nutr Cancer* 50:141
57. Sfakianos J, Coward L, Kirk M, Barnes S (1997) *J Nutr* 127:1260
58. Ridlon JM, Kang DJ, Hylemon PB (2006) *J Lipid Res* 47:241
59. Kilkkinen A, Pietinen P, Klaukka T, Virtamo J, Korhonen P, Adlercreutz H (2002) *Am J Epidemiol* 155:472
60. Setchell KD, Lawson AM, Borriello SP et al (1981) *Lancet* 2:4
61. Cebra JJ (1999) *Am J Clin Nutr* 69:1046S
62. Goodman AL, Kallstrom G, Faith JJ, Reyes A, Moore A, Dantas G, Gordon JI (2011) *Proc Natl Acad Sci USA* 108:6252
63. Becker N, Kunath J, Loh G, Blaut M (2011) *Gut Microbes* 2:25
64. Hanske L, Loh G, Sczesny S, Blaut M, Braune A (2009) *J Nutr* 139:1095
65. Hanske L, Loh G, Sczesny S, Blaut M, Braune A (2010) *Mol Nutr Food Res* 54:1405
66. Bowey E, Adlercreutz H, Rowland I (2003) *Food Chem Toxicol* 41:631
67. Woting A, Clavel T, Loh G, Blaut M (2010) *FEMS Microbiol Ecol* 72:507
68. Qin J, Li R, Raes J et al (2010) *Nature* 464:59
69. Mahowald MA, Rey FE, Seedorf H et al (2009) *Proc Natl Acad Sci USA* 106:5859
70. Tap J, Mondot S, Levenez F et al (2009) *Environ Microbiol*. doi:10.1111/j.1462-2920.2009.01982.x
71. Clavel T, Fallani M, Lepage P et al (2005) *J Nutr* 135:2786
72. Zoetendal EG, Akkermans AD, De Vos WM (1998) *Appl Environ Microbiol* 64:3854
73. Koenig JE, Spor A, Scalfone N, Fricker AD, Stombaugh J, Knight R, Angenent LT, Ley RE (2011) *Proc Natl Acad Sci USA* 108(Suppl 1):4578
74. Hoey L, Rowland IR, Lloyd AS, Clarke DB, Wiseman H (2004) *Br J Nutr* 91:607
75. Cao Y, Calafat AM, Doerge DR, Umbach DM, Bernbaum JC, Twaddle NC, Ye X, Rogan WJ (2009) *J Expo Sci Environ Epidemiol* 19:223
76. Fallani M, Amarri S, Uusijarvi A et al (2011) *Microbiology* 157:1385
77. Dominguez-Bello MG, Costello EK, Contreras M, Magris M, Hidalgo G, Fierer N, Knight R (2010) *Proc Natl Acad Sci USA* 107:11971
78. Roger LC, Costabile A, Holland DT, Hoyles L, McCartney AL (2010) *Microbiology* 156:3329
79. Penders J, Vink C, Driessen C, London N, Thijs C, Stobberingh EE (2005) *FEMS Microbiol Lett* 243:141
80. Willing BP, Russell SL, Finlay BB (2011) *Nat Rev Microbiol* 9:233
81. Xu X, Harris KS, Wang HJ, Murphy PA, Hendrich S (1995) *J Nutr* 125:2307
82. Rowland IR, Wiseman H, Sanders TA, Adlercreutz H, Bowey EA (2000) *Nutr Cancer* 36:27
83. Possemiers S, Bolca S, Eeckhaut E, Depypere H, Verstraete W (2007) *FEMS Microbiol Ecol* 61:372

84. Clavel T, Henderson G, Alpert CA, Philippe C, Rigottier-Gois L, Dore J, Blaut M (2005) *Appl Environ Microbiol* 71:6077
85. Braune A, Maul R, Schebb NH, Kulling SE, Blaut M (2010) *Mol Nutr Food Res* 54:929
86. Selma MV, Espin JC, Tomas-Barberan FA (2009) *J Agric Food Chem* 57:6485
87. Possemiers S, Bolca S, Verstraete W, Heyerick A (2011) *Fitoterapia* 82:53
88. Wang LQ, Meselhy MR, Li Y, Qin GW, Hattori M (2000) *Chem Pharm Bull(Tokyo)* 48:1606
89. Mapesa JO, Waldschmitt N, Schmoeller I, Blume C, Hofmann T, Mahungu S, Clavel T, Haller D (2011) *Mol Nutr Food Res* 55:1850
90. Clavel T, Lippman R, Gavini F, Dore J, Blaut M (2007) *Syst Appl Microbiol* 30:16
91. Bryant MP (1972) *Am J Clin Nutr* 25:1324
92. Dubos RJ, Schaedler RW (1960) *J Exp Med* 111:407
93. Moore WE, Holdeman LV (1974) *Appl Microbiol* 27:961
94. Borriello SP, Setchell KD, Axelson M, Lawson AM (1985) *J Appl Bacteriol* 58:37
95. Wang XL, Hur HG, Lee JH, Kim KT, Kim SI (2005) *Appl Environ Microbiol* 71:214
96. Maruo T, Sakamoto M, Ito C, Toda T, Benno Y (2008) *Int J Syst Evol Microbiol* 58:1221
97. Minamida K, Tanaka M, Abe A, Sone T, Tomita F, Hara H, Asano K (2006) *J Biosci Bioeng* 102:247
98. Minamida K, Ota K, Nishimukai M, Tanaka M, Abe A, Sone T, Tomita F, Hara H, Asano K (2008) *Int J Syst Evol Microbiol* 58:1238
99. Yokoyama S, Suzuki T (2008) *Biosci Biotechnol Biochem* 72:2660
100. Matthies A, Clavel T, Gutschow M, Engst W, Haller D, Blaut M, Braune A (2008) *Appl Environ Microbiol* 74:4847
101. Clavel T, Charrier C, Braune A, Wenning M, Blaut M, Haller D (2009) *Int J Syst Evol Microbiol* 59:1805
102. Schoefer L, Mohan R, Braune A, Birringer M, Blaut M (2002) *FEMS Microbiol Lett* 208:197
103. Shimada Y, Yasuda S, Takahashi M, Hayashi T, Miyazawa N, Sato I, Abiru Y, Uchiyama S, Hishigaki H (2010) *Appl Environ Microbiol* 76:5892
104. Jin JS, Nishihata T, Kakiuchi N, Hattori M (2008) *Biol Pharm Bull* 31:1621
105. Jin JS, Kitahara M, Sakamoto M, Hattori M, Benno Y (2010) *Int J Syst Evol Microbiol* 60:1721
106. Matthies A, Blaut M, Braune A (2009) *Appl Environ Microbiol* 75:1740
107. Tsuji H, Moriyama K, Nomoto K, Miyanaga N, Akaza H (2010) *Arch Microbiol* 192:279
108. Yu ZT, Yao W, Zhu WY (2008) *FEMS Microbiol Lett* 282:73
109. Hur HG, Lay JO Jr, Beger RD, Freeman JP, Rafii F (2000) *Arch Microbiol* 174:422
110. Hur HG, Beger RD, Heinze TM, Lay JO Jr, Freeman JP, Dore J, Rafii F (2002) *Arch Microbiol* 178:8
111. Wang XL, Shin KH, Hur HG, Kim SI (2005) *J Biotechnol* 115:261
112. Zhao H, Wang XL, Zhang HL, Li CD, Wang SY (2011) *Appl Microbiol Biotechnol* 92:803
113. Yokoyama S, Niwa T, Osawa T, Suzuki T (2010) *Arch Microbiol* 192:15
114. Tamura M, Tsushida T, Shinohara K (2007) *Anaerobe* 13:32
115. Adlercreutz H (2007) *Crit Rev Clin Lab Sci* 44:483
116. Thawornkuno C, Tanaka M, Sone T, Asano K (2009) *Biosci Biotechnol Biochem* 73:1435
117. Turnbaugh PJ, Ley RE, Hamady M, Fraser-Liggett CM, Knight R, Gordon JI (2007) *Nature* 449:804
118. Walter J, Mangold M, Tannock GW (2005) *Appl Environ Microbiol* 71:2347
119. Harriott OT, Frazer AC (1997) *Appl Environ Microbiol* 63:296
120. Setchell KD, Clerici C, Lephart ED et al (2005) *Am J Clin Nutr* 81:1072
121. Clavel T, Dore J, Blaut M (2006) *Nutr Res Rev* 19:187
122. Muthyala RS, Ju YH, Sheng S, Williams LD, Doerge DR, Katzenellenbogen BS, Helferich WG, Katzenellenbogen JA (2004) *Bioorg Med Chem* 12:1559
123. Brown NM, Belles CA, Lindley SL, Zimmer-Nechemias LD, Zhao X, Witte DP, Kim MO, Setchell KD (2010) *Carcinogenesis* 31:886
124. EFSA Panel on Dietetic Products (Nutrition and Allergies) (2011) *EFSA J* 9:2264

125. EFSA Panel on Dietetic Products (Nutrition and Allergies) (2009) *EFSA J* 7:1270
126. Akingbemi BT, Braden TD, Kemppainen BW, Hancock KD, Sherrill JD, Cook SJ, He X, Supko JG (2007) *Endocrinology* 148:4475
127. Lewis RW, Brooks N, Milburn GM, Soames A, Stone S, Hall M, Ashby J (2003) *Toxicol Sci* 71:74
128. Su Y, Shankar K, Simmen RC (2009) *J Nutr* 139:945
129. Sharpe RM, Martin B, Morris K, Greig I, McKinnell C, McNeilly AS, Walker M (2002) *Hum Reprod* 17:1692
130. Setchell KD, Zimmer-Nechemias L, Cai J, Heubi JE (1998) *Am J Clin Nutr* 68:1453S
131. Setchell KD, Zimmer-Nechemias L, Cai J, Heubi JE (1997) *Lancet* 350:23
132. Irvine CH, Fitzpatrick MG, Alexander SL (1998) *Proc Soc Exp Biol Med* 217:247
133. Franke AA, Custer LJ, Tanaka Y (1998) *Am J Clin Nutr* 68:1466S
134. Franke AA, Halm BM, Custer LJ, Tatsumura Y, Hebshi S (2006) *Am J Clin Nutr* 84:406
135. Strom BL, Schinnar R, Ziegler EE et al (2001) *JAMA* 286:807
136. Agostoni C, Axelsson I, Goulet O et al (2006) *J Pediatr Gastroenterol Nutr* 42:352
137. Vandenplas Y, De Greef E, Devreker T, Hauser B (2011) *Acta Paediatr* 100:162
138. Chen A, Rogan WJ (2004) *Annu Rev Nutr* 24:33
139. Bernbaum JC, Umbach DM, Ragan NB, Ballard JL, Archer JI, Schmidt-Davis H, Rogan WJ (2008) *Environ Health Perspect* 116:416
140. Cheng E, Story CD, Yoder L, Hale WH, Burroughs W (1953) *Science* 118:164
141. Axelson M, Kirk DN, Farrant RD, Cooley G, Lawson AM, Setchell KD (1982) *Biochem J* 201:353
142. Mueller SO, Simon S, Chae K, Metzler M, Korach KS (2004) *Toxicol Sci* 80:14
143. Morito K, Hirose T, Kinjo J et al (2001) *Biol Pharm Bull* 24:351
144. Hirvonen J, Rajalin AM, Wohlfahrt G, Adlercreutz H, Wahala K, Aarnisalo P (2011) *J Steroid Biochem Mol Biol* 123:46
145. Kostelac D, Rechkemmer G, Briviba K (2003) *J Agric Food Chem* 51:7632
146. Damdimopoulou P, Nurmi T, Salminen A et al (2011) *J Nutr* 141:1583
147. Low YL, Dunning AM, Dowsett M, Luben RN, Khaw KT, Wareham NJ, Bingham SA (2006) *Cancer Res* 66:8980
148. Pino AM, Valladares LE, Palma MA, Mancilla AM, Yanez M, Albala C (2000) *J Clin Endocrinol Metab* 85:2797
149. Stricker R, Eberhart R, Chevailler MC, Quinn FA, Bischof P (2006) *Clin Chem Lab Med* 44:883
150. Saarinen NM, Power KA, Chen J, Thompson LU (2008) *Nutr Cancer* 60:245
151. Rickard SE, Thompson LU (1998) *J Nutr* 128:615
152. Hedlund TE, Maroni PD, Ferucci PG et al (2005) *J Nutr* 135:1400
153. Boccardo F, Lunardi GL, Petti AR, Rubagotti A (2003) *Breast Cancer Res Treat* 79:17
154. Faqi AS, Johnson WD, Morrissey RL, McCormick DL (2004) *Reprod Toxicol* 18:605
155. Guan L, Huang Y, Chen ZY (2008) *Biomed Environ Sci* 21:197
156. Cederroth CR, Auger J, Zimmermann C, Eustache F, Nef S (2010) *Int J Androl* 33:304
157. Beaton LK, McVeigh BL, Dillingham BL, Lampe JW, Duncan AM (2010) *Fertil Steril* 94:1717
158. Chavarro JE, Toth TL, Sadio SM, Hauser R (2008) *Hum Reprod* 23:2584
159. Hamilton-Reeves JM, Vazquez G, Duval SJ, Phipps WR, Kurzer MS, Messina MJ (2010) *Fertil Steril* 94:997
160. Rachner TD, Khosla S, Hofbauer LC (2011) *Lancet* 377:1276
161. Cassidy A, Albertazzi P, Lise Nielsen I et al (2006) *Proc Nutr Soc* 65:76
162. Shu XO, Zheng Y, Cai H, Gu K, Chen Z, Zheng W, Lu W (2009) *JAMA* 302:2437
163. Hooper L, Madhavan G, Tice JA, Leinster SJ, Cassidy A (2010) *Hum Reprod Update* 16:745
164. Cummings SR, Bates D, Black DM (2002) *JAMA* 288:1889
165. Johnson ML, Lara N, Kamel MA (2009) *Genome Med* 1:84
166. Ma DF, Qin LQ, Wang PY, Katoh R (2008) *Clin Nutr* 27:57

167. Ma DF, Qin LQ, Wang PY, Katoh R (2008) *Eur J Clin Nutr* 62:155
168. Taku K, Melby MK, Takebayashi J, Mizuno S, Ishimi Y, Omori T, Watanabe S (2010) *Asia Pac J Clin Nutr* 19:33
169. Taku K, Melby MK, Kurzer MS, Mizuno S, Watanabe S, Ishimi Y (2010) *Bone* 47:413
170. Levis S, Strickman-Stein N, Doerge DR, Krischer J (2010) *Contemp Clin Trials* 31:293
171. Tai TY, Tsai KS, Tu ST et al (2011) *Osteoporos Int* 23:1571
172. Demark-Wahnefried W, Polascik TJ, George SL et al (2008) *Cancer Epidemiol Biomarkers Prev* 17:3577
173. Demark-Wahnefried W, Robertson CN, Walther PJ, Polascik TJ, Paulson DF, Vollmer RT (2004) *Urology* 63:900
174. Sturgeon SR, Heersink JL, Volpe SL et al (2008) *Nutr Cancer* 60:612
175. Thompson LU, Chen JM, Li T, Strasser-Weippl K, Goss PE (2005) *Clin Cancer Res* 11:3828
176. Velentzis LS, Cantwell MM, Cardwell C, Keshtgar MR, Leathem AJ, Woodside JV (2009) *Br J Cancer* 100:1492
177. Bassett CM, Rodriguez-Leyva D, Pierce GN (2009) *Appl Physiol Nutr Metab* 34:965
178. Ward HA, Kuhnle GG, Mulligan AA, Lentjes MA, Luben RN, Khaw KT (2010) *Am J Clin Nutr* 91:440
179. Hallund J, Ravn-Haren G, Bugel S, Tholstrup T, Tetens I (2006) *J Nutr* 136:112
180. Hallund J, Tetens I, Bugel S, Tholstrup T, Bruun JM (2008) *Nutr Metab Cardiovasc Dis* 18:497
181. Hallund J, Tetens I, Bugel S, Tholstrup T, Ferrari M, Teerlink T, Kjaer A, Wiinberg N (2006) *J Nutr* 136:2314
182. Zhang W, Wang X, Liu Y, Tian H, Flickinger B, Empie MW, Sun SZ (2008) *J Med Food* 11:207
183. Chen J, Tan KP, Ward WE, Thompson LU (2003) *Exp Biol Med (Maywood)* 228:951
184. Rickard SE, Yuan YV, Chen J, Thompson LU (1999) *Nutr Cancer* 35:50
185. Thompson LU (1998) *Baillieres Clin Endocrinol Metab* 12:691
186. Tou JC, Thompson LU (1999) *Carcinogenesis* 20:1831
187. Ward WE, Jiang FO, Thompson LU (2000) *Nutr Cancer* 37:187
188. Li D, Yee JA, Thompson LU, Yan L (1999) *Cancer Lett* 142:91
189. Jenab M, Thompson LU (1996) *Carcinogenesis* 17:1343
190. Pajari AM, Smeds AI, Oikarinen SI, Eklund PC, Sjöholm RE, Mutanen M (2006) *Cancer Lett* 233:309
191. Saarinen NM, Warri A, Dings RP, Airio M, Smeds AI, Makela S (2008) *Int J Cancer* 123:1196
192. Penumathsa SV, Koneru S, Thirunavukkarasu M, Zhan L, Prasad K, Maulik N (2007) *J Pharmacol Exp Ther* 320:951
193. Penumathsa SV, Koneru S, Zhan L, John S, Menon VP, Prasad K, Maulik N (2008) *J Mol Cell Cardiol* 44:170
194. Prasad K (2008) *Atherosclerosis* 197:34
195. Jacobs MN, Nolan GT, Hood SR (2005) *Toxicol Appl Pharmacol* 209:123
196. Penttinen P, Jaehrling J, Damdimopoulos AE et al (2007) *Endocrinology* 148:4875
197. Pianjing P, Thiantanawat A, Rangkadilok N, Watcharasit P, Mahidol C, Satayavivad J (2011) *J Agric Food Chem* 59:212
198. Carreau C, Flouriot G, Bennetau-Pelissero C, Potier M (2008) *J Steroid Biochem Mol Biol* 110:176
199. Garreau B, Vallette G, Adlercreutz H, Wahala K, Makela T, Benassayag C, Nunez EA (1991) *Biochim Biophys Acta* 1094:339
200. Schottner M, Spiteller G, Gansser D (1998) *J Nat Prod* 61:119
201. Adlercreutz H, Bannwart C, Wahala K, Makela T, Brunow G, Hase T, Arosemena PJ, Kellis JT Jr, Vickery LE (1993) *J Steroid Biochem Mol Biol* 44:147
202. Brooks JD, Thompson LU (2005) *J Steroid Biochem Mol Biol* 94:461
203. Evans BA, Griffiths K, Morton MS (1995) *J Endocrinol* 147:295
204. Wang C, Makela T, Hase T, Adlercreutz H, Kurzer MS (1994) *J Steroid Biochem Mol Biol* 50:205

205. Sathyamoorthy N, Wang TT, Phang JM (1994) *Cancer Res* 54:957
206. Cosentino M, Marino F, Ferrari M et al (2007) *Pharmacol Res* 56:140
207. Danbara N, Yuri T, Tsujita-Kyutoku M, Tsukamoto R, Uehara N, Tsubura A (2005) *Anticancer Res* 25:2269
208. Fotsis T, Pepper M, Adlercreutz H, Fleischmann G, Hase T, Montesano R, Schweigerer L (1993) *Proc Natl Acad Sci USA* 90:2690
209. Lin X, Switzer BR, Demark-Wahnefried W (2001) *Anticancer Res* 21:3995
210. Mousavi Y, Adlercreutz H (1992) *J Steroid Biochem Mol Biol* 41:615
211. Kitts DD, Yuan YV, Wijewickreme AN, Thompson LU (1999) *Mol Cell Biochem* 202:91
212. Prasad K (2000) *Int J Angiol* 9:220
213. Luiten H, Yuan YV, Rickard SE, Thompson LU (1999) *Nutr Res* 19:1233
214. Yee S, Burdock GA, Kurata Y, Enomoto Y, Narumi K, Hamada S, Itoh T, Shimomura Y, Ueno T (2008) *Food Chem Toxicol* 46:2713
215. Kulling SE, Jacobs E, Pfeiffer E, Metzler M (1998) *Mutat Res* 416:115
216. Cho YM, Imai T, Ito Y, Takami S, Hasumura M, Yamazaki T, Hirose M, Nishikawa A (2009) *Food Chem Toxicol* 47:2150
217. Blaut M, Braune A, Wunderlich S, Sauer P, Schneider H, Glatt H (2006) *Food Chem Toxicol* 44:1940
218. Ozasa K, Nakao M, Watanabe Y et al (2005) *J Epidemiol* 15(Suppl 2):S196
219. Stumpf K, Pietinen P, Puska P, Adlercreutz H (2000) *Cancer Epidemiol Biomarkers Prev* 9:1369
220. Brown NM, Lindley SL, Witte DP, Setchell KD (2011) *Reprod Toxicol* 32:33
221. Orcheson LJ, Rickard SE, Seidl MM, Thompson LU (1998) *Cancer Lett* 125:69
222. Phipps WR, Martini MC, Lampe JW, Slavin JL, Kurzer MS (1993) *J Clin Endocrinol Metab* 77:1215
223. Tou JC, Chen J, Thompson LU (1998) *J Nutr* 128:1861
224. Jumpertz R, Le DS, Turnbaugh PJ, Trinidad C, Bogardus C, Gordon JI, Krakoff J (2011) *Am J Clin Nutr* 94:58
225. Martinez I, Kim J, Duffy PR, Schlegel VL, Walter J (2010) *PLoS One* 5:e15046
226. Sklenickova O, Flesar J, Kokoska L, Vlkova E, Halamova K, Malik J (2010) *Molecules* 15:1270
227. Ozcelik B, Kartal M, Orhan I (2011) *Pharm Biol* 49:396
228. Kim MG, Lee HS (2009) *J Food Sci* 74:M467
229. Hong H, Landauer MR, Foriska MA, Ledney GD (2006) *J Basic Microbiol* 46:329
230. Doerner KC, Takamine F, LaVoie CP, Mallonee DH, Hylemon PB (1997) *Appl Environ Microbiol* 63:1185
231. Lee HC, Jenner AM, Low CS, Lee YK (2006) *Res Microbiol* 157:876
232. Possemiers S, Bolca S, Grootaert C et al (2006) *J Nutr* 136:1862
233. Hanske L, Hussong R, Frank N, Gerhauser C, Blaut M, Braune A (2005) *Mol Nutr Food Res* 49:868
234. Smith AH, Mackie RI (2004) *Appl Environ Microbiol* 70:1104
235. Okubo T, Ishihara N, Oura A, Serit M, Kim M, Yamamoto T, Mitsuoka T (1992) *Biosci Biotechnol Biochem* 56:588
236. Mai V, Katki HA, Harmsen H, Gallaher D, Schatzkin A, Baer DJ, Clevidence B (2004) *J Nutr* 134:473
237. Tzounis X, Rodriguez-Mateos A, Vulevic J, Gibson GR, Kwik-Urbe C, Spencer JP (2011) *Am J Clin Nutr* 93:62
238. Tzounis X, Vulevic J, Kuhnle GG, George T, Leonczak J, Gibson GR, Kwik-Urbe C, Spencer JP (2008) *Br J Nutr* 99:782
239. Wiseman H, Casey K, Bowey EA et al (2004) *Am J Clin Nutr* 80:692
240. Jacobs DM, Deltimple N, van Velzen E, van Dorsten FA, Bingham M, Vaughan EE, van Duynhoven J (2008) *NMR Biomed* 21:615
241. Atkinson C, Berman S, Humbert O, Lampe JW (2004) *J Nutr* 134:596
242. Blair RM, Appt SE, Franke AA, Clarkson TB (2003) *J Nutr* 133:2262

243. Franke AA, Halm BM, Ashburn LA (2008) *Nutr Cancer* 60:627
244. Milder IE, Kuijsten A, Arts IC, Feskens EJ, Kampman E, Hollman PC, Van't Veer P (2007) *J Nutr* 137:1266
245. Atkinson C, Newton KM, Bowles EJ, Yong M, Lampe JW (2008) *Am J Clin Nutr* 87:679
246. Bolca S, Possemiers S, Herregat A et al (2007) *J Nutr* 137:2242
247. Gardana C, Canzi E, Simonetti P (2009) *J Nutr Biochem* 20:940
248. Adlercreutz H, Fotsis T, Heikkinen R, Dwyer JT, Woods M, Goldin BR, Gorbach SL (1982) *Lancet* 2:1295
249. Horner NK, Kristal AR, Prunty J, Skor HE, Potter JD, Lampe JW (2002) *Cancer Epidemiol Biomarkers Prev* 11:121
250. Nurmi T, Mursu J, Penalvo JL, Poulsen HE, Voutilainen S (2010) *Br J Nutr* 103:677
251. Vedrine N, Mathey J, Morand C, Brandolini M, Davicco MJ, Guy L, Remesy C, Coxam V, Manach C (2006) *Eur J Clin Nutr* 60:1039
252. Mazur WM, Uehara M, Wahala K, Adlercreutz H (2000) *Br J Nutr* 83:381
253. Luoto R, Kharazmi E, Saarinen NM, Smeds AI, Makela S, Fallah M, Raitanen J, Hilakivi-Clarke L (2010) *Reprod Health* 7:26
254. Liu B, Qin L, Liu A, Uchiyama S, Ueno T, Li X, Wang P (2010) *J Epidemiol* 20:377
255. Franke AA, Lai JF, Pagano I, Morimoto Y, Maskarinec G (2011) *Br J Nutr* 107:1201–1206
256. Vergne S, Sauviant P, Lamothe V, Chantre P, Asselineau J, Perez P, Durand M, Moore N, Bennetau-Pelissero C (2009) *Br J Nutr* 102:1642
257. Rijkers GT, Bengmark S, Enck P et al (2010) *J Nutr* 140:671S
258. Larkin TA, Price WE, Astheimer LB (2007) *Nutrition* 23:709
259. Larkin TA, Astheimer LB, Price WE (2009) *Eur J Clin Nutr* 63:238
260. Nettleton JA, Greany KA, Thomas W, Wangen KE, Adlercreutz H, Kurzer MS (2005) *J Altern Complement Med* 11:1067
261. Nettleton JA, Greany KA, Thomas W, Wangen KE, Adlercreutz H, Kurzer MS (2005) *J Nutr* 135:603
262. Nettleton JA, Greany KA, Thomas W, Wangen KE, Adlercreutz H, Kurzer MS (2004) *J Nutr* 134:1998
263. Tsangalis D, Wilcox G, Shah NP, Stojanovska L (2005) *Br J Nutr* 93:867
264. McMullen MH, Hamilton-Reeves JM, Bonorden MJ, Wangen KE, Phipps WR, Feirtag JM, Kurzer MS (2006) *J Altern Complement Med* 12:887
265. Bonorden MJ, Greany KA, Wangen KE, Phipps WR, Feirtag J, Adlercreutz H, Kurzer MS (2004) *Eur J Clin Nutr* 58:1635
266. Cohen LA, Crespín JS, Wolper C, Zang EA, Pittman B, Zhao Z, Holt PR (2007) *In Vivo* 21:507
267. Greany KA, Nettleton JA, Wangen KE, Thomas W, Kurzer MS (2004) *J Nutr* 134:3277
268. Kekkonen RA, Holma R, Hatakka K, Suomalainen T, Poussa T, Adlercreutz H, Korpela R (2011) *J Nutr* 141:870
269. Decroos K, Eeckhaut E, Possemiers S, Verstraete W (2006) *J Nutr* 136:946
270. Possemiers S, Rabot S, Espin JC et al (2008) *J Nutr* 138:1310
271. Roberfroid M (2007) *J Nutr* 137:830S
272. Steer TE, Johnson IT, Gee JM, Gibson GR (2003) *Br J Nutr* 90:635
273. Piazza C, Privitera MG, Melilli B, Incognito T, Marano MR, Leggio GM, Roxas MA, Drago F (2007) *Am J Clin Nutr* 86:775
274. Cashman K (2003) *Curr Issues Intest Microbiol* 4:21
275. Mathey J, Mardon J, Fokialakis N et al (2007) *Osteoporos Int* 18:671
276. Wong JM, Kendall CW, de Souza R, Emam A, Marchie A, Vidgen E, Holmes C, Jenkins DJ (2010) *Metabolism* 59:1331
277. Arumugam M, Raes J, Pelletier E et al (2011) *Nature* 473:174
278. Van Duynhoven J, Vaughan EE, Jacobs DM et al (2011) *Proc Natl Acad Sci USA* 108 (Suppl 1):4531
279. Spor A, Koren O, Ley R (2011) *Nat Rev Microbiol* 9:279

PAPER 13

Intestinal microbiota in metabolic diseases

From bacterial community structure and functions to species of pathophysiological relevance

Thomas Clavel,^{1,*} Charles Desmarchelier,^{2,†} Dirk Haller,³ Philippe Gérard,⁴ Sascha Rohn,⁵ Patricia Lepage,⁴ and Hannelore Daniel²

¹Junior Research Group Intestinal Microbiome; ZIEL-Research Center for Nutrition and Food Sciences; Technische Universität München; Freising-Weihenstephan, Germany; ²Molecular Nutrition Unit; ZIEL-Research Center for Nutrition and Food Sciences; Technische Universität München; Freising-Weihenstephan, Germany; ³Chair of Nutrition and Immunology; Biofunctionality Unit; ZIEL-Research Center for Nutrition and Food Sciences; Technische Universität München; Freising-Weihenstephan, Germany; ⁴INRA / AgroParisTech; Micalis UMR1319; Jouy-en-Josas, France; ⁵Institute of Food Chemistry; Hamburg School of Food Science; University of Hamburg; Hamburg, Germany

[†]Current affiliation: UMR 1062 INSERM/ 1260 INRA/ Université d'Aix-Marseille; Faculté de Médecine; Marseille, France

Keywords: obesity, diabetes, high-fat diet, mouse models, intestinal microbiota, metaproteome, metabolomics, bile acids, steroids, *Coriobacteriaceae*

*Correspondence to: Thomas Clavel;
Email: thomas.clavel@tum.de

Submitted: 03/06/2014; Revised:
05/22/2014; Accepted: 05/22/2014;
Published Online: 07/08/2014

<http://dx.doi.org/10.4161/gmic.29331>

Addendum to: Daniel H, Moghaddas Gholami A, Berry D, Desmarchelier C, Hahne H, Loh G, Mondot S, Lepage P, Rothballer M, Walker A, et al. High-fat diet alters gut microbiota physiology in mice. *ISME J* 2014; 8:295–308; PMID:24030595; <http://dx.doi.org/10.1038/ismej.2013.155>

The trillions of bacterial cells that colonize the mammalian digestive tract influence both host physiology and the fate of dietary compounds. Gnotobionts and fecal transplantation have been instrumental in revealing the causal role of intestinal bacteria in energy homeostasis and metabolic dysfunctions such as type-2 diabetes. However, the exact contribution of gut bacterial metabolism to host energy balance is still unclear and knowledge about underlying molecular mechanisms is scant. We have previously characterized cecal bacterial community functions and host responses in diet-induced obese mice using *omics* approaches. Based on these studies, we here discuss issues on the relevance of mouse models, give evidence that the metabolism of cholesterol-derived compounds by gut bacteria is of particular importance in the context of metabolic disorders and that dominant species of the family *Coriobacteriaceae* are good models to study these functions.

Introduction

The communities of microorganisms in our intestinal tract are referred to as the gut microbiota, which is dominated by facultative and strictly anaerobic bacteria of the phyla *Firmicutes*, *Bacteroidetes*,

Actinobacteria, *Verrucomicrobia*, and *Proteobacteria*. These bacteria carry out important metabolic functions for the host via conversion of indigestible dietary substrates and interaction with the immune system.¹

Although the impact of intestinal microbiota on host metabolic functions has been known for decades,² it has recently received attention again following the pioneering work by Jeffrey Gordon and colleagues.³ Massive amounts of data on the gut microbiota in obesity and metabolic disorders has already been obtained by research consortia such as HMP⁴ and MetaHIT⁵ and by many other groups.^{6,7} Most of all, studies on the transfer of gut contents to recipient hosts proved that the presence of specific exogenous microbial communities in the intestine can cause changes in host metabolic phenotypes.^{8–12} State-of-the-art metagenomic work proposed that low bacterial gene counts and shifts in the occurrence of certain species in human feces are associated with obesity and insulin resistance, setting the stage for hypothesis-driven research on bacteria of clinical relevance or for the use of targeted nutritional interventions.^{5,13,14}

In this context, we recently provided novel functional insights into cecal bacterial communities in diet-induced obese mice using a combination of high-resolution

spectrometric techniques.¹⁵ Thereby, we showed that feeding mice a high-fat diet has a major impact on cecal microbiota that extends beyond compositional changes to major alterations in bacterial physiology and metabolite landscape. On the basis of these findings, we review herein some recent highlights in the field of gut microbiota in metabolic diseases, discuss issues on the need for standardized models, and give future perspectives.

Diet Composition and Texture

Recent years have witnessed the popularization of 16S-based analysis of gut bacteria and the use of mice to study diet-induced obesity and associated metabolic complications. Mouse models are helpful to analyze molecular mechanisms underlying metabolic processes and allow direct assessment of the causal role of microorganisms. However, proper comparative analysis between different studies is hampered by highly heterogeneous sample collection, storage, and preparation procedures, as well as various sequencing approaches, animal hygiene status, and feeding protocols. Whereas housing conditions are not easy to standardize due to infrastructure and technical constraints in animal facilities, experimental diets could easily be defined in systematic manners and so could sequencing be improved by utilizing standard samples as references.

Variations between high-fat diets in their ability to cause obesity in germfree mice or to induce shifts in bacterial composition in conventional or re-colonized animals have been reported.¹⁶ With respect to host responses, we showed that a Western-style diet causing obesity via the offered choice of several palatable food items is more detrimental in causing liver pathologies than a classical high-fat diet, which contains more fat but fewer simple sugars.¹⁷ Based on fluorescence in situ hybridization, the Western-style and high-fat diets had also distinct effects on cecal bacterial composition. Compared with control mice on the carbohydrate diet, mice fed the Western-style diet had 3-fold decreased proportions of *Bacteroidaceae*, *Porphyromonadaceae*, and

Prevotellaceae ($P = 0.019$) (Fig. 1A), and increased proportions of the *Clostridium leptum* subgroup ($P = 0.016$), which includes several cellulolytic, butyrate-producing, and bile salt-converting bacteria. Hence, bacterial proportions were mostly affected by the cafeteria diet, supporting the notion that changes in mouse gut microbiota depend more strongly upon diet composition than obesity per se.⁷²

Most importantly, we found that diet-dependent effects not only relate to composition, but also to texture, a parameter that must be taken into consideration in the future. Using standard carbohydrate diets provided either as a powder or in pellet form, we observed that mice became obese due to higher feed intake in the powder group.¹⁷ Interestingly, mice fed the diet as pellets displayed increased cecal weight, pointing at a possible role of the gut microbiota to explain these phenotypic differences. Using high-throughput 16S rRNA gene sequencing,¹⁵ we found that diet texture drives also remarkable shifts in cecal bacterial populations. The powder diet substantially decreased phylotype richness (Fig. 1B) and β -diversity analysis showed a clear clustering between mice fed the powder vs. pellet diet (Fig. 1C). Taxonomic assignment of sequences revealed a marked decrease in the abundance of *Firmicutes*, mainly due to lower sequence proportions of *Lachnospiraceae* and *Ruminococcaceae*. This was accompanied by a bloom of sequences assigned to the genus *Akkermansia* (Fig. 1D), a member of the phylum *Verrucomicrobia* shown to decrease in abundance under high-fat diet feeding and proposed to be negatively associated with fat mass or weight gain, adipose tissue inflammation, endotoxemia, and insulin resistance.^{19,20} It is yet unclear which mechanisms underline the observed effects of diet texture on mouse cecal bacterial diversity and composition. Evidence from the literature suggest that decreased intestinal transit time or increased feed intake related to ingestion of powder diets may affect gut microbial communities.^{21,22}

These examples demonstrate the current limitation of interpreting data on bacterial diversity and composition

obtained in the course of mouse experiments where results largely depend upon experimental conditions, especially feeding protocols. Detailed information on diet composition and texture should be obligatory for publishing and effort in standardization is urgently needed. Moreover, besides collecting descriptive 16S-based data, it is also crucial to analyze bacterial genes or proteins expression and metabolites production in order to generate hypothesis-driven approaches with clear functional targets.

Bacterial Functions with Relevance to Metabolic Disorders

We learnt from studies in gnotobiotic animals that the gut microbiota affects host fat storage, but its exact energetic contribution is not yet defined. Moreover, when compared with many reports on gut bacterial diversity and composition after ingestion of high-energy diets, there is far less functional data available, i.e., knowledge of active bacterial molecules and associated molecular mechanisms is scant.

The gut microbiota can affect host metabolism directly via fermentation processes and the production of bioactive metabolites, or indirectly via for instance modulation of immune responses.¹ Impaired Toll-Like Receptor 5 (TLR5) signaling was shown to drive hyperphagia and hallmarks of the metabolic syndrome in mice, and this phenotype was transmissible via cecal microbiota transfer.²³ Intestinal bacteria are also proposed to affect signaling of the peptide hormones GLP1,²⁴ GLP2,²⁵ and PYY that control intestinal transit, mucosal barrier functions, satiety and numerous processes in peripheral tissues such as the pancreas and liver. Regarding high-fat diet-induced disturbances in bacterial communities and gut barrier, contradictory results have been published, emphasizing again the difficulties in reproducibility of results from different mouse models.²⁶⁻²⁸ In human subjects, there is, to the best of our knowledge, no direct evidence for disturbed intestinal barrier functions associated with obesity besides increased blood levels of lipopolysaccharides.^{29,30} Of

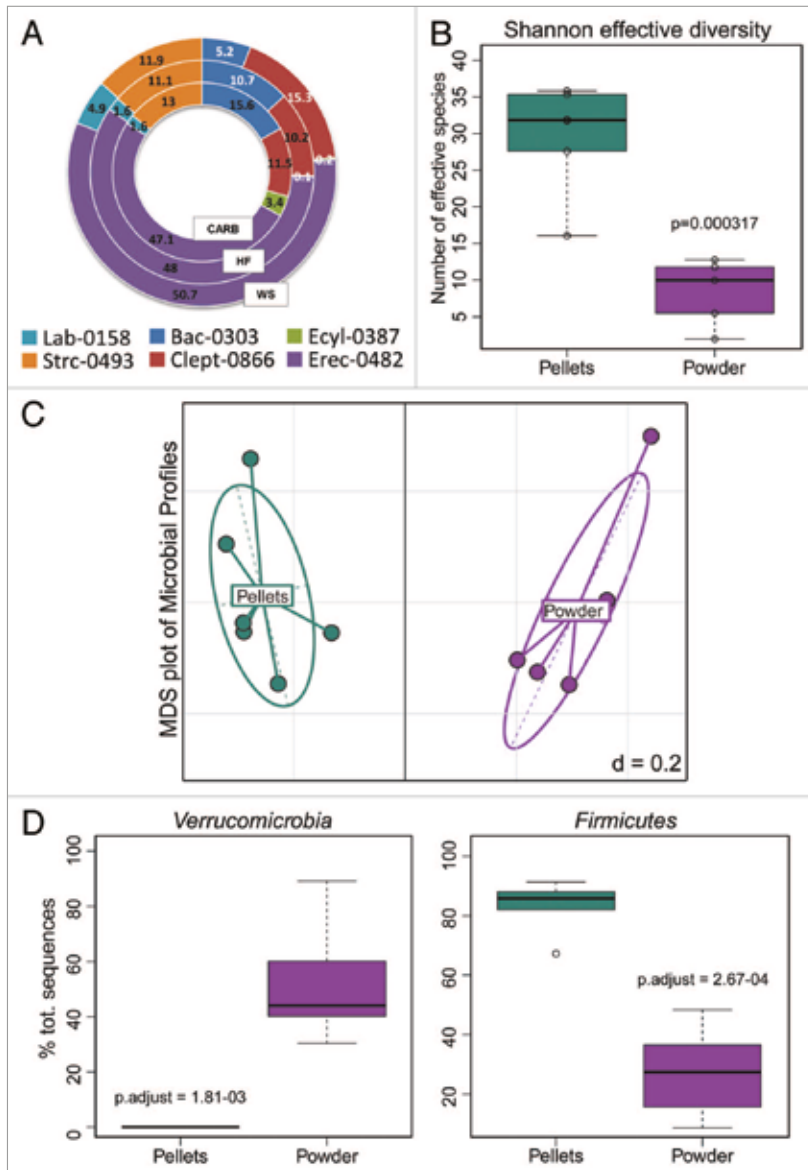


Figure 1. Diet composition and texture alter cecal bacterial populations. **(A)** Mean percentages of total bacteria (probe Eub-0338) using in situ hybridization with flow cytometry (LSRII System, BD Biosciences).⁶⁵ A total of 100 000 events was acquired in duplicate for each sample (n = 6 mice). Values in white differed significantly from controls ($P < 0.05$; ANOVA). Non-parametric data (Bac-0303, Ecyl-0387) were analyzed using Kruskal-Wallis analysis of variance. Tukey's or Dunn's test was used for pairwise comparisons. For the *Lactobacillus-Enterococcus* group (Lab-0158), data could not be analyzed statistically since counts were below detection limit for four of six CARB samples. Diets: CARB, carbohydrate control; HF, high-fat; WS, Western-style.^{15,40} Probes: Bac, *Bacteroides*, and relatives; Clept, *Clostridium leptum* subgroup; Ecyl, *Eubacterium cylindroides* group; Erec, *Eubacterium rectale-Blautia coccoides* group; Strc, *Streptococcaceae*; **(B)** Box plots of Shannon effective species richness⁶⁶ according to diet. Cecal samples from mice fed the powder or pellet diet (n = 5 each) were analyzed by sequencing the V4 region (233 bp) of 16S rRNA genes using the MiSeq system (Illumina Inc.).¹⁵ Data refer to a total of 230 711 quality- and chimera-checked sequences representing a total of 99 OTUs. Demultiplexed samples were processed using usearch following the UPARSE approach.⁶⁷ OTUs were picked at a threshold of 97% similarity, and those OTUs with a relative abundance above 0.5% total sequences in at least one sample were kept. The RDP classifier was used to assign taxonomic classification (80% confidence).⁶⁸ All statistical analyses were performed using the R programming environment; **(C)** Multidimensional scaling analysis of phylogenetic distances (generalized UniFrac)¹⁸ at even sampling of 8 900 sequences; **(D)** Abundance of dominant taxonomic groups significantly different according to diet; p-values were adjusted for multiple testing according to the Benjamini-Hochberg method.

note, experimental endotoxemia has been linked to adipose tissue inflammation and insulin resistance in human subjects.³¹ There is no doubt that the study of bacterial communities associated with the gut mucosa and barrier functions in the context of human metabolic disorders will be of primary interest in the near future.^{19,32} The lipoprotein lipase inhibitor angiopoietin-like 4 (ANGPTL4), which is proposed to regulate hepatic fat accumulation, is also one of the few host candidate molecules through which the gut microbiota may alter host metabolic condition. However, more data are needed here as well to reach consensus in results.^{3,16} Finally, short-chain fatty acids produced via bacterial fermentation regulate many molecular processes involved in epithelial metabolism, cell growth and inflammatory responses. However, there is still no clear overview of their modes of action in metabolic diseases. Effects of the microbiota on hormone secretion by enteroendocrine cells is mainly mediated by short-chain fatty acids acting on G protein-coupled receptors such as GPR41.³³ Human fecal metagenomes with low gene counts linked to insulin resistance were characterized by lower genomic potential for butyrate production.¹⁴ Moreover, lower concentrations of butyrate (-4 mM) were detected in human feces following an 8-wk-intervention using a low-carbohydrate high-fat diet,³⁴ which agrees with findings that carbohydrate-rich diets favor butyrate production in humans.⁸ In contrast, butyrate is proposed to contribute to increased adiposity in mice¹¹ and increased butyrate production has been reported in obese human subjects.³⁵

Our contribution to the identification of bacterial functions that may influence host metabolic condition was to provide the first comparative analysis of cecal samples in diet-induced obese mice via high-resolution mass spectrometry to assess changes in metaproteomes and metabolomes.¹⁵ First, it should be noted that annotation of mass spectra remains challenging as <5% of acquired spectra can usually be matched to protein sequences or metabolite masses, which hampers comprehensive analysis and functional interpretation. Nonetheless, changes in functional categories of

differently detected proteins inferred that the mouse cecal microbiota under high-fat feeding is subject to substrate deprivation characterized by low levels of protein synthesis relative to preformed ribosomal proteins. We also found signs of shift toward utilization of amino acids and simple sugars and adaptation to an environment with altered redox potential, which is in line with findings from shotgun DNA-based analysis of mouse and human intestinal microbiota.^{14,36-39} Diet-induced alterations of the metaproteome were accompanied by clear-cut changes in cecal metabolite profiles in mice fed the control or high-fat diet. In particular, prostaglandins, thromboxanes and several steroids and conjugates thereof were absent in cecal contents from mice fed the high-fat diet,¹⁵ which is in agreement with low cholesterol levels in intestinal and hepatic tissues despite plasma hypercholesterolemia in mice fed the high-fat diet, likely due to an increased cholesterol demand for chylomicron building and proper lipid absorption.⁴⁰ Prostaglandins and steroids can influence bile acids composition and bile secretion.^{41,42} In our study,¹⁵ high-fat feeding diet led to lower intensity of spectra annotated as 3,7,12 α ,26-tetrahydroxy-5 β -cholestane. Altogether, these findings emphasize the importance of investigating bacterial metabolism of cholesterol and its derivatives in the gut, especially steroids and bile salts produced by the host.⁴³

Toward Model Bacterial Species

Microbial community analysis in both humans and mice allows the generation of hypotheses on metabolically important bacterial groups, the relevance of which in metabolic processes can be tested in experimental models. This requires that target bacterial strains are made available, underlining the urgent need to culture bacteria, characterize them properly, and ensure long-term storage, transparent archiving and availability. Although many of the most abundant gut bacterial species as detected by 16S rRNA gene sequencing have nowadays representative strains in culture, some core species and many bacteria at the borderline of dominance

possibly expressing important metabolic functions are still yet uncultured.^{10,44}

There is accumulating evidence that cultivable and dominant commensal anaerobes such as *Akkermansia muciniphila* and *Faecalibacterium prausnitzii* may be beneficial to the host with respect to metabolic health and inflammatory processes,^{19,45} opening ways to novel bacteria-based therapeutic approaches.⁴⁶ On the other hand, the term “pathobiont” is used to describe opportunistic but otherwise harmless bacteria that contribute to various diseases under specific environmental conditions.⁴⁷ Bacteria of the family *Coriobacteriaceae* within the phylum *Actinobacteria* can be seen as paradigm pathobionts. Indeed, they belong to dominant commensal communities in humans and mice, e.g., *Collinsella aerofaciens* is a member of the human gut core microbiome as highlighted by both 16S rRNA gene and metagenomic analysis,^{44,48} and *Eggerthella lenta* has for long been cultivated from human feces⁴⁹ and is detectable in most individuals by molecular techniques.⁵⁰ However, several members have also been implicated in various pathologies such as inflammatory bowel diseases, colon cancer, periodontitis, and bacteremia.⁵¹ It is striking that all 30 species of the family have been recovered only from body habitats in mammals and insects, suggesting that strong evolutionary forces shaped colonization processes and *Coriobacteriaceae*-host interactions. In light of the dominance and prevalence of *Coriobacteriaceae* in the mammalian gut and the importance of steroid and bile salt metabolism by bacteria as mentioned above, the literature speaks in favor of *Coriobacteriaceae* as being particularly relevant for host metabolic processes, as we describe in more details in the following paragraphs.

The occurrence of 16S rRNA gene sequences assigned to the genus *Eggerthella* and *Enterorhabdus*⁵² within the *Coriobacteriaceae* in feces correlated positively with intrahepatic levels triacylglycerol concentrations and non-HDL plasma concentrations in mice or hamsters.⁵³⁻⁵⁵ Moreover, the recent metagenomic study by Qin et al. based on high-throughput analysis of 350 human

Table 1. Facts and needs in the field of gut microbiota and metabolic diseases

Knowledge ▷ Opinions and outlook
The gut microbiota influences host energy homeostasis. ³
<ul style="list-style-type: none"> ▷ The real contribution of microbial metabolism to energy balance must be determined. Increased energy harvest of ca. 150 kcal was associated with a 20% increase in sequence abundance of <i>Firmicutes</i> and corresponding decrease in <i>Bacteroidetes</i> in human feces.²¹ However, the literature on increased <i>Firmicutes</i> to <i>Bacteroidetes</i> ratios and associated butyrate production in obesity is contradictory depending on host species and variations in diet. Concerns about the precision of measures of energy loss in stools have also been raised.⁶⁹ ▷ In-depth standardized calorimetric and heat production measurements should be performed under strictly controlled conditions in experimental models.
The causal effect of shifts in gut microbiota on host metabolism is established. ^{9,11,12}
<ul style="list-style-type: none"> ▷ With respect to therapeutic approaches, fecal transplantation is hitherto not sound in the context of metabolic disorders where benefits to patients relative to safety issues seem to be limited, besides being unknown in the long-term. ▷ From highly complex communities, the challenge is to identify specific bacteria and active molecules thereof with beneficial or detrimental effects. ▷ The establishment of simplified bacterial consortia carrying out specific functions is of primary interest, as done in the case of immune system regulation.⁷⁰
Low-gene counts and several candidate bacterial species (e.g., <i>Akkermansia</i> , <i>Alistipes</i> or <i>Coriobacteriaceae</i> spp.) are proposed to be of clinical relevance in metabolic disorders. ^{5,13,14,19,51}
<ul style="list-style-type: none"> ▷ All data published so far refer to cross-sectional design. Validation in large-scale prospective study cohorts is needed via sequencing (thanks to ever decreasing costs) followed by state-of-the-art data analysis or using targeted quantification methods. Beyond the identification of bacterial species and functions in well-phenotyped cohorts, the appeal lies in the validation of novel marker species preceding disease onset or facilitating prediction of treatment outcomes. ▷ The role of intestinal microorganisms other than bacteria, such as phages and fungi, should also be investigated in the context of obesity and metabolic complications.⁷¹
Pioneering meta-genomic, -transcriptomic or -proteomic analyses have initiated functional assessment of gut microbiota, but clear understanding of central molecular mechanisms that are key to bacteria-host interactions in metabolic diseases is lacking. ^{5,14,15}
<ul style="list-style-type: none"> ▷ Effort must be put into translation of already available descriptive data to hypothesis-driven functional testing of candidate strains or model communities. ▷ In that respect, culture-based work is essential and forms the basis of targeted functional studies in animal models. Initiatives toward standardization of feeding protocols in mice are urgently needed (e.g., feed database with information on supplier, composition, texture, corresponding published studies).

fecal samples from Chinese diabetic and control participants identified *Eggerthella lenta* as one of the molecular species linked to the occurrence of type-2 diabetes.⁵ On the other hand, another recent metagenomic study in 145 European women with diabetes, impaired or normal glucose tolerance reported depletion of metagenomic clusters assigned to *Coriobacteriaceae* in fecal samples from diabetic individuals.¹³ One newly proposed genus of the family *Coriobacteriaceae* was isolated from feces of one obese human female subject.⁷³

We have recently demonstrated in mice and rats that gut bacteria play important roles in the onset and maintenance of fatty liver and obesity.^{9,56} In both studies, members of the *Coriobacteriaceae* in the cecum were more often associated with resistant phenotypes, i.e., animals that were either not getting obese or not developing liver pathology under high-fat feeding. Diversity within the family was however low and mainly related to

Enterorhabdus mucosicola, *Enterorhabdus cecimuris*, and *Atopobium* species. In line with our data, *Enterorhabdus* spp. have previously been highlighted as being specific of lean animals microbiota when compared with db/db diabetic mice.⁵⁷ In the latter study, proportions of *Atopobium* in mouse cecum were significantly positively correlated with the levels of Apelin and its specific G protein-coupled receptor APJ mRNA expression. Apelin (adipokines family) has been shown to control glucose homeostasis and plays a key role in the cardiovascular system by acting on heart contractility, blood pressure, fluid homeostasis, vessel formation, and cell proliferation.⁵⁸ On the other hand, proportions of *Eggerthella* were negatively correlated with APJ mRNA levels. Still, our knowledge of underlying molecular mechanisms remains scarce.

Coriobacteriaceae, including *Enterorhabdus mucosicola* and *Collinsella* spp., seem to be well suited for colonization of mucosal surfaces, which implies peculiar

interactions with the host.⁵¹ Moreover, the metabolism of amino acids is a widespread feature within the family and the production of ammonia and its effect on epithelial cell metabolism seem worth investigating.⁵¹ Some *Coriobacteriaceae* are involved in bile acid metabolism, which is linked to gut barrier and metabolic dysfunctions.^{59,60} Various strains of *Eggerthella lenta* and *Collinsella aerofaciens* possess hydroxysteroid dehydrogenases (HSDH) responsible for stereospecific oxidation and epimerization of bile acids, thereby generating stable oxo-bile acid intermediates.⁶¹ However, the impact of bacterial HSDH activities on bile acid metabolism and host functions in vivo is undefined. Finally, *Eggerthella lenta* is also able to transform corticoids such as deoxycorticosterone to progesterone via 21-dehydroxylase activity.⁶² This species also carries a corticoid-converting 16 α -dehydroxylase⁶³ and a 3 α -HSDH.⁶⁴ Although these findings relate to possible changes in the host hormonal status,

functional studies in experimental animal models have not yet been performed.

Taken together, evidence from the literature strongly suggests that *Coriobacteriaceae* are important constituents of gut microbiomes affecting host physiology. To test this, we have initiated a multi-center project to study whether and how *Coriobacteriaceae* influence lipid metabolism and the development of hepatic steatosis and insulin resistance.

Summary

Despite major breakthroughs in recent years, understanding the involvement of gut microbiota in host energy homeostasis and metabolism is still in its infancy. Our view of the current knowledge and future perspectives in the field is presented in Table 1. At the

community level, efforts must be put into the analysis of bacterial functions in addition to diversity and composition, if possible in the framework of large-scale prospective human cohorts. Moreover, although the use of various experimental procedures may guarantee relevance of findings in the long run, the field suffers from misleading interpretations of huge repositories of descriptive data from artificial models that are difficult—if not impossible—to compare. It needs concerted actions to better define experimental conditions, provide SOPs and reference materials and maybe agree on common analysis processes and data interpretation tools. Researchers who study mechanisms underlying variations in metabolic phenotypes in mice must be encouraged to systematically provide basic description of gut colonization (and corresponding analysis method), especially when mice are obtained from

commercial suppliers prior to experiments. Finally, culture work combined with the use of gnotobiotic animals give us the chance to examine in detail molecular mechanisms underlying the regulation of host metabolic processes by specific bacteria of patho-physiological relevance, such as the *Coriobacteriaceae*.

Disclosure of Potential Conflicts of Interest

No potential conflicts of interest were disclosed

Acknowledgments

As part of the joint DFG/ANR initiative, the authors received financial support from the German Research Foundation (grant no. CL481/1-1) and the French National Research Agency (grant no. ANR-13-ISV3-0008-04). We are grateful to Ilias Lagkouvardos for help with 16S rRNA gene sequence analysis.

References

1. Kau AL, Ahern PP, Griffin NW, Goodman AL, Gordon JI. Human nutrition, the gut microbiome and the immune system. *Nature* 2011; 474:327-36; PMID:21677749; <http://dx.doi.org/10.1038/nature10213>
2. Wostmann BS. The germfree animal in nutritional studies. *Annu Rev Nutr* 1981; 1:257-79; PMID:6764717; <http://dx.doi.org/10.1146/annurev.nu.01.070181.001353>
3. Bäckhed F, Ding H, Wang T, Hooper LV, Koh GY, Nagy A, Semenkovich CF, Gordon JI. The gut microbiota as an environmental factor that regulates fat storage. *Proc Natl Acad Sci U S A* 2004; 101:15718-23; PMID:15505215; <http://dx.doi.org/10.1073/pnas.0407076101>
4. Human Microbiome Project Consortium. A framework for human microbiome research. *Nature* 2012; 486:215-21; PMID:22699610; <http://dx.doi.org/10.1038/nature11209>
5. Qin J, Li Y, Cai Z, Li S, Zhu J, Zhang F, Liang S, Zhang W, Guan Y, Shen D, et al. A metagenome-wide association study of gut microbiota in type 2 diabetes. *Nature* 2012; 490:55-60; PMID:23023125; <http://dx.doi.org/10.1038/nature11450>
6. Delzenne NM, Cani PD. Interaction between obesity and the gut microbiota: relevance in nutrition. *Annu Rev Nutr* 2011; 31:15-31; PMID:21568707; <http://dx.doi.org/10.1146/annurev-nutr-072610-145146>
7. Duncan SH, Lohley GE, Holtrop G, Ince J, Johnstone AM, Louis P, Flint HJ. Human colonic microbiota associated with diet, obesity and weight loss. *Int J Obes (Lond)* 2008; 32:1720-4; PMID:18779823; <http://dx.doi.org/10.1038/ijo.2008.155>
8. Duncan SH, Belenguer A, Holtrop G, Johnstone AM, Flint HJ, Lohley GE. Reduced dietary intake of carbohydrates by obese subjects results in decreased concentrations of butyrate and butyrate-producing bacteria in feces. *Appl Environ Microbiol* 2007; 73:1073-8; PMID:17189447; <http://dx.doi.org/10.1128/AEM.02340-06>
9. Le Roy T, Llopis M, Lepage P, Bruneau A, Rabot S, Bevilacqua C, Martin P, Philippe C, Walker F, Bado A, et al. Intestinal microbiota determines development of non-alcoholic fatty liver disease in mice. *Gut* 2013; 62:1787-94; PMID:23197411; <http://dx.doi.org/10.1136/gutjnl-2012-303816>
10. Walker AW, Duncan SH, Louis P, Flint HJ. Phylogeny, culturing, and metagenomics of the human gut microbiota. *Trends Microbiol* 2014; 22:267-74; PMID:24698744; <http://dx.doi.org/10.1016/j.tim.2014.03.001>
11. Turnbaugh PJ, Ley RE, Mahowald MA, Magrini V, Mardis ER, Gordon JI. An obesity-associated gut microbiome with increased capacity for energy harvest. *Nature* 2006; 444:1027-31; PMID:17183312; <http://dx.doi.org/10.1038/nature05414>
12. Vrieeze A, Van Nood E, Holleman F, Salojärvi J, Kootte RS, Bartsman JF, Dallinga-Thie GM, Ackermans MT, Serlie MJ, Oozeer R, et al. Transfer of intestinal microbiota from lean donors increases insulin sensitivity in individuals with metabolic syndrome. *Gastroenterology* 2012; 143:913-6, e7; PMID:22728514; <http://dx.doi.org/10.1053/j.gastro.2012.06.031>
13. Karlsson FH, Tremaroli V, Nookaew I, Bergström G, Behre CJ, Fagerberg B, Nielsen J, Bäckhed F. Gut metagenome in European women with normal, impaired and diabetic glucose control. *Nature* 2013; 498:99-103; PMID:23719380; <http://dx.doi.org/10.1038/nature12198>
14. Le Chatelier E, Nielsen T, Qin J, Prifti E, Hildebrand F, Falony G, Almeida M, Arumugam M, Batto JM, Kennedy S, et al.; MetaHIT consortium. Richness of human gut microbiome correlates with metabolic markers. *Nature* 2013; 500:541-6; PMID:23985870; <http://dx.doi.org/10.1038/nature12506>
15. Daniel H, Moghaddas Gholami A, Berry D, Desmarchelier C, Hahne H, Loh G, Mondot S, Lepage P, Rothballer M, Walker A, et al. High-fat diet alters gut microbiota physiology in mice. *ISME J* 2014; 8:295-308; PMID:24030595; <http://dx.doi.org/10.1038/ismej.2013.155>
16. Fleissner CK, Huebel N, Abd El-Bary MM, Loh G, Klaus S, Blaut M. Absence of intestinal microbiota does not protect mice from diet-induced obesity. *Br J Nutr* 2010; 104:919-29; PMID:20441670; <http://dx.doi.org/10.1017/S0007114510001303>
17. Desmarchelier C, Ludwig T, Scheundel R, Rink N, Bader BL, Klingenspor M, Daniel H. Diet-induced obesity in ad libitum-fed mice: food texture overrides the effect of macronutrient composition. *Br J Nutr* 2013; 109:1518-27; PMID:22863169; <http://dx.doi.org/10.1017/S0007114512003340>
18. Chen J, Bittinger K, Charlson ES, Hoffmann C, Lewis J, Wu GD, Collman RG, Bushman FD, Li H. Associating microbiome composition with environmental covariates using generalized UniFrac distances. *Bioinformatics* 2012; 28:2106-13; PMID:22711789; <http://dx.doi.org/10.1093/bioinformatics/bts342>
19. Everard A, Belzer C, Geurts L, Ouwerkerk JP, Druart C, Bindels LB, Guiot Y, Derrien M, Muccioli GG, Delzenne NM, et al. Cross-talk between *Akkermansia muciniphila* and intestinal epithelium controls diet-induced obesity. *Proc Natl Acad Sci U S A* 2013; 110:9066-71; PMID:23671105; <http://dx.doi.org/10.1073/pnas.1219451110>
20. Shin NR, Lee JC, Lee HY, Kim MS, Whon TW, Lee MS, Bae JW. An increase in the *Akkermansia* spp. population induced by metformin treatment improves glucose homeostasis in diet-induced obese mice. *Gut* 2014; 63:727-35; PMID:23804561; <http://dx.doi.org/10.1136/gutjnl-2012-303839>
21. Jumpertz R, Le DS, Turnbaugh PJ, Trinidad C, Bogardus C, Gordon JI, Krakoff J. Energy-balance studies reveal associations between gut microbes, caloric load, and nutrient absorption in humans. *Am J Clin Nutr* 2011; 94:58-65; PMID:21543530; <http://dx.doi.org/10.3945/ajcn.110.010132>
22. Kashyap PC, Marcolal A, Ursell LK, Larauche M, Duboc H, Earle KA, Sonnenburg ED, Ferreyra JA, Higginbottom SK, Million M, et al. Complex interactions among diet, gastrointestinal transit, and gut microbiota in humanized mice. *Gastroenterology* 2013; 144:967-77; PMID:23380084; <http://dx.doi.org/10.1053/j.gastro.2013.01.047>

23. Vijay-Kumar M, Aiken JD, Carvalho FA, Cullender TC, Mwangi S, Srinivasan S, Sitarman SV, Knight R, Ley RE, Gewirtz AT. Metabolic syndrome and altered gut microbiota in mice lacking Toll-like receptor 5. *Science* 2010; 328:228-31; PMID:20203013; <http://dx.doi.org/10.1126/science.1179721>
24. Wichmann A, Allahyar A, Greiner TU, Plovier H, Lundén GO, Larsson T, Drucker DJ, Delzenne NM, Cani PD, Bäckhed F. Microbial modulation of energy availability in the colon regulates intestinal transit. *Cell Host Microbe* 2013; 14:582-90; PMID:24237703; <http://dx.doi.org/10.1016/j.chom.2013.09.012>
25. Cani PD, Possemiers S, Van de Wiele T, Guiot Y, Everard A, Rottier O, Geurts L, Naslain D, Neyrinck A, Lambert DM, et al. Changes in gut microbiota control inflammation in obese mice through a mechanism involving GLP-2-driven improvement of gut permeability. *Gut* 2009; 58:1091-103; PMID:19240062; <http://dx.doi.org/10.1136/gut.2008.165886>
26. Cani PD, Neyrinck AM, Fava F, Knauf C, Burcelin RG, Tuohy KM, Gibson GR, Delzenne NM. Selective increases of bifidobacteria in gut microflora improve high-fat-diet-induced diabetes in mice through a mechanism associated with endotoxaemia. *Diabetologia* 2007; 50:2374-83; PMID:17823788; <http://dx.doi.org/10.1007/s00125-007-0791-0>
27. Gruber L, Kislung S, Lichti P, Martin FP, May S, Klingenspor M, Lichtenegger M, Rychlik M, Haller D. High fat diet accelerates pathogenesis of murine Crohn's disease-like ileitis independently of obesity. *PLoS One* 2013; 8:e71661; PMID:23977107; <http://dx.doi.org/10.1371/journal.pone.0071661>
28. Reichardt F, Baudry C, Gruber L, Mazzuoli G, Moriez R, Scherling C, Kollmann P, Daniel H, Kislung S, Haller D, et al. Properties of myenteric neurones and mucosal functions in the distal colon of diet-induced obese mice. *J Physiol* 2013; 591:5125-39; PMID:23940384; <http://dx.doi.org/10.1113/jphysiol.2013.262733>
29. Clemente-Postigo M, Queipo-Ortuño MI, Murri M, Boto-Ordóñez M, Perez-Martinez P, Andres-Lacueva C, Cardona F, Tinahones FJ. Endotoxin increase after fat overload is related to postprandial hypertriglyceridemia in morbidly obese patients. *J Lipid Res* 2012; 53:973-8; PMID:22394503; <http://dx.doi.org/10.1194/jlr.P020909>
30. Dewulf EM, Cani PD, Claus SP, Fuentes S, Puylaert PG, Neyrinck AM, Bindels LB, de Vos WM, Gibson GR, Thissen JP, et al. Insight into the prebiotic concept: lessons from an exploratory, double blind intervention study with inulin-type fructans in obese women. *Gut* 2013; 62:1112-21; PMID:23135760; <http://dx.doi.org/10.1136/gutjnl-2012-303304>
31. Mehta NN, McGillicuddy FC, Anderson PD, Hinkle CC, Shah R, Pruscino L, Tabita-Martinez J, Sellers KF, Rickels MR, Reilly MP. Experimental endotoxaemia induces adipose inflammation and insulin resistance in humans. *Diabetes* 2010; 59:172-81; PMID:19794059; <http://dx.doi.org/10.2337/db09-0367>
32. Berry D, Stecher B, Schintlmeister A, Reichert J, Brugiroux S, Wild B, Wanek W, Richter A, Rauch I, Decker T, et al. Host-compound foraging by intestinal microbiota revealed by single-cell stable isotope probing. *Proc Natl Acad Sci U S A* 2013; 110:4720-5; PMID:23487774; <http://dx.doi.org/10.1073/pnas.1219247110>
33. Samuel BS, Shaito A, Motoike T, Rey FE, Backhed F, Manchester JK, Hammer RE, Williams SC, Crowley J, Yanagisawa M, et al. Effects of the gut microbiota on host adiposity are modulated by the short-chain fatty-acid binding G protein-coupled receptor, Gpr41. *Proc Natl Acad Sci U S A* 2008; 105:16767-72; PMID:18931303; <http://dx.doi.org/10.1073/pnas.0808567105>
34. Brinkworth GD, Noakes M, Clifton PM, Bird AR. Comparative effects of very low-carbohydrate, high-fat and high-carbohydrate, low-fat weight-loss diets on bowel habit and faecal short-chain fatty acids and bacterial populations. *Br J Nutr* 2009; 101:1493-502; PMID:19224658; <http://dx.doi.org/10.1017/S0007114508094658>
35. Schwirtz A, Taras D, Schäfer K, Beijer S, Bos NA, Donus C, Hardt PD. Microbiota and SCFA in lean and overweight healthy subjects. *Obesity (Silver Spring)* 2010; 18:190-5; PMID:19498350; <http://dx.doi.org/10.1038/oby.2009.167>
36. Turnbaugh PJ, Ridaura VK, Faith JJ, Rey FE, Knight R, Gordon JL. The effect of diet on the human gut microbiome: a metagenomic analysis in humanized gnotobiotic mice. *Sci Transl Med* 2009; 1:ra14; PMID:20368178; <http://dx.doi.org/10.1126/scitranslmed.3000322>
37. Turnbaugh PJ, Bäckhed F, Fulton L, Gordon JL. Diet-induced obesity is linked to marked but reversible alterations in the mouse distal gut microbiome. *Cell Host Microbe* 2008; 3:213-23; PMID:18407065; <http://dx.doi.org/10.1016/j.chom.2008.02.015>
38. Yatsunen T, Rey FE, Manary MJ, Trehan I, Dominguez-Bello MG, Contreras M, Magris M, Hidalgo G, Baldassano RN, Anokhin AP, et al. Human gut microbiome viewed across age and geography. *Nature* 2012; 486:222-7; PMID:22699611
39. Xiao Y, Cui J, Shi YH, Sun J, Wang ZP, Le GW. Effects of duodenal redox status on calcium absorption and related genes expression in high-fat diet-fed mice. *Nutrition* 2010; 26:1188-94; PMID:20444574; <http://dx.doi.org/10.1016/j.nut.2009.11.021>
40. Desmarchelier C, Dahloff C, Keller S, Sailer M, Jahreis G, Daniel H. C57Bl/6 N mice on a western diet display reduced intestinal and hepatic cholesterol levels despite a plasma hypercholesterolemia. *BMC Genomics* 2012; 13:84; PMID:22394543; <http://dx.doi.org/10.1186/1471-2164-13-84>
41. Beckh K, Kneip S, Arnold R. Direct regulation of bile secretion by prostaglandins in perfused rat liver. *Hepatology* 1994; 19:1208-13; PMID:8175143; <http://dx.doi.org/10.1002/hep.1840190519>
42. Everson GT, Fennessey P, Kern F Jr. Contraceptive steroids alter the steady-state kinetics of bile acids. *J Lipid Res* 1988; 29:68-76; PMID:3356953
43. Gérard P. Metabolism of cholesterol and bile acids by the gut microbiota. *Pathogens* 2014; 3:14-24; <http://dx.doi.org/10.3390/pathogens3010014>
44. Qin J, Li R, Raes J, Arumugam M, Burgdorf KS, Manichanh C, Nielsen T, Pons N, Levenez F, Yamada T, et al.; MetaHIT Consortium. A human gut microbial gene catalogue established by metagenomic sequencing. *Nature* 2010; 464:59-65; PMID:20203603; <http://dx.doi.org/10.1038/nature08821>
45. Sokol H, Pigneur B, Watterlot L, Lakhdari O, Bermúdez-Humarán LG, Grataudoux JJ, Blugeon S, Bridonneau C, Furet JP, Corthier G, et al. *Faecalibacterium prausnitzii* is an anti-inflammatory commensal bacterium identified by gut microbiota analysis of Crohn disease patients. *Proc Natl Acad Sci U S A* 2008; 105:16731-6; PMID:18936492; <http://dx.doi.org/10.1073/pnas.0804812105>
46. Takiishi T, Korf H, Van Belle TL, Robert S, Grieco FA, Caluwaerts S, Galleri L, Spagnuolo I, Steidler L, Van Huynegem K, et al. Reversal of autoimmune diabetes by restoration of antigen-specific tolerance using genetically modified *Lactococcus lactis* in mice. *J Clin Invest* 2012; 122:1717-25; PMID:22484814; <http://dx.doi.org/10.1172/JCI60530>
47. Devkota S, Wang Y, Musch MW, Leone V, Fehlner-Peach H, Nadimpalli A, Antonopoulos DA, Jabri B, Chang EB. Dietary-fat-induced taurocholic acid promotes pathobiont expansion and colitis in H101 mice. *Nature* 2012; 487:104-8; PMID:22722865
48. Tap J, Mondot S, Levenez F, Pelletier E, Caron C, Furet JP, Ugarte E, Muñoz-Tamayo R, Paslier DL, Nalin R, et al. Towards the human intestinal microbiota phylogenetic core. *Environ Microbiol* 2009; 11:2574-84; PMID:19601958; <http://dx.doi.org/10.1111/j.1462-2920.2009.01982.x>
49. Eggerth AH. The Gram-positive Non-spore-bearing Anaerobic Bacilli of Human Feces. *J Bacteriol* 1935; 30:277-99; PMID:16559837
50. Kageyama A, Benno Y. Rapid detection of human fecal *Eubacterium* species and related genera by nested PCR method. *Microbiol Immunol* 2001; 45:315-8; PMID:11386422; <http://dx.doi.org/10.1111/j.1348-0421.2001.tb02624.x>
51. Clavel T, Lepage P, Charrier C. Family *Coriobacteriaceae*. In: Rosenberg E, DeLong E, Thompson F, Lory S, Stackebrand E, eds. *The prokaryotes*: Springer, 2013.
52. Clavel T, Charrier C, Braune A, Wenning M, Blaut M, Haller D. Isolation of bacteria from the ileal mucosa of TNFdeltaARE mice and description of *Enterorhabdus mucosicola* gen. nov., sp. nov. *Int J Syst Evol Microbiol* 2009; 59:1805-12; PMID:19542111; <http://dx.doi.org/10.1099/ijs.0.003087-0>
53. Claus SP, Ellero SL, Berger B, Krause L, Bruttin A, Molina J, Paris A, Want EJ, de Waziers I, Cloarec O, et al. Colonization-induced host-gut microbial metabolic interaction. *MBio* 2011; 2:e00271-10; PMID:21363910; <http://dx.doi.org/10.1128/MBio.00271-10>
54. Martínez I, Lattimer JM, Hubach KL, Case JA, Yang J, Weber CG, Louk JA, Rose DJ, Kyureghian G, Peterson DA, et al. Gut microbiome composition is linked to whole grain-induced immunological improvements. *ISME J* 2013; 7:269-80; PMID:23038174; <http://dx.doi.org/10.1038/ismej.2012.104>
55. Martínez I, Perdicaro DJ, Brown AW, Hammons S, Carden TJ, Carr TP, Eskridge KM, Walter J. Diet-induced alterations of host cholesterol metabolism are likely to affect the gut microbiota composition in hamsters. *Appl Environ Microbiol* 2013; 79:516-24; PMID:23124234; <http://dx.doi.org/10.1128/AEM.03046-12>
56. Duca FA, Sakar Y, Lepage P, Devime F, Langelier B, Doré J, Covasa M. Replication of obesity and associated signaling pathways through transfer of microbiota from obese-prone rats. *Diabetes* 2014; 63:1624-36; PMID:24430437; <http://dx.doi.org/10.2337/db13-1526>
57. Geurts L, Lazarevic V, Derrien M, Everard A, Van Roye M, Knauf C, Valet P, Girard M, Muccioli GG, François P, et al. Altered gut microbiota and endocannabinoid system tone in obese and diabetic leptin-resistant mice: impact on apelin regulation in adipose tissue. *Front Microbiol* 2011; 2:149; PMID:21808634; <http://dx.doi.org/10.3389/fmicb.2011.00149>
58. Maenhaut N, Van de Voorde J. Regulation of vascular tone by adipocytes. *BMC Med* 2011; 9:25; PMID:21410966; <http://dx.doi.org/10.1186/1741-7015-9-25>
59. Stenman LK, Holma R, Eggert A, Korpela R. A novel mechanism for gut barrier dysfunction by dietary fat: epithelial disruption by hydrophobic bile acids. *Am J Physiol Gastrointest Liver Physiol* 2013; 304:G227-34; PMID:23203158; <http://dx.doi.org/10.1152/ajpgi.00267.2012>
60. Turnbaugh PJ. Microbiology: fat, bile and gut microbes. *Nature* 2012; 487:47-8; PMID:22763552; <http://dx.doi.org/10.1038/487047a>
61. Ridlon JM, Kang DJ, Hylemon PB. Bile salt biotransformations by human intestinal bacteria. *J Lipid Res* 2006; 47:241-59; PMID:16299351; <http://dx.doi.org/10.1194/jlr.R500013-JLR200>
62. Bokkenheuser VD, Winter J, Dehazya P, Kelly WG. Isolation and characterization of human fecal bacteria capable of 21-dehydroxylating corticoids. *Appl Environ Microbiol* 1977; 34:571-5; PMID:303887

63. Bokkenheuser VD, Winter J, O'Rourke S, Ritchie AE. Isolation and characterization of fecal bacteria capable of 16 *alpha*-dehydroxylating corticoids. *Appl Environ Microbiol* 1980; 40:803-8; PMID:7425626
64. Bokkenheuser VD, Winter J, Finegold SM, Sutter VL, Ritchie AE, Moore WE, Holdeman LV. New markers for *Eubacterium lentum*. *Appl Environ Microbiol* 1979; 37:1001-6; PMID:314778
65. Clavel T, Henderson G, Alpert CA, Philippe C, Rigottier-Gois L, Doré J, Blaut M. Intestinal bacterial communities that produce active estrogen-like compounds enterodiol and enterolactone in humans. *Appl Environ Microbiol* 2005; 71:6077-85; PMID:16204524; <http://dx.doi.org/10.1128/AEM.71.10.6077-6085.2005>
66. Jost L. Entropy and diversity. *Oikos* 2006; 113:363-75; <http://dx.doi.org/10.1111/j.2006.0030-1299.14714.x>
67. Edgar RC. UPARSE: highly accurate OTU sequences from microbial amplicon reads. *Nat Methods* 2013; 10:996-8; PMID:23955772; <http://dx.doi.org/10.1038/nmeth.2604>
68. Cole JR, Chai B, Marsh TL, Farris RJ, Wang Q, Kulam SA, Chandra S, McGarrell DM, Schmidt TM, Garrity GM, et al.; Ribosomal Database Project. The Ribosomal Database Project (RDP-II): previewing a new autoaligner that allows regular updates and the new prokaryotic taxonomy. *Nucleic Acids Res* 2003; 31:442-3; PMID:12520046; <http://dx.doi.org/10.1093/nar/gkg039>
69. Heymsfield SB, Pietrobelli A. Individual differences in apparent energy digestibility are larger than generally recognized. *Am J Clin Nutr* 2011; 94:1650-1; PMID:22106417; <http://dx.doi.org/10.3945/ajcn.111.026476>
70. Atarashi K, Tanoue T, Oshima K, Suda W, Nagano Y, Nishikawa H, Fukuda S, Saito T, Narushima S, Hase K, et al. Treg induction by a rationally selected mixture of Clostridia strains from the human microbiota. *Nature* 2013; 500:232-6; PMID:23842501; <http://dx.doi.org/10.1038/nature12331>
71. Reyes A, Wu M, McNulty NP, Rohwer FL, Gordon JL. Gnotobiotic mouse model of phage-bacterial host dynamics in the human gut. *Proc Natl Acad Sci U S A* 2013; 110:20236-41; PMID:24259713; <http://dx.doi.org/10.1073/pnas.1319470110>
72. Hildebrandt MA, Hoffmann C, Sherrill-Mix SA, Keilbaugh SA, Hamady M, Chen YY, Knight R, Ahima RS, Bushman F, Wu GD. High-fat diet determines the composition of the murine gut microbiome independently of obesity. *Gastroenterology* 2009; 137:1716, e1-2; PMID:19706296; <http://dx.doi.org/10.1053/j.gastro.2009.08.042>
73. Mishra AK, Hugon P, Lagier JC, Nguyen TT, Couderc C, Raoult D, Fournier PE. Non contiguous-finished genome sequence and description of *Enorma massiliensis* gen. nov., sp. nov., a new member of the Family Coriobacteriaceae. *Stand Genomic Sci* 2013; 8:290-305; PMID:23991260; <http://dx.doi.org/10.4056/sigs.3426906>

Paper 14-16

Microbe-host interaction: The gut-liver axis

The following selected publications refer to research topic 3 (see detailed description above on p34-37). The impact of gut bacteria on host physiology, and more particularly liver functions, is an emerging field of my research, *i.e.*, it originates from some of the findings published below and forms the basis of ongoing work supported by the German Research Foundation.

14. G Hörmannspurger,* T Clavel,* D Haller (2012) Gut matters: intestinal microbial ecology in allergic diseases, *J Allergy Clin Immunol* 129:1452; *shared first authorship

Paper 14 is an invited, peer-reviewed publication, which highlights mechanisms underlying the regulation host physiology outside the gut, with strong emphasis on immune responses and allergic disorders.

15. H Daniel, A Moghaddas Gholami, D Berry, C Desmarchelier, H Hahne, G Loh, S Mondot, P Lepage, M Rothballer, A Walker, C Böhm, M Wenning, M Wagner, M Blaut, P Schmitt-Kopplin, B Kuster, D Haller, T Clavel (2014) High-fat diet alters gut microbiota physiology in mice, *The ISME Journal* 8:295

This is my first piece of work as a senior author in a top-ranking journal in the field of microbial ecology. This paper reports the functional description of microbial communities in the mouse caecum using *omics* technologies. Metaproteomic data indicated that bacterial communities are not well prepared for efficient energy harvest when 60% of dietary energy originates from fat. Moreover, metabolomics analysis by mass spectrometry pointed at the relevance of studying the conversion of cholesterol-derived compounds by the gut microbiota in the context of metabolic disorders.

16. T Clavel, P Lepage, C Charrier (2014) Family *Coriobacteriaceae*, In *The Prokaryotes*, 4th Edition, E Rosenberg, EF DeLong, F Thompson, S Lory, E Stackebrand (Eds), Springer, ISBN 978-3-642-30137-7

This publication is a symbol of my recognition in the field of bacterial taxonomy (invited peer-reviewed contribution) and was instrumental in obtaining one major financial support by the German Research Foundation for the study of gut bacteria in the onset of fatty liver disease. This book chapter describes the diversity and functions of *Coriobacteriaceae*, their ecological importance and their role in the conversion of steroids and bile acids. Thereby, it highlights the rationale behind our ongoing work about the study of molecular mechanisms underlying the impact of cholesterol-derived compounds on hepatic steatosis and their metabolism by gut bacteria.

PAPER 14

Gut matters: Microbe-host interactions in allergic diseases

Gabriele Hörmannspurger, PhD,* Thomas Clavel, PhD,* and Dirk Haller, PhD *Freising-Weihenstephan, Germany*

The human body can be considered a metaorganism made up of its own eukaryotic cells and trillions of microbes that colonize superficial body sites, such as the skin, airways, and gastrointestinal tract. The coevolution of host and microbes brought about a variety of molecular mechanisms, which ensure a peaceful relationship. The mammalian barrier and immune functions warrant simultaneous protection of the host against deleterious infections, as well as tolerance toward harmless commensals. Because these pivotal host functions evolved under high microbial pressure, they obviously depend on a complex network of microbe-host interactions. The rapid spread of immune-mediated disorders, such as autoimmune diseases, inflammatory bowel diseases, and allergies, in westernized countries is thus thought to be due to environmentally mediated disturbances of this microbe-host interaction network. The aim of the present review is to highlight the importance of the intestinal microbiota in shaping host immune mechanisms, with particular emphasis on allergic diseases and possible intervention strategies. (*J Allergy Clin Immunol* 2012;129:1452-9.)

Key words: *Intestinal microbiota, bacteria, barrier function, allergy, asthma, eczema, immune responses, oral tolerance, functional food, probiotic*

Allergies, including asthma, dermatitis, rhinitis, and food allergies, are chronic inflammatory diseases driven by deregulated immune responses toward minute amounts of harmless antigens (allergens). Epidemiologic and clinical studies indicate that the increased incidence of autoimmune and allergic diseases in developed countries is associated with reduced microbial exposure and alteration of microbial communities in various body sites.¹ Recent advances in high-throughput molecular technologies in the field of metagenomic and metabolomic analysis have opened up new ways to identify core microbial communities linked to the onset of pathologies.²⁻⁵ Nevertheless, it is still challenging to reach consensus in the definition of a “normal healthy” microbiota of the human gut, airway, and skin at the functional level. Moreover, the molecular mechanisms

Abbreviations used

DC: Dendritic cell
MAMP: Microbe-associated molecular pattern
MLN: Mesenteric lymph node
PP: Peyer patch
SCFA: Short-chain fatty acid
Treg: Regulatory T

underlying microbe-host interactions that shape host immune functions are still elusive. In the present review we intend to discuss up-to-date knowledge of how the host microbiota is involved in the regulation of immune responses and the development of allergic disorders. We will provide a brief summary of clinically relevant evidence of the role of microorganisms in allergies, highlight the central role of the gut and its microbiota in regulating peripheral immune functions, and finally discuss data on the use of prebiotics and probiotics for the treatment or prevention of allergic symptoms.

IMPORTANCE OF MICROBE-HOST INTERACTIONS FOR ALLERGIC DISEASES: EVIDENCE FROM HUMAN STUDIES

Our gut harbors the majority of mammalian-associated microbes (10^8 to 10^{12} colony-forming units/g intestinal content). The intestinal microbiota, which is defined as the highly complex and dynamic assemblage of the thousands of microorganisms living in our gut,⁵ has therefore been proposed as a major non-self-factor affecting the development of allergies. Changes in gut microbial composition have been reported in patients with allergic diseases at distant body sites, such as rhinitis and atopic eczema.⁶⁻⁹ Alterations of the intestinal microbiota might actually precede the development of allergic manifestations in children, supporting the hypothesis that microbial dysbiosis is not only a consequence but also a cause of allergy.^{10,11} Beyond the gut, the microbiota of the skin and bronchi was also altered in patients with allergic diseases at the respective sites (eczema or asthma).¹²⁻¹⁵

Potential reasons for microbial dysbiosis in allergic subjects lie in complex individual-specific interactions between genetic predispositions¹⁶ and environmental factors, such as birth delivery mode, diet, hygiene, and medication. Birth delivery mode, for instance, markedly influences initial microbial colonization of newborns.^{17,18} Natural birth, which results in immediate exposure of the child to the mother's vaginal and fecal microbiota, is associated with a reduced incidence of allergies compared with that seen in children born by means of cesarean section.¹⁹ The revised hygiene hypothesis states that reduced microbial exposure in early childhood results in an increased T_H2/T_H1 response ratio and in defective regulatory immune mechanisms that contribute to a

From Biofunctionality, ZIEL—Research Center for Nutrition and Food Science, CDD Center for Diet and Disease, Technische Universität München.

*These authors contributed equally to this work.

Disclosure of potential conflict of interest: The authors declare that they have no relevant conflicts of interest.

Received for publication September 26, 2011; revised December 9, 2011; accepted for publication December 21, 2011.

Available online February 8, 2012.

Corresponding author: Dirk Haller, PhD, ZIEL—Research Center for Nutrition and Food Science, Technische Universität München, Gregor-Mendel-Str 2, 85350 Freising-Weihenstephan, Germany. E-mail: haller@wzw.tum.de.

0091-6749/\$36.00

© 2012 American Academy of Allergy, Asthma & Immunology

doi:10.1016/j.jaci.2011.12.993

higher incidence of immune-mediated diseases, such as allergies, in developed countries.²⁰ In line with the hygiene hypothesis, growing up in a farming environment, including close contact with cows and consumption of raw milk, is strongly associated with reduced incidence of allergic diseases.²¹ Although the farming environment seems to be protective through exposure to increased numbers and varieties of microorganisms,²² its effect on the intestinal and bronchial microbiota, as well as potentially protective microbes, remain to be characterized. Exposure to pathogens, such as *Helicobacter pylori*, parasites, or *Mycoplasma tuberculosis*, have also been associated with reduced incidence of allergic diseases.²³⁻²⁵ However, protective effects are pathogen specific, and early viral infections of the airways are a risk factor for allergic asthma.²⁶ Finally, breast-feeding and the use of antibiotics are 2 additional factors that markedly influence the intestinal and extraintestinal microbiota.²⁷⁻³¹ However, clinical results concerning their effect on allergy development are still conflicting.³²⁻³⁵

In summary, clinical data strongly suggest that microbial inhabitants of the human body, especially the intestinal microbiota, influence the development and severity of allergic diseases. Characterization of microbiota dysbiosis beyond phylogenetic diversity analysis is now essential to identify alterations of core microbial functions that contribute to early immune disturbances in allergic patients.

THE INTESTINE AS GATEKEEPER OF IMMUNITY

The intestine emerged as an important target in the prevention and therapy of allergies because the intestinal immune system has unique regulatory functions that affect local and systemic immune responses.³⁶ In the following paragraphs, we focus on 2 intestinal functions of relevance for systemic immune reactions: gut barrier and oral tolerance.

The intestinal mucosa provides the border between inner tissues and tremendous amounts of mostly harmless food- and bacteria-derived antigens. It is usually very efficient in preventing translocation of microorganisms and reducing the amount of permeating microbe-associated molecular patterns (MAMPs) and antigens.³⁷ However, increased gut permeability in pediatric and adult patients with asthma and eczema was reported in several clinical and *ex vivo* studies.³⁸⁻⁴¹ Both acute and chronic barrier disruption caused by mechanical damage, infection, dysbiosis (eg, resulting in overexpression of bacterial proteases), or dietary components can enhance translocation of microbial triggers that can act in distant body sites, such as the lung or skin.⁴²⁻⁴⁴ For instance, diet-induced barrier alterations can result in increased occurrence of LPSs in the blood, which was in turn found to promote the development of diabetes.^{43,45} Recent studies in mice provided additional evidence linking gut barrier function to inflammatory responses in distant body sites.^{46,47} The authors demonstrated that intestinal epithelial barrier breakdown (eg, enhanced translocation of fluorescein isothiocyanate–dextran and reduced occludin protein levels) contributes to acute lung inflammation after skin burn. By means of surgery (abdominal vagotomy and stimulation of the right cervical nerve), they concluded that the neuroenteric axis is essential for gut barrier–mediated prevention of secondary acute lung injury. All these findings indicate that gut permeability is a promising function worth further investigation in the context of allergy development.

Because inflammatory immune responses toward low levels of penetrating MAMPs and antigens would be detrimental to the host, the intestinal immune system evolved to be highly tolerant toward these structures. An array of innate and adaptive tolerance mechanisms ensures prevention of inflammatory reactions toward harmless MAMPs and antigens.⁴⁸ Anti-inflammatory microenvironments in the intestinal mucosa, the gut-associated lymphoid tissue, and the mesenteric lymph nodes (MLNs) favor the development of IgA-secreting B cells and antigen-specific regulatory T (Treg) cells, 2 major antigen-specific tolerance mechanisms.³⁶ In contrast to other immunoglobulin-driven reactions, antigen binding by IgA results in efficient antigen neutralization without induction of proinflammatory signaling cascades. In addition, the export of high amounts of dimeric IgA toward the intestinal lumen through intestinal epithelial cells results in efficient immune exclusion of the respective antigen and reinforces the intestinal barrier.⁴⁹ Low levels of fecal IgA have been associated with increased development of IgE-mediated allergic diseases in children, supporting the relevance of IgA for systemic immune homeostasis.⁵⁰ Importantly, the induction of antigen-specific Treg cells on oral antigen exposure not only confers gastrointestinal but also peripheral tolerance toward the specific antigen (oral tolerance, Fig 1). Antigen-specific Treg cells exert potent anti-inflammatory activities, either through suppression of cell-cell contacts or secretion of anti-inflammatory cytokines, such as IL-10 and TGF- β .⁵¹ Noticeably, the capacity to induce tolerogenic mechanisms toward antigens can also be referred to as mucosal tolerance because it is not exclusive to the gastrointestinal tract but rather a general feature of mucosal body surfaces, including nasal and bronchial mucosa.

The induction of mucosal tolerance is an important and extensively investigated therapeutic goal in patients with a wide range of chronic inflammatory diseases.⁵²⁻⁵⁵ In the context of allergies, sublingual immunotherapies have been successfully developed to reduce systemic reactivity toward the respective allergen through induction of oral tolerance.⁵⁶ However, deregulated intestinal immune responses, such as those in patients with food allergies, in which the immune system is overreacting toward minute amounts of food antigens, or inflammatory bowel diseases, in which an overreaction toward microbial antigens triggers chronic inflammation, were found to be associated with strongly reduced or loss of oral tolerance.^{57,58} These findings indicate that oral tolerance is dependent on the proper development and function of the intestinal barrier and immune system, which in turn are shaped by microbe-host interactions. In the next section we will provide details on the role of microbe-host interactions in the development of specific immune cell populations and immune mechanisms that are thought to underlie the development of allergies.

EFFECT OF MICROBE-HOST INTERACTIONS ON INTESTINAL AND SYSTEMIC IMMUNE FUNCTIONS

The major role of microbe-host interactions for host health has been underlined by abundant experimental studies using gnotobiotic animal models. The morphology and functions of the immune system in germ-free animals differ from those in colonized animals. Organized immune structures, such as Peyer patches (PPs) and MLNs, are smaller in germ-free animals, contain lower numbers of B and T cells, and lack germinal centers. Furthermore, germ-free animals exhibit decreased

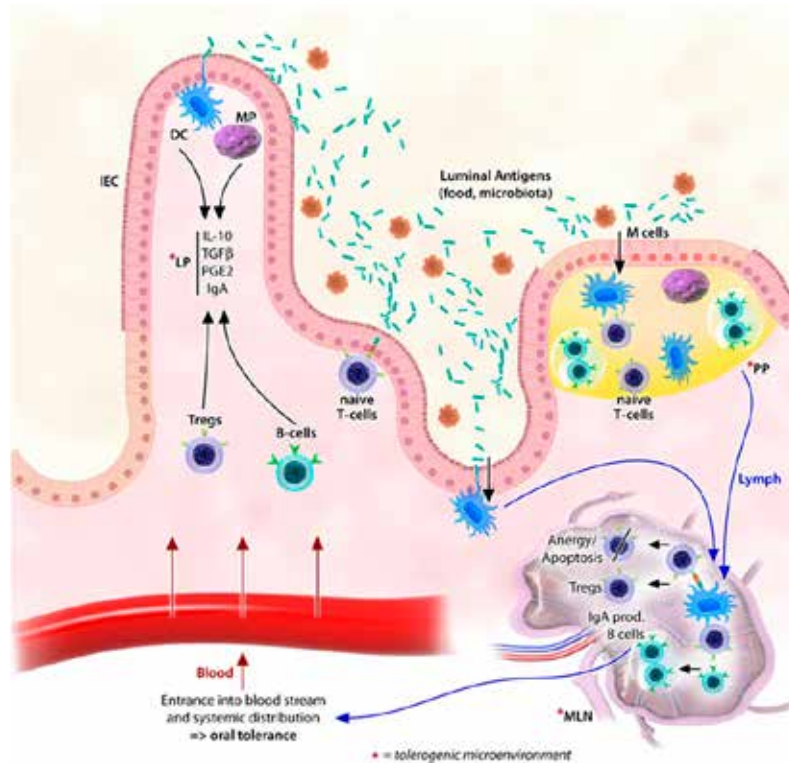


FIG 1. Oral tolerance mechanisms. Innocuous antigens that enter mucosal tissues through organized antigen sampling of M cells in PPs or lamina propria DCs induce tolerogenic mechanisms on antigen presentation. The tolerogenic microenvironment in the mucosal tissue and PPs primes antigen-presenting cells toward reduced antigen responsiveness, resulting either in clonal deletion of antigen-specific T cells through induction of T-cell anergy or apoptosis or the induction of antigen-specific Treg cells on antigen presentation in PPs or MLNs. These Treg cells are subsequently systemically distributed through the bloodstream and enter both mucosal and peripheral tissues, where they can exert anti-inflammatory activities on antigen contact. The induction of IgA-secreting plasma cells contributes to the induction of oral tolerance because IgA not only plays an important role in immune exclusion of antigens but also contributes to mucosal antigen sampling and anti-inflammatory antigen neutralization. IEC, Intestinal epithelial cells; LP, lamina propria; MP, macrophage; PGE₂, prostaglandin E₂.

numbers of dendritic cells (DCs), CD4⁺ T cells, and IgA-producing B cells in the lamina propria, as well as lower numbers of intraepithelial T cells.⁵⁹⁻⁶¹ In addition, the spleen was found to be smaller in germ-free animals and to contain fewer lymphocytes, especially CD4⁺ T cells.⁶² These findings demonstrate that microbial triggers are necessary for the development and maturation of the immune system. In line with these morphologic changes, several immune functions are compromised in germ-free animals, resulting in aberrant immune responses. Germ-free animals produce less IgA⁶³ and are characterized by T_H2-skewed immune responses, indicating that microbial triggers are necessary for counterbalancing T_H2 responses through the induction of T_H1, T_H17, and/or Treg cells.⁶⁴⁻⁶⁶ Colonization of germ-free mice with microbial communities or single bacterial strains or even oral application of specific microbial components, such as polysaccharide A from *Bacteroides fragilis*, is sufficient to normalize the morphology of the immune system and the T_H1/T_H2 balance.^{67,68} However, the highly complex nature of microbe-host interactions that

shape host immune responses is demonstrated by recent findings in the context of T_H17 responses. The induction of T_H17 cells in the lamina propria of germ-free mice was found to be dependent on a specific population of microbes, the segmented filamentous bacteria.⁶⁶ In addition, microbial ATP was shown to induce differentiation of T_H17 cells,⁶⁹ whereas polysaccharide A from *B fragilis* prevents T_H17 responses through induction of Treg cells.⁶⁸ With regard to the development and function of Treg cells, the effect of microbe-host interactions is still controversial.^{70,71} Although germ-free mice do have CD25⁺CD4⁺ regulatory cells in PPs and MLNs, their number and suppressive activity are reduced, resulting in failure to induce oral tolerance in germ-free mice.⁷² Interestingly, colonization with specific bacterial species (eg, *Bifidobacterium infantis*) resulted in normalization of oral tolerance induction, whereas colonization with other species (eg, *Clostridium perfringens*) did not, indicating that species-specific yet unknown bacterial structures or products are crucial for the induction of regulatory mechanisms.⁷³

Consistent with a decreased T_H1/T_H2 ratio, germ-free mice were recently shown to mount an exaggerated allergic airway reaction compared with that seen in colonized mice, indicating the important role of microbe-host interactions in the development of allergic diseases. Ovalbumin challenge in sensitized germ-free mice resulted in increased infiltration of lymphocytes and eosinophils into the airways and increased local levels of ovalbumin-specific IgE and typical T_H2 cytokines compared with those seen in colonized mice. Whereas increased allergic reaction correlated with reduced secretion of bronchial IgA, reduced numbers of plasmacytoid DCs and alveolar macrophages, and increased numbers of basophils, numbers of Treg cells and levels of regulatory cytokines were unchanged.⁷⁴ However, the molecular mechanisms and responsible microbial structures underlying the protective effect of the microbiota on the development of the allergic airway reaction remain to be elucidated. Furthermore, it would be highly interesting to clarify to what extent the observed protection is mediated through the intestinal or bronchial microbiota. In addition to exaggerated allergic airway reaction, germ-free mice seem to be more susceptible to IgE-mediated cow's milk allergy.⁷⁵ Germ-free mice were more responsive to oral sensitization (increased IL-4 secretion by stimulated splenocytes *ex vivo*) and were characterized by greater reduction in body temperature (clinical cow's milk allergy symptom) and higher blood levels of mast cell protease 1 and β -lactoglobulin-specific IgG₁ after oral challenge with β -lactoglobulin compared with colonized mice. Interestingly, whereas sensitization had no significant effect on dominant intestinal bacterial groups (denaturing gradient gel electrophoresis analysis), severe allergic disease was associated with low counts of cecal staphylococci (culture analysis), suggesting that subdominant species might play protective roles. With regard to specific active microbial molecules, short-chain fatty acids (SCFAs) can exert an array of anti-inflammatory effects in experimental models of inflammation. The increased severity of dextran sodium sulfate-induced colitis in germ-free mice compared with that seen in colonized mice can be prevented by giving acetate in drinking water.⁷⁶ Importantly, the protective effect of acetate is dependent on the presence of the SCFA receptor GPR43. Knockout of GPR43 resulted in worsened dextran sodium sulfate-induced acute colitis, 2,4,6-trinitrobenzene sulfonic acid-induced colitis (T_H1 mediated), arthritis, and allergic asthma in colonized mice, indicating that bacterial SCFAs are able to mediate potent anti-inflammatory effects through this pathway.

In summary, the use of gnotobiotic mice and experimental allergy models has been very useful in testing the causative role of microbiota in shaping regulatory immune responses in the gut and the development of allergic responses. However, microbial functions must be further investigated. For instance, the role of specific microbial features (eg, adhesion and enzymatic activities), and microbial structures (eg, MAMPs, antigens, and metabolites) remain to be elucidated at the level of the entire ecosystem. In spite of this lack of knowledge, targeted modulation of the intestinal microbiota is a major goal of basic and clinical research aiming at the development or re-establishment of immune homeostasis.

INTERVENTION STRATEGIES TARGETING THE INTESTINAL MICROBIOTA IN PATIENTS WITH ALLERGIC DISEASES

Although attempts to modulate the microbiota through antibiotics, such as amoxicillin or clarithromycin, have been of no to

low protective relevance in adult asthmatic patients,^{77,78} the application of prebiotics and probiotics is hypothesized to be a safe and efficient approach for the prevention and treatment of allergic diseases.

Prebiotics are food components that cannot be digested by the host but are metabolized by and promote the growth of specific subgroups of endogenous gut bacteria thought to be beneficial for the host.⁷⁹ An array of experimental data indicate that prebiotic-mediated compositional changes in murine intestinal microbiota protect the host against the development of allergic diseases.⁸⁰⁻⁸² Mechanistically, a study in mice showed protective effects of prebiotic uptake on cow's milk allergy through increased oral tolerance induction after oral wheat sensitization.⁸³ In contrast, results from clinical interventions based on the use of prebiotics are heterogeneous. Some studies showed significantly reduced allergic manifestations in prebiotic-treated children, whereas others did not detect any protective effect.⁸⁴⁻⁸⁷ Furthermore, there is still no proof that potential protective effects are due to prebiotic-induced compositional or functional changes in the intestinal microbiota.

Probiotics are live microorganisms that confer a health benefit to the host when administered in adequate amounts (World Health Organization/Food and Agriculture Organization 2001). They are proposed to exert either direct protective effects on the host or to modulate the intestinal microbiota in a protective way. Many different bacterial strains or mixtures thereof, as well as synbiotics (combination of prebiotics and probiotics), have been used in clinical trials to assess protective effects in the context of allergic sensitization and allergic diseases, but results have been conflicting. Several studies reported a significant reduction in the incidence and severity of allergic diseases after probiotic treatment,^{88,89} whereas others did not observe protective effects.⁹⁰ Meta-analysis of data from clinical studies concluded that probiotics cannot be generally recommended for the treatment of eczema⁹¹ or the prevention of allergies in general (eczema, rhinitis, asthma, and food allergy).⁹² These results stress the importance of selecting suitable bacterial strains and application schemes for different patient subgroups.

Microorganisms need to be screened *in vitro* and in experimental studies for protective microbe-microbe or microbe-host interactions to preselect potentially effective probiotic bacteria for targeted application in clinical studies. Until now, the selection of probiotic strains has mostly been performed on a hypothesis-free basis. In addition, the reported effects of probiotic therapy in clinical studies remain mostly descriptive, resulting in a lack of understanding of protective mechanisms. Clinical studies showed that probiotics can improve mucosal barrier function,⁹³ increase allergen-specific IgA levels,⁹⁴ and positively affect an array of other immune-modulatory effects affecting the T_H1/T_H2 balance.⁹⁵⁻⁹⁷ Moreover, in experimental studies the protective effect of probiotics on allergic diseases was mediated by the induction of regulatory mechanisms, such as generation, proliferation, and activity of tolerogenic DCs and T cells.^{94,98,99} However, it is unclear whether probiotic bacteria directly induce these effects or whether protection is conferred through a probiotic-mediated stabilization or modulation of the intestinal microbiota. Studies addressing this question provided contradictory results. Whereas uptake of 2 probiotic strains (*Lactobacillus acidophilus* ATCC 700396 and *Bifidobacterium animalis subsp. lactis* ATCC SD5220) affected neither disease severity (Scoring Atopic Dermatitis score) nor the diversity and composition of

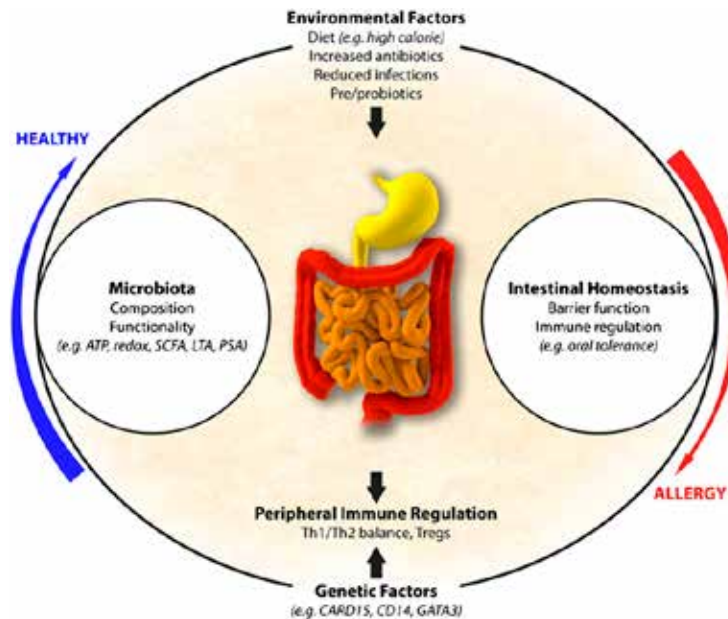


FIG 2. Systemic immune homeostasis depends on intestinal microbe-host interactions. Under the influence of genetic and environmental factors, the activity and antigenic potential of gut microorganisms have a strong influence on barrier maintenance, the development of gut-associated lymphoid tissues, and eventually systemic immune responses. *LTA*, Lipoteichoic acid; *PSA*, polysaccharide A; *redox*, redox potential.

TABLE I. Current knowledge and future research needs

Consensus	Perspective
Alterations of the gut microbiota are associated with the development and severity of allergies.	Dysbiosis of microbial ecosystems in allergic patients must be described at functional levels (metagenome, proteome, or metabolome). Dysbiosis in early-life periods must be further investigated to reach consensus in the definition of “healthy” infant microbiota and to mine microbial parameters involved in the onset of allergic symptoms.
	The causative role of changes in gut microbial communities (dysbiosis) in patients with allergic diseases must be clearly demonstrated, such as through microbial transfer experiments in germ-free murine models of allergy.
The intestinal mucosa is a highly efficient barrier, which prevents translocation of microorganisms, as well as dietary and microbial molecules.	Intestinal barrier dysfunctions must be further investigated in homogeneous populations of allergic patients. The occurrence of specific bacterial molecules (eg, LPS, heat shock proteins, fatty acids, and DNA) in the blood of allergic patients must be analyzed.
There is inconsistent support for the efficacy of probiotics and prebiotics in preventing allergies.	Probiotic structure-function relationships with regard to probiotic-microbiota or probiotic-host interactions need to be elucidated to enable targeted application of probiotics. The clinical relevance of selected prebiotics and probiotics needs to be investigated in a sufficient number of state-of-the-art clinical studies. The effect of prebiotics and probiotics on gut microbial ecosystems must be analyzed beyond the sole level of bacterial diversity.

the main bacterial genera in the intestines of atopic children,¹⁰⁰ uptake of *Lactobacillus rhamnosus* GG and *Lactobacillus gasseri* TMC0356 resulted in reduced allergic rash-induced alterations of the fecal microbiota in Japanese patients with cedar pollinosis,¹⁰¹ suggesting that the effect of probiotics on the intestinal microbiota is strain specific and dependent on the resident microbiota. A synbiotic mixture (*B breve* M-16V and Immunofortis; Nutricia Cuijk BV, Cuijk, The Netherlands) had a strong effect on the

intestinal microbiota (increased proportion of bifidobacteria vs clostridia and eubacteria), which did not translate into improvement in disease severity (Scoring Atopic Dermatitis score).¹⁰² In contrast, uptake of *L rhamnosus* GG affected humoral parameters, such as blood levels of IgA- or IgM-secreting cells but not the number of specific microbial species in intestinal and skin samples from infants with atopic dermatitis.¹⁰³ Furthermore, a combination of *L acidophilus* ATCC 700396 and *B lactis* ATCC

SD5219 did not prevent allergic rash-induced changes in intestinal microbiota but had protective effects with regard to eosinophil infiltration in patients with allergic rhinitis,⁶ which speaks in favor of the direct effects of the ingested strains.

In summary, additional state-of-the-art clinical intervention trials are needed before any recommendation can be made concerning the use of prebiotics and probiotics for the prevention or therapy of allergic diseases. Direct or microbiota-mediated protective effects of probiotic strains on host immune functions are far from being understood. In this respect analyzing changes in gut microbiota only at the level of bacterial diversity is not likely to be sufficient to measure the effect of probiotic microorganisms on intestinal ecosystems.¹⁰⁴

CONCLUSIONS

Fig 2 provides a schematic overview of key issues highlighted in the present review with respect to the role of microbe-host interactions in allergy development. Future research needs are summarized in Table I. Ecologic approaches dedicated to the characterization of ecosystem functions and alteration thereof (dysbiosis) in early-life periods will be essential for characterizing the establishment of a “normal” microbiota (as in the sense of diverse and stable microbial consortia) expressing key functions that affect intestinal and systemic immune homeostasis. Intervention trials could then be designed with the aim of stabilizing or re-establishing these key functions. With regard to the use of specific microorganisms for the prevention or reduction of allergic diseases, experimental studies are required to preselect candidate strains with a high protective potential and to dissect protective molecular mechanisms. The clinical relevance of candidate strains must then be determined in high-quality clinical studies.

REFERENCES

- Okada H, Kuhn C, Feillet H, et al. The “hygiene hypothesis” for autoimmune and allergic diseases: an update. *Clin Exp Immunol* 2010;160:1-9.
- Charlson ES, Bittinger K, Haas AR, et al. Topographical continuity of bacterial populations in the healthy human respiratory tract. *Am J Respir Crit Care Med* 2011;184:957-63.
- Costello EK, Lauber CL, Hamady M, et al. Bacterial community variation in human body habitats across space and time. *Science* 2009;326:1694-7.
- Jansson J, Willing B, Lucio M, et al. Metabolomics reveals metabolic biomarkers of Crohn’s disease. *PLoS One* 2009;4:e6386.
- Qin J, Li R, Raes J, et al. A human gut microbial gene catalogue established by metagenomic sequencing. *Nature* 2010;464:59-65.
- Ouwehand AC, Nermes M, Collado MC, et al. Specific probiotics alleviate allergic rhinitis during the birch pollen season. *World J Gastroenterol* 2009;15:3261-8.
- Penders J, Thijs C, van den Brandt PA, et al. Gut microbiota composition and development of atopic manifestations in infancy: the KOALA Birth Cohort Study. *Gut* 2007;56:661-7.
- Gore C, Munro K, Lay C, et al. *Bifidobacterium pseudocatenulatum* is associated with atopic eczema: a nested case-control study investigating the fecal microbiota of infants. *J Allergy Clin Immunol* 2008;121:135-40.
- Hong PY, Lee BW, Aw M, et al. Comparative analysis of fecal microbiota in infants with and without eczema. *PLoS One* 2010;5:e9964.
- Vael C, Vanheirstraeten L, Desager KN, et al. Denaturing gradient gel electrophoresis of neonatal intestinal microbiota in relation to the development of asthma. *BMC Microbiol* 2011;11:68.
- Nakayama J, Kobayashi T, Tanaka S, et al. Aberrant structures of fecal bacterial community in allergic infants profiled by 16S rRNA gene pyrosequencing. *FEMS Immunol Med Microbiol* 2011;63:397-406.
- Dekio I, Sakamoto M, Hayashi H, et al. Characterization of skin microbiota in patients with atopic dermatitis and in normal subjects using 16S rRNA gene-based comprehensive analysis. *J Med Microbiol* 2007;56:1675-83.
- Hilty M, Burke C, Pedro H, et al. Disordered microbial communities in asthmatic airways. *PLoS One* 2010;5:e8578.
- Huang YJ, Nelson CE, Brodie EL, et al. Airway microbiota and bronchial hyper-responsiveness in patients with suboptimally controlled asthma. *J Allergy Clin Immunol* 2011;127:372-81, e1-3.
- Thompson-Chagoyan OC, Fallani M, Maldonado J, et al. Faecal microbiota and short-chain fatty acid levels in faeces from infants with cow’s milk protein allergy. *Int Arch Allergy Immunol* 2011;156:325-32.
- Torgerson DG, Ampleford EJ, Chiu GY, et al. Meta-analysis of genome-wide association studies of asthma in ethnically diverse North American populations. *Nat Genet* 2011;43:887-92.
- Dominguez-Bello MG, Costello EK, Contreras M, et al. Delivery mode shapes the acquisition and structure of the initial microbiota across multiple body habitats in newborns. *Proc Natl Acad Sci U S A* 2010;107:11971-5.
- van Nimwegen FA, Penders J, Stobberingh EE, et al. Mode and place of delivery, gastrointestinal microbiota, and their influence on asthma and atopy. *J Allergy Clin Immunol* 2011;128:948-55, e1-3.
- Thavagnanam S, Fleming J, Bromley A, et al. A meta-analysis of the association between Caesarean section and childhood asthma. *Clin Exp Allergy* 2008;38:629-33.
- Wills-Karp M, Santeliz J, Karp CL. The germless theory of allergic disease: revisiting the hygiene hypothesis. *Nat Rev Immunol* 2001;1:69-75.
- von Mutius E, Vercelli D. Farm living: effects on childhood asthma and allergy. *Nat Rev Immunol* 2010;10:861-8.
- Ege MJ, Mayer M, Normand AC, et al. Exposure to environmental microorganisms and childhood asthma. *N Engl J Med* 2011;364:701-9.
- Bach JF. The effect of infections on susceptibility to autoimmune and allergic diseases. *N Engl J Med* 2002;347:911-20.
- Feary J, Britton J, Leonardi-Bee J. Atopy and current intestinal parasite infection: a systematic review and meta-analysis. *Allergy* 2011;66:569-78.
- von Mutius E, Pearce N, Beasley R, et al. International patterns of tuberculosis and the prevalence of symptoms of asthma, rhinitis, and eczema. *Thorax* 2000;55:449-53.
- Busse WW, Lemanske RF Jr, Gern JE. Role of viral respiratory infections in asthma and asthma exacerbations. *Lancet* 2010;376:826-34.
- Blaser M. Antibiotic overuse: stop the killing of beneficial bacteria. *Nature* 2011;476:393-4.
- Fallani M, Young D, Scott J, et al. Intestinal microbiota of 6-week-old infants across Europe: geographic influence beyond delivery mode, breast-feeding, and antibiotics. *J Pediatr Gastroenterol Nutr* 2010;51:77-84.
- Makino H, Kushi A, Ishikawa E, et al. Transmission of intestinal *Bifidobacterium longum* subsp. *longum* strains from mother to infant determined by multilocus sequencing typing and amplified fragment length polymorphism. *Appl Environ Microbiol* 2011;77:6788-93.
- Mosconi E, Rekimia A, Seitz-Polski B, et al. Breast milk immune complexes are potent inducers of oral tolerance in neonates and prevent asthma development. *Mucosal Immunol* 2010;3:461-74.
- Willing BP, Russell SL, Finlay BB. Shifting the balance: antibiotic effects on host-microbiota mutualism. *Nat Rev Microbiol* 2011;9:233-43.
- Murk W, Risnes KR, Bracken MB. Prenatal or early-life exposure to antibiotics and risk of childhood asthma: a systematic review. *Pediatrics* 2011;127:1125-38.
- Brew BK, Allen CW, Toelle BG, et al. Systematic review and meta-analysis investigating breast feeding and childhood wheezing illness. *Paediatr Perinat Epidemiol* 2011;25:507-18.
- Batchelor JM, Grindlay DJ, Williams HC. What’s new in atopic eczema? An analysis of systematic reviews published in 2008 and 2009. *Clin Exp Dermatol* 2010;35:823-8.
- Penders J, Kummeling I, Thijs C. Infant antibiotic use and wheeze and asthma risk: a systematic review and meta-analysis. *Eur Respir J* 2011;38:295-302.
- Brandtzaeg P. Food allergy: separating the science from the mythology. *Nat Rev Gastroenterol Hepatol* 2010;7:380-400.
- Turner JR. Intestinal mucosal barrier function in health and disease. *Nat Rev Immunol* 2009;9:799-809.
- Benard A, Desreumeaux P, Huglo D, et al. Increased intestinal permeability in bronchial asthma. *J Allergy Clin Immunol* 1996;97:1173-8.
- Hijazi Z, Molla AM, Al-Habashi H, et al. Intestinal permeability is increased in bronchial asthma. *Arch Dis Child* 2004;89:227-9.
- Jackson PG, Lessof MH, Baker RW, et al. Intestinal permeability in patients with eczema and food allergy. *Lancet* 1981;1:1285-6.
- Majamaa H, Isolauri E. Evaluation of the gut mucosal barrier: evidence for increased antigen transfer in children with atopic eczema. *J Allergy Clin Immunol* 1996;97:985-90.
- Steck N, Hoffmann M, Sava IG, et al. *Enterococcus faecalis* metalloprotease compromises epithelial barrier and contributes to intestinal inflammation. *Gastroenterology* 2011;141:959-71.

43. Cani PD, Possemiers S, Van de Wiele T, et al. Changes in gut microbiota control inflammation in obese mice through a mechanism involving GLP-2-driven improvement of gut permeability. *Gut* 2009;58:1091-103.
44. Fernandez-Blanco JA, Barbosa S, Sanchez de Medina F, et al. Persistent epithelial barrier alterations in a rat model of postinfectious gut dysfunction. *Neurogastroenterol Motil* 2011;23:e523-33.
45. Kau AL, Ahern PP, Griffin NW, et al. Human nutrition, the gut microbiome and the immune system. *Nature* 2011;474:327-36.
46. Costantini TW, Bansal V, Peterson CY, et al. Efferent vagal nerve stimulation attenuates gut barrier injury after burn: modulation of intestinal occludin expression. *J Trauma* 2010;68:1349-56.
47. Krzyzaniak MJ, Peterson CY, Cheadle G, et al. Efferent vagal nerve stimulation attenuates acute lung injury following burn: the importance of the gut-lung axis. *Surgery* 2011;150:379-89.
48. Rescigno M, Lopatin U, Chieppa M. Interactions among dendritic cells, macrophages, and epithelial cells in the gut: implications for immune tolerance. *Curr Opin Immunol* 2008;20:669-75.
49. Mantis NJ, Rol N, Corthesy B. Secretory IgA's complex roles in immunity and mucosal homeostasis in the gut. *Mucosal Immunol* 2011;4:603-11.
50. Kukkonen K, Kuitunen M, Haahela T, et al. High intestinal IgA associates with reduced risk of IgE-associated allergic diseases. *Pediatr Allergy Immunol* 2010;21:67-73.
51. Brandtzaeg P. Homeostatic impact of indigenous microbiota and secretory immunity. *Benef Microbes* 2010;1:211-27.
52. Scurlock AM, Jones SM. An update on immunotherapy for food allergy. *Curr Opin Allergy Clin Immunol* 2010;10:587-93.
53. Fourlanos S, Perry C, Gellert SA, et al. Evidence that nasal insulin induces immune tolerance to insulin in adults with autoimmune diabetes. *Diabetes* 2011;60:1237-45.
54. Hyun JG, Barrett TA. Oral tolerance therapy in inflammatory bowel disease. *Am J Gastroenterol* 2006;101:569-71.
55. Weiner HL, da Cunha AP, Quintana F, et al. Oral tolerance. *Immunol Rev* 2011;241:241-59.
56. Ye YL, Chuang YH, Chiang BL. Strategies of mucosal immunotherapy for allergic diseases. *Cell Mol Immunol* 2011;8:453-61.
57. Scurlock AM, Vickery BP, Hourihane JO, et al. Pediatric food allergy and mucosal tolerance. *Mucosal Immunol* 2010;3:345-54.
58. Kraus TA, Toy L, Chan L, et al. Failure to induce oral tolerance to a soluble protein in patients with inflammatory bowel disease. *Gastroenterology* 2004;126:1771-8.
59. Tlaskalova-Hogenova H, Sterzl J, Stepankova R, et al. Development of immunological capacity under germfree and conventional conditions. *Ann N Y Acad Sci* 1983;409:96-113.
60. Umesaki Y, Setoyama H, Matsumoto S, et al. Expansion of alpha beta T-cell receptor-bearing intestinal intraepithelial lymphocytes after microbial colonization in germ-free mice and its independence from thymus. *Immunology* 1993;79:32-7.
61. Moreau MC, Ducluzeau R, Guy-Grand D, et al. Increase in the population of duodenal immunoglobulin A plasmocytes in axenic mice associated with different living or dead bacterial strains of intestinal origin. *Infect Immun* 1978;21:532-9.
62. Dobber R, Hertogh-Huijbregts A, Rozing J, et al. The involvement of the intestinal microflora in the expansion of CD4+ T cells with a naive phenotype in the periphery. *Dev Immunol* 1992;2:141-50.
63. Macpherson AJ, Gatto D, Sainsbury E, et al. A primitive T cell-independent mechanism of intestinal mucosal IgA responses to commensal bacteria. *Science* 2000;288:2222-6.
64. Bowman LM, Holt PG. Selective enhancement of systemic Th1 immunity in immunologically immature rats with an orally administered bacterial extract. *Infect Immun* 2001;69:3719-27.
65. Gaboriau-Routhiau V, Rakotobe S, Lecuyer E, et al. The key role of segmented filamentous bacteria in the coordinated maturation of gut helper T cell responses. *Immunity* 2009;31:677-89.
66. Ivanov II, Atarashi K, Manel N, et al. Induction of intestinal Th17 cells by segmented filamentous bacteria. *Cell* 2009;139:485-98.
67. Mazmanian SK, Liu CH, Tzianabos AO, et al. An immunomodulatory molecule of symbiotic bacteria directs maturation of the host immune system. *Cell* 2005;122:107-18.
68. Round JL, Lee SM, Li J, et al. The Toll-like receptor 2 pathway establishes colonization by a commensal of the human microbiota. *Science* 2011;332:974-7.
69. Atarashi K, Nishimura J, Shima T, et al. ATP drives lamina propria T(H)17 cell differentiation. *Nature* 2008;455:808-12.
70. Annacker O, Buren-Defranoux O, Pimenta-Araujo R, et al. Regulatory CD4 T cells control the size of the peripheral activated/memory CD4 T cell compartment. *J Immunol* 2000;164:3573-80.
71. Strauch UG, Obermeier F, Grunwald N, et al. Influence of intestinal bacteria on induction of regulatory T cells: lessons from a transfer model of colitis. *Gut* 2005;54:1546-52.
72. Ishikawa H, Tanaka K, Maeda Y, et al. Effect of intestinal microbiota on the induction of regulatory CD25+ CD4+ T cells. *Clin Exp Immunol* 2008;153:127-35.
73. Maeda Y, Noda S, Tanaka K, et al. The failure of oral tolerance induction is functionally coupled to the absence of T cells in Peyer's patches under germfree conditions. *Immunobiology* 2001;204:442-57.
74. Herbst T, Sichelstiel A, Schar C, et al. Dysregulation of allergic airway inflammation in the absence of microbial colonization. *Am J Respir Crit Care Med* 2011;184:198-205.
75. Rodriguez B, Prioult G, Bibiloni R, et al. Germ-free status and altered caecal subdominant microbiota are associated with a high susceptibility to cow's milk allergy in mice. *FEMS Microbiol Ecol* 2011;76:133-44.
76. Maslowski KM, Vieira AT, Ng A, et al. Regulation of inflammatory responses by gut microbiota and chemoattractant receptor GPR43. *Nature* 2009;461:1282-6.
77. Graham VA, Milton AF, Knowles GK, et al. Routine antibiotics in hospital management of acute asthma. *Lancet* 1982;1:418-20.
78. Sutherland ER, King TS, Icitovic N, et al. A trial of clarithromycin for the treatment of suboptimally controlled asthma. *J Allergy Clin Immunol* 2010;126:747-53.
79. Bird AR, Conlon MA, Christophersen CT, et al. Resistant starch, large bowel fermentation and a broader perspective of prebiotics and probiotics. *Benef Microbes* 2010;1:423-31.
80. Fujiwara R, Takemura N, Watanabe J, et al. Maternal consumption of fructo-oligosaccharide diminishes the severity of skin inflammation in offspring of NC/Nga mice. *Br J Nutr* 2010;103:530-8.
81. Yasuda A, Inoue KI, Sanbongi C, et al. Dietary supplementation with fructooligosaccharides attenuates airway inflammation related to house dust mite allergen in mice. *Int J Immunopathol Pharmacol* 2010;23:727-35.
82. Watanabe J, Sasajima N, Aramaki A, et al. Consumption of fructo-oligosaccharide reduces 2,4-dinitrofluorobenzene-induced contact hypersensitivity in mice. *Br J Nutr* 2008;100:339-46.
83. Schouten B, van Esch BC, Hofman GA, et al. Oligosaccharide-induced whey-specific CD25(+) regulatory T-cells are involved in the suppression of cow milk allergy in mice. *J Nutr* 2010;140:835-41.
84. Osborn DA, Sinn JK. Prebiotics in infants for prevention of allergic disease and food hypersensitivity. *Cochrane Database Syst Rev* 2007;(4):CD006474.
85. Arslanoglu S, Moro GE, Schmitt J, et al. Early dietary intervention with a mixture of prebiotic oligosaccharides reduces the incidence of allergic manifestations and infections during the first two years of life. *J Nutr* 2008;138:1091-5.
86. Gruber C, van Stuijvenberg M, Mosca F, et al. Reduced occurrence of early atopic dermatitis because of immunoreactive prebiotics among low-atopy-risk infants. *J Allergy Clin Immunol* 2010;126:791-7.
87. Shibata R, Kimura M, Takahashi H, et al. Clinical effects of kestose, a prebiotic oligosaccharide, on the treatment of atopic dermatitis in infants. *Clin Exp Allergy* 2009;39:1397-403.
88. Kalliomaki M, Salminen S, Poussa T, et al. Probiotics and prevention of atopic disease: 4-year follow-up of a randomized placebo-controlled trial. *Lancet* 2003;361:1869-71.
89. Dotterud CK, Storro O, Johnsen R, et al. Probiotics in pregnant women to prevent allergic disease: a randomized, double-blind trial. *Br J Dermatol* 2010;163:616-23.
90. Gruber C, Wendt M, Sulser C, et al. Randomized, placebo-controlled trial of *Lactobacillus rhamnosus* GG as treatment of atopic dermatitis in infancy. *Allergy* 2007;62:1270-6.
91. Boyle RJ, Bath-Hextall FJ, Leonardi-Bee J, et al. Probiotics for the treatment of eczema: a systematic review. *Clin Exp Allergy* 2009;39:1117-27.
92. Osborn DA, Sinn JK. Probiotics in infants for prevention of allergic disease and food hypersensitivity. *Cochrane Database Syst Rev* 2007;(4):CD006475.
93. Rosenfeldt V, Benfeldt E, Valerius NH, et al. Effect of probiotics on gastrointestinal symptoms and small intestinal permeability in children with atopic dermatitis. *J Pediatr* 2004;145:612-6.
94. Rautava S, Arvilommi H, Isolauri E. Specific probiotics in enhancing maturation of IgA responses in formula-fed infants. *Pediatr Res* 2006;60:221-4.
95. Marschan E, Kuitunen M, Kukkonen K, et al. Probiotics in infancy induce protective immune profiles that are characteristic for chronic low-grade inflammation. *Clin Exp Allergy* 2008;38:611-8.
96. Torii S, Torii A, Itoh K, et al. Effects of oral administration of *Lactobacillus acidophilus* L-92 on the symptoms and serum markers of atopic dermatitis in children. *Int Arch Allergy Immunol* 2011;154:236-45.

97. West CE, Hammarstrom ML, Hernell O. Probiotics during weaning reduce the incidence of eczema. *Pediatr Allergy Immunol* 2009;20:430-7.
98. Kwon HK, Lee CG, So JS, et al. Generation of regulatory dendritic cells and CD4+Foxp3+ T cells by probiotics administration suppresses immune disorders. *Proc Natl Acad Sci U S A* 2010;107:2159-64.
99. Lyons A, O'Mahony D, O'Brien F, et al. Bacterial strain-specific induction of Foxp3+ T regulatory cells is protective in murine allergy models. *Clin Exp Allergy* 2010;40:811-9.
100. Larsen N, Vogensen FK, Gobel R, et al. Predominant genera of fecal microbiota in children with atopic dermatitis are not altered by intake of probiotic bacteria *Lactobacillus acidophilus* NCFM and *Bifidobacterium animalis subsp. lactis* Bi-07. *FEMS Microbiol Ecol* 2011;75:482-96.
101. Kubota A, He F, Kawase M, et al. Lactobacillus strains stabilize intestinal microbiota in Japanese cedar pollinosis patients. *Microbiol Immunol* 2009;53:198-205.
102. van der Aa LB, Heymans HS, van Aalderen WM, et al. Effect of a new synbiotic mixture on atopic dermatitis in infants: a randomized-controlled trial. *Clin Exp Allergy* 2010;40:795-804.
103. Nermes M, Kantele JM, Atosuo TJ, et al. Interaction of orally administered *Lactobacillus rhamnosus* GG with skin and gut microbiota and humoral immunity in infants with atopic dermatitis. *Clin Exp Allergy* 2011;41:370-7.
104. McNulty NP, Yatsunenko T, Hsiao A, et al. The impact of a consortium of fermented milk strains on the gut microbiome of gnotobiotic mice and monozygotic twins. *Sci Transl Med* 2011;3:106ra106.

The Journal of Allergy and Clinical Immunology
&
The Journal of Pediatrics
Announce a
Shared Science Program

These recent articles from *The Journal of Pediatrics* may be of interest to readers of *The Journal of Allergy and Clinical Immunology*:

In the April 2012 issue, Sicherer et al report on a freely available food allergy education program for parents of children with food allergies.

Sicherer SH, Vargas PA, Groetch ME, et al. Development and Validation of Educational Materials for Food Allergy. *J Pediatr* 2012;160:651-6.

In the May 2012 issue, Ross et al report that after 1 year of specialty asthma care, sleep-disordered breathing, but not obesity, is a risk factor for severe asthma.

Ross, KR, Storfer-Isser, A, Hart, MA, et al. Sleep-Disordered Breathing is Associated with Asthma Severity in Children. *J Pediatr* 2012;160:736-42.

These articles may be accessed at no cost to readers of *The Journal of Allergy and Clinical Immunology* at the Shared Science page on the website of *The Journal of Pediatrics* (www.jpeds.com).

This opportunity is made possible through a reciprocal partnership between The Journal of Pediatrics, The Journal of Allergy and Clinical Immunology, and their publisher, Elsevier, Inc.

THE JOURNAL OF
**Allergy AND Clinical
Immunology**

The JOURNAL
of PEDIATRICS

PAPER 15

ORIGINAL ARTICLE

High-fat diet alters gut microbiota physiology in mice

Hannelore Daniel¹, Amin Moghaddas Gholami^{2,13}, David Berry^{3,13}, Charles Desmarchelier^{1,13}, Hannes Hahne^{2,13}, Gunnar Loh⁴, Stanislas Mondot^{5,6}, Patricia Lepage⁵, Michael Rothballer⁷, Alesia Walker⁸, Christoph Böhm³, Mareike Wenning⁹, Michael Wagner³, Michael Blaut⁴, Philippe Schmitt-Kopplin⁸, Bernhard Kuster^{2,10}, Dirk Haller¹¹ and Thomas Clavel^{11,12}

¹Molecular Nutrition Unit, ZIEL-Research Center for Nutrition and Food Sciences, Technische Universität München, Freising-Weihenstephan, Germany; ²Proteomics and Bioanalytics, Technische Universität München, Freising-Weihenstephan, Germany; ³Division of Microbial Ecology, Department of Microbiology and Ecosystem Science, Faculty of Life Sciences, University of Vienna, Vienna, Austria; ⁴Department of Gastrointestinal Microbiology, German Institute of Human Nutrition Potsdam-Rehbrücke (DIfE), Nuthetal, Germany; ⁵INRA/AgroParisTech, Micalis UMR1319, Jouy-en-Josas, France; ⁶CSIRO Livestock Industries, Queensland Bioscience Precinct, St Lucia, Australia; ⁷Research Unit Plant-Microbe Interactions, Helmholtz Zentrum München, Neuherberg, Germany; ⁸Analytical BioGeoChemistry, Helmholtz Zentrum München, Neuherberg, Germany; ⁹Chair of Analytical Food Chemistry, Technische Universität München, Freising-Weihenstephan, Germany; ¹⁰Microbiology, ZIEL-Research Center for Nutrition and Food Sciences, Technische Universität München, Freising-Weihenstephan, Germany; ¹¹Center for Integrated Protein Science Munich, Germany; ¹²Chair of Nutrition and Immunology, Technische Universität München, Freising-Weihenstephan, Germany and ¹³Junior Research Group Intestinal Microbiome, ZIEL-Research Center for Nutrition and Food Sciences, Technische Universität München, Freising-Weihenstephan, Germany

The intestinal microbiota is known to regulate host energy homeostasis and can be influenced by high-calorie diets. However, changes affecting the ecosystem at the functional level are still not well characterized. We measured shifts in cecal bacterial communities in mice fed a carbohydrate or high-fat (HF) diet for 12 weeks at the level of the following: (i) diversity and taxa distribution by high-throughput 16S ribosomal RNA gene sequencing; (ii) bulk and single-cell chemical composition by Fourier-transform infrared-(FT-IR) and Raman micro-spectroscopy and (iii) metaproteome and metabolome via high-resolution mass spectrometry. High-fat diet caused shifts in the diversity of dominant gut bacteria and altered the proportion of *Ruminococcaceae* (decrease) and *Rikenellaceae* (increase). FT-IR spectroscopy revealed that the impact of the diet on cecal chemical fingerprints is greater than the impact of microbiota composition. Diet-driven changes in biochemical fingerprints of members of the *Bacteroidales* and *Lachnospiraceae* were also observed at the level of single cells, indicating that there were distinct differences in cellular composition of dominant phylotypes under different diets. Metaproteome and metabolome analyses based on the occurrence of 1760 bacterial proteins and 86 annotated metabolites revealed distinct HF diet-specific profiles. Alteration of hormonal and anti-microbial networks, bile acid and bilirubin metabolism and shifts towards amino acid and simple sugars metabolism were observed. We conclude that a HF diet markedly affects the gut bacterial ecosystem at the functional level.

The ISME Journal advance online publication, 12 September 2013; doi:10.1038/ismej.2013.155

Subject Category: Microbe-microbe and microbe-host interactions

Keywords: diet-induced obesity; high-fat diet; intestinal microbiota; metabolomics; metaproteome; spectroscopy

Introduction

Over the last century, the field of clinical microbiology has been driven by the study of pathogens (Raoult *et al.*, 2004), but recently, the importance of

commensal microorganisms that colonize various body habitats has been brought to light (Lepage *et al.*, 2013). In particular, the gut microbial ecosystem has emerged as an important factor regulating host health and the onset of chronic diseases such as inflammatory bowel diseases, allergies and obesity (Blaut and Clavel, 2007; Delzenne and Cani, 2011; Kau *et al.*, 2011; Hörmannspurger *et al.*, 2012).

A proof of the causative role of gut microbes in influencing host metabolism was provided by the observation that transfer of gut microbiota from

Correspondence: T. Clavel, Junior Research Group Intestinal Microbiome, ZIEL-Research Center for Nutrition and Food Sciences, Technische Universität München, Gregor-Mendel-Strasse 2, 85350 Freising-Weihenstephan, Germany.
E-mail: thomas.clavel@tum.de

¹³These authors contributed equally to the work.

Received 13 June 2013; accepted 4 August 2013

obese donor mice to germfree mice fed a standard diet promoted adiposity (Backhed *et al.*, 2004; Turnbaugh *et al.*, 2009). Nonetheless, the quantitative contribution of the gut microbiota to host energy balance remains elusive. Jumpertz *et al.*, (2011), recently proposed that an increased energy harvest of *ca.* 150 kcal is associated with an increase of 20% in the sequence occurrence of *Firmicutes* and a corresponding decrease in the *Bacteroidetes* in humans, although the impact of high inter-individual differences in the percentage of energy lost in stools have been discussed (Heymsfield and Pietrobelli, 2011). Driven by the popularization of DNA sequencing-based approaches, many studies have described changes in gut bacterial diversity and composition after ingestion of high-energy diets (Cani *et al.*, 2008; Turnbaugh *et al.*, 2008; Fleissner *et al.*, 2010). However, the consequences of such changes in bacterial diversity on the function of the ecosystem are still unclear. Major advances in the assessment of microbial gene occurrence by large-scale metagenomic sequencing have shed light on the genomic potential of the gut microbiota and have indicated possible changes in microbial activity related to diet and metabolic disorders (Turnbaugh *et al.*, 2006; Qin *et al.*, 2012). Nonetheless, direct proofs of changes in activity and function of the ecosystem in response to dietary challenge are urgently required. Therefore, in the present work, we used a combination of high-resolution spectroscopic and mass spectrometric techniques for in-depth characterization of the cecal ecosystem in mice. We thereby provide novel insights into biochemical alterations of the gut microbiota in response to a high-fat (HF) diet.

Materials and methods

Animals and samples

All procedures were conducted according to the German guidelines for animal care and approved by the state ethics committee (ref. no. 209.1/211-2531-41/03). The design of mouse trials has been described elsewhere (Desmarchelier *et al.*, 2012, 2013). Details are given in the Supplementary Methods. Male C57BL/6NCrl mice ($n = 6$ per group) were fed an experimental carbohydrate (CARB) or HF diet for 12 weeks (Table 1). The data presented in this paper were obtained in the course of four feeding trials with exactly the same design (Supplementary Figure S1). In trial 1–3, after cecal weight determination, the content was divided into two portions that were snap frozen in liquid nitrogen. In trial 4, cecal contents were used in their entirety in order to obtain sufficient starting material (metaproteome via LC-MS/MS, $n = 4$; metabolome via Fourier-transform ion cyclotron resonance mass spectrometry (FT-ICR-MS), $n = 3$). Experiments with germfree mice were performed as explained in the Supplementary Methods.

Table 1 Diet composition

	CARB	HF
GE (MJ kg ⁻¹)	18.0	25.2
ME (MJ kg ⁻¹)	15.0	21.4
% carbohydrate	66.0	21.0
% protein	23.0	19.0
% fat	11.0	60.0
Crude protein	20.8	24.1
Crude fat	4.2	34.0
Crude fiber	5.0	6.0
Crude ash	5.6	6.1
Starch	48.8	1.1
Sugar	10.8	8.2
Dextrins	—	15.6
Sodium	0.2	0.2
Casein	24.0	27.7
Corn starch	49.8	—
Maltodextrin	—	15.8
Glucose	10.0	—
Sucrose	—	8.0
Cellulose	5.0	6.0
Vitamin premix	1.0	1.2
Mineral/trace elements	6.0	6.1
L-cystine	—	0.4
Choline chloride	0.2	0.3
Salt (NaCl)	—	0.1
Butylhydroxytoluol	—	<0.1
Beef tallow (premier jus)	—	31.0
Soybean oil	4.0	3.0

Abbreviations: CARB, carbohydrate; GE, gross energy; HF, high-fat; ME, metabolizable energy calculated with the Atwater factors. Nutrient contents are given in percentages (g 100 g⁻¹). All experimental diets were ordered from Ssniff GmbH (Soest, Germany): CARB, cat. no. E15000-04; HF, E15741-34. The composition of the standard laboratory chow diet (Ssniff GmbH, cat. no. V1534) used for 2 weeks prior to dietary treatment was: dry matter, 87.7; crude protein, 19.0; crude fat, 3.3; crude fiber, 4.9; crude ash, 6.4; starch, 36.5; sugar/dextrins, 4.7; GE, 16.3; ME, 12.8; % carbohydrate, 58; % protein, 33; % fat, 9.

High-throughput sequencing

Cecal samples were analyzed by sequencing the V4 region (233 bp) of 16S ribosomal RNA (rRNA) genes in paired-end modus using the MiSeq system (Illumina, San Diego, CA, USA). Detailed instructions are given in the Supplementary Methods. The first 10 and last 20 nucleotides of all reads were trimmed using the NGS-QC toolkit (New Dehli, India) (Patel and Jain, 2012) to avoid GC bias and non-random base composition as well as low sequence quality at 3'-end. Reads were assembled using Pandaseq with a minimum overlap of 35 bp (Masella *et al.*, 2012). Sequences were further analyzed using the open source software package QIIME (Boulder, CO, USA) (Caporaso *et al.*, 2010) and the Ribosomal Database Project (East Lansing, MI, USA) (Cole *et al.*, 2003). Filtering parameters were as follows: minimum Phred score, 20; minimum number of high-quality calls, 0.65; maximum number of consecutive low-quality base calls, 5. Operational taxonomic units were picked against the Greengenes database (Berkeley, CA, USA) at a threshold of 97% similarity and those occurring in less than three mice and with a total number of less than three sequences were excluded from the analysis.

Fourier-transform infrared spectroscopy

In Fourier-transform infrared (FT-IR) spectroscopy, samples are excited by an infrared beam and transmitted light is recorded, resulting in spectra showing at which wavelengths samples absorb light, depending on the nature of covalent bonds. Thereby, FT-IR spectroscopy gives information on the overall biochemical composition of microbial cells, and can be a useful tool for the identification of pure cultures (Wenning *et al.*, 2006). Saline solution (0.9% NaCl in water) was used for sample preparation by centrifugation to obtain cecal microbial pellets (Supplementary Methods). Re-suspended pellets in saline solution (referred to as cecal suspensions hereon) were analyzed by transmission using a TENSOR 27 spectrometer coupled with a HTS-XT high-throughput device (Bruker Optics, Ettlingen, Germany). The spectrum of each sample was computed from 32 scans. Spectral similarities were assessed by hierarchical cluster analysis using the OPUS software version 6.5 (Bruker).

Confocal Raman microscopy

Fluorescence *in situ* hybridization (FISH) was used to identify target populations for Raman microspectroscopic analysis, which utilizes the principle of Raman scattering to chemically fingerprint individual microbial cells (Huang *et al.*, 2007). The probes used in the present study were Bac-0303 5'-CCA ATG TGG GGG ACC TT-3' (Manz *et al.*, 1996) and Erec-0482 5'-CGC GGC ATT GCT TCA-3' (Franks *et al.*, 1998) (Thermo Fisher Scientific, Vienna, Austria). Cecal samples that had been fixed in 4% paraformaldehyde were hybridized on aluminum slides using a previously described hybridization protocol (Berry *et al.*, 2012). Spectra of cells from target populations were acquired using a LabRAM HR800 confocal Raman microscope (Horiba Jobin-Yvon, Munich, Germany) equipped with a 532 nm Nd:YAG laser as described previously (Haider *et al.*, 2010). Raman spectra were baseline corrected and mean normalized in R using the package 'baseline' (Liland and Mevik, Norway) (Lieber and Mahadevan-Jansen, 2003). Machine-learning classification of spectra was performed with the 'randomForest' package (Liaw and Wiener (2002); Merck Research Laboratories, Whitehouse Station, NJ, USA) in R and plotted using non-metric multidimensional scaling.

Protein identification by liquid chromatography and tandem mass spectrometry

Cecal samples were prepared by centrifugation as for FT-IR spectroscopy and microbial pellets were lysed mechanically in the presence of protease inhibitors (Supplementary Methods). After reduction with 10 mM dithiothreitol (10 min, 95 °C) and alkylation with 50 mM iodoacetamide (30 min, room temperature), proteins were separated on 4–12% NuPAGE Bis-Tris gels (Invitrogen, Darmstadt, Germany; cat. no. NP0321BOX) and stained with colloidal Coomassie.

The complete protein separation lane of each sample was cut into 12 equal gel pieces (Supplementary Figure S2) and in-gel digestion was performed with sequencing grade trypsin (Promega) (Shevchenko *et al.*, 1996). Peptides were measured using an Eksigent nanoLC-Ultra 1D Plus (Eksigent, Dublin, CA, USA) coupled to a LTQ Orbitrap Velos (Thermo Scientific, Bremen, Germany), as described in detail in the Supplementary Methods.

Metaproteome data analysis

Peak picking and processing of raw MS data was performed as in the Supplementary Methods. To minimize the number of hypothetical proteins, spectra were first searched against a compiled database comprising 81 well-annotated genomes recovered from the Integrated Microbial Genomes website of the Joint Genome Institute (Supplementary Methods). Confounder proteins not expected to be present in the cecal samples were added to the database to ensure specificity. Unmatched spectra were subsequently searched against the entire NCBI database (download date 10/26/2011). For all eight samples (each 12 gel pieces), matched spectra obtained from both database searches were compiled using Scaffold version 3.3.1 (Proteome Software, Portland, OR, USA). Threshold parameters were as follows: protein probability, 95%; minimum number of peptides, 1; peptide probability, 95%. Protein abundances were estimated using NSAF (normalized spectral abundance factor) values calculated from the spectral counts of each individual identified protein (Zybailov *et al.*, 2006). Briefly, in order to account for the fact that larger proteins tend to contribute more peptides or spectra, spectral counts were divided by protein length to provide a spectral abundance factor. Spectral abundance factor values were normalized against the sum of all spectral abundance factor values in the corresponding run, allowing comparison of protein levels across different runs. NSAF was used as quantitative measure of protein abundances for subsequent statistical analyses. UniProt accession numbers were obtained using the ID mapping function at www.uniprot.org. Protein sequences were downloaded via batch retrieval at the Protein Information Resource website. Protein sequences were assigned to Clusters of Orthologous Groups (COG) by performing a BLASTP (Altschul *et al.*, 1990) against the COG database (Tatusov *et al.*, 2003). BLAST results were further parsed for best hit with an e-value lower than $1e-5$.

High-resolution metabolomics

Cecal samples were prepared by solid-phase extraction as described in the Supplementary Methods. Ultrahigh resolution mass spectra were acquired using a SOLARIX FT-ICR-MS (Bruker Daltonik GmbH, Bremen, Germany), equipped with a 12 Tesla superconducting magnet and an Apollo II ESI source. FT-ICR-MS settings are given in the Supplementary Methods. Samples were measured

in parallel in positive and negative ESI mode due to ionization and detection of different compounds. Raw spectra were processed with Data Analysis Version 4.0 SP2 (Bruker Daltonik GmbH). They were calibrated internally using reference lists of known masses with an error below 0.1 p.p.m. Calibrated spectra were exported to .asc files with a signal-to-noise ratio of 4. The acquired peak lists were aligned by means of in-house software with an error p.p.m. of 1. The aligned data matrix was filtered and only masses detected in at least two of the three biological replicates were kept for subsequent data processing. The filtered matrix was analyzed using Hierarchical Clustering Explorer (College Park, MD, USA) (Seo and Shneiderman, 2002) for unsupervised multivariate data analysis and MultiExperiment Viewer (Saeed *et al.*, 2006) for calculation of significant masses by two-tailed Student's *t*-test (adjusted *P*-value < 0.01). Possible metabolite identities of significant masses were assigned using the MassTRIX web server (Suhre and Schmitt-Kopplin, 2008) with a maximum error of 1 p.p.m. for both ionization modes. Masses were searched against the KEGG (Kyoto Encyclopedia of Genes and Genomes) (Kanehisa and Goto, 2000), HMDB (Human Metabolome Database) (Wishart *et al.*, 2007) and Lipid Maps (www.lipidmaps.org) databases using *Mus musculus* as reference organism.

Statistics

Unless otherwise stated, statistical tests were done using the R programming environment. For all tests, the bilateral alpha risk was $\alpha = 0.05$. Data were expressed as mean \pm s.d. and tested for normal distribution and equality of variances before statistical testing. Non-parametric data were analyzed using the Mann–Whitney U test. The Benjamini–Hochberg procedure was used for multiple testing corrections. For the metaproteomic NSAF data set, the Bioconductor package PLGEM (Power Law Global Error Model) (Pavelka *et al.*, 2004) was used to fit a PLGEM to the NSAF data set. It has been shown that the use of PLGEM-based standard deviations to calculate signal-to-noise ratios in a NSAF data set improves determination of protein expression changes, as it is more conservative with proteins of low abundance than proteins with high abundance. The goodness-of-fit of the model to the NSAF data and the relevant algorithmic details of the PLGEM method are explained in detail elsewhere (Pavelka *et al.*, 2008). Principal component analysis of exported normalized FT-IR spectra was done using SIMCA-P 12.0.1.

Results

High-fat diet induced obesity and altered microbial diversity and composition

The HF diet caused (i) an increase in body weight over the 12-week-long feeding trial (CARB, 29.9 ± 0.63 g;

HF, 43.2 ± 4.4 g) (Supplementary Figure S3), (ii) fasting hyperglycemia (Supplementary Table S1) and (iii) a marked reduction in mean cecal mass (tissue plus content): CARB, 342 ± 36 mg; HF, 223 ± 37 mg ($P < 0.001$; *t*-test). To assess the impact of experimental feeding on dominant bacterial communities, we sequenced V4 amplicons of 16S rRNA genes. After trimming, assembly and quality filtering, we obtained a total of 82 698 sequences (6892 ± 2419 per sample) of 233 bp length. The HF diet did not significantly affect taxa richness (Shannon diversity index: CARB, 5.37 ± 0.63 ; HF 4.96 ± 0.67) (Supplementary Figure S4). Beta-diversity analysis (unweighted Unifrac) showed that samples clustered according to diet, although intra-group variations were high (Figure 1a). As expected, phylum-level composition was dominated by members of the *Firmicutes* (71 to 98% of total sequences) and *Bacteroidetes* (1–16%) (Supplementary Table S2). Despite marked inter-individual differences at the family level, sequence proportions were significantly lower for *Ruminococcaceae* (phylum *Firmicutes*) and higher for *Rikenellaceae* (phylum *Bacteroidetes*) in HF mice (Figure 1b and Supplementary Table S3). Lactobacilli were detected in higher proportions in mice fed the HF diet (4–29%), but one control mouse had also a very high proportion (49%). Proportions of *Erysipelotrichales* were higher in three of six HF mice compared with CARB mice, reaching up to 43% in HF mouse three (Supplementary Table S3). The occurrence of 19 dominant operational taxonomic units (OTUs) was significantly affected by the HF diet (Supplementary Table S4). Most of them belonged to the order *Clostridiales* and their sequence numbers were lower in HF mice. In agreement with the aforementioned results, HF mice were characterized by increased numbers of two OTUs within the genus *Alistipes* (a genus in the *Rikenellaceae* with up to 3.5% total sequences). Other major operational taxonomic units OTUs with a higher prevalence in HF mice included one dominant member of the *Clostridium* cluster XIVa (0.01 vs 4.33% in HF mice) and two *Clostridium* species.

In order to determine if the HF diet causes not only alterations in the composition of the microbiota but also changes to the biochemical environment and microbiota activity in the gut, we performed spectroscopic and mass spectrometric analyses of cecal samples.

Cecal and single-cell chemical fingerprints were diet-specific

To examine the effect of diets on chemical fingerprints in the cecum, samples were analyzed using FT-IR spectroscopy. Cluster analysis of FT-IR spectra revealed a clear separation of chemical fingerprints according to the diet (Figure 2a). There was a clear correlation between peak height and dietary composition in region 2 and 4, which corresponds to lipids and carbohydrates, respectively (Figure 2b).

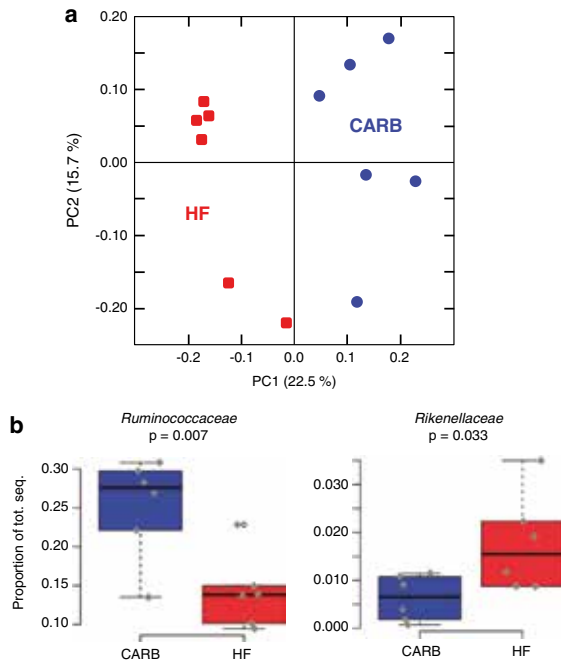


Figure 1 Changes in dominant bacterial diversity and composition. Cecal samples from mice in the CARB and HF group ($n = 6$ each) were analyzed by Illumina sequencing of 16S rRNA gene amplicons (V4 region; 233 bp). Sequences were analyzed using QIIME and the RDP. **(a)** Principal component analysis of sequence numbers (filtered OTUs) revealed grouping of samples according to diet. **(b)** HF feeding was associated with a significant reduction in the proportion of sequences assigned to the family *Ruminococcaceae* and an increase in the proportion of *Rikenellaceae*. Taxa were assigned using the Greengenes Database (released October 2012).

The carbohydrate content was markedly reduced in HF mice, accompanied by a reduced amount of water probably related to reduction in hydration water of carbohydrates and proteins. In spectral region 3 (proteins), the amide I band at 1650 cm^{-1} was clearly reduced in HF samples. In contrast, we observed four new peaks at 1580, 1540 and 1470 as well as one additional peak at 725 cm^{-1} , the absorption of which can be attributed to aromatic rings and heteroaromatic nitro compounds (Colthup *et al.*, 1990). As a proof-of-concept for the impact of bacterial colonization on cecal chemical fingerprints, we compared samples from mice monocolonized with *Bacteroides thetaiotaomicron* to those from conventional mice. As illustrated by microbiota-specific clusters of mice after multivariate analysis, cecal FT-IR spectra were dependent upon the colonization status of mice (Figure 2c). The ability to distinguish altered ecosystem composition on the basis of FT-IR spectra was supported in another mouse cohort by the observation that cecal suspensions after antibiotic treatment clustered distinctly from control samples (cecal preparation from mice on water without antibiotics)

(Supplementary Figure S5). However, spectra were overall most affected by the diet, that is, cluster depth after average linkage clustering of samples from conventional mice and gnotobionts on the CARB or HF diet was about threefold higher for diet vs colonization effects (data not shown).

We then aimed at refining the resolution of analysis by comparing the biochemical composition of cecal communities at the level of single cells. Therefore, we used FISH to target members of the abundant groups *Bacteroidales* and *Lachnospiraceae* and measured cellular chemical composition by Raman microspectroscopy. These groups were selected because they were abundant in all mice and alterations in their phylotype composition were observed due to diet. Using fixed cecal biomass from duplicate mice from the CARB and HF group, we acquired a total of 112 single-cell spectra, with 7–20 cells measured for each FISH-defined population in each sample. Analysis with the Random Forests classifier showed that single-cell spectra from Bac-0303 and Erec-0482 groups were clearly distinguishable from each other under both diets (Figure 3a), due in large part to a much higher peak in the Erec-0482 group at $480\text{--}482\text{ cm}^{-1}$ (Figure 3b). An effect of the two diets was also observed in the single-cell spectra, especially in the case of Erec-0482-positive cells (Figure 3a). No single peaks alone had high discriminative power for the diet-related differences (Figure 3b), but rather small differences in the intensity of many wave numbers in the spectra collectively allowed for discrimination with the machine-learning classifier.

High-fat diet altered the gut bacterial metaproteome

To corroborate the hypothesis that biochemical changes observed using FT-IR and Raman spectroscopy reflect changes in microbial functions, we further analyzed cecal microbiota from mice fed the CARB and HF diet at the proteome level using LC-MS/MS ($n = 4$ mice per diet). The majority of identified proteins (94%) were of bacterial origin. A total of 114 mouse proteins were identified in the samples (Supplementary Results and Supplementary Table S5). After iterative search, 74553 out of 1409370 acquired spectra were matched to 1760 microbial proteins with a false-discovery rate of 0.6% at the protein level (Supplementary Table S5). Of these 1760 proteins, approximately 18% were hypothetical and 29% were housekeeping proteins (ribosomal and chaperone proteins, polymerases, transcription and translation factors). The mean number of spectra and proteins per mouse were as follows: CARB diet, 10481 ± 2445 and 816 ± 68 ; HF diet, 5377 ± 623 and 579 ± 28 . A proportion of 36 and 23% annotated proteins occurred only in CARB and HF mice, respectively (Figure 4a). A heat map including 342 proteins, the occurrence of which was significantly different between the two groups, showed

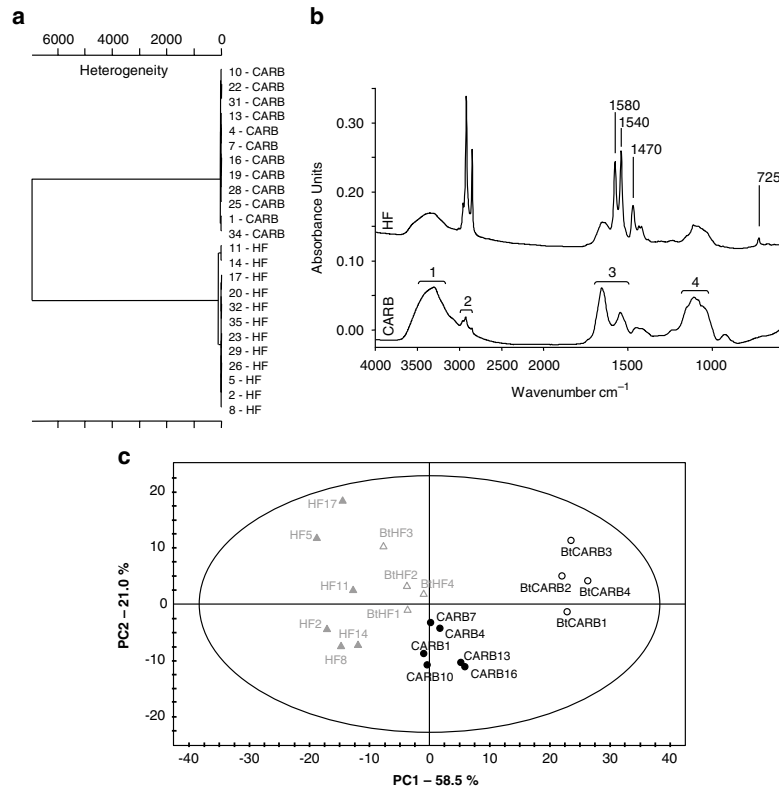


Figure 2 FT-IR-based spectral analysis revealed distinct chemical patterns. **(a)** Cecal microbial pellets from mice fed the same diet clustered together ($n = 12$ mice per diet; trial 1 and 2). Clusters were calculated using the Ward's algorithm and vector normalized first derivatives of the spectra in the range from 3000 to 2800 cm^{-1} and 1800 to 700 cm^{-1} . Mouse ID numbers are shown. Capital letters indicate diets (CARB, carbohydrate; HF, high-fat). **(b)** For each diet, one representative original spectrum is shown. For the sake of clarity, spectra were shifted vertically and the region between 1800 and 700 cm^{-1} was expanded. Regions 1 to 4 depict water-, lipid-, protein- and carbohydrate-specific absorbance wave number ranges, respectively. New peaks arising upon changes in diet are labeled individually. **(c)** Principal component analysis of cecal FT-IR spectra. Input data were spectral intensities from 3000 to 2800 and 1800 to 850 cm^{-1} (598 data points per spectrum). Data were normalized according to integrated spectra (area under the curve) and Pareto scaling. Factor 1 is a projection of mainly lipid (2850 and 2920 cm^{-1}) and protein (1539 and 1576 cm^{-1}) wave numbers. Factor 2 is a projection of mainly carbohydrate (920 to 1080 cm^{-1}) wave numbers. These factors explain 58.5% and 21.0% of the quantitative variations within the wave number span of the spectra, respectively. The mean body weight of mice monocolonized with *B. thetaiotaomicron* was $22.4 \pm 1.3\text{ g}$ (CARB) and $26.2 \pm 1.9\text{ g}$ (HF) after 3 weeks of experimental feeding ($P = 0.017$; t -test). CARB, conventional mice on control diet (black dots); HF, conventional mice on high-fat diet (gray triangles); BtCARB, mice monocolonized with *B. thetaiotaomicron* DSM 2079^T on control diet (circles); BtHF, monocolonized mice on high-fat diet (empty triangles).

homogenous metaproteome patterns between replicate mice (Figure 4b). After principal component analysis, the two groups of mice clustered very distinctly along PC1, which explained 67% of the variability within the data set (Supplementary Figure S6). For each group, variables (differentially detected proteins) that correlated with PC1 are given in Supplementary Table S5. COG category assignment showed that overall functional patterns were similar in the CARB and HF groups (Supplementary Figure S7) and were dominated by enzymes involved in energy production from carbohydrate metabolism originating from a variety of bacterial species (Supplementary Results and Supplementary Table S5). However, functional assignment of differently detected proteins revealed significant variations between the dietary groups (Figure 4c).

The prevalence of functional category C (energy production and conversion), G (carbohydrate metabolism and transport) and O (post-translational modification, protein turnover, chaperone functions) was higher in mice fed the CARB diet whereas the prevalence of category E (amino-acid metabolism and transport), J (translation) and S (unknown functions) was higher in mice fed the HF diet (Supplementary Results and Supplementary Table S5).

Non-targeted metabolome analysis revealed distinct metabolite patterns

To further describe the cecal ecosystem at the functional level, three cecal contents in each the CARB and HF group were analyzed by FT-ICR-MS to obtain high-resolution metabolite profiles.

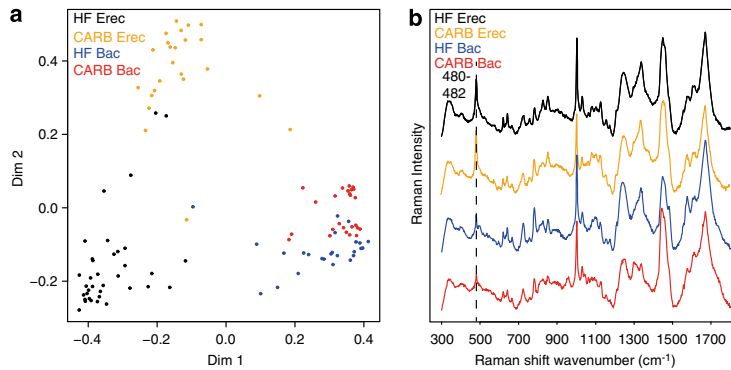


Figure 3 Single-cell characterization of abundant bacterial groups in the cecum by combining FISH and Raman microspectroscopy. Raman spectra were determined for cells from the *Bacteroidales* (identified using probe Bac-0303) and *Lachnospiraceae* (using probe Erec-0482) under high-fat (HF) or carbohydrate (CARB) diet. (a) Analysis with the Random Forests classifier revealed clustering of cell spectra by both group and diet on a non-metric multidimensional scaling ordination plot. (b) Mean spectra for each bacterial population and dietary group show that the major discriminative peak (480–482 cm^{-1}) is indicative for storage of polyglucan compounds in *Lachnospiraceae*.

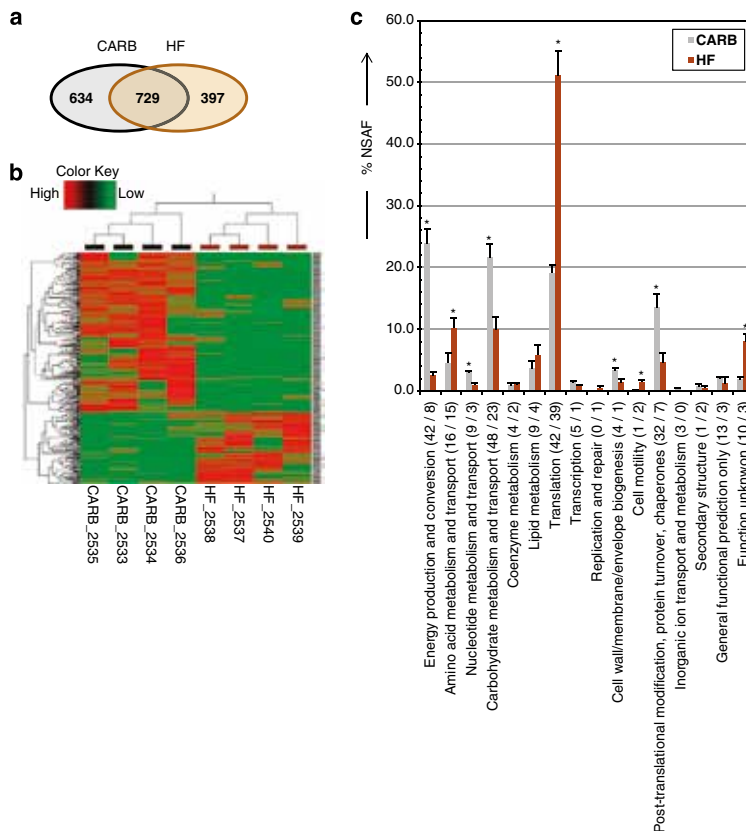


Figure 4 Metaproteome analysis (a) Venn diagram showing the occurrence of the 1760 detected microbial proteins. (b) Heat map of the 342 differently detected proteins revealed homogenous patterns within each of the two dietary groups. The normalized spectral abundance factors data set was imported into the R programming environment for statistical computing. (c) The sequences of dietary group-specific proteins were grouped in COGs functional categories by protein BLAST. Categories marked with asterisk were significantly different based on statistical analysis of NSAF proportions ($P < 0.01$; two-tailed homoscedastic t -test). The number of proteins used for NSAF calculation is given in brackets (CARB/HF) below the x axis.

3

The complete data set (filtered and significant mass values with annotations) is provided in Supplementary Table S6. The distribution of filtered mass values between the two dietary groups showed that most masses were discriminative (Figure 5a). HF and CARB samples shared only 15 and 28% of features in the negative and positive electrospray ionization mode, respectively, underscoring that diet has a profound impact on cecal biochemical composition and molecular diversity. Cluster analysis resulted in a clear separation of CARB and HF samples, that is, diet-induced effects on the metabolome in cecal contents were much higher than inter-individual differences between the three mice in each group (Figure 5b). A total of 2534 features were significantly different between CARB and HF mice ($P < 0.01$). Using MassTRIX annotation and KEGG reference pathways, 86 differently detected metabolites were identified. We noted the presence of fatty acids, steroid hormones, anti-microbial substances (macrolides) and bacterial products such as *cis*-2-carboxycyclohexyl-acetic acid, *cis*-2,3-dihydroxy-2,3-dihydro-p-cumate, pravastatin and urobilinogen. Among these metabolites, fatty acids and urobilinogen were specific for the HF diet (Table 2).

Discussion

The intestinal microbiota has been extensively studied at both the phylogenetic and metagenomic level in the context of metabolic disorders. The novelty of the present work lies in the comparative characterization of microbial communities in the mouse cecum at the biochemical level after feeding a HF diet.

We found that HF feeding alters the diversity and composition of intestinal microbiota. Mice in the HF group were characterized by increased relative abundance of *Rikenellaceae*, which is in agreement with other reports based on qPCR and FISH that found no decrease in *Bacteroidetes* following HF feeding (Cani *et al.*, 2008; Duncan *et al.*, 2008). The presence of *Alistipes*, a genus within the *Rikenellaceae*, has also been recently associated with type-2 diabetes in humans (Qin *et al.*, 2012). In addition, we found that *Ruminococcaceae* (phylum *Firmicutes*) were decreased, which makes sense in light of the fact that *ruminococci* are major utilizers of plant polysaccharides, the amount of which is substantially decreased in HF diets (Flint *et al.*, 2012; Ze *et al.*, 2012). Lactic acid bacteria have been proposed to be key players in host metabolic balance (Armougom *et al.*, 2009; Delzenne and Reid, 2009; Arora *et al.*, 2012). Mean *Lactobacillus* relative abundances were generally higher in the HF group (12.5 vs 9.7%), but diet-associated differences were not statistically significant due to marked inter-individual variations. It is worth mentioning that, when compared with studies showing rapid changes

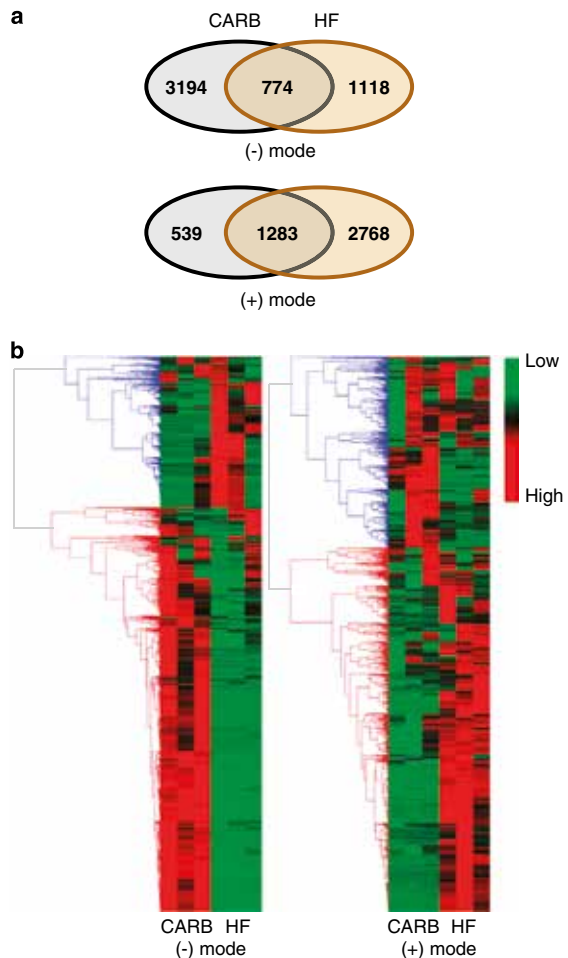


Figure 5 Metabolomic data (a) Venn diagrams for positive and negative ESI-FT-ICR-MS mode showing the number of mass values discriminating cecal metabolite patterns from CARB and HF mice (each $n = 3$). Most features specific for HF mice and distinguishing the two diets were detected after measurement in positive mode (b) Hierarchical cluster analysis using Average Linkage (Unweighted Pair Group Method with Arithmetic Mean) and Pearson correlation coefficient for groups and variables. For each ionization mode, branches within the two main metabolite clusters (y axis) appear in blue (e.g. high in CARB in (+) mode) or red (high in HF). Centered and normalized peak intensities are color coded from low (green) to high (red).

in bacterial communities due to high-calorie diets, the data obtained in the present work relate to adaptation of the gut ecosystem and the host to long-term feeding (12 weeks) (Desmarchelier *et al.*, 2012, 2013), which may explain, together with differences in HF diet composition, some of the variations observed as well as differences with data from the literature (for example, regarding abundance changes of *Bacteroides* or *Erysipelotrichaceae*).

The fact that a HF diet may alter cellular composition of microorganisms is suggested by *in vitro* studies showing that the addition of

Table 2 Identified features contributing to diet-specific FT-ICR-MS profiles

	CARB intensity (n)	HF intensity (n)
<i>CARB diet-specific metabolites</i>		
Steroid hormone biosynthesis		
Allotetra hydrodeoxycorticosterone	6,022,197 (3)	0 (0)
11beta,21-Dihydroxy-5beta-pregnane-3,20-dione ^a	12,256,770 (3)	0 (0)
Aldosterone ^b	40,386,531 (3)	0 (0)
Cortol ^c	19,629,775 (3)	0 (0)
Testosterone glucuronide	3,626,084 (3)	0 (0)
Androsterone glucuronide ^d	16,261,771 (3)	3,900,967 (2)
Microbial metabolism in diverse environments		
cis-2-Carboxycyclohexyl-acetic acid	4,116,462 (3)	0 (0)
cis-2,3-Dihydroxy-2,3-dihydro-p-cumate	2,408,782 (3)	0 (0)
Biosynthesis of 12-, 14- and 16-membered macrolides		
10-Deoxymethynolide	27,444,569 (3)	3,494,241 (2)
8,8a-Deoxyoleandolide	59,777,639 (3)	12,161,516 (3)
Oleandolide	93,629,776 (3)	18,567,187 (3)
6-Deoxyerythronolide B	32,516,089 (3)	3,925,532 (2)
Erythronolide B	63,863,133 (3)	3,720,904 (2)
3-O-alpha-Mycarosylerythronolide B	25,751,484 (3)	0 (0)
Bile acid biosynthesis and bile secretion		
Pravastatin	40,424,347 (3)	9,377,244 (3)
3alpha,7alpha,12alpha,26-Tetra hydroxy-5beta-cholesta ne	4,727,224 (3)	0 (0)
<i>HF diet-specific metabolites</i>		
Fatty acid biosynthesis		
Decanoic acid	0 (0)	2,509,582 (3)
(6Z,9Z,12Z)-Octadecatrienoic acid ^e	3,648,269 (2)	21,133,473 (3)
(9Z)-Hexadecenoic acid (= palmitoleic acid)	5,110,652 (3)	34,486,283 (3)
Linoleate ^f	4,116,114 (2)	49,977,956 (3)
Tetradeca noic acid (= myristic acid)	6,560,960 (3)	35,976,376 (3)
(8Z,11Z,14Z)-Icosatrienoic acid	7,386,592 (2)	72,601,368 (3)
(9Z)-Octadecenoic acid (= oleic acid)	42,947,039 (3)	1,164,910,976 (3)
Hexadecanoic acid (= palmitic acid)	53,440,799 (3)	856,402,496 (3)
Octadecanoic acid (= stearic acid)	155,914,441 (3)	1,067,133,440 (3)
Porphyrin and chlorophyll metabolism		
D-Urobilinogen ^g	0 (0)	4,375,615 (3)
L-Urobilinogen	1,633,985 (1)	88,861,815 (3)
I-Urobilinogen	31,249,205 (3)	592,250,379 (3)
L-Urobilin	26,692,537 (2)	422,294,496 (3)

FT-ICR-MS, Fourier-transform ion cyclotron resonance mass spectrometry;

Significant masses were annotated using MassTRIX searching against the KEGG, HMDB and Lipid Map databases. Values are mean peak intensities in cecal samples from mice fed the carbohydrate (CARB) or high-fat (HF) diet. Numbers of positive mice are given in brackets. Superscript letters refer to masses with several possible annotations:

^a17alpha,21-Dihydroxypregnenolone, 3alpha,21-Dihydroxy-5beta-pregnane-11,20-dione.

^bCortisone.

^cCortolone.

^dEtiocolan-3alpha-ol-17-one 3-glucuronide.

^e(9Z,12Z,15Z)-Octadecatrienoic acid, Crepenynate.

^f9-cis,11-trans-Octadecadienoate.

^gI-Urobilin.

cholesterol and fatty acids to growth media alter lipid and cell membrane composition of lactic acid bacteria (Dambekodi and Gilliland, 1998; Lye *et al.*, 2010). In the present work, we used FT-IR and Raman spectroscopy to show that a HF diet induces changes in chemical composition of the cecum and single cells as a hint for changes in bacterial physiology. The analysis of cecal samples from mice mono-associated with *B. thetaiotaomicron* vs conventional and from antibiotic-treated mice revealed that, for a given diet, samples clustered distinctly, testifying to the ability to discriminate FT-IR spectra on the basis of microbial community structure. However, spectral distances between

diet-dependent clusters were higher than microbiota-driven clusters. Thus, taking into account that the monocolonized, antibiotic-treated and conventional mouse models that we used represent extreme cases, we concluded that diet alters spectra to a higher extent than bacterial composition. It has been shown that the excess of certain nutrients, including lipids, can result in the formation of storage granules or vesicles in the microbial cells (Bauchart *et al.*, 1990), which can have pronounced effects on FT-IR fingerprints (Naumann, 2000) and may even mask differences in microbial composition (Bosch *et al.*, 2008). Still, it is very likely that part of the spectral differences that we observed were not of microbial

origin, that is, due to dietary constituents remaining in the sample or adhering to bacteria. We therefore tested the hypothesis that the differences in diet would result in accumulation of storage compounds by employing single-cell analysis with Raman microspectroscopy. Surprisingly, we found no evidence of increase in storage compounds under either diet, though Erec-0482-positive cells had a higher peak at 480–482 cm^{-1} than Bac-0303-positive cells. This peak is due to intracellular glycogen or polyglucan storage (Movasaghi *et al.*, 2007), which likely reflects the presence of the clostridial-equivalent of glycogen, granulose, a high molecular weight polyglucan important for sporulation (Reysenbach *et al.*, 1986). Nonetheless, analysis of chemical composition at the single-cell level confirmed that the overall cellular composition of bacteria within the abundant bacterial groups *Bacteroidales* and *Lachnospiraceae* was altered by HF feeding, which may be due to the shifting phylotype dynamics that were observed within this group and possibly also altered activity.

While many studies have shown that microbial diversity is altered by dietary changes (Clavel *et al.*, 2005; Martinez *et al.*, 2009; Jumpertz *et al.*, 2011; Kau *et al.*, 2011), much less is known about the impact of diet on the metabolic potential of gut microbiota (Martin *et al.*, 2010; McNulty *et al.*, 2011; Muegge *et al.*, 2011). To our knowledge, this is the first report on the adaptive response of the gut metaproteome to dietary challenge. Since the first gel-based metaproteome published in 2007 (Klaassens *et al.*, 2007) and the state-of-the-art LC-MS/MS work by Verberkmoes *et al.* (2009), the size of genomic databases has been rising exponentially. Nevertheless, annotation of peptide spectra remains challenging and functional interpretation based on the occurrence of dominant proteins is limited, that is, taking into account the high degree of diversity of the intestinal microbial ecosystem, we still profit only from a narrow window of analysis at the proteome level (Rooijers *et al.*, 2011; Haange *et al.*, 2012; Kolmeder *et al.*, 2012; Perez-Cobas *et al.*, 2012). This challenge is reflected in the present study by the fact that only 5% of all tandem MS spectra acquired could be matched to protein sequences from the databases. In contrast, up to 50% of all spectra can be commonly identified for sequenced microorganisms.

The total number of proteins identified in the mouse cecal samples that we analyzed ($n = 1760$) is comparable to results obtained using human fecal samples ($n = 1500$ to 1800 proteins) (Verberkmoes *et al.*, 2009; Kolmeder *et al.*, 2012). After functional category assignment of identified proteins, our data confirmed that, regardless of the diet, the dominant mammalian gut metaproteome is involved in energy production from carbohydrate metabolism. However, in the HF group, we observed a lower spectra occurrence for proteins classified in COG category C (energy production and conversion). These findings

suggest that (i) the microbial ecosystem is not well prepared for efficient energy harvest when 60% of dietary energy originates from fat. The HF diet-induced increase in spectral abundance factors related to category J (translation) may reflect adaptation of microbial cells to meet their needs for survival in a milieu with low energy originating from carbohydrates. For example, *in vitro* studies showed that levels of protein synthesis in marine *Sphingomonas* during starvation were low but reformed ribosomes and whole-cell proteins were retained for at least 7 days in culture (Fegatella and Cavicchioli, 2000). The authors proposed that in starvation, the number of ribosomes is in large excess relative to protein synthesis requirements, which may corroborate increased signals for ribosomal proteins in our HF data sets; and (ii) the depth of analysis (both in terms of biological replicates and protein annotation) is still limiting, that is, only most dominant proteins are detected, which likely prevents better discrimination of the effect of the two diets at the metaproteome level.

Bacterial response to the HF feeding included a sharp decrease in the occurrence of proteins involved in carbohydrate metabolism as well as a reorganization of amino acid metabolism. Indeed, among proteins that best characterized microbiota from mice fed the HF diet, we noted the presence of enzymes metabolizing amino acids (aminotransferases and proteases) that were not detected in CARB mice. We thus propose that shifts in the metabolism of amino acids such as histidine (ammonia-lyase, glutamate formimidoyltransferase, urocanate hydratase) and alanine (alanine and glutamate dehydrogenase) as well as arginine and proline coupled with the use of glutamate as a source of pyruvate for energy production (acetylornithine aminotransferase, glutamate dehydrogenase, (R)-2-hydroxyglutaryl-CoA dehydratase, urease) represent the most prominent metabolic adaptations of the microbial ecosystem to the HF diet (Potrykus *et al.*, 2008). This may corroborate (i) the higher protein to carbohydrate ratio in the HF vs CARB diet (ca. 1:1 vs 1:3), and (ii) increased production of branched-chain fatty acids from the amino acid leucine, isoleucine and valine reported by others after HF feeding in humans or protein fermentation *in vitro* (MacFarlane *et al.*, 1992; Russell *et al.*, 2011). The occurrence of only two of seven enzymes involved in the metabolism of the aforementioned branched-chain amino acids was higher in the HF metaproteome. Of note, in contrast to the suggested increase in the production of short-chain fatty acids linked to higher prevalence of specific members of the *Firmicutes* (for example, *Erysipelotrichaceae*) in diet-induced obesity (Turnbaugh *et al.*, 2008), evidence from human intervention studies clearly indicates decreased short-chain fatty acids, in particular butyrate, yet increased branched-chain fatty acids concentrations after HF feeding (Brinkworth *et al.*, 2009; Russell *et al.*, 2011).

Thus, the notion of increased capacity of the microbiome for energy harvest in the context of diet-induced obesity should be taken with caution, although results may depend on diet composition (for example, content of simple sugars or proteins) and duration of feeding as well as the host phenotype (lean or obese). Most recent metagenomic data suggest that low-diversity (gene count) fecal microbiomes, which seem to be associated with adiposity and metabolic disturbances, are characterized by decreased capability of producing butyrate (Le Chatelier *et al.*, 2013).

The metaproteomic data set is also in agreement with previously published transcriptome analysis and functional prediction of metagenomic sequencing reads (Turnbaugh *et al.*, 2008, 2009). In the aforementioned studies, the authors reported that the cecal metagenome from mice fed a HF/high-sugar Western diet was enriched in genes assigned to glutamate metabolic pathways. They also proposed that the microbiome adapted to the Western diet by increasing transport and conversion of simple sugars and host-derived glycoproteins, which agrees with the higher occurrence of 2-dehydro-3-deoxyglucokinase, 6-phosphofructokinase, *N*-acetylglucosamine-6-phosphate deacetylase and two sugar-binding proteins (gi:282600834 and gi:266619140) in the present HF metaproteomic data set. Also consistent with our results, Yatsunenکو *et al.* (2012) recently proposed that a Westernized diet is associated with metagenomes enriched in amino acid- and simple sugar-degrading enzymes when compared with African populations on rural diets high in complex carbohydrates. Finally, the cecal HF metaproteome was characterized by three enzymes (glutaredoxin, alkyl hydroperoxide and thioredoxin reductase) involved in oxidative stress responses, which may reflect adaptation to an environment with altered redox potential (Xiao *et al.*, 2010).

Holmes *et al.* (2012) have provided evidence that the gut microbiome influences host metabolic phenotypes, based primarily on NMR studies (Claus *et al.*, 2008; Calvani *et al.*, 2010). However, only few papers focused on the analysis of metabolites in intestinal content (Martin *et al.*, 2010). In line with the pioneering work by Jansson *et al.*, (2009), we used a non-targeted metabolomic approach based on ultrahigh resolution mass spectrometry to identify diet-derived, host and microbial metabolites in cecal samples. Antunes *et al.* (2011) have also recently used FT-ICR-MS to assess the effect of antibiotics and *Salmonella* infection on the metabolome in mouse feces. They found that both treatments altered host hormone metabolism, for example, production of steroids and eicosanoids. In the present study, we detected prostaglandins, thromboxanes and several steroids and conjugates thereof, which were essentially absent in cecal samples from mice fed the HF diet. This implies that host steroid hormone homeostasis can also be affected by a HF diet. Although literature data are

inconsistent, studies have demonstrated that HF diets can influence, for instance, serum testosterone levels in mice and humans (Reed *et al.*, 1987; Meikle *et al.*, 1990; Whyte *et al.*, 2007). Interestingly, the absence of cholesterol-derived products like steroids in the cecum of HF mice corroborates with the finding that mice on the same HF diet were characterized by lower intestinal and hepatic levels of cholesterol in spite of plasma hypercholesterolemia, probably due to increased demand for lipid absorption (Desmarchelier *et al.*, 2012).

Samples from CARB mice were also characterized by the identification of (i) metabolites involved in naphthalene and xylene/cymene degradation by bacteria, and (ii) pravastatin, a potent inhibitor of hydroxymethylglutaryl-CoA reductase with cholesterol-lowering effects, which can also be produced by a variety of bacteria (Serizawa, 1996; Park *et al.*, 2003). In addition, the occurrence of various macrolides in CARB samples may partly explain disturbances in gut microbial composition after HF feeding due to changes in the pool of anti-microbial substances present in the cecum. In cecal samples from mice fed the HF diet, fatty acid levels were much higher than in CARB mice, reflecting the proportion of major fatty acids in the HF diet (12% oleic acid, 8% palmitic acid, 6% stearic acid, 2% linoleic acid). We also noted the presence of a ceramide (*N*-acylsphingosine), for which *de novo* synthesis may be promoted by high levels of palmitate in the HF diet. Ceramide production may also be enhanced by hydrolysis of sphingomyelin, which corroborates with the detection of a secreted protein of the sphingomyelinase family (sp|P58242|ASM3B_MOUSE) in the mouse cecal proteome after HF feeding. Of note, ceramides have been implicated in diet-induced insulin resistance (Longato *et al.*, 2011) and have cytotoxic and proapoptotic properties (Haimovitz-Friedman *et al.*, 1997; Jarvis and Grant, 1998). Finally, the conversion of bilirubin to urobilinogen is considered to be a specific feature of the gut microbiota, especially *Clostridium* spp. (Becker *et al.*, 2011). Thus, higher levels of urobilinogen and its oxidized product urobilin in the cecum of HF mice (i) testify to diet-induced functional alterations of the microbial ecosystem, (ii) may be related to the observed HF-induced increase in phylotypes within the *Clostridiales*, an order that includes known converters of bilirubin, and (iii) could explain the appearance of the FT-IR spectral features attributed to aromatic and heteroaromatic ring vibrations in the cecum of HF mice. Due to the relatively limited number of samples analyzed and to the fact that data sets were obtained from different mice and that a minor fraction of metabolite masses can be annotated, we did not integrate data and extrapolate on functional links between the metaproteome and metabolome.

In summary, we demonstrated that (i) diet can alter the biochemical composition of the gut microbiota either by shifting phylotype composition or the

activity of bacterial cells, (ii) changes in bacterial metaproteome after HF feeding are most pronounced for pathways of amino acid metabolism, and (iii) cecal metabolic pathways affected by HF feeding include eicosanoid, steroid hormone, macrolide, bile acid and bilirubin metabolism. These findings show that a HF diet has a major impact on the mouse cecal microbiota that extends beyond compositional changes to major alterations in bacterial physiology and metabolite landscape. Molecular mechanisms underlying the conversion of steroids and amino acids by specific gut bacteria in relation with the onset of metabolic disorders appear to be of particular relevance for future targeted experimental work.

Acknowledgements

Raw files obtained by metaproteomic and metabolomic spectrometry measurements are available upon request. We thank Adelmair Stamford and Pia Baur for helping with statistical analysis, Nico Gebhardt, Ines Grüner, Elmar Jocham, Melanie Klein, Ute Lehmann, Ronny Scheundel and Caroline Ziegler for technical assistance, and Gabriele Hörmannsperger for reviewing the manuscript. Charles Desmarchelier was financed by the EU FP6 project *Nutrient Sensing in Satiety Control and Obesity* (NuSISCO, grant no. MEST-CT-2005-020494). Christoph Böhm, David Berry, and Michael Wagner were supported by the European Research Council (Advanced Grant NITRICARE 294343) and David Berry was supported by the Vienna Science and Technology Fund (WWTF) through project LS12-001.

References

- Altschul SF, Gish W, Miller W, Myers EW, Lipman DJ. (1990). Basic local alignment search tool. *J Mol Biol* **215**: 403–410.
- Antunes LC, Arena ET, Menendez A, Han J, Ferreira RB, Buckner MM *et al.* (2011). Impact of salmonella infection on host hormone metabolism revealed by metabolomics. *Infect Immun* **79**: 1759–1769.
- Antunes LC, Han J, Ferreira RB, Lolic P, Borchers CH, Finlay BB. (2011). Effect of antibiotic treatment on the intestinal metabolome. *Antimicrob Agents Chemother* **55**: 1494–1503.
- Armougom F, Henry M, Vialettes B, Raccach D, Raoult D. (2009). Monitoring bacterial community of human gut microbiota reveals an increase in *Lactobacillus* in obese patients and Methanogens in anorexic patients. *PLoS One* **4**: e7125.
- Arora T, Anastasovska J, Gibson G, Tuohy K, Sharma RK, Bell J *et al.* (2012). Effect of *Lactobacillus acidophilus* NCDC 13 supplementation on the progression of obesity in diet-induced obese mice. *Br J Nutr* **108**: 1382–1389.
- Backhed F, Ding H, Wang T, Hooper LV, Koh GY, Nagy A *et al.* (2004). The gut microbiota as an environmental factor that regulates fat storage. *Proc Natl Acad Sci USA* **101**: 15718–15723.
- Bauchart D, Legay-Carmier F, Doreau M, Gaillard B. (1990). Lipid metabolism of liquid-associated and solid-adherent bacteria in rumen contents of dairy cows offered lipid-supplemented diets. *Br J Nutr* **63**: 563–578.
- Becker N, Kunath J, Loh G, Blaut M. (2011). Human intestinal microbiota: characterization of a simplified and stable gnotobiotic rat model. *Gut Microbes* **2**: 25–33.
- Berry D, Schwab C, Milinovich G, Reichert J, Ben Mahfoudh K, Decker T *et al.* (2012). Phylotype-level 16S rRNA analysis reveals new bacterial indicators of health state in acute murine colitis. *ISME J* **6**: 2091–2106.
- Blaut M, Clavel T. (2007). Metabolic diversity of the intestinal microbiota: implications for health and disease. *J Nutr* **137**: 751S–755S.
- Bosch A, Minan A, Vescina C, Degrossi J, Gatti B, Montanaro P *et al.* (2008). Fourier transform infrared spectroscopy for rapid identification of nonfermenting gram-negative bacteria isolated from sputum samples from cystic fibrosis patients. *J Clin Microbiol* **46**: 2535–2546.
- Brinkworth GD, Noakes M, Clifton PM, Bird AR. (2009). Comparative effects of very low-carbohydrate, high-fat and high-carbohydrate, low-fat weight-loss diets on bowel habit and faecal short-chain fatty acids and bacterial populations. *Br J Nutr* **101**: 1493–1502.
- Calvani R, Miccheli A, Capuani G, Tomassini Miccheli A, Puccetti C, Delfini M *et al.* (2010). Gut microbiome-derived metabolites characterize a peculiar obese urinary metabolite. *Int J Obes (Lond)* **34**: 1095–1098.
- Cani PD, Bibiloni R, Knauf C, Waget A, Neyrinck AM, Delzenne NM *et al.* (2008). Changes in gut microbiota control metabolic endotoxemia-induced inflammation in high-fat diet-induced obesity and diabetes in mice. *Diabetes* **57**: 1470–1481.
- Caporaso JG, Kuczynski J, Stombaugh J, Bittinger K, Bushman FD, Costello EK *et al.* (2010). QIIME allows analysis of high-throughput community sequencing data. *Nat Methods* **7**: 335–336.
- Claus SP, Tsang TM, Wang Y, Cloarec O, Skordi E, Martin FP *et al.* (2008). Systemic multicompartmental effects of the gut microbiome on mouse metabolic phenotypes. *Mol Syst Biol* **4**: 219.
- Clavel T, Fallani M, Lepage P, Levenez F, Mathey J, Rochet V *et al.* (2005). Isoflavones and functional foods alter the dominant intestinal microbiota in postmenopausal women. *J Nutr* **135**: 2786–2792.
- Cole JR, Chai B, Marsh TL, Farris RJ, Wang Q, Kulam SA *et al.* (2003). The Ribosomal Database Project (RDP-II): previewing a new autoaligner that allows regular updates and the new prokaryotic taxonomy. *Nucleic Acids Res* **31**: 442–443.
- Colthup NB, Daly LH, Wiberley SE. (1990). *Introduction to Infrared and Raman Spectroscopy*, 3rd edn Academic Press: Boston.
- Dambekodi PC, Gilliland SE. (1998). Incorporation of cholesterol into the cellular membrane of *Bifidobacterium longum*. *J Dairy Sci* **81**: 1818–1824.
- Delzenne N, Reid G. (2009). No causal link between obesity and probiotics. *Nat Rev Microbiol* **7**: 901, author reply 901.
- Delzenne NM, Cani PD. (2011). Interaction between obesity and the gut microbiota: relevance in nutrition. *Annu Rev Nutr* **31**: 15–31.
- Desmarchelier C, Dahlhoff C, Keller S, Sailer M, Jahreis G, Daniel H. (2012). C57Bl/6 N mice on a western diet display reduced intestinal and hepatic cholesterol levels despite a plasma hypercholesterolemia. *BMC Genomics* **13**: 84.

- Desmarchelier C, Ludwig T, Scheundel R, Rink N, Bader BL, Klingenspor M *et al.* (2013). Diet-induced obesity in *ad libitum*-fed mice: food texture overrides the effect of macronutrient composition. *Br J Nutr* **109**: 1518–1527.
- Duncan SH, Lobleby GE, Holtrop G, Ince J, Johnstone AM, Louis P *et al.* (2008). Human colonic microbiota associated with diet, obesity and weight loss. *Int J Obes (Lond)* **32**: 1720–1724.
- Fegatella F, Cavicchioli R. (2000). Physiological responses to starvation in the marine oligotrophic *ultramicrobacterium Sphingomonas* sp. strain RB2256. *Appl Environ Microbiol* **66**: 2037–2044.
- Fleissner CK, Huebel N, Abd El-Bary MM, Loh G, Klaus S, Blaut M. (2010). Absence of intestinal microbiota does not protect mice from diet-induced obesity. *Br J Nutr* **104**: 919–929.
- Flint HJ, Scott KP, Duncan SH, Louis P, Forano E. (2012). Microbial degradation of complex carbohydrates in the gut. *Gut Microbes* **3**: 289–306.
- Franks AH, Harmsen HJ, Raangs GC, Jansen GJ, Schut F, Welling GW. (1998). Variations of bacterial populations in human feces measured by fluorescent in situ hybridization with group-specific 16S rRNA-targeted oligonucleotide probes. *Appl Environ Microbiol* **64**: 3336–3345.
- Haange SB, Oberbach A, Schlichting N, Hugenholtz F, Smidt H, von Bergen M *et al.* (2012). Metaproteome analysis and molecular genetics of rat intestinal microbiota reveals section and localization resolved species distribution and enzymatic functionalities. *J Proteome Res* **11**: 5406–5417.
- Haider S, Wagner M, Schmid MC, Sixt BS, Christian JG, Hacker G *et al.* (2010). Raman microspectroscopy reveals long-term extracellular activity of Chlamydiae. *Mol Microbiol* **77**: 687–700.
- Haimovitz-Friedman A, Cordon-Cardo C, Bayoumy S, Garzotto M, McLoughlin M, Gallily R *et al.* (1997). Lipopolysaccharide induces dissemination of endothelial apoptosis requiring ceramide generation. *J Exp Med* **186**: 1831–1841.
- Heysfield SB, Pietrobelli A. (2011). Individual differences in apparent energy digestibility are larger than generally recognized. *Am J Clin Nutr* **94**: 1650–1651.
- Holmes E, Li JV, Marchesi JR, Nicholson JK. (2012). Gut microbiota composition and activity in relation to host metabolic phenotype and disease risk. *Cell Metab* **16**: 559–564.
- Huang WE, Stoecker K, Griffiths R, Newbold L, Daims H, Whiteley AS *et al.* (2007). Raman-FISH: combining stable-isotope Raman spectroscopy and fluorescence *in situ* hybridization for the single cell analysis of identity and function. *Environ Microbiol* **9**: 1878–1889.
- Hörmannspurger G, Clavel T, Haller D. (2012). Gut matters: microbe-host interactions in allergic diseases. *J Allergy Clin Immunol* **129**: 1452–1459.
- Jansson J, Willing B, Lucio M, Fekete A, Dicksved J, Halfvarson J *et al.* (2009). Metabolomics reveals metabolic biomarkers of Crohn's disease. *PLoS One* **4**: e6386.
- Jarvis WD, Grant S. (1998). The role of ceramide in the cellular response to cytotoxic agents. *Curr Opin Oncol* **10**: 552–559.
- Jumpertz R, Le DS, Turnbaugh PJ, Trinidad C, Bogardus C, Gordon JI *et al.* (2011). Energy-balance studies reveal associations between gut microbes, caloric load, and nutrient absorption in humans. *Am J Clin Nutr* **94**: 58–65.
- Kanehisa M, Goto S. (2000). KEGG: kyoto encyclopedia of genes and genomes. *Nucleic Acids Res* **28**: 27–30.
- Kau AL, Ahern PP, Griffin NW, Goodman AL, Gordon JI. (2011). Human nutrition, the gut microbiome and the immune system. *Nature* **474**: 327–336.
- Klaassens ES, de Vos WM, Vaughan EE. (2007). Meta-proteomics approach to study the functionality of the microbiota in the human infant gastrointestinal tract. *Appl Environ Microbiol* **73**: 1388–1392.
- Kolmeder CA, de Been M, Nikkila J, Ritamo I, Matto J, Valmu L *et al.* (2012). Comparative metaproteomics and diversity analysis of human intestinal microbiota testifies for its temporal stability and expression of core functions. *PLoS One* **7**: e29913.
- Le Chatelier E, Nielsen T, Qin J, Prifti E, Hildebrand F, Falony G *et al.* (2013). Richness of human gut microbiome correlates with metabolic markers. *Nature* **500**: 541–546.
- Lepage P, Leclerc MC, Joossens M, Mondot S, Blottiere HM, Raes J *et al.* (2013). A metagenomic insight into our gut's microbiome. *Gut* **62**: 146–158.
- Liaw A, Wiener M. (2002). Classification and Regression by randomForest. *R News* **2**: 18–22.
- Lieber CA, Mahadevan-Jansen A. (2003). Automated method for subtraction of fluorescence from biological Raman spectra. *Appl Spectrosc* **57**: 1363–1367.
- Longato L, Tong M, Wands JR, de la Monte SM. (2011). High fat diet induced hepatic steatosis and insulin resistance: Role of dysregulated ceramide metabolism. *Hepatol Res* **42**: 412–427.
- Lye HS, Rusul G, Liong MT. (2010). Removal of cholesterol by lactobacilli via incorporation and conversion to coprostanol. *J Dairy Sci* **93**: 1383–1392.
- MacFarlane GT, Gibson G, Beatty E, Cummings JH. (1992). Estimation of short-chain fatty acid production from protein by human intestinal bacteria based on branched-chain fatty acid measurements. *FEMS Microbiol Ecol* **101**: 81–88.
- Manz W, Amann R, Ludwig W, Vancanneyt M, Schleifer KH. (1996). Application of a suite of 16S rRNA-specific oligonucleotide probes designed to investigate bacteria of the phylum Cytophaga-Flavobacter-Bacteroides in the natural environment. *Microbiology* **142**: 1097–1106.
- Martin FP, Sprenger N, Montoliu I, Rezzi S, Kochhar S, Nicholson JK. (2010). Dietary modulation of gut functional ecology studied by fecal metabonomics. *J Proteome Res* **9**: 5284–5295.
- Martinez I, Wallace G, Zhang C, Legge R, Benson AK, Carr TP *et al.* (2009). Diet-induced metabolic improvements in a hamster model of hypercholesterolemia are strongly linked to alterations of the gut microbiota. *Appl Environ Microbiol* **75**: 4175–4184.
- Masella AP, Bartram AK, Truszkowski JM, Brown DG, Neufeld JD. (2012). PANDAseq: paired-end assembler for illumina sequences. *BMC Bioinformatics* **13**: 31.
- McNulty NP, Yatsunenko T, Hsiao A, Faith JJ, Muegge BD, Goodman AL *et al.* (2011). The impact of a consortium of fermented milk strains on the gut microbiome of gnotobiotic mice and monozygotic twins. *Sci Transl Med* **3**: 106ra106.
- Meikle AW, Stringham JD, Woodward MG, McMurry MP. (1990). Effects of a fat-containing meal on sex hormones in men. *Metabolism* **39**: 943–946.

- Movasaghi Z, Rehman S, Rehman I. (2007). Raman spectroscopy of biological tissues. *Appl Spectrosc Rev* **42**: 493–541.
- Muegge BD, Kuczynski J, Knights D, Clemente JC, Gonzalez A, Fontana L *et al.* (2011). Diet drives convergence in gut microbiome functions across mammalian phylogeny and within humans. *Science* **332**: 970–974.
- Naumann D. (2000). *Infrared Spectroscopy in Microbiology* In Encyclopedia of analytical chemistry. In RA Meyers (ed.) John Wiley & Sons: Chichester; pp 102–131.
- Park JW, Lee JK, Kwon TJ, Yi DH, Kim YJ, Moon SH *et al.* (2003). Bioconversion of compactin into pravastatin by *Streptomyces* sp. *Biotechnol Lett* **25**: 1827–1831.
- Patel RK, Jain M. (2012). NGS QC Toolkit: a toolkit for quality control of next generation sequencing data. *PLoS One* **7**: e30619.
- Pavelka N, Fournier ML, Swanson SK, Pelizzola M, Ricciardi-Castagnoli P, Florens L *et al.* (2008). Statistical similarities between transcriptomics and quantitative shotgun proteomics data. *Mol Cell Proteomics* **7**: 631–644.
- Pavelka N, Pelizzola M, Vizzardelli C, Capozzoli M, Splendiani A, Granucci F *et al.* (2004). A power law global error model for the identification of differentially expressed genes in microarray data. *BMC Bioinformatics* **5**: 203.
- Perez-Cobas AE, Gosalbes MJ, Friedrichs A, Knecht H, Artacho A, Eismann K *et al.* (2012). Gut microbiota disturbance during antibiotic therapy: a multi-omic approach. *Gut*; doi:10.1136/gutjnl-2012-303184.
- Potrykus J, White RL, Bearn SL. (2008). Proteomic investigation of amino acid catabolism in the indigenous gut anaerobe *Fusobacterium varium*. *Proteomics* **8**: 2691–2703.
- Qin J, Li Y, Cai Z, Li S, Zhu J, Zhang F *et al.* (2012). A metagenome-wide association study of gut microbiota in type 2 diabetes. *Nature* **490**: 55–60.
- Raoult D, Fournier PE, Drancourt M. (2004). What does the future hold for clinical microbiology? *Nat Rev Microbiol* **2**: 151–159.
- Reed MJ, Cheng RW, Simmonds M, Richmond W, James VH. (1987). Dietary lipids: an additional regulator of plasma levels of sex hormone binding globulin. *J Clin Endocrinol Metab* **64**: 1083–1085.
- Reysenbach AL, Ravenscroft N, Long S, Jones DT, Woods DR. (1986). Characterization, biosynthesis, and regulation of granulose in *clostridium acetobutylicum*. *Appl Environ Microbiol* **52**: 185–190.
- Rooijers K, Kolmeder C, Juste C, Dore J, de Been M, Boeren S *et al.* (2011). An iterative workflow for mining the human intestinal metaproteome. *BMC Genomics* **12**: 6.
- Russell WR, Gratz SW, Duncan SH, Holtrop G, Ince J, Scobbie L *et al.* (2011). High-protein, reduced-carbohydrate weight-loss diets promote metabolite profiles likely to be detrimental to colonic health. *Am J Clin Nutr* **93**: 1062–1072.
- Saeed A, Bhagabati N, Braisted J, Liang W, Sharov V, Howe E *et al.* (2006). TM4 microarray software suite. DNA microarrays, part B: databases and statistics. *A. Kimmel and B. Oliver*. Elsevier Academic Press: San Diego, Vol. **411**: 134–193.
- Seo J, Shneiderman B. (2002). Interactively exploring hierarchical clustering results. *IEEE Computer* **35**: 80–86.
- Serizawa N. (1996). Biochemical and molecular approaches for production of pravastatin, a potent cholesterol-lowering drug. *Biotechnol Annu Rev* **2**: 373–389.
- Shevchenko A, Wilm M, Vorm O, Mann M. (1996). Mass spectrometric sequencing of proteins silver-stained polyacrylamide gels. *Anal Chem* **68**: 850–858.
- Suhre K, Schmitt-Kopplin P. (2008). MassTRIX: mass translator into pathways. *Nucleic Acids Res* **36**: W481–W484.
- Tatusov RL, Fedorova ND, Jackson JD, Jacobs AR, Kiryutin B, Koonin EV *et al.* (2003). The COG database: an updated version includes eukaryotes. *BMC Bioinformatics* **4**: 41.
- Turnbaugh P, Ridaura V, Faith J, Rey F, Knight R, Gordon J. (2009). The effect of diet on the human gut microbiome: a metagenomic analysis in humanized gnotobiotic mice. *Sci Transl Med* **1**: 6ra14.
- Turnbaugh PJ, Backhed F, Fulton L, Gordon JI. (2008). Diet-induced obesity is linked to marked but reversible alterations in the mouse distal gut microbiome. *Cell Host Microbe* **3**: 213–223.
- Turnbaugh PJ, Ley RE, Mahowald MA, Magrini V, Mardis ER, Gordon JI. (2006). An obesity-associated gut microbiome with increased capacity for energy harvest. *Nature* **444**: 1027–1031.
- Verberkmoes NC, Russell AL, Shah M, Godzik A, Rosenquist M, Halfvarson J *et al.* (2009). Shotgun metaproteomics of the human distal gut microbiota. *Isme J* **3**: 179–189.
- Wenning M, Theilmann V, Scherer S. (2006). Rapid analysis of two food-borne microbial communities at the species level by Fourier-transform infrared microspectroscopy. *Environ Microbiol* **8**: 848–857.
- Whyte JJ, Alexenko AP, Davis AM, Eilersieck MR, Fountain ED, Rosenfeld CS. (2007). Maternal diet composition alters serum steroid and free fatty acid concentrations and vaginal pH in mice. *J Endocrinol* **192**: 75–81.
- Wishart DS, Tzur D, Knox C, Eisner R, Guo AC, Young N *et al.* (2007). HMDB: the Human Metabolome Database. *Nucleic Acids Res* **35**: D521–D526.
- Xiao Y, Cui J, Shi YH, Sun J, Wang ZP, Le GW. (2010). Effects of duodenal redox status on calcium absorption and related genes expression in high-fat diet-fed mice. *Nutrition* **26**: 1188–1194.
- Yatsunenkov T, Rey FE, Manary MJ, Trehan I, Dominguez-Bello MG, Contreras M *et al.* (2012). Human gut microbiome viewed across age and geography. *Nature* **486**: 222–227.
- Ze X, Duncan SH, Louis P, Flint HJ. (2012). Ruminococcus bromii is a keystone species for the degradation of resistant starch in the human colon. *ISME J* **6**: 1535–1543.
- Zybaiov B, Mosley AL, Sardi ME, Coleman MK, Florens L, Washburn MP. (2006). Statistical analysis of membrane proteome expression changes in *Saccharomyces cerevisiae*. *J Prot Res* **5**: 2339–2347.

Supplementary Information accompanies this paper on The ISME Journal website (<http://www.nature.com/ismej>)

Supplementary Materials and Methods

Experimental feeding trials in mice

Conventional 8-week-old male C57BL/6NCrl mice (Charles River Laboratories, Sulzfeld, Germany) were housed individually in a controlled environment (12 h
5 daylight cycle, 22 °C) with free access to water and food. They were fed a standard laboratory chow diet for two weeks (**Table 1**). Thereafter, they were divided into two groups (n = 6 mice/group) with similar mean body weights and were fed an experimental carbohydrate (CARB) or high-fat (HF) diet (**Table 1**). After 12 weeks (83 to 85 days), mice in a non-fasting state were anesthetized using isoflurane and
10 killed by cervical dislocation (2 mice of each group per day over 3 days). Cecal contents were collected within twenty minutes after killing.

Gnotobiology

Experiments were carried out at the germfree facility of the German Institute of
15 Human Nutrition Potsdam-Rehbrücke and were approved by the state institution in charge (approval no. 23-2347-6-2009). Female germfree C3H mice (12-week-old) were fed either the CARB or HF diet (n = 4 mice/group). Diets were irradiated prior to use (50 kGy, Gamma-Service, Radeberg, Germany). After two weeks on the experimental diets, mice were colonized with 1×10^8 cells of *Bacteroides*
20 *thetaiotaomicron* DSM 2079^T and were fed the experimental diets for one extra week. At the end of the three weeks, body weight was recorded and mice were killed by cervical dislocation. Cecal samples were collected and kept frozen until analysis.

Fourier-transform infrared (FT-IR) spectroscopy

25 Samples were kept on ice throughout the procedure. Frozen cecal portions were diluted 1:10 (w/v) in saline solution. Portion weight had been previously determined by weighing tubes before and after collection using a TB-215D precision balance (Denver Instrument). After homogenization by vortexing using sterile glass beads, suspensions (Sp1) were centrifuged ($300 \times g$, 1 min, RT) to sediment debris.

30 Supernatants (S1) were centrifuged ($8\,000 \times g$, 3 min, RT) to pellet microbes. Supernatants (S2) were discarded. Pellets were washed (vortexed in 200 μ L saline solution and centrifuged at $8\,000 \times g$, 3 min, RT) and re-suspended in a volume of saline solution (suspension Sp2) equal to the volume of supernatants S1. Two-fold dilutions of Sp2 (30 μ L) were pipetted onto a zinc/selenide 96-well-plate, allowed to

35 dry (20 min, 45 °C) and analyzed by infrared spectroscopy. As control, supernatants S3 (obtained after centrifugation of Sp2) were analyzed to test for artifacts. No signals were detected.

High-throughput sequencing

40 DNA was isolated from cecal samples after mechanical lysis (FastPrep®-24, MP Biomedicals) in Phenol:Chloroform:IsoAmyl alcohol using the QIAamp® DNA Stool kit (cat. no. 51504, Qiagen) (Wu *et al.*, 2010). DNA concentration was measured using the Nanodrop system (peqlab Biotechnologie GmbH). The V4 region of 16S rRNA genes was amplified from 50 ng template DNA by polymerase chain reaction

45 (25 cycles), as described previously (Caporaso *et al.* 2011; Caporaso *et al.* 2012). The Phusion® High-Fidelity DNA Polymerase (NewEngland BioLabs) was used to minimize amplification artifacts. PCR products were purified from agarose gels using the NucleoSpin Gel and PCR clean-up kit (Macherey-Nagel). The concentration of amplicons in each sample was determined using a Qubit® 2.0 Fluorometer (Life

50 Technologies™) prior to equimolar pooling (2 nM). The amplicon mixture was

sequenced using the MiSeq system (Illumina Inc.). Library preparation was done following the manufacturer's protocol and detailed instructions published elsewhere (Caporaso *et al.* 2012). The final DNA concentration used for sequencing was 4 pM. The PhiX control library was added at a ratio of 30 % (v/v). Samples were sequenced
55 in paired-end modus (2 x 180 bp) using the MiSeq reagent kit 2 (cat. no. MS-102-2001).

Cecal sample preparation for LC-MS/MS

Samples were prepared on ice. After thawing, cecal samples (n = 4 mice in each the
60 CARB and HF group; trial 3) were diluted 1:10 (w/v) in Phosphate Buffered Saline solution supplemented with a protease inhibitor cocktail (Roche, cat. no. 04693124001) (PBS-PIC). After homogenization by vortexing using sterile glass beads, suspensions were centrifuged (300 x g, 1 min, 4 °C) to sediment debris. Microorganisms in supernatants were pelleted by centrifugation (10 000 x g, 3 min, 4
65 °C). Pellets were washed in 400 µl PBS-PIC and re-suspended in 200 µl filter-sterilized deionized water supplemented with 3.75 mM of the serine protease inhibitor phenylmethanesulfonylfluoride (Roche, cat. no. 837091). Microorganisms were lyzed using 100 mg acid-washed glass beads and a FastPrep (3 x 30 sec at 6.5; samples were left to stand on ice for 5 min between each run). After centrifugation (16 000 x
70 g, 30 min, 4 °C), supernatants were diluted 3:4 in 4X LDS sample buffer (Invitrogen, cat. no. NP0008).

Liquid chromatography and tandem mass spectrometry (LC-MS/MS)

After in-gel digestion, peptides were dissolved in 20 µl 0.1 % formic acid. For
75 nanoflow LC-MS/MS, an Eksigent nanoLC-Ultra 1D+ (Eksigent, Dublin, CA) was coupled to a LTQ Orbitrap Velos (Thermo Scientific, Bremen, Germany). Peptides

were delivered to a trap column (100 µm i.d. x 2 cm, packed with 5 µm C18 resin, Reprosil PUR AQ, Dr. Maisch, Ammerbuch, Germany) at a flow rate of 5 µl/min in 100 % buffer A (0.1% FA in HPLC grade water). The injection volume was 10 µl.

80 After 10 min of loading and washing, peptides were transferred to an analytical column (75 µm x 40 cm C18 column Reprosil PUR AQ, 3 µm, Dr. Maisch, Ammerbuch, Germany) and separated using a 110 min gradient from 7 % to 35 % buffer B (0.1 % FA in acetonitrile) at a flow rate of 300 nl/min. The mass spectrometer was operated in data-dependent mode, automatically switching
85 between MS and MS2. Full scan MS spectra were acquired in the Orbitrap at 60,000 resolution, and tandem MS spectra were acquired at 7,500 resolution. Internal calibration was performed using the ion signal (Si(CH₃)₂O)₆H⁺ at m/z 445.120025 present in ambient laboratory air. Tandem mass spectra were generated for up to ten peptide precursors using higher energy collision dissociation (Olsen *et al.* 2007).
90 Precursors were dynamically excluded from fragmentation for 20 sec and unassigned charge states as well as singly charged ions were rejected.

Metaproteome data analysis

Peak picking and processing of raw MS data was performed using the Mascot
95 Distiller software (version 2.3, Matrix Science, London, UK) and peaklist files were submitted to Mascot (version 2.3.01) for peptide and protein identification. The Mascot database search parameters included a precursor tolerance of 10 ppm, a fragment tolerance of 0.02 Da and accounted for the oxidation of methionine (+15.9949 Da) and the carbamidomethylation of cysteine residues (+57.0215 Da) as
100 variable modification. The Mascot built-in target-decoy database search option was enabled.

List of microorganisms included in the compiled database for metaproteome analysis

Acetobacter pasteurianus IFO3283-32, *Alistipes shahi* WAL831, *Akkermansia muciniphila* ATCC BAA835, *Anaerococcus preuotii* DSM 20548, *Atopobium Parvulum* DSM 20469, *Bacillus cellulosilyticus* DSM 2522, *Bacillus cereus* ATCC 10987, *Bacillus licheniformis* DSM 13, *Bacillus subtilis* 168, *Bacteroides fragilis* NCTC 9343, *Bacteroides theatiotaomicron* VPI5482, *Bacteroides vulgatus* ATCC 8482, *Bacteroides xyloxylicus* XB1A, *Bifidobacterium adolescentis* ATCC 15703, 110 *Bifidobacterium animalis subsp. lactis* DSM 10140, *Bifidobacterium bifidum* S17, *Bifidobacterium longum subsp. infantis* ATCC 15697, Butyrate-producing bacterium SM4/1, Butyrate-producing bacterium SS3/4, Butyrate-producing bacterium SSC/2, *Butyrivibrio fibrisolvens* 16/4, *Butyrivibrio proteoclasticus* B316, *Candida glabrata* CBS 138, *Clostridium acetobutylicum* ATCC 824, *Clostridium beijerinckii* NCIM 8052, 115 *Clostridium cellulolyticum* H10, *Clostridium cellulovorans* 743B, *Clostridium difficile* CD196, *Clostridium novyi* NT, *Clostridium perfringens* ATCC 13124, *Clostridium saccharolyticum* DSM 2544, *Coprococcus catus* GD/7, *Desulfotomaculum reducens* MI-1, *Desulfovibrio salexigens* DSM 2638, *Eggerthella lenta* DSM 2243, *Enterobacter cloacae* ATCC 13047, *Enterococcus faecalis* V583, *Escherichia coli* K12, 120 *Eubacterium cylindroides* T2-87, *Eubacterium eligens* ATCC 27750, *Eubacterium limosum* KIST612, *Eubacterium rectale* ATCC 33656, *Faecalibacterium prausnitzii* L2-6, *Fingoldia magna* ATCC 29328, *Fusobacterium nucleatum* ATCC 25586, *Gordonibacter pamela* 7-10-1-b, *Helicobacter pylori* 26695, *Klebsiella pneumonia* 342, *Lactobacillus acidophilus* NCFM, *Lactobacillus brevis* ATCC 367, *Lactobacillus casei* BL23, *L. delbrueckii bulgaricus* ATCC 11842, *Lactobacillus johnsonii* NCC 533, 125 *Lactobacillus plantarum* WCFS1, *Lactobacillus reuteri* JCM 1112, *Lactococcus lactis* II1403, *Listeria monocytogenes* Clip81459, *Methanobrevibacter smithii* ATCC 35061, *Mycobacterium avium* 104, *Neisseria gonorrhoea* NCCP 11945, *Parabacteroides*

distasonis ATCC 8503, *Pediococcus pentosaceus* ATCC 25745, *Prevotella*
130 *ruminicola* 23, *Propionibacterium acnes* SK137, *Pseudomonas putida* KT2440,
Roseburia intestinalis M50/1, *Ruminococcus albus* 7, *Ruminococcus bromii* L2-63,
Ruminococcus obeum L2-14, *Ruminococcus torques* L12-162, *Saccharomyces*
cerevisiae S288c, *Salmonella enterica thyphimurium* D23580, *Shigella dysenteriae*
Sd197, *Slackia heliotrinireducens* DSM 20476, *Staphylococcus aureus* NCTC 8325,
135 *Staphylococcus epidermidis* ATCC 12228, *Staphylococcus agalactiae* A909,
Staphylococcus pneumoniae TCH8431/19A, *Streptococcus thermophilus* LMG 311,
Streptomyces coelicola A3(2), *Yersinia enterocolica* 8081.

Sample preparation and setting parameters for FT-ICR-MS analysis

140 Frozen cecal samples (n = 3 mice in each the CARB and HF group; trial 3) were kept
on dry ice and transferred to lysis tubes (NucleoSpin Bead Tubes, Macherey-Nagel)
containing ceramic beads and one metal bead (Qiagen). Samples were shaken (5
min, 30 Hz, 4 °C) in 1 ml cold (-20 °C) methanol using a TissueLyser II (Qiagen).
After two runs of centrifugation (14,000 rpm, 10 min, 4 °C), supernatants were
145 collected and dried using a SpeedVac Concentrator (Savant SPD 121 P,
Thermoscientific) for subsequent solid phase extraction (SPE) to remove
electrospray ionization (ESI)-suppressing contaminants. Dried samples were solved
in 1 ml aqueous 0.1 % formic acid and extracted using Oasis HLB cartridges (1 cc/30
mg, Waters GmbH). Cartridges were conditioned with 1 ml methanol and 1 ml water
150 prior to loading samples. After washing with 5 % methanol, samples were eluted with
pure methanol. Extracted samples were diluted (1:1000) in methanol and or 0.1 %
formic acid in methanol for negative or positive mode, respectively. They were
infused into the spectrometer with an ESI source at a flow rate of 120 ml/h. Prior to
measurement, the FT-ICR-MS was calibrated with clusters of arginine (m/z of

155 173.10440, 347.21607, 521.32775, 695.43943 and 869.55110) by using 5 mg/l
arginine solution in methanol for positive and negative ionisation mode with
calibration errors below 0.1 ppm for the four selected m/z signals. Two MW time
domains were applied in the mass range of 70-1000 m/z, the ion accumulation time
was set to 0.3 sec and time of flight was set to 0.7 msec. Spectra were accumulated
160 for 300 scans in both modes for all samples.

Supplementary Results

Mouse proteome data

Taking into account the sample preparation by centrifugation to collect bacteria, a
165 relatively high number of host proteins were identified via their peptide masses in the
metaproteome dataset (Supplementary Table S3). This suggests that mouse proteins
or fragments thereof may be bound to bacteria and were retained in the pellets.
Inspection of the list of identified mouse peptide fragments revealed that pancreatic
enzymes and enzyme inhibitors were over-represented, *i.e.*, anionic trypsin,
170 chymotrypsin B, alpha-1-antitrypsin, serine protease inhibitor A3K, serpin B6 and
meprin together with zymogen granule membrane protein 16, which most likely
originate from exocrine pancreatic secretions. In addition, proteins/enzymes
associated with the intestinal epithelium such as aminopeptidase N, angiotensin-
converting enzyme, carboanhydrase, cadherin and mucin-2 fragments were
175 identified. These findings suggest that proteome analysis of cecal samples has the
potential not only to reveal diet-induced changes in the microbiome but also provides
information on adaptive changes in the protein pool derived from pancreatic
secretions and the epithelium in the gastrointestinal tract.

180 *Metaproteome*

After functional category assignment of identified proteins, our data confirmed that, irrespective of diet, the dominant mammalian gut metaproteome is involved in energy production from carbohydrate metabolism (COG category G), including the following dominant proteins originating from a variety of bacterial species: ABC sugar
185 transporters, L-arabinose and -fucose isomerase, beta-galactosidase, glucose-6-phosphate isomerase, fructose-1,6-bisphosphate aldolase, glyceraldehyde-3-phosphate dehydrogenase, glycogen phosphorylase, phosphofructokinase, phosphoglycerate kinase, phosphopyruvate hydratase, pyruvate:flavodoxin oxidoreductase and pyruvate phosphate dikinase. However, in the HF group, we
190 observed a lower spectra occurrence for proteins classified in COG category C (energy production and conversion), *e.g.*, ATP synthase, acetyl-CoA decarboxylase/synthase complex, formate acetyltransferase, fumarate hydratase, glycerol dehydratase, oxaloacetate decarboxylase, phosphate acetyl- and butyryltransferase, pyruvate formate-lyase, flavodoxin oxidoreductase, rubredoxin,
195 molybdenum hydroxylase and acetaldehyde/alcohol, isocitrate, malate and xanthine dehydrogenase.

200 **Supplementary References**

Caporaso JG, Lauber CL, Walters WA, Berg-Lyons D, Huntley J, Fierer N *et al.* (2012). Ultra-high-throughput microbial community analysis on the Illumina HiSeq and MiSeq platforms. *Isme J* **6**: 1621-1624.

205 *et al.* (2011). Global patterns of 16S rRNA diversity at a depth of millions of sequences per sample. *Proc Natl Acad Sci U S A* **108 Suppl 1**: 4516-4522.

Olsen JV, Macek B, Lange O, Makarov A, Horning S and Mann M. (2007). Higher-energy C-trap dissociation for peptide modification analysis. *Nat Methods* **4**: 709-712.

Supplementary Table S1 Final body weight, cumulative energy, water and macronutrient intake according to dietary treatment

	Carbohydrate (C)	High-fat (HF)	p-value ^c
Body weight (g) ^a	29.9 ± 1.5	43.2 ± 4.4	< 0.001
Epididymal fat (g)	0.61 ± 0.19	2.60 ± 0.39	< 0.001
Plasma glucose (mg/dl) ^b	79.5 ± 8.9	129.2 ± 19.5	< 0.001
Water (mL)	313 ± 47	212 ± 12	< 0.001
Energy (kcal)	1 304 ± 22	1 571 ± 60	< 0.001
Protein (g)	58.9 ± 1.0	42.1 ± 1.6	< 0.001
Fat (g)	28.2 ± 0.5	133.0 ± 5.1	< 0.001
Carbohydrate (g)	168.9 ± 2.9	46.5 ± 1.8	< 0.001
Crude fiber (g)	15.3 ± 0.4	15.8 ± 0.5	0.085
Starch (g)	149.6 ± 4.1	2.9 ± 0.1	< 0.001

Values are mean ± s.d. (n = 6). Body weight as well as feed and water intake were measured once per week throughout the feeding trial. To correct feed intake for loss of feed, metal grids were placed below the feed containers allowing collection of spillage. Cumulative energy, water and micronutrient intake were recorded until day 81. Final body weights were obtained at day 83 to 85.

^aSimilar differences were observed in all subsequent cohorts of mice (data not shown).

^bAfter 9 weeks, animals were deprived of food for 14 h and blood was collected from the tail vein. Blood glucose concentrations were measured with an Accu-Check blood glucose meter (Roche Diagnostics).

^cP-values were obtained by Student's t-test using the software SigmaStat. In the case of inhomogeneous variances, Welch's correction was applied to Student's t-test.

Supplementary Table S2 16S rRNA gene sequence proportions at the level of bacterial phyla

P-values were adjusted for multiple testing according to the Benjamini-Hochberg correction. C, mouse on carbohydrate diet; HF, mouse on high-fat diet

Supplementary Table S3 16S rRNA gene sequence proportions at the level of bacterial families

P-values were adjusted for multiple testing according to the Benjamini-Hochberg correction. C, mouse on carbohydrate diet; HF, mouse on high-fat diet

Supplementary Table S4 List of diet-specific operational taxonomic units (OTUs)

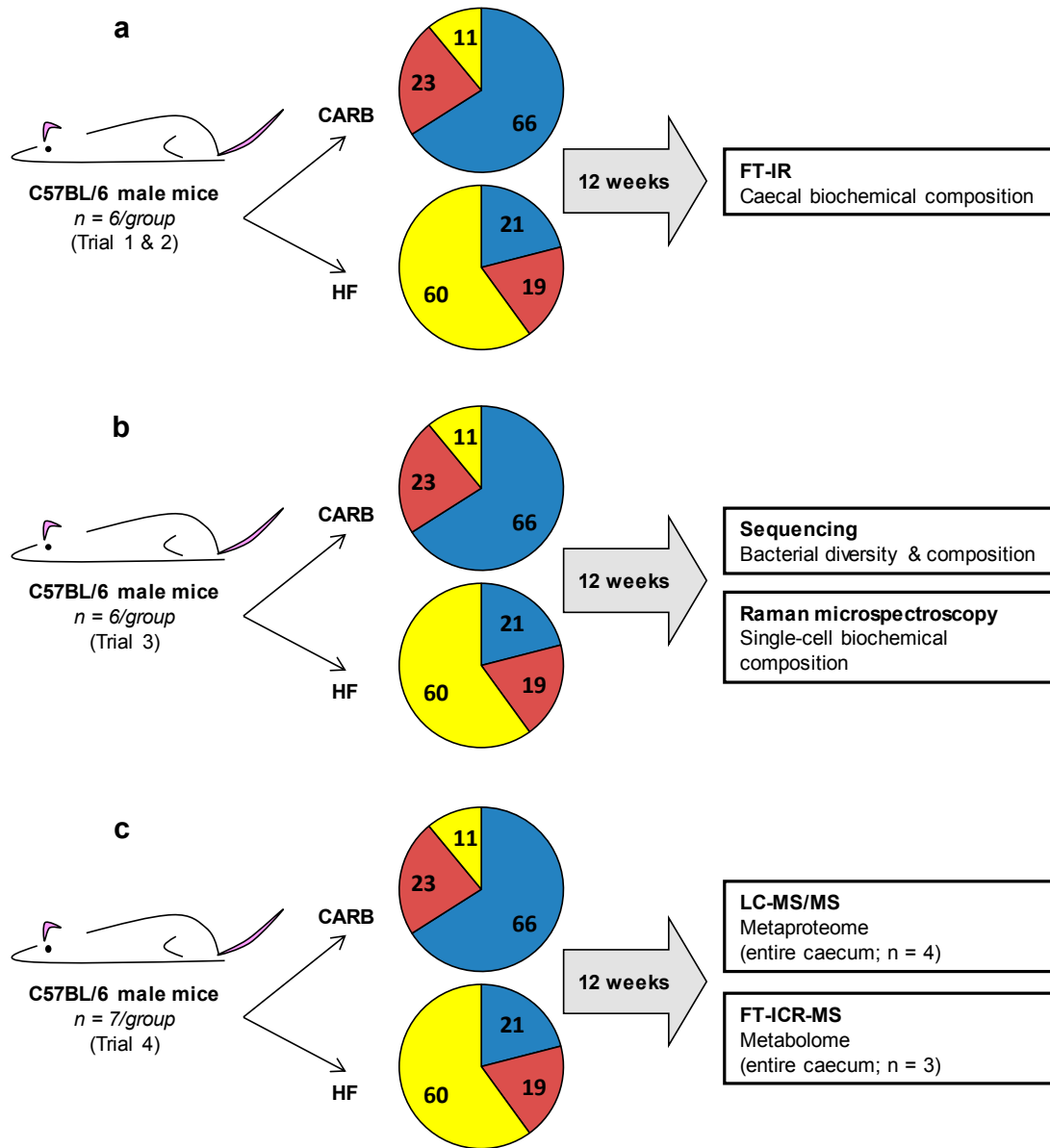
Data are shown as percentage of total sequences per mouse. Sequences (V4 region, 233 bp) were identified using the Seqmatch tool of the RDP.

Supplementary Table S5 Metaproteomic dataset

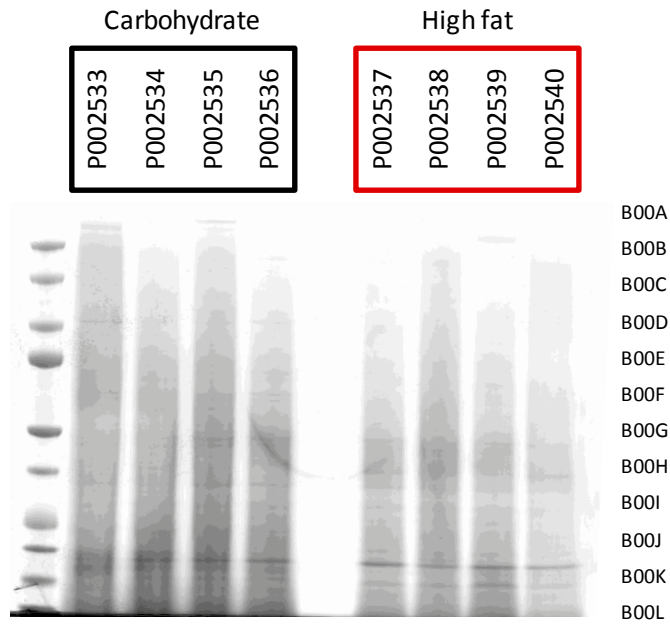
This table gathers the annotation and intensity values of all 1760 bacterial proteins detected in the caecum of mice fed the control carbohydrate (CARB) or high-fat (HF) diet (n = 4 each) (Window 1). Significant diet-specific bacterial proteins (and corresponding COG categories) for each the CARB and HF group as well as the 114 mouse proteins that were annotated are given in Window 2-4, respectively.

Supplementary Table S6 Metabolomic dataset

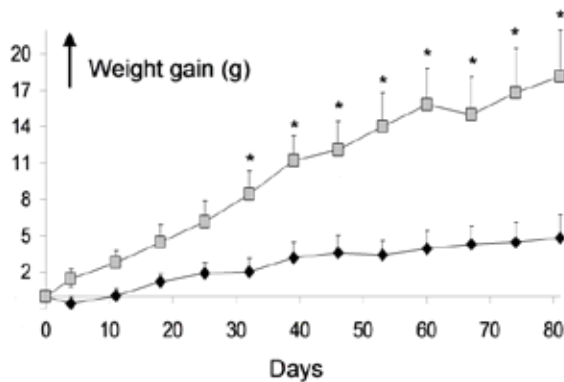
This table includes the list of masses (in Da) detected by FT-ICR-MS in the caecum of mice fed the control carbohydrate (CARB) or high-fat (HF) diet (n = 3 each). The list was filtered so as to include only masses that occurred in at least two of the three biological replicates (Window 1). Masses that significantly differed between mice from the CARB and HF group and those that could be annotated using MasSTRIX are shown in Window 2 and 3, respectively.



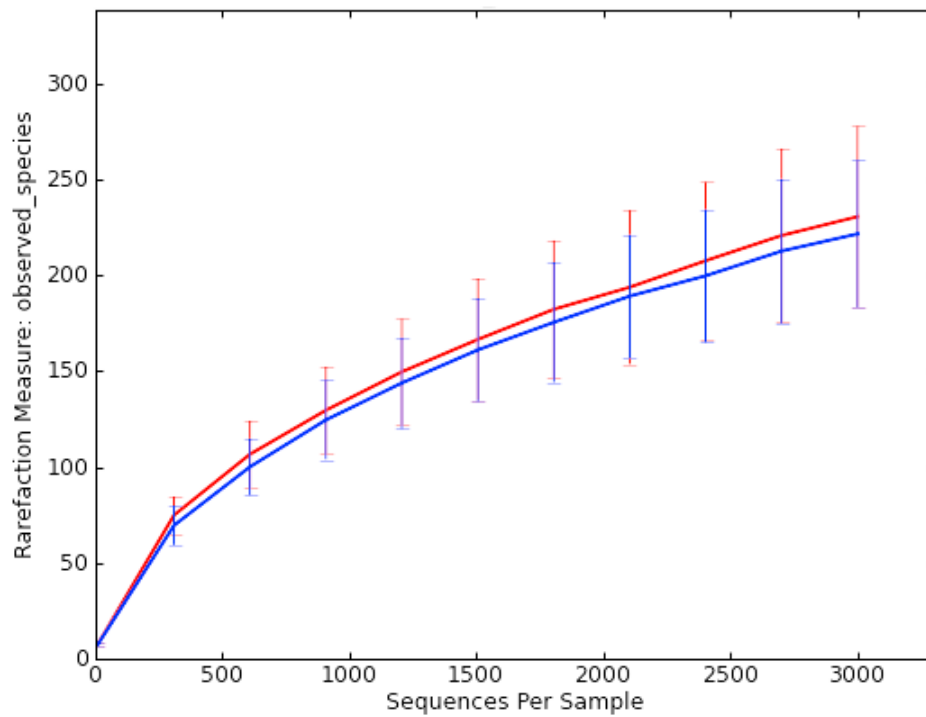
Supplementary Figure S1 Mouse trials and downstream analyses. In all four trials, mice were raised in the same animal facility and were fed exactly the same experimental diets (Ssniff GmbH, Soest, Germany; CARB, carbohydrate diet, cat. no. E15000-04; HF, high-fat diet, E15741-34). Pie charts indicate percentages of metabolizable energy originating from carbohydrates (blue), proteins (red) or fat (yellow) in the two diets.



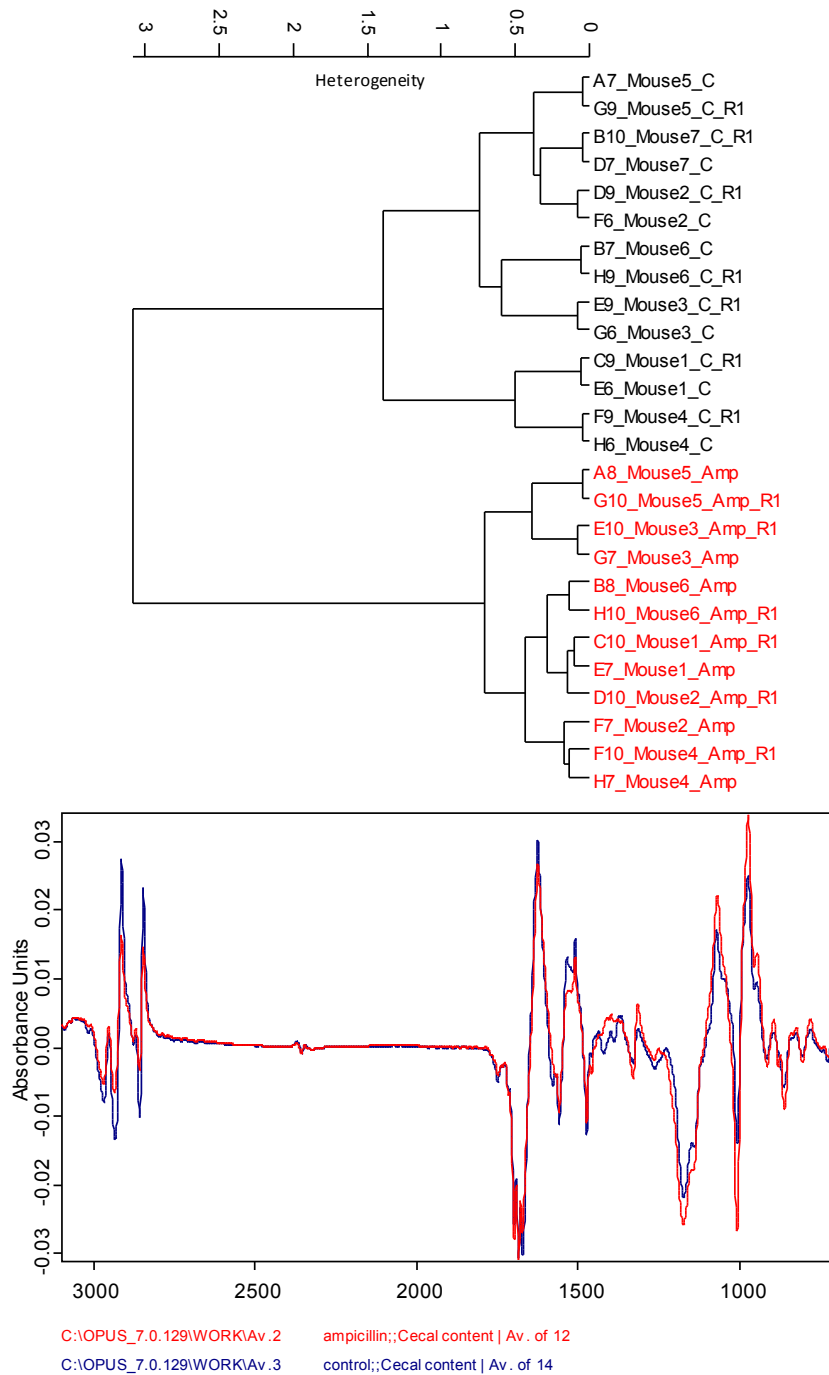
Supplementary Figure S2 Protein smears on denaturing polyacrylamide gels showing the 8 samples analyzed by LC-MS/MS. Proteins were separated on 4-12% NuPAGE Bis-Tris gels (Invitrogen, ca. no. NP0321BOX) and stained with colloidal coomassie. Each lane was cut into 12 gel pieces (B00A-L) prior to in-gel digestion using trypsin.



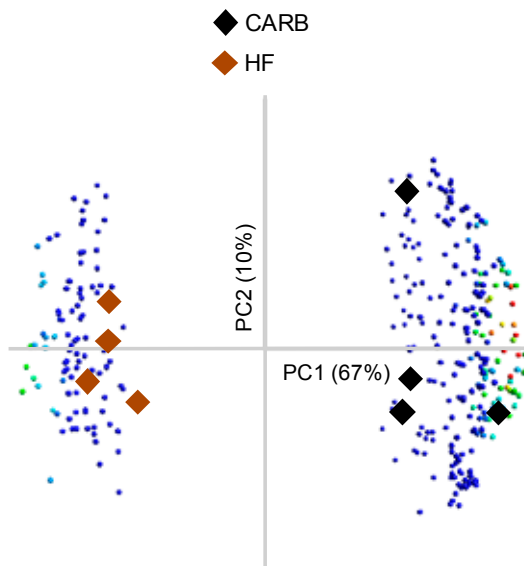
Supplementary Figure S3 Cumulative body weight gain over the 12 week feeding trial. Data are shown as mean \pm s.d. ($n = 6$ mice per group). Symbols: black diamonds, CARB diet; grey squares, HF diet; *, $p < 0.05$ when compared with the control group (Tukey's test). Statistical analyses were done using the MIXED procedure in SAS (Version 9.2; SAS Institute Inc., Cary, USA) with time as a repeated factor. The variables studied were subjected to seven covariance structures: unstructured covariance, compound symmetry, autoregressive order one, autoregressive moving average order one, heterogeneous compound symmetry, heterogeneous autoregressive order one and Toeplitz. The goodness of fit of the models was compared using the Bayesian information criterion (BIC).



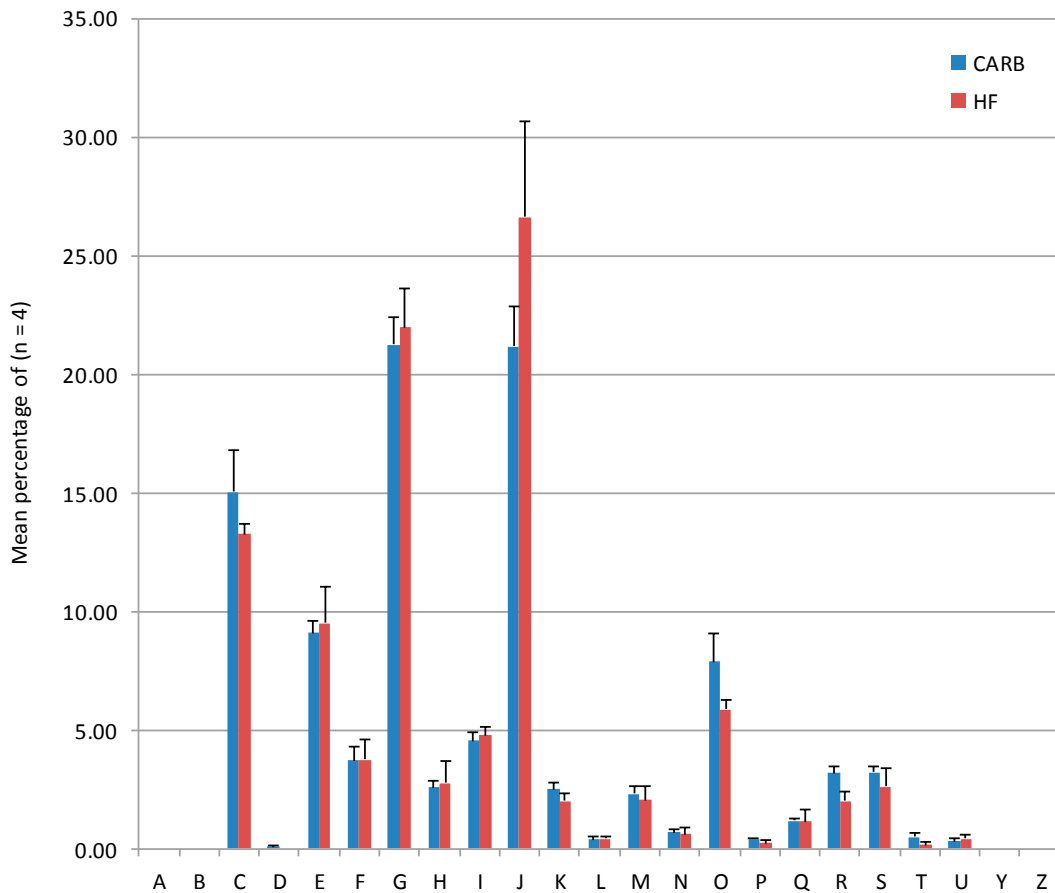
Supplementary Figure S4 Rarefaction plots at a depth of 3000 sequences showing that taxa richness does not differ between the two dietary groups (n = 6 mice/group; blue = HF; red = CARB). Rarefaction curves were obtained using the open source software package QIIME.



Supplementary Figure S5 FT-IR spectroscopy of cecal suspensions from C57BL/6 mice on chow diet treated with antibiotics (red) compared with control mice. Ampicillin (Amp) was given in water for 4 weeks (8 to 12 weeks of age) at 1g/l. The protocol was approved by the state ethics committee (ref. no. 55.2-1-54-2531-75-10). For each mouse, spectra from duplicate suspensions were acquired. Treatment groups clustered separately and spectral differences were visible over whole range of wavenumbers (mean first derivatives spectra are shown).



Supplementary Figure S6 Principal component analysis of metaproteomic NSAF values showing proteins (dots) and individual samples (diamonds) scattered predominantly along PC1 depending on dietary treatment. The percentage of dataset variability explain by each of the two components are given in brackets. The data points (proteins) are colored according to significance (from blue <math>< 0.05</math> to red <math>< 0.002</math>).



Supplementary Figure S7 Occurrence of identified proteins in mice fed the CARB and HF diet according to COG functional categories. **A**, RNA processing and modification; **B**, chromatin Structure and dynamics; **C**, energy production and conversion; **D**, cell cycle control and mitosis; **E**, amino Acid metabolism and transport; **F**, nucleotide metabolism and transport; **G**, carbohydrate metabolism and transport; **H**, coenzyme metabolism, **I**, lipid metabolism; **J**, translation; **K**, transcription; **L**, replication and repair; **M**, cell wall/membrane/envelop biogenesis; **N**, cell motility; **O**, post-translational modification, protein turnover, chaperone functions; **P**, inorganic ion transport and metabolism; **Q**, secondary structure; **R**, general functional prediction only; **S**, function unknown; **T**, signal transduction; **U**, intracellular trafficking and secretion; **Y**, nuclear structure; **Z**, cytoskeleton

PAPER 16

11 The Family *Coriobacteriaceae*

Thomas Clavel¹ · Patricia Lepage² · Cédric Charrier³

¹Junior Research Group Intestinal Microbiome, ZIEL – Research Center for Nutrition and Food Sciences, Technische Universität München, Freising-Weihenstephan, Germany

²INRA, AgroParisTech, Jouy-en-Josas, France

³Redx Anti-infectives Ltd, Alderley Edge, UK

Taxonomy, Historical and Current	201
Molecular Analyses	202
Phylogenetic Structure of the Family and Its Genera ...	202
DNA-Based Analysis and Genome Comparison	203
Phenotypic Analyses	204
<i>Adlercreutzia</i> Maruo et al. (2008)	205
<i>Asaccharobacter</i> Minamida et al. (2008)	210
<i>Atopobium</i> Collins and Wallbanks (1992)	214
<i>Collinsella</i> Kageyama et al. (1999c), Emend. Kageyama and Benno (2000)	215
<i>Coriobacterium</i> Haas and König (1988)	216
<i>Cryptobacterium</i> Nakazawa et al. (1999)	216
<i>Denitrobacterium</i> Anderson et al. (2000)	217
<i>Eggerthella</i> Wade et al. (1999), Emend. Maruo et al. (2008), Emend. Würdemann et al. (2009)	217
<i>Enterorhabdus</i> Clavel et al. (2009), Emend. Clavel et al. (2010)	218
<i>Gordonibacter</i> Würdemann et al. (2009)	218
<i>Olsenella</i> Dewhirst et al. (2001)	218
<i>Paraeggerthella</i> Würdemann et al. (2009)	220
<i>Parvibacter</i> Clavel et al. (2013)	220
<i>Slackia</i> Wade et al. (1999), Emend. Nagai (2010)	220
Isolation, Enrichment, and Maintenance Procedures	221
Ecology	222
Habitat and Occurrence	222
Metabolic Activities	226
Conversion of Cholesterol-Derived Host Metabolites	226
Polyphenol Metabolism	227
Pathogenicity, Clinical Relevance	227
Bacteremia	231
Gastrointestinal Pathologies	232
Allergy	232
Dental Caries and Abscess	232
Bacterial Vaginosis	233
Application	233

Abstract

Coriobacteriaceae is a family within the order *Coriobacteriales* (phylum Actinobacteria), which includes 30 species belonging to 14 genera: *Adlercreutzia*, *Asaccharobacter*, *Atopobium*, *Collinsella*, *Coriobacterium* (type genus), *Cryptobacterium*, *Denitrobacterium*, *Eggerthella*, *Enterorhabdus*, *Gordonibacter*, *Olsenella*, *Paraeggerthella*, *Parvibacter*, and *Slackia*. These bacteria are normal dwellers of mammalian body habitats such as the oral cavity, the gastrointestinal tract, and the genital tract. In the gut, *Coriobacteriaceae* carry out functions of importance such as the conversion of bile salts and steroids as well as the activation of dietary polyphenols. However, they can also be considered as pathobionts, because their occurrence has been associated with a range of pathologies such as bacteremia, periodontitis, and vaginosis. *Coriobacteriaceae* are usually nonmotile, nonspore-forming, nonhemolytic, and strictly anaerobic bacteria that grow as small rods; stain Gram-positive; are negative for oxidase, urease, and indole production; and are characterized by a high G+C content of DNA (around 60 mol%). Many species are asaccharolytic and possess a variety of aminopeptidases. Typical cellular fatty acids are C_{18:1}W9c as well as saturated fatty acids (C_{14:0}, C_{16:0}, C_{18:0}) and derivatives thereof. The production of menaquinone-6 homologues of vitamin K₂ seems also to be an attribute of the family. Taking into account the aforementioned metabolic functions of *Coriobacteriaceae*, their clinical relevance and the fact that an increasing number of novel species have been described very recently, this bacterial family will surely gain an increasing attention in the field of host/bacteria interactions in the near future.

Taxonomy, Historical and Current

The proposal to create the family *Coriobacteriaceae* (Co.ri.o.bac.te.ri.a'ce.ae. M.L. neut. n. *Coriobacterium* type genus of the family; *-aceae* ending to denote a family; M.L. fern. pl. n. *Coriobacteriaceae* the *Coriobacterium* family) was first published in 1997 by Stackebrandt et al. who reported a novel hierarchic classification of the phylum Actinobacteria according to 16S ribosomal RNA (rRNA) gene-based phylogeny (Stackebrandt et al. 1997). The type genus of the family, *Coriobacterium*, includes only one species, *Coriobacterium glomerans*, originally cultured from the intestine of a red soldier bug (Haas and König 1988).

Only five of the current members of the family were isolated before the advent of molecular phylogeny in the mid-1980s. All of them have been subjected to amended description: *Atopobium minutum* (formerly *Bacteroides minutum*, *Eubacterium minutum*, or *Lactobacillus minutus*) (Collins and Wallbanks 1992), *Atopobium parvulum* (formerly *Peptostreptococcus parvulus* or *Streptococcus parvulus*) (Collins and Wallbanks 1992), *Collinsella aerofaciens* (formerly *Bacteroides aerofaciens*, *Eubacterium aerofaciens*, or *Pseudobacterium aerofaciens*) (Kageyama et al. 1999a), *Eggerthella lenta* (formerly *Bacteroides lentus*, *Eubacterium lentum*, or *Pseudobacterium lentum*) (Wade et al. 1999), and *Slackia heliotrinireducens* (formerly *Peptococcus heliotrinireducans* or *Peptostreptococcus heliotrinireducens*) (Wade et al. 1999). The main phenotypic traits still used nowadays for the identification of most family members are as follows: Gram-positive staining; nonmotile (with the exception of *Gordonibacter pamelaeae*); nonspore-forming; nonhemolytic; typically with a relatively narrow range of growth temperatures around the optimum of 37 °C; usually neutrophilic and acidotolerant; strictly anaerobic, albeit some members reported to be aerotolerant (*Eggerthella lenta*, *Enterorhabdus*, and *Parvibacter* spp.) and others microaerophiles (*Olsenella* spp.) or facultative anaerobes (*Atopobium vaginae*); grow as small rods or coccobacilli that mostly occur as single cells, pairs, or chains (e.g., *Adlercreutzia equolifaciens*, *Collinsella aerofaciens*, *Collinsella tanakaei*, *Coriobacterium glomerans*, *Eggerthella* spp., *Olsenella umbonata*, *Paraeggerthella hongkongensis*); grow usually to low optical density in liquid medium (with the exception of *Atopobium*, *Collinsella*, and *Olsenella* spp.); enhanced growth in the presence of arginine (e.g., *Cryptobacterium*, *Eggerthella*, *Gordonibacter*, and *Slackia* spp.) or Tween 80 (e.g., *Atopobium* and *Olsenella* spp.); positive for arginine dihydrolase and a variety of aminopeptidases; and negative for indole production, oxidase, and urease. Many species are asaccharolytic or convert a very limited number of sugars, e.g., *Adlercreutzia equolifaciens*, *Asaccharobacter celatus*, *Eggerthella* spp., *Enterorhabdus* spp., *Paraeggerthella hongkongensis*, *Parvibacter caecicola*, and all *Slackia* species.

Researchers who isolated strains of *Coriobacteriaceae* in the early days focused mainly on the description of isolates from feces, wounds, abscesses, and gingival crevices, which drew attention to the pathogenic potential of these bacteria. To date, however, nearly all species within the *Coriobacteriaceae* are known as commensal members of mammalian microbiota. The last 5 years have seen a bloom in the number of newly described bacteria belonging to the family: 11 of the 30 known species with a standing name in nomenclature have been described since 2008 (Maruo et al. 2008; Minamida et al. 2008; Clavel et al. 2009, 2010, 2013; Matthies et al. 2009; Würdemann et al. 2009; Jin et al. 2010; Nagai et al. 2010; Kraatz et al. 2011). In light of these novel descriptions, chemotaxonomic features have emerged as important parameters for reliable taxonomic classification of isolates. Most members of the *Coriobacteriaceae* contain a high proportion of saturated cellular fatty acids (e.g., C_{14:0}, C_{16:0}, or C_{18:0} and dimethyl acetal thereof) and/or C_{18:1}ω9c. The major menaquinones hitherto reported are

menaquinone-6 (MK-6) (e.g., in *Eggerthella lenta*, *Gordonibacter pamelaeae*, and *Paraeggerthella hongkongensis*), monomethylmenaquinone-6 (MMK-6) (e.g., in *Eggerthella sinensis*, *Enterorhabdus* spp., and *Parvibacter caecicola*), and dimethylmenaquinone-6 (DMMK-6) (e.g., in *Adlercreutzia equolifaciens*, *Eggerthella* spp., and *Enterorhabdus caecimuris*). The latter group of quinones seems to be unique to the *Coriobacteriaceae* (Würdemann et al. 2009). So far analyzed peptidoglycan structures are of type A4a, A4b, as well as A4g or A1g based on the presence of LL- or meso-diaminopimelic acid, respectively. In all species examined for the presence of polar lipids, phosphatidylglycerol and diphosphatidylglycerol as well as up to four glycolipids and three phospholipids were detected.

Molecular Analyses

Phylogenetic Structure of the Family and Its Genera

A 16S rRNA gene sequence-based phylogenetic tree of the 30 members of the family is shown in Fig. 11.1. The trees were reconstructed by using a subset of sequences representative of most closely related genera to stabilize the tree topology.

The first phylogenetic description of the family *Coriobacteriaceae* was published by Stackebrandt et al. (1997). Due to newly described species within the phylum Actinobacteria and the availability of their 16S rRNA gene sequences, an emended description of the family was recently published based on the analysis of 2,642 actinobacterial sequences with >1,300 unambiguous nucleotides (between position 100 and 1,400) (Zhi et al. 2009). The authors reported that the order *Coriobacteriales* (and thus *Coriobacteriaceae*, the sole family within this order) constitutes one of the deepest branches within the phylum Actinobacteria together with the lineages of the order *Rubrobacterales* (e.g., *Thermoleophilaceae*, *Conexibacteraceae*) and *Acidimicrobiales*. The pattern of 16S rRNA signatures of *Coriobacteriaceae* consists of nucleotides at positions 242 : 284 (C–G), 291 : 309 (C–G), 316 : 337 (U–G), 819 (A), 952 : 1229 (U–A), and 1115 : 1185 (C–G). Before the first description of the family by Stackebrandt et al. (1997), 16S rRNA-based phylogeny had already played an important role for the sake of emended description of several misclassified member species, including *Lactobacillus minutus*, *Lactobacillus rimae*, and *Streptococcus parvulus* (Collins and Wallbanks 1992). The genus *Atopobium* has then served, together with *Coriobacterium*, as a phylogenetic core of the *Coriobacteriaceae* and has been used to demonstrate that the inclusion of a broad range of physiologically diverse bacteria and thoughtful selection of out-groups are essential prerequisites for drawing proper phylogenetic conclusion (Rainey et al. 1994; Stackebrandt and Ludwig 1994). Thereafter, 16S rRNA gene-based phylogenetic evidence has largely contributed to the reclassification of additional members of the *Coriobacteriaceae*, e.g., *Atopobium fossor*, *Collinsella aerofaciens*, *Eggerthella lenta*, *Slackia exigua*, and *Slackia heliotrinireducens* (Kageyama et al. 1999a, b; Wade et al. 1999).

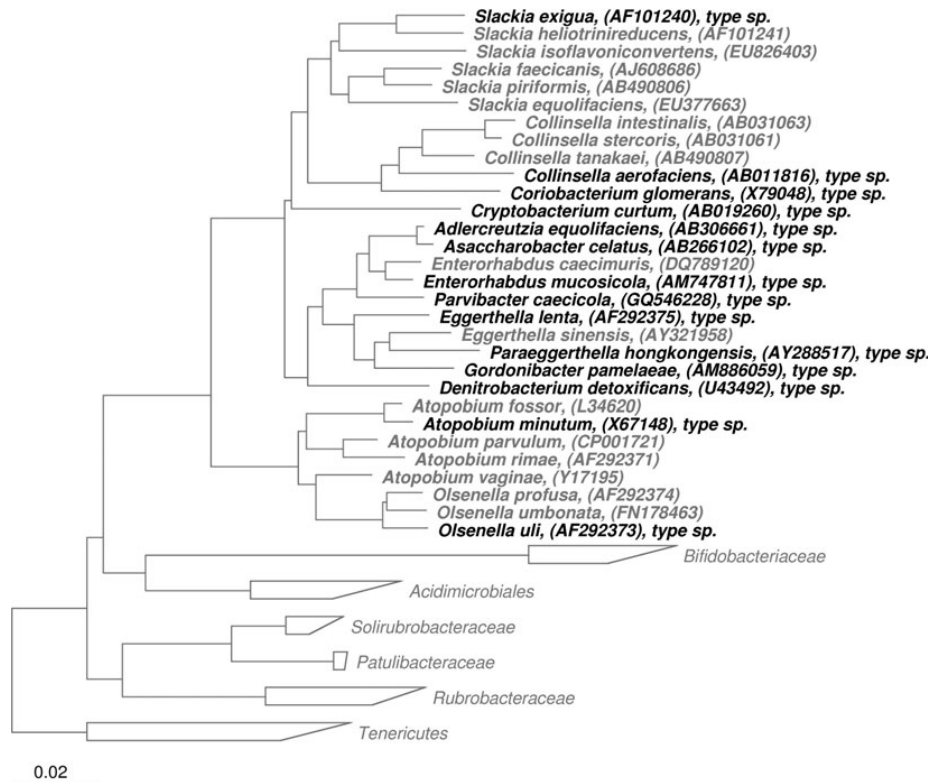


Fig. 11.1

Phylogenetic reconstruction of the family *Coriobacteriaceae* based on 16S rRNA and created using the neighbor-joining algorithm with the Jukes-Cantor correction. The sequence datasets and alignments were used according to the All-Species Living Tree Project (LTP) database (Yarza et al. 2010; <http://www.arb-silva.de/projects/living-tree>). The tree topology was stabilized with the use of a representative set of nearly 750 high-quality-type strain sequences proportionally distributed amongst the different bacterial and archaeal phyla. In addition, a 40 % maximum frequency filter was applied in order to remove hypervariable positions and potentially misplaced bases from the alignment. Scale bar indicates estimated sequence divergence

According to information retrieved from the Ribosomal Database Project, 749 isolates that relate to the *Coriobacteriaceae* family have been described (full and partial 16S rDNA length), most of them from the *Atopobium* genus (337) and unclassified *Coriobacteriaceae* (117), followed by *Olsenella* (94), *Collinsella* (63), *Cryptobacterium* (39), *Eggerthella* (25), *Slackia* (22), *Paraeggerthella* (20), *Coriobacterium* (10), *Adlercreutzia* (9), *Gordonibacter* (6), *Denitrobacterium* (4), *Enterorhabdus* (2), and *Asaccharobacter* (1). Even though the number of 16S rRNA operons varies greatly between species (from 1 operon to 7 in *Collinsella aerofaciens*), their average number is low (2.4) since most of the sequenced strains have only one to two 16S rRNA operons.

DNA-Based Analysis and Genome Comparison

With the exception of *Atopobium* spp. and *Cryptobacterium curtum*, family members are characterized by a high

G+C content of DNA (approximately 60 mol% and above). All DNA-DNA relatedness values available in the literature for members of the *Coriobacteriaceae* are given in Table 11.1.

Table 11.2 gathers most relevant information on genome sequencing projects focused on members of the *Coriobacteriaceae*. Representative genomes are available for 24 species belonging to 8 of the *Coriobacteriaceae* genera: *Atopobium* ($n = 6$ genomes), including *Atopobium parvulum*, *Atopobium rimae*, and *Atopobium vaginae* (3 strains); *Collinsella* ($n = 4$ genomes), including *Collinsella aerofaciens*, *Collinsella intestinalis*, *Collinsella stercoris*, and *Collinsella tanakaei*; *Coriobacterium glomerans* ($n = 1$ genome); *Cryptobacterium curtum* ($n = 1$ genome); *Eggerthella lenta* ($n = 4$ genomes from 3 strains); *Gordonibacter pamelaee* ($n = 1$ genome); *Olsenella* ($n = 2$ genomes), including *Olsenella uli* and *Olsenella* sp. oral taxon 809; *Slackia* ($n = 4$ genomes), including *Slackia exigua*, *Slackia heliotrinireducens*, and *Slackia piriformis* (2 strains); and unclassified *Coriobacteriaceae* ($n = 1$ genome; *Coriobacteriaceae* bacterium JC110).

Table 11.1

DNA-DNA homology between species of *Coriobacteriaceae*

Strain 1	Strain 2	%	Reference
<i>Atopobium minutum</i> VPI 9428 ^T	<i>Atopobium parvulum</i> VPI 0546 ^T	<16	Olsen et al. (1991)
<i>Atopobium minutum</i> VPI 9428 ^T	<i>Atopobium rimae</i> VPI D140H-11A ^T	<11	Olsen et al. (1991)
<i>Atopobium parvulum</i> VPI 0546 ^T	<i>Atopobium rimae</i> VPI D140H-11A ^T	16	Olsen et al. (1991)
<i>Atopobium minutum</i> VPI 9428 ^T	<i>Olsenella uli</i> VPI D76D-27C ^T	4	Olsen et al. (1991)
<i>Atopobium parvulum</i> VPI 0546 ^T	<i>Olsenella uli</i> VPI D76D-27C ^T	5	Olsen et al. (1991)
<i>Atopobium rimae</i> VPI D140H-11A ^T	<i>Olsenella uli</i> VPI D76D-27C ^T	8	Olsen et al. (1991)
<i>Collinsella aerofaciens</i> JCM 10188 ^T	<i>Collinsella intestinalis</i> RCA56-68 ^T	8	Kageyama and Benno (2000)
<i>Collinsella aerofaciens</i> JCM 10188 ^T	<i>Collinsella stercoris</i> RCA 55-54 ^T	8	Kageyama and Benno (2000)
<i>Collinsella intestinalis</i> RCA56-68 ^T	<i>Collinsella stercoris</i> RCA 55-54 ^T	<25	Kageyama and Benno (2000)
<i>Cryptobacterium curtum</i> 12-3 ^T	<i>Eggerthella lenta</i> ATCC 25559 ^T	<5	Nakazawa et al. (1999), Nakazawa and Hoshino (2004)
<i>Cryptobacterium curtum</i> 12-3 ^T	<i>Slackia exigua</i> ATCC 700122 ^T	4	Nakazawa and Hoshino (2004)
<i>Cryptobacterium curtum</i> 12-3 ^T	<i>Slackia heliotrinireducens</i> ATCC 29202 ^T	5	Nakazawa and Hoshino (2004)
<i>Eggerthella lenta</i> ATCC 25559 ^T	<i>Slackia exigua</i> ATCC 700122 ^T	<11	Poco et al. (1996), Nakazawa and Hoshino (2004)
<i>Eggerthella lenta</i> ATCC 25559 ^T	<i>Slackia heliotrinireducens</i> ATCC 29202 ^T	10	Nakazawa and Hoshino (2004)
<i>Enterorhabdus caecimuris</i> B7 ^T	<i>Enterorhabdus mucosicola</i> Mt1-B8 ^T	28	Clavel et al. (2010)
<i>Olsenella profusa</i> CCUG 45371 ^T	<i>Olsenella uli</i> CCUG 31166 ^T	33	Kraatz et al. (2011)
<i>Olsenella profusa</i> CCUG 45371 ^T	<i>Olsenella umbonata</i> lac31 ^T	50	Kraatz et al. (2011)
<i>Olsenella uli</i> CCUG 31166 ^T	<i>Olsenella umbonata</i> lac31 ^T	47	Kraatz et al. (2011)
<i>Slackia exigua</i> ATCC 700122 ^T	<i>Slackia heliotrinireducens</i> ATCC 29202 ^T	33	Nakazawa and Hoshino (2004)
<i>Slackia isoflavoniconvertens</i> HE8 ^T	<i>Slackia exigua</i> CCUG 44588 ^T	18	Matthies et al. (2009)
<i>Slackia isoflavoniconvertens</i> HE8 ^T	<i>Slackia faecicanis</i> DSM 17537 ^T	29	Matthies et al. (2009)
<i>Slackia isoflavoniconvertens</i> HE8 ^T	<i>Slackia heliotrinireducens</i> DSM 20476 ^T	22	Matthies et al. (2009)

A complete genome is available for eight of the sequenced organisms, whereas the others are whole genome shotgun under completion. Fourteen of the 24 sequenced species are human isolates; four of them were isolated from diseased patients (caries, periodontitis, or bacteremia). Genome size ranges from 1,418,601 (*Atopobium vaginae* DSM 15829^T) to 3,632,260 bp (*Eggerthella lenta* DSM 2243^T). No plasmids have been described. One chromosome has been described for each of the sequenced strains. The number of genes is lowest in the *Atopobium* genus and highest in *Eggerthella lenta* DSM 2243^T. On average, 73.2 % of genes can be assigned to Clusters of Orthologous Groups (COGs). This ranges from 66.5 % in *Collinsella* spp. (min. 60.0 % in *Collinsella stercoris*) to 80.7 % in *Coriobacterium glomerans* PW2. In *Eggerthella* sp. YY7918, Yokoyama et al. reported an incomplete carbohydrate metabolic pathway in KEGG, supporting the observation that members of this genus are known to be asaccharolytic (Yokoyama et al. 2011). Several phage-related genes have been described in the genomes of all members of the family (Table 11.3). The highest number of phage-related genes is observed in the genome of *Atopobium rimae* ATCC 49626 ($n = 20$) and *Collinsella stercoris* DSM 13279 ($n = 16$). However, no phages have been described to lyse or infect strains of the *Coriobacteriaceae*.

The complete genomes of six sequenced strains were compared to the biggest genome of the family, i.e., *Eggerthella*

lenta DSM 2243^T, using RAST (Aziz et al. 2008) (Fig. 11.2). Genes were annotated to proteins and results were computed using BLASTP (uni- and bidirectionally) to compare every protein in the reference genome (*Eggerthella lenta*) to every protein in the comparison genomes. Out of the 3,308 total proteins in *Eggerthella lenta*, 115 proteins were shared with the six other sequenced strains at a threshold of 60 % similarity. A major part of these genes were related to ribosomal proteins. Proteins that were not directly related to ribosomal proteins ($n = 73$) belonged to several COGs family, but originated mainly from the family J (translation, ribosomal structure, and biogenesis), L (DNA replication, recombination, and repair), O (posttranslational modification, protein turnover, chaperones), and R (general function prediction only). As expected, the genome of *Eggerthella* sp. YY7918 was the most closely related to that of *Eggerthella lenta*, followed by *Slackia heliotrinireducens*.

Phenotypic Analyses

Unless otherwise stated, all so far described species are Gram-positive, nonspore-forming, nonmotile, strictly anaerobic small rods or coccobacilli (Fig. 11.3) that are negative for oxidase, urease, hemolysis, and indole production. The main

Table 11.2

Coriobacteriaceae family members for which the genome is completely or partially sequenced. Bacteria are listed according to their genome size. Data were extracted from the PATRIC resource (Gillespie et al. 2011). Abbreviations: WGS whole genome shotgun, CDS coding sequences

Genome name	NCBI taxon Id	Genome status	Type strain	Publication (PMID)	GenBank accession	Genome length	GC content	RAST CDS
<i>Atopobium vaginae</i> DSM 15829	525256	WGS	Yes	Unpublished	ADNA000000000	1,418,601	42.7	1,214
<i>Atopobium vaginae</i> DSM 15829	525256	WGS	Yes	Unpublished	ACGK000000000	1,435,317	42.7	1,197
<i>Atopobium vaginae</i> PB189-T1-4	866774	WGS	No	Unpublished	AEDQ000000000	1,448,900		1,282
<i>Atopobium parvulum</i> DSM 20469	521095	Complete	Yes	21304653	CP001721	1,543,805	45.7	1,329
<i>Cryptobacterium curtum</i> DSM 15641	469378	Complete	Yes	21304644	CP001682	1,617,804	50.9	1,351
<i>Atopobium rimae</i> ATCC 49626	553184	WGS	No	Unpublished	ACFE000000000	1,626,291	49.3	1,480
<i>Collinsella intestinalis</i> DSM 13280	521003	WGS	Yes	Unpublished	ABXH000000000	1,809,497	62.5	1,537
<i>Olsenella uli</i> DSM 7084	633147	Complete	Yes	21304694	CP002106	2,051,896		1,805
<i>Slackia</i> sp. CM382	1111137	WGS	No	Unpublished	ALNO01	2,051,910	-	1,803
<i>Slackia exigua</i> ATCC 700122	649764	WGS	No	Unpublished	ACUX000000000	2,096,289	62.1	1,813
<i>Slackia piriformis</i> YIT 12062	742818	WGS	Yes	Unpublished	ADMD01	2,100,457	-	1,967
<i>Coriobacterium glomerans</i> PW2	700015	Complete	No	Unpublished	CP002628	2,115,681	60	1,936
<i>Olsenella</i> sp. oral taxon 809 str. F0356	661087	WGS	No	Unpublished	ACVE01	2,159,805	-	1,905
<i>Coriobacteriaceae</i> bacterium JC110	1034345	WGS	No	Unpublished	CAEM01	2,354,438	62.1	1,973
<i>Atopobium</i> sp. ICM58	1105030	WGS	No	Unpublished	ALIY01	2,390,495	-	1,968
<i>Collinsella aerofaciens</i> ATCC 25986	411903	WGS	Yes	Unpublished	AAVN000000000	2,439,869	60.5	2,110
<i>Collinsella stercoris</i> DSM 13279	445975	WGS	Yes	Unpublished	ABXJ000000000	2,475,429	63.2	1,805
<i>Collinsella tanakaei</i> YIT 12063	742742	WGS	Yes	Unpublished	ADLS01	2,482,197	—	2,190
<i>Eggerthella</i> sp. YY7918	502558	Complete	No	21914883	AP012211	3,123,671		2,715
<i>Slackia heliotrinireducens</i> DSM 20476	471855	Complete	Yes	Unpublished	CP001684	3,165,038	60.2	2,824
<i>Eggerthella</i> sp. HGA1	910311	WGS	No	Unpublished	AEXR000000000	3,362,931		3,021
<i>Eggerthella</i> sp. 1_3_56FAA	665943	WGS	No	Unpublished	ACWN000000000	3,453,272		3,045
<i>Gordonibacter pamelaee</i> 7-10-1-b	657308	Complete	No	Unpublished	FP929047	3,608,022		3,083
<i>Eggerthella lenta</i> DSM 2243	479437	Complete	Yes	21304654	CP001726	3,632,260	64.2	3,212

discriminative features of *Coriobacteriaceae* at the genus level are listed in Table 11.4. Many species possess a range of aminopeptidases likely to be important for amino acid release from the environment, N cycling processes, ammonia production, and which are useful selective parameters for the classification of *Coriobacteriaceae*. Thus, information on arginine dihydrolase and amino acid arylamidases is summarized at the species level in Table 11.5.

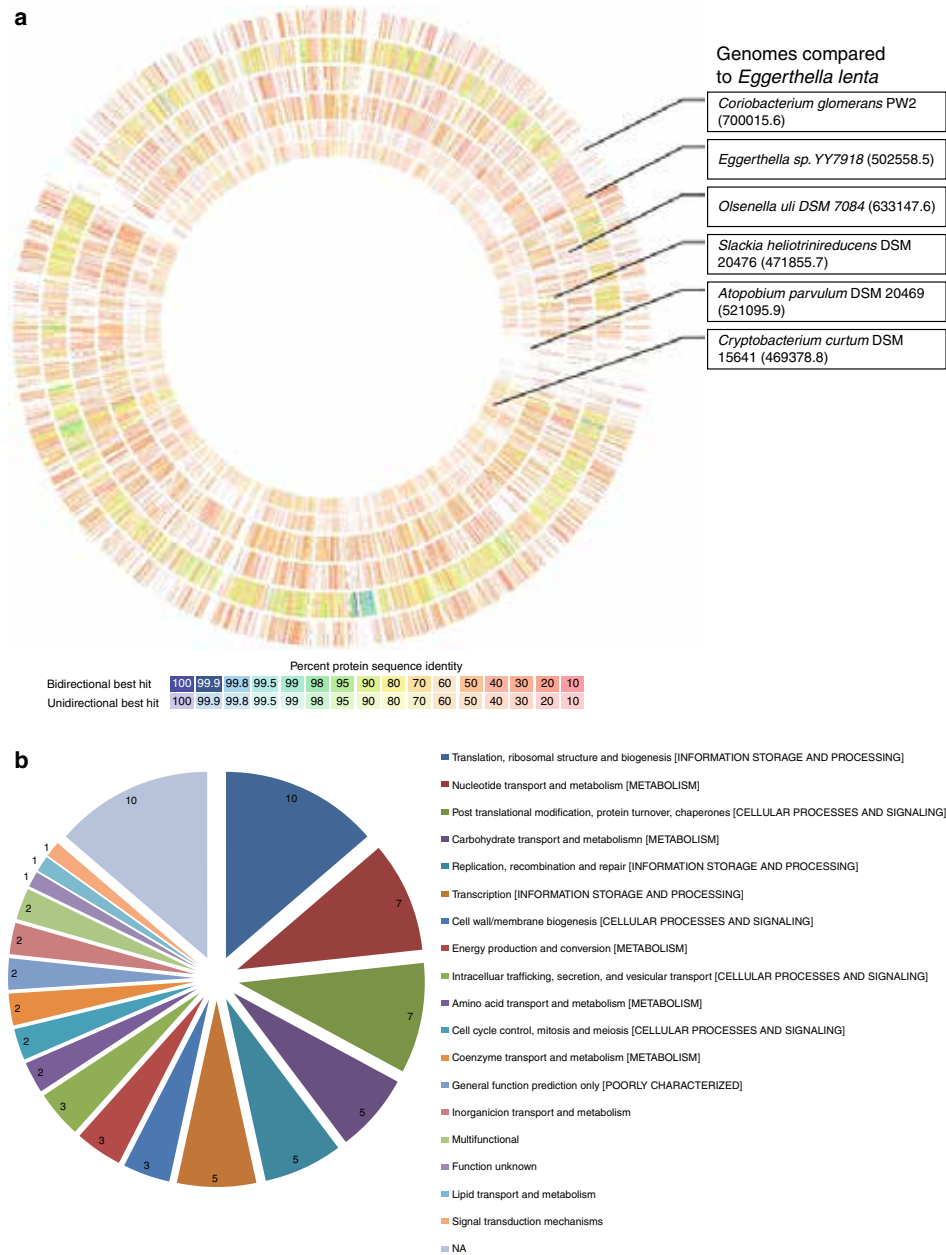
Adlercreutzia Maruo et al. (2008)

Adlercreutzia N.L. fem. n. *Adlercreutzia* named after H. Adlercreutz (Emeritus Professor, University of Helsinki, Finland), for his contributions to research on the effects of phytoestrogens on human health.

The genus is represented only by the type species *Adlercreutzia equolifaciens* (e.quo.li.fa.ci.ens. N.L. n. *equol-olis*

Table 11.3
Listing of phage-related genes in sequenced genomes of *Coriobacteriaceae*

Gene product name (sample locus tag)	Atopobium vaginae DSM 15829	Atopobium vaginae PB189-T1-4	Atopobium rimaе ATCC 49626	Atopobium parvulum IIP 1246, DSM 20469	Collinsella aerofaciens ATCC 25986	Collinsella stercoris DSM 13279	Collinsella intestinalis DSM 13280	Collinsella tanakaе YIT 12063	Cryptobacterium curtum 12-3, DSM 15641	Eggerthella sp. HGA1	Eggerthella sp. 1_3_56FAA	Eggerthella lenta VPI 0255, DSM 2243	Eggerthella sp. YY7918	Gordonibacter pamaeаe 7-10-1-BT, DSM 19378	Stactia heliointrireducens RH51, DSM 20476	Stactiaexigua ATCC 700122	Olsenella uli VPI, DSM 7084	Coriobacterium glomerans PW2, DSM 20642
Conserved hypothetical phage AbiD protein (HMPREF0091_0188)	1																	
Holin, phage phi LC3 family (Apar_0594)			1	1	1	1			1									
Hypothetical membrane protein with similarity to phage infection protein (ATORI0001_0646)			1															
Integrase/recombinase, phage integrase family protein (HMPREF9404_4029)										1								
Lambda family phage portal protein (HMPREF9452_00397)									1									
Phage capsid family (GPA_22850)														1				
Phage DNA replication protein (predicted replicative helicase loader) (COLAER_00687)					1									1	1			
Phage family integrase (ATORI0001_0862)			1															
Phage integrase (HMPREF1023_00378)											4					2		
Phage integrase family protein (ATORI0001_1210)			1															
Phage integrase family (COLAER_00798)					2	3												
Phage integrase, N-terminal SAM domain protein (HMPREF9248_0962)		2																
Phage major capsid protein, HK97 family (Shel_08230)																		1
Phage major tail protein, -1 family (ATORI0001_0997)			1															
Phage major tail protein, phi13 family (COLSTE_02157)						1												
Phage minor capsid protein 2 (COLSTE_01119)						1												
Phage minor structural protein (Elen_2638)												1						
Phage minor structural protein, N-terminal region (COLSTE_01099)																		
Phage N-6-adenine-methyltransferase (Elen_2611)						2												
Phage portal protein (ATORI0001_1181)			1								1	1						



■ Fig. 11.2

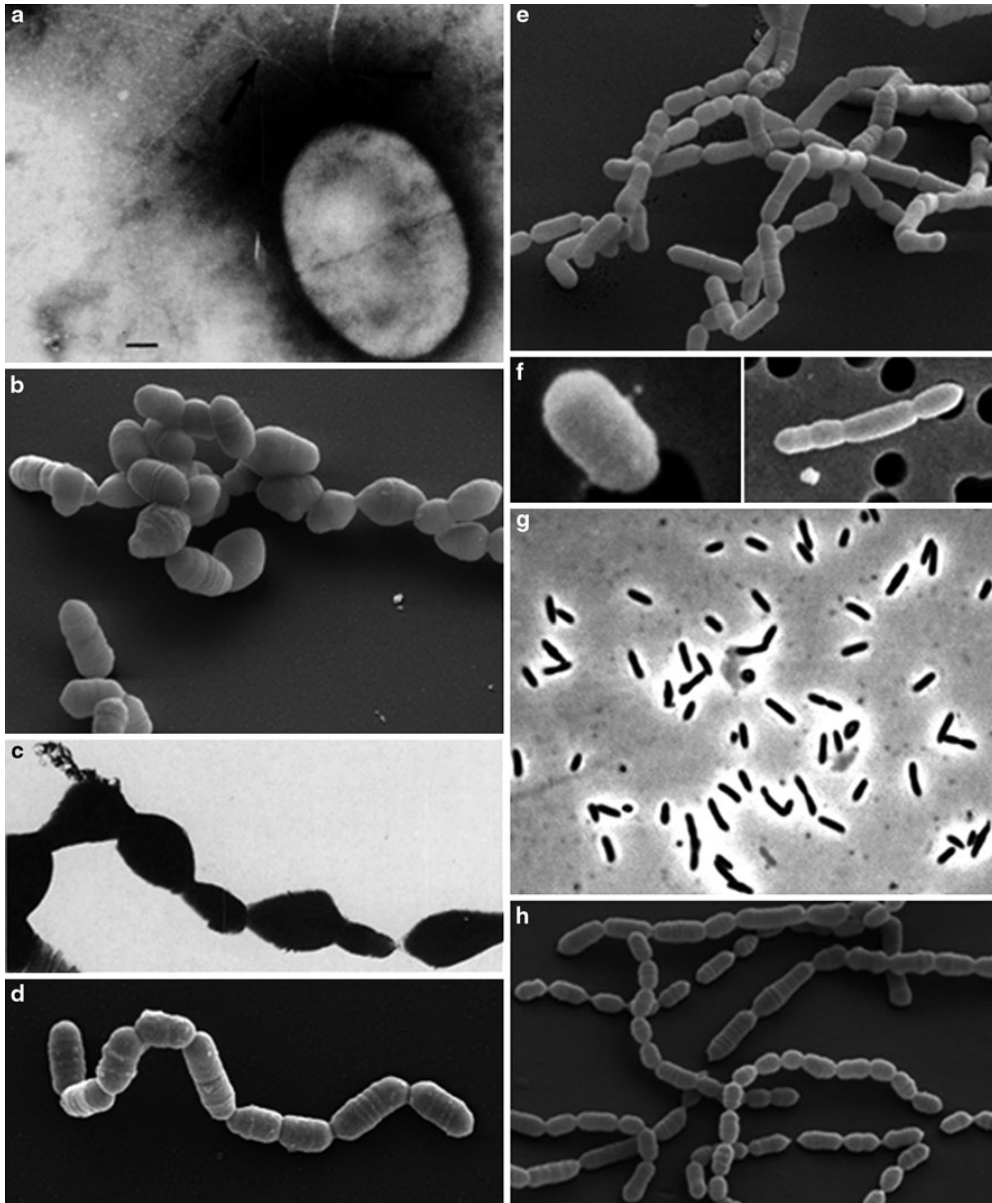
Comparative genome analysis of *Coriobacteriaceae*. (a) Circular map of proteins encoded by the different compared genomes with percent similarity to the reference genome *Eggerthella lenta* (the order of proteins refers to the order of the contigs/genes in the reference genome). The amino acid identity of the query genomes relative to the reference is color coded on a logarithmic scale following the visible spectrum. (b) Functional category distribution of non-ribosomal proteins ($n = 73$) shared by the seven *Coriobacteriaceae* genomes

equol; L. part. adj. *faciens* making; N.L. part. adj. *equolifaciens* equol-producing). Cells are coccobacilli ($0.6\text{--}0.7 \times 1.5\text{--}2.7 \mu\text{m}$) arranged in chains. Colonies on blood agar are 1–2 mm in diameter, grey to off-white grey, circular, entire, slightly

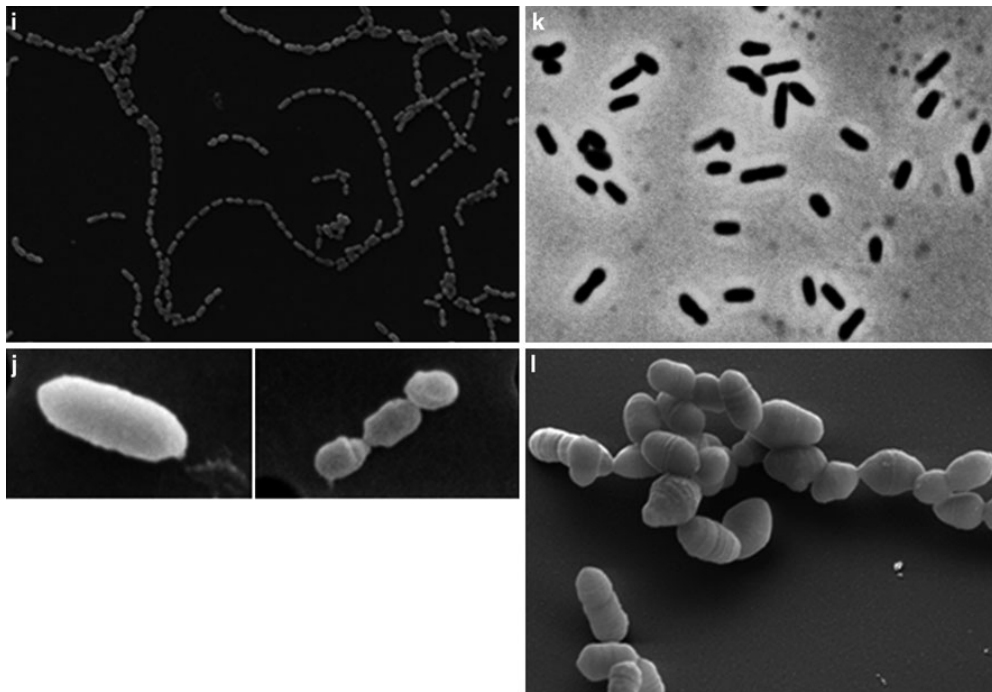
convex, and smooth. The species does not grow in 20 % bile. It is asaccharolytic and positive for arginine dihydrolase as well as arginine and leucine peptylamidase. No metabolic end product is detected in peptone-yeast extract medium

supplemented with glucose. Growth is stimulated by arginine. Nitrate is not reduced. *Adlercreutzia equolifaciens* converts the isoflavone daidzein into equol. Its cell wall contains A1g-type peptidoglycan with an (L-Ala)-D-Glu-m-Dpm peptide subunit. The diamino acid in the peptidoglycan is *meso*-diaminopimelic acid. The principal respiratory quinone is DMMK-6 (70–96 %).

MMK-6 is a minor component (1–29 %). The major cellular fatty acid is C_{18:1 cis9}. The G+C content of DNA is 64–67 mol% (64 mol% for the type strain). The description is based on the study of four strains: FJC-A10, FJC-B9, FJC-B20, and FJC-D53. The type strain is FJC-B9^T (= JCM 14793^T = DSM 19450^T = CCUG 54925^T).



■ Fig. 11.3 (Continued)



■ Fig. 11.3

Cell morphology of members of the Coriobacteriaceae. (a) *Atopobium fossor* (Bailey and Love 1986), (b) *Atopobium parvulum* (Copeland et al. 2009), (c) *Coriobacterium glomerans* (Haas and König 1988), (d) *Cryptobacterium curtum* (Mavrommatis et al. 2009), (e) *Eggerthella lenta* (Saunders et al. 2009), (f) *Eggerthella sinensis* (Lau et al. 2004b), (g) *Enterorhabdus mucosicola* (Clavel et al. 2009), (h) *Olsenella uli* (Goker et al. 2010), (i) *Olsenella umbonata* (Kraatz et al. 2011), (j) *Paraeggerthella hongkongensis* (Lau et al. 2004a), (k) *Parvibacter caecicola* (Clavel et al. 2013), (l) *Slackia heliotrinireducens* (Pukall et al. 2009)

Asaccharobacter Minamida et al. (2008)

A.sac.cha.ro.bac'ter. Gr. pref. *a-* not; Gr.n.*saccharon* sugar; N.L. masc. n. *bacter* a rod; N.L. masc. n. *Asaccharobacter* rod that does not digest sugar.

The genus is represented only by the type species *Asaccharobacter celatus* (ce.la'tus. L. masc. adj. *celatus* conceal, hide, keep secret). This species is phylogenetically closely related to *Adlercreutzia equolifaciens* FJC-B9^T and strain Julong 732 (>99 % similarity) based on partial 16S rRNA gene sequence analysis. DNA-DNA hybridization analysis of these three isolates has not been performed so far. In contrast to *Adlercreutzia equolifaciens*, *Asaccharobacter celatus* can grow in 20 % bile, is negative for leucine arylamidase, and is characterized by the presence of a dominant lipoquinone that is not MK, MMK, DMMK, ubiquinone, or rhodoquinone. Cells are rod-shaped (0.45 × 2.3–2.7 μm). Colonies are smooth, clear, and colorless on GAM agar, reaching 1 mm in diameter after 2 days at 37 °C. Growth is enhanced in the presence of arginine, but not Tween 80. The species does not reduce nitrate, is asaccharolytic, and produces trace amounts of organic

acids (lactic, acetic, and succinic acid) in medium containing peptone, yeast extract, and glucose. It is capable of converting the isoflavone daidzein to equol. Cells do not produce acid from/show negative test results in the API 50 CH system with the following substrates: glycerol, glucose, erythritol, D-arabinose, L-arabinose, ribose, D-xylose, L-xylose, adonitol, methyl *b*-D-xyloside, galactose, fructose, mannose, sorbose, rhamnose, dulcitol, inositol, mannitol, sorbitol, methyl *a*-D-mannoside, methyl *a*-D-glucoside, *N*-acetylglucosamine, amygdalin, arbutin, esculin, salicin, cellobiose, maltose, lactose, melibiose, sucrose, trehalose, inulin, melezitose, raffinose, starch, glycogen, xylitol, gentiobiose, D-turanose, D-lyxose, D-tagatose, D-fucose, L-fucose, D-arabitol, L-arabitol, gluconate, 2-ketogluconate, and 5-ketogluconate. Cells show strong naphthol-AS-BI-phosphohydrolase activity, medium acid phosphatase activity, and weak alkaline phosphatase and esterase (C4) activities. The cell-wall peptidoglycan contains *meso*-diaminopimelic acid, alanine, and glutamic acid. The predominant cellular fatty acid is C_{18:1 cis9}. The G+C content of DNA is 63 mol%. The type strain is do03^T (= JCM 14811^T = DSM 18785^T = AHU 1763^T).

■ Table 11.4

Comparison of selected characteristics of genera within the family *Coriobacteriaceae*

Characteristic	<i>Adlercreutzia</i>	<i>Asaccharobacter</i>	<i>Atopobium</i>	<i>Collinsella</i>	<i>Coriobacterium</i>
Growth requirement	Strictly anaerobic	Strictly anaerobic	Strictly or facultative anaerobic	Strictly anaerobic	Strictly anaerobic
Motility	–	–	–	–	–
Growth stimulated by arginine	+	+	–	ND	ND
Growth stimulated by Tween 80	–	–	+	+	ND
Nitrate reduction	–	–	–	–	–
Catalase	–	–	–	–	–
Esculin hydrolysis	ND	–	v	v	ND
Asaccharolytic	+	+	v	–	–
Lactate production	–	trace	+	trace	+
Main CFA	C _{18:1} w9c	C _{18:1} w9c	C _{18:1} w9c FAME/DMA	C _{18:1} w9c; C _{18:1} w9c DMA	ND
% saturated CFA (major sCFA)	67 (C _{18:0} DMA)	20 (C _{18:0})	14–16 (C _{10:0} FAME; C _{16:0} DMA)	3–30 (C _{16:0} DMA; C _{18:0} DMA)	ND
Major respiratory quinone	DMMK-6	Unidentified	ND	Not detected	ND
G+C mol%	64–67	63	39–46	60–64	60–61
Characteristic	<i>Cryptobacterium</i>	<i>Denitrobacterium</i>	<i>Eggerthella</i>	<i>Enterorhabdus</i>	<i>Gordonibacter</i>
Growth requirement	Strictly anaerobic	Strictly anaerobic	Strictly anaerobic	Strictly anaerobic	Strictly anaerobic
Motility	–	–	–	–	+
Growth stimulated by arginine	+	ND	+	ND	+
Growth stimulated by Tween 80	–	ND	–	ND	ND
Nitrate reduction	–	+	v	–	–
Catalase	–	–	+	–	+
Esculin hydrolysis	–	ND	–	v	ND
Asaccharolytic	+	+	+	+	–
Lactate production	–	ND	trace	ND	ND
Main CFA	ND	C _{14:0} FAME; C _{16:0} DMA	C _{16:0} DMA	C _{16:0}	ai-C _{15:0} ; C _{16:0} DMA
% saturated CFA (major sCFA)	ND	87 (C _{14:0} FAME; C _{16:0} DMA)	61–76 (C _{16:0} DMA)	70–71 (C _{16:0})	89 (ai-C _{15:0} ; C _{16:0} DMA)
Major respiratory quinone	ND	ND	MK-6; MMK-6; DMMK-6	MMK-6	MK-6
G+C mol%	50–51	56–60	62–66	64–65	66

Table 11.4 (continued)

Characteristic	<i>Olsenella</i>	<i>Paraeggerthella</i>	<i>Parvibacter</i>	<i>Slackia</i>
Growth requirement	Microaerophilic or strictly anaerobic	Strictly anaerobic	Strictly anaerobic	Strictly anaerobic
Motility	–	–	–	–
Growth stimulated by arginine	–	ND	ND	+
Growth stimulated by Tween 80	+	ND	ND	–
Nitrate reduction	–	–	–	v
Catalase	–	+	–	–
Esculin hydrolysis	v	ND	ND	–
Asaccharolytic	–	+	+	+
Lactate production	+	ND	ND	–
Main CFA	C _{14:0} ; C _{18:0} ; C _{18:1} W9C; C _{18:1} W9c DMA	C _{18:1} W9c	C _{16:0}	C _{18:1} W9c; C _{18:1} W9c DMA
% saturated CFA (major sCFA)	54–100 (C _{14:0} ; C _{18:0})	49 (C _{16:0} DMA)	75 (C _{16:0})	16–42 (C _{14:0} ; C _{16:0} DMA; C _{18:0} DMA)
Major respiratory quinone	ND	MK-6	MMK-6	ND or not detected
G+C mol%	63–64	61–62	63	58–64

Symbols and abbreviations: + positive, – negative, *ai* anteiso, *DMA* dimethyl acetal, *FAME* fatty acid methyl ester, *MK* menaquinone, *MMK* methylmenaquinone, *DMMK* dimethylmenaquinone, *ND* not determined, *v* variable depending on species, *CFA* cellular fatty acids

Table 11.5

Detection of aminopeptidase activity in *Coriobacteriaceae* species

Aminopeptidase	<i>Adlercreutzia equolifaciens</i> ^T	<i>Asaccharobacter celatus</i> ^T	<i>Atopobium minutum</i> ^T	<i>Atopobium parvulum</i>	<i>Atopobium rimae</i>
Arginine dihydrolase	+	ND	v	–	–
Alanine arylamidase	ND	ND	v	+	–
Arginine arylamidase	+	ND	+	+	–
Cystine arylamidase	ND	–	ND	ND	ND
Glycine arylamidase	ND	ND	V	+	–
Histidine arylamidase	ND	ND	V	–	–
Leucine arylamidase	+	–	V	+	–
Leucyl glycine arylamidase	ND	ND	+	ND	ND
Lysine arylamidase	ND	ND	ND	ND	ND
Phenylalanine arylamidase	ND	ND	–	ND	ND
Proline arylamidase	ND	ND	v	–	–
Serine arylamidase	ND	ND	–	–	–
Tyrosine arylamidase	ND	ND	–	+	–
Valine arylamidase	ND	–	ND	ND	ND
Aminopeptidase	<i>Atopobium vaginae</i>	<i>Collinsella aerofaciens</i> ^T	<i>Collinsella intestinalis</i>	<i>Collinsella stercoris</i>	<i>Collinsella tanakaei</i>
Arginine dihydrolase	+	+	+	+	+
Alanine arylamidase	–	–	–	+	–
Arginine arylamidase	+	+	+	+	+
Cystine arylamidase	ND	–	–	–	–
Glycine arylamidase	+	+	+	+	+
Histidine arylamidase	+	+	+	+	+
Leucine arylamidase	+	+	+	+	+

Table 11.5 (continued)

Aminopeptidase	<i>Atopobium vaginae</i>	<i>Collinsella aerofaciens</i> ^T	<i>Collinsella intestinalis</i>	<i>Collinsella stercoris</i>	<i>Collinsella tanakaei</i>
Leucyl glycine arylamidase	ND	+	+	+	+
Lysine arylamidase	ND	ND	ND	ND	ND
Phenylalanine arylamidase	ND	—	—	—	—
Proline arylamidase	+	+	—	—	+
Serine arylamidase	+	—	—	+	—
Tyrosine arylamidase	—	—	—	+	—
Valine arylamidase	ND	—	—	—	—
Aminopeptidase	<i>Cryptobacterium curtum</i> ^T	<i>Eggerthella lenta</i> ^T	<i>Eggerthella sinensis</i>	<i>Enterorhabdus caecimuris</i>	<i>Enterorhabdus mucosicola</i> ^T
Arginine dihydrolase	+	+	+	+	+
Alanine arylamidase	ND	—	—	—	+
Arginine arylamidase	ND	v	+	—	—
Cystine arylamidase	ND	ND	ND	ND	ND
Glycine arylamidase	ND	—	—	—	+
Histidine arylamidase	ND	—	—	—	+
Leucine arylamidase	ND	—	—	—	+
Leucyl glycine arylamidase	ND	—	—	—	—
Lysine arylamidase	ND	ND	+	—	+
Phenylalanine arylamidase	ND	—	—	—	+
Proline arylamidase	ND	—	—	—	+
Serine arylamidase	ND	—	—	—	+
Tyrosine arylamidase	ND	—	—	—	+
Valine arylamidase	ND	ND	ND	ND	ND
Aminopeptidase	<i>Gordonibacter pamelaeae</i> ^T	<i>Olsenella profusa</i>	<i>Olsenella uli</i> ^T	<i>Olsenella umbonata</i>	<i>Paraeggerthella hongkongensis</i> ^T
Arginine dihydrolase	+	+	+	+	+
Alanine arylamidase	—	+	+	+	v
Arginine arylamidase	v	+	+	+	v
Cystine arylamidase	ND	+	+	+	ND
Glycine arylamidase	—	+	+	+	—
Histidine arylamidase	—	+	+	+	—
Leucine arylamidase	—	+	+	+	v
Leucyl glycine arylamidase	ND	+	+	+	—
Lysine arylamidase	ND	ND	ND	ND	v
Phenylalanine arylamidase	—	+	+	+	—
Proline arylamidase	—	+	+	+	—
Serine arylamidase	—	+	+	+	—
Tyrosine arylamidase	—	+	+	+	—
Valine arylamidase	ND	+	+	+	ND

Table 11.5 (continued)

Aminopeptidase	<i>Parvibacter caecicola</i> ^T	<i>Slackia equolifaciens</i>	<i>Slackia exigua</i> ^T	<i>Slackia faecicanis</i>	<i>Slackia heliotrinireducens</i>
Arginine dihydrolase	–	+	+	+	+
Alanine arylamidase	+	+	+	–	+
Arginine arylamidase	–	–	+	–	–
Cystine arylamidase	ND	ND	+	–	v
Glycine arylamidase	+	+	+	–	+
Histidine arylamidase	–	+	+	–	+
Leucine arylamidase	+	+	+	–	+
Leucyl glycine arylamidase	–	v	–	–	–
Lysine arylamidase	ND	ND	ND	ND	ND
Phenylalanine arylamidase	+	+	+	–	+
Proline arylamidase	+	+	+	–	+
Serine arylamidase	+	+	+	v	+
Tyrosine arylamidase	+	+	+	–	+
Valine arylamidase	ND	ND	+	–	+
Aminopeptidase	<i>Slackia isoflavoniconvertens</i>		<i>Slackia piriformis</i>		
Arginine dihydrolase	+		+		
Alanine arylamidase	–		+		
Arginine arylamidase	–		–		
Cystine arylamidase	–		+		
Glycine arylamidase	–		+		
Histidine arylamidase	–		+		
Leucine arylamidase	–		+		
Leucyl glycine arylamidase	–		–		
Lysine arylamidase	ND		ND		
Phenylalanine arylamidase	–		+		
Proline arylamidase	–		+		
Serine arylamidase	–		+		
Tyrosine arylamidase	–		+		
Valine arylamidase	–		+		

Atopobium fossor, *Coriobacterium glomerans*, and *Denitrobacterium detoxificans* were not included in the table since, to the best of our knowledge, no information is available in the literature on any of the listed enzymes for these species

Symbols and abbreviations: + positive, – negative, v variable depending on strains, ND not determined

Atopobium Collins and Wallbanks (1992)

A.to.po'bi.um. Gr. adj. *atopos* having no place, strange; Gr. neu. part. used as noun; *bion* living thing; N.L. neu. n. *Atopobium* strange living thing.

The genus name *Atopobium* was initially proposed in 1992 following the pioneering 16S rRNA-based phylogenetic analysis of 40 lactic acid bacteria by Collins and Wallbanks. The genus was created to accommodate the species formerly classified as follows: (a) *Lactobacillus minutus* (synonyms: *Bacteroides minutum*, *Eubacterium minutum*) → *Atopobium minutum* comb. nov. (mi.nu'tum. L. neut. adj. *minutum* little, small); (b) *Lactobacillus rimae* → *Atopobium rimae* comb. nov. (L. gen. n. *rimae* of a fissure, here pertaining to the gingival crevice); and

(c) *Streptococcus parvulus* (synonym: *Peptostreptococcus parvulus*) → *Atopobium parvulum* comb. nov. (L. neut. dim. adj. *parvulum* very small) (Collins and Wallbanks 1992). The genus also includes *Atopobium vaginae* (va.gi'nae. L. n. *vagina* vagina; L. gen. n. *vaginae* of the vagina) (Rodríguez Jovita et al. 1999) and *Atopobium fossor* (fos'sor. L.n. *fossor*, a digger, delver), originally described as [*Eubacterium fossor*] (Bailey and Love 1986; Kageyama et al. 1999b). The type species of the genus is *Atopobium minutum*. Of note, Olsen et al. published already in 1991 an amended description of [*Lactobacillus minutus*] and [*Streptococcus parvulus*] (Olsen et al. 1991), which were originally described in 1937 (Hauduroy et al. 1937; Weinberg et al. 1937). The transfer of [*Peptostreptococcus parvulus*] to the genus *Streptococcus* was published by Cato in 1983 (Cato 1983).

Table 11.6

Phenotypic features of *Atopobium* spp.

Characteristic	<i>Atopobium fossor</i>	<i>Atopobium minutum</i> ^T	<i>Atopobium parvulum</i>	<i>Atopobium rimae</i>	<i>Atopobium vaginae</i>
Growth atmosphere	Strictly anaerobic	Strictly anaerobic	Strictly anaerobic	Strictly anaerobic	Facultative anaerobic
Esculin hydrolysis	–	–	+	v	–
<i>b</i> -Galactosidase	ND	–	+	–	–
Pyroglutamic acid arylamidase	ND	v	+	+	–
Growth in 6.5 % NaCl	ND	v (4/11)	v (6/67)	–	ND
G+C content of DNA (mol%)	43–46	44	39	45	44
Type strain	ATCC 43386 = CIP 106638 = JCM 9981 = NCTC 11919 = VPB 2127	VPI 9428 = ATCC 33267 = CCUG 31167 = DSM 20586 = JCM 1118 = LMG 9439 = NCIMB 702751 (NCFB 2751)	IPP 1246 = ATCC 33793 = CCUG 32760 = CIP 102970 = DSM 20469 = JCM 10300 = VPI 0546	VPI D140H-11A = ATCC 49626 = CCUG 31168 = DSM 7090 = IFO (now NBRC) 15546 = JCM 10299 = LMG 11476	ATCC BAA-55 = CCUG 38953 = CIP 106431

Symbols: v variable (number of positive strains/total number of strains tested)

The growth of *Atopobium* spp. is usually stimulated by the presence of Tween 80. Cells consist of short rods, often with central swellings, or small cocci that may appear to be elliptical. Cells occur singly, in pairs, or short chains. The major fermentation products from glucose are lactic acid, together with acetic and formic acid; trace amounts of succinic acid may also be formed. H₂ is not produced. Gelatin is not liquefied; meat is not digested. These bacteria are usually strictly anaerobic, but *Atopobium vaginae* can also grow under aerobic conditions (5 % CO₂). The G+C content of DNA is 35–46 mol%. Discriminative features of *Atopobium* spp. are shown in Table 11.6.

Collinsella Kageyama et al. (1999c), Emend. Kageyama and Benno (2000)

Col.lin.sel'la. M.L. fem. dim. ending *-ella*, M.L. fem. n. *Collinsella* named to honor Matthew D. Collins, a contemporary English microbiologist, for his outstanding contribution to microbial taxonomy and phylogeny.

The genus *Collinsella* was created in 1999 to accommodate [*Eubacterium*] *aerofaciens* (ae.ro.fa'ci.ens. Gr. n. *aer* gas; L. v. *facere* to make, to produce; M.L. part. adj. *aerofaciens* gas-producing), which had been previously published as *Bacteroides aerofaciens* (Eggerth 1935). The proposal to create *Collinsella* gen. nov. was based on 16S rRNA gene sequence analysis showing that three strains of [*Eubacterium*] *aerofaciens* (JCM 10188^T, JCM 7790, and JCM 7791) formed a cluster closest to *Atopobium* spp. and *Coriobacterium glomerans*. The three strains were also characterized by higher G+C content of DNA

(60–61 vs. 45–47 mol%) when compared with *Eubacterium sensu stricto* (*Eubacterium limosum*, *Eubacterium barkeri*, *Eubacterium callanderi*). The genus currently comprises four species: *Collinsella intestinalis* (in'test.in.alis. N. L. adj. *intestinalis* pertaining to the intestine) (Kageyama and Benno 2000), *Collinsella stercoris* (ster'co.ris. L. n. *stercus* feces; L. gen. n. *stercoris* of feces, referring to the source of the isolate) (Kageyama and Benno 2000), *Collinsella tanakaei* (ta.na.ka'e.i. N.L. masc. gen. n. *tanakaei* of Tanaka, to honor Ryuichiro Tanaka, a Japanese microbiologist, for his contribution to increased knowledge about human intestinal microbiota and probiotics) (Nagai et al. 2010), and the type species *Collinsella aerofaciens*. *Collinsella* spp. occur in chains of rod-shaped cells (0.5–1.0 × 1–3 μm). Fermentation products of glucose are H₂, ethanol, formate, and lactate. All strains are positive for naphthol-AS-BI-phosphohydrolase, acid from glucose and D-mannose. They are negative for *a*-arabinosidase, *a*-fucosidase, *a*-galactosidase, *a*-mannosidase, chymotrypsin, esterase (C4), esterase lipase (C8), glutamic acid decarboxylase, glutamyl glutamic acid arylamidase, lipase (C14), pyroglutamic acid arylamidase and acid from L-arabinose, glycerol, D-mannitol, melezitose, raffinose, L-rhamnose, D-sorbitol, and D-xylose. It has been reported that the growth of *Collinsella* is stimulated by Tween 80 (Dewhirst et al. 2001; Maruo et al. 2008), but this characteristic is absent from the single description of all *Collinsella* species (Kageyama et al. 1999a; Kageyama and Benno 2000; Nagai et al. 2010). Cells of *Collinsella tanakaei* are resistant to 20 % bile (no data available for the other species). The cell wall contains a A4-type peptidoglycan. Respiratory quinones are not detected. The G+C content of DNA is

Table 11.7

Phenotypic features of *Collinsella* spp.

Characteristic	<i>Collinsella aerofaciens</i> ^T	<i>Collinsella intestinalis</i>	<i>Collinsella stercoris</i>	<i>Collinsella tanakaei</i>
Acid produced from				
Cellobiose	–	+	+	+
Lactose	+	–	+	+
Maltose	+	–	+	+
Acid phosphatase	–	+	+	+
Alkaline phosphatase	–	+	+	+
<i>b</i> -Galactosidase	+	–	+	–
<i>a</i> -Glucosidase	+	–	–	–
<i>b</i> -Glucosidase	–	v	+	+
<i>b</i> -Glucuronidase	–	–	–	+
<i>N</i> -Acetyl <i>b</i> -glucosaminidase	–	+	+	–
6-phospho- <i>b</i> -galactosidase	–	+	–	–
Esculin hydrolysis	–	v	–	+
Peptidoglycan type	A4b [(L-Ala)-D-Glu-L-Orn-D-Asp]	A4a [(L-Ala)-D-Glu-L-Lys-D-Glu]	A4b [(L-Ala)-D-Glu-L-Orn-D-Asp]	ND
% saturated CFA	31	3	3	18
Type strain	VPI 1003 = ATCC 25986 = CCUG 28087 = DSM 3979 = JCM10188 = NCTC 11838	RCA56-68 = CCUG45296 = CIP 106914 JCM 10643 = DSM 13280	RCA55-54 = CCUG45295 = CIP 106913 = DSM 13279 = JCM 10641	YIT 12063 = DSM 22478 = JCM 16071

CFA cellular fatty acids

60–64 mol%. All strains were isolated from human feces. Discriminative features of the *Collinsella* spp. are shown in Table 11.7.

Coriobacterium Haas and König (1988)

Co.ri.o.bac.te'ri.um. Gr. fem. n. *koris* bug; Gr. neut. n. *bakterion* a small rod; M.L. neut. n. *Coriobacterium* rodlet associated with bugs.

The genus is represented only by the type species *Coriobacterium glomerans* (glo'me.rans. L. part. adj. *glomerans* agglomerating; the cells form flocculent, wooly sediments with a clear supernatant in fluid media). Cells grow as long chains (>150 µm) of pear-shaped to irregularly shaped rods (0.44–1.80 µm long). Spherical involution forms are common. The filamentous cell chains are attached to the epithelia in the intestine of bugs. The organisms grow on Columbia blood agar, supplemented Schaedler agar (BBL), and TPY agar at 25 and 30 °C. When grown in TPY medium, the fermentation products of glucose (–7.8 µmol/mL) are acetic acid (7.5 µmol/mL), L-lactic acid (6.5 µmol/mL), ethanol (6.1 µmol/mL), CO₂, and H₂. D-Lactic acid, formic acid, volatile short-chain

alcohols, or other volatile fatty acids are not formed. The cells ferment glucose, L-arabinose, D-xylose, D-ribose, mannose, sucrose, maltose, cellobiose, mannitol, and salicin. Lactose, melibiose, raffinose, inulin, starch, and inositol are not fermented. The cells have an electron-dense Gram-positive 40-nm-wide cell wall. The peptidoglycan belongs to the Lys-Asp type. The G+C content of the DNA is 60–61 mol%. The type strain is PW2^T (= DSM 20642^T = ATCC 49209^T = JCM 10262^T). The species was originally reported to occur in the third bulbous midgut portion of all stages of the red soldier bug (*Pyrrhocoris apterus*), except the eggs. However, recent in situ hybridization experiments and sterilization of eggs revealed that vertical transmission of *Coriobacterium glomerans* occurs via the egg surface (Kaltenpoth et al. 2009).

Cryptobacterium Nakazawa et al. (1999)

Crypt.o.bac.te'ri.um. Gr. n. *kryptos* hidden; Gr. n. *bakterion* a small rod; M.L. neut. n. *Cryptobacterium* a hidden rod-shaped bacterium.

The genus is represented only by the type species *Cryptobacterium curtum* (cur'tum. L. neut. adj. *curtum*

shortened, a shortened cell of this organism). Cells are asaccharolytic short rods. On BHI-blood agar, minute, circular, convex, and translucent colonies less than 1 mm in diameter are formed, even after prolonged incubation. Growth in broth media is poor with or without carbohydrates. Starch is not hydrolyzed and no liquefaction of gelatin occurs. Ammonia is produced from arginine (Uematsu et al. 2006). Adonitol, amygdalin, arabinose, cellobiose, erythritol, fructose, galactose, glucose, glycogen, inositol, lactose, maltose, mannitol, mannose, melezitose, melibiose, rhamnose, ribose, salicin, sorbitol, starch, sucrose, trehalose, and xylose are not utilized. No metabolic end product is detected in peptone-yeast extract medium supplemented with glucose. Maruo et al. (2008) reported that growth is stimulated by arginine but not Tween 80, yet this statement is not found in the original description by Nakazawa et al., and no amended description has been proposed. The G+C content of DNA is 50–51 mol%. The type strain is 12-3^T (= ATCC 700863^T = DSM 15641^T).

Denitrobacterium Anderson et al. (2000)

De.nit.ro.bac.te'ri.um. L. pref. *de* from; L. n. *nitro* nitro-compound; Gr. neut. dim.n. *bakterion* a small rod; M.L. neut. n. *Denitrobacterium* nitro-compound-reducing rod.

The genus is represented only by the type species *Denitrobacterium detoxificans* (de.tox.if'i.cans. L. pref. *de* from; L. n. *toxicum* poison; L. neut. n. *detoxificans* poison reducer). Cells are chemoorganotrophic and rod-shaped (0.5–1.0 × 1.0–1.5 μm); bulbous ends may be present. The species grows equally well at 32, 37, and 39 °C. Growth occurs in media containing clarified rumen fluid, peptone, and a suitable electron acceptor, including nitrate, 3-nitropropanol, 2-nitropropanol, 3-nitropropionate, nitroethanol, nitroethane, 1-nitropropane, 2-nitrobutane, DMSO, trimethylamine oxide, hydrogen, formate, or (DL)-lactate. H₂S is not produced, and gelatin is not hydrolyzed. Little if any acid is produced during growth in medium with hydrogen or formate as electron donor. Acetate is the major product after growth on lactate; D-lactate is used more readily than L-lactate. The G+C content of DNA ranges from 56 to 60 mol% (thermal denaturation method). A *c*-type cytochrome was found in the type strain NPOH1^T (= ATCC 700546^T = CCUG 56741^T), isolated from a population of ruminal microbes enriched for enhanced metabolism of 3-nitropropanol, the toxic aglycone of miserotoxin (3-nitro-1-propyl-β-D-glucopyranoside) (Anderson et al. 1996). Strain NPOH1^T differs from other strains of the species (NPOH2 = ATCC 700547; NPOH3 = ATCC 700548; and MAJ1 = ATCC 700549) in that it has the ability to reduce nitrate.

Eggerthella Wade et al. (1999), Emend. Maruo et al. (2008), Emend. Würdemann et al. (2009)

Eg.ger.thel'la. L. dim. ending *-ella*; M.L. fem. n. *Eggerthella* named after Arnold H. Eggerth, an American microbiologist

who was the first person to report the isolation of [*Eubacterium lentum*] from human feces in 1935 (Eggerth 1935).

The genus *Eggerthella* comprises two species: *Eggerthella sinensis* (M.L. gen. n. *sinae* of China; N.L. fem. adj. *sinensis* pertaining to China, the country where the bacterium was discovered) (Lau et al. 2004b) and the type species *Eggerthella lenta* (len'ta. L. fem. adj. *lenta* slow). *Eggerthella lenta* was originally referred to as *Eubacterium lentum* (Moore et al. 1971; Holdeman et al. 1977). Other synonyms of this species include [*Bacteroides lentus*] and [*Pseudobacterium lentum*]. The proposal to create the name *Eggerthella lenta* was first published in 1999 by Wade et al. on the basis of 16S rRNA gene-based phylogenetic evidence, which showed that [*Eubacterium lentum*], [*Eubacterium exiguum*], and [*Peptostreptococcus heliotrinireducens*] formed a coherent cluster closely related to *Atopobium* spp. and *Coriobacterium glomerans* but only distantly related to *Eubacterium limosum*, the type species of the genus *Eubacterium* (Wade et al. 1999). Kageyama et al. also published a similar study in 1999 and proposed to create the name *Eggerthella* gen. nov. to accommodate [*Eubacterium lentum*] (Kageyama et al. 1999c). However, the work by Wade et al. has priority. Kageyama et al. reported as well that the cell wall of *Eggerthella lenta* contains type A3 peptidoglycan, yet this information cannot be found in the original work by Schleifer and Kandler to which Kageyama et al. referred (Schleifer and Kandler 1972). In their amended description of the genus *Eggerthella*, Maruo et al. stated that the cell wall contains A4g-type peptidoglycan with an (L-Ala)-D-Glu-m-Dpm-D-Glu peptide subunit and an inter-peptide bridge that consists only of D-Glu (Maruo et al. 2008). In 2009, Saunders et al. published the genome sequence of the type strain of *Eggerthella lenta* and stated that its cell wall contains A1g-type peptidoglycan (Saunders et al. 2009). The latest description with standing in nomenclature is the one by Maruo et al. 2008. The major respiratory quinones are MK-6 (dominant in *Eggerthella lenta*) and MMK-6 (dominant in *Eggerthella sinensis*). DMMK-6 is also detected in *Eggerthella sinensis*. Polar lipids consist of two phospholipids, phosphatidylglycerol and diphosphatidylglycerol, and four glycolipids. The main cellular fatty acid is C_{16:0} DMA. The proportion of saturated cellular fatty acids is 61–76%. Growth is stimulated by arginine (Sperry and Wilkins 1976a). Cells are usually arranged in chains. They are catalase- and arginine dihydrolase-positive. Colonies on blood agar are as follows: 0.25–1.0 mm, circular, entire, slightly raised, smooth, grey, and translucent to semiopaque (*Eggerthella lenta*) and greyish white, 0.5 mm in diameter after 48 h at 37 °C (*Eggerthella sinensis*). *Eggerthella lenta* reduces nitrate and has been found to produce ammonia from arginine and to contain cytochromes *a*, *b*, and *c* and a carbon monoxide-binding pigment (Sperry and Wilkins 1976b). The G+C content of DNA is 61–64 mol% (*Eggerthella lenta*) and 65–66 mol% (*Eggerthella sinensis*). The type strain of *Eggerthella lenta* is DSM 2243^T (= ATCC 25559^T = CCUG 17323A^T = CIP 106637^T = JCM 9979^T = NCAIM B.01418^T = NCTC 11813^T). The type strain of *Eggerthella sinensis* is HKU14^T (= DSM 16107^T = JCM 14551^T = LMG 22123^T). Discriminative features of *Eggerthella* spp. are shown in ► Table 11.8.

■ Table 11.8

Phenotypic features of *Eggerthella* spp.

Characteristic	<i>Eggerthella lenta</i> ^T	<i>Eggerthella sinensis</i>
Nitrate reduction	+	–
Major respiratory quinone	MK-6 (64 %)	MMK-6 (60 %)
Bile resistance	+	ND
Lysine arylamidase	ND	+

Abbreviations: MK menaquinone, MMK methylmenaquinone

■ Table 11.9

Phenotypic features of *Enterorhabdus* spp

Characteristic	<i>Enterorhabdus caecimuris</i>	<i>Enterorhabdus mucosicola</i> ^T
Diamino pimelic acid	meso	LL
Respiratory quinone	MMK-6 (60 %); DMMK-6 (40 %)	MMK-6 (100 %)
Glucose in whole-cell sugars	+	–
Polar lipids	DPG, PG, 2 GL, 1PL, 1 L	DPG, PG, 4 GL, 3 PL
Aminopeptidases	–	+
Glutamic acid decarboxylase	+	–
Equol production	–	+

Abbreviations: DPG diphosphatidylglycerol, GL glycolipids, L unidentified lipid, MMK methylmenaquinone, PG phosphatidylglycerol, PL phospholipids

Enterorhabdus Clavel et al. (2009), Emend. Clavel et al. (2010)

En.te.ro.rhab'dus. Gr. n. *enteron* intestine; Gr. fem. n. *rhabdos* a rod; N.L. fem. n. *Enterorhabdus* a rod isolated from the intestine.

The genus *Enterorhabdus* comprises two species: *Enterorhabdus caecimuris* (ca.e.ci.mu'ris. L. n. *caecum* caecum; L. n. *mus muris* mouse; N.L. gen. n. *caecimuris* of the caecum of a mouse) and the type species *Enterorhabdus mucosicola* (mu.co.si'co.la. N.L. n. *mucosa* mucosa from L. adj. *mucosus* -a -um mucous; L. suff. -cola (from L. n. *incola*) inhabitant, dweller; N.L. n. *mucosicola* inhabitant of the intestinal mucosa). These species are mesophilic, aerotolerant anaerobes that grow as single short rods (0.5 × 2.0 μm) that do not produce glycosidases. Cultures in the stationary phase of growth in anoxic Wilkins-Chalgren-Anaerobe broth are characterized by stable pH (6.9–7.1) and a typically low turbidity (<0.5 McFarland standard). They grow well in the temperature range 30–40 °C. No growth occurs in the presence of 0.5 % (w/v) bile salts. *Enterorhabdus caecimuris* grows in the presence of 2 % (w/v) NaCl. Both species form pinpoint colonies on blood agar.

The major cellular fatty acids are C_{14:0}, C_{16:0}, and C_{16:0} DMA. Whole-cell sugars include galactose and ribose. The most dominant respiratory quinone is MMK-6. The G+C content is 64.2–64.5 mol%. The major polar lipids are diphosphatidylglycerol and two glycolipids. The type strain of *Enterorhabdus mucosicola* is Mt1B8^T (= DSM 19490^T = CCUG54980^T). The type strain of *Enterorhabdus caecimuris* is B7^T (= DSM 21839^T, =CCUG 56815^T). Discriminative features of *Enterorhabdus* spp. are shown in ● Table 11.9.

Gordonibacter Würdemann et al. (2009)

Gor.do'ni.bac'ter. N.L. masc. n. *Gordon* named after Jeffrey I. Gordon, MD, the Dr Robert J. Glaser Distinguished University Professor and Director of the Center for Genome Sciences at Washington University School of Medicine, St. Louis, MO, USA; N.L. masc. n. *bacter* a rod; N.L. masc.n. *Gordonibacter* a rod named after Jeffrey I. Gordon.

The genus is represented only by the type species *Gordonibacter pamelaeeae* (pa.me'la.eae. N.L. fem. n. *pamelaeeae* named after Dr Pamela Lee Oxley (née Fredericks), biochemist, environmentalist, teacher, mentor, and mother). Cells are catalase-positive coccobacilli (0.5–0.6 × 0.8–1.2 μm) with a conical cell apex. They are motile and characterized by the presence of a subpolarly inserted flagella when grown in BHI medium. Of note, one clinical isolate identified as *Gordonibacter pamelaeeae* on the basis of 16S rRNA gene sequencing and phenotypic analysis was reported to be nonmotile (Woo et al. 2010). Growth is generally slow on BHI and Schaedler anaerobic media (Oxoid) supplemented with 5 % defibrinated horse blood, with pale-white, semitranslucent colonies forming after 48–72 h at 37 °C. Growth is enhanced by 1 % (w/v) arginine-HCl. Arabinose, glucose, mannose, raffinose, trehalose, xylose, L-methionine, L-phenylalanine, L-valine, L-valine plus L-aspartic acid, dextrin, and D-glucose 6-phosphate are not metabolized. Nitrate is not reduced. Only weak conversion of pyruvic acid and pyruvic acid methyl ester is observed. All other organic substrates included in the Biolog AN MicroPlate are not metabolized. Cellular fatty acids consist mainly (approximately 90 %) of saturated fatty acids (predominantly C₁₅ and C₁₆). The major respiratory lipoquinone present is MK-6; MMK-6 is a minor component. The major polar lipids are phosphatidylglycerol, diphosphatidylglycerol, and four glycolipids. The G+C content of DNA is 66 mol%. The type strain is 7-10-1-b^T (= DSM 19378^T = CCUG55131^T).

Olsenella Dewhirst et al. (2001)

Olsen.el'la. L. fem. dim. ending -ella, N.L. fem. n. *Olsenella* of Olsen, named to honor Ingar Olsen, a contemporary Norwegian microbiologist, who first described *Lactobacillus uli*.

The genus currently comprises three species: (a) *Olsenella profusa* (pro.fus'a. L. adj. *profusus* profuse, referring to the good growth of the organism), (b) *Olsenella umbonata* (um.bo.na'ta. N.L. fem. adj. *umbonata* bossed, umbonate (from L. masc. n.

Table 11.10
Phenotypic features of *Olsenella* spp.

Characteristic	<i>Olsenella profusa</i>	<i>Olsenella uli</i> ^T	<i>Olsenella umbonata</i>
Cell morphology	Single, pairs, or chains	Single, pairs, or chains	Short to very long serpentine chains
Acid produced from			
Mannitol	+	–	–
Lactose	+	v	–
Arabinose	+	–	–
Cellobiose	+	–	–
Raffinose	+	–	–
Alkaline phosphatase	+	–	–
<i>b</i> -Galactosidase	+	–	–
<i>α</i> -Glucosidase	+	–	+
<i>b</i> -Glucosidase	+	+	–
<i>N</i> -Acetyl- <i>b</i> -glucosaminidase	+	–	–
6-phospho- <i>b</i> -galactosidase	+	–	–
Growth stimulation by Tween 80	slight	+	+
Esculin hydrolysis	+	v	–
% saturated CFA (main)	93–97 (ai-C _{14:0})	54–87 (C _{18:0})	85–100 (C _{14:0} ^o ; C _{18:0})
Type strain	D315A-29 = CCUG 45371 = CIP 106885 = DSM 13989 = JCM 14553	VPI D76D-27C = ATCC 49627 = CCUG 31166 = DSM 7084 = JCM 12494 = LMG 11480 = VPI D76D-27C	lac31 = CCUG 58604 = DSM 22620 = JCM 16156

Abbreviations: ai, anteiso, CFA cellular fatty acids

umbo, *umbonis* a shield boss), referring to the umbonate elevations of outgrown colonies on solid culture media) (Kraatz et al. 2011), and (c) the type species *Olsenella uli* (u'li. Gr. n. *oulon* the gum; N.L. gen. n. *uli* of the gum). Cells are microaerotolerantly (moderately obligately) anaerobic (less than 5 % O₂, v/v). They grow as small, elliptical rods that occur singly, in pairs, or short to very long serpentine chains. Convert a variety of sugars. Lactic acid is the major product from glucose. Minor products are formic and acetic acid. Able to grow on mucin from porcine stomach. All strains are negative for urease, *a*-galactosidase, *a*-arabinosidase, *b*-glucuronidase, *a*-mannosidase, *a*-fucosidase, raffinose fermentation, acidification of glycerol and melezitose, trypsin, *a*-chymotrypsin, reduction of nitrate, pyroglutamic acid arylamidase, glutamic acid decarboxylase, and glutamyl glutamic acid arylamidase. All strains are positive for mannose fermentation, acidification of glucose, and gelatin hydrolysis. Growth is stimulated by Tween 80 but not arginine. The cellular fatty acids consist mainly of saturated fatty acids. The G+C content of DNA is 63–64 mol%. Original values reported for [*Lactobacillus*] *uli* were C_{18:1} cis9 (major cellular fatty acid)

and 53 mol% (G+C content of DNA) (Olsen et al. 1991). Göker et al. recently reported that *Olsenella uli* is characterized by the presence of a A4b-type peptidoglycan based on L-Orn-D-Asp (Goker et al. 2010). *Olsenella profusa* was previously designated *Eubacterium* group D52 (Holdeman et al. 1977). The description of *Olsenella umbonata* refers to the analysis of four strains (A2, lac 15, lac 16, and lac31^T). All lac strains were isolated from pig jejunal mucosa (Kraatz and Taras 2008), whereas strain A2 was isolated from sheep rumen as part of a study focusing on ammonia-producing bacteria (Eschenlauer et al. 2002). *Olsenella umbonata* was found to produce ammonium from peptone under anaerobic and un-reduced microaerobic conditions (ca. 12 and 9 mmol/l, respectively). Growth of this species is positive in 20 % bile but absent in 6.5 % NaCl. Strain A2 (=CCUG 58212 = DSM 22619 = JCM 16157), which had been informally named [*Olsenella* (*Atopobium*) *oviles*] (Dewhirst et al. 2001; Eschenlauer et al. 2002), can be differentiated from the type strain lac31^T by a negative result for acidification of trehalose in the API 20 A strip. Discriminative features of *Olsenella* spp. are shown in Table 11.10.

***Paraeggerthella* Würdemann et al. (2009)**

Pa'ra.eg.ger.thel'la. L. prep. *para* beside; N.L. fem. n. *Eggerthella* a bacterial genus name; N.L. fem. n. *Paraeggerthella* beside *Eggerthella*, named in recognition of the close relationship to the genus *Eggerthella*.

The genus is represented only by the type species *Paraeggerthella hongkongensis* (N.L. fem. adj. *hongkongensis*, pertaining to Hong Kong, the city where the bacterium was discovered). This species had been previously described as [*Eggerthella*] *hongkongensis* (Lau et al. 2004b), for which an emended description was published by Maruo et al. (2008). The type strain is HKU10^T (= DSM 16106^T = CCUG 49250^T), isolated in 1998 from the blood of a 30-year-old male patient suffering from alcoholic cirrhosis, portal hypertension, and epilepsy and diagnosed with perianal abscess (Lau et al. 2004a). Additional strains (HKU11, HKU12, HKU13) were isolated from blood cultures of a patient with an infected rectal tumor, a liver abscess, and acute appendicitis, respectively. These additional strains were not further studied in amended descriptions. The rationale for reclassifying [*Eggerthella*] *hongkongensis* into the novel genus *Paraeggerthella* was based on several major differences observed between strain HKU10^T and *Eggerthella* species: (a) 16S rRNA gene similarity values <95 %, (b) a lower amount of saturated cellular fatty acids (45 vs. 61–63 %), (c) the presence of C_{18:1} w9c instead of C_{16:0} DMA as major cellular fatty acid, (d) different polar lipid profiles (three instead of four glycolipids), and (e) the ability of *Paraeggerthella hongkongensis* to metabolize 3-methyl-D-glucose, palatinose, L-rhamnose, L-methionine, L-valine, L-valine plus L-aspartic acid, and uridine 5'-monophosphate. Physiological testing using Rapid ID32A and API 20A revealed just one positive reaction, for arginine dihydrolase. Lau et al. reported a positive reaction for *b*-glucosidase, which was not confirmed by Würdemann and colleagues. Results obtained with Biolog AN MicroPlates indicated that urocanic acid and L-threonine are metabolized. Weak conversion of rhamnose is observed. The other organic substrates included in the Biolog AN MicroPlate are not metabolized. No significant conversion of the flavonoids quercetin, rutin, genistein, and phloretin is observed. Cells are catalase-positive coccobacilli arranged in chains. They grow on blood agar as greyish white colonies of 0.5 mm in diameter after 48 h at 37 °C. The cell wall contains the A4g-type peptidoglycan. According to Würdemann et al., the major respiratory lipoquinone is MK-6 (68 %); MMK-6 is a minor component (32 %). Maruo et al. found that the principal respiratory quinone is MMK-6 and that minor menaquinones are MK-6 and DMMK-6. This discrepancy is likely due to growth conditions and technical issues, e.g., the fact that DMMK-6 can be difficult to detect using HPLC. Polar lipids consist of phosphatidylglycerol, diphosphatidylglycerol, and three glycolipids (GL1, GL2, and GL4). The G+C content of DNA of strain HKU10^T is 61–62 mol%.

***Parvibacter* Clavel et al. (2013)**

Par.vi.bac'ter. L. adj. *parvus* small; N.L. masc. n. *bacter* rod; N.L. masc. n. *Parvibacter* small rod.

The genus is represented only by the type species *Parvibacter caecicola* (ca.e.ci'co.la. N.L. n. *caecum* blind pouch, caecum; L. suff. *-cola* (from L. n. *incola*), dweller, inhabitant; N.L. n. *caecicola* caecum dweller). Cells are aerotolerant small rods (0.5 × 1.5 µm) that grow only under strictly anoxic conditions in the temperature range from 25 to 37 °C. After 48 h at 37 °C on Wilkins-Chalgren-Anaerobe agar under anoxic conditions, colonies are circular, entire, pinpoint, and grey. Positive for proline, phenylalanine, leucine, tyrosine, alanine, glycine, and serine arylamidase. Negative for urease activity, arginine dihydrolase, *a*- and *b*-galactosidase, *a*- and *b*-glucosidase, *a*-arabinosidase, *b*-glucuronidase, *b*-N-acetylglucosamine, mannose and raffinose fermentation, glutamic acid decarboxylase, *a*-fucosidase, nitrate reduction, indole production, and alkaline phosphatase as well as arginine, leucyl glycine, pyroglutamic acid, histidine, and glutamyl glutamic acid arylamidase. The major cellular fatty acids are C_{16:0} (26 %) and i-C_{15:0} (11 %). Galactose, glucose, and ribose are detected as whole-cell sugars. The principal respiratory quinone is MMK-6. The diamino acid in the peptidoglycan is *meso*-diaminopimelic acid. The major polar lipids are diphosphatidylglycerol, phosphatidylglycerol, three phospholipids, four glycolipids, and one unidentified lipid. The G+C content of DNA is 62.5 %. The type strain is NR06^T (= DSM 22242^T = CCUG 57646^T).

***Slackia* Wade et al. (1999), Emend. Nagai (2010)**

Slack'ia. M.L. fem. n. named to honor Geoffrey Slack, distinguished British microbiologist and dental researcher.

The rationale for creating the genus name *Slackia* was to accommodate [*Eubacterium exiguum*] (Poco et al. 1996) and [*Peptococcus heliotrinireducans*] (Lanigan 1976) on the basis of 16S rRNA phylogenetic evidence showing that these two species formed a distinct cluster within the *Coriobacteriaceae*. The genus *Slackia* currently comprises six species: (a) *Slackia equolifaciens* (e.quo.li.fa'ci.ens. N.L. n. *equol-olis* equol; L. part. adj. *faciens* making; N.L. part. adj. *equolifaciens* equol-producing) (Jin et al. 2010), (b) *Slackia faecicanis* (fae.ci.ca'nis. L. n. *faex*, *faecis* feces; L. gen. n. *canis* dog; N.L. gen. n. *faecicanis* from dog feces) (Lawson et al. 2005), (c) *Slackia heliotrinireducens* (he.li.o.trin.i.re.duc.ens. M.L. n. *heliotrinum* derived from heliotrine, a pyrrolizidine alkaloid; L. adj. *reducans* reducing M.L. adj. *heliotrinireducens* referring to the ability to bring about oxidative cleavage of the heliotrine molecule), (d) *Slackia isoflavoniconvertens* (i.so fla.vo.ni.con.ver'tens. N.L. neut. n. *isoflavonum* isoflavone; L. part. adj. *convertens* converting; *isoflavoniconvertens* isoflavone-converting) (Matthies et al. 2009), (e) *Slackia piriformis* (pi.ri.for'mis. L. n. *pirum* pear; L. adj.

Table 11.11

Phenotypic features of *Slackia* spp.

Characteristic	<i>Slackia equolifaciens</i>	<i>Slackia exigua</i> ^T	<i>Slackia faecicanis</i>	<i>Slackia heliotrinireducens</i>	<i>Slackia isoflavoniconvertens</i>	<i>Slackia piriformis</i>
Nitrate reduction	–	–	v	+	–	–
Bile resistance	ND	–	w ^a	–	ND	w ^a
% saturated CFA (main)	42 (C _{14:0})	22–35 (C _{14:0} ; C _{16:0} DMA)	18–30 (C _{14:0} ; C _{18:0} DMA)	16 (i-C _{14:0})	ND	26 (C _{18:0} DMA)
G+C content of DNA (mol%)	61	60–64	61	61	58.5	58
Colony morphology (agar medium)	1–2 mm, translucent grey (GAM ^b + 0.5 % arginine-HCl)	<1 mm, circular, convex, translucent (BHI-blood)	1–2 mm, translucent to grey, uneven surface, irregular edges (anaerobic blood)	1–2 mm, effuse, entire edge, colorless, transparent (tryptone-yeast-mineral salts)	1 mm, smooth, translucent (Columbia blood)	0.1–1.0 mm, translucent to beige, circular, uneven surface, irregular edges (GAM ^b)
Type strain	DZE (=CCUG 58231 = JCM 16059)	S-7 = ATCC 700122 = CIP 105133 = JCM 11022 = CCUG 44588	5WC12 = CCUG 48399 = CIP 108281 = JCM 14555 = DSM 17537	RHS1 = ATCC 29202 = CCUG 47954 = DSM 20476 = JCM 14554 = NCTC 11029	HE8 = CCUG57679 = DSM 22006 = JCM 16137	YIT 12062 = DSM 22477 = JCM 16070

Abbreviations: BHI brain-heart infusion, DMA dimethyl acetal, i iso, ND not determined, w weak

^aw weak, cells grew on medium containing 2 % oxgall, but the number of colonies was decreased compared with control medium without oxgall (5 % and 50 % cfu for *Slackia faecicanis* and *Slackia piriformis*, respectively)

^bGeneral anaerobic medium, Nissui Pharmaceutical, Tokyo, Japan

suffix-*formis*-like, in the shape of; N.L. fem. adj. *piriformis* pear-shaped, referring to the cell shape) (Nagai et al. 2010), and (f) the type species *Slackia exigua* (ex.i.gu'a. L. adj. *exigua* scanty, small, referring to the scanty or poor growth of this organism). Cells are cocci, coccobacilli, or short bacilli, the growth of which is stimulated by 0.5 % arginine. Sugars are not fermented. Positive for naphthol-AS-BI-phosphohydrolase but negative for alkaline phosphatase, *a*-arabinosidase, *N*-acetyl-*b*-glucosaminidase, chymotrypsin, *a*-fucosidase, *a*-galactosidase, *b*-galactosidase, *a*-glucosidase, *b*-glucosidase, *b*-glucuronidase, glutamic acid decarboxylase, glutamyl glutamic acid arylamidase, lipase (C14), *a*-mannosidase, 6-phospho-*b*-galactosidase, pyroglutamic acid arylamidase, trypsin, urease, and esculin hydrolysis. The main cellular fatty acids are C_{18:1}w9c and C_{18:1}w9c DMA. Respiratory quinones have not been detected in *Slackia piriformis*, *Slackia exigua*, *Slackia heliotrinireducens*, and *Slackia faecicanis* (*Slackia equolifaciens* and *Slackia isoflavoniconvertens* have not been analyzed). *Slackia heliotrinireducens* was isolated for its ability to reductively cleave hepatotoxic pyrrolizidines found in forages. It also contains a *c*-type cytochrome. This species was originally published as *Peptococcus heliotrinireducans* (Lanigan 1976), before its transfer to the

genus *Peptostreptococcus* as *Peptostreptococcus heliotrinireducens* in 1986 on the basis of its high G+C content of DNA and the presence of various aminopeptidases (Ezaki and Yabuuchi 1986). Discriminative features of *Slackia* spp. are shown in Table 11.11.

Isolation, Enrichment, and Maintenance Procedures

It is striking that all members of the *Coriobacteriaceae* have been so far isolated only from body habitats of mammals and insects, which hints at evolutionary driving forces that made these bacteria best suited for efficient colonization and survival in such environments. The first cultivable representatives of the family, i.e., *Collinsella aerofaciens* and *Eggerthella lenta*, were recovered from human feces (Eggerth 1935). All strains of so far described species have been isolated by chance using either nonselective rich media or selective media and isolation procedures targeting specific metabolic functions or bacterial populations, e.g., conversion of isoflavones (*Asaccharobacter celatus*, *Slackia equolifaciens*, *Slackia isoflavoniconvertens*), mucosa-associated bacteria

(*Gordonibacter pamelaee*, *Enterorhabdus mucosicola*, *Olsenella umbonata*), reduction of nitro-compounds (*Denitrobacterium detoxificans*), or ammonia production (*Olsenella umbonata*, *Slackia heliotrinireducens*). For this reason, and due as well to the metabolic versatility of the 30 species of the family, there is to date no selective medium available for exhaustive enrichment of *Coriobacteriaceae*. The efficacy of blood, arginine, or Tween 80 to stimulate growth as well as the resistance towards bile and antibiotics has hitherto not been tested for all species. Moreover, while strictly anoxic culture techniques are suited for cultivation of most species, *Olsenella* spp. grow under microaerophilic conditions and *Atopobium vaginae* is a facultative anaerobe. The isolation and maintenance conditions reported for the 30 species of the family are summarized in [Table 11.12](#).

Ecology

The family *Coriobacteriaceae* includes a large majority of strictly anaerobic strains with fastidious growth requirements. They frequently coexist with a number of other microorganisms in complex ecosystems. As a result, the ecology of this family (as in the sense of the occurrence and functions of its members) was poorly studied until the emergence (and affordability) of culture-independent techniques such as polymerase chain reaction (PCR), sequencing of 16S rRNA genes as well as metabolomics and system biology approaches (Woo et al. 2008; Claus et al. 2011). It is now becoming clear that these previously understudied bacterial species carry out important physiological functions within their hosts.

Habitat and Occurrence

At the time of writing, the family accommodates 14 genera, 13 of which originate from the gastrointestinal tract of mammals (human, mouse, rat, dog, cow, and sheep). *Coriobacterium glomerans*, the type species of the family, has been so far retrieved only from the gut of insects (Haas and König 1988; Kaltenpoth et al. 2009). The diversity and composition of the human intestinal microbiota varies greatly between individuals (Qin et al. 2010). Nevertheless, *Coriobacteriaceae* can be considered as prevalent and dominant dwellers of the human intestine (and by extension of the mammalian intestine in general). Dominant means that certain species can be found at cell densities above 10^8 cells per gram intestinal content. Still, actinobacteria, and thus *Coriobacteriaceae*, represent usually a minor fraction of gut bacterial diversity (<2–5 % of total 16S rRNA gene sequences) when compared with members of the phyla Bacteroidetes and Firmicutes.

Culture-independent studies have demonstrated that the genus *Collinsella* is the most abundant human gut taxon of the family (Kageyama et al. 2000). The species *Collinsella aerofaciens* seems to be a member of the core human gut microbiome,

i.e., “a set of bacterial molecular species that are altogether dominant and prevalent within the fecal microbiota of healthy humans” (Tap et al. 2009; Qin et al. 2010). Based on the use of specific 16S rRNA-targeted oligonucleotide probes for fluorescence in situ hybridization, Harmsen et al. found that the *Collinsella* and *Atopobium* phylogenetic groups were part of the dominant microbiota in 26 of 33 adult subjects, with cell counts $>10^9$ cell/g dry feces (Harmsen et al. 2000). In another similar study, mean proportions of the *Atopobium* group were >3 % of dominant bacteria in 39 postmenopausal women (Clavel et al. 2005). Thus, *Atopobium* spp. also seem to be predominant in human feces. However, it is important to note that the specificity of 16S probes warrants detection of relatively broad phylogenetic groups rather than specific species (e.g., the *Atopobium* probe S-⁺-Ato-0291-a-A-17 targets also other *Coriobacteriaceae*). In one study based on the use of quantitative PCR, *Slackia* spp. were detected in 16 of 40 fecal samples from healthy Japanese adults at a mean population density of $\log_{10} 6.4 \pm 2.4$ cell/g wet weight (Tsuji et al. 2010). PCR-based assays have been used as well to assess the occurrence of *Eggerthella lenta* in human feces, revealing that this species is detected in 30–40 % of tested samples (Schwartz et al. 2000; Kageyama and Benno 2001). In fact, part of the aforementioned molecular data confirmed the pioneering culture-based work by W. E. C. Moore, S. M. Finegold, and L. V. Holdeman, who readily isolated a number of strains of [*Eubacterium*] *aerofaciens* and [*Eubacterium*] *lentum* from feces of healthy human adults. These isolates were usually recovered from 50 % of analyzed subjects at mean densities of $>10^9$ cfu/g dry weight (Moore and Holdeman 1974; Finegold et al. 1983). Some *Coriobacteriaceae* have also been detected in sewage samples using massively parallel pyrosequencing of hypervariable regions in microbial rRNA genes (McLellan et al. 2010). The genus *Collinsella* was detected at 0.27 % and 1.07 % total sequences in sewage and human fecal samples, respectively, but not in surface water. The presence of fecal microbial taxa in sewage water appears to be the consequence of human fecal pollution of the wastewater treatment plants rather than such environmental samples being the natural habitat of *Coriobacteriaceae*.

Regarding more recently described taxa within the family, *Enterorhabdus* spp. have been repeatedly found in high-throughput 16S rRNA gene sequence datasets from the mouse, human, and bovine intestinal tract (Benson et al. 2010; Werner et al. 2011; Hristov et al. 2012; Martinez et al. 2012). This speaks in favor of a widespread occurrence in various gut ecosystems, yet most likely at lower population densities. With respect to specific niches occupied by *Coriobacteriaceae* in the gut, it is worth noting that some members may be well suited for colonization of mucosal surfaces, as suggested by (a) the isolation of strains from mucosal samples or using selective culture media containing mucin (*Enterorhabdus mucosicola*, *Gordonibacter pamelaee*, *Olsenella umbonata*), (b) the symbiotic relationship they may have with their hosts (*Coriobacterium glomerans*), and (c) their detection in mucosal samples using molecular-based techniques (*Atopobium* and *Collinsella* spp.) (Collado and Sanz 2007a, b; Nadal et al. 2007; Lyra et al. 2012).

Table 11.12

Origin, isolation, and growth conditions of type strains of *Coriobacteriaceae*

	<i>Adlercreutzia equolifaciens</i>	<i>Asaccharobacter celatus</i>	<i>Atopobium fossor</i>	<i>Atopobium minutum</i>	<i>Atopobium parvulum</i>
Publication	2008	2008	1986	1937 ^a	1937 ^a
Sample type	Feces of a 25-year-old healthy woman	Caecal content (frozen glycerol stock) of a male Sprague–Dawley rat ^b	Pharyngeal tonsillar surface of normal horses	Human oral cavity	Human oral cavity
Agar medium	BL ^c + 5 % horse blood	GAM ^c + 2 g Fujiflavone P10 ^d	Sheep blood (5 %) + vitamin K-hemin + formate-fumarate ^e	Nonselective D4 ^f	Nonselective D4 ^f
Incubation	3 d, 37 °C	2 d, 37 °C	NR (d), 37 °C	5 d, NR (t°C)	5 d, NR (t°C)
Atmosphere	Anaerobic ^g	N ₂ /H ₂ /CO ₂ (85:5:10)	N ₂ /H ₂ /CO ₂ (80:10:10)	N ₂ /H ₂ /CO ₂ (85:3:12)	N ₂ /H ₂ /CO ₂ (85:3:12)
Additional maintenance media	GAM ^c + 0.5 % arginine, pH 7.0	GAM ^c	Tryptose agar ^h	/	/
References	Maruo et al. (2008)	Minamida et al. (2008)	Bailey and Love (1986)	Moore et al. (1982), Moore et al. (1983)	Moore et al. (1982), Moore et al. (1983)
	<i>Atopobium rimae</i>	<i>Atopobium vaginae</i>	<i>Collinsella aerofaciens</i>	<i>Collinsella intestinalis</i>	<i>Collinsella stercoris</i>
Publication	1991	1999	1935	2000	2000
Sample type	Human gingival crevice	Human vagina	Human feces	Human feces	Human feces
Medium	NR	NR	Beef-heart infusion agar ⁱ	EG agar ^j	EG agar ^j
Incubation	NR	NR	5–6 d, NR (t°C)	2 d, 37 °C	2 d, 37 °C
Atmosphere	NR	NR	Anaerobic ^g As for <i>Adlercreutzia</i>	100 % CO ₂	100 % CO ₂
Additional maintenance media	Reduced and unreduced PYG (DSMZ medium 104)	Columbia CNA (Difco) + 5 % horse blood; 37 °C; 5 % CO ₂ in air	Liver infusion agar	/	/
References	Olsen et al. (1991)	Rodriguez Jovita et al. (1999)	Eggerth (1935)	Kageyama and Benno (2000)	Kageyama and Benno (2000)
	<i>Collinsella tanakaei</i>	<i>Coriobacterium glomerans</i>	<i>Cryptobacterium curtum</i>	<i>Denitrobacterium detoxificans</i>	<i>Eggerthella lenta</i>
Publication	2010	1988	1999	1996	1935
Sample type	Human feces	Intestinal tract of a red soldier bug (<i>Pyrrhocoris apterus</i>)	Human periodontal pocket	Rumen content, cow #1 reared at NADC ^k and fed an alfalfa/corn (9:1) diet	Human feces
Medium	GAM ^c + 1 % (w/v) NaCl + fosfomycin (60 µg/mL)	Blood agar (BD)	NR	Enrichment in medium A ^l	Beef-heart infusion agar ⁱ
Incubation	3 d, 37 °C	10–20 d, 25–30 °C	NR	24 h of consecutive batch cultures; 39 °C	5–6 d, NR (t°C)

■ Table 11.12 (continued)

	<i>Collinsella tanakaei</i>	<i>Coriobacterium glomerans</i>	<i>Cryptobacterium curtum</i>	<i>Denitrobacterium detoxificans</i>	<i>Eggerthella lenta</i>
Atmosphere	N ₂ /H ₂ /CO ₂ (88:7:5)	N ₂ /CO ₂ (80:20)	NR	H ₂ /CO ₂ (50:50)	Anaerobic (Eggerth 1935)
Additional maintenance media	GAM ^c	TPY medium (11) + Na ₂ S + cysteine-HCl (each 0.45 g/l)	BHI-blood agar; 3 d, 37 °C; N ₂ /H ₂ /CO ₂ (80:10:10)	Medium B and C ^m	Liver infusion agar
References	Nagai et al. (2010)	Haas and König (1988)	Sato et al. (1998), Nakazawa et al. (1999)	Anderson et al. (1996), Anderson et al. (2000)	Eggerth (1935)
	<i>Eggerthella sinensis</i>	<i>Enterorhabdus caecimuris</i>	<i>Enterorhabdus mucosicola</i>	<i>Gordonibacter pamelaiae</i>	<i>Olsenella profusa</i>
Publication	2004	2010	2009	2009	2001
Sample type	Blood of a 59-year-old female patient with acute proctitis and a history of cervical carcinoma	Caecum of a C3H/HeJBir mouse	Ileal mucosa of a 12-week-old female heterozygous TNF ^{deltaARE} C57BL/6 mouse with ileitis	Sigmoid region of the colon of a 33-year-old male patient suffering from active Crohn's disease ⁿ	Human subgingival plaque in adults with periodontitis
Medium	BACTEC 9240 blood culture system (Becton Dickinson, Sparks, MD, USA)	ATCC medium 602E	Mucin-containing medium ^p	Schaedler basal agar (Oxoid) with 5 % defibrinated horse blood	NR
Incubation	NR	3 d, 37 °C	9 d, 37 °C	37 °C	NR
Atmosphere	Anaerobic ^g	N ₂ /H ₂ /CO ₂ (90:5:5)	AnaeroGen catalyzer (Oxoid)	N ₂ /H ₂ /CO ₂ (80:10:10)	NR
Additional maintenance media	Blood agar	BHI (BD 211059) + 2 g/l each yeast extract and glucose + 0.05 % (w/v) cysteine; 100 % N ₂	BHI (BD 211059) + 2 g/l each yeast extract and glucose + 0.05 % (w/v) cysteine; 100 % N ₂	Pre-reduced BHI + 1 % (w/v) arginine-HCl	Fastidious anaerobe agar (LabM) with 5 % horse blood
References	Lau et al. (2004a), Lau et al. (2004b)	Duck et al. (2007)	Clavel et al. (2009)	Würdemann et al. (2009)	Holdeman et al. (1977), Dewhirst et al. (2001)
	<i>Olsenella uli</i>	<i>Olsenella umbonata</i>	<i>Paraeggerthella hongkongensis</i>	<i>Parvibacter caecicola</i>	<i>Slackia equolifaciens</i>
Publication	1991	2011	2004	2013	2010
Sample type	Human gingival crevice	Jejunal mucosa of a healthy 62-day-old pig	Blood of a 30-year-old male patient ^p	Caecal content of a 25-week-old male heterozygous TNF ^{deltaARE} C57BL/6 mouse with ileitis	Human fecal enrichment in GAM broth + 0.1 mM daidzein
Medium	NR	LAB selective medium with porcine gastric mucin (type III; Sigma) ^q	BACTEC 9240 blood culture system (Becton Dickinson, Sparks, MD, USA)	WCA + 1 % (v/v) autoclaved rumen fluid, 0.05 % (w/v) cysteine and 0.02 % DTT	GAM ^c agar
Incubation	NR	7–14 d, 37 °C	NR	6 d, 37 °C	3 d, 37 °C
Atmosphere	NR	Anaerocult A (Merck)	Anaerobic ^g	N ₂ /H ₂ /CO ₂ (85:5:10)	100 % CO ₂

Table 11.12 (continued)

	<i>Olsenella uli</i>	<i>Olsenella umbonata</i>	<i>Paraeggerthella hongkongensis</i>	<i>Parvibacter caecicola</i>	<i>Slackia equolifaciens</i>
Additional maintenance media	Reduced and unreduced PYG (DSMZ medium 104)	Reduced and unreduced PYG (DSMZ medium 104)	Blood agar	WCA with cysteine and DTT; 100 % N ₂	GAM ^c + 0.5 % arginine-HCl
References	Olsen et al. (1991)	Eschenlauer et al. (2002), Kraatz and Taras (2008)	Lau et al. (2004a), Lau et al. (2004b)	Clavel et al. (2013)	Jin et al. (2010)
	<i>Slackia exigua</i>	<i>Slackia faecicanis</i>	<i>Slackia heliotrinireducens</i>	<i>Slackia isoflavoniconvertens</i>	<i>Slackia piriformis</i>
Publication	1996	2005	1976	2009	2010
Sample type	Human deciduous teeth with endodontic lesions	Feces of a healthy male Labrador dog	Sheep rumen	Feces of a healthy 37-year-old woman	Human feces
Medium	BHI-blood agar	<i>Bacteroides</i> agar ^f	Rich medium with rumen fluid and heliotrine (2 mg/mL)	BHI + 100 µM daidzein + 10 µg/mL tetracyclin	GAM + 6 % Bacto oxgall (Difco)
Incubation	7 d, 37 °C	2 d, 37 °C	7d, 38 °C	Enrichment by limiting dilution; cycles of 37 °C, 72 h	3 d, 37 °C
Atmosphere	N ₂ /H ₂ /CO ₂ (80:10:10)	N ₂ /H ₂ /CO ₂ (80:10:10)	CO ₂	CO ₂ /H ₂ (80:20)	N ₂ /H ₂ /CO ₂ (88:7:5)
Additional maintenance media	/	Chocolate or blood agar	/	BHI or Columbia agar	GAM
References	Sato et al. (1993), Poco et al. (1996)	Lawson et al. (2005)	Lanigan (1976)	Matthies et al. (2009)	Nagai et al. (2010)

Abbreviations: BHI brain-heart infusion, d days, GAM general anaerobic medium, NR not reported, PYG peptone-yeast-glucose

^aThe isolation procedure in the table refers to the work by Moore et al. 1982, 1983

^bSLC Japan, Tokyo; the rat was fed an AIN-93G casein diet for 3 weeks

^cNissui Pharmaceutical, Tokyo, Japan

^dFujicco, Kobe, Japan

^eSmibert and Holdeman (1976), Holdeman et al. (1977)

^fDetails on gas phase were not provided

^gPer L, 37 g brain-heart infusion, 5 g yeast extract, 5 mL 6 % (w/v) ammonium formate solution, 0.5 g cysteine-HCl, 5 mg hemin, 2.5 mg resazurin, 1 mg vitamin K₁, 4 % rabbit blood, pH 7.0

^hPer L, 5 g NaCl, 15 g agar, 20 g tryptose, 2.5 g tryptone, 1 g yeast extract, 1 g of glucose, pH 7.4–7.6

ⁱ1.5 % agar, 1 % Parke Davis peptone, 0.4 % Na₂HPO₄ · 12H₂O, 5 % blood, 0.15 % glucose, pH 7.6

^jPer L: 3 g beef extract, 5 g yeast extract, 10 g peptone, 1.5 g glucose, 0.5 g L-cysteine · HCl, 0.2 g L-cystine, 4 g Na₂HPO₄, 0.5 g soluble starch, 0.5 g Tween 80, 0.5 g silicone, 15 g agar, 5 % horse blood, pH 7.7

^kThe National Animal Disease Center in Ames (IA, USA)

^lContained Na₂CO₃, resazurin, L-cysteine-HCl, and vitamins at concentrations that were the same as in the complete medium of Bryant and Robinson (Bryant and Robinson 1961). Also contained (in 1 L) 800 mg phytone peptone, 5 µg lipoic acid, 2 µg vitamin B₁₂, 40 % (v/v) clarified rumen fluid, and the same minerals as in the non-rumen fluid medium of Dawson et al. (Dawson et al. 1980). Supplemented for enrichment with milk vetch or alfalfa forage + 4.2 mM nitropropanol

^mSame as medium A with 8 and 0 % rumen fluid, respectively

ⁿTreated with azathioprine, mutaflo and cortisone

^oPer L, 5 g mucin (Sigma M1778), 0.5 % (v/v) ethanol, 500 mg L-cysteine, 1 mg yeast extract, 20 mg folic acid, 20 mg vitamin B₁₂, 50 mmol NaHCO₃, 10 mmol sodium acetate, 5 mmol Na₂HPO₄, 5 mmol NaCl, 3 mmol KH₂PO₄, 1 mmol CaCl₂, 1 mmol MgCl₂, 10 mmol FeCl₃, 1 % (w/v) agar, pH 7.7

^pSuffered from alcoholic cirrhosis, portal hypertension, and epilepsy and diagnosed with perianal abscess

^qPer L, 10.0 g mucin, 0.01 g peptone, 0.01 g yeast extract, 0.01 g glucose, 0.3 g NaCl, 0.1 g CaCl₂, 6.0 g KH₂PO₄, 5 mL Rogosa's salt solution, 1 mL modified (lacking elements already included in Rogosa's salt solution) Pfennig's SL8 trace element solution, 0.2 mL vitamin solution, 0.5 mg resazurin, 4–7.5 g agar, pH 5 (Kraatz and Taras 2008)

^rHoldeman et al. (1977)

A number of species of the family have also been isolated from mammalian body habitats other than the gut. However, their prevalence in these other environments has not been investigated, apart from *Atopobium* spp. in the mouth and vagina (Zhou et al. 2004; Ravel et al. 2011; Belda-Ferre et al. 2012; Liu et al. 2012; Santiago et al. 2012). The other body origins of *Coriobacteriaceae* include:

- (a) The blood: *Atopobium rimae* (Angelakis et al. 2009), *Eggerthella sinensis* and *Paraeggerthella hongkongensis* (Lau et al. 2004b), and *Gordonibacter pamelaiae* (Woo et al. 2010).
- (b) The perineum region and vagina: *Atopobium minutum* (Hauduroy et al. 1937; Collins and Wallbanks 1992) and *Atopobium vaginae* (Rodriguez Jovita et al. 1999). The latter species is usually found in biofilms adherent to the vaginal mucosa rather than in the vaginal fluid (Verhelst et al. 2004; Swidsinski et al. 2005; Polatti 2012).
- (c) The oral cavity and respiratory tract: *Atopobium fossor* (Bailey and Love 1986; Kageyama et al. 1999b), *Atopobium parvulum* and *Atopobium rimae* (Weinberg et al. 1937; Olsen et al. 1991; Collins and Wallbanks 1992), *Cryptobacterium curtum* (Nakazawa et al. 1999), *Olsenella profusa* and *Olsenella uli* (Dewhirst et al. 2001), and *Slackia exigua* (Poco et al. 1996; Wade et al. 1999). Using 16S rRNA gene sequencing, Dewhirst et al. identified *Olsenella uli* and *Olsenella profusa* from subgingival plaques in patients with severe periodontal disease, suggesting that, similarly to other *Coriobacteriaceae* in the gut and vaginal mucosa, *Olsenella uli* and *Olsenella profusa* favor an adherent mode of growth. However, in sheep rumen, *Olsenella umbonata* was isolated from ruminal fluid, indicating variability in the mode of growth of this genus (Kraatz et al. 2011).

Metabolic Activities

Conversion of Cholesterol-Derived Host Metabolites

The potential of *Coriobacteriaceae* to modulate host metabolism in vivo has been recently brought to light by reports of significant correlations between their occurrence and altered metabolic parameters, including (a) higher intestinal cholesterol absorption and higher levels of plasma non-high-density lipoprotein (non-HDL) cholesterol in hamsters (Martinez et al. 2009, 2012) and (b) energy metabolism via decreased glycogenesis and enhanced triglycerides synthesis as well as hepatic detoxification pathways (higher 2*b*- and 6*b*-hydroxylase activity) in mice (Claus et al. 2011). Moreover, a recent metagenomic analysis of fecal samples from approximately 350 human subjects indicated that the prevalence of *Eggerthella lenta* is linked to type-2 diabetes (Qin et al. 2012). However, these data are descriptive and there is yet no direct proof of molecular mechanisms underlying

the impact of *Coriobacteriaceae* on host metabolism. In other words, research on bacteria/host interactions with respect to *Coriobacteriaceae* is in its infancy.

The best studied metabolic functions of *Coriobacteriaceae* are the dehydrogenation and dehydroxylation of cholesterol-derived host factors (Ridlon et al. 2006). The type and various strains of *Eggerthella lenta* and *Collinsella aerofaciens* possess hydroxysteroid dehydrogenases (HSDH), which are responsible for stereospecific oxidation and epimerization (change from *a* to *b* configuration or vice versa) of bile acids, thereby generating stable oxo-bile acid intermediates. Hitherto detected dehydrogenases include both 3*a*- and 12*a*-HSDH in *Eggerthella lenta* and 7*b*-HSDH in *Collinsella aerofaciens* (Eyssen and Verhulst 1984; Ridlon et al. 2006). This hints at metabolic chains between *Coriobacteriaceae* and other bacteria, since the combined activity of two position-specific, stereochemically distinct HSDH (e.g., 3*a* and 3*b*) is required for epimerization of bile salts (Ridlon et al. 2006).

Although early work reported that *Eubacterium* spp., especially strain VPI 12708, were also capable of dehydroxylating free primary bile acids (cholic and chenodeoxycholic acid) into secondary bile acids (deoxycholic and lithocholic acid) (White et al. 1988; Takamine and Imamura 1995), deeper taxonomic assignment revealed that these bacteria actually belong to the genus *Clostridium* (Kitahara et al. 2000). There is to date no report on bile acid dehydroxylase activity in *Eggerthella lenta* or other *Coriobacteriaceae*. One paper referred to 7*a*-dehydroxylation by one isolate related to [*Eubacterium lentum*] without standing in nomenclature (Hirano and Masuda 1982). Bacterial dehydroxylation renders bile acids more hydrophobic, thereby favoring passive reabsorption in the proximal colon (enterohepatic circulation). However, secondary bile salts may also contribute to the pathogenesis of cholesterol gallstones and colon cancer (Ridlon et al. 2006). Altered bile acid metabolism has also been associated with chronic intestinal inflammation (Gnewuch et al. 2009; Devkota et al. 2012; Duboc et al. 2012).

Transformation of bile salts by HSDH and dehydroxylases is believed to serve as an energy source for the bacteria and reduce the levels of bile acids with antimicrobial activities (Ridlon et al. 2006). Several *Coriobacteriaceae* are reported to be bile resistant, e.g., *Asaccharobacter celatus*, *Eggerthella lenta*, *Olsenella umbonata*, and *Slackia piriformis*. Additionally, the favorable generation of oxo-bile acids by *a*-HSDH at higher redox potentials such as those encountered at mucosal surfaces may be one additional reason for the colonization of these areas by some *Coriobacteriaceae* (Ridlon et al. 2006). Finally, *Eggerthella lenta* is also able to dehydroxylate corticoids such as deoxycorticosterone to form progesterone via 21-dehydroxylase activity (Bokkenheuser et al. 1977). This species also carries a corticoid-converting 16*a*-dehydroxylase (Bokkenheuser et al. 1980) and a 3*a*-HSDH (Bokkenheuser et al. 1979). Strikingly, despite the apparent implication for the host of this bacterial rearrangement of hormonal networks in the gut, related functional studies in experimental animal models have not yet been performed.

Polyphenol Metabolism

One of the most peculiar enzymatic properties of *Coriobacteriaceae* is the conversion of food polyphenols, especially the activation of the isoflavone daidzein to the bioactive metabolite equol (Clavel and Mapesa 2013). Isoflavones are dietary phytoestrogens that are abundant in soybean and soy-derived products. They share structural similarities with steroid hormones such as 17-*b*-estradiol and thus have low binding affinity to estrogen receptors (Kuijper et al. 1998; Kostelac et al. 2003). Equol is known to be the most potent isoflavone metabolite, e.g., it has stronger affinity to estrogen receptors than its substrate (Clavel and Mapesa 2013). The biological properties of equol have been given attention since the 1930s when reproductive failures started to affect sheep grazing on clover containing high amounts of isoflavones and later in the 1980s in captive cheetahs fed a soy-based diet (Setchell et al. 1987; Messina 2010). Since then, equol has been associated with protective effects against cardiovascular diseases, bone disorders, prostate and breast cancer, and other hormone-related conditions, even though gold-standard randomized control trials are urgently needed to substantiate results (Clavel and Mapesa 2013). In humans, only 30–50 % of individuals are able to produce equol from daidzein, possibly due to the absence of specific equol-producing bacteria in the rest of the population (Xu et al. 1995; Rowland et al. 2000).

Evidence of intestinal microbial equol production dates back from the early 1980s (Axelson and Setchell 1981). However, it was only in 2005 that the first equol-producing isolate, strain Julong 732, was cultured from human feces (Wang et al. 2005). To date, only ten bacterial strains capable of producing equol from daidzein have been isolated from intestinal samples of pigs, rodents, and humans. Nearly all of them ($n = 9$) fall into the family *Coriobacteriaceae* based on 16S rRNA gene sequence analysis. These strains include five type strains, which have been fully described and assigned valid names (human isolates are marked with stars in the following list): (1) *Adlercreutzia equolifaciens** FJC-B9^T (=DSM 19450^T) (GenBank accession AB306661) (Maruo et al. 2008), (2) *Asaccharobacter celatus* do03^T (=DSM 18785^T) (AB266102) (Minamida et al. 2006, 2008), (3) *Enterorhabdus mucosicola* Mt1B8^T (=DSM 19490^T) (AM747811) (Matthies et al. 2008; Clavel et al. 2009), (4) strain Julong 732* (AY310748) (Wang et al. 2005), (5) '*Eggerthella*' sp. YY7918* (AB379693) (Yokoyama and Suzuki 2008), (6) *Slackia equolifaciens** DZE^T (=CCUG 58231^T) (EU377663) (Jin et al. 2010), (7) *Slackia isoflavoniconvertens** HE8^T (=DSM 22006^T) (EU826403) (Matthies et al. 2009), (8) '*Slackia*' sp. NATTS* (AB505075) (Tsuji et al. 2010), and (9) strain D1 (DQ904563) (Yu et al. 2008). Of note, *Adlercreutzia equolifaciens*, *Asaccharobacter celatus*, and strain Julong 732 share >99 % similarity based on 16S rRNA-based phylogeny (Maruo et al. 2008). One additional equol-producing isolate, strain D2, seems not to belong to the *Coriobacteriaceae* based on 16S rRNA gene sequencing (DQ904564) (Yu et al. 2008). Interestingly, the production of equol from daidzein by '*Slackia*' sp. NATTS was found to be two to fourfold higher after addition of 1 g/L autoclaved

adonitol, arabinose, galactose, lactitol, inositol, melezitose, ribose, sorbitol, sorbose, trehalose, or xylose to the culture medium (Tsuji et al. 2010). Conversely, the addition of fructooligosaccharides, galactooligosaccharides, inulin, lactose, raffinose, or sucrose inhibited equol production. This may fit with the observation that resistant polysaccharides do not enhance equol production in vivo (Larkin et al. 2007; Mathey et al. 2007).

In addition to isoflavones, dietary lignans are phytoestrogens that can also be activated by *Coriobacteriaceae*. Conversion of plant lignans (pinoresinol, lariciresinol, secoisolariciresinol, matairesinol, and corresponding glycosides) by gut bacteria involves two to five different reactions (deglycosylation, reduction, demethylation, dehydroxylation, and dehydrogenation) to form the enterolignans enterodiol and enterolactone (Clavel et al. 2006). Enterolignans were actually thought to be new steroid hormones after their first detection in urine samples from female primates and human adults (Setchell et al. 1980; Stich et al. 1980). Their bacterial origin was highlighted shortly thereafter (Setchell et al. 1981; Borriello et al. 1985). Several strains of *Eggerthella lenta* were found to reduce and dehydroxylate plant lignans and intermediate metabolites thereof (Clavel 2006). Thus, beyond the metabolism of host-derived bile acids and steroid hormones, the species *Eggerthella lenta* is also involved in metabolic chains leading to the production of bioactive molecules from plant substrates in the gut. Recently, this species was also found to reductively cleave the heterocyclic C-ring of the flavanols epicatechin and catechin (Kutschera et al. 2011). Most importantly, the successful isolation and cultivation of phytoestrogen-converting strains open ways to assess the effects of bacterial metabolites on host health in detail using, for instance, gnotobiotic approaches (i.e., colonization of germfree animals with specific strains of interest) (Woting et al. 2010; Becker et al. 2011; Mabrok et al. 2012).

Pathogenicity, Clinical Relevance

As seen above, members of the *Coriobacteriaceae* carry out functions of importance for their hosts. However, several members of the genera *Atopobium*, *Eggerthella*, *Gordonibacter*, *Olsenella*, and *Paraeggerthella* have been also implicated in the development of various clinical pathologies including abscesses, intestinal diseases and tumors, periodontitis, vaginosis, and bacteremia. *Coriobacteriaceae* can thus be considered as pathobionts, i.e., potentially pathogenic commensal species of host body microbiota (Chow et al. 2011). However, one can say that nearly all published studies on *Coriobacteriaceae* refer to descriptive work, for instance, the enumeration of bacteria in diseased versus healthy tissues/subjects or the isolation of bacteria from clinical specimens. Hence, fundamental knowledge on how and when *Coriobacteriaceae* start to be detrimental to their hosts is lacking. The antimicrobial susceptibility profile of some family members has been well defined in various studies and is summarized in Table 11.13.

Table 11.13
Antimicrobial susceptibility profiles of *Coriobacteriaceae*

Antibiotic class	Antibiotic	<i>Atopobium parvulum</i>	<i>Atopobium rima</i>	<i>Atopobium vaginae</i>	<i>Collinsella aerofaciens</i>	<i>Eggerthella lenta</i>	<i>Eggerthella sinensis</i>	<i>Enterorhabdus caecimuris</i>	<i>Enterorhabdus mucosicola</i>	<i>Olsenella uli</i>	<i>Paraegethella hongkongensis</i>	<i>Parvibacter cecticola</i>	<i>Stackia exigua</i>
Penicillins	Amoxicillin				1	1							
	Ampicillin	0.125	0.023	<0.016–0.94	≤0.03–1	0.5–2							0.094–0.19
	Oxacillin							36	4.667			6	
	Penicillin		0.064	0.008–0.25	≤0.03–2	1–4	0.5			≤0.03–1	0.25–2		0.064–0.125
Tetracyclines	Piperacillin					1–16							
	Doxycycline			0.19–0.75									
	Minocycline	0.25											
	Tetracycline				0.06–8	6		0.12	0.115	0.125–32		0.069	
Macrolides	Tigecycline					0.12–25					0.06–0.25		
	Azithromycin		<0.016	<0.016–0.32	≤0.03–0.25								
	Clarithromycin	<0.004						<0.016	<0.016			<0.016	
	Erythromycin		<0.016		≤0.03–0.25	3		<0.016	0.048			<0.016	0.016–0.023
Aminoglycosides	Kanamycin			8–16									
	Tobramycin							4.333	2.667			0.6	
	Ciprofloxacin		0.06	0.023–0.25	≤0.5–2			0.305	>32	≤0.5–>8		0.061	
	Levofloxacin	0.25–0.5			≤0.06–2	0.5				0.25–8			
	Moxifloxacin			0.06–1		0.25–>32					0.25–4		
	Nalidixic acid			>256									
	Nemofloxacin			0.125–1		0.25–>32					0.5–2		
	Nifuratel			<0.015–2									
Polypeptides	Trovafoxacin												
	Bacitracin			1–4									
Lincosamides	Colistin			>1,024					>256			>256	
	Clindamycin	1		<0.016–2	≤0.03–0.25	<0.06–>32		0.105	<0.016	≤0.03–>32	>4	<0.016	0.016–0.023

Table 11.13 (continued)

Antibiotic class	Antibiotic	<i>Atopobium parvulum</i>	<i>Atopobium rima</i>	<i>Atopobium vaginae</i>	<i>Collinsella aerofaciens</i>	<i>Eggerthella lenta</i>	<i>Eggerthella sinensis</i>	<i>Enterorhabdus caecimuris</i>	<i>Enterorhabdus mucosicola</i>	<i>Olsenella uli</i>	<i>Parasggerthella hongkongensis</i>	<i>Parvibacter cecicola</i>	<i>Slackia exigua</i>
Rifamycin	Rifampicin			<0.002									
Streptogramins	Quinupristin/dalfopristin				0.06–8	0.25–2							
References		a, b	c	d, e, f, g, h, i	j, k	a, l, m, n, o, p, q	q	r	s	k	q, m	t	u

The shaded boxes show antimicrobial resistance according to the 2012 CLSI MIC breakpoints for anaerobes (M100-S22)

References (when more than one strain was analyzed, the number of strains is shown within brackets after the corresponding reference):

- ^aTanaka et al. (2006)
^bHirokawa et al. (2008)
^cAngelakis et al. (2009)
^dKnoester et al. (2011)
^eSalimnia et al. (2008)
^fPolatti (2012)
^gFerris et al. (2004) (3)
^hDe Backer et al. (2006) (9)
ⁱChan et al. (2012)
^jGoldstein et al. (2003) (9)
^kMerriam et al. (2006) (7)
^lLidert et al. (2010)
^mLee et al. (2012) (8)
ⁿMosca et al. (1998) (29)
^oSneath et al. (1986) (12)
^pCredito and Appelbaum (2004) (10)
^qLau et al. (2004b)
^rClavel et al. (2010)
^sClavel et al. (2009)
^tClavel et al. (2013)
^uKim et al. (2010) (6)

Bacteremia

Five of the 14 genera of the family include species which have been already isolated from blood samples of human patients: *Atopobium*, *Eggerthella*, *Gordonibacter*, *Olsenella*, and *Paraeggerthella*. There seems to be a consensus about the reservoir of infection as being the natural habitats of *Coriobacteriaceae*, i.e., the mouth and the gastrointestinal or genital tract, or acutely infected organs (Lau et al. 2004a; Salimnia et al. 2008; Angelakis et al. 2009; Woo et al. 2010; Thota et al. 2011).

The best documented cases of *Coriobacteriaceae*-driven bacteremia relate to *Eggerthella* spp. and closely related species. In Hong Kong, between 1998 and 2001, *Eggerthella lenta* was associated with five of 16 clinically relevant cases of bacteremia, whereas five additional cases were associated with the presence of its relatives *Eggerthella sinensis* and *Paraeggerthella hongkongensis* (Lau et al. 2004a, b). Lee et al. very recently published 10 additional cases of bacteremia due to *Eggerthella lenta* and *Paraeggerthella hongkongensis* in Taiwanese subjects hospitalized between 2001 and 2010 (Lee et al. 2012). Landais et al. also reported two cases of bacteremia in France that were associated with the presence of *Eggerthella lenta* based on 16S rRNA gene sequencing of isolates (the authors erroneously cited the genus name as 'Eggerthella') (Landais et al. 2007). In this study, patient 1 was admitted to the hospital with fecal peritonitis related to intestinal perforation, whereas patient 2 had acute appendicitis. They received imipenem (1.5 g/day for 3 weeks) and amoxicillin/clavulanic acid (3 g/day), respectively, with favorable outcomes. Two additional clinically relevant strains of *Eggerthella lenta* have been reported, including one strain identified on the basis of the VITEK system after isolation from the blood of a 21-year-old African-American woman diagnosed with Crohn's disease who developed bacteremia after ileocecal resection (Chan and Mercer 2008; Thota et al. 2011). This case of *Eggerthella lenta* bacteremia was successfully treated with a combination of meropenem, metronidazole, and vancomycin. Finally, one case of polymicrobial bloodstream infection with *Eggerthella lenta* and *Desulfovibrio desulfuricans* was reported in Sweden in one 86-year-old woman who was successfully treated with cefuroxime and amoxicillin (Liderot et al. 2010). Of note, a rather broad range of diseases may underlie translocation of *Eggerthella* spp. from the gut to the blood stream, since patients positive for these species in blood cultures were hospitalized for a variety of reasons (pelvic inflammatory disease, infected bed sore, perianal abscess, infected rectal tumor, liver abscess, acute appendicitis, and proctitis) and suffered from a variety of chronic diseases (lung, cervical and colon cancer, alcoholic cirrhosis, diabetes, cardiovascular disorders, recurrent pyogenic cholangitis) (Lau et al. 2004a; Landais et al. 2007). Finally, *Eggerthella lenta* was also isolated from (a) the pus of a hepatic abscess from a 42-year-old patient who was treated favorably with a course of metronidazole (1.5 g/day) (Landais et al. 2007) and (b) bone biopsy samples of the spine in one 82-year-old Chinese woman with spondylodiscitis who was treated with trimethoprim/sulfamethoxazole and metronidazole (Bok and Ng 2009).

The genus *Atopobium* also gained attention following the isolation of strains from clinical samples (Olsen et al. 1991; Kumar et al. 2005). *Atopobium rimae*, together with *Streptococcus gordonii*, was recently associated with a case of septic shock in a 77-year-old woman in France, from whom two isolates were recovered from blood cultures on two separate occasions during hospitalization for pneumonia (Angelakis et al. 2009). Treatment of the patient with intravenous amoxicillin-clavulanate (2 g/200 mg) led to full recovery within 7 days. Beforehand, *Atopobium rimae* had been already identified in blood samples from a 47-year-old man with liver cirrhosis, who was treated with success using metronidazole and imipenem (Chung et al. 2007). Another *Atopobium* species phylogenetically closely related to *Atopobium rimae* (98 % 16S rRNA gene sequence identity) has also been associated with bacteremia (Salimnia et al. 2008). This species, provisionally named "*Atopobium detroitii*", was isolated from the blood of a 38-year-old paraplegic male patient hospitalized for presumed sepsis and characterized by a necrotic decubitus ulcer of the hip and poor oral hygiene after physical examination. Finally, the species *Atopobium vaginae* has also been identified in the context of intrauterine infection leading to fetal death and maternal bacteremia in a 40-year-old woman undergoing transcervical chorionic villus sampling (Knoester et al. 2011). Unlike *Eggerthella lenta*, *Atopobium vaginae* has been associated with metronidazole resistance (Ferris et al. 2004; De Backer et al. 2006; Knoester et al. 2011), and successful treatment of *Atopobium vaginae* bacteremia usually involves a course of *b*-lactam antibiotics alone or in combination with *b*-lactamase inhibitors or clindamycin (Knoester et al. 2011; Chan et al. 2012).

Less frequently reported cases of *Coriobacteriaceae*-driven bacteremia relate to bacteria other than *Eggerthella* and *Atopobium*. One isolate identified as *Gordonibacter pamelaeeae* based on 16S rRNA gene sequencing and phenotypic description was recently recovered from the blood of an 82-year-old Chinese man diagnosed to have rectosigmoid carcinoma with lung metastasis (Woo et al. 2010). In contrast to the type strain of the species, this isolate was found to be nonmotile and positive for arginine arylamidase. The patient was successfully treated with a course of intravenous amoxicillin-clavulanate for 9 days. Finally, one case of bacteremia associated with a strain of *Olsenella uli* obtained from the blood of one 43-year-old male subject suffering from acute cholangitis has been reported (Lau et al. 2004a).

In summary, when compared with bacteremia due to usual suspects such as *Bacteroides fragilis*, enterobacteria, enterococci, or staphylococci, cases of *Coriobacteriaceae*-driven bacteremia seem to be relatively rare, but are very often clinically relevant. More research effort is needed to identify environmental factors and molecular mechanisms that favor initial colonization and survival of *Coriobacteriaceae* in the blood. Of note, only three genera within the family are positive for catalase activity: *Eggerthella*, *Gordonibacter*, and *Paraeggerthella*. All three have been associated with cases of bacteremia. The presence of catalase may help these organisms coping with oxidative stress during infection.

Gastrointestinal Pathologies

Although there are an increasing number of studies investigating the gut microbiota in colorectal cancer (CRC), the exact contribution of bacteria to molecular mechanisms underlying disease remains unclear. Intestinal bacteria are proposed to play a role in CRC via two main mechanisms: (1) the production of metabolites such as hydrogen sulfide or ammonia, which can have detrimental effects on host cell functions (Blaut and Clavel 2007), and (2) the alteration of innate immune mechanisms (Rakoff-Nahoum and Medzhitov 2007).

The role of a variety of bacteria such as enterotoxigenic *Bacteroides fragilis*, *Enterococcus faecalis*, *Fusobacterium* spp., *Prevotella* spp., and *Streptococcus bovis* in CRC has already been discussed (Wu et al. 2009; Al-Jashamy et al. 2010; Sobhani et al. 2011; Kostic et al. 2012). *Coriobacteriaceae* have gained attention in this field very recently. The occurrence of *Collinsella*, *Eggerthella*, *Olsenella*, and *Slackia* spp. was significantly higher on tumor site versus adjacent nonmalignant tissue in six Dutch patients who underwent resection for primary colon adenocarcinoma (Marchesi et al. 2011). Other recent studies on bacterial diversity in CRC patients found an increased prevalence of 16S rRNA gene sequences classified as *Actinobacteria*, including *Collinsella* spp., in feces from CRC versus healthy control subjects (Chen et al. 2012; Wang et al. 2012). In the study by Chen et al., the prevalence of sequences assigned to the *Coriobacteriaceae* was 1.19 % in CRC patients versus 0.74 % in healthy individuals. Still, these data refer only to the density of bacterial populations, and there is no indication that *Coriobacteriaceae* have overall positive or negative effects on tumorigenesis. *Coriobacteriaceae* have recently been referred to as “passenger” bacteria in CRC, in contrast to “driver” bacteria such as *Bacteroides fragilis* which seem to be involved in the initiation of disease (Tjalsma et al. 2012). Passenger bacteria are proposed to be best suited for colonization of disturbed microenvironments in the vicinity of tumors. In that context, the effect of local production of equol by *Slackia* spp. that colonize tumor sites in the gut may be worth investigating considering the biological properties of this bacterial product (Magee et al. 2006; Choi 2009). The effects of ammonia production by, for instance, *Olsenella* spp. or *Eggerthella lenta* may be worth investigating too (Eschenlauer et al. 2002; Kraatz et al. 2011).

Apart from cancer, the role of *Coriobacteriaceae* in other pathologies associated with gastrointestinal dysfunctions is ill defined. Isolates of *Eggerthella lenta* identified on the basis of fermentation and biochemical reactions were recovered in 44 % of 41 appendix tissue samples from children with suspected acute appendicitis (Rautio et al. 2000). Moreover, although clinical case reports and targeted isolation procedures hint at the relevance of *Coriobacteriaceae* in inflammatory bowel diseases, there is to date no corresponding quantitative or functional data available (Clavel et al. 2009, 2013; Würdemann et al. 2009; Joossens et al. 2011; Thota et al. 2011). Finally, there is an increasing body of evidence pointing at the involvement of gut bacteria in host energy balance and metabolic disorders (Backhed et al. 2004; Qin et al. 2012). *Coriobacteriaceae* have been detected

in the feces of 14 overweight and obese human volunteers with no history of gastrointestinal disease (Walker et al. 2011). As previously reported in healthy individuals (Harmsen et al. 2000; Kageyama et al. 2000; Tap et al. 2009), *Collinsella aerofaciens* was amongst the most abundant taxonomic units (3.7 % of 16S rRNA clones) after *Faecalibacterium prausnitzii* (8.0 %), *Eubacterium rectale* (4.4 %), and *Clostridium clostridioforme* (3.8 %) in the fecal sample from six of the 14 volunteers. The proportion of *Collinsella aerofaciens* was significantly reduced to 0.6 % after consumption of a protein-rich, fat, and carbohydrate-reduced weight-loss diet. In another study, the number of 16S rRNA gene sequences assigned to *Coriobacteriaceae* in the feces of three obese subjects was found to be higher than in lean controls and in subjects after gastric bypass-induced weight loss (Zhang et al. 2009). Based on these descriptive findings on the dominance of *Coriobacteriaceae* in the gut and considering their metabolic potential with regard to hepatic functions and lipid homeostasis (see metabolic activities), their role in the regulation of host metabolic disorders is worth investigating in more details.

Allergy

Commensal gut microbial communities are known to influence host immune responses beyond the gut. For instance, they have been implicated in the regulation of molecular mechanisms underlying allergies (Hormannspurger et al. 2012). A molecular study comparing the fecal microbiota in <12-month-old infants with cow’s milk protein allergy versus nonallergic infants ($n = 46$ each) found higher median counts of the *Atopobium* group in allergic infants (0.6 vs. 0.0 % of total bacteria) (Thompson-Chagoyan et al. 2011). Of note, in a former study, the *Atopobium* and *Collinsella* group represented a substantial proportion of the gut microbiota in the feces of formula-fed infants when compared with breast-fed infants (>17 vs. 0.5 % of total bacteria; $n = 6$ each) (Harmsen et al. 2000). Breast-feeding is proposed to have protective effects on the development of atopic disorders, although more data are needed to reach consensus in results (Mimouni Bloch et al. 2002; Batchelor et al. 2010; Brew et al. 2011).

Dental Caries and Abscess

In the human oral cavity, *Coriobacteriaceae*, including *Atopobium parvulum*, *Atopobium rimae*, and *Olsenella profusa*, have been detected during the final phase of caries extension in dental pulp with established and advanced infection (Nadkarni et al. 2010). The spatial distribution of these bacteria suggested an intricate association with members of the *Bacteroidetes* in tightly concentrated biomass, even though underlying reasons were unclear. Identification of bacterial pathogens by 16S rRNA gene-targeted PCR in the oral cavity of 21 patients suffering from primary or persistent endodontic infections revealed that some *Coriobacteriaceae* were amongst the most prevalent phylotypes: *Olsenella uli*,

Olsenella profusa, and *Atopobium parvulum* were identified in 33, 9.5, and 5 % of cases of infection, respectively (Siqueira and Rocas 2005). *Olsenella uli* was also identified in persistent endodontic infections in this study. This species was also found to be one of the most prevalent species in root canals from 139 teeth with apical periodontitis (Dewhirst et al. 2001; Chavez de Paz et al. 2004). A number of additional papers reported the detection of *Coriobacteriaceae*, especially *Atopobium* and *Olsenella* spp., in oral clinical samples (Kumar et al. 2003, 2005; Aas et al. 2008; Preza et al. 2008; Subramanian and Mickel 2009; Lima et al. 2011). In one additional study, high-throughput sequencing of 16S rRNA genes allowed the identification of *Coriobacteriaceae* in the oral cavity, infected root canal, and periapical abscess of eight patients (Hsiao et al. 2012). The genus *Atopobium* was mostly found in root canal samples, whereas the genus *Collinsella* was significantly overrepresented in abscess samples. Other *Coriobacteriaceae*, including *Olsenella*, *Slackia*, *Cryptobacterium*, and *Eggerthella* were seldom identified in oral cavity samples.

Bacterial Vaginosis

Bacterial vaginosis is a frequently reported polymicrobial infection in which the commensal microbiota usually dominated by lactobacilli is replaced by obligate anaerobes (Danielsson et al. 2011). The type strain of *Atopobium vaginae* was isolated from the vagina of a healthy woman (Rodriguez Jovita et al. 1999). The pathogenic potential of this species was highlighted in 2003 by a case of tubo-ovarian abscess following transvaginal oocyte recovery (Geissdorfer et al. 2003). Clinical isolates have also been recovered in the context of uterine endometritis (Yamagishi et al. 2011) and intrauterine infection (Knoester et al. 2011). Thanks to molecular techniques, this bacterium has been frequently detected in vaginal infections and is thought to be involved in 55–95 % of cases and responsible for therapeutic failures (Ferris et al. 2004; Verhelst et al. 2004; Polatti 2012). A recent evaluation of the microbiota in vaginal swabs from 220 women using pyrosequencing of 16S rRNA gene amplicons showed that women with vaginosis are characterized by diverse heterogeneous communities with a high prevalence of *Atopobium vaginae* and *Eggerthella* species (Srinivasan et al. 2012).

Atopobium vaginae is commonly identified alongside *Gardnerella vaginalis* in clinical samples, and their association appears to provide a reliable diagnosis (Lamont et al. 2011; Srinivasan et al. 2012). Fluorescence in situ hybridization analysis of vaginal biopsies provided further evidence of the strong co-occurrence of these species, which accounts for more than 90 % of the biofilm mass on vaginal epithelial surfaces (Swidsinski et al. 2005). The biofilm-forming properties of *Atopobium vaginae* and *Gardnerella vaginalis* contribute to the recalcitrance of infection by conferring a protective environment against both antibacterial therapies and immune responses. A 5-day treatment of polymicrobial *Gardnerella*, *Atopobium*, and *Lactobacillus* spp. biofilm using 400 mg/day moxifloxacin

in women with bacterial vaginosis showed a significant decrease in *Atopobium* and *Gardnerella* coupled to an increase in lactobacilli in biofilms (Swidsinski et al. 2011). However, despite short-term clinical efficacy, moxifloxacin (similarly to metronidazole and clindamycin) fails to prevent the recurrence of vaginosis (Swidsinski et al. 2011; Bradshaw et al. 2012).

The antibiotic susceptibility profile of *Atopobium vaginae* reveals resistance to the antibiotics nalidixic acid and colistin with MIC values higher than 256 and 1,024 µg/mL, respectively, while metronidazole resistance was reported for a number of strains (Ferris et al. 2004; De Backer et al. 2006; Polatti 2012). Also, *Atopobium vaginae* was found to be susceptible to a range of antibiotics including clindamycin, the antibiotic of choice for bacterial vaginosis, as well as ampicillin, ampicillin-sulbactam, azithromycin, ceftriaxone, ciprofloxacin, imipenem, linezolid, meropenem, moxifloxacin, penicillin, rifampicin, and trovafloxacin (Ferris et al. 2004; De Backer et al. 2006). It was recently suggested that the nitrofurantoin derivative, nitrofurantoin, provides an alternative therapy for bacterial vaginosis involving the common pathogens *Atopobium vaginae* and *Gardnerella vaginalis*, without affecting the commensal microbiota of the vagina (Togni et al. 2011; Polatti 2012).

Application

Due to the recent description of a substantial number of *Coriobacteriaceae* species and to the even more recent reports that highlight some of their physiologically and clinically relevant functions, the use of these bacteria for application purposes has been very limited so far, but is at favorable odds for the near future.

The ability of *Coriobacteriaceae* to convert dietary isoflavones into the bioactive product equol is of particular interest for potential nutraceutical or pharmaceutical applications. The observation that two thirds of the human population cannot produce equol has spurred considerable interest on applied microbiological approaches aimed at triggering equol production in non-equol producers, along with the hypothesis that people hosting equol-producing *Coriobacteriaceae* are more likely to benefit from potentially beneficial health effects of soyfood and isoflavone intake. However, most attempts fell short of their target. First, there is to date no official nutritional recommendation on the benefit of dietary soy isoflavones on human health and state-of-the-art intervention trials are needed (Clavel and Mapesa 2013). Second, a number of animal and human studies examined the use of probiotic strains to boost equol production but failed to establish clear evidence (Larkin et al. 2007; Clavel and Mapesa 2013). Finally, the intake of *Coriobacteriaceae* themselves as probiotic strains in human subjects is for obvious safety issues not sound. However, the use of already isolated and characterized *Coriobacteriaceae* can be of great value in several ways: (1) for gathering functional evidence that equol is indeed directly linked to beneficial health effects using gnotobiotic mouse models of diseases colonized with, for instance, equol-producing or steroid-dehydroxylating versus

non-active strains (Woting et al. 2010; Becker et al. 2011), (2) for studying the production and effects of so far unknown isoflavone products such as 5-hydroxy-euol (Matthies et al. 2008), and (3) for large-scale affordable production of euol, for instance, for the sake of intervention trials that require large quantity of pure material. With respect to the latter point, the enantiospecificity of euol production is noteworthy. Gut bacteria are known to produce exclusively the *S*-enantiomer of euol, which seems to be more biologically active than its counterpart *R*-euol (Setchell et al. 2005; Wang et al. 2005, 2007; Shinkaruk et al. 2010). Patents related to the bacterial or synthetic production of enantiomeric euol and to the isolation of involved bacterial enzymes have already been registered (Setchell et al., US2009/7528267, Shimada et al., US2010/0330627; Isono et al., US2011/0189134; Tsuji et al., US2011/0318309). *Coriobacteriaceae*-based applications for the sake of metabolite production are also valid with respect to secondary bile acids, as recently studied using a 7 β -HSDH from *Collinsella aerofaciens* (Braun et al. 2012).

The aforementioned use of *Coriobacteriaceae* in gnotobiotic mouse models can actually be extended to the study of host metabolic functions. Such experiments would help deciphering, for instance, the health implication of *Eggerthella*-encoded bile acid and steroid dehydroxylases as well as the role of these bacteria on hepatic functions, e.g., lipid metabolism and detoxification pathways (Ridlon et al. 2006; Claus et al. 2011; Martinez et al. 2012). In addition, one member of the *Coriobacteriaceae* isolated from the bovine rumen, *Denitrobacterium detoxificans*, is capable of metabolizing the nitrotoxins 3-nitro-1-propanol and 3-nitro-1-propionate found in forages, thereby providing potential industrial application for clearance of nitro-compounds from environmental samples or enhancement of tolerance towards environmental toxins in cattle (Anderson et al. 2000, 2005). *Slackia heliotrinireducens* may also be of interest for the reduction of pyrrolizidine alkaloid poisoning in cattle (Hovermale and Craig 2002).

References

- Aas JA, Griffen AL, Dardis SR et al (2008) Bacteria of dental caries in primary and permanent teeth in children and young adults. *J Clin Microbiol* 46:1407–1417
- Al-Jashamy K, Murad A, Zeehaida M et al (2010) Prevalence of colorectal cancer associated with *Streptococcus bovis* among inflammatory bowel and chronic gastrointestinal tract disease patients. *Asian Pac J Cancer Prev* 11:1765–1768
- Anderson RC, Rasmussen MA, Allison MJ (1996) Enrichment and isolation of a nitropropanol-metabolizing bacterium from the rumen. *Appl Environ Microbiol* 62:3885–3886
- Anderson RC, Rasmussen MA, Jensen NS et al (2000) *Denitrobacterium detoxificans* gen. nov., sp. nov., a ruminal bacterium that respire on nitrocompounds. *Int J Syst Evol Microbiol* 50(2):633–638
- Anderson RC, Majak W, Rasmussen MA et al (2005) Toxicity and metabolism of the conjugates of 3-nitropropanol and 3-nitropropionic acid in forages poisonous to livestock. *J Agric Food Chem* 53:2344–2350
- Angelakis E, Roux V, Raoult D et al (2009) Human case of *Atopobium rimae* bacteremia. *Emerg Infect Dis* 15:354–355
- Axelsson M, Setchell KD (1981) The excretion of lignans in rats—evidence for an intestinal bacterial source for this new group of compounds. *FEBS Lett* 123:337–342
- Aziz RK, Bartels D, Best AA et al (2008) The RAST server: rapid annotations using subsystems technology. *BMC Genomics* 9:75
- Backhed F, Ding H, Wang T et al (2004) The gut microbiota as an environmental factor that regulates fat storage. *Proc Natl Acad Sci USA* 101:15718–15723
- Bailey GD, Love DN (1986) *Eubacterium fossor* sp. nov. An agar-corroding organism from normal pharynx and oral and respiratory tract lesions of horses. *Int J Syst Bacteriol* 36:383–387
- Batchelor JM, Grindlay DJ, Williams HC (2010) What's new in atopic eczema? An analysis of systematic reviews published in 2008 and 2009. *Clin Exp Dermatol* 35:823–827
- Becker N, Kunath J, Loh G et al (2011) Human intestinal microbiota: characterization of a simplified and stable gnotobiotic rat model. *Gut Microbes* 2:25–33
- Belda-Ferre P, Alcaraz LD, Cabrera-Rubio R et al (2012) The oral metagenome in health and disease. *ISME J* 6:46–56
- Benson AK, Kelly SA, Legge R et al (2010) Individuality in gut microbiota composition is a complex polygenic trait shaped by multiple environmental and host genetic factors. *Proc Natl Acad Sci USA* 107:18933–18938
- Blaut M, Clavel T (2007) Metabolic diversity of the intestinal microbiota: implications for health and disease. *J Nutr* 137:751S–755S
- Bok CW, Ng YS (2009) *Eggerthella lenta* as a cause of anaerobic spondylodiscitis. *Singapore Med J* 50:e393–e396
- Bokkenheuser VD, Winter J, Dehazya P et al (1977) Isolation and characterization of human fecal bacteria capable of 21-dehydroxylating corticoids. *Appl Environ Microbiol* 34:571–575
- Bokkenheuser VD, Winter J, Finegold SM et al (1979) New markers for *Eubacterium lentum*. *Appl Environ Microbiol* 37:1001–1006
- Bokkenheuser VD, Winter J, O'Rourke S et al (1980) Isolation and characterization of fecal bacteria capable of 16 alpha-dehydroxylating corticoids. *Appl Environ Microbiol* 40:803–808
- Borriello SP, Setchell KD, Axelsson M et al (1985) Production and metabolism of lignans by the human faecal flora. *J Appl Bacteriol* 58:37–43
- Bradshaw CS, Pirotta M, De Guingand D et al (2012) Efficacy of oral metronidazole with vaginal clindamycin or vaginal probiotic for bacterial vaginosis: randomised placebo-controlled double-blind trial. *PLoS One* 7:e34540
- Braun M, Sun B, Anselment B et al (2012) Novel whole-cell biocatalysts with recombinant hydroxysteroid dehydrogenases for the asymmetric reduction of dehydrocholic acid. *Appl Microbiol Biotechnol* 95:1457–1468
- Brew BK, Allen CW, Toelle BG et al (2011) Systematic review and meta-analysis investigating breast feeding and childhood wheezing illness. *Paediatr Perinat Epidemiol* 25:507–518
- Bryant MP, Robinson IM (1961) Some nutritional requirements of the genus *Ruminococcus*. *Appl Microbiol* 9:91–95
- Cato EP (1983) Transfer of *Peptostreptococcus parvulus* (Weinberg, Nativelle, and Prévot 1937) Smith 1957 to the Genus *Streptococcus*: *Streptococcus parvulus* (Weinberg, Nativelle, and Prévot 1937) comb. nov., nom. rev., emend. *Int J Syst Bacteriol* 33:82–84
- Chan RC, Mercer J (2008) First Australian description of *Eggerthella lenta* bacteraemia identified by 16S rRNA gene sequencing. *Pathology* 40:409–410
- Chan JF, Lau SK, Curreem SO et al (2012) First report of spontaneous intrapartum *Atopobium vaginae* bacteremia. *J Clin Microbiol* 50:2525–2528
- Chavez de Paz LE, Molander A, Dahlen G (2004) Gram-positive rods prevailing in teeth with apical periodontitis undergoing root canal treatment. *Int Endod J* 37:579–587
- Chen W, Liu F, Ling Z et al (2012) Human intestinal lumen and mucosa-associated microbiota in patients with colorectal cancer. *PLoS One* 7:e39743
- Choi EJ (2009) Evaluation of euol function on anti- or prooxidant status in vivo. *J Food Sci* 74:H65–H71
- Chow J, Tang H, Mazmanian SK (2011) Pathobionts of the gastrointestinal microbiota and inflammatory disease. *Curr Opin Immunol* 23:473–480
- Chung HY, Sung H, Lee MY et al (2007) A case of bacteremia by *Atopobium rimae* in a patient with liver cirrhosis. *Korean J Lab Med* 27:351–354
- Claus SP, Ellero SL, Berger B et al (2011) Colonization-induced host-gut microbial metabolic interaction. *MBio* 2:e00271–00210
- Clavel T (2006) Metabolism of the dietary lignan secoisolariciresinol diglucoside by human intestinal bacteria. Logos Verlag, Berlin. ISBN 3-8325-1192-X

- Clavel T, Mapesa JO (2013) Phenolics in human nutrition: importance of the intestinal microbiome for isoflavone and lignan bioavailability. In: Ramawat KG, Merillon JM (eds) Handbook of natural products. Elsevier, Amsterdam
- Clavel T, Fallani M, Lepage P et al (2005) Isoflavones and functional foods alter the dominant intestinal microbiota in postmenopausal women. *J Nutr* 135:2786–2792
- Clavel T, Dore J, Blaut M (2006) Bioavailability of lignans in human subjects. *Nutr Res Rev* 19:187–196
- Clavel T, Charrier C, Braune A et al (2009) Isolation of bacteria from the ileal mucosa of TNFdeltaARE mice and description of *Enterorhabdus mucosicola* gen. nov., sp. nov. *Int J Syst Evol Microbiol* 59:1805–1812
- Clavel T, Duck W, Charrier C et al (2010) *Enterorhabdus caecimuris* sp. nov., a member of the family Coriobacteriaceae isolated from a mouse model of spontaneous colitis, and emended description of the genus *Enterorhabdus* Clavel et al. 2009. *Int J Syst Evol Microbiol* 60:1527–1531
- Clavel T, Charrier C, Wenning M et al (2013) *Parvibacter caecicola* gen. nov., sp. nov., a new bacterium of the family Coriobacteriaceae isolated from the caecum of a mouse. *Int J Syst Evol Microbiol* 63(7):2642–2648
- Collado MC, Sanz Y (2007a) Quantification of mucosa-adhered microbiota of lambs and calves by the use of culture methods and fluorescent in situ hybridization coupled with flow cytometry techniques. *Vet Microbiol* 121:299–306
- Collado MC, Sanz Y (2007b) Characterization of the gastrointestinal mucosa-associated microbiota of pigs and chickens using culture-based and molecular methodologies. *J Food Prot* 70:2799–2804
- Collins MD, Wallbanks S (1992) Comparative sequence analyses of the 16S rRNA genes of *Lactobacillus minutus*, *Lactobacillus rimae* and *Streptococcus parvulus*: proposal for the creation of a new genus *Atopobium*. *FEMS Microbiol Lett* 74:235–240
- Copeland A, Sikorski J, Lapidus A, Nolan M, Del Rio TG, Lucas S, Chen F, Tice H, Pitluck S, Cheng JF, Pukall R, Chertkov O, Brettin T, Han C, Detter JC, Kuske C, Bruce D, Goodwin L, Ivanova N, Mavromatis K, Mikhailova N, Chen A, Palaniappan K, Chain P, Rohde M, Göker M, Bristow J, Eisen JA, Markowitz V, Hugenholtz P, Kyrpides NC, Klenk HP, Detter JC (2009) Complete genome sequence of *Atopobium parvulum* type strain (IPP 1246). *Stand Genomic Sci* 1(2):166–173. doi: 10.4056/sigs.29547. PubMed PMID: 21304653; PubMed Central PMCID: PMC3035223
- Credito KL, Appelbaum PC (2004) Activity of OPT-80, a novel macrocycle, compared with those of eight other agents against selected anaerobic species. *Antimicrob Agents Chemother* 48:4430–4434
- Danielsson D, Teigen PK, Moi H (2011) The genital econiche: focus on microbiota and bacterial vaginosis. *Ann N Y Acad Sci* 1230:48–58
- Dawson KA, Allison MJ, Hartman PA (1980) Characteristics of anaerobic oxalate-degrading enrichment cultures from the rumen. *Appl Environ Microbiol* 40:840–846
- De Backer E, Verhelst R, Verstraelen H et al (2006) Antibiotic susceptibility of *Atopobium vaginae*. *BMC Infect Dis* 6:51
- Devkota S, Wang Y, Musch MW et al (2012) Dietary-fat-induced taurocholic acid promotes pathobiont expansion and colitis in IL10^{-/-} mice. *Nature* 487:104–108
- Dewhirst FE, Paster BJ, Tzellas N et al (2001) Characterization of novel human oral isolates and cloned 16S rDNA sequences that fall in the family Coriobacteriaceae: description of *Olsenella* gen. nov., reclassification of *Lactobacillus uli* as *Olsenella uli* comb. nov. and description of *Olsenella profusa* sp. nov. *Int J Syst Evol Microbiol* 51:1797–1804
- Duboc H, Rajca S, Rainteau D et al (2013) Connecting dysbiosis, bile-acid dysmetabolism and gut inflammation in inflammatory bowel diseases. *Gut* 62(4):531–539
- Duck LW, Walter MR, Novak J et al (2007) Isolation of flagellated bacteria implicated in Crohn's disease. *Inflamm Bowel Dis* 13:1191–1201
- Eggerth AH (1935) The gram-positive non-spore-bearing anaerobic bacilli of human feces. *J Bacteriol* 30:277–299
- Eschenlauer SC, McKain N, Walker ND et al (2002) Ammonia production by ruminal microorganisms and enumeration, isolation, and characterization of bacteria capable of growth on peptides and amino acids from the sheep rumen. *Appl Environ Microbiol* 68:4925–4931
- Eyssen H, Verhulst A (1984) Biotransformation of linoleic acid and bile acids by *Eubacterium lentum*. *Appl Environ Microbiol* 47:39–43
- Ezaki T, Yabuuchi E (1986) Transfer of *Peptococcus heliotrinreducens* corrig. to the Genus *Peptostreptococcus*: *Peptostreptococcus heliotrinreducens* Lanigan 1983 comb. nov. *Int J Syst Bacteriol* 36:107–108
- Ferris MJ, Maszta A, Martin DH (2004) Use of species-directed 16S rRNA gene PCR primers for detection of *Atopobium vaginae* in patients with bacterial vaginosis. *J Clin Microbiol* 42:5892–5894
- Finegold SM, Sutter VL, Mathisen GE (1983) Normal indigenous intestinal flora. In: Hentges DJ (ed) Human intestinal microflora in health and disease. Academic, New York, pp 3–31
- Geissdorfer W, Bohmer C, Pelz K et al (2003) Tuboovarian abscess caused by *Atopobium vaginae* following transvaginal oocyte recovery. *J Clin Microbiol* 41:2788–2790
- Gillespie JJ, Wattam AR, Cammer SA et al (2011) PATRIC: the comprehensive bacterial bioinformatics resource with a focus on human pathogenic species. *Infect Immun* 79:4286–4298
- Gnewuch C, Liebisch G, Langmann T et al (2009) Serum bile acid profiling reflects enterohepatic detoxification state and intestinal barrier function in inflammatory bowel disease. *World J Gastroenterol* 15:3134–3141
- Goker M, Held B, Lucas S et al (2010) Complete genome sequence of *Olsenella uli* type strain (VPI D76D-27C). *Stand Genomic Sci* 3:76–84
- Goldstein EJ, Citron DM, Merriam CV et al (2003) In vitro activities of dalbavancin and nine comparator agents against anaerobic gram-positive species and corynebacteria. *Antimicrob Agents Chemother* 47:1968–1971
- Haas F, König H (1988) *Coriobacterium glomerans* gen. nov., sp. nov. from the intestinal tract of the red soldier bug. *Int J Syst Bacteriol* 38:382–384
- Harmsen HJ, Wildeboer-Veloo AC, Grijpstra J et al (2000) Development of 16S rRNA-based probes for the *Coriobacterium* group and the *Atopobium* cluster and their application for enumeration of Coriobacteriaceae in human feces from volunteers of different age groups. *Appl Environ Microbiol* 66:4523–4527
- Hauduroy P, Ehringer G, Urbain A et al (1937) Dictionnaire des bactéries pathogènes. Masson et Cie, Paris
- Hirano S, Masuda N (1982) Enhancement of the 7 alpha-dehydroxylase activity of a gram-positive intestinal anaerobe by Bacteroides and its significance in the 7-dehydroxylation of ursodeoxycholic acid. *J Lipid Res* 23:1152–1158
- Hirokawa Y, Kinoshita H, Tanaka T et al (2008) Water-soluble pleuromutilin derivative with excellent in vitro and in vivo antibacterial activity against gram-positive pathogens. *J Med Chem* 51:1991–1994
- Holdeman LV, Cato EP, Moore WE (1977) Anaerobe laboratory manual, 4th edn. Virginia Polytechnic and State University, Blacksburg, VA
- Hormannspurger G, Clavel T, Haller D (2012) Gut matters: microbe-host interactions in allergic diseases. *J Allergy Clin Immunol* 129:1452–1459
- Hovermale JT, Craig AM (2002) Metabolism of pyrrolizidine alkaloids by *Peptostreptococcus heliotrinreducens* and a mixed culture derived from ovine ruminal fluid. *Biophys Chem* 101–102:387–399
- Hristov AN, Callaway TR, Lee C et al (2012) Rumen bacterial, archaeal, and fungal diversity of dairy cows in response to lauric or myristic acids ingestion. *J Anim Sci* 90(12):4449–4457
- Hsiao WW, Li KL, Liu Z et al (2012) Microbial transformation from normal oral microbiota to acute endodontic infections. *BMC Genomics* 13:345
- Jin JS, Kitahara M, Sakamoto M et al (2010) *Slackia equalifaciens* sp. nov., a human intestinal bacterium capable of producing equol. *Int J Syst Evol Microbiol* 60:1721–1724
- Joossens M, Huys G, Cnockaert M et al (2011) Dysbiosis of the faecal microbiota in patients with Crohn's disease and their unaffected relatives. *Gut* 60:631–637
- Kageyama A, Benno Y (2000) Emendation of genus *Collinsella* and proposal of *Collinsella stercoris* sp. nov. and *Collinsella intestinalis* sp. nov. *Int J Syst Evol Microbiol* 50(5):1767–1774
- Kageyama A, Benno Y (2001) Rapid detection of human fecal *Eubacterium* species and related genera by nested PCR method. *Microbiol Immunol* 45:315–318
- Kageyama A, Benno Y, Nakase T (1999a) Phylogenetic and phenotypic evidence for the transfer of *Eubacterium aerofaciens* to the genus *Collinsella* as *Collinsella aerofaciens* gen. nov., comb. nov. *Int J Syst Bacteriol* 49(2):557–565

- Kageyama A, Benno Y, Nakase T (1999b) Phylogenetic and phenotypic evidence for the transfer of *Eubacterium fossor* to the genus *Atopobium* as *Atopobium fossor* comb. nov. *Microbiol Immunol* 43:389–395
- Kageyama A, Benno Y, Nakase T (1999c) Phylogenetic evidence for the transfer of *Eubacterium lentum* to the genus *Eggerthella* as *Eggerthella lenta* gen. nov., comb. nov. *Int J Syst Bacteriol* 49(4):1725–1732
- Kageyama A, Sakamoto M, Benno Y (2000) Rapid identification and quantification of *Collinsella aerofaciens* using PCR. *FEMS Microbiol Lett* 183:43–47
- Kaltenpoth M, Winter SA, Kleinhammer A (2009) Localization and transmission route of *Coriobacterium glomerans*, the endosymbiont of pyrrhocorid bugs. *FEMS Microbiol Ecol* 69:373–383
- Kim KS, Rowlinson MC, Bannion R et al (2010) Characterization of *Slackia exigua* isolated from human wound infections, including abscesses of intestinal origin. *J Clin Microbiol* 48:1070–1075
- Kitahara M, Takamine F, Imamura T et al (2000) Assignment of *Eubacterium* sp. VPI 12708 and related strains with high bile acid 7 α -dehydroxylating activity to *Clostridium scindens* and proposal of *Clostridium hylemonae* sp. nov., isolated from human faeces. *Int J Syst Evol Microbiol* 50(3):971–978
- Knoester M, Lashley LE, Wessels E et al (2011) First report of *Atopobium vaginae* bacteremia with fetal loss after chorionic villus sampling. *J Clin Microbiol* 49:1684–1686
- Kostelac D, Rechkemmer G, Briviva K (2003) Phytoestrogens modulate binding response of estrogen receptors alpha and beta to the estrogen response element. *J Agric Food Chem* 51:7632–7635
- Kostic AD, Gevers D, Pedamallu CS et al (2012) Genomic analysis identifies association of *Fusobacterium* with colorectal carcinoma. *Genome Res* 22:292–298
- Kraatz M, Taras D (2008) *Veillonella magna* sp. nov., isolated from the jejunal mucosa of a healthy pig, and emended description of *Veillonella ratti*. *Int J Syst Evol Microbiol* 58:2755–2761
- Kraatz M, Wallace RJ, Svensson L (2011) *Olsenella umbonata* sp. nov., a microaerotolerant anaerobic lactic acid bacterium from the sheep rumen and pig jejunum, and emended descriptions of *Olsenella*, *Olsenella uli* and *Olsenella profusa*. *Int J Syst Evol Microbiol* 61:795–803
- Kuiper GG, Lemmen JG, Carlsson B et al (1998) Interaction of estrogenic chemicals and phytoestrogens with estrogen receptor beta. *Endocrinology* 139:4252–4263
- Kumar PS, Griffen AL, Barton JA et al (2003) New bacterial species associated with chronic periodontitis. *J Dent Res* 82:338–344
- Kumar PS, Griffen AL, Moeschberger ML et al (2005) Identification of candidate periodontal pathogens and beneficial species by quantitative 16S clonal analysis. *J Clin Microbiol* 43:3944–3955
- Kutschera M, Engst W, Blaut M et al (2011) Isolation of catechin-converting human intestinal bacteria. *J Appl Microbiol* 111:165–175
- Lamont RE, Sobel JD, Akins RA et al (2011) The vaginal microbiome: new information about genital tract flora using molecular based techniques. *BJOG* 118:533–549
- Landais C, Doudier B, Imbert G et al (2007) Application of rrs gene sequencing to elucidate the clinical significance of *Eggerthella lenta* infection. *J Clin Microbiol* 45:1063–1065
- Lanigan GW (1976) *Peptococcus heliotrinreducans*, sp. nov., a cytochrome-producing anaerobe which metabolizes pyrrolizidine alkaloids. *J Gen Microbiol* 94:1–10
- Larkin TA, Price WE, Astheimer LB (2007) Increased probiotic yogurt or resistant starch intake does not affect isoflavone bioavailability in subjects consuming a high soy diet. *Nutrition* 23:709–718
- Lau SK, Woo PC, Fung JM et al (2004a) Anaerobic, non-sporulating, gram-positive bacilli bacteraemia characterized by 16S rRNA gene sequencing. *J Med Microbiol* 53:1247–1253
- Lau SK, Woo PC, Woo GK et al (2004b) *Eggerthella hongkongensis* sp. nov. and *Eggerthella sinensis* sp. nov., two novel *Eggerthella* species, account for half of the cases of *Eggerthella* bacteremia. *Diagn Microbiol Infect Dis* 49:255–263
- Lawson PA, Greetham HL, Gibson GR et al (2005) *Slackia faecianis* sp. nov., isolated from canine faeces. *Int J Syst Evol Microbiol* 55:1243–1246
- Lee MR, Huang YT, Liao CH et al (2012) Clinical and microbiological characteristics of bacteremia caused by *Eggerthella*, *Paraeggerthella*, and *Eubacterium* species at a university hospital in Taiwan from 2001 to 2010. *J Clin Microbiol* 50:2053–2055
- Liderot K, Larsson M, Borang S et al (2010) Polymicrobial bloodstream infection with *Eggerthella lenta* and *Desulfovibrio desulfuricans*. *J Clin Microbiol* 48:3810–3812
- Lima KC, Coelho LT, Pinheiro IV et al (2011) Microbiota of dental caries as assessed by reverse-capture checkerboard analysis. *Caries Res* 45:21–30
- Liu B, Faller LL, Klitgord N et al (2012) Deep sequencing of the oral microbiome reveals signatures of periodontal disease. *PLoS One* 7:e37919
- Lyra A, Forssten S, Rolny P et al (2012) Comparison of bacterial quantities in left and right colon biopsies and faeces. *World J Gastroenterol* 18:4404–4411
- Mabrok HB, Klopffleisch R, Ghanem KZ et al (2012) Lignan transformation by gut bacteria lowers tumor burden in a gnotobiotic rat model of breast cancer. *Carcinogenesis* 33:203–208
- Magee PJ, Raschke M, Steiner C et al (2006) Equol: a comparison of the effects of the racemic compound with that of the purified S-enantiomer on the growth, invasion, and DNA integrity of breast and prostate cells in vitro. *Nutr Cancer* 54:232–242
- Marchesi JR, Dutilh BE, Hall N et al (2011) Towards the human colorectal cancer microbiome. *PLoS One* 6:e20447
- Martinez I, Wallace G, Zhang C et al (2009) Diet-induced metabolic improvements in a hamster model of hypercholesterolemia are strongly linked to alterations of the gut microbiota. *Appl Environ Microbiol* 75:4175–4184
- Martinez I, Lattimer JM, Hubach KL et al (2013) Gut microbiome composition is linked to whole grain-induced immunological improvements. *ISME J* 7(2):269–280
- Maruo T, Sakamoto M, Ito C et al (2008) *Adlercreutzia equolifaciens* gen. nov., sp. nov., an equol-producing bacterium isolated from human faeces, and emended description of the genus *Eggerthella*. *Int J Syst Evol Microbiol* 58:1221–1227
- Mathey J, Mardon J, Fokialakis N et al (2007) Modulation of soy isoflavones bioavailability and subsequent effects on bone health in ovariectomized rats: the case for equol. *Osteoporos Int* 18:671–679
- Matthies A, Clavel T, Gutschow M et al (2008) Conversion of daidzein and genistein by an anaerobic bacterium newly isolated from the mouse intestine. *Appl Environ Microbiol* 74:4847–4852
- Matthies A, Blaut M, Braune A (2009) Isolation of a human intestinal bacterium capable of daidzein and genistein conversion. *Appl Environ Microbiol* 75:1740–1744
- McLellan SL, Huse SM, Mueller-Spitz SR et al (2010) Diversity and population structure of sewage-derived microorganisms in wastewater treatment plant influent. *Environ Microbiol* 12:378–392
- Merriam CV, Citron DM, Tyrrell KL et al (2006) In vitro activity of azithromycin and nine comparator agents against 296 strains of oral anaerobes and 31 strains of *Eikenella corrodens*. *Int J Antimicrob Agents* 28:244–248
- Messina M (2010) A brief historical overview of the past two decades of soy and isoflavone research. *J Nutr* 140:1350S–1354S
- Mimouni Bloch A, Mimouni D, Mimouni M et al (2002) Does breastfeeding protect against allergic rhinitis during childhood? A meta-analysis of prospective studies. *Acta Paediatr* 91:275–279
- Minamida K, Tanaka M, Abe A et al (2006) Production of equol from daidzein by gram-positive rod-shaped bacterium isolated from rat intestine. *J Biosci Bioeng* 102:247–250
- Minamida K, Ota K, Nishimukai M et al (2008) *Asaccharobacter celatus* gen. nov., sp. nov., isolated from rat caecum. *Int J Syst Evol Microbiol* 58:1238–1240
- Moore WE, Holdeman LV (1974) Human fecal flora: the normal flora of 20 Japanese-Hawaiians. *Appl Microbiol* 27:961–979
- Moore WEC, Cato EP, Holdeman LV (1971) *Eubacterium lentum* (Eggerth) Prévot 1938: emendation of description and designation of the neotype strain. *Int J Syst Bacteriol* 21:299–303
- Moore WE, Holdeman LV, Smibert RM et al (1982) Bacteriology of experimental gingivitis in young adult humans. *Infect Immun* 38:651–667
- Moore WE, Holdeman LV, Cato EP et al (1983) Bacteriology of moderate (chronic) periodontitis in mature adult humans. *Infect Immun* 42:510–515
- Mosca A, Summanen P, Finegold SM et al (1998) Cellular fatty acid composition, soluble-protein profile, and antimicrobial resistance pattern of *Eubacterium lentum*. *J Clin Microbiol* 36:752–755

- Mavrommatis K, Pukall R, Rohde C, Chen F, Sims D, Brettin T, Kuske C, Dettler JC, Han C, Lapidus A, Copeland A, Glavina Del Rio T, Nolan M, Lucas S, Tice H, Cheng JF, Bruce D, Goodwin L, Pitluck S, Ovchinnikova G, Pati A, Ivanova N, Chen A, Palaniappan K, Chain P, D'haeseleer P, Göker M, Bristow J, Eisen JA, Markowitz V, Hugenholtz P, Rohde M, Klenk HP, Kyrpides NC (2009) Complete genome sequence of *Cryptobacterium curtum* type strain (12-3). *Stand Genomic Sci* 1(2):93–100. doi: 10.4056/signs.12260. PubMed PMID: 21304644; PubMed Central PMCID: PMC3035227
- Nadal I, Donat E, Ribes-Koninckx C et al (2007) Imbalance in the composition of the duodenal microbiota of children with coeliac disease. *J Med Microbiol* 56:1669–1674
- Nadkarni MA, Simonian MR, Harty DW et al (2010) Lactobacilli are prominent in the initial stages of polymicrobial infection of dental pulp. *J Clin Microbiol* 48:1732–1740
- Nagai F, Watanabe Y, Morotomi M (2010) *Slackia piriformis* sp. nov. and *Collinsella tanakaei* sp. nov., new members of the family Coriobacteriaceae, isolated from human faeces. *Int J Syst Evol Microbiol* 60:2639–2646
- Nakazawa F, Hoshino E (2004) DNA-DNA relatedness and phylogenetic positions of *Slackia exigua*, *Slackia heliotrinireducens*, *Eggerthella lenta*, and other related bacteria. *Oral Microbiol Immunol* 19:343–346
- Nakazawa F, Poco SE, Ikeda T et al (1999) *Cryptobacterium curtum* gen. nov., sp. nov., a new genus of gram-positive anaerobic rod isolated from human oral cavities. *Int J Syst Bacteriol* 49(3):1193–1200
- Olsen I, Johnson JL, Moore LV et al (1991) *Lactobacillus uli* sp. nov. and *Lactobacillus rimae* sp. nov. from the human gingival crevice and emended descriptions of *Lactobacillus minutus* and *Streptococcus parvulus*. *Int J Syst Bacteriol* 41:261–266
- Poco SE Jr, Nakazawa F, Ikeda T et al (1996) *Eubacterium exiguum* sp. nov., isolated from human oral lesions. *Int J Syst Bacteriol* 46:1120–1124
- Polatti F (2012) Bacterial vaginosis, *Atopobium vaginae* and nifuratel. *Curr Clin Pharmacol* 7:36–40
- Preza D, Olsen I, Aas JA et al (2008) Bacterial profiles of root caries in elderly patients. *J Clin Microbiol* 46:2015–2021
- Pukall R, Lapidus A, Nolan M, Copeland A, Glavina Del Rio T, Lucas S, Chen F, Tice H, Cheng JF, Chertkov O, Bruce D, Goodwin L, Kuske C, Brettin T, Dettler JC, Han C, Pitluck S, Pati A, Mavrommatis K, Ivanova N, Ovchinnikova G, Chen A, Palaniappan K, Schneider S, Rohde M, Chain P, D'haeseleer P, Göker M, Bristow J, Eisen JA, Markowitz V, Kyrpides NC, Klenk HP, Hugenholtz P (2009) Complete genome sequence of *Slackia heliotrinireducens* type strain (RHS 1). *Stand Genomic Sci* 1(3):234–241. doi: 10.4056/signs.37633. PubMed PMID: 21304663; PubMed Central PMCID: PMC3035243
- Qin J, Li R, Raes J et al (2010) A human gut microbial gene catalogue established by metagenomic sequencing. *Nature* 464:59–65
- Qin J, Li Y, Cai Z et al (2012) A metagenome-wide association study of gut microbiota in type 2 diabetes. *Nature* 490:55–60
- Rainey FA, Weiss N, Stackebrandt E (1994) *Coriobacterium* and *Atopobium* are phylogenetic neighbors within the Actinomycetes line of descent. *Syst Appl Microbiol* 17:202–205
- Rakoff-Nahoum S, Medzhitov R (2007) Regulation of spontaneous intestinal tumorigenesis through the adaptor protein MyD88. *Science* 317:124–127
- Rautio M, Saxen H, Siitonen A et al (2000) Bacteriology of histopathologically defined appendicitis in children. *Pediatr Infect Dis J* 19:1078–1083
- Ravel J, Gajer P, Abdo Z et al (2011) Vaginal microbiome of reproductive-age women. *Proc Natl Acad Sci USA* 108(Suppl 1):4680–4687
- Ridlon JM, Kang DJ, Hylemon PB (2006) Bile salt biotransformations by human intestinal bacteria. *J Lipid Res* 47:241–259
- Rodriguez Jovita M, Collins MD, Sjoden B et al (1999) Characterization of a novel *Atopobium* isolate from the human vagina: description of *Atopobium vaginae* sp. nov. *Int J Syst Bacteriol* 49(4):1573–1576
- Rowland IR, Wiseman H, Sanders TA et al (2000) Interindividual variation in metabolism of soy isoflavones and lignans: influence of habitual diet on equol production by the gut microflora. *Nutr Cancer* 36:27–32
- Salimnia H, Noronha A, Sobel JD et al (2008) Sepsis associated with a new *Atopobium* species, provisionally named *Atopobium detroitii*: case report and review of the current status of the species *Atopobium*. *Scand J Infect Dis* 40:679–681
- Santiago GL, Tency I, Verstraelen H et al (2012) Longitudinal qPCR study of the dynamics of *L. crispatus*, *L. iners*, *A. vaginae*, (sialidase positive) *G. vaginalis*, and *P. bivia* in the vagina. *PLoS One* 7:e45281
- Sato T, Hoshino E, Uematsu H et al (1993) Predominant obligate anaerobes in necrotic pulps of human deciduous teeth. *Microbiol Ecol Health Dis* 6:269–275
- Sato T, Sato M, Matsuyama J et al (1998) Restriction fragment-length polymorphism analysis of 16S rDNA from oral asaccharolytic *Eubacterium* species amplified by polymerase chain reaction. *Oral Microbiol Immunol* 13:23–29
- Saunders E, Pukall R, Abt B et al (2009) Complete genome sequence of *Eggerthella lenta* type strain (IPP VPI 0255). *Stand Genomic Sci* 1:174–182
- Schleifer KH, Kandler O (1972) Peptidoglycan types of bacterial cell walls and their taxonomic implications. *Bacteriol Rev* 36:407–477
- Schwartz A, Le Blay G, Blaut M (2000) Quantification of different *Eubacterium* spp. in human fecal samples with species-specific 16S rRNA-targeted oligonucleotide probes. *Appl Environ Microbiol* 66:375–382
- Setchell KD, Lawson AM, Mitchell FL et al (1980) Lignans in man and in animal species. *Nature* 287:740–742
- Setchell KD, Lawson AM, Borriello SP et al (1981) Lignan formation in man—microbial involvement and possible roles in relation to cancer. *Lancet* 2:4–7
- Setchell KD, Gosselin SJ, Welsh MB et al (1987) Dietary estrogens—a probable cause of infertility and liver disease in captive cheetahs. *Gastroenterology* 93:225–233
- Setchell KD, Clerici C, Lephart ED et al (2005) S-equol, a potent ligand for estrogen receptor beta, is the exclusive enantiomeric form of the soy isoflavone metabolite produced by human intestinal bacterial flora. *Am J Clin Nutr* 81:1072–1079
- Shinkaruk S, Carreau C, Flouriot G et al (2010) Comparative effects of R- and S-equol and implication of transactivation functions (AF-1 and AF-2) in estrogen receptor-induced transcriptional activity. *Nutrients* 2:340–354
- Siqueira JF Jr, Rocas IN (2005) Uncultivated phylotypes and newly named species associated with primary and persistent endodontic infections. *J Clin Microbiol* 43:3314–3319
- Smbert RM, Holdeman LV (1976) Clinical isolates of anaerobic gram-negative rods with a formate-fumarate energy metabolism: *Bacteroides corrodens*, *Vibrio succinogenes*, and unidentified strains. *J Clin Microbiol* 3:432–437
- Sneath PHA, Mair NS, Elisabeth Sharpe M (1986) Bergey's manual of systematic bacteriology, vol 2. Williams & Wilkins, Baltimore
- Sobhani I, Tap J, Roudot-Thoraval F et al (2011) Microbial dysbiosis in colorectal cancer (CRC) patients. *PLoS One* 6:e16393
- Sperry JE, Wilkins TD (1976a) Arginine, a growth-limiting factor for *Eubacterium lentum*. *J Bacteriol* 127:780–784
- Sperry JE, Wilkins TD (1976b) Cytochrome spectrum of an obligate anaerobe, *Eubacterium lentum*. *J Bacteriol* 125:905–909
- Srinivasan S, Hoffman NG, Morgan MT et al (2012) Bacterial communities in women with bacterial vaginosis: high resolution phylogenetic analyses reveal relationships of microbiota to clinical criteria. *PLoS One* 7:e37818
- Stackebrandt E, Ludwig W (1994) The importance of using outgroup reference organisms in phylogenetic studies: the *Atopobium* case. *Syst Appl Microbiol* 17:39–43
- Stackebrandt E, Rainey FA, Ward-Rainey NL (1997) Proposal for a new hierarchical classification system, *Actinobacteria* classis nov. *Int J Syst Bacteriol* 47:479–491
- Stitch SR, Toumba JK, Groen MB et al (1980) Excretion, isolation and structure of a new phenolic constituent of female urine. *Nature* 287:738–740
- Subramanian K, Mickel AK (2009) Molecular analysis of persistent periradicular lesions and root ends reveals a diverse microbial profile. *J Endod* 35:950–957
- Swidsinski A, Mendling W, Loening-Baucke V et al (2005) Adherent biofilms in bacterial vaginosis. *Obstet Gynecol* 106:1013–1023
- Swidsinski A, Dorffel Y, Loening-Baucke V et al (2011) Response of *Gardnerella vaginalis* biofilm to 5 days of moxifloxacin treatment. *FEMS Immunol Med Microbiol* 61:41–46
- Takamine F, Imamura T (1995) Isolation and characterization of bile acid 7-dehydroxylating bacteria from human feces. *Microbiol Immunol* 39:11–18
- Tanaka K, Mikamo H, Nakao K et al (2006) In vitro antianaerobic activity of DX-619, a new des-fluoro(6) quinolone. *Antimicrob Agents Chemother* 50:3908–3913

- Tap J, Mondot S, Levenez F et al (2009) Towards the human intestinal microbiota phylogenetic core. *Environ Microbiol* 11:2574–2584
- Thompson-Chagoyan OC, Fallani M, Maldonado J et al (2011) Faecal microbiota and short-chain fatty acid levels in faeces from infants with cow's milk protein allergy. *Int Arch Allergy Immunol* 156:325–332
- Thota VR, Dacha S, Natarajan A et al (2011) *Eggerthella lenta* bacteremia in a Crohn's disease patient after ileocecal resection. *Future Microbiol* 6:595–597
- Tjalsma H, Boleij A, Marchesi JR et al (2012) A bacterial driver-passenger model for colorectal cancer: beyond the usual suspects. *Nat Rev Microbiol* 10:575–582
- Togni G, Battini V, Bulgheroni A et al (2011) In vitro activity of nifuratel on vaginal bacteria: could it be a good candidate for the treatment of bacterial vaginosis? *Antimicrob Agents Chemother* 55:2490–2492
- Tsuji H, Moriyama K, Nomoto K et al (2010) Isolation and characterization of the equol-producing bacterium *Slackia* sp. strain NATTS. *Arch Microbiol* 192:279–287
- Uematsu H, Sato N, Djais A et al (2006) Degradation of arginine by *Slackia exigua* ATCC 700122 and *Cryptobacterium curtum* ATCC 700683. *Oral Microbiol Immunol* 21:381–384
- Verhelst R, Verstraelen H, Claeys G et al (2004) Cloning of 16S rRNA genes amplified from normal and disturbed vaginal microflora suggests a strong association between *Atopobium vaginae*, *Gardnerella vaginalis* and bacterial vaginosis. *BMC Microbiol* 4:16
- Wade WG, Downes J, Dymock D et al (1999) The family Coriobacteriaceae: reclassification of *Eubacterium exiguum* (Poco et al. 1996) and *Peptostreptococcus heliotrinireducens* (Lanigan 1976) as *Slackia exigua* gen. nov., comb. nov. and *Slackia heliotrinireducens* gen. nov., comb. nov., and *Eubacterium lentum* (Prevot 1938) as *Eggerthella lenta* gen. nov., comb. nov. *Int J Syst Bacteriol* 49(2):595–600
- Walker AW, Ince J, Duncan SH et al (2011) Dominant and diet-responsive groups of bacteria within the human colonic microbiota. *ISME J* 5:220–230
- Wang XL, Hur HG, Lee JH et al (2005) Enantioselective synthesis of S-equol from dihydrodaidzein by a newly isolated anaerobic human intestinal bacterium. *Appl Environ Microbiol* 71:214–219
- Wang XL, Kim HJ, Kang SI et al (2007) Production of phytoestrogen S-equol from daidzein in mixed culture of two anaerobic bacteria. *Arch Microbiol* 187:155–160
- Wang T, Cai G, Qiu Y et al (2012) Structural segregation of gut microbiota between colorectal cancer patients and healthy volunteers. *ISME J* 6:320–329
- Weinberg M, Nativelle R, Prévot AR (1937) Les microbes anaérobies. Masson et Cie, Paris
- Werner T, Wagner SJ, Martinez I et al (2011) Depletion of luminal iron alters the gut microbiota and prevents Crohn's disease-like ileitis. *Gut* 60:325–333
- White WB, Coleman JP, Hylemon PB (1988) Molecular cloning of a gene encoding a 45,000-Da polypeptide associated with bile acid 7-dehydroxylation in *Eubacterium* sp. strain VPI 12708. *J Bacteriol* 170:611–616
- Woo PC, Lau SK, Teng JL et al (2008) Then and now: use of 16S rDNA gene sequencing for bacterial identification and discovery of novel bacteria in clinical microbiology laboratories. *Clin Microbiol Infect* 14:908–934
- Woo PC, Teng JL, Lam KK et al (2010) First report of *Gordonibacter pamelaee* bacteremia. *J Clin Microbiol* 48:319–322
- Woting A, Clavel T, Loh G et al (2010) Bacterial transformation of dietary lignans in gnotobiotic rats. *FEMS Microbiol Ecol* 72:507–514
- Wu S, Rhee KJ, Albesiano E et al (2009) A human colonic commensal promotes colon tumorigenesis via activation of T helper type 17 T cell responses. *Nat Med* 15:1016–1022
- Würdemann D, Tindall BJ, Pukall R et al (2009) *Gordonibacter pamelaee* gen. nov., sp. nov., a new member of the Coriobacteriaceae isolated from a patient with Crohn's disease, and reclassification of *Eggerthella hongkongensis* Lau et al. 2006 as *Paraeggerthella hongkongensis* gen. nov., comb. nov. *Int J Syst Evol Microbiol* 59:1405–1415
- Xu X, Harris KS, Wang HJ et al (1995) Bioavailability of soybean isoflavones depends upon gut microflora in women. *J Nutr* 125:2307–2315
- Yamagishi Y, Mikamo H, Tanaka K et al (2011) A case of uterine endometritis caused by *Atopobium vaginae*. *J Infect Chemother* 17:119–121
- Yokoyama S, Suzuki T (2008) Isolation and characterization of a novel equol-producing bacterium from human feces. *Biosci Biotechnol Biochem* 72:2660–2666
- Yokoyama S, Oshima K, Nomura I et al (2011) Complete genomic sequence of the equol-producing bacterium *Eggerthella* sp. strain YY7918, isolated from adult human intestine. *J Bacteriol* 193:5570–5571
- Yu ZT, Yao W, Zhu WY (2008) Isolation and identification of equol-producing bacterial strains from cultures of pig faeces. *FEMS Microbiol Lett* 282:73–80
- Zhang H, DiBaise JK, Zuccolo A et al (2009) Human gut microbiota in obesity and after gastric bypass. *Proc Natl Acad Sci USA* 106:2365–2370
- Zhi XY, Li WJ, Stackebrandt E (2009) An update of the structure and 16S rRNA gene sequence-based definition of higher ranks of the class *Actinobacteria*, with the proposal of two new suborders and four new families and emended descriptions of the existing higher taxa. *Int J Syst Evol Microbiol* 59:589–608
- Zhou X, Bent SJ, Schneider MG et al (2004) Characterization of vaginal microbial communities in adult healthy women using cultivation-independent methods. *Microbiology* 150:2565–2573

The intestine of mammals harbors diverse and complex bacterial communities dominated by members of the phylum *Firmicutes* and *Bacteroidetes*, and referred to as the intestinal microbiome.

The symbiotic to pathogenic relationships between host and bacteria in the gut, and the underlying influence of bacterial activities on host functions, are still largely unknown.

Nutritional factors are also intrinsic elements of the intestinal ecosystem and interact with both host and bacterial cells.

To understand the intestinal microbiome and its implication in terms of health maintenance, bacteriological studies applied to nutrition and medicine are essential.

The present manuscript summarizes main outputs of my research in the field of gut microbial ecology, with emphasis on the study of bacterial diversity and diet-bacteria interactions, especially in the context of metabolic diseases.